The origin and evolution of granites: an in-situ study of zircons from Scottish Caledonian intrusions

Sarah Kristina Appleby

PhD

University of Edinburgh

2007

Declaration

This thesis is entirely my own work except where indicated otherwise.

Sarah Kristina Appleby

Abstract

Granitic magmatism in collision belts is widely regarded as a major mechanism for generating continental crust. This hypothesis can be tested by identifying the source rocks of granitic magmas, and in particular the contribution by pristine mantle material. The complexity of granites, and their susceptibility to post-crystallisation alteration, has until recently provided a major obstacle to progress. Zircon, a common and chemically robust accessory mineral in granitoid rocks, retains a record of the composition of the magma it grew from. Recent developments in micro-analysis (ion microprobe and laser ablation ICP-MS) now enable in-situ analysis of zircon crystals at high spatial resolution and precision, providing access to this record at the previously inaccessible intra-crystal scale. The resulting data have enormous potential to provide new insights into the nature and age of source rocks and the processes driving magma evolution. This project used an integrated in-situ O, U-Pb and Hf isotope, trace and rare earth element study of zircon to identify the sources and chart the evolution of two 'I-type' (igneous/infracrustal precursor) Scottish late Caledonian (~430-400 Ma) granite plutons. I have constrained models of magma generation, the relative contributions of mantle and crust, the ages and identities of their lower crustal sources, and have shown that the plutons played, at most, a minor role in crustal growth. In addition, I have been able to resolve the extent to which open-system changes like magma mixing affected the magma compositions. The same approach was used in a pilot study of three Caledonian (~460 Ma) 'S-type' (sedimentary/supracrustal precursor) granite plutons, which theoretically represent magmas formed by melting of a purely supracrustal source. The data confirm that Dalradian country rocks were the primary source, but reveal remarkable isotopic diversity within and amongst the three plutons. The most important general conclusion from this PhD study is that the complexity and scale of isotopic heterogeneity between plutons, amongst samples of the same pluton, in single samples and within individual crystals is far greater than previously recognised, consistent with the incremental assembly of plutons from multiple melt batches of differing composition, sources and petrogenetic evolution.

Acknowledgements

Many people have accompanied and helped me over the course of the last three years to get this PhD to completion. Firstly, I would like to thank my supervisor team Colin Graham, Martin Gillespie, Grahame Oliver and Richard Hinton, who not only designed an excellent PhD project with clearly defined aims, but also did an incredible job with respect to providing a wealth of background information, always being available for meetings that could last a few minutes or several hours, getting my papers into publishable form and always having an open ear for PhD-related as well as personal issues.

Secondly, I would like to express gratitude to the people who have provided me with high-quality data and have supervised me on the great instruments I had the privilege to use. At the University of Edinburgh these are the EMMAC crew John Craven, Simone Kasemann, Nicola Cayzer, Paula McDade and David Steele, Godfrey Fitton, Nic Odling and Mike Hall. Other people who have been kind enough to offer assistance, training and analytical support include Kate Breward (BGS) for whole-rock ICP-MS REE data, Angus Calder (St Andrews) for assisting during grain separation, Tony Fallick for whole-rock oxygen isotope data, and Matt Horstwood (NIGL) for LA-ICP-MS Hf analysis.

I would also like to thank my funding sources without whom this project would have never been possible in the first place: BGS for a UCAC grant to support fieldwork and analyses, Gottlieb Daimler- und Karl Benz-Stiftung, the DAAD (German Academic Exchange Service) and the School of GeoSciences, University of Edinburgh, for doctoral scholarships.

I have also benefited from scientific discussions with John Valley, Aaron Cavosie, Zeb Page and Tony Kemp, who have been great inspiration over the three years.

My Mum and Dad, who provided moral support on a daily basis, certainly deserve a very big ‘Thank You’. Even though they have different backgrounds they were always willing to listen and offer an opinion. They also helped me greatly to keep in touch with reality when things weren’t going so well.

My ‘Mouse House’ office mates – Ruth, Amber, Antoine, Leon, Clare and especially Janette have been wonderful companions. I think we had a great time together, helped each other out or gave each other space when necessary.

The last person I would like to mention here is my partner and colleague Nigel Kelly, who probably had the toughest part during my PhD. Not only did he always motivate me during the rough patches of my PhD and personal life of which there have been unfortunately quite a few. He was also a fantastic colleague, who shared my excitement and was always very willing to discuss ideas.

Table of Contents

II. Paper 1: A cryptic record of magma mixing in diorites revealed by high-precision SIMS oxygen isotope analysis of zircons

III. Paper 2: A tale of two plutons: an integrated ion microprobe study of $^{18}O/^{16}O$, U-Pb, trace elements and REE in zircons from Scottish Caledonian granites

IV. Paper 3: Using in-situ O and Hf isotope analysis of zircons to constrain the sources of late Caledonian granites in Scotland

V. Paper 4: An integrated O, U-Pb and Hf isotope study of zircons in S-type granites

VI. Conclusions

IX. Appendices

List of Figures

I. Introduction

II. Paper 1

III. Paper 2

IV. Paper 3

V. Paper 4

List of Tables

I.

Introduction

Introduction

1. Introduction

The formation of the Earth's crust is widely envisaged to be at least a two-stage process involving generation of basaltic magmas by melting of the mantle and subsequent production of more evolved magmas such as granites by either differentiation or re-melting of basaltic magmas (Kelemen, 1995; Rudnick, 1995). Differentiation is thought to occur within large magma chambers, which ascend rapidly through the crust by diapirism or stoping until they reach shallow crustal levels where they are either emplaced as plutons or form sub-volcanic magma chambers (e.g. Buddington, 1959; Paterson et al., 1996; Petford et al., 2000; Pitcher and Berger, 1972).

Granites are widely viewed as the end-products of growth of the Earth's crust either directly from mantle-derived magmas or by re-melting of pre-existing crust (e.g. Atherton and Petford, 1993; Chappell and White, 2001; Gill, 1981; Grove et al., 2002, 2003; Grove and Kinzler, 1986; Izebekov et al., 2004; Müntener et al., 2001; Musselwhite et al., 1989; Petford and Atherton, 1996; Prouteau and Scaillet, 2003; Rapp and Watson, 1995; Rogers and Hawkesworth, 1989; Smith and Leeman, 1987; Tepper et al., 1993). In order to understand processes of crust formation and the evolution of the continental crust, granites from different locations and tectonic settings and of varying ages have been studied for many decades. A principal aim of granite research has been to identify granite sources, and in particular the contribution made by the mantle.

Previously it has been suggested that granites have simple petrogenetic histories and comprise either igneous/infracrustal (I-types) or sedimentary/supracrustal (S-types) sources (Chappell and White, 1974). However, after much further research, the development of new analytical techniques and improved precisions of conventional techniques, it has been shown that in reality the majority of granites comprise multiple sources (John and Wooden, 1990; Kemp et al., 2007; Kemp and Hawkesworth, 2003; Miller et al., 1990), which leaves the relationship between granite genesis and crustal growth unresolved.

While the origin of S-type granites by melting of crustal sedimentary rocks is widely accepted, the origin of I-type granites is much more complicated and controversial. The latter may represent mixtures of melts of different (crustal or mantle) origins, may contain unmelted or partially melted remnants of their sources, and may have evolved and differentiated extensively from their parental mafic melts. Furthermore, whole-rock geochemical studies of granites have been complicated by their susceptibility to post-crystallisation alteration by fluid-rock exchange, in particular the usually abundant feldspars (e.g. King and Valley, 2001; Taylor and Huston, 1998; Valley and Graham, 1996); whole-rock data commonly do not represent the magma composition from the time of crystallisation, and may lead to incorrect interpretations and models.

In recent years studies using the mineral zircon ($ZrSiO_4$), a common accessory phase in granitoid rocks, have made significant contributions to our understanding of the origin and evolution of granites, and hence of the continental crust (e.g. Coleman et al., 2004; Hawkesworth and Kemp, 2006a, b; Kemp et al., 2007; Matzel et al., 2006). Zircon has been widely used to determine the U-Pb crystallisation ages of granitic rocks (e.g. Pidgeon and Aftalion, 1978; Pidgeon and Compston, 1992). As zircon is resistant to chemical modification following crystallisation, even at magmatic temperatures, it also contains a wealth of further information about the origin and evolution of its host granite. Due to its significant concentrations of U, Th, Hf, trace and rare earth elements (REEs) (ppm to percent level) (Kinny and Maas, 2003) it is suitable not only for U-Pb dating, but also for oxygen and Hf isotope, and trace element/REE analyses, which may be used to trace the entire petrogenetic history of the host granite from genesis to post-crystallisation alteration. Zircon crystals may now be analysed in-situ at high spatial resolution and precision by ion microprobe (SIMS) and laser ablation ICPMS. Due to the high spatial resolution of these techniques multiple analyses may be made within a single crystal, providing information about previously inaccessible intra-grain changes in composition. In addition, as SIMS analysis consumes only very small amounts of sample material oxygen, U-Pb isotope, trace elements/REEs and Hf isotopes can be measured in exactly the same area enabling direct correlation of the data sets.

In this PhD study, I have applied these new micro-analytical techniques to zircons of Scottish Caledonian I- and S-type granite plutons. Even though this classic granite suite has been studied extensively over the last four decades the sources and petrogenesis of the voluminous late Caledonian (~430-400 Ma) I-type granites in particular, and hence their role in crustal growth remain largely unresolved due to the limitations of whole-rock data. The objectives of this study were to:

- Constrain the ages and origins of selected Scottish Caledonian granite plutons. Characterise their mantle and/or lower crustal sources.
- Test models of lower crustal age and composition beneath the Scottish Highlands.
- Evaluate the contribution of these voluminous magmas to continental growth.
- Use information stored in zircon to test existing models and provide new insights into granite genesis, ascent and emplacement.

2. The origin and evolution of granites – previous and recent models

2.1. Granite sources

In order to establish a link between granite magmatism and crustal growth, the main aim of past and ongoing granite research has been to identify the sources of granites, and in particular to constrain the proportion of primitive mantle-derived versus crustal material. Chappell and White (1974) conducted an extensive whole-rock study of granites in the Lachlan Fold Belt (LFB) of southeastern Australia, based on which they proposed that granites are derived from either an igneous/infracrustal (I-types) or a sedimentary/supracrustal source (S-types), which can easily be distinguished by whole-rock geochemical and isotopic compositions, and major and accessory phase assemblage (see Table 1 for characteristics of I- and S-type granites). They further suggested that granitoid rocks inherit their geochemical composition and possibly even some petrographic features from their source, and closely reflect the composition of the latter.

Table 1
Characteristics of I- and S-type granites (Chappell and White, 2001)

I-type granites	S-type granites
relatively high Na, Na_2O typically > 3.2 % in felsic varities decreasing to > 2.2 % in mafic samples	relatively low Na, Na_2O typically < 3.2 % in rocks with c. 5 % K_2O, decreasing to < 2.2 % in rocks with c. 2 % K_2O (due to removal of Na into sea water (or evaporites) during sedimenatry fractionation)
Mol. $Al_2O_3/(Na_2O+K_2O+CaO)$ < 1.1	Mol. $Al_2O_3/(Na_2O+K_2O+CaO)$ > 1.1
CIPW normative diopside or < 1 % normative corundum	> 1 % CIPW normative corundum
broad spectrum of compositions from felsic to mafic	relatively restricted in composition to high SiO_2 types
regular inter-element variations within plutons; linear or near-linear variation diagram	variation diagrams more irregular
hornblende common	muscovite, up to 35 % biotite (in more mafic S-types), garnet and cordierite common, no hornblende
sphene; apatite inclusions in biotite and hornblende	monazite, apatite in larger discrete crystals
$(^{87}Sr/^{86}Sr)_i$ = 0.704-0.706 (McCulloch and Chappell (1982) report values of up to 0.711)	$(^{87}Sr/^{86}Sr)_i$ > 0.708
mafic hornblende-bearing igneous xenoliths	metasedimentary xenoliths

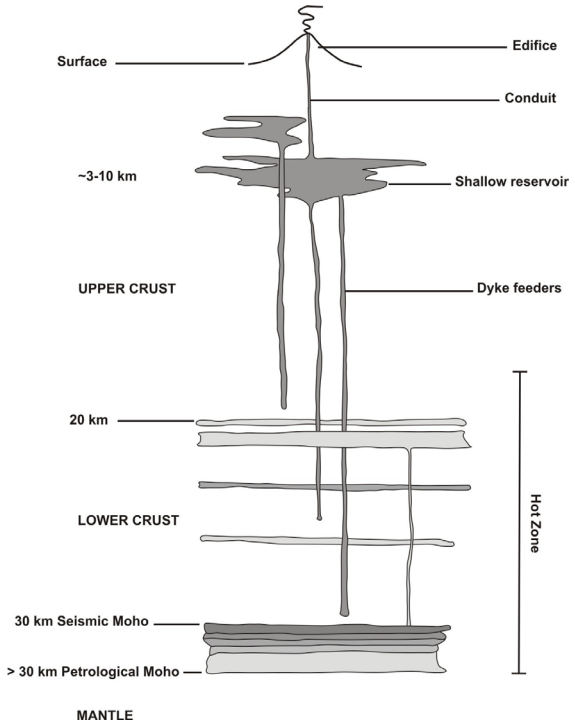

Fig. 1: Deep crustal hot zone model (after Annen et al., 2006). See text for description.

Since then, numerous whole-rock geochemical and isotopic studies of the LFB granites and other granites worldwide have shown that in reality the majority of intrusions display to some extent the characteristics of both I- and S-type granites, and appear to comprise multiple sources (e.g. Chappell et al., 1987, 2000; Collins, 1998, 1999; Kemp and Hawkesworth, 2003; Vernon, 1983; Wall et al., 1987). This has recently been confirmed for selected LFB I-type granites (Cobargo, Jindabyne and Why Worry suites) by an integrated in-situ oxygen and Hf isotope study of zircons, which was able to demonstrate that these intrusions were formed by interaction (magma mixing or assimilation) between mantle-derived juvenile and supracrustal materials (Kemp et al., 2007), and were not solely sourced from the mantle or igneous precursors. Another important outcome of this study was that by using an integrated micro-analytical approach it was possible to show that the I-type granites incorporate between 50 % and 85 % pristine contemporaneous mantle material, and hence have made a significant contribution to Lower Palaeozoic continental crustal growth.

2.2. Melt generation, ascent and emplacement

The generation of intermediate and silicic magmas has been widely considered to occur predominantly in the crust or close to the Moho by differentiation of mantle-derived basalt or basaltic andesite (e.g. Gill, 1981; Grove et al., 2002, 2003; Grove and Kinzler, 1986; Müntener et al., 2001; Musselwhite et al., 1989; Prouteau and Scaillet, 2003; Rogers and Hawkesworth, 1989) and by partial melting of pre-existing crustal rocks following mafic underplating (e.g. Atherton and Petford, 1993; Chappell and White, 2001; Izebekov et al., 2004; Petford and Atherton, 1996; Rapp and Watson, 1995; Smith and Leeman, 1987; Tepper et al., 1993). The depths at which chemical differentiation, magma mixing or melting and assimilation take place are not well constrained; the traditional view has been that these processes predominantly occur in crustal magma chambers. These are envisaged as large bodies of magma, which ascend rapidly through the crust by diapirism or stoping (e.g. Buddington, 1959; Paterson et al., 1996; Petford et al., 2000; Pitcher and Berger, 1972), and are either emplaced as plutons or form sub-volcanic reservoirs.

However, a number of problems have been identified with these traditional and relatively simple models. (1) Even though the existence of some ephemeral shallow sub-volcanic magma chambers has been proven, seismic techniques have failed to locate large bodies of magma (e.g. Detrick et al., 1990). (2) To produce intermediate and silicic magmas, which in large batholiths may occupy hundreds to thousands of km^3, approximately twice as much primary mantle-derived magma has to undergo fractional crystallisation (Foden and Green, 1992; Müntener et al., 2001). However, this would also produce huge amounts of mafic cumulates of which to date no evidence has been found. (3) Thermal modelling has demonstrated that it is difficult to maintain even small permanent magma chambers in a molten state in the cold shallow crust, and that high rates of magma replenishment would be required (e.g. Lister, 1983). (4) The diapiric ascent of magma is too slow and energetically inefficient to be geologically important (e.g. Clemens and Mawer, 1992; Petford et al., 2000), and stoping is not volumetrically significant in the emplacement of most plutons (Glazner and Bartley, 2006).

Recent thermal models suggest that 'deep crustal hot zones' may play an important role in the generation of intermediate and silicic igneous rocks (Annen et al., 2006; Annen and Sparks, 2002). The development of these hot zones results from repeated intrusion of mantle-derived hydrous basalt sills into the lower and/or middle crust, where melts are generated either by (1) differentiation of the basalt to produce residual and more siliceous H_2O-rich melts, by (2) mixing between silicic melts, possibly generated by partial melting of crustal rocks (e.g. Druitt et al., 1999), and mantle-derived mafic magmas, or by (3) partial melting of pre-existing crustal rocks including early basalt sills or older mafic lower crust (Fig. 1). Mixing of residual melts (or mafic mantle melts) and crustal partial melts creates a large range of intermediate and silicic melts. Thus, the 'deep crustal hot zone model' provides a conceptual framework and theoretical underpinning for models of mafic underplating (Raia and Spera, 1997), basalt differentiation near the Moho (Gill, 1981; Grove et al., 2002), and assimilation and fractional crystallisation (AFC) (e.g. DePaolo, 1981). The efficiency of melt production in deep crustal hot zones largely depends on the amount of intruding basalt, spacing of the basalt sills, the level of emplacement in the crust, the rate of emplacement and the composition of lower and middle crust.

Residual melts are most efficiently produced by differentiation of basalt at deep crustal levels. However, in the model of Annen et al. (2006) the largest amounts of crustal partial melts are generated either by random basalt sill injection over extended periods of time at different mid- and lower crustal levels, heating the crust from below and above, or by emplacement of sills at the contact with a fertile upper crust. After melt generation, the melts segregate and, depending on their H_2O content, density, viscosity and ascent path, ascend more or less rapidly into shallow reservoirs where they undergo crystallisation by degassing and cooling. Entrained material from the source will be partially or entirely digested, but contamination by xenocrystic wall-rock material may occur during ascent (Annen et al., 2006). Melt extraction is generally envisaged to take place in pulses, their frequency being dependent on the timescales of melt generation and segregation (Annen et al., 2006; Bons et al., 2004). Thus, magma reservoirs and plutons are thought to grow by incremental assembly of melt batches of commonly differing composition (Annen et al., 2006).

The 'deep crustal hot zone' model is in good agreement with a growing body of field and geochronological evidence, which suggests that some (and perhaps most) plutons were emplaced incrementally as a series of sheet- or dyke-like intrusions over time spans an order of magnitude longer than the thermal lifetime of large magmatic masses and never existed as a large molten magma body (Brown and McClelland, 2000; Coleman et al., 1995; Wiebe, 1993; Wiebe and Collins, 1998). For example, TIMS dating of the Tuolomne Intrusive Suite in California demonstrated that it was incrementally assembled over a period of at least 10 m.y. (Coleman et al., 2004). In addition, a recent detailed TIMS study of the Mount Stuart batholith located in the North Cascades of Washington State was able to resolve that it was constructed by four major magma pulses over a period of ~5.5 m.y. (Matzel et al., 2006). Contacts between different magma batches may be sharp, gradational or cryptic depending on the time between injection events and the degree of homogenisation by post-emplacement annealing (Glazner et al., 2004). Hence, the chemical heterogeneity previously interpreted to result from fractional crystallisation (e.g. Bateman and Chappell, 1979; Sisson and Moore, 1994; Tindle and Pearce, 1981) and/or magma mixing (Frost and Mahood, 1987; Kistler et al., 1986) in large

magma chambers, might reflect processes operating at much deeper levels (Glazner et al., 2004), for example in deep crustal hot zones.

3. The Scottish Caledonian granites

The majority of the classic Scottish Caledonian I- and S-type granites are located in the Grampian terrane of the Scottish Highlands **(Fig. 2)** where they intruded metasedimentary rocks of the Dalradian Supergroup, a c. 25 km thick sequence of deformed and metamorphosed late Neoproterozoic to Lower Ordovician shallow- and deep-water sediments and volcanics (Harris et al., 1978, 1994; Stephenson and Gould, 1995). The Caledonian granites are in many respects (e.g. emplacement age, occurrence of both I- and S-type granites) similar to the LFB granites of southeastern Australia. However, in the LFB I- and S-type granites intruded contemporaneously (~450-340 Ma) (Gray and Foster, 1997) and share several chemical features, which led to the interpretation that their generation was coupled and involved melting of similar source materials (Kemp and Hawkesworth, 2003). In contrast, the Caledonian I- and S-type granites intruded at different times (S-types: ~470-465 Ma; I-types: 430-400 Ma) and involved different sources.

The Caledonian S-type granites are thought to have been produced by melting of a supracrustal source, most likely the Dalradian country rocks (Harris et al., 1978, 1994; Stephenson and Gould, 1995), and to date no evidence exists for the involvement of infracrustal or mantle-derived components. The origin and sources of the late Caledonian I-type granites have caused much debate and are still not fully resolved. Proposed models suggest that the granites were predominantly derived from the mantle (Brown and Locke, 1979; Simpson et al., 1979), from the crust (Hamilton et al., 1980; Leake, 1978; Pankhurst, 1979; Pidgeon and Aftalion, 1978; Pitcher and Berger, 1972), or from mixed sources comprising mantle and crustal components (Clayburn et al., 1983; Frost and O'Nions, 1985; Halliday, 1984; Halliday et al., 1979, 1980, 1984; Harmon and Halliday, 1980); the latter model is generally favoured today. However, little is known about the composition of the mantle and lower crustal basement beneath the Grampian terrane; thus the identities

and compositions of the sources and their relative contributions to granitic magmas have not been constrained.

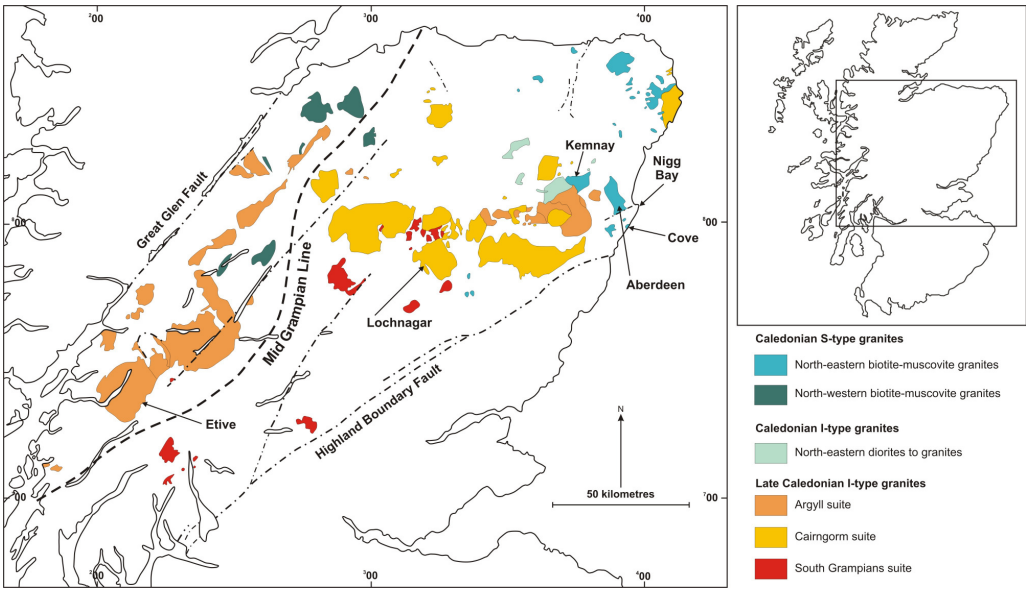

Fig. 2: Map of the Grampian terrane (located between Great Glen and Highland Boundary faults) in Scotland showing the locations of the Caledonian I- and S-type granites and of the plutons studied in this PhD project (after Stephenson and Gould, 1995).

3.1. The Caledonian S-type granites

The Caledonian S-type granites intruded contemporaneously with and subsequent to the Grampian Event, which occurred between c. 480 Ma and 465 Ma (Oliver, 2001) and resulted from the collision of the Laurentian continental margin with a southeast-dipping subduction zone and a volcanic arc that developed during closure of the Iapetus Ocean. Evidence of the volcanic arc was found in western Ireland (South Mayo Trough) (Dewey and Ryan, 1990); indirect evidence for the existence of this arc was discovered in the Midland Valley of Scotland, buried underneath the post-Caledonian sedimentary cover (Bluck, 1983, 1984). The Grampian Event is considered to be the main tectonic and metamorphic event in the Grampian Highlands, involving overthrusting of an ophiolite nappe, regional deformation and

Barrovian metamorphism of the Dalradian metasedimentary rocks (Dewey and Ryan, 1990; Dewey and Shackleton, 1984).

The Grampian Event was accompanied by syn- and late-tectonic plutonism. This included mafic and ultramafic plutons - the 'Newer Gabbros' (Read, 1961), and two suites of syn- to late-tectonic diorites and granites (Strachan et al., 2002). The majority of granites are peraluminous, have high initial $^{87}Sr/^{86}Sr$ ratios (> 0.71), contain a high proportion of country rock xenoliths and older inherited zircons, and have thus been interpreted as S-type granites (Harmon, 1983; Pankhurst, 1974; Pidgeon and Aftalion, 1978); few intrusions show I-type characteristics (Oliver et al., 2000). The S-type granites were probably produced by melting of Dalradian Supergroup country rocks at structural levels not far below the present level of exposure (Kneller and Aftalion, 1987; Richardson and Powell, 1976). The heat required for melt generation was most likely provided by crustal thickening and Barrovian metamorphism following arc-continent collision, aided in the Buchan area of the northeast Scottish Highlands by intrusion of the 'Newer Gabbros' (Oliver, 2001).

3.2. The late Caledonian I-type granites

Following the Grampian Event (465 Ma to 435 Ma) the Grampian terrane experienced cooling, isostatic uplift and decompression (Dempster et al., 1995; Dewey and Mange, 1999; Oliver, 2001; Oliver et al., 2000; Soper et al., 1999). Closure of the Iapetus Ocean culminated in the collision of Laurentia, Baltica and Avalonia (Pickering et al., 1988; Soper et al., 1992; Soper and Hutton, 1984). At approximately 435 Ma oblique collision of Baltica and Laurentia resulted in the Scandian Event; this caused major ductile thrusting, folding and metamorphism within the Northern Highland terrane (Coward, 1990; Dallmeyer et al., 2001; Dewey and Mange, 1999; Kinny et al., 2003; Strachan et al., 2002), however in the Grampian terrane its effects appear to have been limited to large-amplitude folding and brittle faulting. Between c. 430 Ma and 400 Ma, broadly contemporaneous with - and subsequent to - the Scandian Event, the late Caledonian I-type granites were emplaced into Dalradian metasediments of the Grampian terrane (Oliver, 2001;

Rogers and Dunning, 1991; Stewart et al., 2001). Recent age dating has shown that the main phase of emplacement took place at approximately 425 ± 5 Ma (Fraser et al., 2004; Rogers and Dunning, 1991). However, the connection between the collision and the voluminous I-type magmatism is unclear.

The predominantly shoshonitic and high-K calc-alkaline Caledonian I-type plutons have geochemical features typical of modern continental arcs, with the majority showing a metaluminous affinity (except for granites with > 70 wt% SiO_2, which are peraluminous) (Frost et al., 2001). They are commonly hornblende-bearing (Soper, 1986) and contain high Rb/Sr and K/Na, low K/Rb and relatively low initial Sr ratios (0.704-0.708) (Halliday et al., 1985; Oliver et al., 2001; Stephens, 1988; Thirlwall, 1988). Previously they have been interpreted to have formed above an Andean-style subduction zone that dipped beneath the Laurentian continental margin (Brown, 1991; Brown et al., 1985; Oliver, 2001; Soper, 1986; Stephens and Halliday, 1984; Stephenson et al., 1999; Thirlwall, 1981, 1982, 1988). However, due to temporal, spatial and chemical discrepancies between the late Caledonian I-type plutons and typical subduction-related melts, this model has recently been challenged and an alternative slab-breakoff model has been proposed (Atherton and Ghani, 2002). The exact tectonic setting that led to emplacement of the late Caledonian I-type granites in Scotland remains controversial.

On the basis of whole-rock geochemical and isotopic data, the late Caledonian I-type granites have been subdivided into three distinct granite suites - the Argyll, Cairngorm and South Grampians suites (Stephens and Halliday, 1984). The *Argyll suite* consists of hornblende-biotite granodiorite and biotite granodiorite plutons with minor dioritic, appinitic and monzogranitic components (Stephens and Halliday, 1984; Strachan et al., 2002). The plutons are strongly metaluminous and are enriched in Ba, Sr and Na relative to the plutons of the other suites, whereas Nb, Th and Rb are present only at low concentrations (Fowler et al., 2001; Halliday, 1984; Halliday et al., 1985; Stephens and Halliday, 1984; Tarney and Jones, 1994; Thirlwall, 1988). The *Cairngorm suite* consists almost entirely of biotite monzogranite, which varies texturally between microgranite and coarse-grained, K-feldspar megacrystic granite. The intrusions contain high concentrations of Rb, Nb, Th and U, but have low Ba, Sr, Ti, P contents (Stephens and Halliday, 1984) relative to the Argyll suite. The *South*

Grampians suite is dominated by diorites, granodiorites and monzogranites, and comprises a higher proportion of gabbroic and appinitic intrusions than the other suites. In general, this suite is strongly metaluminous with higher K and Th abundances than the Argyll suite, but lower concentrations of Zr, La, Ce, Ba and Rb (Stephenson et al., 1999).

To date the compositional differences between the suites are not fully understood; they may reflect heterogeneities in the composition and age of the underlying lower crustal basement and/or mantle, or differences in the relative mantle and crustal contributions. Halliday (1984) proposed the existence of an important boundary in the deep basement and possibly in the mantle beneath the Grampian terrane separating the Argyll suite plutons in the northwest from the Cairngorm and South Grampians suite plutons in the southeast; he referred to this inferred structure as the Mid Grampian Line (MGL) (Fig. 2).

4. Aims and objectives of this study

Recent micro-analytical studies of zircons from granitoid rocks integrating oxygen, U-Pb, Hf isotope, and trace element/REE data (e.g. Kemp et al., 2007) have made significant advances in our understanding of the complex origin and evolution of granite suites, and their relationship to crustal growth. In addition, the ultra-high precision geochronological studies of zircon from granite plutons of (e.g.) the Sierra Nevada in California (Tuolomne Intrusive Suite, Coleman et al., 2004) and the Cretaceous North Cascades in Washington State (Mount Stuart batholith, Matzel et al., 2006) have provided important insights into pluton assembly and emplacement mechanisms.

However, to date only a limited number of such studies have been carried out and many uncertainties remain. Some aspects of pluton assembly and emplacement mechanisms have been largely resolved by ultra-high precision geochronology, but they provide no information about granite sources, genesis or magmatic processes that may have occurred during ascent and at shallower levels.

The aims and objectives of *this* study were to use an in-situ and integrated micro-analytical study of isotopic and trace element/REE signatures in zircons from the Scottish Caledonian granites to:

- Constrain the relative contributions to I-type granites made by contemporaneous mantle melts and recycled lower continental crust, and hence to quantify their contribution to Phanerozoic continental growth.
- Test previous and recent models of magma generation, ascent and emplacement.
- Identify open-system processes such as magma mixing, assimilation and hydrothermal alteration.
- Evaluate the scales of heterogeneity, and hence the complexity of plutonic magma systems, by combining information obtained on pluton-, sample-, crystal- and intra-crystal scales.
- Assess the applicability - and identify the limitations - of integrated multi-isotope and trace element studies of zircon to answering the above questions.
- Resolve the compositions and ages of the sources of Caledonian granite suites in more detail, explaining their observed whole-rock geochemical differences, and test existing models of the nature, ages and origins of the basement underlying the Grampian terrane.

To achieve these aims, several plutons from the classic late Caledonian granites were chosen for more detailed study. Like the LFB granites, the Caledonian granites have been studied for decades and an extensive data base of field, petrographic, whole-rock geochemical and isotopic data exists. Nevertheless, their origin, sources and petrogenetic histories remain largely unresolved. Thus, they represent an ideal location to use such an integrated approach, and to test existing regional and global models on the origin and evolution of granites.

For this purpose two I-type granites (Lochnagar and Etive) were selected (Fig. 2). The reasons for choosing these two plutons were that both are relatively well exposed, and have previously been mapped and studied in detail, providing a large data set of field relationships, petrographic descriptions, whole-rock and mineral chemical and isotopic data; these provide the basis for this integrated micro-

analytical study. In addition, based on the existing data the selected plutons differ in their complexity. The Lochnagar pluton represents a relatively simple composite pluton, comprising two main granite facies (L1 and L2), a third, locally developed, granite facies (L3), microgranites and several marginal diorites (Smith et al., 2001). In contrast, the Etive pluton comprises four main intrusive phases (the Meall Odhar, Cruachan, Starav and Quarry intrusions), which range in composition from granite to monzodiorite/diorite (Clayburn et al., 1983). Whole-rock geochemical and isotopic evidence suggests that both the Cruachan and Starav intrusions were emplaced in multiple pulses, and that the Starav Intrusion sourced different material than the other phases (Batchelor, 1987; Clayburn et al., 1983). Furthermore, based on differing whole-rock geochemical and isotopic compositions, the Lochnagar and Etive plutons are interpreted to belong to different granite suites – the Cairngorm and Argyll suites (Stephens and Halliday, 1984). To date the origin of these compositional differences is largely unresolved, but it has been suggested that they either reflect variations in the relative contributions of mantle and crust or differences in the nature of the underlying lower crustal and mantle reservoirs (Halliday, 1984).

In addition to the I-type granites, samples of three S-type granites (Kemnay, Cove and Nigg Bay) (Fig. 2) were collected. As previous studies suggest the S-type granites formed by melting of their current Dalradian Supergroup country rocks they are thought to have simple petrogenetic histories, which is in contrast to the late Caledonian I-type granites. The Kemnay, Cove and Nigg Bay granites are hosted by the same lithological unit of the Dalradian Supergroup, the Aberdeen Formation, hence probably have similar source rocks. However, they vary significantly in size (Kemnay: c. 36 km^2, Cove: c. 1.7 km^2, Nigg Bay: exact size unknown, but probably considerably smaller than Cove). The Dalradian Supergroup also comprises the host rocks to the I-type granites, and thus the S-type granites provide an important constraint on the types of crustal melts that might have contributed to the formation of the Lochnagar and Etive I-type plutons.

The main focus of this PhD study has been on zircons from the late Caledonian I-type granites as they have previously caused the most debate. As little or no work has been published to date on the S-type granites, this part of the project was considered a pilot study.

5. Methods

Recent developments in micro-analytical techniques enable analyses of oxygen, U-Pb isotopes, and trace and rare earth elements by ion microprobe (SIMS) and Hf isotopes by laser ablation-multi-collector ICP-MS (LA-MC-ICPMS) at high spatial resolution and precision in-situ in zircon. Due to the high spatial resolution of ion microprobe and laser ablation systems (~20 µm and ~50 µm respectively) multiple analyses may be made on a single zircon crystal (e.g. core and rim) enabling correlation of multiple isotopic and trace element data sets with textural information obtained from cathodoluminescence (CL) and backscattered electron (BSE) images, thereby providing access to otherwise inaccessible intra-grain variation. Furthermore, as in-situ analysis by SIMS consumes only very small amounts of sample material isotopes and trace elements may be measured in exactly the same area within each crystal, which permits direct correlation of the different data sets. The following sections give a background to the techniques employed in this study, including the utility of zircon as a petrogenetic indicator, and the applicability of isotopic and trace element/REE information stored in zircon to achieving the aims and objectives of this study.

5.1. Zircon

Zircon ($ZrSiO_4$) is a common accessory mineral in igneous rocks of intermediate to silicic composition (Hoskin and Schaltegger, 2003). As it is chemically and mechanically extremely robust, it is able to preserve compositional information about the melt it crystallised from. Due to its refractory nature, crystals of zircon in igneous rocks commonly contain pre-magmatic 'inherited' cores (Fig. 3a) that are either inherited from the source region or assimilated from country rocks. Since the 1950s empirical and experimental studies have aimed to establish the temperatures and conditions under which zircon crystallises (e.g. Baker et al., 2002; Dickinson and Hess, 1982; Harrison et al., 2007; Keppler, 1993; Linnen and Keppler, 2002; Poldervaart, 1955, 1956; Watson, 1979, 1996b; Watson et al., 2006; Watson and Harrison, 1983, 2005). For the system SiO_2-Al_2O_3-Na_2O-K_2O Watson (1979)

demonstrated that the Zr saturation level required for zircon to crystallise strongly depends on a melt's molar proportions of $(Na_2O+K_2O)/Al_2O_3$, but only little on temperature, SiO_2 content or Na_2O/K_2O. He also showed that in peraluminous melts less than 100 ppm Zr is needed to saturate the melt and crystallise zircon, which suggests that zirconium saturation is commonly reached early in their magmatic evolution (Corfu et al., 2003). Hence, zircon is likely to record information about the melt's primary composition and also any subsequent changes in melt composition, temperature or crystallisation conditions arising from either local closed-system processes or large-scale open-system changes (e.g. magma mixing, assimilation) (Hoskin and Schaltegger, 2003; Shore and Fowler, 1996; Vavra, 1990, 1993, 1994).

Igneous zircons typically vary in size between 20 μm and 250 μm, and are sub- or euhedral with a range of external morphologies (Hoskin and Schaltegger, 2003). Since the 1950s studies have attempted to use zircon morphologies as petrogenetic indicators (Hoffmann, 1981; Kostov, 1973; Larsen and Poldervaart, 1957; Poldervaart, 1955, 1956; Pupin and Turco, 1972a, b, c); the most widely used classification scheme was published by Pupin (1980). More recently it has been demonstrated that external zircon morphologies are of very limited use as petrogenetic indicators because zircons from a single rock and age population are often highly variable in their morphologies, those from different rock types may have similar morphologies, and the morphologies of zircon crystals commonly change during growth due to local kinetic factors such as diffusion rates and adsorption (Dowty, 1980; Vavra, 1990, 1993).

Zircons can incorporate large amounts of trace elements, such as Hf, Y, REE, P, U and Th (ppm to percent level) (Kinny and Maas, 2003), which are substituted into the crystal lattice either by simple (e.g. $U^{4+} = Zr^{4+}$) (Frondel, 1953) or coupled (e.g. $(Y, REE)^{3+} + P^{5+} = Zr^{4+} + Si^{4+}$ = 'xenotime substitution') substitution (Speer, 1982). Intra-grain variations in Hf, P, Y, REEs, U and Th typically result in the development of oscillatory growth zoning (Fig. 3b), which is a common feature of magmatic zircon (e.g. Benisek and Finger, 1993; Fowler et al., 2002; Hanchar and Rudnick, 1995; Köppel and Sommerauer, 1974). Quite commonly growth zoning is interrupted by resorption surfaces, which reflect periods of Zr undersaturation in the

magma caused by either large-scale mixing events or local kinetic phenomena (Corfu et al., 2003).

In the past, zircons have been widely used for U-Th-Pb geochronology. However, they are also commonly used in trace element studies, in both igneous and metamorphic petrology. As recent developments in micro-analysis now allow measurement of oxygen and Hf isotopes at high spatial resolution and precision in-situ in zircon, they have become increasingly important in studies of crustal growth and evolution (e.g. Hawkesworth and Kemp, 2006a, b; Kemp et al., 2005, 2006, 2007).

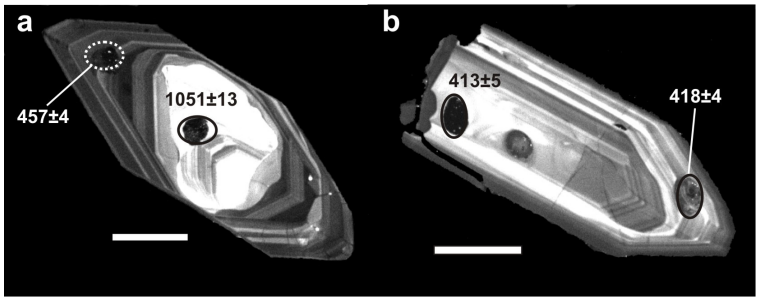

Fig. 3: CL images of (a) a zircon comprising an old inherited core (Kemnay Granite, grain 23) and (b) a magmatic zircon grown from the granite melt (L2 (Lochnagar pluton), grain 11).

5.2. Oxygen isotopes

The fractionation of oxygen isotopes between coexisting phases increases with decreasing temperatures, with Si-rich phases being enriched in ^{18}O relative to Fe-rich and Si-poor phases. This contributes to the characteristic enrichment of ^{18}O in crustal rocks relative to that of the Earth's mantle (Fig. 4). Thus, oxygen isotopes have been widely used in petrogenetic evolution studies of granitic rocks to constrain the relative contributions of mantle and crust. However, as the oxygen isotope compositions of granites and their constituent minerals are sensitive to modification by assimilation of ^{18}O-enriched crustal rocks, magma mixing and hydrothermal alteration by ^{18}O-depleted and/or ^{18}O-enriched fluids (e.g. King et al., 1997, 2000; Monani and Valley, 2001; Valley and Graham, 1996), whole-rock studies often deliver ambiguous or controversial results.

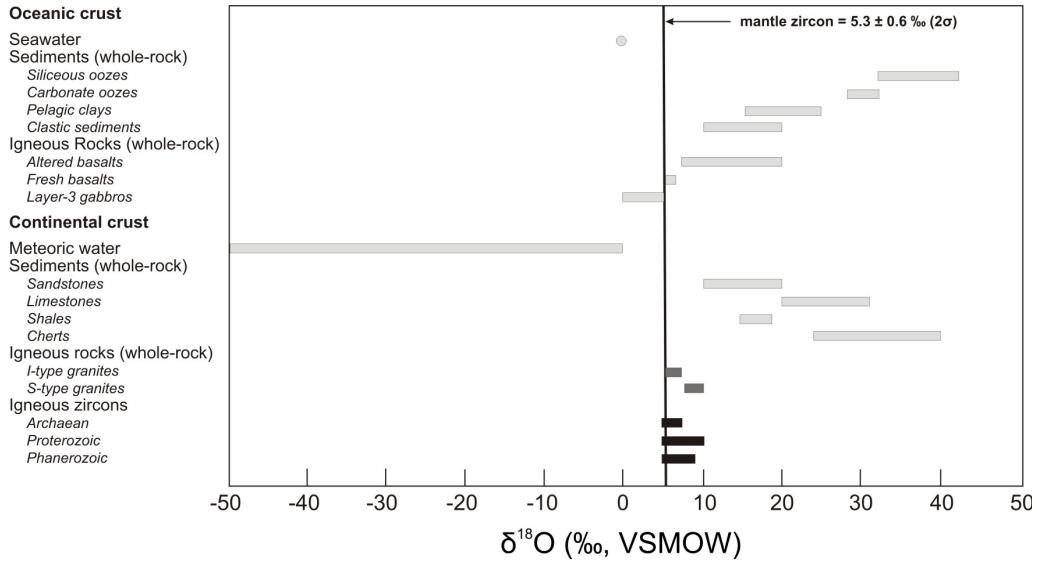

Fig. 4: Typical oxygen isotope compositions of sediments, igneous rocks and igneous zircons (modified from Eiler (2001) and Valley et al. (2005)).

Previous studies have shown that zircons preserve their $\delta^{18}O$ values from the time of crystallisation due to very slow oxygen diffusion rates and high closure temperatures in comparison to most other minerals (Dodson, 1973; Page et al., 2007; Peck et al., 2003; Valley, 2003; Watson and Cherniak, 1997). Furthermore, zircon oxygen isotopes have been found to be insensitive to fractional crystallisation. In a closed system where all minerals are in isotopic equilibrium, whole-rock $\delta^{18}O$ and the melt-zircon equilibrium fractionation factor (Δ(melt-Zrc)) increase in parallel as differentiation and accompanying increase of SiO_2 proceed (Valley et al., 1994). Thus, zircons may show mantle-like $\delta^{18}O$ values of 5.3 ± 0.6 ‰ (2σ) (Valley et al., 1998), even if the host rock has a more evolved oxygen isotope composition due to differentiation. This makes oxygen isotope analysis of zircon a powerful tool to discriminate crustal and mantle sources.

Oxygen isotope analysis of zircon may also be used to investigate magmatic processes such as magma mixing, assimilation or hydrothermal alteration (Valley, 2003). As a change in $\delta^{18}O$ (zircon) can only be achieved by adding material of differing oxygen isotope composition, an increase or decrease in $\delta^{18}O$ with zircon growth can be considered evidence of open-system processes such as magma mixing or assimilation of crustal material (Valley, 2003). Contamination or assimilation that

occurs at a later stage in magma evolution can be evaluated by examining the state of isotopic equilibrium between zircon, which commonly precipitates early in the crystallisation sequence, and a mineral like quartz, which typically crystallises in the later stages (e.g. Bindeman and Valley, 2001; Criss and Taylor, 1986; Monani and Valley, 2001; Valley et al., 1994). Furthermore, by comparing the oxygen isotope compositions of zircon, quartz and their host rock it is possible to identify post-crystallisation hydrothermal alteration, which usually causes a change in $\delta^{18}O$ of the whole-rock but not of zircon or quartz.

5.3. U-Pb dating

The U-Th-Pb dating method is based on the radioactive decay of U and Th to stable isotopes of Pb, and has been used to date zircons since the 1950s (e.g. Larsen et al., 1952). Zircon is particularly suitable for U-Pb dating as it is chemically and mechanically extremely robust and readily incorporates U and Th. However, due to the large difference in ionic radii substitution does not occur between Zr and Pb. Thus, in principle all measured Pb stems from the radioactive decay of U and Th, and by determining the concentrations of U, Th and Pb and the isotopic composition of Pb the crystallisation age of the zircon crystal can be calculated (Faure and Mensing, 2004). Due to the precision of ~1 % of SIMS U-Pb analysis this age is considered to represent the most reliable estimate of the timing of pluton crystallisation in older granitoid rocks. However, on young (115 ± 3 ka) rhyolite lavas from the Long Valley Caldera, California it has been demonstrated that zircons can remain suspended for long periods (> 100 ka) in the convecting portions of a magma (Reid et al., 1997). Here crystallisation ages represent the time at which the zircon saturation temperature was reached in the magma, which in the case of the Long Valley rhyolite lavas occurred approximately 100 ka prior to eruption. Recently, U-Pb dating has also become a very important tool in identifying differences in ages between individual melt batches, which led to the model of incremental assembly (e.g. Coleman et al., 2004). In addition, U-Pb dating can also provide critical evidence of the age of magma source rocks, as igneous rocks commonly contain older zircon

cores which were either inherited from the source region or by late-stage assimilation of a supracrustal component (Corfu et al., 2003; Pidgeon and Aftalion, 1978).

5.4. Trace elements/REEs

Zircon is known to incorporate up to 25 different elements, the most abundant being Hf, Y, REEs, P, U and Th, which are incorporated into the crystal lattice by simple or coupled substitutions. Normalised against chondrite, crustal zircons typically show REE patterns with slopes rising steeply from the LREE to the HREE, a positive Ce anomaly (Ce/Ce*) and a negative Eu anomaly (Eu/Eu*), which is a result of differences in compatibility (Hoskin and Schaltegger, 2003).

The ability of zircon to record and retain information about its parental melt inspired several authors to assess the applicability of trace element/REE concentrations and variations to petrogenesis and provenance-indicator studies (Belousova et al., 2002; Heaman et al, 1990; Hoskin and Ireland, 2000). These studies showed that crustal zircons from rocks ranging in composition from mafic to felsic have generally similar REE patterns. In addition, REE abundances in zircon commonly vary at an inter- and intra-grain scale (between c. 250 ppm to 5000 ppm) (e.g. Black et al., 1986). The processes that control the incorporation of trace elements and REEs into zircon are not well constrained, and little is known about how much the zircon chemistry is affected by crystallisation conditions and the overall growth environment (e.g. Guo et al., 1996; Hinton and Upton, 1991). These factors led to the conclusion that the REE chemistry of zircons is of limited use as a petrogenetic tool (Hoskin and Schaltegger, 2003). However, it was also shown that mantle zircons lack significant Eu anomalies and have flatter HREE patterns, hence are distinctly different from crustal zircons. These differences may be used to discriminate between rocks with mantle affinities and those with crustal affinities (Belousova et al., 1998; Heaman et al., 1990; Hoskin, 1998; Hoskin and Ireland, 2000).

5.5. Hf isotopes

Like the Sm-Nd system, the Lu-Hf isotopic system can be used to decipher the differentiation history of the Earth's mantle and crust. During mantle melting ^{176}Hf, the stable decay product of ^{176}Lu, is more incompatible than Lu, which leads to depletion in Hf of the residual mantle and enrichment in the crust (Patchett et al., 1981) (Fig. 5). Thus, the generation of basaltic magmas has caused the originally uniform and approximately chondritic initial Lu/Hf ratio of the Bulk Silicate Earth (or Chondritic Universal Reservoir = CHUR) to be progressively modified, resulting in a Lu/Hf ratio higher than CHUR in the depleted mantle and lower than CHUR in the enriched crust (Kinny and Maas, 2003).

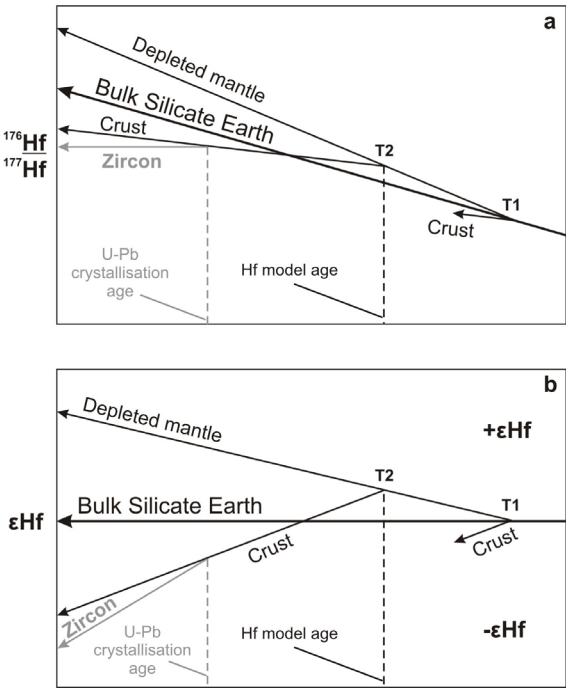

Fig. 5: Evolution of the Bulk Silicate Earth, depleted mantle and continental crust (see text). T1 and T2 represent two melting events (modified from Scherer et al., 2007).

Since Hf isotopes may now be measured at relatively high spatial resolution and precision in-situ in zircon they have become an essential tool in crustal evolution studies. Zircon is particularly suitable for Hf isotope analysis as most zircon crystals contain 0.5-2.0 wt% Hf_2O (Hoskin and Schaltegger, 2003). In addition, as the $^{176}Lu/^{177}Hf$ ratio of zircon is usually < 0.0005, in-situ decay of ^{176}Lu in the zircon crystal typically has a negligible effect. Hence, zircons preserve close to their initial

$^{176}Hf/^{177}Hf$ ratio and that of their parent magma from their time of crystallisation. This ratio may be used to determine εHf values (deviations in Hf isotopic composition from CHUR in parts per ten thousand) and to calculate Hf model ages, i.e. the approximate time at which the protolith separated from the depleted mantle (Kinny and Maas, 2003). Thus, in the study of granites, Hf isotopes of zircons provide valuable information on the compositions and ages of granite sources, especially when used in combination with oxygen and U-Pb isotope data. These may be used to constrain the presence and proportion of pristine mantle material in the zircons, and hence a granite's contribution to continental growth. The Hf model ages may be compared with the crystallisation ages of granites determined by U-Pb dating; if the model ages are much older than the crystallisation ages, the contribution of contemporaneous juvenile mantle melts may be discounted.

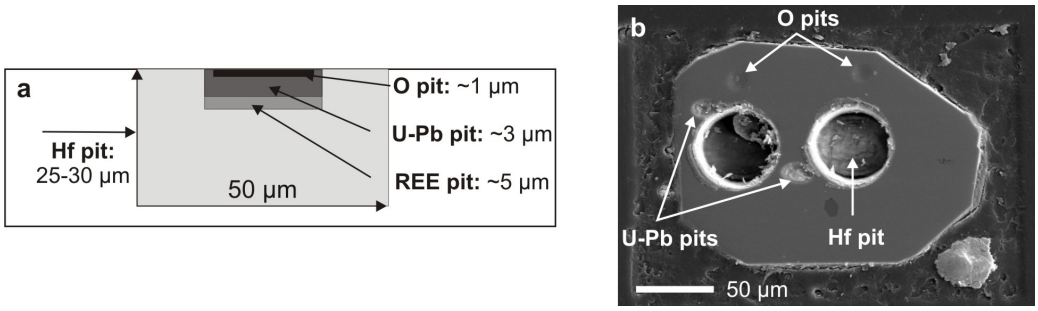

Fig. 6: (a) Sketch of pit sizes of SIMS oxygen, U-Pb isotope and trace element/REE analyses, and of laser ablation ICPMS Hf isotope analysis; (b) Secondary Electron image of zircon crystal with oxygen, U-Pb and Hf isotope pits.

5.6. Analytical protocols

As each type of analysis consumes different amounts of material, with oxygen isotope analysis consuming the least and Hf isotope analysis the most, analyses must be carried out in a particular order with oxygen isotopes measured first and Hf isotopes last (Fig. 6). Furthermore, oxygen isotope analysis by SIMS is very sensitive to surface irregularities, and may be affected by topography created by previous analyses. In addition, oxygen flooding of the sample surface is employed during U-Pb analysis to enhance Pb ion yields, which may lead to abnormal $\delta^{18}O$ values. Assuming the zircon does not contain older components, this order of analysis can be

reversed, but only if the sample surface is re-polished and an undisturbed layer of the crystal exposed prior to oxygen isotope analysis.

Prior to analysis approximately 100 zircons per sample were hand-picked and mounted into epoxy, and subsequently imaged under transmitted and reflected light, and using CL and BSE imaging techniques. For oxygen isotope analysis, which produces the smallest and shallowest ion probe pits (~18 µm across and ~1 µm deep) (Fig. 6), between 20 and 30 ideally clear, crack- and inclusion-free zircons per sample were selected. Zircons were selected for analysis if they were considered to be representative with respect to grain size, morphology and internal zoning. To enable detection of changes in oxygen isotope composition with zircon growth multiple analyses were typically made on a single zircon crystal. However, due to the poor grain quality in some samples this was not always possible. Analyses of U-Pb isotopes and trace elements/REEs, which generate slightly larger pits (~25 µm across and ~3-5 µm deep) (Fig. 6), were carried out next. Due to much longer data acquisition times (O: c. 3.5 minutes, U-Pb and trace elements/REEs: c. 30 minutes) U-Pb isotope, trace element and REE data were obtained on only a sub-set (between 10 and 15 zircons per sample) of crystals. Commonly, analyses were made in the same area or at least within the same CL zone as the oxygen isotope analysis. Because analysis by LA-MC-ICPMS consumes a much larger amount of sample material than ion microprobe analysis, typically ablation pits that are 50 µm across and ~25-30 µm deep (Fig. 6), Hf isotopes were analysed last. Generally, the aim was to obtain Hf isotope data from zircon crystals and areas within the crystal for which U-Pb and oxygen isotope data already existed. However, this objective was greatly limited by the much larger size of the laser beam, and resulted in a much smaller data set. Thus, some analyses were also made on crystals for which either no oxygen or no U-Pb data existed. Nevertheless, outermost zircon rims were often too narrow to analyse by laser ablation and are therefore generally under-represented in the data set.

Subsequent to analysis, zircons were again imaged by CL and BSE to determine the exact position of each analysis, and to check for inclusions and cracks in the bottom of each pit. Data from dubious locations were rejected. Further data were rejected from zircons showing high concentrations of common Pb, discordance (U-

Pb: > 10 %, O: > 20 % discordance), and more than 1000 ppm U. This resulted in a considerably smaller, but very robust, data set.

6. Thesis layout

This PhD thesis comprises four papers. Papers 1 to 3 focus on the genesis of the late Caledonian I-type granites, and paper 4 on the S-type granites.

The first zircon oxygen isotope data obtained in this PhD project showed that the Lochnagar pluton comprises homogeneous and heterogeneous samples. The objective of Paper 1 was to investigate this in more detail by comparing the zircon, quartz and whole-rock oxygen isotope data of two representative samples, one homogeneous in zircon $\delta^{18}O$ (Cul nan Gad diorite) and one heterogenous (Allt Darrarie diorite). By combining the different data sets it was possible to study the petrogenetic histories from genesis to post-crystallisation hydrothermal alteration of both samples. Paper 2 presents oxygen, U-Pb isotope and trace element/REE data of zircons from the remaining Lochnagar samples and of the Etive samples in order to constrain their emplacement histories, and to assess the role of mantle, infracrustal and supracrustal sources in their genesis. One major outcome of this part of the study was that the $\delta^{18}O$ (zircon) data of the Lochnagar and Etive plutons are very similar, hence fail to explain the whole-rock differences between the plutons. The zircon oxygen isotope data also revealed that both plutons appear to contain only a small proportion of zircons with mantle-like $\delta^{18}O$ values. However, from these data alone it was not possible to investigate whether these mantle-like zircons represent involvement of contemporary (~420 Ma) mantle-derived material, thus indicate crustal growth, or represent melting of mafic lower crust, thus crustal recycling. To resolve this, and to explain the whole-rock geochemical differences between the plutons Paper 3 integrates the zircon oxygen isotope data presented in Paper 2 with zircon Hf isotope data. The aim of Paper 4 was to determine the crystallisation ages (which had previously not been determined) and sources of the Kemnay, Cove and Nigg Bay S-type granites by integrating oxygen, U-Pb and Hf isotope data of

zircons. The following sections give a more detailed summary of the objectives, results and conclusions of each paper.

Paper 1: A cryptic record of magma mixing in diorites revealed by high-precision SIMS oxygen isotope analysis of zircons

The combination of oxygen isotope data for zircon, quartz and whole-rock in granitic rocks has been shown to provide detailed insights into the petrogenetic and post-crystallisation alteration history of plutons (e.g. King et al., 1997; King and Valley, 2001; Monani and Valley, 2001). Previous studies have assessed the state of equilibrium between zircon, quartz and whole-rock based on conventional laser fluorination data (King et al., 1997, 1998, 2001, 2004; Lackey et al., 2005, 2006; Monani and Valley, 2001). However, this paper presents high-precision in-situ ion microprobe oxygen isotope analyses of zircon and quartz, supported by whole-rock oxygen isotope data, for two diorite intrusions forming part of the late Caledonian Lochnagar pluton.

The Allt Darrarie (AD) and Cul nan Gad (CnG) diorites form two small intrusions (areal dimensions of 0.6 x 0.4 km and 4-5 x 1.8 km, respectively) along the margin of the Lochnagar pluton. Based on petrographic and field data they have been interpreted to be related to, but older than, the Lochnagar pluton (Smith et al., 2001). However, new U-Pb SIMS dating of the diorites shows that they were emplaced contemporaneously with and subsequent to the main granite body (Paper 2). Compositionally and texturally the diorites are very similar; both are dark grey, fine- to medium-grained, and comprise plagioclase (45-50 %), biotite (c. 40 %), hornblende (< 5-10 %) and interstitial quartz (c. 5 %), with accessory ilmenite and magnetite, titanite (absent in CnG), zircon and apatite. Evidence of restitic or cumulate material was not found in either sample.

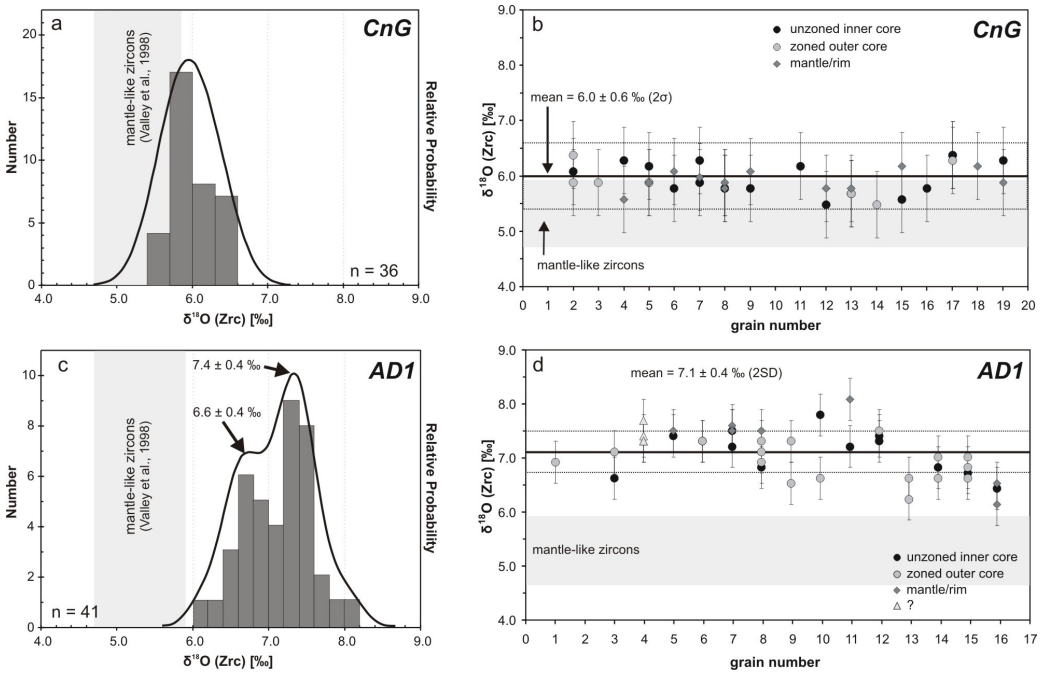

Fig. 7: Cumulative probability-histograms and grain-scale variation plot of zircon crystals from the Cul nan Gad (a & b)and Allt Darrarie diorites (c & d).
a) CnG zircons show a narrow range in $\delta^{18}O$ values and a single mode (bin widths of histograms equal 1σ, error bars are 2σ).
b) All data from the CnG zircons lie within 2 of the mean (dotted area).
c) AD1 zircons display a much larger range than CnG zircons and an apparent bimodal distribution (bin widths of histograms equal 1σ, error bars are 2σ).
d) Data are more scattered and not all lie within error of the mean. Prominent inter-grain variation in $\delta^{18}O$ occurs between e.g. grains 7 and 16, intra-grain variation between inner and outer core (grain 9), core and rim (grain 11). $\delta^{18}O$ commonly increases with zircon growth except in grain 10.

Despite these similarities, oxygen isotope analyses of zircons from the Allt Darrarie and Cul nan Gad diorites reveal large differences in the degree of heterogeneity, data distribution and mean $\delta^{18}O$ compositions (Fig. 7). Zircon crystals from the Cul nan Gad diorite show a unimodal distribution of oxygen isotope values ($\delta^{18}O$ = 6.0 ± 0.6 ‰ (2σ, n=36)) with a standard deviation comparable to that of the homogeneous analytical zircon standard, and no - or only minor - intra-grain variation. In contrast, those from the Allt Darrarie diorite display a large range in $\delta^{18}O$, an apparent bimodal distribution with modes of 6.6 ± 0.4 ‰ and 7.3 ± 0.4 ‰ (n=41), and inter- and intra-grain variations of up to 1.2 ‰. Where intra-grain variations were detected both an increase and decrease in $\delta^{18}O$ with zircon growth was observed. As the $\delta^{18}O$ composition of growing zircon can only evolve by open-system changes to the magma composition, i.e. if material of contrasting $\delta^{18}O$

composition is added to the magma, the intra-grain variation in zircons of the Allt Darrarie diorite is interpreted to represent a cryptic record of magma mixing of which no other evidence was found in the sample. As simple mixing with a supracrustal component would result in an increase in $\delta^{18}O$, but never a decrease, the Allt Darrarie magma must have had a more complicated mixing history.

Recently, it has been proposed that 'deep crustal hot zones', which result from repeated intrusion of mantle-derived basalt sills into the lower crust, are a likely site for formation of intermediate and silicic magmas. Magmas are either produced by differentiation of basaltic sills, mixing of residual melts and crustal partial melts or by melting of lower crustal rocks, which creates a large range of intermediate and silicic melts of varying oxygen isotope composition (Annen et al., 2006). Based on the large inter- and intra-grain variations in $\delta^{18}O$ (zircon) in the Allt Darrarie diorite, generation in a deep crustal hot zone appears possible. Mantle-derived zircon has a $\delta^{18}O$ value of 5.3 ± 0.6 ‰ (2σ, Valley et al., 1998). The $\delta^{18}O$ range of zircon from the Allt Darrarie diorite is 6.1-8.1 ‰, hence none of the zircon in this intrusion has a mantle-like composition. By contrast, a $\delta^{18}O$ range of 5.5-6.4 ‰ for zircon from the Cul nan Gad diorite includes a number of analyses with mantle-like values. From oxygen isotope data alone it is not possible to decipher whether the diorites represent a mixture of mantle-derived and crustal material or were generated by recycling of infra- and supracrustal sources.

In contrast to the zircon data, the quartz oxygen isotope data from the Cul nan Gad and Allt Darrarie diorites display only minor variation (CnG: 10.9 ± 0.5 ‰ (2σ, n=22), AD1: 11.7 ± 0.6 ‰ (2σ, n=27)) within each sample, with no evidence of mixing. As quartz and zircon display isotopic disequilibrium (Fig. 8) in both diorites quartz probably crystallised later in the crystallisation sequence; in the Allt Darrarie diorite it precipitated after the inferred magma mixing from a homogenised, higher $\delta^{18}O$ melt.

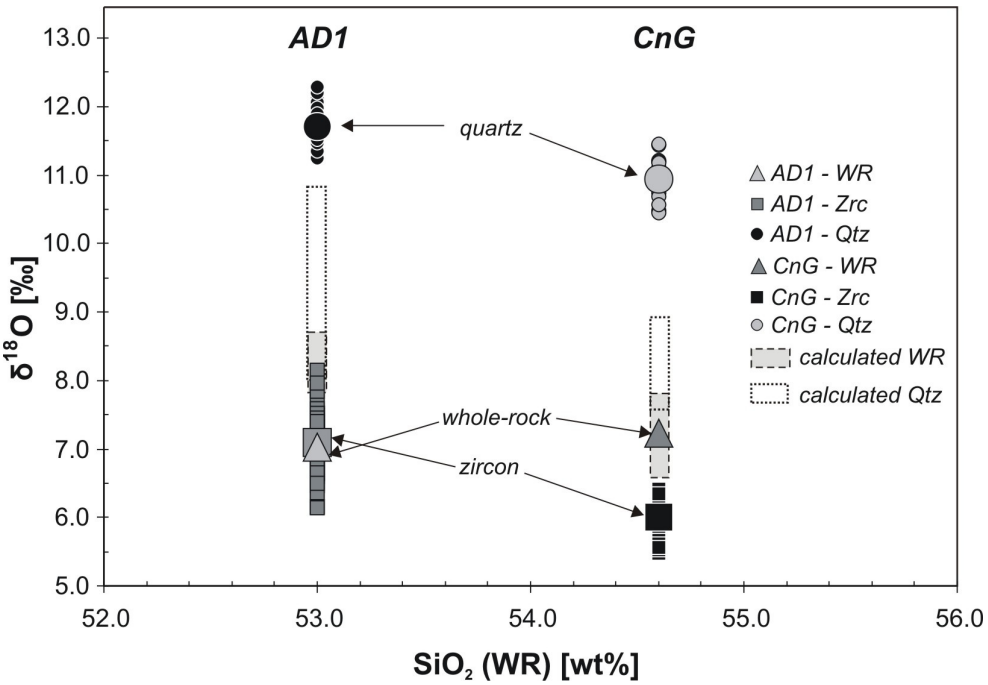

Fig. 8: Evaluation of equilibrium between zircon (Zrc), quartz (Qtz) and whole-rock (WR). 'Calculated WR' and 'calculated quartz' are calculated using equations (1) and (2) (see text); calculations include the error on the zircon analysis.
AD1: Zircon is not in equilibrium with quartz or whole-rock. Measured whole-rock is too low to be in equilibrium with zircon, which suggests it was affected by hydrothermal alteration after zircon crystallisation.
CnG: Zircon and quartz are not in equilibrium as measured quartz $\delta^{18}O$ is considerably higher than the calculated quartz value, which suggests quartz crystallised late in sequence. Zircon and whole-rock are in equilibrium. Low modal percentage of elevated quartz in whole-rock (< 5 %) did not shift whole-rock out of equilibrium.

Comparison of whole-rock and zircon $\delta^{18}O$ data shows them to be in equilibrium in the Cul nan Gad diorite, whereas in the Allt Darrarie diorite the whole-rock $\delta^{18}O$ value is too low (Fig. 8) indicating that it probably experienced hydrothermal alteration that did not affect zircon or quartz.

This study shows that a combination of zircon, quartz and whole-rock data is a powerful tool to reconstruct the petrogenetic evolution of plutons from early crystallisation to late alteration. In addition, high-precision SIMS oxygen isotope analysis of zircon provides a new approach to identifying and resolving previously undetected early-stage magma mixing events and constraining the compositions and origins of the component magmas.

Paper 2: A tale of two plutons: an integrated ion microprobe study of $^{18}O/^{16}O$, U-Pb, trace elements and REE in zircons from Scottish Caledonian granites

Based on their differing whole-rock geochemical compositions the Lochnagar and Etive plutons have been interpreted to belong to different granite suites – the Cairngorm and Argyll suites, respectively (Fig. 2). To date the reasons for these whole-rock differences are not resolved, but it has been proposed that they may reflect heterogeneities in the composition and age of the underlying lower crust and/or mantle, or differences in the relative contributions made by the crust and mantle (Halliday, 1984).

To resolve the sources and petrogenetic evolutions of the Lochnagar and Etive plutons oxygen isotope analyses together with U-Pb isotope and trace element/REE analyses were carried out on zircons from a suite of granite and diorite samples of both plutons.

Zircons from the Lochnagar and Etive plutons have the same mean $\delta^{18}O$ values (Lochnagar: 6.6 ± 0.6 ‰ (2σ, n=230); Etive: 6.5 ± 0.4 ‰ (n=209), and each pluton yielded a similar small proportion (c. 18 %) of analyses with mantle-like values (5.3 ± 0.6 ‰ (2σ, Valley et al., 1998)). This leads to two important conclusions: (1) The relative contributions of mantle and crust to magma genesis have probably been similar in both plutons, and therefore the whole-rock differences between them most likely reflect compositional differences between their lower crustal sources. Zircon trace element and REE data have been found to be overall similar in both plutons, and hence do not provide further information on the sources. (2) Based on the small proportion of mantle-like zircons, the Lochnagar and Etive plutons, and possibly the late Caledonian I-type granites as a whole, probably made some contribution to net crustal growth. However, from oxygen isotope data alone it is not clear whether the small proportion of zircon analyses with mantle-like values reflects sourcing of contemporary ~420 Ma mantle, and thus generation of new crust, or of ancient mafic material, e.g. a mafic underplate, and thus crustal recycling.

Samples from both plutons may be homogeneous or heterogeneous in terms of the distribution of $\delta^{18}O$ values in zircon (Fig. 9). In heterogeneous samples, resolvable variations in $\delta^{18}O$ occur between zircon crystals of a single sample and

even within individual zircons. This degree and scale of heterogeneity have not previously been reported. Where resolvable intra-grain variations were detected, both decreases and increases of $\delta^{18}O$ with zircon growth were observed, providing evidence for magma mixing.

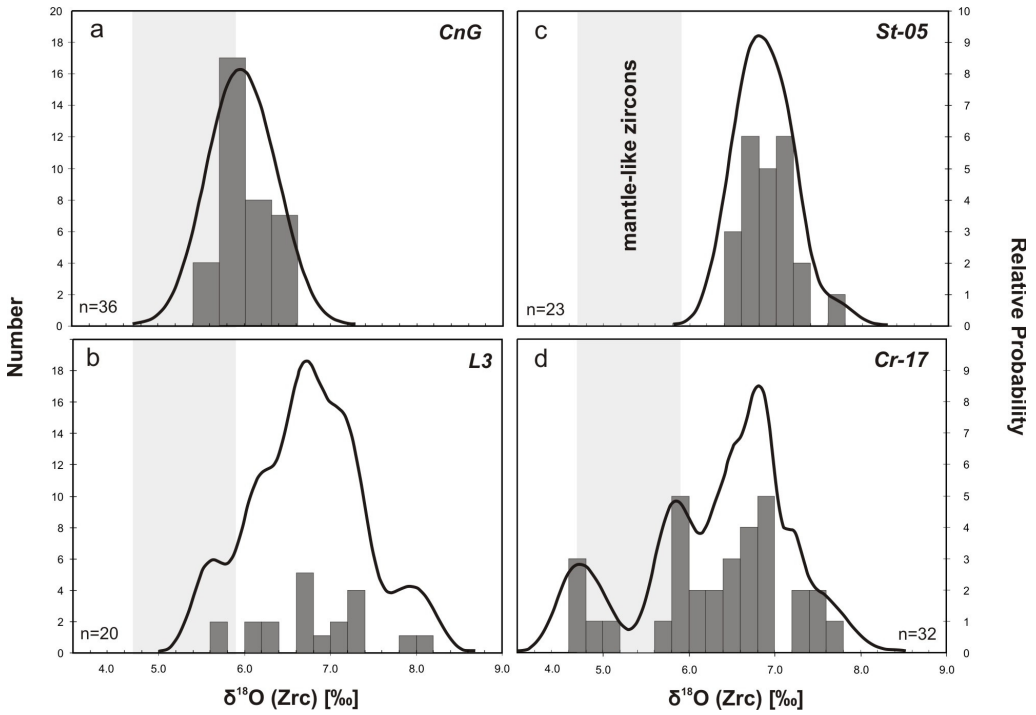

Fig. 9: Oxygen isotope probability-histograms of zircons from homogeneous and heterogeneous Lochnagar (a & b) and Etive (c & d) pluton samples.
(CnG = Cul nan Gad diorite, St-05 = Starav Intrusion, Cr-17 = Cruachan Intrusion; bin width = 1σ, probability curves were calculated at 1σ).

Evidence for the complex petrogenetic evolution and assembly of the plutons was also found in the U-Pb isotope data, which revealed that the emplacement histories of both plutons are more protracted and complicated than previously recognised, with magmatic activity at the Lochnagar pluton lasting for c. 11 m.y. (424 ± 5 Ma to 413 ± 4 Ma) and at the Etive pluton for c. 16 m.y. (423 ± 2 Ma and 407 ± 2 Ma).

The large variation in $\delta^{18}O$ in zircons of the Allt Darrarie and Cul nan Gad diorites is attributed to magma generation in a 'deep crustal hot zone' (Annen et al., 2006) where mantle melts differentiated, inducing partial melting of the lower/middle crust and extensive mixing of melts with differing $\delta^{18}O$. Based on intra-grain variations in $\delta^{18}O$ further mixing occurred during zircon growth during

ascent and at shallower levels. Magmas were subsequently emplaced incrementally in small batches over extended periods of time, consistent with the U-Pb data.

To summarise, even though the reasons for whole-rock geochemical differences between the Lochnagar and Etive plutons have not been fully resolved by this study, integrating $\delta^{18}O$ and U-Pb isotope data is a powerful tool to constrain the petrogenesis of the plutons, their very complex evolution and the mechanisms of emplacement.

Paper 3: Using in-situ O and Hf isotope analysis of zircons to constrain the sources of late Caledonian granites in Scotland

Oxygen and U-Pb isotope analyses of zircons from the Lochnagar and Etive plutons gave some insight into the relative contributions made by crust and mantle, and furthermore deciphered important aspects of the plutons' genesis, evolution, emplacement mechanisms and histories. However, three questions could not be resolved: (1) Do the zircons with mantle-like $\delta^{18}O$ values represent contemporary mantle (~420 Ma), thus generation of new crust, or melting of ancient mafic material in the lower crust (e.g. a mafic underplate), thus recycling of crust? (2) What caused the whole-rock compositional differences between the plutons? (3) What are the compositions and ages of the lower crustal sources that contributed to the plutons, and hence of the basement beneath the Grampian Highlands?

The integration of oxygen and Hf isotopes of zircons has been shown to be a powerful approach to constrain the amount of contemporary mantle melting, and the compositions and approximate ages of sources (e.g. Kemp et al., 2007). Thus, in order to resolve the above questions this integrated approach is applied here to zircons of the Lochnagar and Etive plutons.

Initial εHf values of zircons from the Lochnagar pluton spread from +3.4 to -5.8 ± 1.0 (2σ) (=9.2 εHf units) (Fig. 10). The spread results from differences in εHf between samples and between zircons of a single sample; where multiple analyses were made on a single zircon crystal from either pluton εHf values are always within error. This variability supports the model of generation in a deep crustal hot zone and incremental assembly proposed in Papers 1 and 2. The majority of samples display

values between +2.7 and -2.8 εHf, but two samples are clearly different. Zircons from one sample of L1 granite show only negative εHf values (-1.5 to -5.8) while those from a second sample of L1 granite display values between +1.2 and -2.3; zircons from the marginal Allt Darrarie diorite extend to even more negative values and are overall much more heterogeneous than the main data cluster (+3.4 to -4.8).

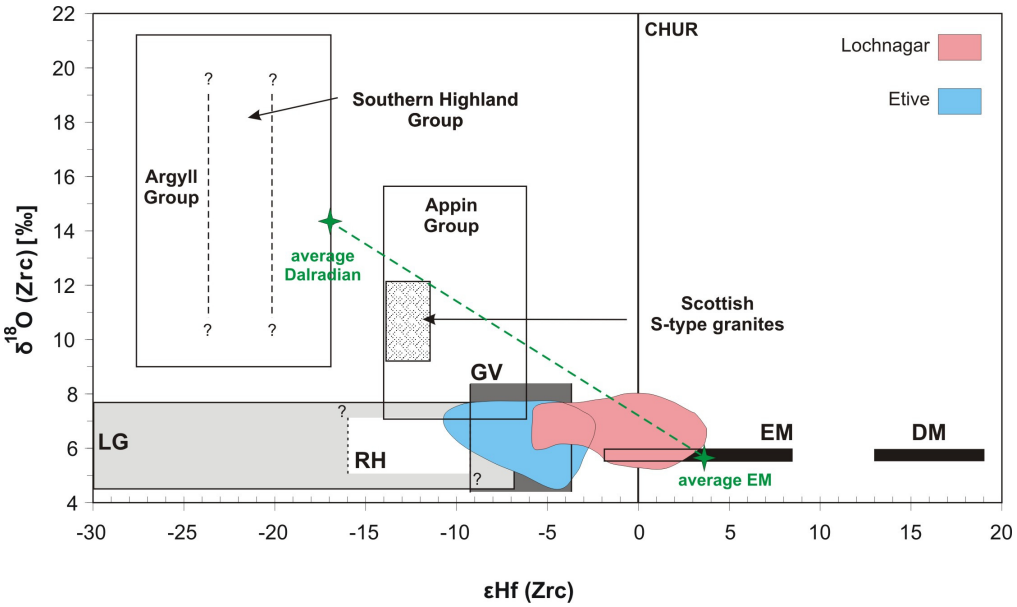

Fig. 10: εHf vs. $\delta^{18}O$ of zircons from the Lochnagar and Etive plutons showing the relationship to their potential supracrustal and infracrustal sources.
Zircons from both plutons show no overlap with the field defined by depleted mantle (DM, re-calculated at 420 Ma), but those from the Lochnagar pluton show strong overlap with enriched mantle (EM). The mixing line (green dashed line) reflects simple two-component mixing between EM and average Dalradian (i.e. Appin, Argyll and Southern Highland groups). Based on this mixing modelling both plutons may contain up to 30 % Dalradian material. However, the complexity and variation observed in the zircon oxygen isotope data indicates involvement of more than two sources. Large overlap exists with fields representing the plutons' potential lower crustal source rocks (i.e. Lewisian granulites = LG, Rhinns Complex = RH, Grenville-age basement = GV). Hf isotope data (at 420 Ma) of potential sources were calculated based on published Nd isotope data (assuming a Hf-Nd correlation of the terrestrial array (Vervoort and Blichert-Toft, 1999)) by Anderson et al. (2004), Canning et al. (1998), Frost and O'Nions, (1985), Halliday (1984), Hamilton et al. (1980), Harmon (1983), Kay (1980), Muir et al. (1994), O'Nions et al. (1983), Restrepo-Pace et al. (1997), Thirlwall (1982).

Zircons from the Etive pluton show εHf values of -3.0 to -10.6 ± 1.0 (2σ) (=7.6 εHf units) (Fig. 10). In contrast to zircons from the Lochnagar pluton, they form two distinct data clusters. The first cluster ranges from -3.0 to -7.3 εHf and comprises zircons from the Meall Odhar, Cruachan and Quarry intrusions; the second cluster is

represented by zircons from the Starav Intrusion and spreads between -8.3 and -10.6 εHf.

The εHf data indicate that the Lochnagar and Etive plutons comprise material of at least two sources of different εHf. With a data range of +3.4 to -5.8 for zircons from the Lochnagar pluton and -3.0 to -10.6 for zircons from the Etive pluton a significant contribution by contemporary depleted mantle, which had an εHf value of approximately +16 (Vervoort and Blichert-Toft, 1999), can be precluded. Little is known about the composition of the mantle beneath the Grampian terrane. However, εNd values for Old Red Sandstone lavas (Thirlwall, 1982) and for two lamprophyre suites (Canning et al., 1998) indicate that the mantle below Scotland is highly heterogeneous and at least locally enriched. Thus, for the Lochnagar pluton involvement of a small enriched mantle component may be possible, but much more negative εHf values for the Etive pluton make it less likely here. Simple two-component magma mixing modelling between the two obvious end-members, i.e. enriched mantle and rocks of the Dalradian Supergroup shows that the Lochnagar pluton may comprise a large enriched mantle (70-100 %) component. However, the complexity and variation observed in the zircon oxygen isotope data indicates a much more complex mixing scenario involving more than two sources.

Variations in composition between the potential mafic components may in part be responsible for the whole-rock differences between the plutons. However, compositional differences between the unknown crustal sources will have also played an important role. This is supported by Hf model ages (calculated based on the $^{176}Lu/^{177}Hf$ ratio of the average crust and on the $^{176}Lu/^{177}Hf$ ratio of each whole-rock sample), which indicate that the Lochnagar pluton melted lower crustal material that separated from the mantle between approximately 1.7 Ga and 1.0 Ga, whereas the Etive pluton sourced material with Hf model ages between 2.1 Ga and 1.2 Ga (Fig. 11). As Hf model ages strongly depend on the $^{176}Lu/^{177}Hf$ ratio used for the calculation, the above ages have to be considered as rough estimates. Nevertheless, they clearly show that the Etive pluton melted at least some older material, which supports the εHf data and indicates that the basement beneath the pluton is different in part to that beneath the Lochnagar pluton.

Due to lack of outcrop, little is known about the basement beneath the Grampian Highlands. Based on geophysical constraints, geochemical and isotopic data for the late Caledonian granites, U-Pb ages of inherited zircons found in the granites and wider geological arguments, it has been proposed that rocks of the Lewisian Complex (c. 2.9 Ga), the Rhinns Complex (c. 1.8), Grenvillian basement (1.2-1.0 Ga), and of the Dava and Glen Banchor successions (i.e. gneisses, locally migmatised psammites, semi-pelites and subordinate quartzites that were derived from Palaeoproterozoic- and Grenville-age sedimentary protoliths) underlie the Grampian Highlands. However, due to the ambiguities of calculating Hf model ages these cannot be easily linked to the Hf model ages of the plutons. Thus, perhaps the most reasonable model for the lower crust beneath the Grampian terrane is that it comprises a range of Archaean- to Neoproterozoic-age material. The contributions from these sources vary between the plutons, with the Lochnagar pluton predominantly representing larger proportions of Mesoproterozoic-age, and the Etive pluton of Meso- and Palaeoproterozoic age lower crust.

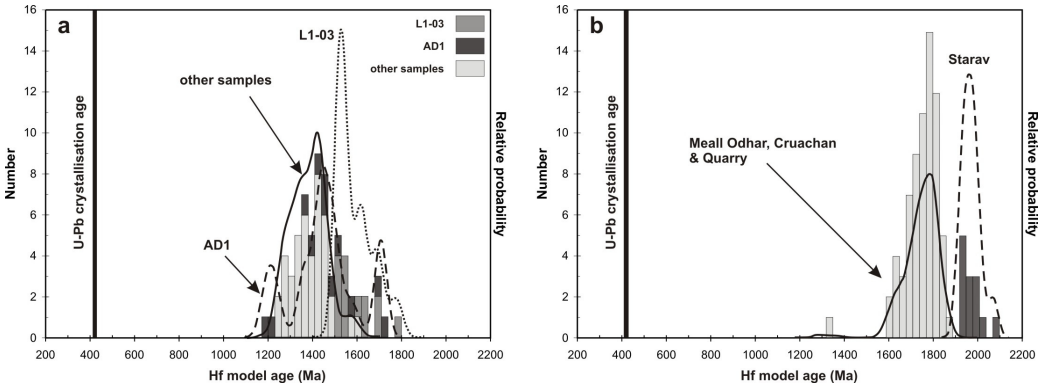

Fig. 11: Hf model ages (TDM_C) of zircons from (a) the Lochnagar pluton and (b) the Etive pluton (probability curves were calculated at 1σ, bin width = 1σ).

In summary, this study shows that the basement beneath the Grampian Highlands is variable in composition and age. This lends support to the hypothesis that the geochemical differences between the Lochnagar and Etive plutons, and on a wider scale between the Cairngorm and Argyll suites, lie dominantly in the differences in

the ages and compositions of their underlying lower crustal sources, and not in differences in the relative contributions made by crust and mantle.

Paper 4: An integrated zircon O, U-Pb and Hf isotope study of zircons in S-type granites

Previous studies have shown that most I-type granites comprise multiple sources and have complicated petrogenetic histories (e.g. Kemp et al., 2007; Papers 1 to 3). S-type granites are widely considered to typically comprise only a single supracrustal/sedimentary source and therefore provide the opportunity to study one of the end-members that commonly contribute to I-type granites.

Papers 1 to 3 showed that the origin and evolution of complex I-type granites may now be deciphered by integrated in-situ ion microprobe and laser ablation ICPMS oxygen, U-Pb and Hf isotope analyses of zircons. Thus, the same approach is applied here to zircons from the Scottish Caledonian Kemnay, Cove and Nigg Bay S-type granites in order to constrain their crystallisation ages (which had previously not been determined) and sources.

The Kemnay, Cove and Nigg Bay granites are all located in the northeastern Grampian Highlands, and crop out in the Aberdeen Formation of the Dalradian Supergroup (Stephenson and Gould, 1995). Some controversy exists over the affinity of the Aberdeen Formation; previous studies suggested that it was part of the Argyll Group (Munro, 1986), whereas more recently it has been interpreted to be part of the Southern Highland Group (Gould, 1997; Stephenson and Gould, 1995). Based on gradational contacts between the granites and their country rocks it has been suggested that the magmas were generated more or less in-situ (Kneller and Aftalion, 1987; Richardson and Powell, 1976), by melting of the host metasedimentary rocks. However, as the granites vary greatly in size (Kemnay: ~36 km^2; Cove: ~1.7 km^2; Nigg Bay: even smaller than the Cove Granite), it is quite likely that the larger granite bodies also contain material of source(s) located at deeper levels in the crust.

U-Pb dating of magmatic zircons from the Kemnay, Cove and Nigg Bay granites shows that all three crystallised at approximately the same time at 457 ± 3 Ma, 458 ± 5 Ma and 465 ± 5 Ma, respectively, shortly after the peak of regional metamorphism

at 470 Ma (e.g. Strachan et al., 2002). Inherited cores, which occur in 60-95 % of all analysed zircon crystals, yield similar concordant $^{207}Pb/^{206}Pb$ of c. 1.8 to 1.05 Ga in the Kemnay Granite, c. 1.5 to 1.0 Ga in the Cove Granite and c. 1.6 to 0.9 Ga in the Nigg Bay Granite. When the data are considered collectively, dominant peaks exist at c. 1.45 Ga and 1.05-1.0 Ga. Discordant ages form an additional peak at c. 2.7-2.5 Ga. These age ranges are essentially the same as those reported for detrital zircons from the Dalradian Supergroup (Cawood et al., 2003).

εHf values of magmatic zircons are broadly similar amongst the granites (Kemnay: -9.9 to -17.3; Cove: -12.6 to -20.3; Nigg Bay: -12.2 to -18.5) and overlap with Hf isotope data calculated from published Nd isotope data of the Dalradian Appin and Argyll groups. The U-Pb data of inherited cores and the Hf isotope data of magmatic zircons therefore suggest that the three granites share the same source material, most likely their current Dalradian Supergroup country rocks.

However, zircon oxygen isotope data reveal large differences between the granites (Fig. 12). Magmatic zircons from the Kemnay Granite span a large range of values between 7.0 ‰ and 12.0 ‰ (mean = 9.2 ‰). Inherited cores show an even larger spread between 6.7 ‰ and 13.3 ‰. Resolvable intra-grain variation was detected in one crystal, which comprises a magmatic core of 7.7 ‰ and a rim of 9.1 ‰. In contrast, magmatic and inherited zircon crystals from the Cove Granite form much more homogeneous oxygen isotope populations, and display values between 8.8 ‰ and 11.6 ‰ (mean = 10.0 ‰), and 6.9 ‰ and 9.0 ‰ (mean = 7.6 ‰), respectively. Inherited and magmatic zircons of the Nigg Bay Granite are even more homogeneous, and in addition considerably less evolved with $\delta^{18}O$ values of magmatic zircons between 6.1 ‰ and 8.4 ‰ (mean = 7.3 ‰) and of inherited cores between 4.1 ‰ and 7.7 ‰ (one outlier at 9.7 ‰, mean = 5.8 ‰). Intra-grain variations were not detected in zircons of either the Cove or Nigg Bay granites. Based on these data the Kemnay and Cove granites display compositions typical of S-type granites, whereas the Nigg Bay Granite shows $\delta^{18}O$ values more commonly observed in I-type granites (Papers 1 and 2), which suggests that the granites did not melt the same source materials.

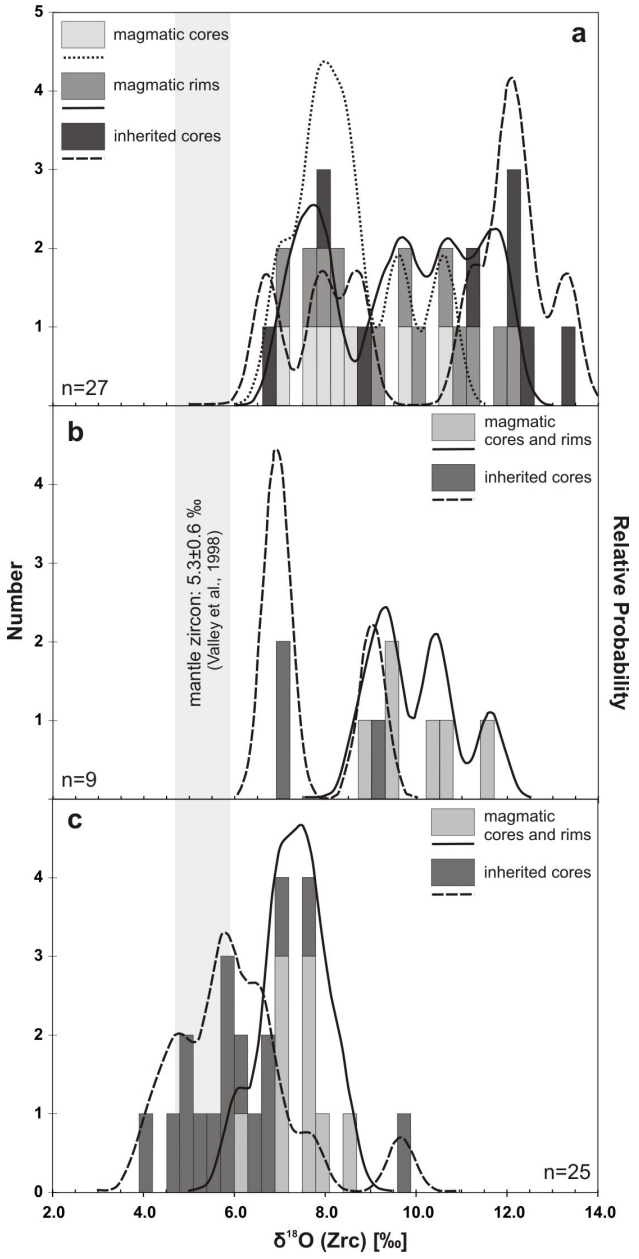

Fig. 12: Cumulative probability plots of zircon oxygen isotope data (probability curves and histograms were calculated at 1σ) from the Kemnay, Cove and Nigg Bay S-type granites.

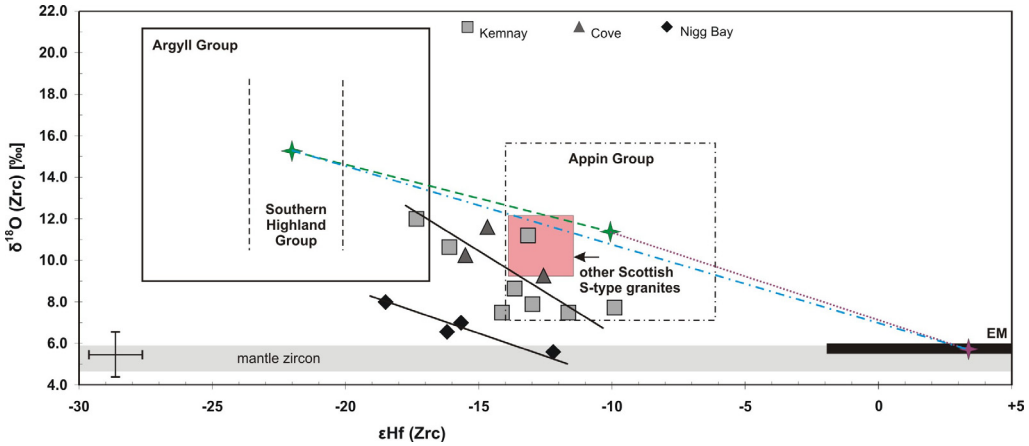

Fig. 13: εHf values (at emplacement age) vs. $\delta^{18}O$ of magmatic zircons of the Kemnay, Cove and Nigg Bay granites (precision on zircon $\delta^{18}O$ and εHf = 0.6 ‰ and 1.0 units (2σ), respectively). Also shown are fields for whole-rock $\delta^{18}O$ and estimated εHf data of the Appin, Argyll and Southern Highland groups, and other Scottish S-type granites (data from Anderson et al., 2004; Frost and O'Nions, 1985; Halliday, 1984; Hamilton et al., 1980; Harmon, 1983; Kay, 1980; O'Nions et al., 1983) and mixing lines (green, purple and blue) between the potential end-members.

Plotting the data of the Kemnay, Cove and Nigg Bay granites in an εHf vs. $\delta^{18}O$ diagram (Fig. 13) shows that all three lie on two negatively-sloping linear mixing trends, which partly overlap fields for the Argyll and (stratigraphically older) Appin groups. These trends may be explained in one of three ways: (1) All three granites sourced rocks of the Argyll and Appin groups, possibly at lower lithostratigraphical and structural levels than their Aberdeen Formation host rocks. In the Cove and Nigg Bay granites melts mixed thoroughly, which led to homogenous oxygen isotope compositions, whereas incomplete mixing resulted in the oxygen isotope heterogeneities observed in the Kemnay Granite. The low $\delta^{18}O$ values observed in the Nigg Bay Granite were produced by melting of a local low-$\delta^{18}O$, possibly hydrothermally altered, unit within the Appin or Argyll groups. (2) Only the Kemnay and Cove granites were generated by melting of Appin Group and Argyll ± Southern Highland Group rocks. The Nigg Bay Granite formed by mixing between Argyll ± Southern Highland Group rocks and an infracrustal source with primitive, mantle-like oxygen and crustal Hf isotope characteristics. (3) All three granites comprise a mixture of melts derived from a mafic lower crustal source and a supracrustal component, possibly the Aberdeen Formation. Based on the high proportion of low-$\delta^{18}O$ zircons the Nigg Bay Granite comprises a larger infracrustal component

whereas the Kemnay and Cove granites contain higher proportions of a supracrustal source. Involvement of pristine contemporaneous Lower Palaeozoic mantle can be precluded on the base of Hf isotope data.

To fully resolve the origin and evolution of the Kemnay, Cove and Nigg Bay granites a more extensive study is required. Nevertheless, this pilot study of S-type granites shows that either supracrustal materials do not always have evolved oxygen isotope compositions, or alternatively that S-type granites, even if compositionally very similar, have complex petrogenetic histories and possibly comprise multiple sources.

II.

PAPER 1

A cryptic record of magma mixing in diorites revealed by high-precision SIMS oxygen isotope analysis of zircons

A cryptic record of magma mixing in diorites revealed by high-precision SIMS oxygen isotope analysis of zircons

S.K. Appleby [a,*], C.M. Graham [a], M.R. Gillespie [b], R.W. Hinton [a], G.J.H. Oliver [c], EIMF [d]

[a] *Grant Institute of Earth Science, University of Edinburgh, West Mains Road, Edinburgh, EH9 3JW, UK*

[b] *British Geological Survey, Murchison House, West Mains Road, Edinburgh, EH9 3LA, UK*

[c] *School of Geography & Geosciences, Crustal Geodynamics Group, University of St. Andrews, St. Andrews, KY16 9AL, UK*

[d] *Edinburgh Ion Microprobe Facility, University of Edinburgh, West Mains Road, Edinburgh, EH9 3JW, UK*

Manuscript

In press at Earth and Planetary Science Letters

Abstract

High-precision in-situ ion microprobe (SIMS) oxygen isotope analysis of zircons from two diorite intrusions associated with the late Caledonian Lochnagar pluton in Scotland has revealed large differences in the degree of heterogeneity in zircon $\delta^{18}O$ between the diorites. Zircon crystals from the Cul nan Gad diorite (CnG) show a unimodal distribution of oxygen isotope values ($\delta^{18}O = 6.0 \pm 0.6$ ‰ (2σ)) and no or only minor grain-scale variation. Those from the Allt Darrarie diorite (AD1) show a large range in $\delta^{18}O$ and an apparent bimodal distribution with modes of 6.6 ± 0.4 ‰ and 7.3 ± 0.4 ‰. Variations of up to 1.2 ‰ occur between and within grains; both an increase and decrease in $\delta^{18}O$ with zircon growth has been observed. The $\delta^{18}O$ composition of growing zircon can only change if open-system processes affect the magma composition, i.e. if material of contrasting $\delta^{18}O$ composition is added to the magma. The variability in AD1 is interpreted to represent a cryptic record of magma mixing. A 'deep crustal hot zone' is a likely site for generation of the dioritic magmas which developed by mixing of residual melts and crustal partial melts or by

melting of mafic lower crustal rocks. The overall small number of zircons with mantle-like $\delta^{18}O$ values (5.3 ± 0.6 ‰ (2σ)) in the Lochnagar diorites is largely the product of crustal differentiation rather than crustal growth.

The $\delta^{18}O$ of quartz from the CnG and AD1 diorites shows only minor variation (CnG: 10.9 ± 0.5 ‰ (2σ), AD1: 11.7 ± 0.6 ‰ (2σ)) within single populations, with no evidence of mixing. Quartz-zircon isotopic disequilibrium is consistent with later crystallisation of quartz from late magmatic fluids, and in case of the AD1 diorite after the inferred magma mixing from a homogenised, higher $\delta^{18}O$ melt.

High-precision SIMS oxygen isotope analysis of zircon provides a new approach to identifying and resolving previously undetected early-stage magma mixing and constraining the compositions and origins of the component magmas. A combination of zircon, quartz and whole-rock data has proven to be a powerful tool in reconstructing the petrogenetic evolution of diorite from early crystallisation to late alteration.

1. Introduction

Oxygen isotopes have been widely used in petrogenetic evolution studies of granitic rocks to constrain the relative contributions of mantle and crust and the roles of fractional crystallisation, assimilation and magma mixing. The oxygen isotope compositions of granites and their constituent minerals are sensitive to modification by assimilation of ^{18}O-enriched crustal rocks, magma mixing and/or hydrothermal alteration by ^{18}O-depleted fluids (e.g. King et al., 1997, 2000; Monani and Valley, 2001; Valley and Graham, 1996).

Zircon is a common accessory mineral in intermediate and silicic plutonic rocks. Due to extremely slow rates of oxygen diffusion and high closure temperatures (Dodson, 1973; Peck et al., 2003; Valley, 2003; Watson and Cherniak, 1997) it is insensitive to hydrothermal alteration and fractional crystallisation during cooling, and therefore retains its oxygen isotope composition from the time of crystallisation (e.g. Kemp et al., 2005a, 2005b, 2006, 2007; King et al., 1998, 2002, 2004; King and Valley, 2001; Lackey et al., 2005, 2006). New developments in micro-analytical techniques now permit the rapid in-situ analysis of oxygen isotopes in zircon at high precision (here 0.4-0.6 ‰ (2σ)) by ion microprobe. With a beam diameter of only c. 20 μm, multiple analyses may be made in a single zircon crystal, which enables detection of differences in $\delta^{18}O$ between growth zones and between cores and rims in individual crystals, and allows detailed comparison between crystals. The high analytical precision and high spatial resolution of modern ion microprobes offers the potential to identify previously undetectable variations in oxygen isotope composition, providing more detailed insights into granite magma genesis and evolution.

Quartz, which commonly crystallises in the later stages of magmatic evolution, is also more resistant to isotopic modification than its host rock, and hence may also preserve isotopic signatures derived directly from the melt (e.g. Bindeman and Valley, 2001; Criss and Taylor, 1986; Monani and Valley, 2001; Valley et al., 1994). Conventional laser fluorination oxygen isotope data have commonly been used to assess the state of equilibrium between zircon, quartz and whole-rock samples in silicic magmatic rocks as a useful guide to the petrological and geochemical

evolution of magmas and rocks (King et al., 1997, 1998, 2004; King and Valley, 2001; Lackey et al., 2005, 2006; Monani and Valley, 2001).

This paper presents high-precision in-situ ion microprobe oxygen isotope data for zircon and quartz, supported by whole-rock $\delta^{18}O$ analyses, from two diorite intrusions forming part of the late Caledonian (424-413 Ma) (Paper 2) Lochnagar pluton in Scotland. It introduces a new approach to deciphering the detailed grain-scale petrogenetic information stored in zircon and quartz, and tests the results against recent models for the generation and evolution of intermediate and silicic calc-alkaline igneous rocks (e.g. Annen et al., 2006).

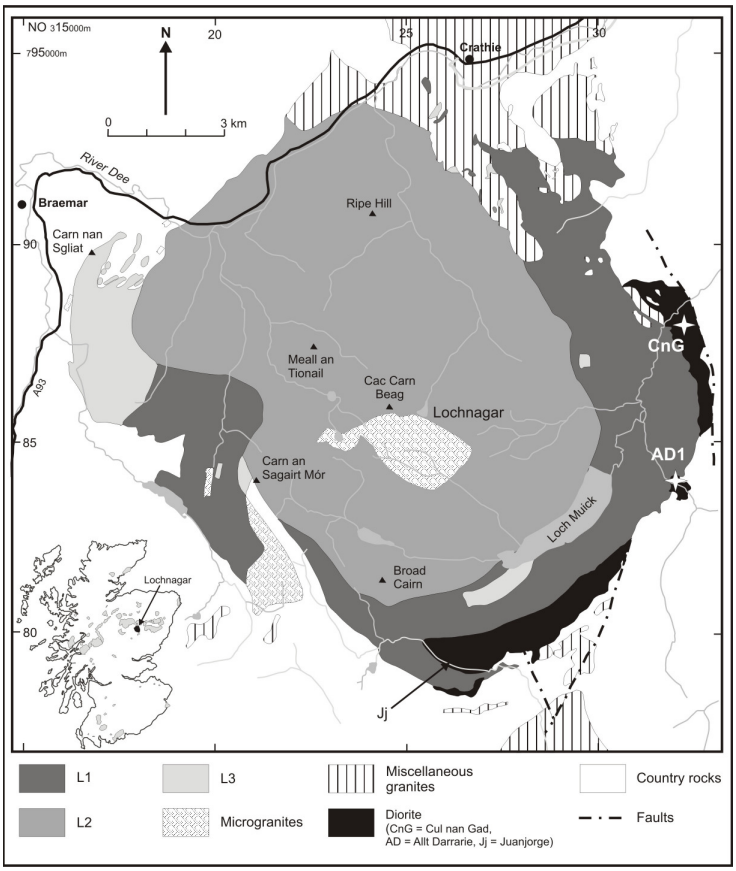

Fig. 1: Geological sketch map of the Lochnagar pluton (after Smith et al., 2001). Lochnagar comprises three main granite (L1, L2, L3) intrusions, several marginal diorite intrusions and late intrusions of microgranite. This paper focuses on the Cul nan Gad (CnG) and Allt Darrarie (AD1) diorites (stars indicate sample locations).

2. Geological background and sample details

The Lochnagar pluton, which crops out over an area of c. 150 km^2, is located in the Grampian Highlands of Scotland and belongs to the classic suite of late Caledonian 'I-type' intrusions that were emplaced at 430-400 Ma, after the c. 470 Ma Grampian Event and broadly contemporaneously with the oblique collision of Baltica and Laurentia (the Scandian Event) (Coward, 1990; Dallmeyer et al., 2001; Dewey and Mange, 1999; Kinny et al., 2003). However, the connection between this collision and the voluminous I-type magmatism is unclear. Based on field relationships and whole-rock geochemical and isotopic data, the Lochnagar pluton has been described as composite, comprising three main granite facies (L1, L2, L3) distinguished by textural and modal variations, a late intrusion of microgranite, and several marginal intrusions of diorite (Fig. 1) (Halliday, 1984; Halliday et al., 1979; Oldershaw, 1974; Smith et al., 2001). Two small diorite intrusions, Cul nan Gad (CnG) and Allt Darrarie (AD1) (with areal dimensions of 4-5 x 1.8 km (CnG) and 0.6 x 0.4 km (AD1); Smith et al. 2001), are the subject of this study. Based on field relationships these were interpreted to be consanguineous with, but cut by, the granite (Smith et al. 2001).

The diorites are dark grey, fine- to medium-grained (< 1-3 mm), and have a calc-alkaline metaluminous composition. They comprise plagioclase (45-50 %), biotite (c. 40 %), hornblende (< 5-10 %) and interstitial quartz (c. 5 %), with accessory ilmenite and magnetite, titanite (absent in CnG), zircon and apatite. All minerals are distributed evenly, which suggests that they do not contain cumulate or restite material and that the diorites represent melt compositions. Plagioclase crystals are sometimes zoned, commonly twinned and weakly altered to sericite in the centre. Biotites are often partially or entirely altered to chlorite, which is particularly prominent in the CnG diorite.

3. Methodology

3.1. Zircon sample preparation

Zircon separation was carried out at the University of St. Andrews Mineral Separation Facility. Rock samples of approximately 5 kg were crushed and sieved to obtain the < 500 µm fraction from which zircon crystals were separated using a Wilfley Table, heavy liquids and a Frantz magnetic separator. Approximately 100 zircon crystals were hand-picked from the remaining heavy, non-magnetic fraction, providing a range of grain size, morphology, transparency, alteration and occurrence of inclusions or cracks. The crystals were mounted into epoxy (Araldite) and the zircon mounts polished to about half thickness to expose the crystal interiors. The polished surfaces were imaged in secondary electron (SE), back-scattered electron (BSE) and cathodoluminescence (CL) mode using a Philips XL30CP Scanning Electron Microscope (SEM) at the University of Edinburgh to identify internal zoning features, inherited material, inclusions and cracks. Suitable crystals for in-situ oxygen isotope analysis were selected using this information.

3.2. Zircon SIMS oxygen isotope analysis

Zircon oxygen isotope data were obtained using a Cameca ims-1270 ion microprobe at the University of Edinburgh following the methods of Cavosie et al. (2005) and Kemp et al. (2006). A 6nA primary $^{133}Cs^{+}$ ion beam with a diameter of c. 20 µm was used, charge was neutralised using a normal-incidence electron flood gun, secondary ions were extracted at 10 kV, and $^{18}O^{-}$ and $^{16}O^{-}$ ions were monitored simultaneously on dual Faraday cups. Secondary ion beam centring, pre-sputtering for 50 seconds and subsequent data collection over 10 cycles (total counting time: 40 seconds = 4 seconds per cycle) resulted in a total acquisition time of c. 200 seconds. The secondary yield of ^{18}O under these conditions was typically between 4.5 x 10^6 and 5.5 x 10^6 counts per second. To correct for instrumental mass fractionation (IMF) and instrumental drift, all data were normalised to zircon standard 91500 ($\delta^{18}O$ = 9.86 ‰) (Wiedenbeck et al., 2004), which was analysed in blocks of 5 to 10

after every 10 to 15 unknown zircon analyses. During stable instrument conditions the unknown zircon analyses were normalised to the daily average $^{18}O/^{16}O$ value obtained for 91500. In cases where instrumental drift was recognised, the analytical conditions changed or sample exchange was carried out, the data were divided into sessions in which unknowns were normalised to the linearly interpolated $^{18}O/^{16}O$ value derived from analyses of the bracketing 91500 standard.

Prior to oxygen isotope analysis, HfO_2 concentrations in the zircons were measured by electron microprobe as variations in HfO_2 have been shown to cause variations in IMF (Peck et al., 2001). This has been shown to be particularly important when conducting analysis using e.g. a Cameca ims-4f at high-energy offset. However, in this study oxygen isotope analysis were carried out using a Cameca ims-1270 ion microprobe, and in both diorite samples HfO_2 variations in zircons were $\leq$ 0.5 wt %; therefore corrections for IMF were unnecessary. The internal precision of individual point analyses based on counting statistics varied between 0.1-0.2 ‰. External precision based on the reproducibility of standard 91500 ranged from 0.4 ‰ (n=57) to 0.6 ‰ (n=38) (2SD) and 0.040 to 0.087 (1 s.e.m.).

Analyses were conducted in clear, crack- and inclusion-free areas of representative zircon crystals. Where possible, multiple analyses (core to rim) were carried out on single zircon crystals to document zircon growth histories, and occasionally also in adjacent spots within crystals to assess reproducibility. The ion probe pits were subsequently imaged in BSE and SE mode using an SEM to determine the exact position of the analyses and to ensure that no cracks in the bottom of the pit might have influenced the results. Data obtained from suspect locations were rejected. In addition, data were excluded when the correction on the position of the secondary ion beam was anomalously large.

3.3. Quartz SIMS oxygen isotope analysis

Oxygen isotope analysis of quartz was carried out on polished thin sections using the Cameca ims-1270 ion microprobe, employing the same instrument set-up as for zircon oxygen isotope analysis. Quartz data were normalised to quartz standard

NBS28 ($\delta^{18}O$ = 9.58 ‰) (National Institute of Standards & Technology, 1992), which was analysed after every 15-20 unknowns. Internal precision calculated from NBS28 varied between 0.1 ‰ and 0.2 ‰. The external precision was 1.1 ‰ (2SD, n=59) and 0.072 (1 s.e.m.). In comparison, uncertainties on the unknowns were considerably lower (0.5 ‰ (n=22) and 0.6 ‰ (n=27) (2SD), 0.057 (1 s.e.m.) for CnG and AD1 respectively). Thus, the uncertainties on the unknown quartz crystals most closely reflect the analytical precision.

Where possible, multiple ion microprobe analyses were obtained between the centre and edge of each crystal in order to identify potential oxygen isotope zoning arising either from changes in the magma chemistry or from oxygen volume diffusion.

3.4. Whole-rock analyses

Oxygen isotope analyses of whole-rock samples were carried out at the Scottish Universities Environmental Research Centre (SUERC) at East Kilbride following the Macaulay et al. (2000) modification of the laser fluorination methodology of Sharp (1990). Approximately 1 mg of powdered sample was reacted with ClF_3 whilst being heated with a CO_2 laser. The resultant oxygen was purified, converted to CO_2 on platinised graphite, and the yield measured with a capacitance manometer. The oxygen isotope composition of the CO_2 was measured by a Micromass PRISM 3 dual inlet, triple collector mass spectrometer with a working standard gas calibrated against international reference materials. The accuracy and precision are ± 0.4 ‰ (2σ), and NBS28 gives a value of 9.56 ‰.

Major element concentrations were determined at the University of Edinburgh using a PANalytical PW2404 wavelength-dispersive sequential X-ray spectrometer.

4. Results

4.1. Zircon description

Zircon crystals show a similar range of sizes, morphologies and internal zoning textures in both diorites. This is a common phenomenon and is generally interpreted to be the result of varying local kinetic factors such as diffusion rates and adsorption (Dowty, 1980; Vavra, 1990, 1993). The only obvious difference between CnG and AD1 zircons lies in their CL character. AD1 zircons are overall more strongly luminescent and usually show only smaller luminescence contrast between growth zones.

In both diorite samples zircons vary in size between c. 200 µm and ≥ 700 µm along the c-axis, and have equant, stubby and elongated morphologies (aspect ratios AD1: 1:1.1 to 1:≥5.6, CnG: 1:1.2 to 1:1:≥7.3) with stubby and elongated crystals being dominant. With respect to internal zoning, all zircons consist of a core, which usually comprises most of the crystal, and up to three mantles and a rim varying in width from c. 5 µm to 100 µm. Cores, mantles and rims, are separated by resorption surfaces, which are generally interpreted to reflect periods of Zr undersaturation in the magma for which the dominant controls are either large-scale mixing events or local kinetic phenomena (Corfu et al., 2003). U-Pb dating by ion microprobe has shown that none of these cores contains inherited (significantly older) components. Hence, they represent magmatic cores that precipitated from the diorite magma, but reflect a different (early) evolution stage than the surrounding rims. Magmatic cores are either completely unzoned (c1) (Fig. 2a), comprise a relatively large inner unzoned domain (c1) and a surrounding outer oscillatory zoned domain (c2) (Fig. 2b-d) or appear to be entirely zoned (c2) (Fig. 2e). In the latter case a c1 domain is usually either difficult or impossible to identify. In terms of CL intensity, c1 domains are always moderately to weakly luminescent, whereas zones within the c2 domain vary between strongly and weakly luminescent. Mantles and rims consist of either a single or multiple zones.

Based on these characteristics it is likely that both diorites contain only a single zircon population in which c1, c2 and the surrounding mantles and rims vary in size due to local differences in growth rate or Zr saturation level in the magma.

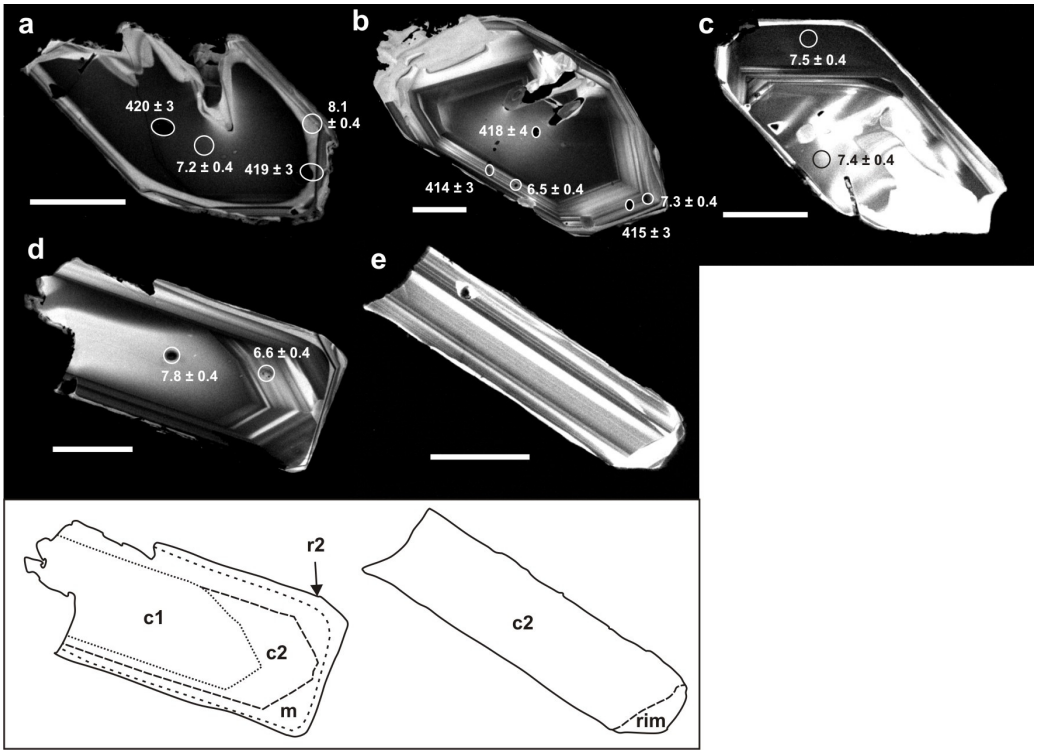

Fig. 2: CL images of zircon crystals representative of zircons from the CnG and AD1 diorites with oxygen isotope and U-Pb data (circles indicate position of oxygen isotope analyses, ovals of U-Pb analyses; error on $\delta^{18}O$ is ± 0.4‰ (2σ); scale bar = 50 µm).
a) Zircon grain (AD1 grain 11) consisting of large resorbed, weakly luminescent core (c1) and moderately luminescent rim. Note the large increase in $\delta^{18}O$ between core and rim.
b) Crystal (AD1 grain 9) comprises weakly luminescent unzoned inner core (c1), oscillatory zoned outer core (c2) and a rim. Both $\delta^{18}O$ values are from within c2, but vary by 0.8‰.
c) Zircon (AD1 grain 5) shows similar zoning pattern as b), but has two resorption surfaces. Core and rim analyses are identical within error.
d) Zoning is similar to b) and c) with c1, c2, mantles (m) and a rim (AD1 grain 10). Here c1 is 1.2‰ higher than c2, thus zoning is opposite to a).
e) Zircon grain lacks obvious c1 core domain (AD1 grain 17).

4.2. Zircon oxygen isotope data

All oxygen isotope values reported here are in per mil (‰) and relative to VSMOW (Vienna Standard Mean Ocean Water). Oxygen isotope data are presented in Figures 3a and 4a as histograms with overlaid cumulative probability curves, which were calculated by summing the probability distributions of a suite of data

with normally distributed errors (Isoplot ver.3.00, Ludwig, 2003). The bin widths of the histograms were chosen according to the precision (1σ) obtained from analyses of standard 91500 in the same analytical session, as this best represents the instrument performance during each session. Heterogeneities larger than those detected in 91500, which is assumed to be homogeneous in $\delta^{18}O$, are considered to reflect real variations in oxygen isotope composition. The data are also shown in grain-scale variation plots (Fig. 3c & 4c) to establish whether heterogeneities mainly occur between or within grains; these diagrams also illustrate whether the data lie within the error of the mean.

The $\delta^{18}O$ values of zircons from CnG lie between 5.5 ‰ and 6.4 ‰, with a mean value of 6.0 ‰ (n=36) and a standard deviation of 0.6 ‰ (2SD) (Table 1, Appendix 1). Zircon standard 91500 analysed in the same analytical session displays the same standard deviation (n=38) and degree of heterogeneity (2SD = 0.6 ‰). From this we interpret that the analytical precision of this session approximates 0.6 ‰ (2σ). The cumulative probability-histogram for CnG (Fig. 3a) shows a unimodal distribution with a mode of 5.9 ‰; a similar distribution is observed for 91500. Neither intra-grain and inter-grain variations in $\delta^{18}O$ nor systematic differences between cores, mantles and rims were detected (Fig. 3b). The grain-scale variation plot (Fig. 3c) reveals that all analyses lie within 2σ error of the mean and that only minor variation exists between and within crystals. However, these variations are not resolvable within the limits of analytical uncertainty.

Zircons from AD1 are relatively enriched in ^{18}O and display a much larger range in $\delta^{18}O$ than those from CnG, ranging from 6.1 ‰ to 8.1 ‰ with a mean of 7.1 ‰ (n=41). A standard deviation of 0.9 ‰ (2SD) is more than twice as large as for the 91500 standard analysed in the same analytical session (0.4 ‰, 2SD, n=57) and must therefore be considered to represent real isotopic heterogeneity. The cumulative probability-histogram (Fig. 4a) shows an apparent bimodal distribution with partly overlapping modes of 6.6 ‰ and 7.3 ‰. Based on this observation the data were separated into two apparent oxygen isotope populations with mean $\delta^{18}O$ values of 6.6 ± 0.4 ‰ (population 1, 2σ) and 7.4 ± 0.4 ‰ (population 2, 2σ). Plotting the probability-histogram of the same data separated into c1, c2 core domains, and mantles and rims (Fig. 4b) shows that each textural component (cores, rims etc.) also

displays a bimodal distribution. Thus, bimodality in AD1 cannot be attributed to systematic intra-grain differences or zonations in $\delta^{18}O$. The grain-scale variation plot reveals that, as indicated by the cumulative probability-histogram, several values lie above and below the field defining the 2σ error of the mean for the whole AD1 data set (Fig. 4c). It also demonstrates that the large range in values results from variations both between grains (e.g. grain 16: 6.1-6.5 ‰, grain 11: 7.2-8.1 ‰) and within grains (core-mantle/rim, c1-c2 core domains and even within core domains). The largest *intra-grain* variation of 1.2 ‰ in grain 10 occurs between c1 (7.8 ‰) and c2 (6.6 ‰) core domains, and represents only about half of the full range of variation of $\delta^{18}O$ in AD1 zircons. The largest variation *between a magmatic core and rim* can be observed in grain 11 (0.9 ‰) (core: 7.2 ‰, rim: 8.1 ‰) (Fig. 2a) and the largest range *within a single domain* in grain 9 (c2a: 6.5‰, c2b: 7.3‰) (Fig. 2b). This demonstrates that changes in $\delta^{18}O$ do not always conform to occurrence of resorption surfaces, but also exist within a single zone. Evidence was also found of cores and rims in some zircon crystals showing no - only minor - intra-grain variations, such as grain 5 (core: 7.4 ‰, rim: 7.5‰), despite being separated by resorption surfaces (Fig. 2c). Commonly AD1 zircon crystals show an increase in $\delta^{18}O$ with zircon growth in grains where multiple analyses (core to rim) were carried out, but grain 10 very clearly displays the opposite trend (Fig. 2d).

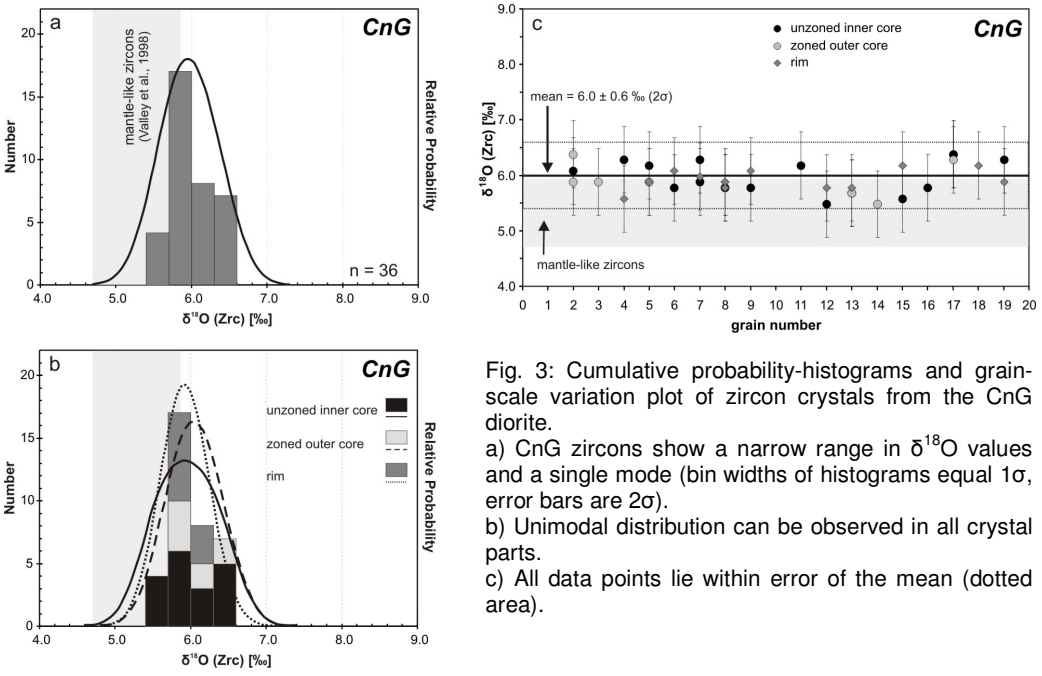

Fig. 3: Cumulative probability-histograms and grain-scale variation plot of zircon crystals from the CnG diorite.
a) CnG zircons show a narrow range in $\delta^{18}O$ values and a single mode (bin widths of histograms equal 1σ, error bars are 2σ).
b) Unimodal distribution can be observed in all crystal parts.
c) All data points lie within error of the mean (dotted area).

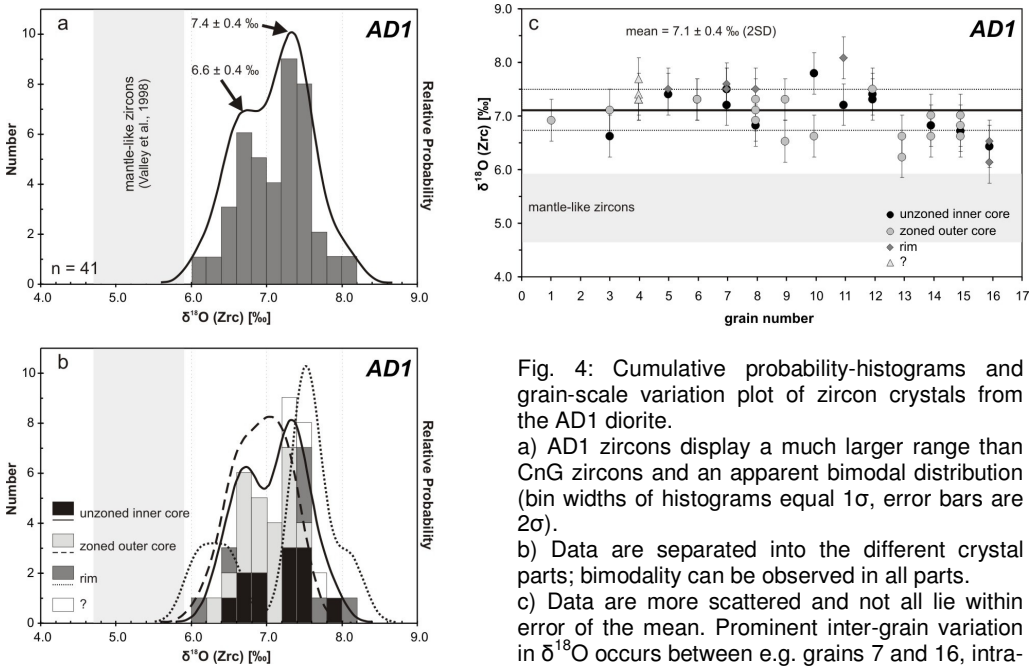

Fig. 4: Cumulative probability-histograms and grain-scale variation plot of zircon crystals from the AD1 diorite.
a) AD1 zircons display a much larger range than CnG zircons and an apparent bimodal distribution (bin widths of histograms equal 1σ, error bars are 2σ).
b) Data are separated into the different crystal parts; bimodality can be observed in all parts.
c) Data are more scattered and not all lie within error of the mean. Prominent inter-grain variation in $\delta^{18}O$ occurs between e.g. grains 7 and 16, intra-grain variation between inner and outer core (grain 9), core and rim (grain 11). $\delta^{18}O$ commonly increases with zircon growth except in grain 10.

4.3. Quartz oxygen isotope data

In both intrusions, quartz crystals from tens of microns to approximately 1 mm are weakly to moderately luminescent. Almost all crystals have annealed and open cracks, with typically more weakly luminescent areas along them (Fig. 5); these are a common feature in quartz crystals (e.g. Valley and Graham, 1996). CL evidence of growth zoning was not generally observed, but numerous crystals have weakly luminescent rims.

CnG quartz oxygen isotope data range from 10.4 ‰ to 11.4 ‰ with a mean of 10.9 ± 0.5 ‰ (2SD, n=22) (Table 1, Appendix 2). One analysis in a weakly luminescent (possibly hydrothermally altered) area yields a value of 12.0 ‰. AD1 quartz oxygen isotope values range from 11.3 ‰ to 12.3 ‰ with a mean of 11.7 ± 0.6 ‰ (2SD, n=27). The values from both samples display unimodal distributions (Fig. 7), and all data other than the possibly altered sample lie within error of the mean. A systematic change in composition between grain centres and rims or between grain sizes was not observed.

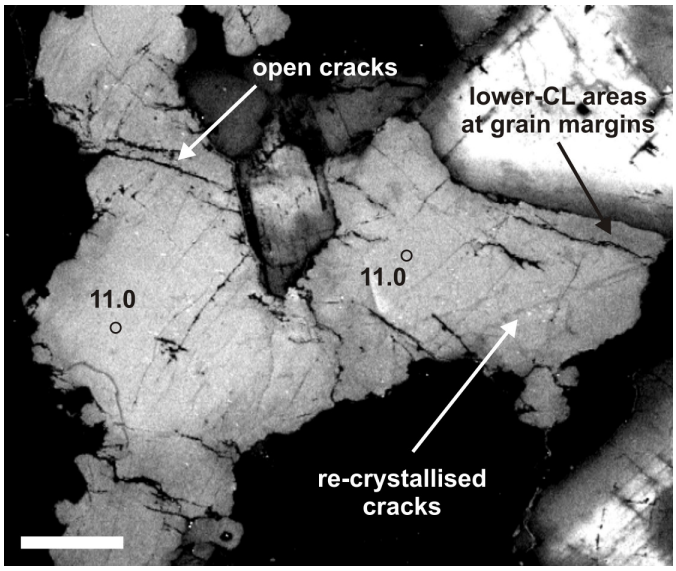

Fig. 5: CL image of representative quartz crystal (CnG, grain 9) with oxygen isotope data. Quartz contains open and re-crystallised cracks as well as lower-CL areas along its grain margins. Error: ± 0.5 ‰ (2σ), scale bar = 200 µm.

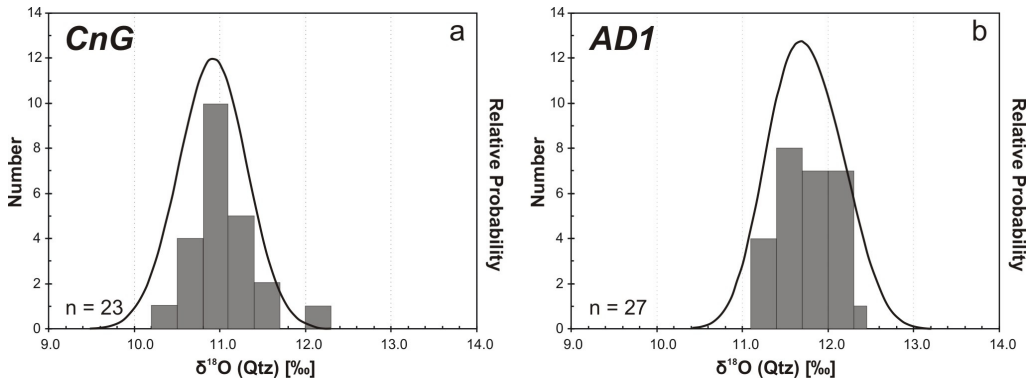

Fig. 6: Cumulative probability-histograms of quartz $\delta^{18}O$ data. Both diorites comprise single quartz populations. Outlier in CnG represents analysis on altered area along a microcrack.

Table 1

$\delta^{18}O$ values and fractionation factors for Lochnagar diorites

Sample	SiO_2 [wt%]	$\delta^{18}O$ (Zrc) [‰]	2σ	n	$\delta^{18}O$ (WR) [‰]	2σ	n	$\delta^{18}O$ (Qtz) [‰]	2σ	n	Δ(Zrc-WR) [‰]	Δ(Qtz-Zrc) [‰]	2σ
CnG	54.6	6.0	0.6	36	7.2	0.4	2	10.9	0.5	17	-1.8 to -0.6	+4.9	1.1
AD1	53.0	7.1	0.4	41	7.0	0.4	2	11.7	0.6	22	-0.3 to +0.5	+5.6 to +3.6	1.0

5. Discussion

The results of this study show that zircon crystals from the Lochnagar diorites display significant differences in their degree of isotopic heterogeneity. All zircons from the CnG diorite sample are homogeneous (within 2σ error of the mean) in their oxygen isotope composition, with a population mean of 6.0 ± 0.6 ‰ (2σ). Those from the AD1 diorite are heterogeneous and yield two apparent populations of 6.6 ± 0.4 ‰ and 7.4 ± 0.4 ‰.

Comparison of the $\delta^{18}O$ of zircons with those of co-existing quartz and their host whole-rocks may be used to assess whether any of the oxygen isotope populations revealed in zircon are in isotopic equilibrium with either quartz or host rocks. In addition, it enables us to resolve the contrasting magmatic evolution and processes of the two diorites in more detail.

5.1. Whole-rock – zircon equilibrium fractionation

Equilibrium oxygen isotope fractionation factors between whole-rock and zircon Δ(WR-Zrc) vary systematically with temperature and SiO_2 concentration (Valley et al., 1994, 2005). Higher silica concentrations in more evolved rocks reflect higher abundances of quartz and feldspar, which are enriched in ^{18}O relative to zircon and responsible for higher whole-rock $\delta^{18}O$ values. Hence, Δ(WR-Zrc) at any temperature increases with increasing whole-rock SiO_2 content. Differentiation in magmas therefore has no measurable effect on $\delta^{18}O$ values in zircon (Valley et al., 1994). At magmatic temperatures, equilibrium values for Δ(Zrc-WR) range from ~-0.5 ‰ for mafic rocks to ~-2.0 ‰ for granites according to the relationship (Lackey, 2005; Valley et al., 1994, 2005):

$$\Delta^{18}O(\text{Zrc-WR}) = \delta^{18}O\ (\text{Zrc}) - \delta^{18}O\ (\text{WR}) \sim -0.0612\ (\text{wt\% } SiO_2) + 2.5 \qquad (1)$$

For the CnG diorite ($\delta^{18}O$ (WR) = 7.2 ± 0.4 ‰ (n=2); SiO_2 (WR) = 54.6 wt%; $\delta^{18}O$ (Zrc) = 6.0 ± 0.6 ‰) Δ(Zrc-WR) values lie between -1.8 ‰ and -0.6 ‰ (taking the error on the analyses into account), which is in agreement with a calculated

equilibrium Δ(Zrc-WR) of -0.8. Thus, CnG zircons appear to be in isotopic equilibrium with their host rock (Fig. 6). Zircon crystals in the AD1 diorite ($\delta^{18}O$ (WR) = 7.0 ± 0.4 ‰ (n=2); SiO_2 (WR) = 53.0 wt%; $\delta^{18}O$ (Zrc) = 7.1 ± 0.4 ‰) contain two apparent populations of oxygen isotope values that cannot both be in isotopic equilibrium with the host rock, and in themselves indicate isotopic disequilibrium.

A change in $\delta^{18}O$ (zircon) can only be achieved by adding material of a different oxygen isotope composition to a magma (Valley, 2003), which implies that the two apparent $\delta^{18}O$ populations in the AD1 zircons must represent mixing of at least two components. In most cases where zircon grains show resolvable variation in $\delta^{18}O$ between different parts of the crystal, this is manifested as an increase in $\delta^{18}O$ from core to rim reflecting mixing of a higher-$\delta^{18}O$ melt with the magma. However, the reverse trend has also been observed (grain 10), which suggests components less enriched in ^{18}O were also mixed into the magma at some stage. We conclude that the two apparent populations do not represent simple mixing of only two components. Instead, a more complicated scenario is envisaged in which there were at least two melt batches (a high-$\delta^{18}O$ melt with ≥ 8.1 ‰ and a lower-$\delta^{18}O$ melt with ≤ 6.6 ‰ representing the highest and lowest measured zircon values (rim in grain 11 and c2 domain in grain 10, respectively)). Plausibly, multiple batches mixed with the magma *during* zircon growth. Imperfect mixing may also have led to some of the variation observed between zircon crystals. Due to this complicated mixing history we conclude that neither major zircon population in AD1 can have been in equilibrium with the present host rock. Independent textural or geochemical evidence for magma mixing has not been recognised in AD1.

The outer rims of zircon crystals are most likely to be in equilibrium with the current host rock. Comparing zircon rim and whole-rock $\delta^{18}O$ data is complicated as zircon rims fall into low-$\delta^{18}O$ (6.1-6.5 ‰) (1 grain) and high-$\delta^{18}O$ (7.5-7.6 ‰) (5 grains) groups. Considering a calculated Δ(Zrc-WR) value of -0.7 ‰ (53.0 wt% SiO_2) and the AD1 whole-rock composition of 7.0 ± 0.4 ‰, only the low-$\delta^{18}O$ rims can be in isotopic equilibrium (Fig. 7). To be in equilibrium with the high-$\delta^{18}O$ rims, the whole-rock oxygen isotope composition would have to lie between 7.8 ‰ and 8.7 ‰, and as high-$\delta^{18}O$ rims appear to be more common they may be more

representative of the bulk magma from which the zircons crystallised. This would suggest that the current host rock underwent depletion in ^{18}O, possibly by further mixing with low-$\delta^{18}O$ components, or by hydrothermal alteration, for example by interaction with heated meteoric water (Farver and Yund, 1991; Smith, 1981) after zircon had crystallised. Since plagioclase and biotite show only minor signs of alteration, any hydrothermal alteration would have occurred at or close to magmatic temperatures. The fact that zircons and whole-rock are in isotopic equilibrium in the CnG diorite suggests that it was unaffected by alteration even though the CnG and AD1 intrusions are located only approximately 1.5 km apart from each other. Hydrothermal fluids typically have heterogeneous flow paths, differing flow durations and fluid/rock ratios, and the intensity of alteration can vary at µm to km scales (Valley and Graham, 1996). Alternatively, isotopic equilibrium between zircon and whole-rock in the CnG diorite is fortuitous.

5.2. Quartz – zircon equilibrium fractionation

Quartz in granite is less susceptible to hydrothermal alteration than its whole-rock host, reflecting the susceptibility of feldspar to rapid isotopic exchange with hydrothermal fluid down to temperatures of 300-400ºC. Quartz exchanges oxygen isotopes mainly by solution/re-precipitation and by slow temperature-dependent volume diffusion, exploiting fractures and crystal boundaries (Valley and Graham, 1996). Hence, if annealed cracks and obviously altered areas are avoided during analysis, the $\delta^{18}O$ of zircon and quartz may provide a reliable indication of the state of isotopic equilibrium and of magmatic evolution.

In contrast to the zircon oxygen isotope data, $\delta^{18}O$ (Qtz) analyses from both the CnG and AD1 diorites yield unimodal oxygen isotope populations (Fig. 6) . Hence, $\delta^{18}O$ (Qtz) in AD1 and CnG provide no evidence of magma mixing. Examining the equilibrium fractionation between zircon and quartz may potentially explain this phenomenon.

Equilibrium oxygen isotope fractionation factors between quartz and zircon (Δ(Qtz-Zrc)) as a function of temperature are given by the empirical equation (Valley et al., 2003):

$$\delta^{18}O_{Qtz}-\delta^{18}O_{Zrc} = \Delta_{Qtz-Zrc} \approx 1000 \ln (\alpha_{Qtz-Zrc}) = A_{Qtz-Zrc}\ 10^6/T^2 \quad (2)$$

where $A_{Qtz-Zrc}$ = 2.64 (‰K^2); T = temperature in degrees Kelvin.

At 800ºC the equilibrium value of Δ(Qtz-Zrc) is 2.3 ‰. However, for diorite CnG (mean $\delta^{18}O$ (Zrc) = 6.0 ± 0.6, mean $\delta^{18}O$ (Qtz) = 10.9 ± 0.5‰) the calculated Δ(Qtz-Zrc) is 4.9 ± 1.1 ‰. Due to the complex $\delta^{18}O$ (Zrc) distribution in AD1, the mean oxygen isotope value of zircon cannot be used for this calculation. Instead we use the lowest and highest measured zircon values ($\delta^{18}O$ (Zrc) = 6.1-8.1 ± 0.4 ‰, mean $\delta^{18}O$ (Qtz) = 11.7 ± 0.6 ‰), yielding Δ(Qtz-Zrc) of 5.6-3.6 ± 1.0 ‰. Taking the error into account, the Δ(Qtz-Zrc) value is at least 1.2 ‰ higher in CnG and 0.3 ‰ higher in AD1 than the calculated value of 2.3 ‰ for isotopic equilibrium at 800ºC using equation (2). A temperature of 700ºC would permit equilibrium between only the highest $\delta^{18}O$-zircons observed in the AD1 diorite and quartz (and only if the error is taken into account). We conclude that zircon and quartz are not in isotopic equilibrium.

Other authors (e.g. King and Valley, 2001; Monani and Valley, 2001) have found that quartz does not always preserve magmatic $\delta^{18}O$ values as robustly as zircon, due to post-magmatic hydrothermal diffusive oxygen exchange and alteration. However, the lack of oxygen isotope heterogeneity along cracks and crystal boundaries or between different quartz crystal sizes in AD1 and CnG suggests that in both samples quartz has essentially retained its oxygen isotope composition from the time of crystallisation and therefore high $\delta^{18}O$ (Qtz) was not caused by hydrothermal alteration or closed-system exchange with feldspar. We conclude that in the CnG diorite quartz crystallised (or completely recrystallised) from late magmatic or high-temperature post-magmatic (subsolidus) fluids with high $\delta^{18}O$ after zircon had ceased to crystallise. The analysed zircons may comtain a very thin outer rim that is in equilibrium with quartz, but due to the spatial resolution of the ion microprobe this is not detectable. Quartz in AD1 also forms a homogeneous oxygen isotope population in contrast to co-existing zircon, and hence disequilibrium between quartz and zircon, and a similar may also be assumed.

In summary, both zircon and quartz in the Lochnagar diorites preserve their oxygen isotope compositions from the time of crystallisation. However, textural and isotopic evidence strongly suggests that zircon and quartz crystallised at different times, and hence we conclude that they represent different magma (or fluid) compositions. As oxygen isotope evidence of magma mixing was only found in AD1 zircons and not in quartz, the $^{18}O/^{16}O$ of the AD1 magma (or late magmatic fluid) must have been completely homogenised and relatively more ^{18}O-enriched at the stage of quartz crystallisation.

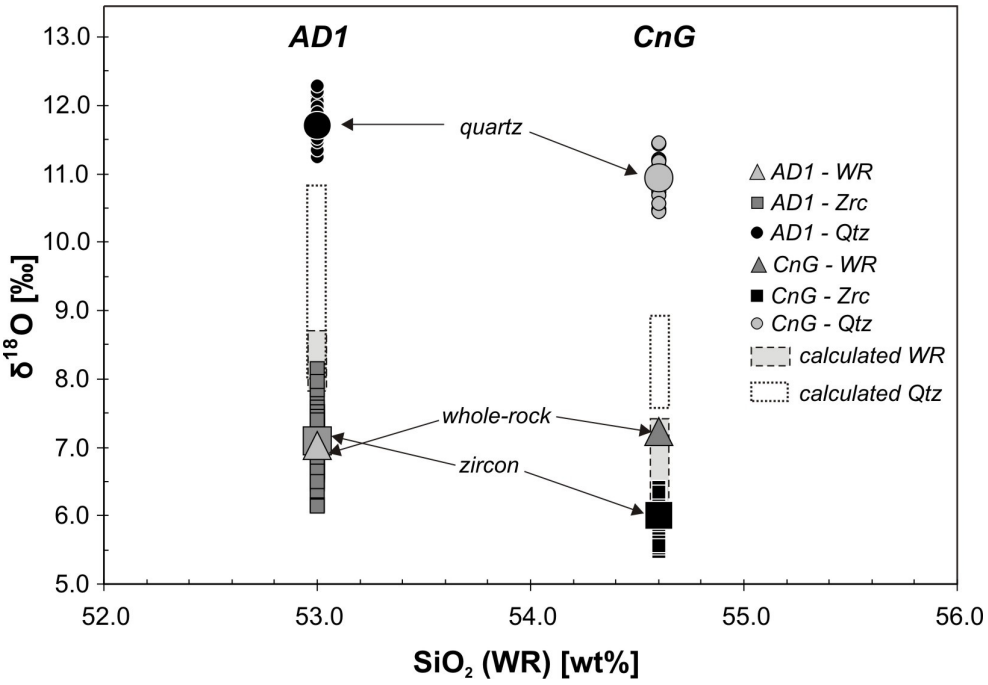

Fig. 7: Evaluation of equilibrium between zircon (Zrc), quartz (Qtz) and whole-rock (WR). 'Calculated WR' and 'calculated quartz' are calculated using equations (1) and (2) (see text); calculations include the error on the zircon analysis.
AD1: Zircon is not in equilibrium with quartz or whole-rock. Measured whole-rock is too low to be in equilibrium with zircon, which suggests it was affected by hydrothermal alteration after zircon crystallisation.
CnG: Zircon and quartz are not in equilibrium as measured quartz $\delta^{18}O$ is considerably higher than the calculated quartz value, which suggests quartz crystallised late in sequence. Zircon and whole-rock are in equilibrium. Low modal percentage of elevated quartz in whole-rock (<5 %) did not shift whole-rock out of equilibrium.

5.3. Petrogenetic evolution model

The granites and diorites of the Lochnagar pluton belong to a suite of late Caledonian I-type intrusions in Scotland whose protoliths are thought to be "igneous" or "infracrustal" insofar as these protoliths have not experienced a weathering cycle (Chappell and Stephens, 1988). I-type granitic rocks are widely considered to be the products of either (1) (re)melting of deep-crustal igneous rocks, implying that they are the products of crustal differentiation and recycling rather than crustal growth; or (2) the interaction (by melting or assimilation) of mantle-derived (mafic) magmas with older crustal rocks, implying the generation and growth of new continental crust (e.g. Kemp and Hawkesworth, 2005).

Zircons in equilibrium with pristine mantle melts have $\delta^{18}O$ of 5.3 ± 0.6 ‰ (2σ, Valley et al., 1998). This value is insensitive to modification by differentiation since whole-rock $\delta^{18}O$ and Δ(melt -Zrc) increase in parallel as differentiation and accompanying increase of SiO_2 proceed (Valley et al., 1994). The occurrence of zircons with $\delta^{18}O > 5.6$ ‰ in dioritic rocks thus indicates that the protoliths contained an ^{18}O-enriched supracrustal component or an altered igneous source, and/or represent the the interaction of mantle-derived magmas with supracrustal materials.

Zircon crystals in the Lochnagar diorites are enriched in ^{18}O by an average of 0.7 ‰ to 2.1 ‰ relative to pristine mantle values ($\delta^{18}O$ (CnG) = 6.0 ± 0.6 ‰; $\delta^{18}O$ (AD1) = 7.1 ± 0.4 ‰), indicating the involvement of ^{18}O-enriched crustal protoliths (supracrustal rocks or altered igneous rocks) in the their generation or evolution, either as remelted protoliths or by assimilation or mixing of such protoliths in mantle-derived mafic magmas. Evidence for the involvement of mantle-derived melts may be preserved in zircon crystals with $\delta^{18}O < 5.9$ ‰ in the CnG diorites that overlap into the mantle field (Fig. 3). These may have crystallised early in the crystallisation history of the CnG diorite in order to capture evidence of a mantle component before any magma mixing processes took place similar to those recorded in diorite AD1. On a wider scale, mafic enclaves in granites and the occurrence of appinites, lamprophyres and rare gabbroic intrusions of late Caledonian (430-400 Ma) age indicate an indirect role for mantle-derived melts in the genesis of the late

Caledonian granites in Scotland (Strachan et al., 2002). However, the absence of any persuasive evidence of a pristine mantle source in the $\delta^{18}O$ (Zrc) data for the Lochnagar diorites suggest an origin dominated by remelting of mafic lower crustal sources and crustal differentiation rather than crustal growth. On the other hand, the $\delta^{18}O$ (Zrc) values are not strongly ^{18}O-enriched, and a large supracrustal contribution by for example Dalradian Supergroup metasedimentary host rocks can therefore be ruled out.

Several models have been proposed for the origin of intermediate and silicic calc-alkaline magmas. These include fractional crystallisation of mantle-derived basalt or basaltic andesite in shallow crustal magma chambers (e.g. Grove et al., 1997; Pichavant et al., 2002; Sisson and Grove, 1993) or at/close to the Moho (e.g. Annen and Sparks, 2002; Mortazavi and Sparks, 2003; Müntener et al., 2001; Prouteau and Scaillet, 2003), and dehydration melting in lower or middle crust induced by intrusion of hot, hydrous, mafic, mantle-derived magma (e.g. Jackson et al., 2003; Petford and Atherton, 1996; Smith and Leeman, 1987). Based on numerical modelling and experimental data Annen and Sparks (2002) have proposed the existence of 'deep crustal hot zones' and have recently applied this model (Annen et al., 2006) to the generation of intermediate and silicic igneous rocks in subduction zone settings.

The development of deep crustal hot zones results from repeated intrusion of mantle-derived hydrous basalt sills into the lower crust, where melts are generated either by (1) differentiation of the basalt sills to produce residual and more siliceous H_2O-rich melts, or by (2) partial melting of pre-existing crustal rocks (including early basalt sills). Mixing of residual melts (or mafic mantle melts) and crustal partial melts creates a large range of intermediate and silicic melts with variably ^{18}O-enriched compositions. The efficiency of melt production in deep crustal hot zones largely depends on the amount of intruding basalt, the level of emplacement in the crust, the rate of emplacement and the composition of the lower and middle crust. Residual melts are most efficiently produced by differentiation of basalt at deep crustal levels. In contrast, the largest amounts of crustal partial melts are generated either by random basalt sill injection over extended periods of time at different mid- and lower crustal levels, heating the crust from below and above, or by emplacement

of sills at the contact with a fertile upper crust. Thus, the basalt sills predominantly act as a heat source required for generation of crustal partial melts, but do not necessarily represent the dominant component in the generated melts. After melt generation, melts segregate and, depending on their H_2O content, density, viscosity and ascent path, ascend more or less rapidly into shallow reservoirs in the upper crust where they undergo crystallisation by degassing and cooling (Annen et al., 2006).

The tectonic setting that led to intrusion of the late Caledonian 'I-type' magmatism in Scotland is still controversial. The late Caledonian granites have commonly been linked to a subduction zone setting (Brown, 1991; Brown et al., 1985; Soper, 1986; Stephens and Halliday, 1984; Stephenson et al., 1999; Thirlwall, 1981, 1982, 1988), and more recently a slab-breakoff model has been proposed (Atherton and Ghani, 2002). Based on the complexity of the zircon oxygen isotope data observed in the AD1 diorite magma generation in a 'deep crustal hot zone' may provide a suitable model to explain the generation of the Lochnagar diorites. As neither CnG nor AD1 diorites contain populations of zircons with pristine mantle $\delta^{18}O$ signatures the diorites do not appear to have formed by simple closed-system fractional crystallisation of contemporaneous mantle-derived melts. Assimilation and fractional crystallisation may explain the zircon oxygen isotope composition of the CnG diorite. However, the observed increase and decrease in $\delta^{18}O$ (zircon) with zircon growth in the AD1 diorite, which indicates mixing or assimilation of lower and higher $\delta^{18}O$ materials, is inconsistent with this process. We therefore propose that the diorites formed in a deep crustal hot zone either by (1) mixing of residual melts and crustal partial melts, or by (2) partial melting of a mafic lower crust. Model 1 implies that zircons with mantle-like $\delta^{18}O$ values represent a contemporary ~420 Ma mantle-derived component, hence new crust, whereas in model 2 mantle-like zircons reflect melting of old lower crust with a mantle-like composition, hence crustal differentiation. Based on oxygen isotope data alone it is not possible to distinguish between these two models, but due to the overall small number of mantle-like zircons crustal recycling appears to have been the dominant process.

Valuable information was also gained about the magmatic evolution of the dioritic magmas, which appear to differ significantly. The homogeneity in $\delta^{18}O$ of the CnG zircons suggests they precipitated from a single homogeneous magma and

did not experience open-system processes during zircon growth. In contrast, the AD1 magma experienced *at least* two mixing events involving a high $\delta^{18}O$ ($\geq$ 8.1 ‰) and a lower-$\delta^{18}O$ melt ($\leq$ 6.6 ‰). As these mixing events appear to have occurred during zircon growth, they probably took place at shallow crustal levels after ascent. The juxtaposition of two or more magmas of differing $\delta^{18}O$ is consistent with a model of incremental assembly of melt batches in the AD diorite pluton. Resorption surfaces between cores and rims or between mantles do not appear to represent the timing of mixing as (1) a shift in $\delta^{18}O$ between cores and rims was not always observed, (2) variations in $\delta^{18}O$ exist within single zones, and (3) zircons from both the CnG and AD1 diorites contain resorption surfaces, but no evidence of mixing was found in CnG. Thus, these surfaces are more likely to represent local differences in the growth environment due to fluctuations in Zr content. In both diorites quartz crystallised late from homogenised, high-$\delta^{18}O$ melt or fluid, is thus not in equilibrium with zircon and shows no evidence of magma mixing. After zircon and quartz crystallisation, diorite AD1, and perhaps also the CnG diorite, may have been affected by high-temperature hydrothermal alteration by infiltration of hot meteoric fluids, resulting in a decrease in whole-rock oxygen isotope composition.

6. Conclusions

1) High-precision in-situ SIMS oxygen isotope analysis reveals small (<< 1 ‰) variations in oxygen isotope composition in zircon and quartz crystals in Scottish late Caledonian diorites at a spatial resolution of around 20 µm.
2) Zircon in the Cul nan Gad diorite intrusion yields a unimodal distribution of oxygen isotope values with a mean of 6.0 ± 0.6 ‰, whereas zircon in the Allt Darrarie diorite intrusion yields two apparent populations with means of 6.6 ± 0.4 ‰, and 7.4 ± 0.4 ‰. The $\delta^{18}O$ composition of zircon preserved in growing crystals in the latter diorite can only evolve by open-system changes to the magma composition, so the presence of two populations of oxygen isotope values in zircon represents a cryptic record of magma mixing during zircon crystallisation. Detailed examination of the grain-scale variations reveals

increases as well as decreases in $\delta^{18}O$ with zircon growth. This suggests that the two apparent populations do not represent simple mixing between two components, but indicates a more complicated process involving additional magma component(s).

3) Quartz oxygen isotope data show no evidence of a mixing event. Evaluation of Δ(Qtz-Zrc) values shows that quartz and zircon are not in equilibrium in either diorite host. This is interpreted to reflect quartz crystallisation late in the sequence, at lower temperatures and from a higher-$\delta^{18}O$ magma well after the mixing events in the Allt Darrarie magma.
4) Whole-rock and zircon oxygen isotope values appear to be in equilibrium in the Cul nan Gad diorite, although this may be fortuitous. In the Allt Darrarie diorite, the whole-rock $\delta^{18}O$ value is too low, which indicates that it experienced further mixing or more likely hydrothermal alteration that did not affect either zircon or quartz.
5) The Lochnagar diorites are thought to have been generated in a 'deep crustal hot zone' by either (1) mixing of residual melts and crustal partial melts indicating that they incorporate new crust, or (2) melting of mafic lower crustal rocks, indicating crustal recycling. Based on oxygen isotope data alone it is not possible to distinguish between these two models, but the small number of zircons with mantle-like $\delta^{18}O$ values is consistent with an origin dominated by crustal differentiation rather than crustal growth. A large supracrustal contribution can be ruled out.
6) Zircons from the Cul nan Gad diorite crystallised from a homogeneous melt; its magma did not experience open-system changes during zircon growth. Allt Darrarie diorite zircons experienced at least two mixing events during zircon growth.
7) A combined zircon, quartz and whole-rock oxygen isotope approach is a powerful way to constrain the petrogenetic evolution of plutons from early crystallisation to late alteration. However, only high-precision in-situ ion microprobe analysis of zircon is capable of revealing the cryptic record of multiple magma mixing events observed in the Allt Darrarie diorite.

III.

PAPER 2

A tale of two plutons: an integrated ion microprobe study of $^{18}O/^{16}O$, U-Pb, trace elements and REE in zircons from Scottish Caledonian granites

A tale of two plutons: an integrated ion microprobe study of $^{18}O/^{16}O$, U-Pb, trace elements and REE in zircons from Scottish Caledonian granites

S.K. Appleby [a,*], C.M. Graham [a], M.R. Gillespie [b],
R.W. Hinton [a], N.M. Kelly [a], G.J.H. Oliver [c], EIMF [d]

[a] *Grant Institute of Earth Science, University of Edinburgh, West Mains Road, Edinburgh, EH9 3JW, UK*

[b] *British Geological Survey, Murchison House, West Mains Road, Edinburgh, EH9 3LA, UK*

[c] *School of Geography & Geosciences, Crustal Geodynamics Group, University of St. Andrews, St. Andrews, KY16 9AL, UK*

[d] *Edinburgh Ion Microprobe Facility, University of Edinburgh, West Mains Road, Edinburgh, EH9 3JW, UK*

* corresponding author. Email: S.K.Appleby@sms.ed.ac.uk

Manuscript
Intended for submission to Journal of Petrology

Abstract

Integrating in-situ SIMS U-Pb, oxygen isotope, trace element and REE analyses of zircons provides the opportunity to access grain-scale information that cannot be detected by conventional techniques in order to decipher the petrogenetic histories of granitic plutons. We have used this approach to study zircons from two Scottish late Caledonian (c. 430-400 Ma) 'I-type' granites, the Lochnagar and Etive plutons. The plutons show large differences in their whole-rock trace element compositions, which have been interpreted to reflect either compositional variations in their sources or variations in the relative contributions of different sources (e.g. mantle vs. crust).

U-Pb dating has revealed that the emplacement histories of both plutons are more protracted and complicated than previously recognised, with magmatic activity at the Lochnagar pluton lasting for c. 11 m.y. (424-413 Ma) and at the Etive pluton for c.

16 m.y. (423-407 Ma). Oxygen isotope analyses of zircons show that the plutons comprise samples with both homogeneous and heterogeneous distributions of $\delta^{18}O$. In heterogeneous samples, resolvable variations occur both between zircon crystals within a single sample and within individual crystals (e.g. between cores and rims). Commonly, both decreases and increases in $\delta^{18}O$ with zircon growth were observed, providing evidence for magma mixing. This scale and degree of this heterogeneity has not previously been reported.

The majority of zircon crystals (c. 80 %) are enriched in ^{18}O relative to zircons with mantle-like $\delta^{18}O$ values (5.3 ± 0.6 ‰ (2σ)). This suggests that the plutons contain only a small pristine mantle component, are either derived from a mixture of mantle-derived and crustal materials or solely from infracrustal sources. Simple two-component magma mixing between mantle-derived melts and a suprcrustal component, e.g. the Dalradian Supergroup country rocks, can account for the range of zircon $\delta^{18}O$ values found in the Lochnagar and Etive plutons. However, the observed variation in zircon oxygen isotope composition indicates a more complex mixing/assimilation scenario involving several sources, which cannot be identified based on oxygen isotope data alone. In addition, it is impossible to decipher whether zircons with mantle-like $\delta^{18}O$ values reflect a contribution by contemporary depleted and/or enriched mantle or actually represent pre-existing mafic lower crust. Minor inheritance of pre-magmatic zircon indicates a supracrustal component, most likely Dalradian Supergroup country rocks.

The large variation in $\delta^{18}O$ measured in zircons from the Lochnagar and Etive pluton is attributed to a 'deep crustal hot zone' where mantle melts differentiated, inducing partial melting of the lower/middle crust and extensive mixing of melts with differing $\delta^{18}O$. Further mixing occurred during zircon growth during ascent and at shallower levels. Magmas were subsequently emplaced incrementally in small batches over extended periods of time. The processes and the relative contributions of mantle and crust involved in the genesis of the Lochnagar and Etive plutons were very similar. Thus, the whole-rock differences must be attributed to compositional differences between the sources.

1. Introduction

Due to the complexity and diversity of granitic rocks, and the difficulty of recognising unambiguous geochemical and petrological signatures of their sources, their petrogenesis and magmatic evolution have remained controversial. Following the classic study of Chappell and White (1974) on the origin of the granitic rocks of the Lachlan Fold Belt, southeastern Australia, plutons have been widely considered to have either igneous (infracrustal) or sedimentary (supracrustal) precursors, which may be distinguished by their whole-rock chemistry. However, more recent studies have demonstrated that granites rarely have a single source, but commonly represent complicated mixtures of melts derived from the mantle and from infra- and/or supracrustal sources (John and Wooden, 1990; Kemp et al., 2007; Kemp and Hawkesworth, 2003; Miller et al., 1990). The relative proportions of mantle and crustal contributions in the voluminous I-type granites that characterise collision belts and volcanic arcs have key significance for the role of granite genesis in the growth and differentiation of the Earth's continental crust (e.g. Hawkesworth and Kemp, 2006a; Kemp et al., 2007).

Recent advances in in-situ microanalysis permit the study of granites using the geochemical record stored in zircon. Due to its refractory nature, zircon retains information about its parental melt(s). Changes in melt composition, temperature or crystallisation conditions with time arising from either local closed-system processes or large-scale open-system changes (e.g. magma mixing, assimilation) are recorded in zircon growth zones (Hoskin and Schaltegger, 2003; Shore and Fowler, 1996; Vavra, 1990, 1993, 1994), which may be imaged by cathodoluminescence (CL) and back-scatter electron (BSE) imaging techniques. With significant concentrations of U, Th and REEs (ppm level) (Kinny and Maas, 2003), zircon is suitable for oxygen isotope, U-Pb and trace element/REE analysis. Due to the high spatial resolution of the ion microprobe, multiple analyses may be made within a single zircon grain, which permits correlation of elemental and isotopic changes with zircon growth (e.g. changes between zircon cores and rims). Furthermore, oxygen, U-Pb and REE analyses may now be carried out on the same c. 20 μm spot, which enables direct spatial correlation to be made between the different data sets. This approach may be

used to constrain the emplacement ages of plutons (U-Pb data), and their sources (mantle, infracrustal and/or supracrustal) (O and REE data), and to resolve processes such as magma mixing (Paper 1).

In this paper we apply these integrated techniques to zircons from the Lochnagar and Etive plutons, which are representative of the Scottish late Caledonian (c. 430-400 Ma) I-type granites, in order to constrain their emplacement histories, and to assess the role of mantle, infracrustal and supracrustal sources in the genesis of this classic and voluminous suite of I-type granites.

2. The late Caledonian granites

The Caledonian I- and S-type granites represent a classic granite suite that is mostly located in the Grampian Highlands of Scotland. The main focus of previous research has been the late Caledonian calc-alkaline I-type granites, which were emplaced into Dalradian metasediments in the Grampian Highlands between c. 430 Ma and 400 Ma (Fig. 1) (Oliver, 2001; Rogers and Dunning, 1991; Stewart et al., 2001). The main phase of emplacement, between 425 and 430 Ma (Oliver, 2001), was broadly contemporaneous with - and subsequent to - the Scandian event, which involved the oblique collision of Baltica and Laurentia (Brown et al., 1985; Brown, 1991; Coward, 1990; Dallmeyer et al., 2001; Dewey and Mange, 1999; Kinny et al., 2003; Soper, 1986; Stephens and Halliday, 1984; Stephenson et al., 1999; Thirlwall, 1981, 1982, 1988). However, the connection between the collision and the voluminous I-type magmatism is unclear.

The Caledonian I-type plutons have geochemical features typical of modern continental arcs with the majority showing a metaluminous affinity (except for granites with > 70 wt% SiO_2, which are peraluminous) (Frost et al., 2001). They are commonly hornblende-bearing (Soper, 1986) and contain high Rb/Sr and K/Na, low K/Rb and relatively low initial Sr isotope ratios (Halliday et al., 1985; Stephens, 1988; Thirlwall, 1988). Their origin has previously been linked to a subduction zone setting (Brown, 1991; Brown et al., 1985; Soper, 1986; Stephens and Halliday, 1984; Stephenson et al., 1999; Thirlwall, 1981, 1982, 1988), but more recently a slab-

breakoff model has been proposed (Atherton and Ghani, 2002). However, the exact tectonic setting that led to emplacement of the late Caledonian I-type granites in Scotland is still controversial.

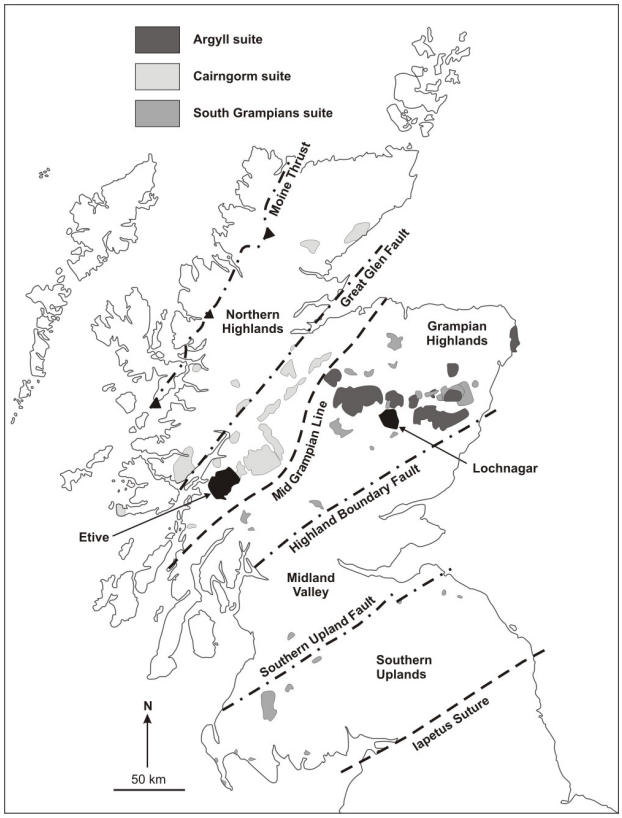

Fig. 1: Map of the late Caledonian granites (after Stephenson et al., 1999).

On the basis of whole-rock geochemical and isotopic data three late Caledonian I-type granite suites - the Argyll, Cairngorm and South Grampians suites - have been distinguished (Fig. 1) (Stephens and Halliday, 1984). The *Argyll suite* consists of hornblende-biotite granodiorite and biotite granodiorite plutons with minor dioritic, appinitic and monzogranitic components (Stephen and Halliday, 1984; Strachan et al., 2002). The plutons are strongly metaluminous and are enriched in Ba, Sr and Na relative to the plutons of the other suites, whereas Nb, Th and Rb are present only at low concentrations (Fowler et al., 2001; Halliday, 1984; Halliday et al., 1985; Stephens and Halliday, 1984; Tarney and Jones, 1994; Thirlwall, 1988). The *Cairngorm suite* consists of biotite monzogranite with minor granodiorite, which

varies texturally between microgranite and coarse-grained, K-feldspar megacrystic granite. The intrusions contain high concentrations of Rb, Nb, Th and U, but have low Ba, Sr, Ti, P contents (Stephens and Halliday, 1984). The *South Grampians suite* is dominated by granodiorites and monzogranites, and has a higher proportion of gabbroic and appinitic intrusions. In general, this suite is strongly metaluminous with higher K and Th abundances than the Argyll suite, but lower concentrations of Zr, La, Ce, Ba and Rb (Stephenson et al., 1999).

To date the compositional differences between the suites are not fully understood; they may reflect heterogeneities in the composition and age of the underlying lower crustal basement and/or mantle, or differences in the relative mantle and crustal contributions. Halliday et al. (1984) proposed the existence of the Mid Grampian Line (MGL) separating the Argyll suite plutons in the northwest from the Cairngorm and South Grampians suite plutons in the southeast, which may represent an important boundary in the deep basement and possibly in the mantle.

3. Methodology

3.1. Whole-rock analysis

Major and trace elements were determined at the University of Edinburgh using a PW2404 wavelength-dispersive sequential X-ray spectrometer. Rare earth elements (REEs) and some trace elements (Y, Hf, Th, U) were analysed at the British Geological Survey (BGS) in Nottingham. The samples were fused with Na_2O_2 and then leached with deionised water and HCl before analysis by ThermoElemental PQ Excel quadrupole ICP-MS. Matrix-matched standards were used throughout (data are presented in Appendix 2a).

3.2. Zircon sample preparation

Zircon separation was carried out at the University of St. Andrews Mineral Separation Facility. Rock samples of approximately 5 kg were crushed and sieved to

obtain the < 500 µm fraction from which zircon crystals were separated using a Wilfley Table, heavy liquids and a Frantz magnetic separator. Approximately 100 zircon crystals were hand-picked from the remaining heavy, non-magnetic fraction, providing a range of grain sizes, morphologies, degrees of transparency, alteration and occurrence of inclusions or cracks. The crystals were mounted in epoxy (Araldite/Epothin) along with fragments of the "91500" and "Temora 2" zircon standards. Subsequently, the zircon mounts were polished to about half thickness to expose the crystal interiors. The polished surfaces were imaged in back-scattered electron (BSE) and cathodoluminescence (CL) mode using a Philips XL30CP Scanning Electron Microscope (SEM) at the University of Edinburgh to identify internal zoning features, inherited material, inclusions and cracks. Suitable crystals for in-situ oxygen isotope analysis were selected based on this grain characterisation.

3.3. Zircon oxygen isotope analysis

Zircon oxygen isotope data were obtained using a Cameca ims-1270 ion microprobe at the University of Edinburgh following the methods of Cavosie et al. (2005) and Kemp et al. (2006). A 6nA primary $^{133}Cs^{+}$ ion beam with a diameter of c. 20 µm was used, charge was neutralised using a normal-incidence electron flood gun, secondary ions were extracted at 10 kV, and $^{18}O^{-}$ and $^{16}O^{-}$ ions were monitored simultaneously on dual Faraday cups. Secondary ion beam centring, pre-sputtering for 50 seconds and subsequent data collection over 10 cycles (total counting time: 40 seconds = 4 seconds per cycle) resulted in a total acquisition time of c. 200 seconds. The secondary yield of ^{18}O under these conditions was typically between 4.5 x 10^6 and 5.5 x 10^6 counts per second. To correct for instrumental mass fractionation (IMF) and instrumental drift, all data were normalised to zircon standard 91500 ($\delta^{18}O$ = 9.86 ‰) (Wiedenbeck et al., 2004), which was analysed in blocks of 5 to 10 after every 10 to 15 unknown zircon analyses. During stable instrument conditions the unknown zircon analyses were normalised to the daily average $^{18}O/^{16}O$ value obtained for 91500. In cases where instrumental drift was recognised, the analytical conditions changed or sample exchange was carried out, the data were divided into

sessions in which unknowns were normalised to the linearly interpolated $^{18}O/^{16}O$ value derived from analyses of the bracketing 91500 standard.

Prior to oxygen isotope analysis, HfO_2 concentrations in the zircons were measured by electron microprobe as variations in HfO_2 have been shown to cause variations in IMF (Peck et al., 2001). This has been shown to be particularly important when conducting analysis using e.g. a Cameca ims-4f at high-energy offset. However, in this study oxygen isotope analysis were carried out using a Cameca ims-1270 ion microprobe, and in both diorite samples HfO_2 variations in zircons were ≤ 0.5 wt %; therefore corrections for IMF were unnecessary. The internal precision of individual point analyses based on counting statistics varied between 0.1-0.4 ‰ (1SD). External precision based on the reproducibility of standard 91500 ranged from 0.2-0.7 ‰ and 0.031 to 0.145 (1 s.e.m.).

Analyses were conducted in clear, crack- and inclusion-free areas on representative zircon crystals. Where possible, multiple analyses (core to rim) were carried out on single zircon crystals to collect information about the zircon growth history, and occasionally also in adjacent spots within crystals to assess reproducibility. The ion probe pits were subsequently imaged in BSE and Secondary Electron (SE) mode using an SEM to determine the exact position of the analyses and to ensure that no cracks in the bottom of pits might have influenced the results. Data obtained from suspect locations were rejected. Furthermore, since metamict zircon grains generally have lighter $\delta^{18}O$ values than non-metamict crystals (Booth et al. 2005; Valley et al. 1994), all data obtained from areas of crystals showing ≥ 20 % discordance were also excluded. In addition, data were rejected when the correction on the position of the secondary ion beam was anomalously large (summarised data are presented in Tables 2 and 4 and full data set in Appendices 2b and 2e.

3.4. U-Th-Pb analysis

Subsequent to oxygen isotope analysis, U-Th-Pb analyses were carried out also using the Cameca ims-1270 at the EIMF. Analytical procedures are similar to those described by Schuhmacher et al. (1994) and Whitehouse et al. (1997), and are described in detail in Kelly et al. (accepted). Zircons were analysed using a ~4nA O_2^-

primary ion source with 22.5 keV net impact energy. The beam was focused using Köhler illumination, with primary beam alignment giving ellipsoidal analysis pits (~25 μm max. dimension). Spatial resolution of the analysed area was further limited by the use of the field aperture. U, Th and Pb were analysed at a mass resolution (M/ΔM) of ~4000R using a peak switching routine. An energy window of 60 eV was used throughout, with energy centring on each analysis using the HfO peak. Oxygen flooding on the surface of the sample was employed to enhance Pb ion yields. Prior to analysis the sample surface was pre-rastered over an area of ~40 μm for 120 seconds to remove any surface contamination.

Calibration of Pb/U ratios followed procedures employed by other SHRIMP and/or Cameca ims-1270 laboratories and were based on the observed relationship between Pb/U and ratios of UO/U (e.g. Claoué-Long et al., 1995; Compston et al., 1984; Schuhmacher et al., 1994; Williams, 1998; Williams and Claesson, 1987; Whitehouse et al., 1997). However, the relationship ln(Pb/U) vs. ln(UO_2/UO) was found to give a better within-session reproducibility than the conventional ln(Pb/U) vs. ln(UO/U) or ln(Pb/U) vs. ln(UO_2/U) methods.

U/Pb ratios were calibrated against measurements on standard 91500 (Wiedenbeck et al., 1995: ~1062.5 Ma; assumed $^{206}Pb/^{238}U$ ratio = 0.17917), which is measured after 3-4 unknowns. Temora 2 was analysed as a secondary standard after every 10-15 analyses. Th/U ratios in unknowns were calculated by reference to measurements of Th/U and $^{208}Pb/^{206}Pb$ on the 91500 standard (Th/U = 0.362), assuming closed system behaviour. Elemental concentrations were determined based on the observed oxide ratios of the standard (UO_2/Zr_2O_2 and HfO/Zr_2O_2; assuming U = 81.2 ppm, Hf = 5880 ppm).

Corrections were carried out for dead time, detector background (~0.025 counts/second) and common Pb. Common Pb corrections were made using the measured ^{204}Pb counts above detector background and the modern day composition of common Pb. Typically ^{204}Pb count rates approached those of the background, which led to corrections of < 15 ppb on ^{206}Pb.

Uncertainties on the Pb/U ratios include an error based on observed uncertainty from each measured ratio, which is generally close to that expected from counting statistics. Observed uncertainties on the U/Pb ratio of 91500 are generally an

additional 0.3% in excess of that expected from counting statistics alone. This is assumed to be a random error (see also Ireland and Williams, 2003) and has been propagated (in both standards and unknowns) together with the observed variation in Pb/U ratios measured for each analysis (typically close to the counting errors). For measurement of the 91500 standard, uncertainties are typically between 0.7-1.0 % per analysis. Uncertainties on $^{207}Pb/^{206}Pb$ ratios are based on observed variations from cycle to cycle during each analysis and commonly approach those expected from counting statistics. Uncertainties on ages quoted in the text and in tables for *individual analyses* (ratios and ages) are at the 1σ level. All uncertainties in calculated *group* ages are reported at 2σ level or 95 % confidence.

Plots and age calculations have been made using the computer program ISOPLOT/EX v3 (Ludwig, 2003). Ages of magmatic grains are presented as weighted mean $^{206}Pb/^{238}U$ average ages and include only concordant data points; ages of inherited grains (> 1000 Ma) are $^{207}Pb/^{206}Pb$ ages. Following analysis, the ion probe pits were imaged in BSE and SE mode to check for inclusions and cracks in the bottom of the pit; where either one was accidentally analysed data were rejected. During data processing we noticed that zircons with high U concentrations (>1000 ppm) commonly give older ages or lie off Concordia. Electron back-scatter diffractometry (EBSD) of these zircons showed disturbance and even complete destruction of their crystal structure. To provide a robust data set we excluded all data obtained from zircons showing above 1000 ppm U. In addition, zircons displaying high common Pb concentrations and/or > 10 % discordance were also rejected (summarised data are presented in Tables 2 and 4; full data sets in Appendices 2c and 2f).

3.5. Zircon REE/trace element analysis

Trace element and REE concentrations were analysed on the Cameca ims-4f at the EIMF. Analytical and correction procedures followed those described by Hinton and Upton (1991). Zircons were analysed using a 14.5 keV primary beam of O^- at ~5nA primary current, with secondary ions measured at ~120 V offset. Due to relatively low REE abundances in zircon, 10 cycles were made through the selected

masses. Analyses were standardised against NIST SRM-610 glass standard and concentrations were referenced against Si. Zircon standard 91500 was used as a secondary standard. Elements analysed were Si, P, Ca, Ti, Sr, Y, Nb, Zr, Ba, Hf and the REE. Corrections were made for $ZrSiO^+$ overlap on $^{138}Ba^+$, $^{139}La^+$, $^{140}Ce^+$ and $^{141}Pr^+$ using count rates measured at mass 134. The interference of LREE on HREE and Hf^{2+} on Y were corrected based on analysis of zircon standard 91500 (summarised data are presented in Tables 2 and 4, full data sets in Appendices 2d and 3g).

4. The Lochnagar pluton

The Lochnagar pluton, which is representative of the Cairngorm suite, crops out in the surrounding Dalradian metasediments over an area of c. 150 km^2, and comprises three main granite facies (L1, L2, L3), microgranites and several marginal diorites (Fig. 2) (Smith et al., 2001). *L1*, which represents the oldest part of the pluton, is a predominantly coarse-grained and porphyritic circular pluton with a diameter of c. 15 km. It has been found in sharp contact with a coarse-grained but inequigranular variant, which has been interpreted to indicate a separate intrusive pulse of L1 (Smith et al., 2001).

L2, an oval intrusion (dimensions 12 x 9 km) that intruded L1, comprises mostly medium- to coarse-grained, inequigranular, unfoliated grey and pink leucocratic rocks. However, Oldershaw (1974) also reported several variants of L2, between which no sharp contacts were discovered, that range from inequigranular to porphyritic and may represent separate intrusive pulses. Both L1 and L2 granites were subsequently intruded by several pink quartz-K-feldspar-plagioclase-phyric microgranites, which are compositionally similar to their host granites (Smith et al., 2001).

L3 granites are predominantly pink (also white) equigranular leucocratic biotite granites, which can be found in various locations within L1. As their contacts with L2 are not exposed, their relation is unclear. Compositionally the L3 granites are

more evolved than L1 and L2, hence may not be related to the main granite body (Smith et al., 2001).

The marginal *diorites* (dimensions: 4-5 x 1.8 km (Cul nan Gad diorite) and 0.6 x 0.4 km (Allt Darrarie diorite)) mostly consist of medium-grained, sometimes foliated, inequigranular quartz diorites. They are interpreted to be separate intrusive bodies that are related, but based on cross-cutting relationships older than the granite (Smith et al., 2001) (for a more detailed description of the petrography and field relationships see Table 1).

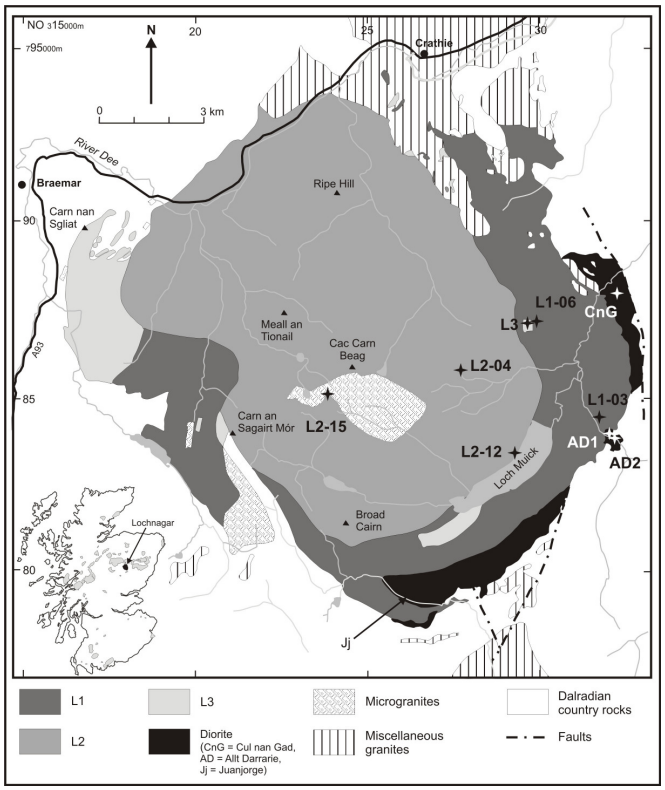

Fig. 2: Geological sketch map of the Lochnagar pluton with sample locations (Smith et al., 2001).

In summary, based on field relationships the order of pluton emplacement is (oldest to youngest) diorites, L1, L2, microgranite, L3 (Halliday, 1984; Halliday et al., 1979; Oldershaw, 1974; Smith et al., 2001). This order is supported by TIMS age data, which indicate that L1 and L2 were emplaced at c. 425 ± 5 Ma (U-Pb zircon) and L3 some time later at c. 417 ± 1 Ma (monazite age) (Smith et al., 2001).

Table 1
Summary of published petrographic and field relationship data of the Lochnagar pluton

	lithology	colour	grain size	texture	major phases	accessory phases	field relationships
Lochnagar							
L1	granite	grey and pink	coarse-grained	mostly Kspar-phyric (up to 15 mm), can be inequigranular	plag (39%), Kspar (28%), qtz (23%), bt (8%), hbl (1%)	titanite, opaques, apatite, zircon	sharp contact between variants; cuts diorites
L2	granite	grey and pink	medium- to coarse-grained	inequigranular, may grade into Kspar-phyric; qtz clusters, isolated bt flakes	plag (41%), qtz (29%), Kspar (26%), bt (4%)	titanite, opaques, apatite, zircon	
L3	granite	pink	medium- to coarse-grained	equigranular	Kspar (40%), plag (33%), qtz (25%), bt (2%)	titanite, opaques, apatite, zircon	5 separate locations, intrudes L1, relation with L2 unknown
Allt Darrarie diorite	qtz diorite	dark grey	medium-grained	inequigranular, in places foliated, plag-phyric, clusters of hbl	plag, hbl, relict pyx, bt, qtz, Kspar		cut by L1, contains country rock xenoliths
Cul nan Gad diorite	qtz diorite, small area of granodiorite	dark grey	medium-grained	inequigranular, in places foliated, plag-phyric, clusters of hbl	plag (38%), hbl+relict pyx (38%), bt (6%), qtz (10%), Kspar (7%)	titanite, opaques, apatite, zircon	cut by L1, contains country rock xenoliths
microgranites	granite	pink	fine-grained	Kspar-plag-phyric	qtz (45%), Kspar (26%), plag (27%), bt (1%)	muscovite, titanite, opaques, apatite, zircon	cut L1, L2, L3

data from Oldershaw (1974) and Smith et al. (2001)

Nd and Sr isotope data for the Lochnagar pluton are scarce. However, Halliday et al. (1984) reported one $\varepsilon Nd_{415\ Ma}$ value of -2.7 and one initial $^{87}Sr/^{86}Sr$ ratio of 0.7063 (n=1), and Halliday et al. (1979) an average initial $^{87}Sr/^{86}Sr$ value of 0.7065 (n=5), which led to the interpretation that the pluton comprises both mantle and crustal sources.

4.1. Samples

Nine samples representing the main granite phases L1 (L1-03, L1-06), L2 (L2-04, L2-12, L2-15), L3, and the Allt Darrarie (AD1, AD2) and Cul nan Gad (CnG) diorites were chosen for analysis. Most samples vary texturally and/or compositionally from the published data to some extent (see Table 1) and also from each other when sampled from the same facies. For example, L1-03 is overall a typical K-feldspar-phyric L1 granite, but lacks hornblende. L1-06 is inequigranular to weakly porphyritic and contains less biotite (< 5 %). According to the literature, L2 comprises c. 40 % plagioclase, but sample L2-04 consists of equal amounts of K-feldspar, plagioclase and quartz (each c. 30 %) and c. 10 % biotite, and L2-12 and L2-15 are dominated by K-feldspar (40-45 %) and quartz (30-35 %) with less plagioclase (15-20 %) and biotite (≤ 5 %). In addition, L2-04 and L2-12 contain euhedral allanite, which has not been reported before. On a microscopic scale L2-15 contains a 5 x 2 mm large, fine-grained (c. 0.5 mm) equigranular cluster of either restitic or entrained material, which comprises equal amounts of quartz, biotite, plagioclase and opaques (ilmenite and magnetite). The selected L3 sample is similar to the published data apart from the absence of accessory titanite. The proportion of mafic to felsic minerals in the three diorite samples (Allt Darrarie diorite = AD1, AD2; Cul nan Gad diorite = CnG) is as published, but the assemblage of the mafic minerals is very different. Diorites described in the literature contain c. 40 % hornblende plus relict pyroxene and 6 % biotite, whereas these samples contain 35-40 % biotite and ≤ 10 % hornblende.

4.2. Zircon morphologies

Zircon crystals are euhedral and show oscillatory and/or sector zoning (Fig. 3a) typical of igneous zircon (Benisek and Finger, 1993; Hanchar and Miller, 1993; Hoskin and Schaltegger, 2003; Vavra, 1990). In each Lochnagar sample a range of sizes, morphologies and internal zoning textures were observed, which is a common phenomenon generally interpreted to be the result of varying local kinetic factors such as diffusion rates and adsorption (Dowty, 1980; Vavra, 1990, 1993). Zircon grain sizes vary between c. 200 μm and ≥ 700 μm along the c-axis with a higher abundance of elongated grains occurring in the diorites. With respect to internal zoning, all zircons consist of a core, which often defines most of the crystal, one or more rims. Cores and rims are separated by resorption surfaces, which are usually interpreted to reflect periods of Zr undersaturation in the magma for which the dominant controls are either large-scale mixing events or local kinetic phenomena (Corfu et al., 2003). Cores are either completely unzoned (c1) (Fig. 3b), comprise a relatively large unzoned inner domain (c1) and a surrounding outer oscillatory zoned domain (c2) (Fig. 3c) or appear to be entirely zoned (c2) (Fig. 3d). In terms of CL intensity, inner core domains are always moderately to weakly luminescent, whereas zones within the oscillatory-zoned domains vary between strongly and weakly luminescent. Rims consist of either a single or multiple zones, which may vary in CL intensity.

One striking difference was observed between samples L1-06, L2-12 and the remaining Lochnagar granite and diorite samples. Despite representing L1 and L2, respectively, samples L1-06 and L2-12 each comprise a very similar-looking homogeneous population of zircons, which display weak luminescence (Fig. 3e). The grains also contain cores and rims. These are commonly separated by a thin and more strongly luminescent resorption surface. Similar looking grains were not observed in any of the other Lochnagar granite or diorite samples.

Inherited zircon cores were found only in L2 samples L2-04 (n=1) and L2-15 (n=6). Some were easily identifiable as pre-magmatic cores with magmatic rims (Fig 3f), whereas others differed only slightly from the magmatic grains (Fig. 3g) and were only detected during U-Pb age dating.

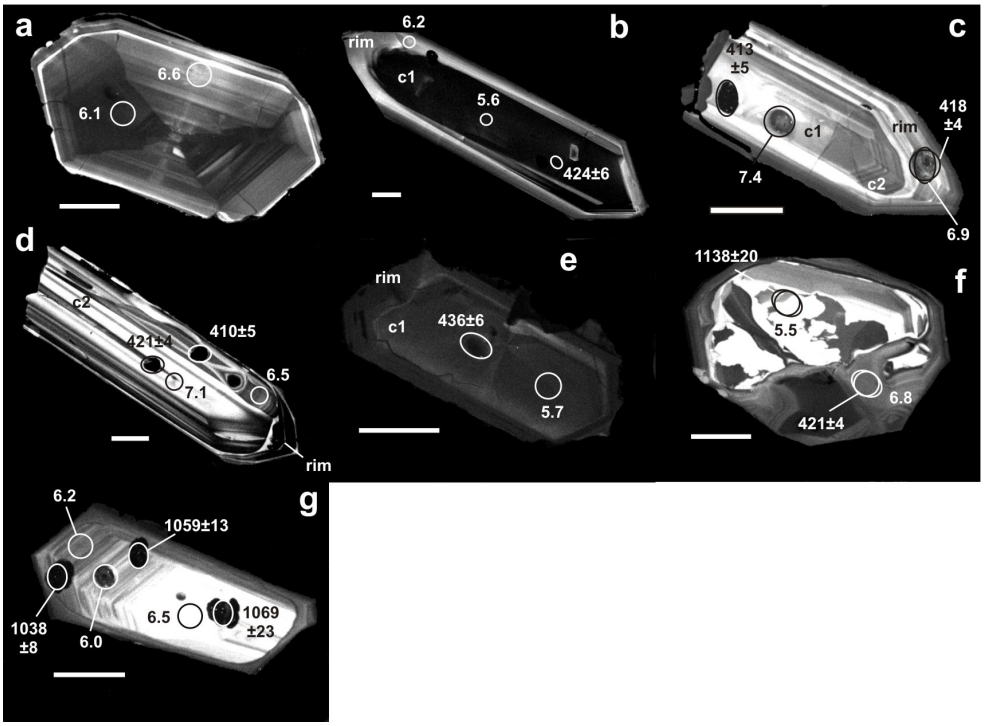

Fig. 3: CL images of representative zircons from the Lochnagar pluton with correlating $\delta^{18}O$ values and U-Pb ages.
a) Sector zoning observed in L1, L2 and L3 zircons (grain 23, L1-03).
b) Elongated zircon crystal with resorbed weakly luminescent core (c1) and moderately luminescent rim (grain 15, CnG diorite).
c) Zircon with moderately luminescent, unzoned inner core domain (c1), outer oscillatory zoned domain (c2) and surrounding rim (grain 11, L2-04).
d) Zoned zircon core (c2) with surrounding rim (grain 13, AD2 diorite).
e) Weakly luminescent zircon typical of L1-06 and L2-12. Weakly luminescent core (c1) shows resorption surface (stronger luminescent) and is mantled by very weakly luminescent rim (grain 36, L2-06).
f) Inherited grain (grain 29) from L2-15. Grain consists of large pre-magmatic core and outer magmatic rim.
g) Inherited grain from L2-04 (grain 15). Grain is indistinguishable from magmatic zircons.
(Scale bar = 50 μm; circles indicate oxygen isotope analyses; ovals U-Pb analyses; quoted U-Pb error = 1σ, $\delta^{18}O$ error = 0.5-0.7 (2σ)).

4.3. U-Pb data

Sample L2-04 represents the oldest phase of the Lochnagar pluton with a weighted average age of 424 ± 5 Ma. All remaining samples, with the exception of diorite AD2, give similar $^{206}Pb/^{238}U$ ages that lie within 2σ error of each other, ranging from 423 ± 2 Ma for L3 to 422 ± 2 Ma for L2-15, 420 ± 2 Ma for L1-03, 420 ± 4 Ma for L1-06, 419 ± 4 Ma for L2-12, 419 ± 2 Ma for diorite AD1 and 418 ± 3

Ma for diorite CnG. However, diorite AD2 is younger at 413 ± 4 Ma. Thus, the pluton intruded over a period of c. 11 m.y. (Fig. 4 & 5).

Inherited older material was found only in L2 (L2-04 and L2-15). L2-04 contains one inherited grain (out of 11 analysed grains), which has a $^{207}Pb/^{206}Pb$ age of 1046 ± 33 Ma. L2-15 comprises six grains (out of 16 analysed grains), which fall into three age groups; analyses are weakly discordant and yield $^{207}Pb/^{206}Pb$ ages of 1149 ± 18 Ma, 1235 ± 45 Ma and 1397 ± 9 Ma.

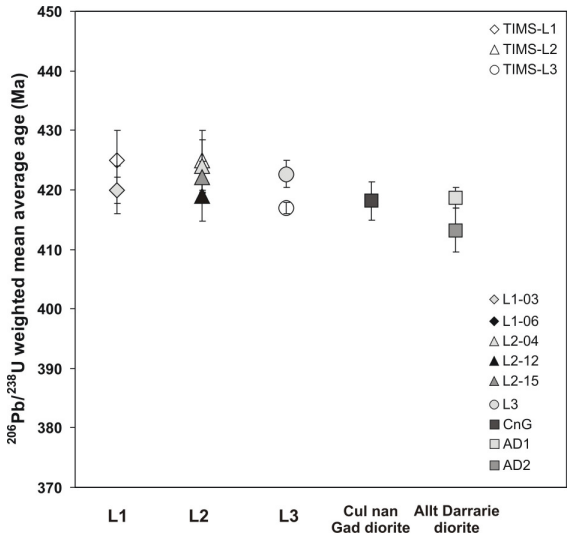

Fig. 4: Weighted mean $^{206}Pb/^{238}U$ ages of the Lochnagar pluton (error bars = 2σ).

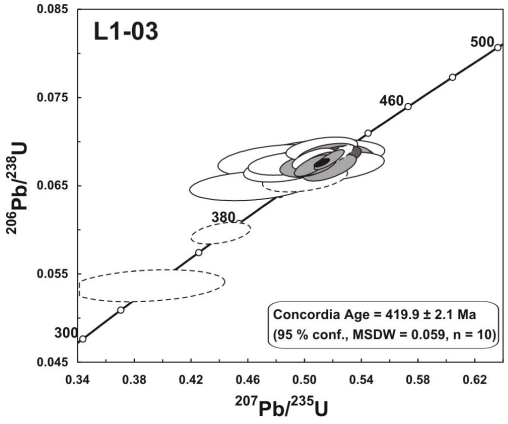
L1-03
500
460
380
300
Concordia Age = 419.9 ± 2.1 Ma
(95 % conf., MSDW = 0.059, n = 10)
$^{206}Pb/^{238}U$
$^{207}Pb/^{235}U$

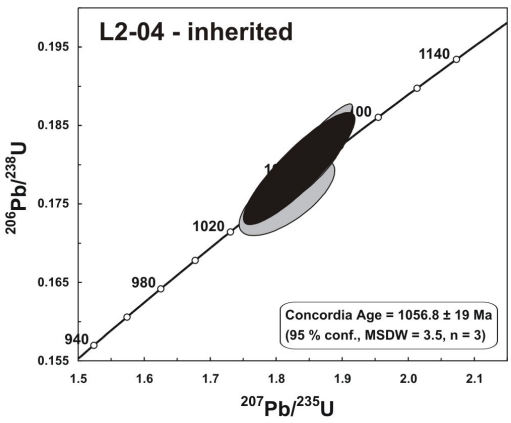
L2-04 - inherited
1140
1020
980
940
Concordia Age = 1056.8 ± 19 Ma
(95 % conf., MSDW = 3.5, n = 3)
$^{206}Pb/^{238}U$
$^{207}Pb/^{235}U$

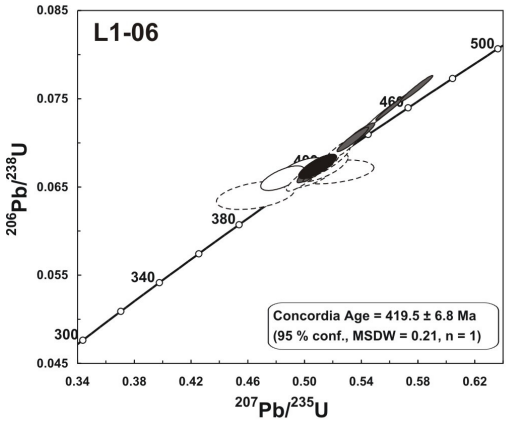
L1-06
500
460
380
340
300
Concordia Age = 419.5 ± 6.8 Ma
(95 % conf., MSDW = 0.21, n = 1)
$^{206}Pb/^{238}U$
$^{207}Pb/^{235}U$

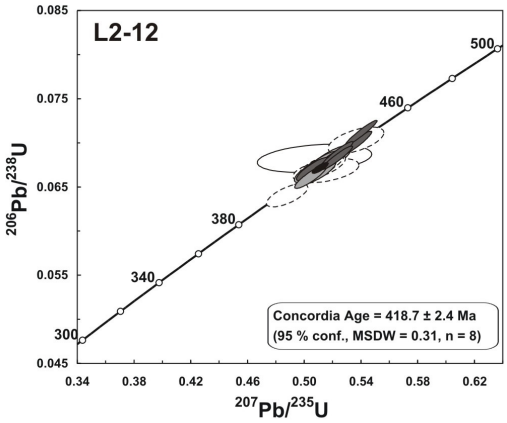
L2-12
500
460
380
340
300
Concordia Age = 418.7 ± 2.4 Ma
(95 % conf., MSDW = 0.31, n = 8)
$^{206}Pb/^{238}U$
$^{207}Pb/^{235}U$

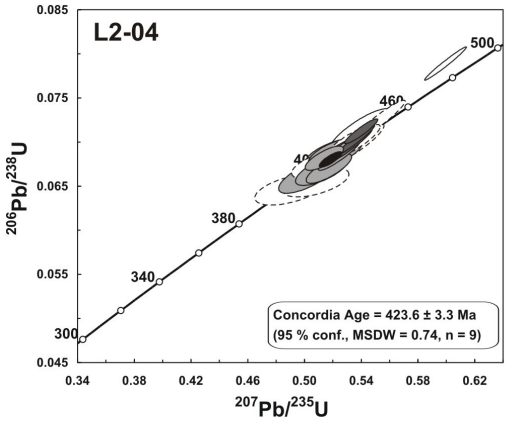
L2-04
500
460
380
340
300
Concordia Age = 423.6 ± 3.3 Ma
(95 % conf., MSDW = 0.74, n = 9)
$^{206}Pb/^{238}U$
$^{207}Pb/^{235}U$

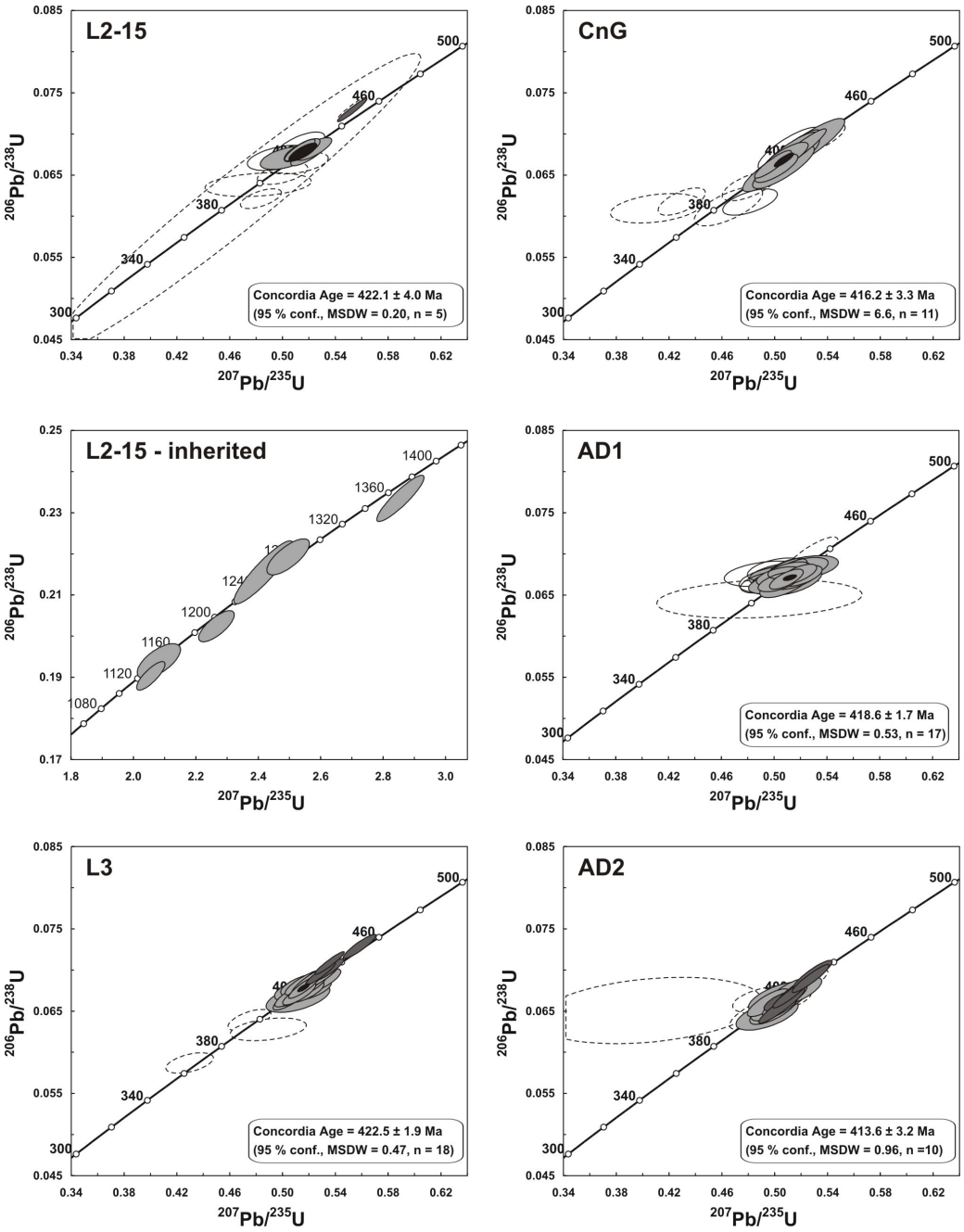

Fig. 5: Concordia diagrams of zircons from the Lochnagar pluton (light grey ellipses = concordant data, dark grey ellipses = data with > 1000 ppm U, white ellipses = > 10 % discordant data, white dashed ellipses = data from cracks, inclusions and with high common Pb; error ellipses = 2σ).

Table 2
Averaged zircon data from the Lochnagar pluton

Sample	L1-03			L1-06			L2-04			L2-12			L2-15			L3		
Age [Ma]	420		n=10	420		n=1	424		n=9	419		n=8	422		n=5	423		n=18
1σ	2			4			5			4			3			2		
Trace elements [ppm]																		
Th	140	(30-742)	n=16	1224	(182-3593)	n=12	333	(68-711)	n=7	883	(363-1598)	n=13	252	(77-512)	n=10	538	(21-1334)	n=16
U	243	(57-997)		2932	(258-8198)		1456	(229-4419)		1475	(661-3801)		698	(166-1561)		885	(49-2295)	
P	319	(85-1016)		869	(175-1239)		552	(230-948)		640	(349-1286)		514	(269-1023)		586	(179-1643)	
Ti	10	(5-16)		6	(2-14)		6	(2-10)		8	(4-20)		52	(2-464)		8	(3-14)	
Y	769	(217-2192)		3436	(676-6100)		1584	(925-2694)		2471	(1261-4248)		1229	(526-1748)		1756	(238-3185)	
HfO_2 [wt%]	1.3	(1.2-1.5)		1.5	(0.9-1.7)		1.7	(1.1-3.5)		1.3	(1.1-1.4)		1.4	(1.1-2.0)		1.3	(1.1-1.4)	
REEs [ppm]																		
La	0.6	(0.0-7.7)		2.6	(0.1-19.3)		0.7	(0.0-3.9)		2.6	(0.1-19.0)		1.1	(0.0-9.6)		1.5	(0.0-13.5)	
Ce	31.0	(10.0-88.6)		196.3	(13.7-730.1)		44.2	(4.9-87.7)		109.0	(47.5-215.7)		46.3	(22.6-79.6)		73.0	(8.6-173.5)	
Pr	0.6	(0.0-6.8)		3.6	(0.1-23.7)		0.4	(0.1-1.7)		2.2	(0.2-11.3)		1.4	(0.1-11.7)		1.1	(0.0-7.3)	
Nd	5.4	(0.5-48.4)		24.6	(2.2-130.9)		3.9	(0.5-9.3)		16.0	(3.1-49.8)		9.8	(1.2-71.8)		9.0	(0.4-34.6)	
Sm	4.5	(1.0-22.0)		20.3	(4.0-58.3)		6.0	(1.8-9.5)		15.8	(6.5-31.6)		7.3	(2.0-29.7)		9.8	(0.9-18.3)	
Eu	1.3	(0.4-4.4)		1.9	(0.9-4.7)		1.2	(0.4-2.4)		3.1	(1.1-8.1)		1.8	(0.4-8.2)		2.2	(0.3-4.5)	
Gd	20	(5-62)		89	(17-169)		35	(21-61)		75	(34-120)		29	(12-45)		48	(5-88)	
Tb	7	(2-21)		32	(5-58)		13	(9-23)		25	(12-42)		10	(4-15)		16	(2-27)	
Dy	81	(20-257)		395	(60-714)		166	(107-294)		287	(142-507)		120	(47-178)		195	(22-320)	
Ho	30	(7-90)		139	(23-252)		62	(37-108)		99	(50-176)		45	(19-65)		71	(9-123)	
Er	146	(37-404)		651	(118-1178)		299	(158-508)		450	(227-797)		217	(89-301)		334	(42-579)	
Tm	32	(10-82)		133	(28-239)		64	(30-105)		91	(49-162)		48	(20-68)		69	(9-123)	
Yb	260	(91-617)		997	(265-1760)		516	(220-811)		684	(368-1202)		402	(162-569)		544	(76-955)	
Lu	61	(24-137)		220	(70-375)		116	(46-180)		154	(84-266)		101	(40-144)		123	(20-215)	
Yb_N/La_N	606	(84-18453)		556	(67-13264)		1089	144-18351)		373	(59-14050)		519	(65-17351)		510	(380-4776)	
Yb_N/Gd_N	18	(10-27)		15	(9-20)		20	(9-41)		12	(8-17)		18	(12-25)		14	(14-17)	
Eu/Eu*	0.48	(0.26-0.66)		0.19	(0.09-0.70)		0.26	(0.13-0.34)		0.27	(0.15-0.61)		0.33	(0.17-0.68)		0.32	(0.30-0.39)	
Ce/Ce*	67.3	(2.9-133.7)		44.4	(8.2-120.5)		71.1	(3.5-131.8)		55.1	(3.5-191.5)		84.3	(1.8-222.2)		53.4	(9.8-78.4)	
Oxygen isotopes																		
$\delta^{18}O$ [‰]	6.4	(5.3-7.1)	n=36	6.3	(5.7-6.8)	n=12	7.3	(6.6-7.9)	n=15	6.4	(5.4-7.3)	n=14	6.6	(5.9-7.8)	n=24	6.7	(5.6-8.1)	n=20
2σ	0.6			0.5			7.3			6.4			0.7			0.5		

Sample	CnG			inherited zircons AD1			AD2			inh L2-04			inh L2-15 (1)			inh L2-15 (2)			inh L2-15 (3)		
Age [Ma]	418		n=11	419		n=17	413		n=10	1046		n=3	1149		n=2	1235		n=3	1397		n=1
1σ	3			2			4			33			18			45			9		
Trace elements [																					
Th	293	(40-928)	n=14	168	(29-1001)	n=18	1309	(49-5255)	n=7	94	(35-173)	n=3	64	(83-86)	n=3	85	(37-89)	n=2	102		n=1
U	345	(80-641)		153	(45-461)		1044	(297-2935)		207	(59-398)		153	(149-225)		187	(92-242)		278		
P	205	(61-533)		291	(172-534)		211	(35-599)		332	(270-365)		245	(244-279)		262	(72-332)		296		
Ti	8	(4-14)		14	(7-26)		5	(2-12)		17	(11-25)		13	(8-9)		8	(12-15)		4		
Y	734	(162-2102)		1160	(420-4174)		1600	(129-5311)		743	(634-862)		1156	(1229-2260)		1745	(767-1626)		1766		
HfO_2 [wt%]	1.1	(0.9-1.7)		1.2	(0.9-1.6)		1.3	(1.0-1.5)		1.5	(1.3-1.7)		1.3	(1.1-1.5)		1	(1.0-1.5)		1.6		
REEs [ppm]																					
La	0.4	(0.0-3.5)		0.1	(0.0-0.7)		0.4	(0.0-2.1)		0.0	(0.05-0.31)		0.0	(0.15-0.23)		0.0	(0.10-0.26)		0.0		
Ce	14.8	(6.1-20.7)		20.3	(7.0-73.0)		53.2	(3.7-177.6)		33.4	(35.6-77.7)		16.9	(25.23-38.67)		19.3	(19.98-41.18)		7.3		
Pr	0.3	(0.0-0.6)		0.3	(0.1-1.1)		0.9	(0.0-2.9)		0.1	(0.8-1.3)		0.2	(1.50-7.18)		0.4	(0.83-4.44)		0.2		
Nd	3.3	(0.3-6.8)		4.4	(1.0-15.9)		10.4	(0.2-40.7)		1.8	(2.5-5.4)		3.8	(4.29-20.87)		5.7	(3.01-18.24)		3.8		
Sm	3.6	(0.6-12.2)		5.7	(1.8-19.4)		10.9	(0.2-47.8)		3.0	(14-27)		6.2	(30-99)		9.5	(19-82)		6.7		
Eu	1.9	(0.2-7.0)		2.3	(0.7-7.4)		4.8	(0.1-21.2)		0.5	(7-11)		1.0	(3-10)		0.4	(4-43)		0.8		
Gd	18	(3-67)		30	(9-110)		48	(1-194)		16	(60-99)		31	(138-325)		45	(74-275)		44		
Tb	6	(1-20)		10	(3-37)		15	(1-59)		6	(125-185)		12	(288-606)		16	(156-518)		16		
Dy	70	(13-227)		121	(39-460)		180	(8-662)		75	(242-365)		134	(541-1040)		192	(316-878)		189		
Ho	26	(5-79)		46	(15-169)		63	(4-218)		28	(409-604)		47	(890-1594)		69	(513-1276)		71		
Er	137	(27-385)		230	(80-833)		307	(27-997)		146	(739-1120)		213	(1486-2493)		316	(874-1912)		337		
Tm	33	(7-86)		51	(19-181)		67	(8-206)		32	(1118-1629)		42	(2037-3101)		62	(1228-2362)		70		
Yb	296	(70-762)		427	(165-1465)		553	(83-1647)		269	(1406-2056)		314	(2381-3333)		464	(1475-2378)		577		
Lu	77	(20-177)		103	(42-339)		129	(27-352)		63	(2271-3126)		66	(3573-5150)		106	(2313-3082)		135		
Yb_N/La_N	1076	(45-18225)		5655	(776-22406)		1918	(436-12758)		8552	(6594-29113)		11234	(14376-15566)		14971	(9239-15206)		25314		
Yb_N/Gd_N	30	(18-40)		20	(11-30)		32	(10-79)		20	(15.1-23.3)		15	(10.3-17.3)		14	(8.7-19.9)		15.8		
Eu/Eu*	0.68	(0.46-0.90)		0.56	(0.47-0.65)		0.58	(0.48-0.69)		0.20	(0.16-0.23)		0.16	(0.0-0.1)		0.05	(0.1-0.3)		0.14		
Ce/Ce*	30.0	(3.4-84.3)		41.8	(8.8-143.5)		40.6	(8.0-109.2)		153.9	(68.3-269.5)		48.2	(30.0-52.6)		41.3	(35.8-70.3)		21.4		
Oxygen isotopes																					
$\delta^{18}O$ [‰]	6.0	(5.5-6.4)	n=36	7.1	(6.1-8.1)	n=41	6.6	(5.9-7.5)	n=32	6.2		n=3	5.9		n=2	5.9		n=5	6.8		n=3
2σ	0.5			0.4			0.5			0.5			0.5			0.5			0.9		

4.4. Zircon REE/trace element data

Lochnagar zircons display REE patterns typical of zircons from granitoid rocks, with strong HREE-enrichment (Yb_N/La_N=45-22406), a positive Ce anomaly (Ce/Ce*) and a negative Eu anomaly (Eu/Eu*) (Fig. 6). Minor variation in the overall REE abundances and in the degree of Eu/Eu* occurs between and within samples and even within single grains; however no systematic change was recognised. On average, zircons from diorite CnG contain the lowest REE abundances (except La and Eu), whereas those of granite L1-06 contain the highest. The diorite zircons have the weakest Eu anomalies (Eu/Eu* = 0.56-0.68 (AD1 and CnG, respectively) and L1-06 zircons the strongest (Eu/Eu* = 0.19). This suggests the melt experienced more calcic-feldspar fractionation prior to zircon crystallisation in the granites than in the diorites.

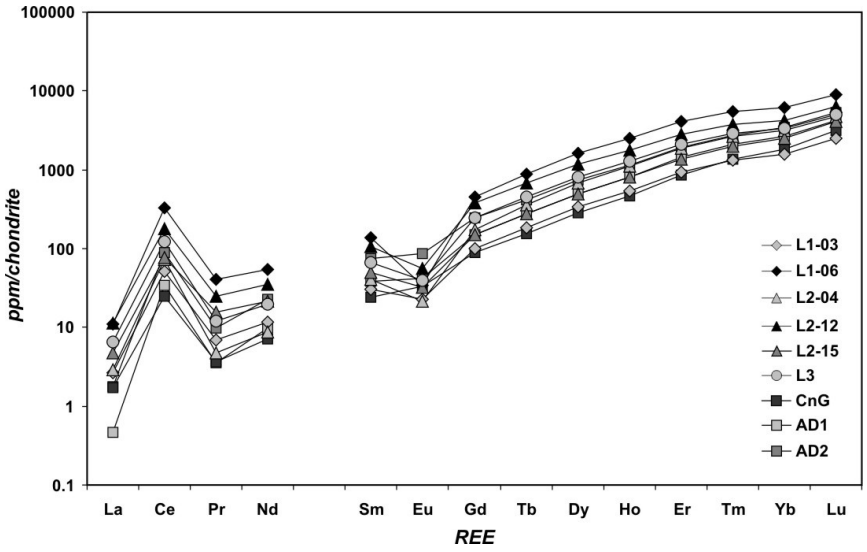

Fig. 6: Average zircon REE patterns of the Lochnagar pluton normalised to chondrite using values of Anders and Grevesse (1989).

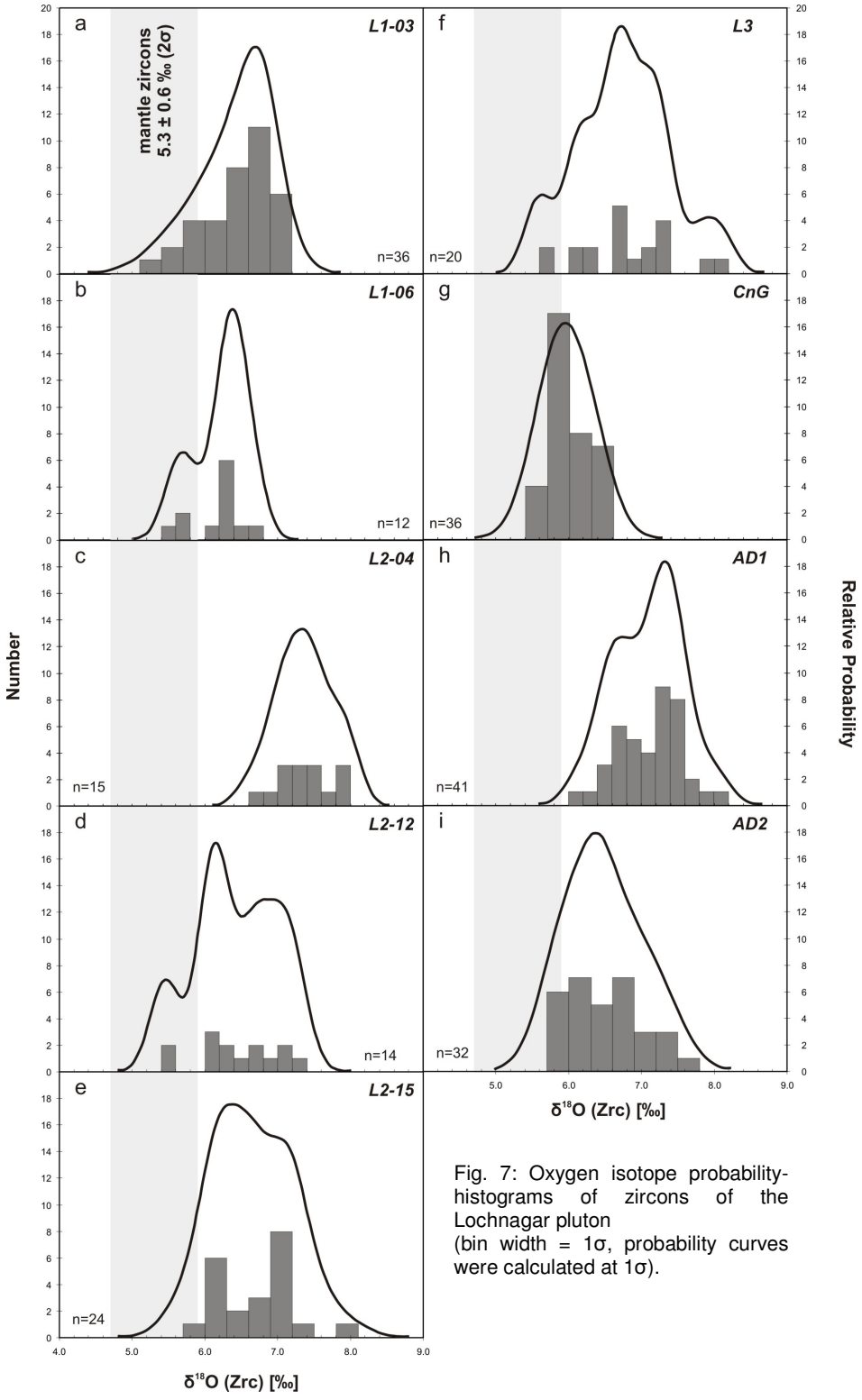

Fig. 7: Oxygen isotope probability-histograms of zircons of the Lochnagar pluton
(bin width = 1σ, probability curves were calculated at 1σ).

4.5. Zircon oxygen isotope data

Lochnagar zircons range in $\delta^{18}O$ from 5.3 to 8.1 ± 0.6 ‰ (n=230, 2σ) (Fig. 7a-i) with a mean of 6.6 ± 0.6 ‰ (2σ). For comparison, mantle zircons have $\delta^{18}O$ values of 5.3 ± 0.6 ‰ (2σ, Valley et al. 1998). On a sample scale each sample displays a different mean $\delta^{18}O$ value; the lowest value occurs in zircons of the CnG diorite (6.0 ± 0.4 ‰ (2σ)) and the highest in those of granite sample L2-04 (7.3 ± 0.5 ‰ (2σ)). However, the main differences between samples, both within a single Lochnagar facies and between different facies, lie in the range and distribution of oxygen isotope values. Zircons in diorite CnG form the tightest data group with a clear unimodal distribution and a spread of 0.9 ‰ (5.5-6.4 ‰), which is similar to the degree of heterogeneity observed in standard 91500 analysed in the same analytical session. All other samples are more heterogeneous and show $\delta^{18}O$ ranges from 1.1 ‰ (L1-06) to 2.5 ‰ (L3). Distribution patterns vary between almost unimodal (diorite AD2, L1-03, L2-04), bimodal (diorite AD1, L1-06, L2-15) and random with no distinct modes (L2-12, L3). Detailed examination of the inter- and intra-grain scale variation of the samples shows that the spread in $\delta^{18}O$ results predominantly from variation between zircon crystals. However, in zircons of diorites AD2 and CnG, and in granite L3 resolvable variation was also found within crystals (between cores and rims, within core domains c1 and c2, and within the same zone). In these samples both an increase and a decrease in $\delta^{18}O$ with zircon growth was observed.

Inherited grains were also analysed for their oxygen isotope composition. The single inherited zircon discovered in L2-04 displays a mean $\delta^{18}O$ value of 6.2 ± 0.5 ‰ (n=3); five inherited grains of sample L2-15 show a much larger range (5.2-7.5 ‰), but the same mean of 6.2 ± 0.5‰ (n=9).

5. The Etive pluton

The Etive pluton, which is representative of the Argyll suite, intruded into Dalradian metasediments and is exposed over an elliptical area of approximately 300 km^2 (Fig. 8). It can be described as a major composite pluton, which comprises four

main intrusive phases ranging in composition from granite to monzodiorite/diorite (Stephenson et al., 1999).

The medium- to coarse-grained *Quarry Intrusion* represents the outermost intrusion of the pluton and is exposed as a small lens of diorite/quartz-diorite. It commonly contains metasedimentary country rock xenoliths and microdioritic or appinitic enclaves (Clayburn et al., 1983; Stephenson et al., 1999).

The largest part of the pluton comprises the compositionally heterogeneous *Cruachan Intrusion*, which ranges from granite through tonalite/granodiorite to monzodiorite and contains abundant microgranitoid enclaves (Jacques and Reavy, 1994). Two main rock types have been distinguished – pale grey, medium-grained, equigranular monzogranites with occasional mafic clots and metasedimentary xenoliths, which predominantly occur in the northern lobe of the intrusion, and grey, medium- to fine-grained monzodiorites, which are abundant in the southern lobe (Batchelor, 1987).

The *Meall Odhar Intrusion* has been described as a pink K-feldspar and quartz granite sheet and dyke intrusion, which cross-cuts all the earlier phases. However, field work carried out for this study has identified numerous locations where the Cruachan Intrusion intrudes the Meall Odhar Intrusion. Similar to the other facies, it is compositionally variable and comprises fine- to medium-grained syenogranites and monzogranites (Stephenson et al., 1999).

The centre of the Etive pluton is composed of the elliptical *Starav Intrusion*. It comprises at least two separate magma pulses, which are represented by two concentric intrusions – the porphyritic, medium- to coarse-grained Outer Starav Facies and the medium-grained non-porphyritic Inner Starav Facies (Batchelor, 1987; Clayburn et al., 1983; Jacques and Reavy, 1994).

To summarise, based on field relationships the pluton becomes younger towards the centre with the order of emplacement being Quarry Intrusion, approximately contemporaneously Cruachan and Meall Odhar intrusions, and Starav Intrusion (Bailey, 1960) (for a more detailed description of the facies' petrography and field relationships see Table 3).

Early radiometric data for the pluton obtained by Rb-Sr, Ar-Ar, K-Ar and U-Pb zircon TIMS dating methods yielded ages ranging from 410 Ma to 373 Ma (Brown,

1975; Brown et al., 1968; Clayburn, 1981; Clayburn et al. 1983; Halliday et al., 1979; Harmon and Halliday, 1980; Pankhurst, 1982; Pidgeon and Aftalion, 1978). Based on these dates and their interpretation, Clayburn et al. (1983) concluded that the Etive Complex was emplaced approximately contemporaneously at 400 Ma. However, more recently Morris et al. (2005) obtained Ar-Ar biotite ages of 415 ± 1.8 Ma and 414 ± 2 Ma for the Etive dyke swarm, which they interpreted to mark the end of magmatism.

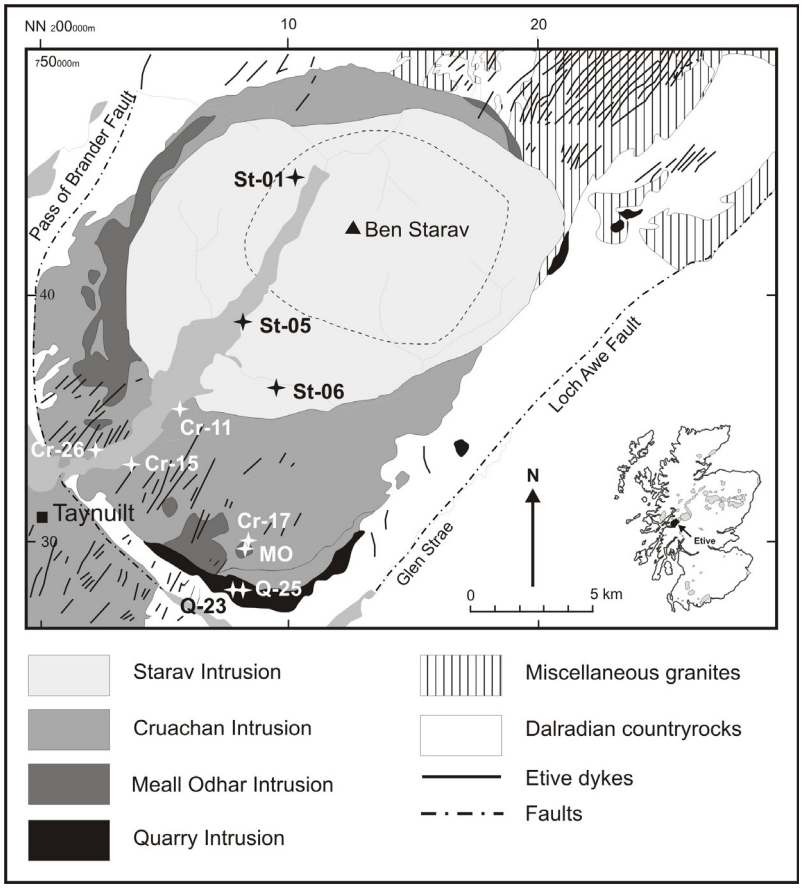

Fig. 8: Geological sketch map of the Etive pluton with sample locations (after Anderson, 1937; Batchelor, 1987).

The Etive pluton has been studied more extensively than the Lochnagar pluton in terms of its Nd and Sr isotope composition, and data exist for all intrusive phases. All have negative $\varepsilon Nd_{400\ Ma}$ values ranging from -4.7 to -9.3, with the Cruachan Intrusion displaying the least negative εNd and the Starav Intrusion and one sample of the Quarry Intrusion showing the most negative εNd values (Frost and O'Nions, 1985).

Initial $^{87}Sr/^{86}Sr$ values range from 0.7043 to 0.7068. Based on the Nd isotope data, the Etive pluton contains a larger crustal component than the Lochnagar pluton, although Sr isotope data do not support this. The petrogenetic model of Clayburn et al. (1983) interpreted the Etive pluton to be the result of melting of a lower crustal and a mantle component. The different phases are assumed to be derived from the same source, with the later phases such as the Starav Intrusion containing a larger crustal component (Clayburn et al., 1983). However, a later detailed whole-rock geochemical study (Batchelor, 1987) has suggested that the Etive pluton has a much more complicated petrogenetic history; it was not entirely derived from the same source and was emplaced as numerous separate magma pulses. At present, the nature of the crustal component and the individual mantle and crustal proportions that have been involved in the generation of the Etive pluton are still unresolved.

5.1. Samples

Ten samples representative of the four main Etive pluton facies, the Quarry Intrusion (Q-23 & Q-25), Cruachan Intrusion (Cr-11, Cr-15, Cr-17 & Cr-26), Meall Odhar Intrusion (MO) and Starav Intrusion (St-01, St-05 & St-06), were selected for analyses. All samples, except those of the Starav Intrusion, differ to some degree from the published petrographic data (see Table 3). The Quarry Intrusion samples contain higher abundances of plagioclase (55-60 %) and biotite (20 %), but less quartz (5 %) than previously reported, while pyroxene was not observed. Of the Cruachan Intrusion samples (all were collected in the southern lobe) only Cr-26 is consistent with the published data. Cr-11 and Cr-17 contain 10-20 % hornblende, which has not been reported in the literature, and only Cr-17 comprises K-feldspar. The Meall Odhar Granite sample is strongly biotite- and plagioclase-phyric (up to 3 mm) and compositionally resembles the monzogranitic variant described in the literature.

Table 3
Summary of published petrographic and field relationship data of the Etive pluton

	lithology	colour	grain size	texture	major phases	accessory phases	field relationships
Etive							
Quarry Intrusion	qtz diorite		medium- to coarse-grained	plag-phyric (up to 15 mm)	plag (46%), hbl (20%), qtz (12%), bt (12%), pyx (9%)	titanite, apatite, zircon, opaques	transitional contact beween variants, contains country rock xenoliths
	diorite		medium-grained	pyx-phyric (up tp 8 mm), mafic clusters of amph + bt after pyx			
Cruachan Intrusion	monzogranite (northern lobe)	pale grey	medium-grained (2-5 mm)	equigranular with mafic clusters	plag (30-46%), Kspar (23-34%), qtz (16-28%), bt (4.5-6.5%), hbl (3-9.5%)	titanite, apatite, zircon, opaques	intrudes Meall Odhar I., contains country rock xenoliths
	monzodiorite (southern lobe)	grey to dark-grey	medium- to fine-grained (1-5 mm)	equigranular	subhedral plag (54-63%); interstitial Kspar (7-25%), bt (6-21%), qtz (5-12%)	titanite, Fe-Ti oxides, zircon, apatite	
Meall Odhar Intrusion	syenogranite	pink	fine- to medium-grained (< 3 mm)		Kspar (50-67%), qtz (27-37%), plag (4.5-12%), hbl (0.2-2%)	chlorite, zircon, opaques, titanite, apatite	intrudes Cruachan I. as sheets and dykes, but also cut by Cruachan I.; cut by Starav I.
	monzogranite	pink	fine- to medium-grained (< 3 mm)		qtz (30-42%), Kspar (33-41%), plag (20-28%), bt (0.5-1%)	titanite, opaques, apatite, zircon	
Starav Intrusion	monzogranite (Outer Facies)	pink-grey	medium- to coarse-grained (1-10 mm)	Kspar (up to 30 mm) + hbl (0.5-2 mm) phyric; mafic clusters of hbl, bt, opaques	Kspar (27-46%), plag (23-41%), qtz (21-32%), bt (3-6%), hbl (0.2-6%)	titanite, apatite, zircon, opaques	
	monzogranite (Inner Facies)		medium-grained (2-5 mm)	equigranular	Kspar (27-48%), qtz (28-40%), plag (22-36%), bt (1-3%)	titanite, apatite, zircon, opaques, monazite, thorite	

data from Batchelor (1987) and Stephenson et al. (2000)

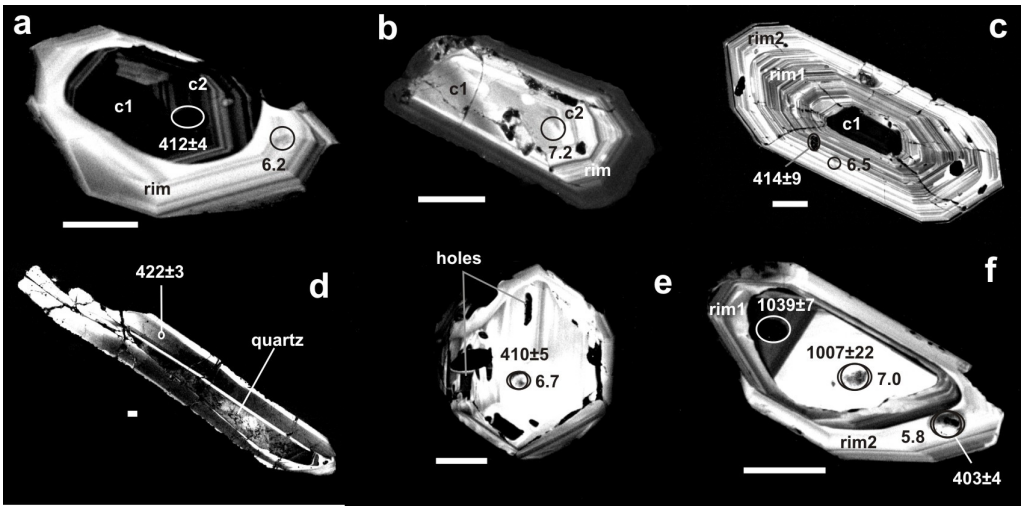

Fig. 9: CL images of representative zircons from the Etive pluton with correlating $\delta^{18}O$ values and U-Pb ages.
a) Zircon comprising weakly luminescent core (unzoned inner domain (c1) + zoned outer domain (c2)) and single strongly luminescent zoned rim. CL intensity varies only little between zones (grain 17, Cr-26)
b) Zircon with strongly luminescent core (c1 + c2) and single zoned rim found in samples of the Starav Intrusion. Rim comprises two main zones, which vary strongly in CL intensity (grain 7, St-01).
c) Crystal showing small weakly luminescent resorbed core and two large zoned rims. Zones within rims are very narrow and vary strongly in CL intensity (grain 19, St-01).
d) Acicular very large zircon crystal with quartz in the centre; crystals were observed in Cr-11 of the Cruachan Intrusion, and Q-23 and Q-25 of the Quarry Intrusion (grain 21, Cr-11).
e) Equant zircon crystal with holes found in Cr-11 of the Cruachan Intrusion, and Q-23 and Q-25 of the Quarry Intrusion (grain 22, Q-23).
f) Xenocrystic core with two magmatic rims (grain 4, Cr-15).
(Scale bar = 50 µm; circles indicate oxygen isotope analyses; ovals U-Pb analyses; quoted U-Pb error = 1σ, $\delta^{18}O$ error = 0.3-0.5 (2σ)).

5.2. Zircon morphologies

Zircon crystals from the Etive pluton share the majority of features described for zircons of the Lochnagar pluton, including a range of sizes (75 µm to > 2 mm, mostly 200-250 µm), morphologies (equant to acicular, mostly stubby) and internal zoning patterns (sector zoning was only observed in zircons from the Meall Odhar Intrusion sample). In the Meall Odhar, Cruachan and Starav intrusions all zircon crystals also comprise obvious cores and rims, which are separated by resorption surfaces. Commonly cores are weakly to moderately luminescent in CL (Fig. 9a), but in the Starav samples approximately half the crystals consist of a strongly luminescent core (Fig. 9b). Cores are either unzoned (c1) or zoned (c2) and commonly represent the largest part in a crystal. In the latter case crystals usually comprise an inner unzoned (c1) domain and an outer zoned (c2) domain (Fig. 9a &

b). Zircon rims commonly consist of zones, which may vary in width and CL intensity between crystals (Fig. 9a & c).

Zircons from Cruachan Intrusion sample Cr-11 and those of the Quarry Intrusion have very different morphology and internal zoning to those of the other Etive samples. All three samples comprise two zircon populations, with the more prominent one consisting of elongated to acicular grains that may be larger than 2 mm (Fig. 9d). The second population displays smaller (up to 250 µm) equant to stubby crystals (Fig. 9e). In both populations grain centres commonly contain quartz or holes, which are surrounded by moderately to strongly luminescent broad zones. It is not clear whether the central quartz represents restitic material on which the zircons nucleated, which may explain the large grain size, or if the zircons contained holes and were subsequently infilled by quartz.

Inherited grains occurring in Cruachan Intrusion samples Cr-15 and Cr-17 were only detected by U-Pb age dating, as the zoning patterns are not strikingly different (Fig. 9f).

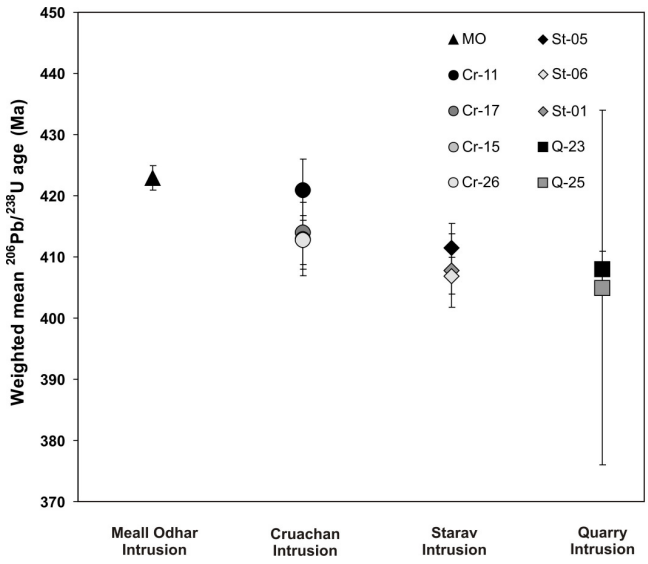

Fig. 10: Weighted mean $^{206}Pb/^{238}U$ ages of the Etive pluton (error bars = 2σ).

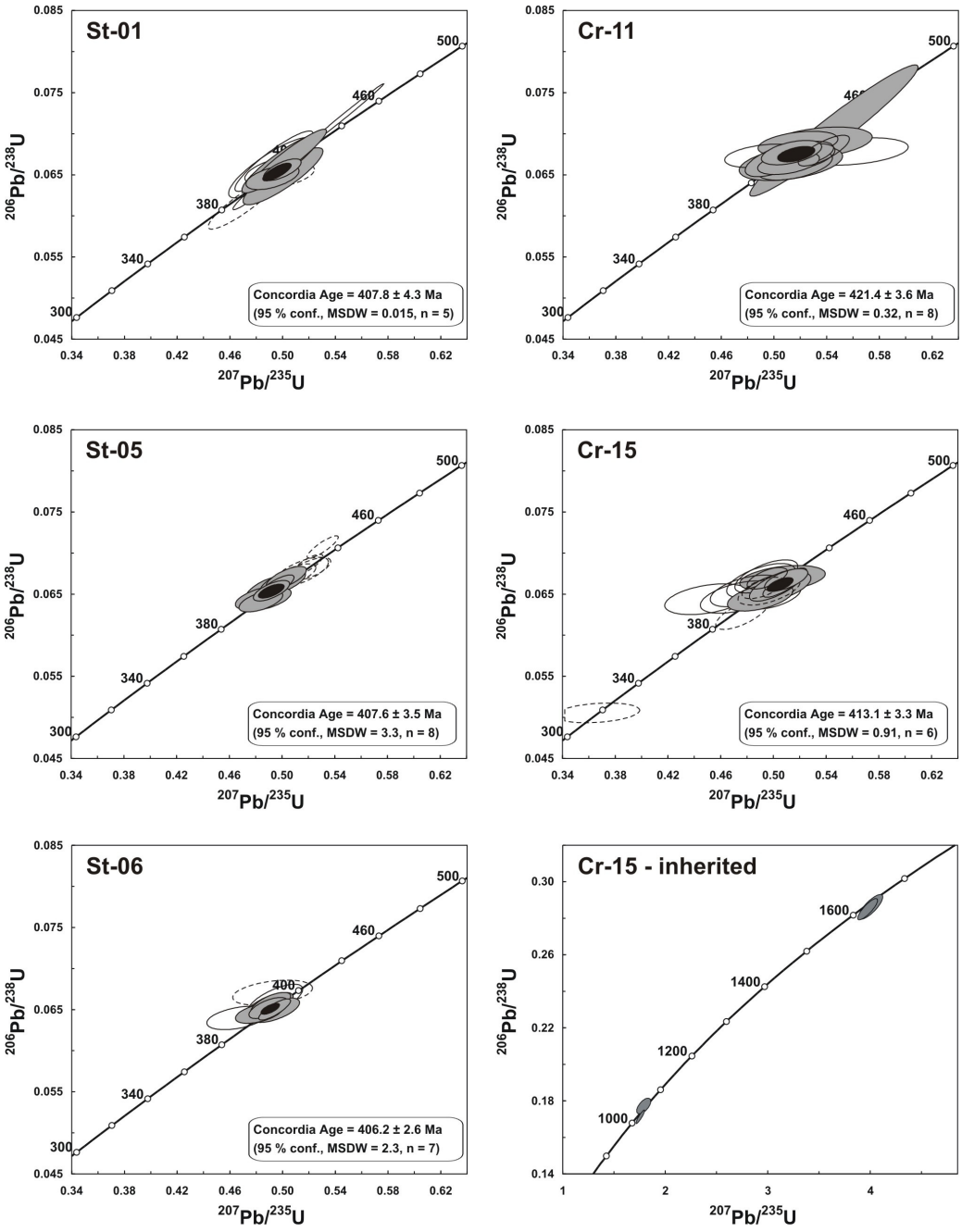
St-01
Concordia Age = 407.8 ± 4.3 Ma
(95 % conf., MSDW = 0.015, n = 5)
Cr-11
Concordia Age = 421.4 ± 3.6 Ma
(95 % conf., MSDW = 0.32, n = 8)
St-05
Concordia Age = 407.6 ± 3.5 Ma
(95 % conf., MSDW = 3.3, n = 8)
Cr-15
Concordia Age = 413.1 ± 3.3 Ma
(95 % conf., MSDW = 0.91, n = 6)
St-06
Concordia Age = 406.2 ± 2.6 Ma
(95 % conf., MSDW = 2.3, n = 7)
Cr-15 - inherited
206Pb/238U
207Pb/235U

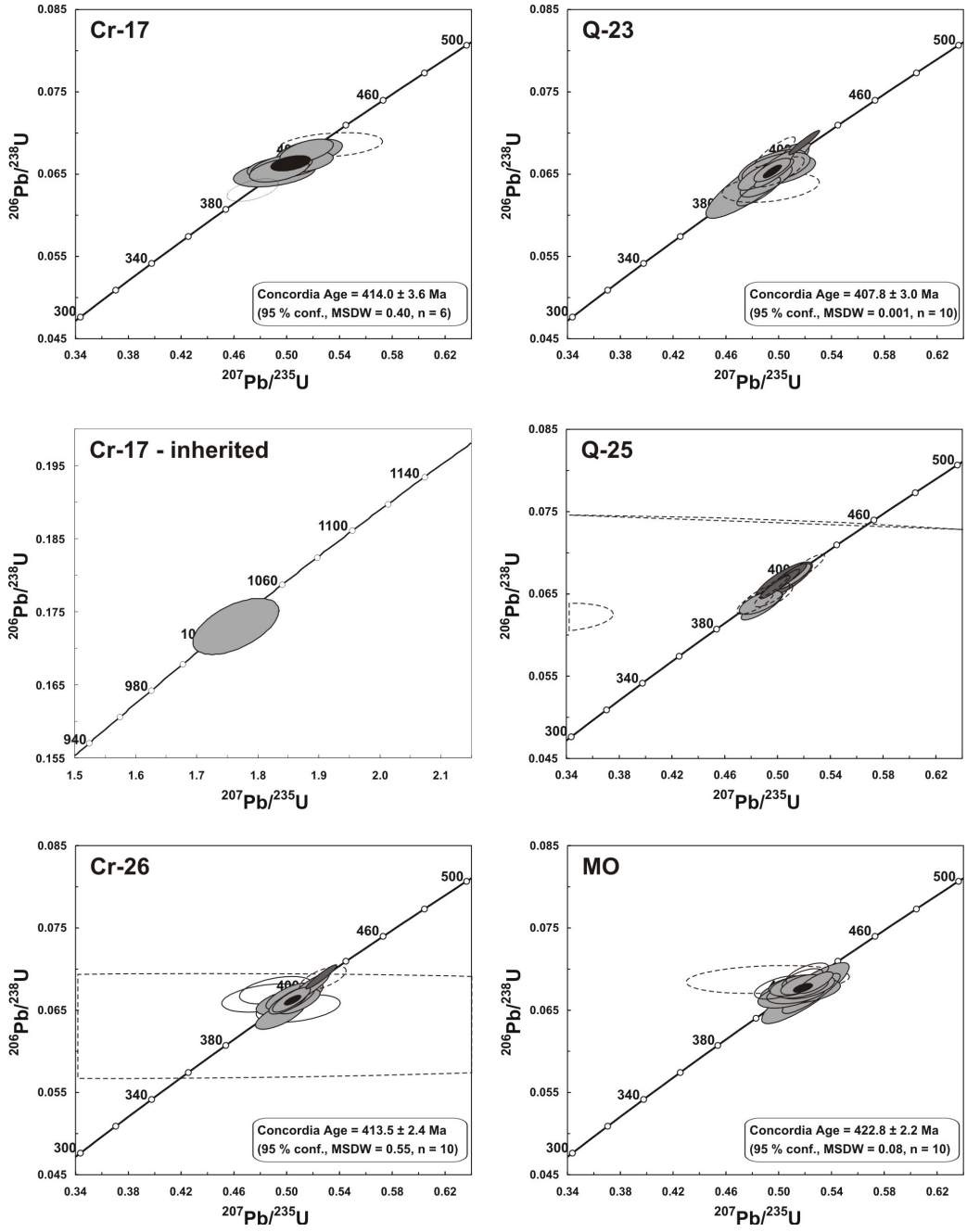

Fig. 11: Concordia diagrams of zircons from the Etive pluton (light grey ellipses = concordant data, dark grey ellipses = data with > 1000 ppm U, white ellipses = > 10 % discordant data, white dashed ellipses = data from cracks, inclusions and with high common Pb; error ellipses = 2σ).

5.3. U-Pb data

The oldest samples from the Etive pluton are the Meall Odhar Intrusion, with an age of 423 ± 2 Ma, and Cr-11 of the Cruachan Intrusion at 421 ± 5 Ma. The remaining Cruachan samples yield younger ages of 414 ± 6 Ma (Cr-17), 413 ± 6 Ma (Cr-15) and 413 ± 4 Ma (Cr-26). St-05 of the Starav Intrusion intruded at 412 ± 6 Ma (contemporaneously with the Cruachan samples), and the remaining Starav intrusion samples St-01 and St-06 somewhat later at 408 ± 4 Ma and 407 ± 3 Ma, while the Quarry Intrusion is dated at 408 ± 3 Ma (Q-23) and 405 ± 29 (Q-25). Thus, the Etive pluton was emplaced over a period of approximately 16 m.y. (Fig. 10 & 11).

Inherited zircon crystals were observed only in Cr-15 and Cr-17 of the Cruachan Intrusion. Cr-15 contains two inherited grains (out of 14 analysed grains) with $^{207}Pb/^{206}Pb$ ages of 1036 ± 110 Ma and 1646 ± 10 Ma. In Cr-17 only one older grain (out of 12 analysed grains) was found, which gives a $^{207}Pb/^{206}Pb$ age of 1040 ± 25 Ma.

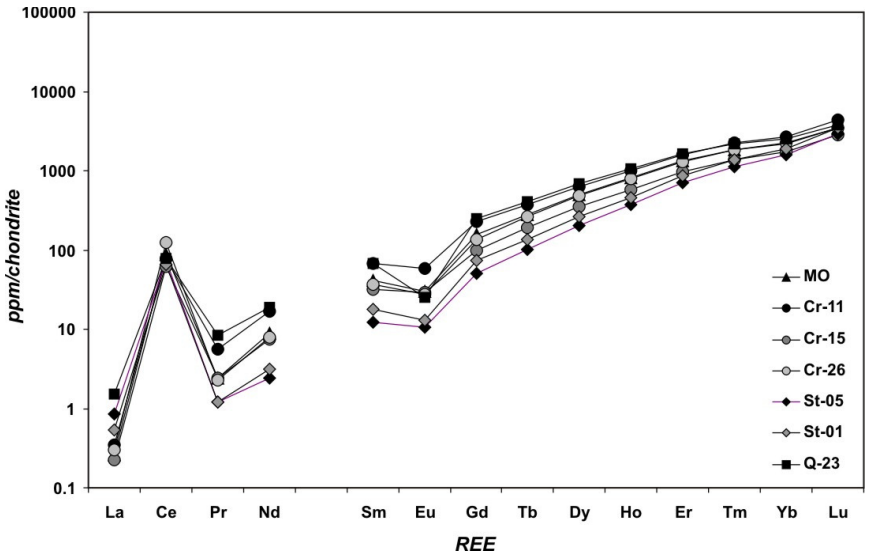

Fig. 12: Average zircon REE patterns of the Etive pluton normalised to chondrite using values of Anders and Grevesse (1989).

Table 4

Averaged zircon data from the Etive pluton

Sample	**MO**			**Cr-11**			**Cr-17**			**Cr-15**			**Cr-26**		
Age [Ma]	423 ± 2		n=10	421 ± 5		n=8	414 ± 6		n=7	413 ± 6		n=6	413 ± 4		n=10
Trace elements [ppm]															
Th	136	(53-325)	n=11	235	(120-564)	n=11	89	(49-219)	n=7	100	(44-286)	n=9	453	(30-2680)	n=8
U	174	(82-315)		234	(184-412)		110	(74-206)		134	(60-473)		490	(48-2933)	
P	364	(285-534)		280	(170-480)					271	(161-392)		329	(131-812)	
Ti	21	(10-107)		9	(5-12)					12	(4.8-26.5)		11	(7-16)	
Y	1152	(742-1871)		1404	(783-2839)					820	(400-1234)		1117	(266-3909)	
HfO_2 [wt%]	1.0	(1.0-1.1)		1.0	(0.9-1.2)					1.0	(0.9-1.4)		1.1	(0.9-1.4)	
REEs [ppm]															
La	0	(0.0-0.1)		0	(0.0-0.2)					0	(0.0-0.1)		0	(0.0-0.2)	
Ce	53	(23.5-101.1)		48	(35.2-85.0)					38	(19.2-80.2)		75	(25.2-282)	
Pr	0	(0.1-0.3)		0	(0.1-1.2)					0	(0.1-0.5)		0	(0.0-0.5)	
Nd	4	(1.7-6.4)		8	(2.2-17.1)					3	(1.2-8.2)		4	(0.5-8.1)	
Sm	6	(3.7-9.2)		10	(3.4-23.7)					5	(1.8-8.5)		5	(1.1-13)	
Eu	2	(1.1-2.5)		3	(1.0-8.1)					2	(0.8-3.3)		2	(0.4-3.2)	
Gd	31	(19-43)		45	(17-110)					19	(10-38)		27	(6-79)	
Tb	10	(6-15)		14	(6-32)					7	(3-12)		10	(2-32)	
Dy	121	(78-186)		153	(71-337)					86	(42-140)		117	(25-412)	
Ho	45	(28-73)		55	(29-115)					32	(16-48)		44	(11-155)	
Er	212	(134-351)		256	(150-504)					154	(76-237)		207	(50-740)	
Tm	45	(29-74)		54	(34-103)					34	(16-55)		44	(12-156)	
Yb	356	(226-594)		440	(297-812)					280	(141-495)		365	(100-1262)	
Lu	83	(54-138)		106	(77-186)					69	(35-121)		85	(25-277)	
Yb_N/La_N	8318	(4025-11637)		7835	(5289-11210)					7706	(3737-13806)		7516	(2403-16849)	
Yb_N/Gd_N	14	(11-17)		14	(9-22)					19	(11-43)		17	(10-22)	
Eu/Eu*	0.37	(0.32-0.42)		0.47	(0.41-0.50)					0.52	(0.42-0.66)		0.45	(0.15-0.54)	
Ce/Ce*	118	(51.6-184.2)		74	(34.7-135.6)					110	(20.9-249.3)		167	(31.0-345.6)	
Oxygen isotopes															
$\delta^{18}O$ [‰]	6.5 ± 0.5	(5.5-8.2)	n=30	6.9 ± 0.4	(5.7-7.9)	n=26	4.7 ± 0.4	(4.6-7.5)	n=32	6.2 ± 0.4	(5.3-6.9)	n=16	6.4 ± 0.3	(5.3-7.6)	n=26

Table 4
Averaged zircon data from the Etive pluton

Sample	MO			Cr-11			Cr-17			Cr-15			Cr-26			St-05			St-06		
Age [Ma]	423		n=10	421		n=8	414		n=7	413		n=6	413		n=10	412		n=11	407		n=7
1σ	2			5			6			6			4			6			3		
Trace elements	**[ppm]**																				
Th	136	(53-325)	n=11	235	(120-564)	n=11	89	(49-219)	n=7	100	(44-286)	n=9	453	(30-2680)	n=8	181	(59-369)	n=9	115	(75-150)	n=8
U	174	(82-315)		234	(184-412)		110	(74-206)		134	(60-473)		490	(48-2933)		357	(192-587)		188	(150-242)	
P	364	(285-534)		280	(170-480)					271	(161-392)		329	(131-812)		174	(41-338)				
Ti	21	(10-107)		9	(5-12)					12	(4.8-26.5)		11	(7-16)		3	(1-5)				
Y	1152	(742-1871)		1404	(783-2839)					820	(400-1234)		1117	(266-3909)		620	(208-1283)				
HfO_2 [wt%]	1.0	(1.0-1.1)		1.0	(0.9-1.2)					1.0	(0.9-1.4)		1.1	(0.9-1.4)		1.3	(1.0-1.5)				
REEs [ppm]																					
La	0	(0.0-0.1)		0	(0.0-0.2)					0	(0.0-0.1)		0	(0.0-0.2)		0	(0.0-1.0)				
Ce	53	(23.5-101.1)		48	(35.2-85.0)					38	(19.2-80.2)		75	(25.2-282)		45	(14.9-85.9)				
Pr	0	(0.1-0.3)		0	(0.1-1.2)					0	(0.1-0.5)		0	(0.0-0.5)		0	(0.0-0.3)				
Nd	4	(1.7-6.4)		8	(2.2-17.1)					3	(1.2-8.2)		4	(0.5-8.1)		1	(0.1-2.5)				
Sm	6	(3.7-9.2)		10	(3.4-23.7)					5	(1.8-8.5)		5	(1.1-13)		2	(0.4-4.3)				
Eu	2	(1.1-2.5)		3	(1.0-8.1)					2	(0.8-3.3)		2	(0.4-3.2)		1	(0.2-1.5)				
Gd	31	(19-43)		45	(17-110)					19	(10-38)		27	(6-79)		10	(2-24)				
Tb	10	(6-15)		14	(6-32)					7	(3-12)		10	(2-32)		4	(1-9)				
Dy	121	(78-186)		153	(71-337)					86	(42-140)		117	(25-412)		49	(12-117)				
Ho	45	(28-73)		55	(29-115)					32	(16-48)		44	(11-155)		21	(6-47)				
Er	212	(134-351)		256	(150-504)					154	(76-237)		207	(50-740)		112	(37-235)				
Tm	45	(29-74)		54	(34-103)					34	(16-55)		44	(12-156)		28	(10-53)				
Yb	356	(226-594)		440	(297-812)					280	(141-495)		365	(100-1262)		259	(114-449)				
Lu	83	(54-138)		106	(77-186)					69	(35-121)		85	(25-277)		71	(36-119)				
Yb_N/La_N	8318	(4025-11637)		7835	(5289-11210)					7706	(3737-13806)		7516	(2403-16849)		1854	(355-15320)				
Yb_N/Gd_N	14	(11-17)		14	(9-22)					19	(11-43)		17	(10-22)		37	(23-63)				
Eu/Eu*	0.37	(0.32-0.42)		0.47	(0.41-0.50)					0.52	(0.42-0.66)		0.45	(0.15-0.54)		0.45	(0.37-0.59)				
Ce/Ce*	118	(51.6-184.2)		74	(34.7-135.6)					110	(20.9-249.3)		167	(31.0-345.6)		149	(22.5-248.4)				
Oxygen isotopes																					
$\delta^{18}O$ [‰]	6.5	(5.5-8.2)	n=30	6.9	(5.7-7.9)	n=26	4.7	(4.6-7.5)	n=32	6.2	(5.3-6.9)	n=16	6.4	(5.3-7.6)	n=26	6.9	(6.4-7.7)	n=23	6.4		n=14
2σ	0.5			0.4			0.4			0.4			0.3			0.4			0.5		

Sample	St-01			Q-23			Q-25			inh Cr-15		inh Cr-15		inh Cr-17	
Age [Ma]	408		n=5	408		n=10	405		n=3	1036	n=2	1646	n=2	1040	
1σ	4			3			29			110		10		25	
Trace elements															
Th	175	(69-528)	n=9	378	(46-1261)	n=12	568	(221-1103)	n=3	14	n=1	71	n=1		n=1
U	403	(165-1372)		403	(91-889)		396	(216-639)		30		86			
P	249	(90-507)		403	(268-769)					470		307			
Ti	3	(2-6)		17	(11-28)					35.29		21.89			
Y	766	(401-1199)		1490	(514-4027)					827		658			
HfO_2 [wt%]	1.2	(1.0-1.4)		1.2	(1.1-1.3)					1.2		1.2			
REEs [ppm]															
La	0	(0.0-0.7)		0	(0.0-1.5)					0.0		0.0			
Ce	40	(24.1-55.5)		47	(21.7-91.0)					21.6		35.7			
Pr	0	(0-0.3)		1	(0.1-2.3)					0.2		0.1			
Nd	1	(0.6-2.5)		9	(2.5-20.3)					2.9		1.7			
Sm	3	(1.6-4.7)		10	(2.7-23.7)					5.3		3.0			
Eu	1	(0.3-1.3)		1	(0.5-3.3)					1.3		0.6			
Gd	14	(7-24)		48	(15-134)					24		15			
Tb	5	(3-8)		15	(5-42)					8		6			
Dy	64	(32-94)		167	(53-466)					94		67			
Ho	26	(13-36)		59	(19-160)					33		25			
Er	138	(73-212)		263	(86-692)					145		123			
Tm	33	(18-56)		53	(19-136)					30		28			
Yb	310	(171-548)		412	(152-1012)					238		238			
Lu	85	(47-156)		92	(36-217)					53		57			
Yb_N/La_N	3544	(568-13800)		1654	461-14721)					8713		7937			
Yb_N/Gd_N	28	(16-50)		12	(9-22)					12		19			
Eu/Eu*	0.36	(0.23-0.41)		0.22	(0.17-0.28)					0.34		0.26			
Ce/Ce*	155	(14.8-257.8)		61	(8.0-190.5)					64.9		135.0			
Oxygen isotopes															
$\delta^{18}O$ [‰]	6.9	(6.3-7.4)	n=17	6.3	(5.5-7.2)	n=16	6	(4.9-6.9)	n=9	7.0	n=1	5.9	n=1	6.2	n=1
2σ	0.5			0.3			0.3			0.4		0.4		0.4	

5.4. Zircon REE/trace element data

REE and trace element analyses were carried out on seven of the ten Etive samples (MO, Cr-11, Cr-15, Cr-26, St-05, St-01, Q-23). Etive zircons show the same features (HREE enrichment, positive Ce/Ce* and negative Eu/Eu*) as the Lochnagar zircons, but the variation between and within samples is even less pronounced (Fig. 12). The highest concentrations of REEs occur in zircons of the Cruachan and Quarry intrusions, and the lowest in zircons of the Starav Intrusion. Eu/Eu* range from 0.22 in Quarry Intrusion sample Q-23 to 0.52 in Cr-15 of the Cruachan Intrusion.

5.5. Zircon oxygen isotope data

Zircons of the Etive pluton have a mean $\delta^{18}O$ value of 6.5 ± 0.4 ‰ (2σ, n=209), which is essentially the same as that of the Lochnagar zircons. Again, each sample displays a different mean composition, range in $\delta^{18}O$ and data distribution (Fig. 13a-j). Sample Q-25 of the Quarry Intrusion has the lowest mean $\delta^{18}O$ (6.0 ± 0.3 ‰ (2σ)); Cr-11 of the Cruachan Intrusion, and St-05 and St-01 of the Starav Intrusion have the highest mean $\delta^{18}O$ values (6.9 ± 0.4-0.5 ‰ (2σ)). Thus, no systematic differences in mean oxygen isotope composition can be observed between facies.

Some systematic differences occur in the range of values and distribution patterns. All samples of the Starav Intrusion (St-01, St-05, St-06) show the least variation with data ranges of 1.1 ‰ (St-01: 6.3-7.4 ‰) to 1.4 ‰ (St-06: 5.6-7.0 ‰) and unimodal to weakly bimodal (St-01) distributions. The largest heterogeneities can be observed in the Meall Odhar Intrusion sample (2.7 ‰), and in samples of the Cruachan Intrusion (except Cr-15). Cr-17 displays a 3 ‰ range between 4.6-7.6 ‰, which falls into three modes. Similarly, sample Cr-11 has two dominant and one less pronounced mode. All other Etive samples display unimodal to bimodal distributions.

As in zircons of the Lochnagar pluton, the large variation in oxygen isotope composition within samples largely results from differences in $\delta^{18}O$ between zircon

crystals. However, resolvable intra-grain variations (both increase and decrease with zircon growth) may be observed in the Meall Odhar Intrusion, Cr-11, Cr-17 and Cr-26 of the Cruachan Intrusion and Q-23 of the Quarry Intrusion.

The inherited components found in the Cruachan Intrusion give oxygen isotope values of 6.2 ± 0.4‰ (n=1) for Cr-17 and 5.9 ± 0.4 (n=1) and 7.0 ± 0.4 (n=1) for Cr-15.

6. Discussion

6.1. Age data and emplacement histories of the Lochnagar and Etive plutons

TIMS age dating of the main Lochnagar pluton facies L1, L2 and L3 suggested that L1 and L2 were emplaced approximately contemporaneously at 425 ± 4 Ma (zircon age) and L3 somewhat later at 417 ± 1 Ma (monazite age) (Smith et al., 2001). Based on cross-cutting field relationships the diorites were interpreted to be older than the Lochnagar granite facies (Smith et al., 2001). Our new U-Pb SIMS zircon data are in good agreement with the published ages of L1 and L2 (SIMS data: 424 ± 5 Ma to 419 ± 4 Ma). However, the SIMS age for L3 of 423 ± 2 Ma is at least 3 m.y. older than that reported by Smith et al. (2001). As L3 intrudes L1 in at least five different locations, it may be that not all of these locations actually belong to L3 and therefore differ in age. Two of the diorite samples, AD1 and CnG, intruded broadly contemporaneously with the main granite body at 419 ± 2 Ma and 418 ± 3 Ma, while the second sample of the Allt Darrarie diorite (AD2) was emplaced somewhat later at 413 ± 4 Ma. Hence, the Allt Darrarie diorite was assembled in at least two separate magma batches – the first batch prior to or contemporaneously with L1, L2 and L3 and the second batch later than the main granite body. Based on these ages the emplacement history of the pluton is more complicated than previously assumed and magmatic activity lasted for approximately 11 m.y..

Based on field relationships the Etive pluton intruded from the rim to the centre in the following sequence: Quarry Intrusion, Cruachan Intrusion, Meall Odhar Intrusion, Starav Intrusion (Bailey, 1960). Published Rb-Sr, Ar-Ar and K-Ar ages

range from 410 Ma to 373 Ma (Brown, 1975; Brown et al., 1968; Clayburn, 1981; Clayburn et al., 1983; Halliday et al., 1979; Harmon and Halliday, 1980; Pankhurst, 1982), while U-Pb zircon TIMS dating by Pidgeon and Aftalion (1978) gave ages of 405 Ma and 390 ± 6 Ma. Based on these ages Clayburn et al. (1983) concluded that the Etive Complex was emplaced approximately contemporaneously at 400 Ma. However, more recently Morris et al. (2005) obtained Ar-Ar biotite ages of 415 ± 1.8 Ma and 414 ± 2 Ma for the Etive dyke swarm, which they interpreted to mark the end of magmatism in the Etive pluton, indicating that the pluton is at least 15 m.y. older than previously assumed.

The SIMS U-Pb zircon ages from this study do not agree with the published data. Our data show that the Etive pluton intruded over a period of approximately 16 m.y. between 423 ± 2 Ma and 407 ± 3 Ma (or 405 ± 29 Ma). Hence the earliest phases of the pluton are much older and the end of magmatic activity in the area was at least 10 m.y. later than proposed by Morris et al. (2005). The emplacement sequence also differs from the published data insofar as the Meall Odhar Intrusion (423 ± 2 Ma) and Cr-11 (421 ± 5 Ma) of the Cruachan Intrusion represent the oldest phases in this study. This is followed by the remaining samples of the Cruachan Intrusion, which were emplaced between 414 ± 6 Ma and 413 ± 6 Ma. This is consistent with our observed field relationships between the Cruachan and Meall Odhar intrusions.

Contemporaneously and subsequently the Starav Intrusion (412 ± 6 Ma to 403 ± 2 Ma) and the marginal Quarry intrusion (408 ± 3 Ma) were emplaced. Thus, the main part of the pluton was emplaced from the rim inwards, but in the final stage intrusion also occurred along its fringes.

This detailed U-Pb zircon SIMS study of the Lochnagar and Etive plutons demonstrates that both plutons have much longer and more complicated emplacement histories than previously assumed. Some facies (e.g. Lochnagar: Allt Darrarie diorite, Etive: Cruachan Intrusion) appear to comprise two or more magma batches, which may have assembled incrementally to form the plutons.

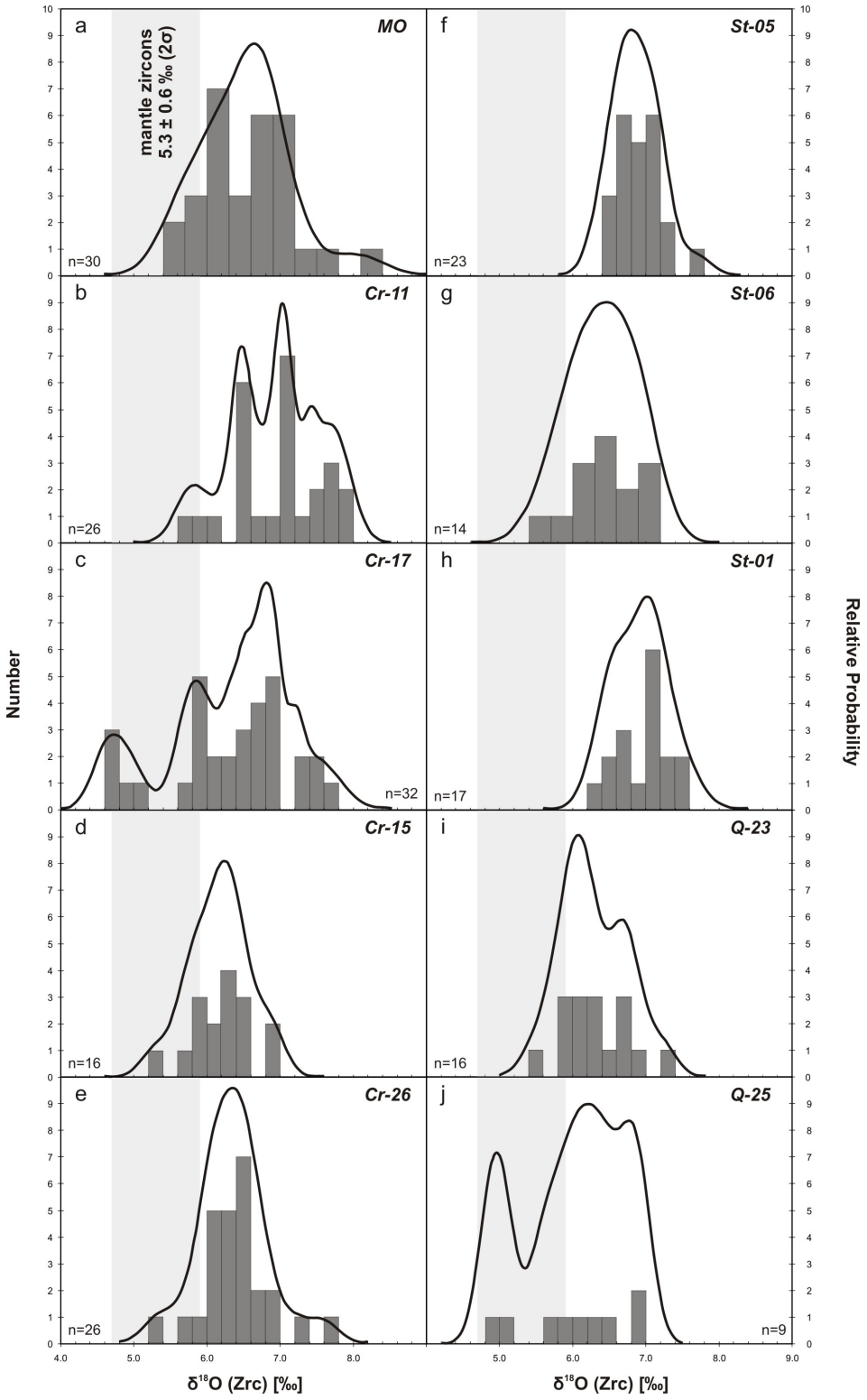

Fig. 13: Oxygen isotope probability-histograms of zircons of the Etive pluton (bin width = 1σ, probability curves were calculated at 1σ).

6.2. Crustal recycling vs. crustal growth

Oxygen isotope compositions of whole-rocks and zircons are commonly used to distinguish between mantle and crustal origins. As oxygen isotopes fractionate more strongly with decreasing temperature and $\delta^{18}O$ increases with increasing SiO_2 content, the crust is more enriched in ^{18}O than the mantle. Studies of zircons from mantle-derived xenoliths in kimberlites have demonstrated that mantle reservoirs display a narrow range of oxygen isotope compositions of 5.3 ± 0.6 ‰ (Valley et al., 1998). The oxygen isotope compositions of zircons in granitic rocks are a key indicator of their sources (pristine mantle, lower and/or middle crustal (infracrustal), and supracrustal sources). Recently, this approach has gained importance in crustal growth studies, which have attempted to quantify the extent to which I-type granites represent the growth of new crust versus the recycling of pre-existing lower crust. A study by Kemp et al. (2007) has demonstrated that up to 85 % new crust was generated during formation of the Lachlan Fold Belt I-type granites.

Zircon crystals yield oxygen isotope compositions of 5.3-8.1 ± 0.6 ‰ (mean=6.6 ‰) in the Lochnagar pluton and 4.6-8.2 ± 0.4 ‰ (mean=6.5 ‰) in the Etive pluton. The vast majority of zircon $\delta^{18}O$ values in both plutons (c. 82 %) lie outside the $\delta^{18}O$ range for mantle zircons (5.9 ‰). In the Lochnagar pluton zircons with mantle-like $\delta^{18}O$ signatures predominantly occur in the Cul nan Gad diorite, where they comprise c. 58 % of the data set. All other samples contain only rare zircon crystals with mantle-like signatures, representing low- $\delta^{18}O$ outliers within their populations. Overall, none of the samples contain entire zircon populations with $\delta^{18}O$ values expected from mantle zircons.

In the Etive pluton samples of the Cruachan Intrusion contain the highest proportion of mantle-like zircons; sample Cr-17 contains a small but distinct sub-population of five mantle-like zircons (out of 32). However, as in the Lochnagar pluton, all other samples comprise only few or no mantle-like zircons, and these represent the low-$\delta^{18}O$ tails of higher-$\delta^{18}O$ populations.

The oxygen isotope compositions of zircons are essentially unaffected by fractional crystallisation and hydrothermal alteration; a change in $\delta^{18}O$ can only be achieved by open-system processes such as magma mixing or assimilation (Valley,

2003). Thus, our data suggest that both plutons contain only a very small distinct and pristine mantle-derived component. The vast majority of zircons grew from melts that had either experienced magma mixing or assimilation of higher-$\delta^{18}O$ components prior to zircon crystallisation, or were derived by melting of infracrustal source rocks enriched in ^{18}O relative to mantle values. The occurrence of minor amounts of inherited zircon and magmatic zircons with $\delta^{18}O$ values of up to 8.2 ± 0.5 ‰ in the Lochnagar and Etive plutons indicates that assimilation of a supracrustal component such as the surrounding Dalradian country-rocks is possible.

Due to lack of outcrop the mantle and crustal components present underneath the Grampian Highlands are not well constrained. In order to explain the zircon $\delta^{18}O$ values observed in the Lochnagar and Etive plutons we carried out simple two-component magma mixing modelling involving the two most obvious end-members, i.e. a mantle component ($\delta^{18}O$ = 5.5 ‰) and the Dalradian Supergroup country rocks (average $\delta^{18}O$ = 14.2 ‰). According to this model the Lochnagar and Etive plutons comprise 70-100 % mantle and 0-30 % of a Dalradian-like supracrustal component. This would suggest that the Lochnagar and Etive plutons, like the Lachlan Fold Belt I-type granites (Kemp et al., 2007), were predominantly derived from the mantle, hence played an important role in Phanerozoic crustal growth. However, several facts suggest that a more complex petrogenetic evolution model for the Lochnagar and Etive plutons a scenario involving other infra- and/or supracrustal sources appears more realistic. (1) Field observations show that country rock xenoliths are rare and generally undigested in the plutons indicating late-stage assimilation during emplacement. (2) Whole-rock geochemical and isotopic data of the Lochnagar and Etive plutons are complex and differ from each other suggesting involvement of different sources. (3) Zircon $\delta^{18}O$ values vary between plutons, samples of a single pluton, crystals of a single sample and even within individual zircon crystals providing strong evidence for a complex petrogenetic evolution. As based on oxygen isotope data alone, it is impossible to identify and decipher between these unknown crustal sources the role and importance of the late Caledonian I-type granites in crustal growth cannot be unambiguously assessed.

6.3. Evidence for magma mixing

A striking feature of the oxygen isotope data for zircons of the Lochnagar and Etive plutons is the heterogeneity between samples of the same facies, within single samples (e.g. Lochnagar: AD1, Etive: Cr-17) and within individual crystals. As the degree of heterogeneity within these samples is much larger than in zircon standard 91500 analysed in the same analytical session, these variations cannot be the result of differences in instrument performance. Furthermore, as all dubious data were rejected from the data sets, we interpret these variations to reflect real compositional changes in the magmas from which the zircons crystallised.

Detailed examination of each zircon crystal has shown that variations in $\delta^{18}O$ do not correlate with zircon morphologies or CL zoning. Heterogeneities predominantly occur between crystals. However, some samples, mostly from the Cruachan Intrusion, contain individual zircon crystals that show large resolvable variations in $\delta^{18}O$. These variations are not systematic and are not spatially related to resorption surfaces; they occur between cores and rims, between different core domains and commonly even within a single zone. A further observation is that $\delta^{18}O$ values increase as well as decrease with zircon growth in zircons from an individual sample. The same pattern has been described for zircons of the Lochnagar Allt Darrarie diorite (AD1), where it has been proposed that the diorite is the product of mixing of several melt batches of differing oxygen isotope composition, which mixed before and during zircon growth (Paper 1). Our detailed study of the Lochnagar and Etive plutons indicates that this pattern of $\delta^{18}O$ variation in zircons is not peculiar to the Allt Darrarie diorite. Similar magma mixing processes to those deduced for the Allt Darrarie diorite are characteristic of the majority of samples of both plutons.

6.4. Petrogenetic model

The application of new and more precise analytical techniques such as those employed in this study now permit fundamental questions about granite genesis, ascent and emplacement remain to be addressed more rigorously. Plutons were believed to represent large bodies of siliceous magma generated either by fractional

crystallisation of mantle-derived basalt or basaltic andesite in shallow crustal magma chambers (e.g. Grove et al., 1997; Pichavant et al., 1992; Sisson and Grove, 1993) or close to the Moho (e.g. Annen and Sparks, 2002; Mortazavi and Sparks, 2003; Müntener et al., 2001; Prouteau and Scaillet, 2003), or by dehydration melting in the lower or middle crust induced by intrusion of hot, hydrous, mafic, mantle-derived magma (e.g. Jackson et al., 2003; Petford and Atherton, 1996; Smith and Leeman, 1987). After formation they were thought to ascend rapidly by diapirism or stoping to shallower emplacement levels (e.g. Buddington, 1959; Paterson et al., 1996; Petford et al., 2000; Pitcher and Berger, 1972). However, these models are problematic for the following reasons: (1) seismic techniques have only rarely been able to locate large molten magma bodies (e.g. Detrick et al., 1990); (2) thermal modelling has demonstrated that it is difficult to maintain even small permanent magma chambers (e.g. Lister, 1983), and (3) it has been shown that diapiric ascent of magma is too slow and energetically inefficient to be geologically important (e.g. Clemens and Mawer, 1992; Petford et al., 2000).

Recent thermal models suggest that 'deep crustal hot zones' may play an important role in the generation of intermediate and silicic igneous rocks (Annen et al., 2006; Annen and Sparks, 2002). The development of deep crustal hot zones results from repeated intrusion of mantle-derived hydrous basalt sills into the lower and/or middle crust, where melts are generated either by differentiation of the basalt sills to produce residual and more siliceous H_2O-rich melts or by partial melting of pre-existing crustal rocks including early basalt sills or older mafic lower crust. Mixing of residual melts (or mafic mantle melts) and crustal partial melts creates a large range of intermediate and silicic melts. Depending on their H_2O content and ascent path, these melts will ascend more or less rapidly into a shallow reservoir in the upper crust where they undergo crystallisation by degassing and cooling. Thus, chemical diversity is primarily acquired at depth and textural diversity at shallow levels (Annen et al., 2006).

The 'deep crustal hot zone' model is in good agreement with field and geochronological evidence, which suggests that some (and perhaps most) plutons were emplaced incrementally as a series of sheet-like or dyke-like intrusions over time spans an order of magnitude longer than the thermal lifetime of large magmatic

masses and never existed as a large molten magma body (Brown and McClelland, 2000; Coleman et al., 1995; Wiebe, 1993; Wiebe and Collins, 1998). For example, TIMS dating of the Tuolomne Intrusive Suite in California provided evidence for incremental assembly over a period of at least 10 m.y. (Coleman et al., 2004). Contacts between different granite facies may be sharp, gradational or cryptic depending on the time between injection events and the degree of homogenisation by post-emplacement annealing (Glazner et al., 2004). Hence, the chemical heterogeneity previously interpreted to result from fractional crystallisation (e.g. Bateman and Chappell, 1979; Sisson and Moore, 1994; Tindle and Pearce, 1981) and/or magma mixing (Frost and Mahood, 1987; Kistler et al., 1986) in large magma chambers, actually reflects processes operating at much deeper levels (Glazner et al., 2004), for example in deep crustal hot zones.

The Lochnagar and Etive plutons both comprise a range of magma compositions varying between gabbro-diorite and alkali-granite, consistent with formation in a deep crustal hot zone. The majority of zircons of the Lochnagar and Etive plutons show values more enriched in ^{18}O than expected for mantle-like zircons (5.3 ± 0.6 ‰ (Valley et al., 1998)), and hence crystallised either from melts that were produced by magma mixing between mantle melts and infra- and/or supracrustal melts, or solely from lower crustal or mid-crustal partial melts. Simple closed-system fractional crystallisation from a basaltic end member can be precluded as neither the Lochnagar nor the Etive pluton comprises populations of zircons with pristine mantle $\delta^{18}O$ signatures. Assimilation and fractional crystallisation may explain the zircon oxygen isotope composition of the homogeneous samples (e,g, CnG diorite, Starav Intrusion). However, the majority of samples display resolvable oxygen isotope variations between and even within individual crystals, which indicates a more complex mixing or assimilation scenario involving several sources. Where resolvable differences in zircon $\delta^{18}O$ between cores and rims were detected, increases as well as decreases in $\delta^{18}O$ with zircon growth were observed, demonstrating that mixing between magma batches also occurred during growth, probably during ascent and at emplacement level. SIMS dating has revealed a range of U-Pb ages for zircons from the Lochnagar and Etive plutons. The $^{18}O/^{16}O$ and U-Pb data together support a model of incremental granite and diorite assembly over extended periods of time (c.

11 m.y. at Lochnagar and c. 16 m.y. at Etive). In both plutons, few sharp contacts have been identified in the field; while this may be in part due to poor outcrop quality, it is probably also due to textural homogenisation of magma batches after emplacement.

Inherited zircons in the Lochnagar and Etive plutons give U-Pb ages similar to detrital zircons found in the Dalradian country rocks, possibly suggesting assimilation. However, since the identity of the basement beneath the Grampian Highlands remains speculative, more precise interpretation of the origins of the inherited zircon cores is not yet possible.

6.5. Comparison of the Lochnagar and Etive plutons

Whole-rock geochemical data from the Cairngorm and Argyll suites (Fowler et al., 2001; Halliday, 1984; Halliday et al., 1985; Stephens and Halliday, 1984; Tarney and Jones, 1994; Thirlwall, 1988) display several compositional differences such as enrichment in the majority of trace elements and REEs in the Cairngorm Suite plutons relative to the Argyll Suite plutons (Fowler et al., 2001; Halliday, 1984; Halliday et al., 1985; Stephens and Halliday, 1984; Tarney and Jones, 1994; Thirlwall, 1988). This has been interpreted to reflect either compositional variations between their crustal and mantle sources, and/or differences in the relative crust and mantle contributions (Halliday, 1984).

Similarly, zircons show on average higher REE and trace element abundances in the Lochnagar than in the Etive pluton. This may be evidence that the sources that contributed to the Lochnagar pluton were more enriched than those of the Etive pluton. However, as REE abundances in zircon vary at an inter- and intra-grain scale (between c. 250 ppm to 5000 ppm) (e.g. Black et al., 1986; Chen and Williams, 1990), the processes that control the incorporation of trace elements and REEs into zircon are not well constrained and little information is known about how much the zircon chemistry is affected by crystallisation conditions and the overall growth environment (e.g. Guo et al., 1996; Hinton and Upton, 1991), the usefulness of REE and trace element concentrations in zircon as petrogenetic indicators is limited (Hoskin and Schaltegger, 2003).

The other difference between the plutons is the range of ages of inherited zircons. The L2 facies of the Lochnagar pluton contains inherited zircons ranging from 1.4 Ga to 1.05 Ga, whereas in the Cruachan Intrusion (Etive pluton) ages range from 1.65 Ga to 1.05 Ga. This may suggest that the basement beneath the Etive pluton contains older components, but due to the ambiguities that surround the origin of inherited zircons, this cannot be treated as unequivocal.

No other systematic characteristics were observed that help to explain the two plutons' distinct whole-rock compositions. Rather, zircon U-Pb and oxygen isotope data have identified a number of commonalities between them: (1) Both show a range of U-Pb ages and heterogeneous $\delta^{18}O$ distributions within and between samples, providing strong evidence for incremental pluton assembly; (2) The ranges and means of zircon $\delta^{18}O$ distributions and their absolute values are within error the same in both plutons, and indicate a similarly small proportion of zircons with mantle-like values. The plutons probably comprise a similar mix of sources consisting of pristine mantle, lower crust and/or middle crust and possibly of Dalradian country rocks; (3) The degree and scale of heterogeneity in $\delta^{18}O$ is the same within the plutons. Variation occurs between granite facies, within the same facies, between samples, between zircon crystals of a single sample and also within individual crystals. However, both plutons also contain homogeneous samples. These are source heterogeneities that are potentially produced in a 'deep crustal hot zone'.

In summary, the relative source contributions and the processes with respect to melt generation, ascent and emplacement were probably the same for the Lochnagar and Etive plutons, and hence cannot be responsible for the whole-rock geochemical differences between the plutons. We conclude that the latter are therefore probably the result of compositional differences between the plutons' infracrustal and/or mantle sources.

6.6. Implications for future granite studies

This study has provided detailed new insights into the complexity of plutonic systems and processes. Plutons are mapped, subdivided into facies and interpreted based on field evidence, petrographic, whole-rock geochemical and isotopic data.

More recently, zircon data have been obtained by single- and/or multi-grain techniques and now by in-situ techniques; these have provided a basis for major progress towards identifying and quantifying granite sources (e.g. Kemp et al., 2007), and ascent and emplacement mechanisms (Coleman et al., 2004; Glazner et al., 2004). Samples are commonly selected from the main facies on the basis of interpretations of geological mapping and petrographic description. The U-Pb and $^{18}O/^{16}O$ heterogeneities that are evident at various (intra-grain to hand specimen to pluton) scales amongst the zircon populations in this study call into question whether any one sample collected from a granitic pluton can ever be considered to be representative of an entire pluton. Based on in-situ high-precision oxygen isotope and U-Pb analysis we have been able to demonstrate that the degree and scales of heterogeneity that have been identified are much greater than can be resolved by conventional analytical methods. This raises two fundamental questions: (1) What do granite facies within plutons really reflect and how should they be interpreted? Our study suggests that even small intrusions such as the Allt Darrarie diorite of the Lochnagar pluton (dimensions: 0.6 x 0.4 km) comprise several magma batches, which may vary in their geochemical and isotopic characteristics. Evidence for this may be found in the two Allt Darrarie samples AD1 and AD2, which differ in age (AD1: 419 ± 2 Ma, AD2: 413 ± 4 Ma), mean oxygen isotope composition (AD1: 7.1 ± 0.4 ‰, AD2: 6.6 ± 0.5 ‰), range of $\delta^{18}O$ values (AD1: 6.1-8.1 ‰, AD2: 5.9-7.5 ‰) and in $\delta^{18}O$ data distribution (AD1: bimodal, AD2: unimodal). (2) How representative are the results of many traditional granite studies, especially when undertaken on a very small number of samples?

The philosophy underlying these questions was addressed by Krauskopf (1968) in his “tale of ten plutons” from the Sierra Nevada batholith. He suggested that granite magmas form, ascend, differentiate and mix in an apparently random fashion making it impossible to establish a complete “stratigraphy” of intrusive units even if more precise data were available. On the one hand this is correct as the deeper we delve into the detail of granitic rocks the greater is the emerging complexity. On the other hand, the integration of new micro-analytical techniques applied to zircons and recent theoretical models have led to major progress in understanding and interpreting the complexity of granitic rocks. In the process new insights into the

mechanisms and processes of granite intrusion have been revealed, and much tighter and more quantitative constraints on their sources and on the role granites play in the generation and differentiation of the continental crust have been set.

7. Conclusions

1. The Lochnagar pluton intruded Dalradian metasedimentary country rocks between 424 ± 5 Ma and 413 ± 4 Ma (over c. 11 m.y.), and the Etive pluton intruded similar rocks between 423 ± 2 Ma and 407 ± 2 Ma (over c. 16 m.y.). The large ranges of U-Pb ages observed within the plutons suggest both were probably assembled incrementally and never existed as large molten bodies of magma.
2. Zircons of the Lochnagar and Etive plutons have the same mean oxygen isotope composition (Lochnagar: 6.6 ± 0.6 ‰ (2σ), Etive: 6.5 ± 0.4 ‰ (2σ)) and the same proportion of mantle zircons (c. 18 %). This suggests that the relative mantle and crust contribution must have been similar in both plutons. The majority of zircons display oxygen isotope compositions that are more ^{18}O-enriched than pristine mantle values, which indicates that the plutons are either the products mixing between mantle and infra- and/or supracrustal sources or of recycled infra- and/or supracrustal components. Simple two-component mixing between mantle-derived melts and supracrustal material (e.g. Dalradian Supergroup country rocks) appears to be too simplistic and fails to explain the zircon oxygen isotope variations observed in the Lochnagar and Etive plutons. From oxygen isotope data alone it is not possible to identify the unknown crustal sources, hence to quantify the amount of new crust in the plutons.
3. Most of the Lochnagar and Etive pluton samples show a large range in zircon $\delta^{18}O$. Heterogeneity in oxygen isotope composition occurs between and within facies, between samples, between zircon crystals of a single sample and even within individual zircons. In the latter case, an increase as well as decrease in $\delta^{18}O$ with zircon growth can be observed, which may be interpreted as evidence of magma mixing between melts of differing oxygen isotope composition. This

degree of complexity and scale of heterogeneity has not previously been reported.

4. The complexity observed in the Lochnagar and Etive plutons supports melt generation in a 'deep crustal hot zone'. The observed geochemical and isotopic variations were in part produced by mixing of melts before zircon crystallisation, but also by subsequent mixing during zircon growth. Melts ascended as melt batches to shallower levels where they were incrementally assembled to form the plutons.
5. The processes and relative mantle vs. crust contributions appear to be similar in the Lochnagar and Etive plutons, and hence fail to explain their whole-rock geochemical differences. The only differences have been found in zircon trace element and REE data, which demonstrate that the Lochnagar zircons on average contain higher abundances than those of the Etive pluton. However, in general REE and trace elements in zircon have been found of limited use as petrogenetic indicators. In addition, U-Pb dating of inherited zircons has identified slightly older ages in the Etive pluton. However, this cannot be considered unambiguous evidence for older basement beneath the Etive pluton as detrital zircons found in the Dalradian country rocks also display these ages.

IV.

PAPER 3

Using in-situ O and Hf isotope analysis of zircons to constrain the sources of late Caledonian granites in Scotland

Using in-situ O and Hf isotope analysis of zircons to constrain the sources of late Caledonian granites in Scotland

S.K. Appleby [a,*], C.M. Graham [a], M.R. Gillespie [b],
R.W. Hinton [a], G.J.H. Oliver [c], M.S.A. Horstwood [d], EIMF [e]

[a] *Grant Institute of Earth Science, University of Edinburgh, West Mains Road, Edinburgh, EH9 3JW, UK*

[b] *British Geological Survey, Murchison House, West Mains Road, Edinburgh, EH9 3LA, UK*

[c] *School of Geography & Geosciences, Crustal Geodynamics Group, University of St. Andrews, St. Andrews, KY16 9AL, UK*

[d] *NERC Isotope Geosciences Laboratory, Kingsley Dunham Centre, Keyworth, Nottingham, NG12 5GG, UK*

[e] *Edinburgh Ion Microprobe Facility, University of Edinburgh, West Mains Road, Edinburgh, EH9 3JW, UK*

* corresponding author. Email: S.K.Appleby@sms.ed.ac.uk

Manuscript
Intended for submission to Chemical Geology

Abstract

Previous whole-rock geochemical and isotopic studies of the Scottish late Caledonian (~430-400 Ma) I-type granites produced controversial results regarding the contribution of crust and mantle sources to their genesis. In-situ oxygen and Hf isotope data of zircons from the Scottish Lochnagar and Etive plutons show that with $\delta^{18}O$ (zircon) values of 5.3-8.1 ± 0.6 ‰ (2σ) and initial εHf values of +3.4 to -5.8 ± 1.0 (2σ), the Lochnagar pluton probably contains an enriched mantle component. Zircons from the Etive pluton display a similar range of $\delta^{18}O$ values (4.6-8.2 ± 0.4 ‰), but less radiogenic Hf isotope compositions (εHf = -3.0 to -10.6 ± 1.0), which make derivation from the mantle less plausible. Based on these data the Etive pluton, and possibly also the Lochnagar pluton, played an insignificant role in Phanerozoic crustal growth.

Large whole-rock compositional differences between the Lochnagar and Etive plutons have been interpreted to either reflect compositional variations between their sources or in the relative contributions of crust and mantle sources. This may now be resolved. The range of zircon oxygen and Hf isotope compositions identified in each pluton and the differences in εHf between the plutons indicate that the lower crust beneath the Grampian Highlands is very heterogeneous and comprises components of differing age and composition. Calculated Hf model ages show that the Lochnagar pluton has predominantly sourced lower crust of Mesoproterozoic age, and the Etive pluton crust of Palaeo- and Mesoproterozoic age. Thus, the whole-rock compositional differences predominantly reflect variations in the underlying crustal and mantle sources and not in the relative contributions of mantle vs. crust.

1. Introduction

Determining the relative contributions of mantle and crust in the genesis of granites has been the primary aim of many whole-rock geochemical and isotopic studies that have attempted to constrain the role of granite magmatism in the crust's evolution. 'I-type' granites (igneous or infracrustal precursors) (Chappell and White, 1974) have been of particular interest. Controversy persists over whether these are predominantly derived from the mantle, and thus actively contribute to growth of continental crust, or are the products of melting and recycling of pre-existing lower crust.

Traditionally, petrogenetic studies of granites have used geochemical and isotopic data derived from whole-rock samples. These deliver 'averaged' information for all minerals in the rock and are commonly affected by alteration. Therefore, they are unrepresentative of the magma composition at the time of crystallisation, which limits their usefulness in petrogenetic studies. Recent advances in in-situ microanalysis now enable access to the geochemical and isotopic information stored in zircons at high spatial resolution and analytical precision, providing insight into a previously inaccessible record of magma evolution. Zircon is a common accessory mineral in granitoid rocks. Its highly refractory nature allows individual crystals to retain a direct record of magma composition, and in many cases this record may span much of the magmatic history. In addition, older 'inherited' cores may be preserved, which yield age and compositional information about source rocks and assimilates. Changes in melt composition, temperature or crystallisation conditions arising from either local closed-system processes or large-scale open-system changes (e.g. magma mixing, assimilation) are recorded in concentric zircon growth zones (Hoskin and Schaltegger, 2003; Shore and Fowler, 1996; Vavra, 1990, 1993, 1994) and may be imaged by cathodoluminescence (CL) and back-scatter electron (BSE) imaging techniques. As zircon contains significant concentrations of U, Th, REEs (all ppm level) and Hf (percent level) (Kinny and Maas, 2003) it is suitable for oxygen, Hf and U-Pb isotope analysis, and trace element/REE analysis. The high spatial resolution of the ion microprobe enables oxygen and U-Pb isotope and REE/trace element data to be obtained on the same c. 20 μm diameter spot. Subsequent in-situ

Hf isotope analysis by laser ablation (LA-MC-ICPMS), made on a c. 50 µm diameter spot, can be positioned over the ion probe spots. This approach allows integration of the various data sets and correlation with textural information (e.g. comparisons of zircon cores and rims within and between crystals), and can hence be used to constrain: the emplacement ages of plutons (U-Pb data); the relative mantle and crustal contributions (REE, O and Hf isotope data); the crustal residence age(s) of the source(s) (Hf isotope data); and, based on the latter, the contribution of the magma to crustal growth. Collectively, these offer a major step forward in deciphering granite sources and petrogenetic histories.

A study applying this integrated approach has recently been carried out on zircons from I-type granite suites (Why Worry, Jindabyne and Cobargo suites) of the Lachlan Fold Belt (LFB) of southeastern Australia (Kemp et al., 2007). The data from that study, which indicate mixing between mantle-derived juvenile material and a supracrustal component, led to two important conclusions: (1) the I-type granites predominantly represent new crust and are therefore major contributors to continental growth, and (2) each granite magma comprises multiple sources.

The same integrated analytical approach is applied here to zircons from late Caledonian (~430-400 Ma) plutons emplaced in the Grampian block of the Scottish Highlands. Despite numerous studies utilising whole-rock data the origin of the late Caledonian I-type granites remains controversial. Most studies favour a mixed source origin comprising juvenile (mantle) and infracrustal components (Clayburn et al., 1983; Halliday, 1984; Halliday et al., 1979, 1980; Harmon and Halliday, 1980), which suggests they contributed to crustal growth. However, some authors propose that the plutons have predominantly recycled one or more infracrustal sources and experienced assimilation of a supracrustal component (Frost and O'Nions, 1985). We address this issue by integrating new in-situ Hf data with O and U-Pb data (Papers 1 & 2) from zircons in the late Caledonian Lochnagar and Etive plutons.

2. Geological background

2.1. The late Caledonian granites

The late Caledonian I-type granites were emplaced into mainly metasedimentary rocks of the Dalradian Supergroup in the Grampian Highlands of Scotland between c. 430 Ma and 400 Ma (Fig. 1) (Oliver, 2001; Rogers and Dunning, 1991; Stewart et al., 2001); the main phase of emplacement appears to have been at approximately 425 ± 5 Ma (Fraser et al., 2004; Rogers and Dunning, 1991; Paper 2), broadly contemporaneously with the Scandian Event, involving the oblique collision of Baltica and Laurentia (Brown, 1991; Brown et al., 1985; Coward, 1990; Dallmeyer et al., 2001; Dewey and Mange, 1999; Kinny et al., 2003; Soper, 1986; Stephens and Halliday, 1984; Stephenson et al., 1999; Thirlwall, 1981, 1982, 1988). However, a robust genetic link between the Scandian Event and the voluminous I-type magmatism has yet to be established. Thus, the exact tectonic setting that led to emplacement of the late Caledonian I-type granites in Scotland is still controversial and several models exist. The favoured model linking the I-type granites to a subduction zone setting (Brown, 1991; Brown et al., 1985; Soper, 1986; Stephens and Halliday, 1984; Stephenson et al., 1999; Thirlwall, 1981, 1982, 1988) has recently been challenged by a slab-breakoff model (Atherton and Ghani, 2002).

The majority of late Caledonian I-type granites are hornblende bearing (Soper 1986), show a metaluminous affinity (except for granitoids with > 70 wt% SiO_2, which are commonly peraluminous) (Frost et al., 2001), high Rb/Sr and K/Na, low K/Rb and relatively low initial Sr ratios (Halliday et al., 1985; Stephens, 1988; Thirlwall, 1988). Based on whole-rock geochemical and isotopic data the granites have been divided into three suites (Fig. 1) (Stephens and Halliday, 1984). The *Argyll suite* consists mainly of hornblende-biotite granodiorite and biotite granodiorite plutons, with some diorite and monzogranite; small intrusions of appinitic rock are commonly associated with the plutons (Stephens and Halliday, 1984; Strachan et al., 2002). The rocks are typically strongly metalumimous in comparison to those of the other suites, with high concentrations of Ba, Sr and Na, and low concentrations of Nb, Th and Rb (Fowler et al., 2001; Halliday, 1984;

Halliday et al., 1985; Stephens and Halliday, 1984; Tarney and Jones, 1994; Thirlwall, 1988). The *Cairngorm suite* consists of biotite monzogranite with minor granodiorite, and varies texturally between microgranite and coarse-grained, K-feldspar megacrystic granite. The intrusions contain high concentrations of Rb, Nb, Th and U, but have low Ba, Sr, Ti, P contents. Appinitic intrusions are essentially absent (Stephens and Halliday, 1984). The *South Grampians suite* is dominated by granodiorites and monzogranites, and has a higher proportion of gabbroic and appinitic intrusions. The suite is strongly metaluminous with higher K and Th abundances than the Argyll suite, but lower concentrations of Zr, La, Ce, Ba and Rb (Stephenson et al., 1999)

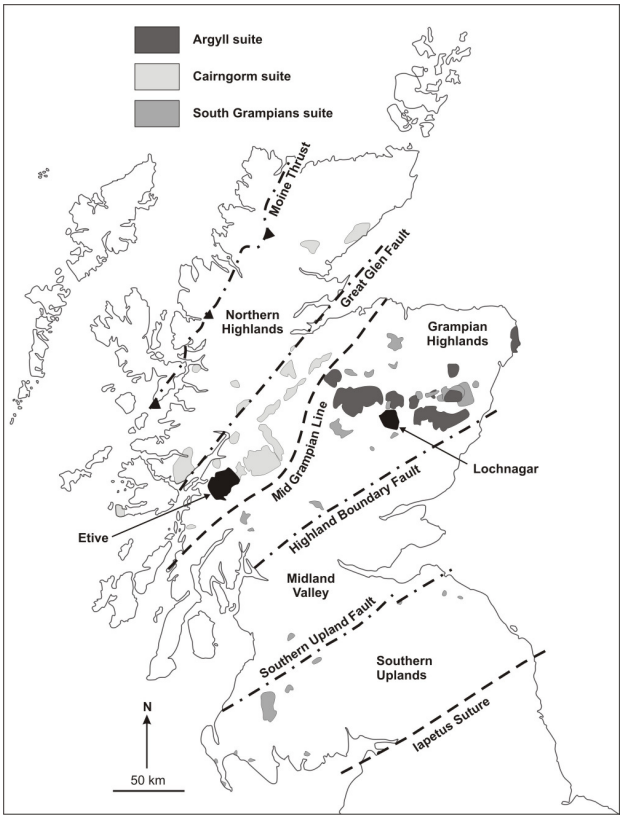

Fig. 1: Map of the late Caledonian granites and showing the locations of the target plutons Lochnagar and Etive (after Stephenson et al., 1999).

To date the reasons for the compositional differences between the suites are not fully resolved. However, it has been proposed that a major concealed discontinuity,

the Mid Grampian Line (MGL), separates Argyll suite plutons from the South Grampians and Cairngorm suite plutons (Fig. 1) (Halliday, 1984). As the whole-rock geochemical differences between the suites may reflect compositional variations in the lower crust beneath the Grampian block and/or variations in the composition and proportion of the mantle contribution to the melts, the MGL may represent an important boundary in the deep basement (Halliday, 1984) with some expression in the mantle. Supporting evidence has been found in inherited zircons, which show that plutons west of the MGL (i.e. in the Argyll suite) contain inherited cores that are older (c. 1600 Ma) than those in plutons to the east (Cairngorm suite) (c. 1100-1000) (Halliday, 1984). However, these ages have also been observed in detrital zircons from the surrounding Dalradian Supergroup (Cawood et al., 2003), which makes the origin of the inherited zircons ambiguous.

The basement onto which the Dalradian Supergroup was deposited is not exposed in the Grampian Highlands. However, based on exposures elsewhere in the surrounding region and in Ireland the Grampian terrane is conceivably underlain by the Lewisian Complex (c. 2.9 Ga), the Rhinns Complex (c. 1.8 Ga), Grenville-age basement (1.2-1.0 Ga) and/or rocks of the Dava and Glen Banchor successions (i.e. gneissose and locally migmatised psammite and semi-pelite with subordinate quartzite that were predominantly derived from Palaeoproterozoic- and Grenville-age sedimentary protoliths (Highton et al., 1999; Piasecki, 1980)).

2.2. The Lochnagar and Etive plutons

2.2.1. The Lochnagar pluton

The Lochnagar pluton, which is representative of the Cairngorm suite, crops out over an area of c. 150 km^2 and comprises three main granite facies (L1, L2, L3), microgranites and several marginal diorites (Fig. 2). The oldest part of the pluton is formed by L1, a circular pluton with a diameter of c. 15 km. It is commonly coarse-grained and inequigranular to porphyritic, and comprises plagioclase (39 %), K-feldspar (28 %), quartz (23 %), bitotite (8 %) and hornblende (1 %). L1 was intruded by L2 (dimensions 12 x 9 km), which comprises mostly grey and pink medium- to coarse-grained, inequigranular to weakly porphyritic, unfoliated leucocratic rocks

that contain plagioclase (41 %), quartz (29 %), K-feldspar (26 %) and biotite (4 %). Both L1 and L2 granites were subsequently intruded by several pink quartz-K-feldspar-plagioclase-phyric microgranites, which are compositionally similar to their host granites. L3 granites are predominantly pink medium- to coarse-grained equigranular granites that contain K-feldspar (40 %), plagioclase (33 %), quartz (25 %) and biotite (2 %), and can be found in various locations within L1. As they have not been discovered in contact with L2, their relationship to L2 is unclear. Compositionally the L3 granites are much more evolved than L1 and L2, and hence may not be related to the main granite body (Smith et al., 2001). The marginal diorites (dimensions: 4-5 x 1.8 km (Cul nan Gad diorite) and 0.6 x 0.4 km (Allt Darrarie diorite) mostly consist of medium-grained, sometimes foliated, inequigranular quartz diorites containing plagioclase (38 %), hornblende and relict pyroxene (38 %), quartz (10 %), K-feldspar (7 %) and biotite (6 %). These were previously interpreted to be separate intrusive bodies that are related, but based on cross-cutting relationships older than the granite (Smith et al., 2001). However, new zircon REE and oxygen isotope data suggest that the diorites are part of the Lochnagar pluton (Paper 2). Thus, based on field relationships the order of intrusion is diorites, L1, L2, microgranite, L3 (Halliday, 1984; Halliday et al., 1979; Oldershaw, 1974; Smith et al., 2001).

Previous TIMS age data indicated that the Lochnagar pluton had a relatively simple emplacement history with intrusion of L1 and L2 approximately contemporaneously at c. 425 ± 5 Ma (U-Pb zircon) and L3 some time later at c. 417 ± 1 Ma (monazite age) (Smith et al., 2001). However, recent U-Pb zircon SIMS dating (Paper 2) showed that the Lochnagar pluton was emplaced incrementally over a period of c. 11 m.y. between 424 ± 5 Ma and 413 ± 4 Ma. At least one of the L3 granite intrusions was emplaced broadly contemporaneously with rather than subsequent to the L1 and L2 granites at 423 ± 2 Ma. Furthermore, U-Pb dating detected that at least part of the Allt Darrarie diorite intruded after emplacement of the granites at 413 ± 4 Ma. Hence the pluton has a much more complicated petrogenetic history than previously recognised.

There is little information on the sources that contributed to the Lochnagar pluton. Based on an $\varepsilon Nd_{415\ Ma}$ value of -2.7 and initial $^{87}Sr/^{86}Sr$ values of 0.7063

(n=1), Halliday et al. (1984) proposed that the pluton comprises both mantle and crustal sources. Recent zircon oxygen isotope data have made a major contribution towards deciphering the pluton's sources and petrogenesis in more detail (Paper 2). Zircons from the Lochnagar pluton yielded a range of $\delta^{18}O$ values between 5.3 ‰ and 8.1 ‰ and a mean of 6.6 ± 0.6 ‰ (n=230, 2σ). Thus, the majority of zircons (c. 82 %) show $\delta^{18}O$ values more enriched in ^{18}O than those of mantle-like zircons (5.3 ± 0.6 ‰ (Valley et al., 1998), but insufficiently ^{18}O-enriched to have been derived from a solely supracrustal component. The presence of inherited cores in some zircons in the pluton is however consistent with a small supracrustal component such as the Dalradian Supergroup. Thus, based on these data the Lochnagar pluton appears to have been predominantly produced by (1) mixing between mantle-derived and infra- and/or supracrustal melts, or (2) recycling of pre-existing lower crust (Paper 2).

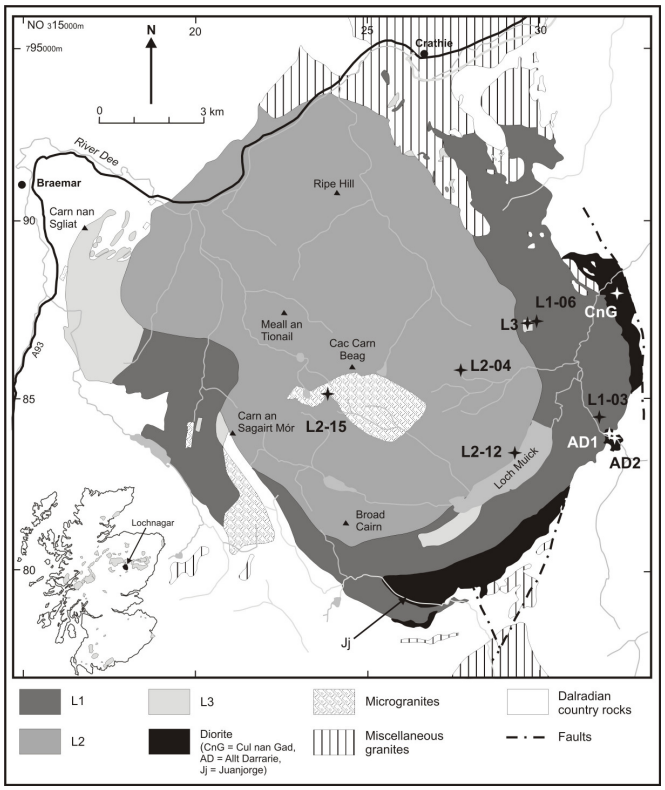

Fig. 2: Geological sketch map of the Lochnagar pluton with sample locations (Smith et al., 2001).

Oxygen isotope analysis of zircons has shown that the majority of samples display a range in zircon $\delta^{18}O$ larger than expected from a homogeneous magma with variability occurring between samples, between crystals and even within individual crystals. This may be further evidence that the pluton represents an accumulation of a series of incrementally-assembled heterogeneous melt batches. Melts of differing $\delta^{18}O$ are thought to have been generated in a deep crustal hot zone (Annen et al., 2006; Annen and Sparks, 2002; Papers 1 & 2). Mixing of melts probably occurred during ascent and also within a shallow magma chamber before final emplacement (Papers 1 & 2).

2.2.2. The Etive pluton

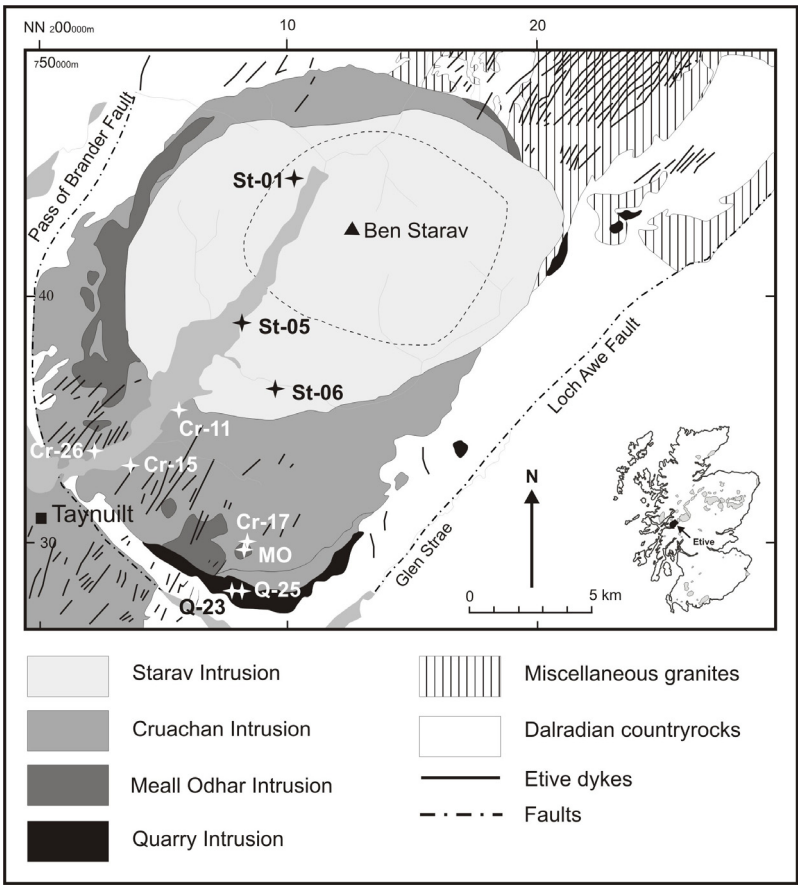

Fig. 3: Geological sketch map of the Etive pluton with sample locations (after Anderson, 1937; Batchelor, 1987).

The Etive pluton, which is representative of the Argyll suite, is exposed over an elliptical area of approximately 300 km^2 (Fig. 3). It is a major composite pluton comprising four main intrusive phases ranging in composition from granite to monzodiorite/diorite. Like the Lochnagar pluton, it has a predominantly calc-alkaline composition with the silicic phases showing a peraluminous and the more mafic phases a metaluminous affinity.

The Quarry Intrusion represents the outermost phase of the pluton and intruded as a small lens of granodiorite to diorite/quartz-diorite (Clayburn et al., 1983; Paper 2) containing country rock xenoliths and microdioritic or appinitic enclaves. Rocks of the Quarry Intrusion are commonly dark-grey, medium- to coarse-grained and plagioclase- or pyroxene-phyric, and contain plagioclase (46 %), hornblende (20 %), quartz (12 %), biotite (12 %) and pyroxene (9 %) (Batchelor, 1987). The largest part of the pluton is concealed by the compositionally heterogeneous Cruachan Intrusion, which ranges from granite through tonalite/granodiorite to monzodiorite and contains microgranitoid enclaves (Jacques and Reavy, 1994). The Cruachan Intrusion has been divided into two main varieties. In the northern lobe of the intrusion pale-grey, medium-grained, equigranular monzogranites are exposed, which contain occasional mafic clusters and metasedimentary xenoliths and comprise plagioclase (30-46 %), K-feldspar (23-34 %), quartz (16-28 %), biotite (4.5-6.5 %) and hornblende (3-9.5 %). The southern lobe comprises grey, medium- to fine-grained, equigranular monzodiorites, which show higher abundances of plagioclase (54-63 %) and often biotite (6-21 %), but only interstitial K-feldspar (7-25 %) and less quartz (5-12 %) (Batchelor, 1987). The Meall Odhar Intrusion has been described as a pink K-feldspar and quartz granite sheet and dyke intrusion, which cross-cuts all the earlier phases. However, field work carried out for this study has revealed numerous locations where the Cruachan Intrusion has intruded the Meall Odhar Intrusion. Similar to the other facies, it is compositionally variable and comprises fine- to medium-grained syenogranites and monzogranites (Stephenson et al., 1999). Syenogranites contain K-feldspar (50-67 %), quartz (27-37 %) and only small amounts of plagioclase (4.5-12 %) and hornblende (0.2-2 %), whereas monzogranites comprise quartz (30-42 %), K-feldspar (33-41 %), plagioclase (20-28 %) and biotite (0.5-1 %) (Batchelor, 1987). The centre of the Etive pluton contains the elliptical

Starav Intrusion, consisting of two concentric intrusions, which have been interpreted to represent at least two separate magma pulses. (Batchelor, 1987; Clayburn et al., 1983; Jacques and Reavy, 1994). The Outer Starav Facies is a medium- to coarse-grained K-feldspar- and hornblende-phyric syenogranite containing K-feldspar (27-46 %), plagioclase (23-41 %), quartz (21-32 %), biotite (3-6 %) and hornblende (0.2-6 %). Rocks of the Inner Starav Facies are medium-grained and equigranular. Compositionally they are similar to the Outer Starav Facies with the exception of higher abundances of quartz (28-40 %) and the absence of hornblende (Batchelor, 1987). To summarise, based on field relationships the pluton becomes younger towards the centre with the order of emplacement being Quarry Intrusion, Cruachan Intrusion and Starav Intrusion (Bailey, 1960). The Meall Odhar Intrusion probably intruded broadly contemporaneously with the Cruachan Intrusion.

Early radiometric dating of the pluton by Rb-Sr, Ar-Ar, K-Ar and U-Pb zircon TIMS methods delivered ages ranging from 410 Ma to 373 Ma (Brown, 1975; Brown et al., 1968; Clayburn, 1981; Clayburn et al., 1983; Halliday et al., 1979; Harmon and Halliday, 1980; Pankhurst, 1982; Pidgeon and Aftalion, 1978). Based on these dates Clayburn et al. (1983) concluded that the constituent parts of the Etive Complex were emplaced approximately contemporaneously at 400 Ma. However, more recently Morris et al. (2005) obtained Ar-Ar biotite ages of 415 ± 1.8 Ma and 414 ± 2 Ma for the Etive dyke swarm, which they interpreted to mark the end of magmatism. New U-Pb zircon SIMS data (Paper 2) indicate that the pluton, like Lochnagar, intruded over an extended time period of approximately 16 m.y., between 423 ± 2 Ma and 407 ± 3 Ma rather than contemporaneously. Based on these data, magmatic activity started with intrusion of the Meall Odhar Intrusion and parts of the Cruachan Intrusion, which was followed by the remaining phases of the Cruachan Intrusion, and ended with emplacement of the Starav Intrusion in the pluton's centre and the Quarry Intrusion along its outer margin.

The Nd and Sr isotope composition of the Etive pluton has been determined in more detail than the Lochnagar pluton, and data exist for all intrusive phases. All have negative $\varepsilon Nd_{400\ Ma}$ values ranging from -4.7 to -9.3 with the Cruachan Intrusion displaying the least negative and the Starav Intrusion and one sample of the Quarry Intrusion displaying the most negative values (Frost and O'Nions, 1985). Initial

$^{87}Sr/^{86}Sr$ values range from 0.7043 to 0.7068. Based on the Nd isotope data the Etive pluton contains a larger crustal component than the Lochnagar pluton, although Sr isotope data do not support this. Clayburn et al. (1983) proposed that the Etive pluton is the result of melting of both lower crustal and mantle components. The different phases are assumed to be derived from the same source, with the later phases such as the Starav Intrusion containing a larger crustal component (Clayburn et al., 1983). At present, the nature of the crustal component and the individual mantle and crustal proportions that have been involved in the generation of the Etive pluton remain unresolved.

Zircon oxygen isotope analyses of the Etive pluton gave a similar result to the Lochnagar pluton. $\delta^{18}O$ values span a similar range from 4.6 ± 0.4‰ up to 8.2 ± 0.4‰ (2σ, n=209) with a mean value of 6.5 ± 0.4‰ (Paper 2). Again c. 82 % of zircons yielded $\delta^{18}O$ values too high for mantle-like zircons (5.3 ± 0.6 ‰ (Valley et al., 1998) but too low for supracrustal sources. Thus, the Etive pluton also appears to comprise a small pristine mantle component and multiple crustal sources (Paper 2). The degree of heterogeneity observed within individual samples and crystals is similar and in some samples of the Cruachan Intrusion, in particular, even greater than in zircons of the Lochnagar pluton, which suggests that the pluton has a very similar petrogenetic and intrusion history to the Lochnagar pluton (Paper 2).

3. Samples

Zircons from eight representative Lochnagar samples (AD1, CnG, L1-03, L1-06, L2-04, L2-12, L2-15, L3) and from nine Etive samples (MO, Cr-11, Cr-17, Cr-15, Cr-26, St-05, St-01, Q-23 and Q-25) were selected for in-situ Hf isotope analysis. Zircons from the Lochnagar and Etive plutons are broadly similar, displaying features typical of igneous zircon such as euhedral grain shapes, and oscillatory and/or sector zoning (Benisek and Finger, 1993; Hanchar and Miller, 1993; Hoskin and Schaltegger, 2003; Vavra, 1990). Each sample covers a range of grain sizes, morphologies (equant to acicular), zoning patterns and CL intensities and contains at least one and commonly multiple overgrown resorption surfaces. Resorbed cores

may comprise ~95 % of a crystal and are commonly overgrown by multiple rims. Cores are often weakly luminescent in CL, and are either entirely unzoned or consist of an inner unzoned domain and an outer oscillatory zoned domain. Some crystals, which predominantly occur in the more mafic phases of intrusion, contain only a very small unzoned core domain or lack it entirely. For a more detailed description of the zircons see Paper 2.

4. Methodology

4.1. Whole-rock analyses

REEs and some trace elements were analysed at the British Geological Survey (BGS) in Nottingham. The samples were fused with Na_2O_2 and then leached with deionised water and HCl before analysis using a ThermoElemental PQ Excel quadrupole ICP-MS. Matrix-matched calibration standards were used throughout.

4.2. Zircon sample preparation

Zircon separation was carried out in the University of St. Andrews Mineral Separation Facility. Rock samples of approximately 5 kg were crushed and sieved to obtain the < 500 µm fraction from which zircon crystals were separated using a Wilfley Table, heavy liquids and a Frantz magnetic separator. Approximately 100 zircon crystals were hand-picked from the remaining heavy, non-magnetic fraction, providing a range of grain size, morphology, transparency, alteration and occurrence of inclusions or cracks. The crystals were mounted into epoxy (Araldite) and the zircon mounts polished to about half thickness to expose the crystal interiors. The polished surfaces were imaged in back-scattered electron (BSE) and cathodoluminescence (CL) mode using a Philips XL30CP Scanning Electron Microscope (SEM) at the University of Edinburgh to identify internal zoning features, inherited material, inclusions and cracks. Suitable crystals for in-situ oxygen isotope analysis were selected using this information.

4.3. Hf isotope analysis

Hafnium isotope analysis was carried out at the NERC Isotope Geosciences Laboratory (NIGL) in Nottingham, using a Nu Instruments Nu-Plasma HR multi-collector ICP-MS coupled to a New Wave Research UP193SS 193nm solid state laser ablation system. For an improved wash-out a low volume ablation cell (NIGL zircon cell) was employed. Ablation was conducted in a He atmosphere (0.8-1.0 l/min). Ar make-up gas was sourced from a Nu Instruments DSN-100 desolvating nebuliser whilst aspirating 2 % HNO_3 and 0.1 molar HF to maintain constant plasma conditions.

At the time of analysis the mass spectrometer was fitted with a specially designed U-Pb collector block, which limits the number of Faraday cups available for Hf isotope analysis to seven. The instrument is therefore restricted to measuring ^{173}Yb, ^{174}Lu, ^{175}Lu, ^{176}(Yb, Lu, Hf), ^{177}Hf, ^{178}Hf and ^{179}Hf. The stable isotopes ^{180}Hf and ^{181}Hf are not analysed and emphasis is placed on the ^{178}Hf/^{177}Hf stable isotope ratio for monitoring of data quality. A peak jumping routine including ^{172}Yb, to allow assessment of the effect of using a Yb mass bias correction for the Yb interference correction rather than the Hf mass bias correction, has been investigated but was found unnecessary with the data for both being equivalent within the increased uncertainty reflected by the low Yb concentrations.

The isobaric interference correction for ^{176}Yb was determined prior to each analytical session using Yb doped JMC475 Hf standards. This correction was determined for total Yb/Hf ratios of up to 0.3. These data were used to calculate a ratio for the ^{176}Yb/^{173}Yb ratio of 0.79488. The Lu interference correction used the accepted ratio of ^{176}Lu/^{175}Lu = 0.02653. During measurement the ^{173}Yb and ^{175}Lu peaks were monitored and corrections applied according to these ratios. Each day spiked and unspiked solution standards were analysed to monitor instrument performance and effectiveness of the corrections.

Ablation data were acquired using a static spot ablation protocol, a 50 µm beam and a 5-10 Hz laser pulse repetition rate. A fluence of 4-6 J/cm^2 and ablation time of 70 seconds resulted in an ablation rate of 0.05-0.09 µm/pulse (0.5-0.9 µm/sec). Total Hf signals varied between 4.5-6.5 V resulting in reproducibilities of the Mud Tank

reference material between 0.7 and 1.0 εHf units (2σ). The Mud Tank zircon reference material was used to normalise the sample zircons and assess the reproducibility of all ratios. This included normalisation of the Lu-Hf ratio required for age correction. All values for Mud Tank were taken from Woodhead and Hergt (2005). All uncertainty components, including those for age and normalisation, were factored into the expanded uncertainty quoted.

For Hf isotope analysis zircons were selected for which U-Pb and (in most cases) oxygen isotope data already existed in order to enable correlation of the different data sets. Where possible multiple analyses were made on a single crystal. However, due to the much larger spot size of the laser in comparison to the ion probe this was seldom possible. Most data were obtained from crystal cores, which were easier to analyse as they often define the largest part of the crystal, and only rarely of the rim. Cracks and inclusions were always avoided and all analyses were carried out on the already existing SIMS spots or at least within the same CL growth zone. The ablation data were normalised to Mud Tank ($^{176}Hf/^{177}Hf_{solution}$= 0.282507 ± 6 and $^{176}Lu/^{177}Hf_{solution}$ = 0.000042 (Woodhead and Hergt, 2005)). Reproducibility of the Mud Tank standard was propagated into the uncertainty of the sample analysis.

In the rare cases where the laser drilled through the zircon grains or from an older inherited core into the surrounding magmatic rim, the analyses were examined using NIGL's time-resolved software, which allowed identification of the most stable parts of the profile and of distinguishable Hf isotope zones.

εHf values were calculated using a ^{176}Lu decay constant of 1.865 x $10^{-11}y^{-1}$ (Scherer et al., 2001), the present-day chondritic $^{176}Lu/^{177}Hf$ value of 0.0332 and $^{176}Hf/^{177}Hf$ ratio of 0.282772 (Blichert-Toft and Albarède, 1997). To calculate two-stage Hf model ages the $^{176}Lu/^{177}Hf$ ratios of the average crust (TDM_C) ($^{176}Lu/^{177}Hf$ = 0.015 (Griffin et al., 2002)) and of the depleted mantle ($^{176}Lu/^{177}Hf$ = 0.0384 (Griffin et al., 2000)), the initial $^{176}Hf/^{177}Hf$ ratios of the zircon and the depleted mantle (present-day $^{176}Hf/^{177}Hf$ ratio of the depleted mantle = 0.28325 (Nowell et al., 1998)), and the U-Pb SIMS age were used. For comparison, two-stage Hf model ages were also calculated based on the whole-rock $^{176}Lu/^{177}Hf$ ratio of each sample (TDM_W). A summary of the data can be found in Table 1, the full data set in Appendices 3a and 3b.

Table 1
Summary of oxygen and Hf isotope of zircons from the Lochnagar and Etive plutons

Sample	Age [Ma]	1SD	$\delta^{18}O$ [‰]		$^{176}Lu/^{177}Hf$ (WR)	$^{176}Hf/^{177}Hf$		$^{176}Lu/^{177}Hf$		$^{176}Hf/^{177}Hf$ (initial)		εHf		95% con.	TDMC [Ma]		95% con.	TDMW [Ma]		95% con.	n
Lochnagar																					
AD1	419	4	7.0	(6.4-7.8)	0.008	0.282500	(0.282384-0.282614)	0.00114	(0.00055-0.00114)	0.282491	(0.282376-0.282606)	-0.7	(+3.4 to -4.8)	1.0	1459	(1198-1715)	60	1221	(1020-1419)	45	12
CnG	418	6	5.9	(5.5-6.4)	0.007	0.282553	(0.282495-0.282584)	0.00080	(0.00031-0.00205)	0.282546	(0.282492-0.282577)	1.2	(+2.3 to -0.7)	1.0	1334	(1264-1455)	61	1102	(1050-1193)	45	12
L1-03	420	3	6.6	(5.8-7.1)	0.007	0.282436	(0.282355-0.282473)	0.00065	(0.00031-0.00118)	0.282431	(0.282347-0.282469)	-2.8	(-1.5 to -5.8)	0.9	1592	(1507-1779)	56	1296	(1232-1436)	41	14
L1-06	420	4	6.4	(5.9-6.8)	0.004	0.282520	(0.282452-0.282562)	0.00185	(0.00092-0.00247)	0.282506	(0.282445-0.282545)	1.4	(+1.2 to -2.3)	1.3	1424	(1335-1560)	78	1105	(1044-1198)	52	5
L2-04	424	6	6.6		0.006	0.282494		0.00147		0.282483		-0.9		1.6	1473		95	1184		67	1
L2-12	419	4	6.3	(6.2-7.1)	0.004	0.282531	(0.282520-0.282548)	0.00154	(0.00127-0.00185)	0.282519	(0.282510-0.282534)	0.3	(+0.8 to -0.1)	0.9	1394	(1362-1415)	57	1084	(1062-1099)	38	6
L2-15	422	3	6.7	(6.0-7.5)	0.006	0.282521	(0.282435-0.282591)	0.00083	(0.00025-0.00187)	0.282515	(0.282430-0.282585)	0.2	(+2.7 to -2.8)	1.4	1403	(1245-1593)	86	1132	(1017-1270)	62	8
L3	423	5	6.6	(5.6-8.1)	0.004	0.282527	(0.282488-0.282583)	0.00107	(0.00055-0.00141)	0.282518	(0.282478-0.282518)	0.3	(+2.3 to -1.1)	0.9	1394	(1267-1484)	55	1086	(999-1147)	36	10
inherited zircons																					
L2-04_15.28	1046	15	6.5		0.006	0.282147		0.00049		0.282138		0.7		1.0	1855		50	1632		32	1
L2-04_15.29	1046	15	6.0		0.006	0.282157		0.00042		0.282149		1.1		1.1	1829		59	1613		38	1
L2-15_29a	1149	8	5.5		0.006	0.282355		0.00097		0.282334		10.0		1.5	1341		89	1288		62	1
L2-15_35b	1149	8	6.3		0.006	0.282198		0.00027		0.282192		4.9		1.3	1664		74	1521		51	1
L2-15_36a	1235	19	5.2		0.006	0.281760		0.00078		0.281742		-9.1		1.5	2622		82	2240		54	1
L2-15_32a	1235	19	5.7		0.006	0.282173		0.00048		0.282162		5.8		1.7	1676		95	1554		64	1
Etive																					
MO	423	3	6.4	(5.6-6.9)	0.005	0.282390	(0.282354-0.282432)	0.00061	(0.00034-0.00099)	0.282386	(0.282349-0.282425)	-4.4	(-3.0 to -5.7)	1.0	1692	(1605-1773)	62	1315	(1253-1372)	43	12
Cr-11	421	9	7.1	(6.4-7.9)	0.009	0.282339	(0.282315-0.282339)	0.00089	(0.00039-0.00146)	0.282332	(0.282305-0.282361)	-6.3	(-5.3 to -7.3)	0.8	1814	(1749-1872)	44	1532	(1481-1579)	34	13
Cr-17	414	6	6.6	(4.6-7.5)	0.009	0.282353	(0.282331-0.282390)	0.00051	(0.00034-0.00062)	0.282349	(0.282328-0.282386)	-5.9	(-4.6 to -6.6)	0.9	1778	(1697-1827)	50	1503	(1437-1541)	39	11
Cr-26	413	5	6.5	(5.3-7.6)	0.009	0.282356	(0.282324-0.282379)	0.00072	(0.00036-0.00118)	0.282350	(0.282316-0.282374)	-5.8	(-5.0 to -7.1)	1.0	1777	(1724-1853)	60	1501	(1459-1562)	46	11
Cr-15	413	5	6.2	(5.3-6.9)	0.009	0.282378	(0.282333-0.282413)	0.00077	(0.00049-0.00077)	0.282372	(0.282329-0.282408)	-5.1	(-3.8 to -6.6)	1.0	1728	(1647-1823)	62	1462	(1397-1539)	49	8
St-05	412	6	7.1	(6.9-7.2)	0.008	0.282281	(0.282275-0.282290)	0.00092	(0.00039-0.00138)	0.282274	(0.282265-0.282283)	-8.6	(-8.3 to -8.9)	0.8	1947	(1928-1968)	46	1597	(1583-1614)	34	3
St-01	408	6	7.0	(6.5-7.4)	0.008	0.282266	(0.282229-0.282293)	0.00077	(0.00051-0.00129)	0.282260	(0.282219-0.282284)	-9.2	(-8.3 to -10.6)	0.8	1981	(1928-2071)	44	1623	(1582-1693)	33	10
Q-23	408	4	6.2	(5.5-6.7)	0.007	0.282361	(0.282330-0.282385)	0.00084	(0.00033-0.00134)	0.282354	(0.282324-0.282382)	-5.8	(-4.8 to -6.9)	1.1	1770	(1710-1839)	68	1427	(1381-1478)	50	8
Q-25	405	12	6.0	(4.9-6.9)	0.007	0.282417	(0.282331-0.282565)	0.00128	(0.00076-0.00167)	0.282407	(0.282320-0.282553)	-4.0	(+1.1 to -7.1)	1.5	1655	(1328-1848)	83	1339	(1094-1484)	59	7
inherited zircons																					
Cr-15_4a	1036	22	7.0		0.009	0.282256		0.00039		0.282249		4.4		1.3	1611		73	1494		50	1
Cr-15_8a	1646	6	5.9		0.009	0.281749		0.00053		0.281733		-0.1		1.0	2374		75	2227		48	1

5. Results

5.1. Hf isotope data

5.1.1 Lochnagar

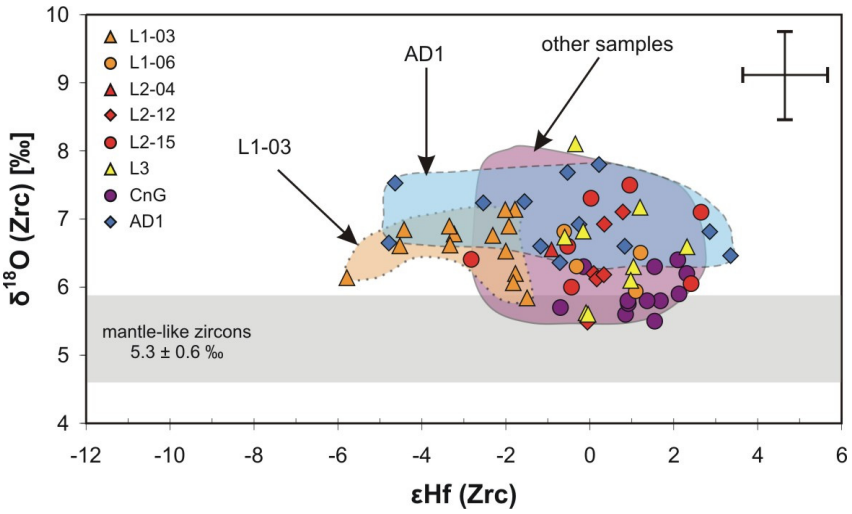

Fig. 4: εHf vs. $\delta^{18}O$ of zircons from the Lochnagar pluton (2σ error: ± 1.0 εHf, ± 0.6 ‰). The majority of samples plot in the purple shaded area; samples L1-03 and AD1 are clearly different. L1-03 may comprise a different source, whereas AD1 may represent a mixture of at least two sources. Also note the difference in εHf between L1-03 and L1-06, which were both collected within the same mapped unit.

Initial zircon εHf values span 9.2 εHf units and range from +3.4 to -5.8 ± 1.0 (2σ) (Fig. 4, Table 1). Resulting TDM_C Hf model ages vary between 1198 ± 65 Ma and 1779 ± 60 Ma (Table 1). The majority of samples (granite samples L1-06, L2-04, L2-12, L2-15, L3 and diorite sample CnG) have similar Hf isotope compositions and form a cluster between +2.7 and -2.8 εHf (Fig. 4). However, zircons of granite sample L1-03 and diorite sample AD1 are distinctly different. Zircons of L1-03 show only negative εHf values and form a cluster at -1.5 to -5.8. L1-03 hence has a different composition than zircons of L1-06 (+1.2 to -2.3) even though both samples were collected from the same mapped granite facies. Zircons of diorite AD1 also extend to much more negative values, but overall form a very heterogeneous population (εHf = +3.4 to -4.8; =8.2 εHf units), which spreads over nearly the entire

range of values detected in zircons of the Lochnagar pluton (Fig. 4). This spread results from differences in εHf between individual zircons; where multiple analyses were made on a single crystal εHf values are always within error, and thus not resolvable (Fig. 5a-d). Therefore, in contrast to the results from $\delta^{18}O$ data, resolvable variations occur between granite facies, between samples of the same facies and between zircon crystals of a single sample, but not within individual grains.

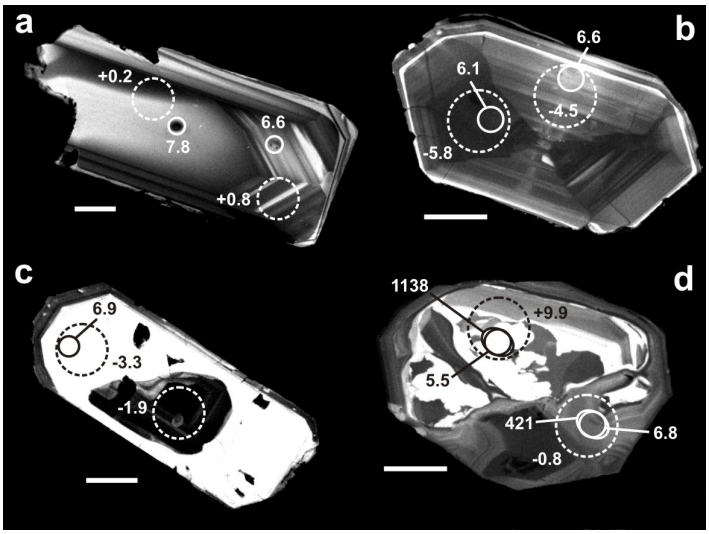

Fig. 5: Representative zircons with Hf isotope data (scale bar = 50 µm, dashed circles: εHf ± 1.0 (2σ), circles: $\delta^{18}O$ ± 0.4-0.6 ‰, ellipses: U-Pb ± 1 %).
a-c) Resolvable variation occurs between, but not within individual magmatic crystals (AD1 grain 10, L1-03 grain 16, L1-03 grain 23).
a) Unzoned inner core domain and outer oscillatory zoned domain show resolvable variation in $\delta^{18}O$, but not in εHf (L1-03, grain 16).
d) Inherited grain with large xenocrystic core and magmatic rim. Core and rim display large variation (L2-15, grain 29).

Six analyses were carried out on older inherited zircons found in L2-04 (n=2) and L2-15 (n=4) (Table 1). One inherited zircon in L2-04 (U-Pb age = 1046 ± 33 Ma) shows initial εHf values of +1.1 to +0.7 ± 1.0 and TDM_C model ages of 1829 ± 59 Ma to 1855 ± 50 Ma; at 424 Ma εHf values were -12.5 to -12.9 +0.8. Three inherited cores in L2-15 with $^{207}Pb/^{206}Pb$ ages between 1149 ± 8 Ma and 1235 ± 19 Ma have positive initial εHf values of $+10.0_{(1149\ Ma)}$, $+5.8_{(1235\ Ma)}$ and $+4.9_{(1149\ Ma)}$ ± 1.5, and corresponding TDM_C ages of 1341 ± 89 Ma, 1676 ± 95 Ma and 1664 ± 74 Ma. At 422 Ma εHf values ranged from -5.7 to -12.1 ± 1.3. A fourth inherited core has the

same U-Pb age (1149 ± 8 Ma), but a very different initial εHf value of -9.1 ± 1.5 and TDM_C model age of 2622 ± 82 Ma. At 422 Ma it had an εHf value of -26.8 ± 1.1.

5.1.2. Etive

Zircons from the Etive pluton range in initial εHf from -3.0 to -10.6 ± 1.0 (=7.6 units) (Fig. 6) and show TDM_C model ages of 1605 ± 69 Ma to 2071 ± 45 Ma (Table 1). One outlier found in sample Q-25 of the Quarry Intrusion has an εHf value of +1.1 ±1.7 and a TDM_C of 1328 ± 97 Ma.

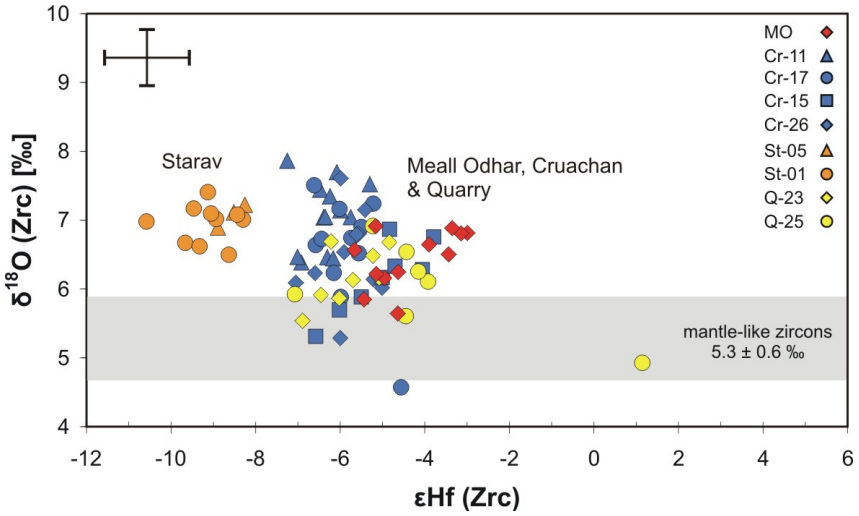

Fig. 6: εHf vs. $\delta^{18}O$ of zircons from the Etive pluton (error: ± 1.0 εHf, ± 0.4 ‰ (2σ)).

The range in εHf of 7.6 ± 1.0 units is well outside the analytical uncertainty and similar to the spread found amongst zircons of the Lochnagar pluton (9.2 ± 1.0 units). However, in the Etive pluton this spread is defined by two distinct clusters of homogeneous samples, which both display negative εHf values (Fig. 6). One cluster, which consists of zircons representing the Meall Odhar, Cruachan and Quarry Intrusions, has εHf values of -3.0 to -7.3 ± 1.0 and TDM_C ages of 1605 ± 69 Ma to 1872 ± 43 Ma. Of these samples zircons of the Meall Odhar Intrusion have the least negative εHf values (-3.0 to -5.7 ± 1.0) and those of Cruachan Intrusion sample Cr-11 the most negative (-5.3 and -7.3 ± 0.8). The second cluster represents zircons from the Starav Intrusion (St-05 and St-01), which display more negative εHf values

of -8.3 to -10.6 ± 0.8 and older model ages of 1928 ± 52 Ma to 2071 ± 45 Ma (TDM_C).

Two εHf values were obtained from older inherited zircons found within Cr-15 (Table 1). They were dated using U-Pb zircon SIMS analysis at 1036 ± 22 Ma and 1646 ± 6 Ma (Paper 2). Their initial εHf values are +4.4 ± 1.3 and -0.1 ± 1.0, corresponding TDM_C ages are 1611 ± 73 Ma and 2374 ± 75 Ma respectively; at 413 Ma their εHf values were -9.3 ± 0.9 and -27.2 ± 0.9.

6. Discussion

6.1. Crustal growth vs. crustal recycling

The origin of the late Caledonian I-type granites and the reasons for the compositional differences between the granite suites have been the focus of numerous whole-rock studies. It has been proposed that the I-type granites represent the products of mixing between at least two different sources. However, whether these are mixtures of mantle (depleted and/or enriched) and infracrustal components (Clayburn et al., 1983; Halliday, 1984; Halliday et al., 1979, 1980; Harmon and Halliday, 1980) or of infracrustal and supracrustal components (possibly plus a mantle component) (Frost and O'Nions 1985) is unclear. Thus, it is uncertain whether the late Caledonian I-type magmatism may have played an important role in crustal growth. New in-situ zircon oxygen isotope data for the Lochnagar and Etive plutons (Paper 2) show that both plutons contain at most a small pristine mantle component, and were either derived from a mixture of mantle-derived and crustal sources or entirely from the crust since very few zircons have mantle-like $\delta^{18}O$ values of 5.3 ± 0.6 ‰ (Valley et al., 1998). Simple two-component magma mixing modelling based on zircon $\delta^{18}O$ indicates that a contribution of up to 30 % by a supracrustal source such as the Dalradian metasedimentary country rocks may explain the range of $\delta^{18}O$ values found in the plutons (Fig. 7). However, based on the lack of field evidence (e.g. xenoliths - pristine or partly digested - are very rare) (Frost and O'Nions, 1985) and the complexity observed in the plutons' zircon

oxygen isotope data observed we envisage a more complex mixing/assimilation scenario involving more than two sources. From oxygen isotope data alone it is not possible to identify these sources, hence at present three questions remain unresolved:

(1) Does the proposed low $\delta^{18}O$ mantle component represent contemporary mantle (c. 420 Ma) or melting of an ancient mafic lower crust source (e.g. mafic underplate), and therefore did the Caledonian I-granites involve any crustal growth?

(2) Which other crustal sources contributed to the Lochnagar and Etive plutons?

(3) What is the explanation for the observed whole-rock geochemical differences between the plutons? Zircon oxygen isotope compositions of the Lochnagar and Etive plutons are very similar, and therefore do not explain the observed whole-rock differences between the plutons, and on a wider scale between the Cairngorm and Argyll suites. This is not surprising considering that published whole-rock oxygen isotope data of the Lewisian Complex, Rhinns Complex, and Grenvillian basement, thus of rocks that may underlie the Grampian terrane, have very similar whole-rock $\delta^{18}O$ values (Frost and O'Nions, 1985; Muir et al., 1994; Restrepo-Pace et al., 1997) (Fig. 7). Therefore the whole-rock differences are probably related to compositional variations amongst the lower crustal (or mantle) sources rather than being the result of varying degrees of crustal and mantle contribution.

In contrast to the zircon oxygen isotope data, the in-situ Hf isotope data of the plutons reveal large differences in εHf between the plutons, potentially providing an explanation for their whole-rock differences. Zircons from the Etive pluton have negative εHf values between -3.0 and -10.6 ± 1.0 (2σ) with the exception of one outlier (grain 10 in Q-25: εHf = +1.1 ± 1.7), whereas zircons from the Lochnagar pluton display positive as well as negative εHf values between +3.4 and -5.8 ± 1.0 (2σ). Positive εHf values are generally interpreted as evidence for a mantle origin, whereas negative values reflect melting of ancient crust (e.g. Amelin et al., 1999; Vervoort et al., 2000). Based on this the Etive pluton is predominantly derived from a crustal source and does not contain a ~420 Ma mantle component, whereas the Lochnagar pluton appears to be the product of melts derived from the mantle and from a crustal source. However, in both plutons a contribution by contemporary depleted mantle can be precluded on the base of εHf data, which show that even the

most positive εHf value in Lochnagar (i.e. +3.4 ± 1.1) indicates a strong crustal affinity in comparison to the ~420 Ma depleted mantle (+16 ± 3 (Vervoort and Blichert-Toft, 1999) (range of ± 3 εHf units represents the range observed in present-day MORB (Griffin et al., 2000)). Further evidence is provided by calculated Hf model ages, which are considerably older than the zircon U-Pb crystallisation ages (Lochnagar: U-Pb = 424-413 Ma, TDM_C ~ 1.7-1.1 Ga, TDM_W ~ 1.4-1.0 Ga; Etive: U-Pb = 423-407 Ma, TDM_C ~ 2.1-1.3 Ga, TDM_W ~ 1.8-1.2 Ga) (Fig. 8 & 9). However, enriched mantle typically has εHf values closer to CHUR (εHf = 0).

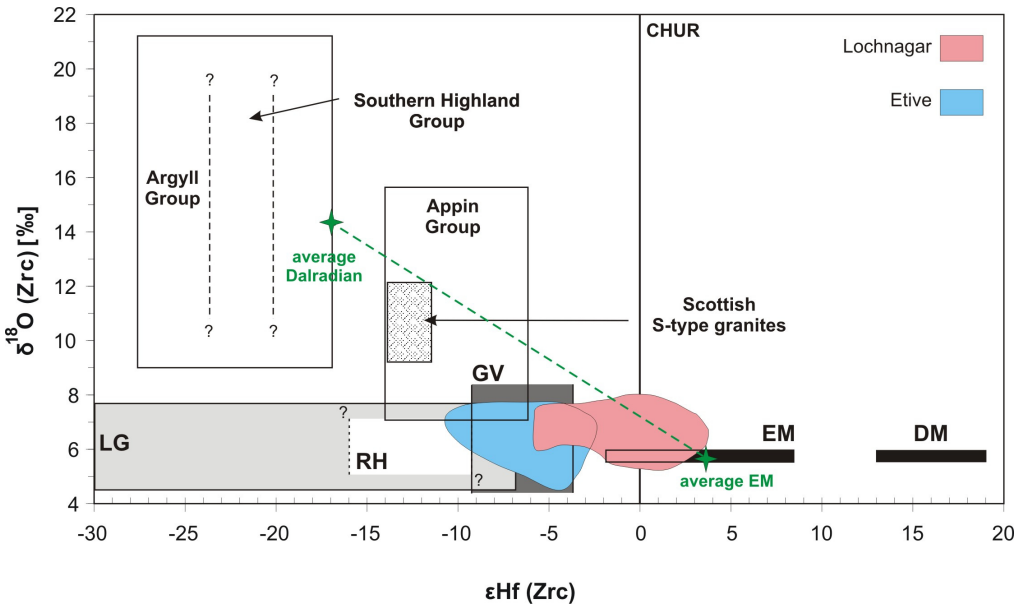

Fig. 7: εHf vs. $\delta^{18}O$ of zircons from the Lochnagar and Etive plutons showing the relationship to their potential supracrustal and infracrustal sources.
Zircons from both plutons show no overlap with the field defined by depleted mantle (DM, re-calculated at 420 Ma), but those from the Lochnagar pluton show strong overlap with enriched mantle (EM). The mixing line (green dashed line) reflects simple two-component mixing between EM and average Dalradian (i.e. Appin, Argyll and Southern Highland groups). Based on this mixing modelling both plutons may contain up to 30 % Dalradian material. However, the complexity and variation observed in the zircon oxygen isotope data indicates involvement of more than two sources. Large overlap exists with fields representing the plutons' potential lower crustal source rocks (i.e. Lewisian granulites = LG, Rhinns Complex = RH, Grenville-age basement = GV). Hf isotope data (at 420 Ma) of potential sources were calculated based on published Nd isotope data (assuming a Hf-Nd correlation of the terrestrial array (Vervoort and Blichert-Toft, 1999)) by Anderson et al. (2004), Canning et al. (1998), Frost and O'Nions, (1985), Halliday (1984), Hamilton et al. (1980), Harmon (1983), Kay (1980), Muir et al. (1994), O'Nions et al. (1983), Restrepo-Pace et al. (1997), Thirlwall (1982).

Strong evidence exists from Nd isotope data that the mantle below Scotland is highly heterogeneous and contains depleted as well as enriched mantle domains.

Evidence for this was provided by Thirlwall (1982), who carried out a study on Scottish Old Red Sandstone lavas located to the north and south of the Highland Boundary Fault (HBF) and demonstrated that lavas to the south of the HBF display $\varepsilon Nd_{410\ Ma}$ values up to +6.4 (estimated εHf = +11.7 assuming a Hf-Nd correlation of the terrestrial array (Vervoort et al., 1999)), which indicates involvement of a depleted mantle source in their genesis. However, lavas to the north of the HBF, which may be representative of the mantle below the Lochnagar and Etive plutons, display εNd values between +1.1 to -3.6 (estimated εHf = +4.5 to -1.9), which was interpreted as evidence for an enriched mantle domain. In addition, Canning et al. (1998) carried out Nd isotope analyses on two lamprophyre suites from northern and southern Scotland and found two distinct mantle domains separated by the Great Glen Fault. The northern domain ranged in $\varepsilon Nd_{400\ Ma}$ from -6.4 to -12.8 (estimated εHf = -5.7 to -14.4), and the southern domain from +3.9 to -3.4 (estimated εHf = +8.3 to -1.6). The εNd data of the southern domain extends to more positive values, but is generally similar to the data reported by Thirlwall (1982) for lavas north of the HBF, and may therefore be a reasonable estimate of the mantle composition below the plutons. Thus, based on this data and our Hf isotope data a contribution by a contemporary enriched mantle source for the Lochnagar pluton cannot be ruled out and is consistent with the zircons with mantle-like $\delta^{18}O$ values. As zircons from the Etive pluton display much more negative εHf values than those of the Lochnagar pluton the contribution by c. 420 Ma enriched mantle was probably considerably smaller. Melting of an ancient mafic underplate to produce zircons with negative εHf and mantle-like $\delta^{18}O$ values may account for the mantle-like zircons observed in the Etive pluton.

By combining the new Hf and oxygen isotope data the questions of continental growth vs. crustal recycling may now be partially resolved. Neither the Lochnagar nor the Etive pluton contain a significant contemporary depleted mantle component; based on the number of zircons with mantle-like $\delta^{18}O$ values and positive εHf values a contribution by enriched mantle is likely for the Lochnagar pluton, but due to generally crustal εHf values less so for the Etive pluton. Both plutons appear to contain a large crustal component, which probably represents a mixture of supra- and infracrustal sources. Thus, we conclude that at least for the Lochnagar pluton it

cannot be ruled out that it made a significant contribution to crustal growth. However, without more detailed information on the composition and ages of the mantle and crustal sources, which would permit us to carry out AFC modelling (DePaolo, 1981), the proportion of new crust cannot be accurately quantified.

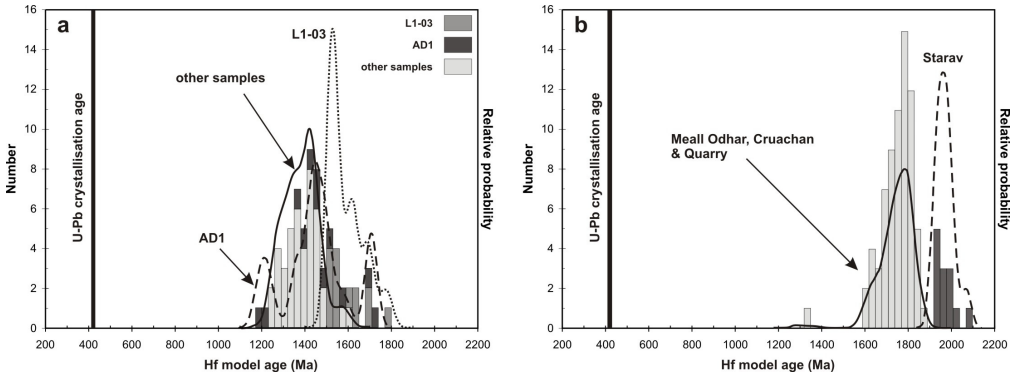

Fig. 8: Hf model ages (TDM_C) of zircons from (a) the Lochnagar pluton and (b) the Etive pluton (probability curves were calculated at 1σ, bin width = 1σ).

6.2. Lower crustal sources

εHf values indicate that the whole-rock geochemical differences between the two plutons are partly the result of compositional variations between the mafic components involved, an enriched contemporary component in the Lochnagar pluton and an ancient mafic underplate in the Etive pluton. However, variations between their infracrustal sources will also be a controlling factor.

Several models have been proposed for the nature, age and affinity of the lower crust below the Grampian Highlands. These are based on geophysical constraints, geochemical and isotopic data for the late Caledonian granites, U-Pb ages of inherited zircons from the granites and wider geological arguments, since appropriate rocks are not exposed in this part of Scotland. U-Pb ages of inherited zircons cannot be considered clear evidence as their origin is ambiguous in the late Caledonian I-type granites. Detrital zircons from the Dalradian Supergroup, the country rocks hosting the granites, display the same ages as inherited zircons in the granites. Thus it is likely that the latter represent minor assimilation of Dalradian rather than lower crustal source material (Paper 2).

The *Lewisian Complex* crops out on the Outer Hebrides, on the coastal mainland of western Scotland, and as inliers within the Moine metasediments located to the east of the Moine Thrust (Park et al., 2002). Geophysical data indicate that these exposures form part of a broad area, which extends further to the north and west. The Lewisian Complex predominantly consists of granulite facies tonalitic gneisses (c. 70 %), which contain mafic and ultramafic enclaves and supracrustal metasediments (e.g. Park, 1991). Nd isotope data show that the gneisses are derived from an igneous protolith that separated from the mantle at c. 2.9 Ga (Muir et al., 1994).

The *Rhinns Complex* is exposed on the islands of Islay and Colonsay in the west of Scotland and on Inishtrahull in Ireland, but it is not clear how far this basement extends beneath the Grampian Highlands. Based on Nd isotope data from Caledonian I-type granites it has been proposed that it forms the basement onto which the Dalradian metasediments (at least in an area of c. 100 km x 600 km) south of the Great Glen Fault were deposited (Dickin and Bowes, 1991; Upton et al., 1998). However, no contacts between the Rhinns Complex and any younger metasedimentary strata can be found (Rollin, 1994). The Rhinns Complex comprises deformed syenites, gabbros and minor felsic and mafic intrusions that were derived from a juvenile mantle source at c. 1.8 Ga (Daly et al., 1991; Muir, 1990).

Grenvillian basement (c. 1.2-1.0 Ga) can be found in only a single location, i.e. in the Glenelg-Attadale Inlier in the northwest Highlands. The inlier contains two units; the Western Unit is believed to represent correlatives of the Lewisian Complex (Barber and May, 1975; May et al., 1993), but the Eastern Unit comprises eclogites, which formed and retrogressed during the Grenville orogeny (Brewer et al., 2003; Sanders et al., 1984) as constrained by zircon and titanite dating (Brewer et al., 2003).

Rocks of the *Dava and Glen Banchor successions*, i.e. gneissose and locally migmatitic psammite and semi-pelite with subordinate quartzite, are known to also underlie parts of the Dalradian Supergroup (Highton et al., 1999; Piasecki, 1980). Dating of detrital zircons has shown that at least rocks of the Dava Succession were predominantly derived from Palaeoproterozoic- and Grenville-age sedimentary protoliths (Highton et al., 1999).

Although these potential lower crustal source rocks are exposed in only relatively small areas and predominantly in the west of Scotland, U-Pb SHRMIP dating of detrital zircons from the Dalradian Supergroup (Cawood et al., 2003) has shown that Archaean- (2.8-2.7 Ga), Palaeoproterozoic- (1.8-1.5 Ga) and Grenville-age (1.1-0.9 Ga) crust must exist across a much larger area.

Two-stage Hf model ages are commonly used to constrain the crustal residence ages of granite protoliths. However, interpretations based on Hf model ages can be ambiguous for the following reasons:

(1) Lu and Hf fractionate during magmatic processes, which leads to significant differences in the $^{176}Lu/^{177}Hf$ ratio between primitive and evolved rocks. For example, high Lu/Hf ratios, typical of mafic crust, will give maximum Hf model ages, whereas low Lu/Hf ratios representative of felsic crust will give minimum Hf model ages (Nebel et al., 2007). Unfortunately it is not possible to determine the $^{176}Lu/^{177}Hf$ ratio of the protolith, and therefore calculations have to be based on approximate (assumed) values. Using the $^{176}Lu/^{177}Hf$ ratio of the granite whole-rock should be the most logical choice as it should be representative of the protolith. However, this assumes that the magma did not undergo any Lu/Hf fractionation during its evolution. Alternatively the $^{176}Lu/^{177}Hf$ of the average crust ($^{176}Lu/^{177}Hf$ = 0.015; Griffin et al., 2002), the average felsic lower crust ($^{176}Lu/^{177}Hf$ = 0.0093; Vervoort and Patchett, 1996) or the average mafic crust ($^{176}Lu/^{177}Hf$ = 0.022; Vervoort and Patchett, 1996) may be used, which is as large an assumption as using the first approach.

(2) In an environment where multiple sources were mixed, a likely scenario based on the large spread in zircon $\delta^{18}O$ and εHf data found in both plutons, the Hf model ages will reflect an intermediate age between the different end-members. Thus, only if a granite has a simple source, did not undergo any mixing and the correct $^{176}Lu/^{177}Hf$ was used, will the Hf model ages reflect the true time of separation from the mantle.

In this study we calculated Hf model ages using the $^{176}Lu/^{177}Hf$ of the average crust (TDM_C), and for comparison also using the whole-rock $^{176}Lu/^{177}Hf$ ratio of each granite sample (TDM_W) (Fig. 9). The resulting model ages differ by ~150-300 m.y., with TDM_C ages representing the older ages. For Lochnagar, TDM_C ~ 1.8-1.2

Ga and TDM_W ~ 1.4-1.0 Ga; for Etive, TDM_C ~ 2.1-1.3 Ga and TDM_W ~ 1.8-1.2 Ga. Thus, linking the ages to any of the potential lower crustal sources is difficult. The best example to illustrate this is the Starav Intrusion of the Etive pluton, for which TDM_C ages range from 2.1 Ga to 1.9 Ga and TDM_W from 1.7 Ga to 1.6 Ga. Based on TDM_C ages the Starav Intrusion comprises magmas derived from melting of Rhinns and Lewisian lower crust, whereas based on TDM_W ages it is sourced in the Rhinns Complex and Grenville-age basement (1.2-1.0 Ga). Nevertheless, TDM_C and TDM_W Hf model ages provide strong evidence that the lower crust beneath the Etive pluton is, at least in parts, older than beneath the Lochnagar pluton.

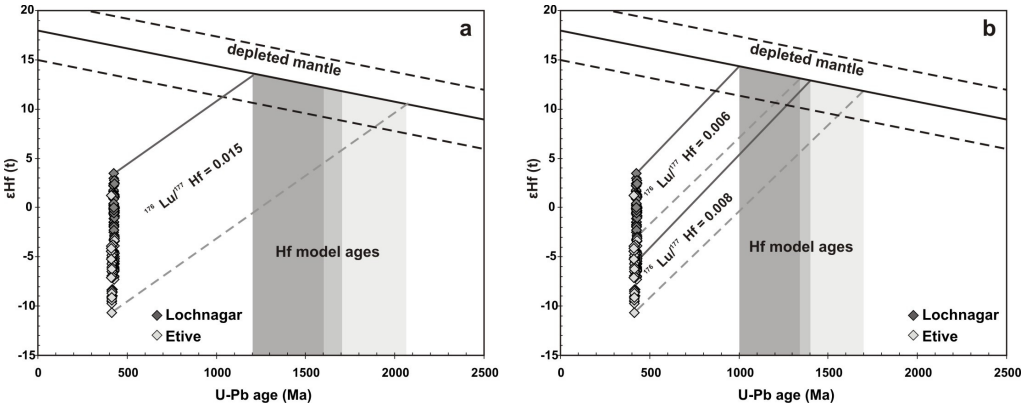

Fig. 9: Hf model ages of the Lochnagar and Etive plutons calculated based on (a) the $^{176}Lu/^{177}Hf$ ratio of the average crust, and (b) the plutons' average whole-rock $^{176}Lu/^{177}Hf$ ratios.

In general, the lower crust is known to be highly heterogeneous due to melting and intracrustal differentiation (Rudnick, 1995). Thus, the most likely model for the lower crust beneath the Lochnagar and Etive plutons is that it represents a complicated mixture of Archaean- to Neoproterozoic-age material. The proportional contributions from different sources varies between the plutons, with the Lochnagar pluton predominantly representing larger proportions of Mesoproterozoic-age lower crust, and the Etive pluton of Palaeo- and Mesoproterozoic-age lower crust. This is supported by the εHf vs. $\delta^{18}O$ diagram (Fig. 7), which for zircons from the Lochnagar pluton shows large overlap with the field for the Grenville basement, and for zircons from the Etive pluton with fields for the Lewisian granulites, Rhinns Complex and Grenville basement. Evidence for the involvement of several sources

can be found in both plutons. For Lochnagar this can be demonstrated in samples of the L1 granite and the Allt Darrarie diorite. Even though both L1 samples were collected within the same mapped unit, they have distinct Hf isotope compositions (L1-03: -1.5 to -5.8; L1-06: +1.2 to -2.3), which overlap by only 0.8 εHf units. This suggests that the L1 granite and therefore the Lochnagar pluton comprise at least two sources of differing Hf isotope compositions. All analysed samples except the Allt Darrarie diorite were predominantly derived from either one of those sources; zircons of the Allt Darrarie diorite, which display nearly the same range of εHf values (8.2 units) as the entire pluton, appear to represent a mixture of both sources. Evidence of at least two sources was also discovered in the Etive pluton. Zircons of the Meall Odhar, Cruachan and Quarry intrusions were derived from a source with εHf values between -3.0 and -7.3, whereas zircons of the Starav Intrusion form a separate cluster at -8.3 and -10.6. In contrast to the Lochnagar pluton, these sources do not appear to have mixed with each other. The observed Hf isotope heterogeneities between the plutons' mapped units, within units and between zircon crystals provide further evidence that magma generation most likely occurred in a deep crustal hot zone and pluton emplacement by incremental assembly as has been proposed by (Paper 1 & 2).

6. Conclusions

1) εHf and Hf model ages indicate different sources for the Lochnagar and Etive plutons. Based on in-situ zircon oxygen isotope analysis both plutons comprise a mantle component. From εHf values a major contemporary depleted mantle component ($\varepsilon Hf_{420\ Ma}$ = +16) can be precluded. However, with εHf values between +3.4 and -5.8 ± 1.0 (2σ) an enriched mantle component cannot be excluded in the Lochnagar pluton. As zircons from the Etive pluton display more negative εHf values between -3.0 and -10.6 ± 1.0 (2σ) melting of an ancient mafic underplate is proposed. Without knowing the composition and ages of the plutons' potential mantle and crustal sources in more detail it is not possible to unambiguously quantify the proportion of new crust. For the Lochnagar pluton a

significant contribution to crustal growth cannot be precluded, however, this appears less likely for the Etive pluton.

2) Both plutons appear to comprise multiple sources. In the Lochnagar pluton one L1 granite sample melted older material than the other granite samples; evidence of mixing between the sources can be observed in the Allt Darrarie diorite. In the Etive pluton the Starav Intrusion melted much older lower crustal material than the Meall Odhar, Cruachan and Quarry intrusions. Evidence for mixing between these sources was not found in the Hf isotope data.
3) The Lochnagar and Etive plutons also show variations between their lower crustal sources. Hf model ages provide strong evidence that the Etive pluton has sourced much older lower crust than the Lochnagar pluton. However, due to the ambiguities of calculating Hf model ages, the potential sources (Lewisian Complex, Rhinns Complex and Grenvillian basement) cannot be easily or quantitatively linked to the plutons. Thus, the most likely model for the lower crust beneath the Lochnagar and Etive plutons is that it represents a complex mixture of remelted material of Archaean- to Neoproterozoic-age material. The contributions from these sources varies between the plutons, with the Lochnagar pluton predominantly representing larger proportions of Mesoproterozoic-age, and the Etive pluton of Palaeo- and Mesoproterozoic-age lower crust. If the two plutons are representative of the Argyll and Cairngorm suites, this study lends support to the hypothesis that the geochemical distinction between these suites lies dominantly in the differences in the ages and compositions of their underlying lower crustal and potentially their mantle sources.

V.

PAPER 4

An integrated O, U-Pb and Hf isotope study of zircons in S-type granites

An integrated O, U-Pb and Hf isotope study of zircons in S-type granites

S.K. Appleby [a,*], M.R. Gillespie [b], C.M. Graham [a],
R.W. Hinton [a], G.J.H. Oliver [c], EIMF [d]

[a] *Grant Institute of Earth Science, University of Edinburgh, West Mains Road, Edinburgh, EH9 3JW, UK*

[b] *British Geological Survey, Murchison House, West Mains Road, Edinburgh, EH9 3LA, UK*

[c] *School of Geography & Geosciences, Crustal Geodynamics Group, University of St. Andrews, St. Andrews, KY16 9AL, UK*

[d] *Edinburgh Ion Microprobe Facility, University of Edinburgh, West Mains Road, Edinburgh, EH9 3JW, UK*

* corresponding author. Email: S.K.Appleby@sms.ed.ac.uk

Manuscript
Intended for submission to Journal of the Geological Society, London

Abstract

In contrast to I-type granites, which are known to comprise multiple sources with complex petrogenetic histories, S-type granites are thought to typically form by melting of a single supracrustal/sedimentary source. However, this integrated oxygen, U-Pb and Hf isotope study of zircons from three Scottish Caledonian (~460 Ma) S-type granites (Kemnay, Cove and Nigg Bay) demonstrates that all three comprise two or more sources. This conflicts with field evidence, which has been interpreted to indicate that the granites were generated in-situ by melting their current country rocks. As zircons from the Kemnay and Cove granites show ^{18}O-enriched $\delta^{18}O$ values of 9.2 ± 0.6 ‰ (2σ) and 10.0 ± 0.6 ‰, respectively they are likely to have sourced predominantly supracrustal material including their current host country rocks. By contrast, zircons from the Nigg Bay Granite have much lower $\delta^{18}O$ values of 7.3 ± 0.6 ‰ suggesting mixing between a supracrustal source and a

1. Introduction

The distinction of I-type (igneous or infracrustal precursor) granites from S-type (sedimentary or supracrustal precursor) granites, based on extensive whole-rock geochemical studies of the Lachlan Fold Belt granites of southeastern Australia (Chappell and White 1974), implies that granites have distinct and recognisable sources that may be identified from their mineralogy and geochemistry. Subsequent studies have shown that granites have complicated petrogenetic histories and commonly comprise multiple sources (John and Wooden, 1990; Kemp et al., 2007; Kemp and Hawkesworth, 2003; Miller et al., 1990). More recent work in the Lachlan Fold Belt has demonstrated that I-type granites may contain 50 % - and S-types up to 10 % - of a component with a mantle-like signature (Collins, 1996, 1998; Gray, 1984), indicating mixing between crustal- and mantle-derived melts.

Traditionally, studies of granite petrogenesis have been based on whole-rock geochemical and isotopic data. These deliver averaged information and are sensitive to mineralogical modification and chemical exchange. Thus, whole-rock data often do not represent the magma composition from the time of crystallisation, and may lead to incorrect interpretations and models.

By exploiting recent advances in in-situ microanalysis we may address the question of granite sources using geochemical information stored in zircon, a common refractory accessory mineral in granitoid rocks that retains information about its host melt. As zircon typically represents an early-crystallising phase in silicic magmas, it records early-stage melt compositions, and in the form of growth zones, any subsequent changes in melt composition during zircon growth (Hoskin and Schaltegger, 2003; Shore and Fowler, 1996; Vavra, 1990, 1993, 1994). Since zircon contains significant concentrations of U and Th (ppm level) and Hf (percent level) (Kinny and Maas, 2003), it is suitable not only for oxygen isotope analysis but also for U-Pb and Hf isotope analysis. Due to the high spatial resolution of ion microprobes (SIMS) multiple analyses may be made in a single crystal, enabling detection of previously inaccessible intra-grain variations and correlation with textural information. In addition, as SIMS analysis is essentially non-destructive, oxygen and U-Pb isotope analyses may be made on the same c. 20 µm spot, followed

by Hf isotope analysis by laser ablation (LA-MC-ICPMS) on a c. 50 µm spot, allowing integration of the data sets. This approach may be used to constrain the emplacement ages of plutons (U-Pb data), the relative mantle and crustal contributions (O and Hf isotope data) and the crustal residence ages of their sources (Hf isotope data), thus providing a major advance in deciphering the sources and petrogenetic histories of granites. Studies applying this integrated zircon approach have already been carried out on zircons from the Lachlan Fold Belt (Kemp et al., 2007) and from the Scottish late Caledonian (c. 430-400 Ma) I-type granites (Paper 3). However, to our knowledge no such studies have to date been undertaken on zircons from S-type granites. In contrast to I-type granites, which have been shown to commonly represent a complex mixture of mantle-like, infra- and/or supracrustal components (e.g. Kemp et al., 2007), S-type granites commonly comprise only supracrustal/sedimentary source material(s) (e.g. Chappell and White, 1974). By studying zircons from S-type granites it may be possible to obtain essentially unmodified information about their supracrustal precursor, and therefore of one commonly inferred end-member component in I-type granites.

The Scottish late Caledonian I-type granites have been shown to contain a small proportion of older inherited zircons (e.g. Pidgeon and Aftalion, 1978; Paper 2). However, to date it has not been possible to resolve whether these were inherited from an infracrustal or supracrustal source (e.g. their Dalradian Supergroup country rocks). In order to characterise the supracrustal component we selected three representative Caledonian S-type granites (Kemnay, Cove and Nigg Bay), which are thought to have been generated more or less in-situ by melting of a supracrustal precursor, most likely within the Dalradian Supergroup. All three granites are currently hosted by the same country rocks (i.e. the Aberdeen Formation) and are petrographically and geochemically very similar, but differ greatly in size. The specific aims of this study were to use high-precision in-situ oxygen, U-Pb and Hf isotope data from zircons to constrain and compare the isotopic composition of their sources and their petrogenetic evolution, which may differ due to their different pluton sizes.

2. Geological background

2.1. The Caledonian S-type granites

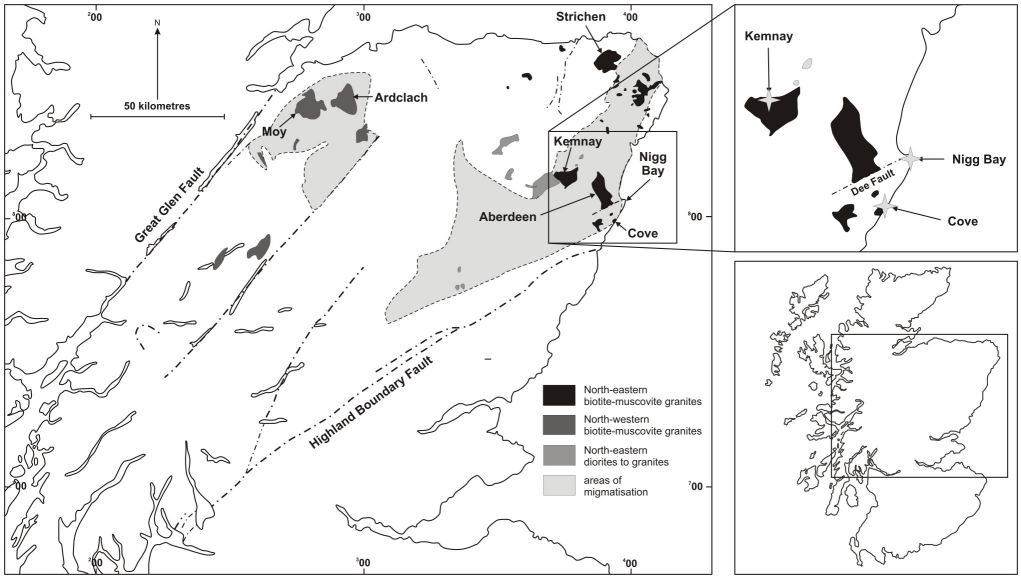

Fig. 1: Map showing the locations of the syn- and late-tectonic granites and diorites that intruded the Grampian Highlands, of the target plutons Kemnay, Cove and Nigg Bay and of collected samples (after Stephenson and Gould, 1995).

The Caledonian S-type granites of the Grampian Highlands of Scotland intrude the Dalradian Supergroup, a c. 25 km thick sequence of deformed and metamorphosed late Neoproterozoic to Lower Ordovician shallow- and deep-water sediments and volcanics (Harris et al., 1978, 1994; Stephenson and Gould, 1995). They were generated contemporaneously with and subsequent to the Grampian Event (c. 480 Ma and 465 Ma; Oliver, 2001), which resulted from the collision of the Laurentian continental margin with a volcanic arc that developed during closure of the Iapetus Ocean. The Grampian Event has been divided into four episodes of deformation (D1-D4) (Strachan et al., 2002). D1 defines the onset of deformation and created major folds, ductile shears, tectonic fabrics and greenschist-facies metamorphism. D2 (c. 470 Ma) represents the main phase of deformation and involved rotation and stacking of fold nappes, and Barrovian metamorphism. In the northeastern and possibly in the northwestern Grampian Highlands D2-induced regional metamorphism caused large-scale migmatisation (Fig. 1). Some migmatites

formed by diffusion of elements via a water-rich fluid phase, but the majority were produced by partial melting of the host rock (Munro, 1986). D3 caused localised lower to middle amphibolite-facies metamorphism and in-situ generation of granitic melts and pegmatites. D4 was the weakest deformational episode and created broad upright folds and brittle structures (Strachan et al., 2002). Following crustal thickening, the Grampian terrane experienced cooling, isostatic uplift and decompression in the later stages of the Grampian Event and subsequent to it (465 Ma to 435 Ma) (Dempster et al., 1995; Dewey and Mange, 1999; Oliver, 2001; Oliver et al., 2000; Soper et al., 1999).

The Grampian Event was accompanied by syn- and late-tectonic magmatism. The syn-tectonic mafic and ultramafic 'Newer Gabbros' are large, layered intrusions of cumulate peridotite, gabbro, norite and syenite (Read, 1961), for which Dempster et al. (2002) reported a zircon TIMS age of 470 ± 9 Ma. The late-tectonic biotite-muscovite granites display peraluminous compositions, high initial $^{87}Sr/^{86}Sr$ values (> 0.71), and high proportions of Dalradian country rock xenoliths and older inherited zircons, all features typical of S-type granites (Harmon, 1983; Pankhurst, 1974; Pidgeon and Aftalion, 1978) (Fig. 1; Stephenson and Gould, 1995; Strachan et al., 2002). They predominantly occur in the previously migmatised areas in northeastern and northwestern Grampian Highlands where they were probably generated due to crustal thickening and radiogenic heating following arc-continent collision, and locally by intrusion of the 'Newer Gabbros' (Gould, 1997; Oliver, 2001).

The North-eastern biotite-muscovite granites, which formed between 475 Ma and 465 Ma (Kneller and Aftalion, 1987; Oliver, 2001; Pidgeon and Aftalion, 1978), range in size from small lensoid or sheet-like bodies (e.g. Nigg Bay Granite) to larger masses (e.g. Cove: ~1.7 km^2, Kemnay: 36 km^2, Aberdeen: 90 km^2). Gradational contacts with the surrounding migmatitic Dalradian country rocks and the occurrence of partly or fully digested and modified metasedimentary xenoliths led to the interpretation that the granites were generated more or less in-situ. However, as many granites show magmatic foliations, sharp contacts with their country rocks, and contain country rock xenoliths with sharp, angular boundaries it has been suggested

that while partial melting of their current country rocks has played an important part, many granites may have been generated at deeper levels (Munro, 1986).

The North-western biotite-muscovite granites comprise variably foliated and recrystallised granites and granodiorites with subordinate leucogranites and pegmatites. Only two U-Pb ages exist for these granites - 455 +27/-15 Ma (monazite) for the Moy Granite (Zaleski, 1983) and 475 ± 7 Ma (monazite) for the Ardclach Granite (Zaleski, 1983). The North-western biotite-muscovite granites were interpreted to have formed towards the end of the Grampian orogenic activity, possibly during decompression following isostatic uplift (Oliver, 2001; Stephens, 1988).

2.2. The Kemnay, Cove and Nigg Bay granites

The Kemnay, Cove and Nigg Bay granites are located close to Aberdeen in the northeastern Grampian Highlands where they crop out over areas of c. 36 km^2, 1.7 km^2 and less than 1 km^2, respectively, in migmatised rocks of the Aberdeen Formation (Fig. 1). Early studies considered the Aberdeen Formation, which comprises psammites, semi-pelites and subsidiary pelites with sparse calc-silicate ribs, to be part of the Argyll Group of the Dalradian Supergroup (Munro, 1986); however, evidence has been found that at least the area south of the river Dee is stratigraphically equivalent to the lower units of the Southern Highland Group (Gould, 1997; Stephenson and Gould, 1995).

2.2.1. The Kemnay Granite

The Kemnay Granite forms a c. 36 km^2 large body around Kemnay and Kintore. It comprises a dominant homogeneous central part and a c. 500 m wide gradational contact zone, which grades into the surrounding migmatitic semi-pelites and feldspathic psammites. In the contact zone the granite is heterogeneous, and shows diffuse compositional layering and abundant partially digested migmatitic country rocks (Gould, 1997).

The central part of the Kemnay Granite consists of medium-grained (1.5-2.5 mm), white biotite-muscovite granite, which displays a weak magmatic foliation

defined by biotite and to a lesser extent by feldspar. It occasionally contains biotite-rich schlieren that are typically 5-10 cm wide and 10 cm long. Some areas show evidence of recrystallisation, hydrothermal alteration and a later tectonic fabric (Gould, 1997).

The inequigranular to weakly porphyritic granite comprises phenocrysts of plagioclase (up to 7.5 mm), quartz (up to 5mm, but recrystallised to smaller crystals of 1.5 mm), K-feldspar (up to 5 mm), and less commonly, biotite (up to 5 mm), and a matrix (1.5-2.5 mm) of the same minerals. Plagioclase (c. 35 %) is typically strongly altered to sericite and in parts replaced by secondary muscovite. Oscillatory zoning and twinning are visible in few crystals. Quartz (c. 30 %) forms anhedral crystals, which are commonly recrystallised to mosaics of smaller crystals. K-feldspar (c. 25 %) crystals commonly show microcline twinning or perthitic exsolution. Generally fresh, strongly pleochroic (beige to dark brown or green) biotite (5 %) occurs as lath-shaped phenocrysts, in interstices, and in the matrix. Muscovite is predominantly present as primary lath-shaped crystals that are up to 2.5 mm long and in interstices; secondary muscovite can be found replacing plagioclase (total muscovite c. 5 %).

2.2.2. The Cove Granite

The Cove Granite crops out over an area of 2 km along the coastal cliffs south of Cove. The contact with the surrounding migmatised country rocks is mostly gradational, but at its southern margin it intruded the country rocks in sheet-like apophyses (Munro, 1986). Biotite clusters and schlieren, which may represent restitic material, as well as pegmatites and quartz veins, are common features.

The unfoliated Cove Granite is dark-grey in colour, fine- to medium-grained (< 1-3.5 mm) and shows an equigranular to weakly inequigranular texture. Plagioclase (c. 30 %), which forms up to 2.5 mm long crystals is typically strongly altered to sericite and replaced by secondary muscovite. Quartz (c. 30 %) predominantly occurs as crystals that are approximately 2.5 mm long, but also in interstices; it is typically strained and shows development of subgrains. K-feldspar (c. 25 %), which forms the largest crystals (up to 3.5 mm) always displays microcline twinning. Pleochroic (beige to dark brown or dark green) biotite (c. 15 %, up to 2 mm) is mostly evenly distributed in thin section, but has also been observed in small possibly restitic biotite

clusters in hand specimen. Muscovite makes up only c. 5 % of the mineral assemblage and is always fine-grained (c. 1 mm). Some may be primary, but most is secondary and replaces plagioclase.

2.2.3. The Nigg Bay Granite

The Nigg Bay Granite is by far the smallest of the three S-type granites, but as it grades into the surrounding strongly migmatised country rocks and contains a high proportion of country rock xenoliths, a reliable estimate of its size cannot be given. Large biotite clots (several cm) and biotite schlieren are common, and in places the original metamorphic fabric is still visible. In addition, a weak magmatic foliation (defined by biotite) may be observed.

The Nigg Bay Granite is dark-grey in colour and has an inequigranular (predominantly < 0.5-4 mm) to porphyritic texture in which plagioclase, K-feldspar and quartz phenocrysts may be up to 1 cm in size. Plagioclase (c. 30 %) is commonly altered, but not as extensively as in the Kemnay and Cove granites, and some crystals show oscillatory zoning. Quartz (c. 30 %) is always strained and K-feldspar (c. 20 %) displays microcline twinning. In contrast to the Kemnay and Cove granites, biotite in the Nigg Bay Granite (15 %) displays red-brown to dark-brown pleochroism. It mostly occurs in clusters with muscovite and has a maximum size of 2 mm. Muscovite (5 %) is predominantly secondary, occurs in clusters with biotite and most often in plagioclase.

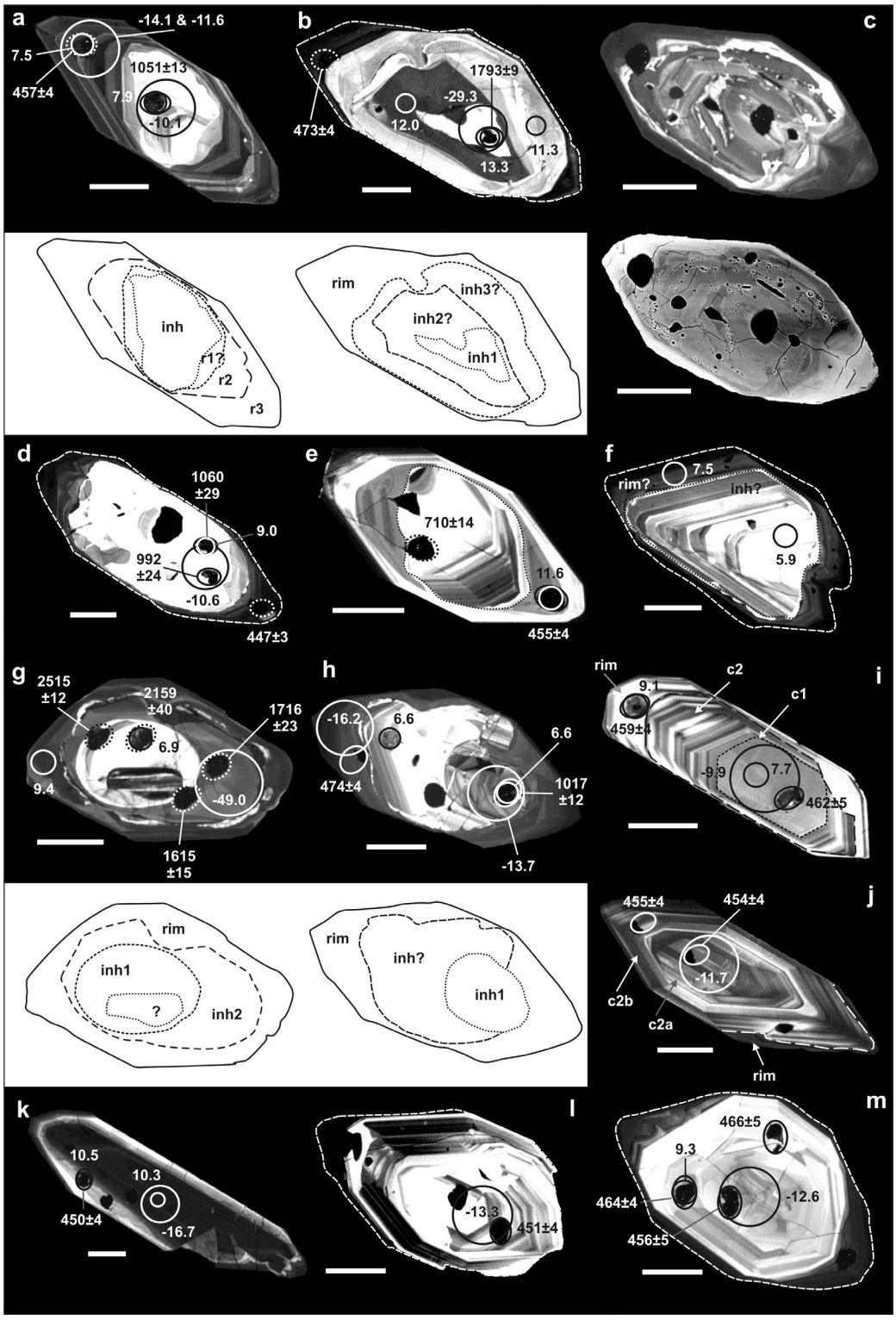
a
-14.1 & -11.6
7.5
1051±13
457±4
7.9
-10.1
b
1793±9
-29.3
473±4
12.0
11.3
13.3
c
inh
r1?
r2
r3
rim
inh3?
inh2?
inh1
d
1060
±29
9.0
992
±24
-10.6
447±3
e
710±14
11.6
455±4
f
rim?
7.5
inh?
5.9
g
2515
±12
2159
±40
1716
±23
6.9
9.4
-49.0
1615
±15
h
-16.2
6.6
6.6
474±4
1017
±12
-13.7
rim
9.1
c2
c1
459±4
-9.9
7.7
462±5
i
rim
inh1
?
inh2
rim
inh?
inh1
455±4
454±4
-11.7
c2b
c2a
rim
j
k
10.5
10.3
450±4
-16.7
l
-13.3
451±4
m
466±5
9.3
464±4
-12.6
456±5

Fig. 2: SEM images of representative inherited and magmatic zircons from the Kemnay, Cove and Nigg Bay granites
a) Zircon comprising strongly luminescent oscillatory zoned inherited core and oscillatory zoned rims (Kemnay, grain 23).
b) Zircon with an inherited core showing an oxygen isotope composition of 13.3 ± 0.6 ‰ in the inner part, 12.0 ± 0.6 ‰ in the outer part of the core and 11.3 ± 0.6 ‰ in the rim (Kemnay, grain 35).
c) CL and BSE images of zircon crystal with large inherited core showing porous, mottled texture (Cove, grain 16).
d) Zircon with unzoned, strongly luminescent inherited core and oscillatory zoned weakly luminescent rim (Cove, grain 9).
e) Zircon with oscillatory zoned and strongly to moderately luminescent inherited core and multiple rims (Cove, grain 12).
f) Zircon crystal comprising an inherited core and magmatic rim representative of the Nigg Bay Granite. Note the variation in $\delta^{18}O$ between the inherited core (5.9 ± 0.6 ‰) and the magmatic rim (7.5 ± 0.6 %) (Nigg Bay, grain 19).
g) Zircon comprising an inherited inner resorbed, unzoned, strongly luminescent core, an inherited outer resorbed, unzoned, moderately luminescent zone and a convoluted weakly luminescent magmatic rim (Cove, grain 20). Note the large variation in $\delta^{18}O$ between the inherited component (6.9 ± 0.6 ‰) and the magmatic rim (9.4 ± 0.6 ‰).
h) Zircon crystal comprising an inherited core and magmatic rim representative of the Nigg Bay Granite (grain 31).
i) Magmatic zircon with a moderately luminescent unzoned inner core domain, an outer oscillatory zoned domain and, separated by a resorption surface, a thin outer weakly luminescent rim (Kemnay, grain 9). Note the large difference in $\delta^{18}O$ between the inner core (7.7 ± 0.6 ‰ (2σ)) and rim (9.1 ± 0.6 ‰).
j) Magmatic zircon crystal with zoned core and oscillatory narrowly zoned rim (separated by strongly luminescent resorption surface) (Kemnay, grain 40).
k) Magmatic zircon with large weakly luminescent unzoned core and oscillatory zoned rim (Cove, grain 7).
l) Magmatic zircon comprising a strongly luminescent unzoned inner core domain, zoned outer core domain and multiple oscillatory zoned rims (Cove, grain 14).
m) Magmatic zircon with strongly luminescent oscillatory zoned core and weakly luminescent rim (Cove, grain 5).
(scale bar = 50 µm; small circles indicate ion probe pit of oxygen isotope analysis, ellipse of U-Pb analysis and large circle of laser Hf isotope analysis; precision of $\delta^{18}O$ = 0.6 ‰ (2σ), of εHf = on average 1.1 units).

3. Samples

As this study has to be considered a pilot study only one sample of the Kemnay, Cove and Nigg Bay granites was chosen for analysis. Zircon crystals in the Kemnay, Cove and Nigg Bay granites are 100-400 µm long and typically stubby; only a few are markedly elongate. In the Kemnay and Cove granites approximately 60 % of crystals, and c. 90-95 ‰ of crystals in the Nigg Bay Granite, comprise a large older inherited core and a narrow weakly or moderately luminescent oscillatory-zoned magmatic rim interpreted to have grown from the granite magma. Zircon crystals commonly contain numerous cracks, and sometimes have a porous, mottled texture, hence poor grain quality.

In the Kemnay Granite inherited cores are commonly more strongly luminescent (Fig. 2a), and in some cases oscillatory zoning is visible. Crystals without an older inherited component are broadly of two types: some comprise a moderately luminescent unzoned inner core domain, an outer oscillatory zoned domain with narrow zones of varying CL intensities and, separated by an obvious resorption surface, a thin outer weakly luminescent rim (Fig. 2i); others consist of an oscillatory-zoned core, a first narrowly zoned rim of similar CL intensity to the core, and a second weakly luminescent rim (Fig. 2j).

In the Cove and Nigg Bay granites crystals with inherited cores display a range of textures and CL intensities. Zoning patterns are commonly complex (Fig. 2b-h), and in at least one crystal multiple inherited components of differing age were found (Fig. 2g). Similarly, magmatic crystals are texturally more variable and do not show any systematic patterns (Fig. 2k-m).

4. Methodology

Major and trace elements were determined at the University of Edinburgh using a PW2404 wavelength-dispersive sequential X-ray spectrometer. Rare earth elements (REEs) and some trace elements (Y, Hf, Th, U) were analysed at the British Geological Survey (BGS) in Nottingham. Zircon separation followed conventional methods and was carried out in the University of St. Andrews Mineral Separation Facility.

Zircon oxygen isotope data were obtained using a Cameca ims-1270 at the Edinburgh Ion Microprobe Facility (EIMF). The method closely followed that of Cavosie et al. (2005), Kemp et al. (2006). Subsequent to oxygen isotope analyses, U-Th-Pb analyses were carried out also using the Cameca ims-1270 at the EIMF. Analytical procedures are similar to those described by Schuhmacher et al. (1994) and Whitehouse et al. (1997), and are described in detail in Kelly et al. (accepted).

Hafnium isotope analysis was carried out at the NERC Isotope Geosciences Laboratory (NIGL) in Nottingham, using a Nu Instruments Nu-Plasma HR multi-collector ICP-MS coupled to a New Wave Research UP193SS 193nm solid state

laser ablation system (a summary data table can be found in Table 1; detailed analytical protocols and full data sets are in Appendices 4a-4f).

5. Results

5.1. Zircon U-Pb data

5.1.1. The Kemnay Granite

Twenty-four zircon crystals from the Kemnay Granite were dated by U-Pb analysis; of these thirteen crystals contain an older inherited core. Magmatic grains and magmatic rims yield a weighted average $^{206}Pb/^{238}U$ age of 457 ± 3 Ma (n=10) (Fig. 3a). Ten concordant inherited zircons give $^{207}Pb/^{206}Pb$ ages of 1047 ± 19 Ma (weighted average age, n=3), 1442 ± 13 (weighted average age, n=3), 1473 ± 16 Ma (n=1), 1525 ± 11 Ma (n=1), 1740 ± 9 Ma (n=1) and 1793 ± 9 Ma (n=1). Discordant inherited zircons yield minimum $^{207}Pb/^{206}Pb$ ages of 794 ± 22 Ma, 899 ± 23 Ma, 997 ± 19 Ma, 1352 ± 11 Ma, 1417 ± 9 Ma and 2556 ± 24 Ma (all n=1) (Fig. 3b).

5.1.2. The Cove Granite

Magmatic cores and rims have a weighted average $^{206}Pb/^{238}U$ age of 458 ± 5 Ma (n=10) (Fig. 3c). Ten out of eighteen analysed crystals have an inherited core. However, only four analyses of these yield concordant $^{207}Pb/^{206}Pb$ ages, of 992 ± 24 Ma, 1060 ± 29 Ma, 1158 ± 32 Ma and 1472 ± 7 Ma (Fig. 3d). Three discordant analyses yield minimum $^{207}Pb/^{206}Pb$ ages of 702 ± 79 Ma, 1716 ± 23 Ma, 2159 ± 40 Ma, 2515 ± 12 Ma and 2685 ± 6 Ma.

5.1.3. Nigg Bay Granite

Seven analyses of magmatic rims give a weighted average $^{206}Pb/^{238}U$ age of 465 ± 5 Ma (n=7) (Fig. 3e). Inherited components were identified in thirteen out of fifteen analysed grains, which have concordant $^{207}Pb/^{206}Pb$ ages of 919 ± 10 Ma (n=1), 997 ± 22 Ma (weighted average age, n=4), 1136 ± 31 Ma (weighted average age, n=2) and 1600 ± 6 Ma (n=1) (Fig. 3f).

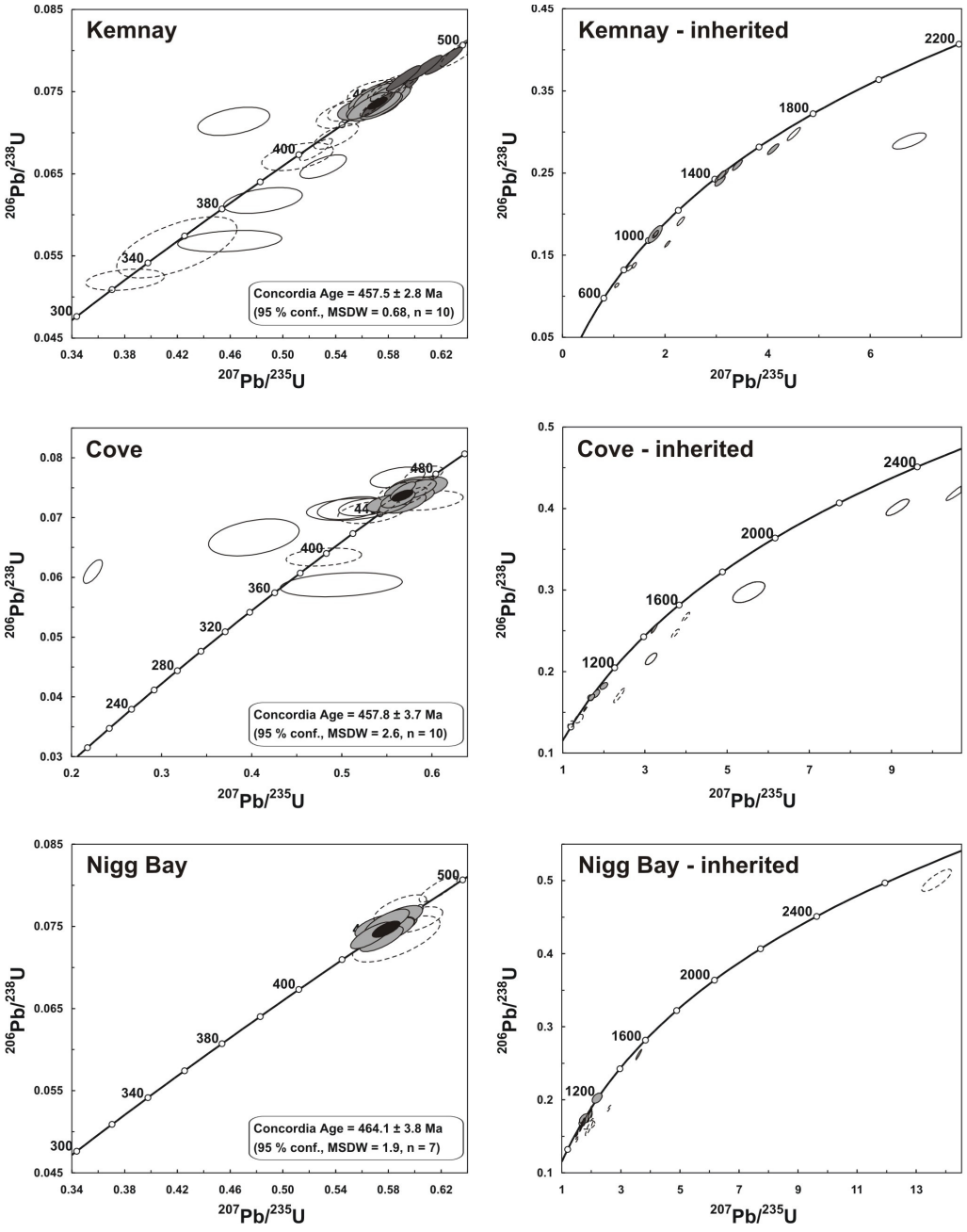

Fig. 3: Concordia diagrams of magmatic zircons and pre-magmtic inherited cores. Grey ellipses represent concordant, white ellipses discordant, white dashed ellipses rejected data points. Data point error ellipses are 2σ.

low-$\delta^{18}O$ component, possibly hydrothermally altered, supracrustal rocks or a mafic infracrustal source. Thus, this pilot study of S-type granites shows that, while field and whole-rock geochemical data have been interpreted to suggest simple melting of supracrustal sources, S-type granites, like I-type granites, may have complex petrogenetic histories and may comprise a mixture of supracrustal ± infracrustal sources.

Table 1
Summary of zircon U-Pb, O and Hf isotope data

sample	U-Pb age [Ma]	2σ	n	$\delta^{18}O$ [‰]		2σ	n	εHf		95% conf.	TDM_C [Ma]	95% conf.	n
Kemnay													
magmatic	457	3	10	9.2	(7.0-12.0)	0.6	19	-13.1	(-9.9 to -17.3)	1.1	2066-2531	67	11
inherited (concordant)	1047-1793	30	10	10.5	(6.7-13.3)	0.6	8	-19.7	(-9.0 to -29.3)	0.9	1647-2456	64	6
inherited (discordant)	794-2556	36	6										
Cove													
magmatic	458	5	10	10.0	(8.8-11.6)	0.6	6	-15.4	(-12.6 to -20.3)	0.9	2234-2718	54	7
inherited (concordant)	992-1472	46	3	7.6	(6.9-9.0)	0.6	3	-30.5	(-10.6 to -49.0)	0.8	1796-3737	59	3
inherited (discordant)	702-2685	55	3										
Nigg Bay													
magmatic	465	5	7	7.3	(6.1-8.4)	0.6	7	-15.6	(-12.2 to -18.5)	0.9	2217-2609	52	4
inherited (concordant)	919-1600	40	8	6.0	(4.1-9.7)	0.6	16	-11.3	(-9.5 to -13.7)	1.0	1662-2310	74	4

5.2. Zircon oxygen isotope data

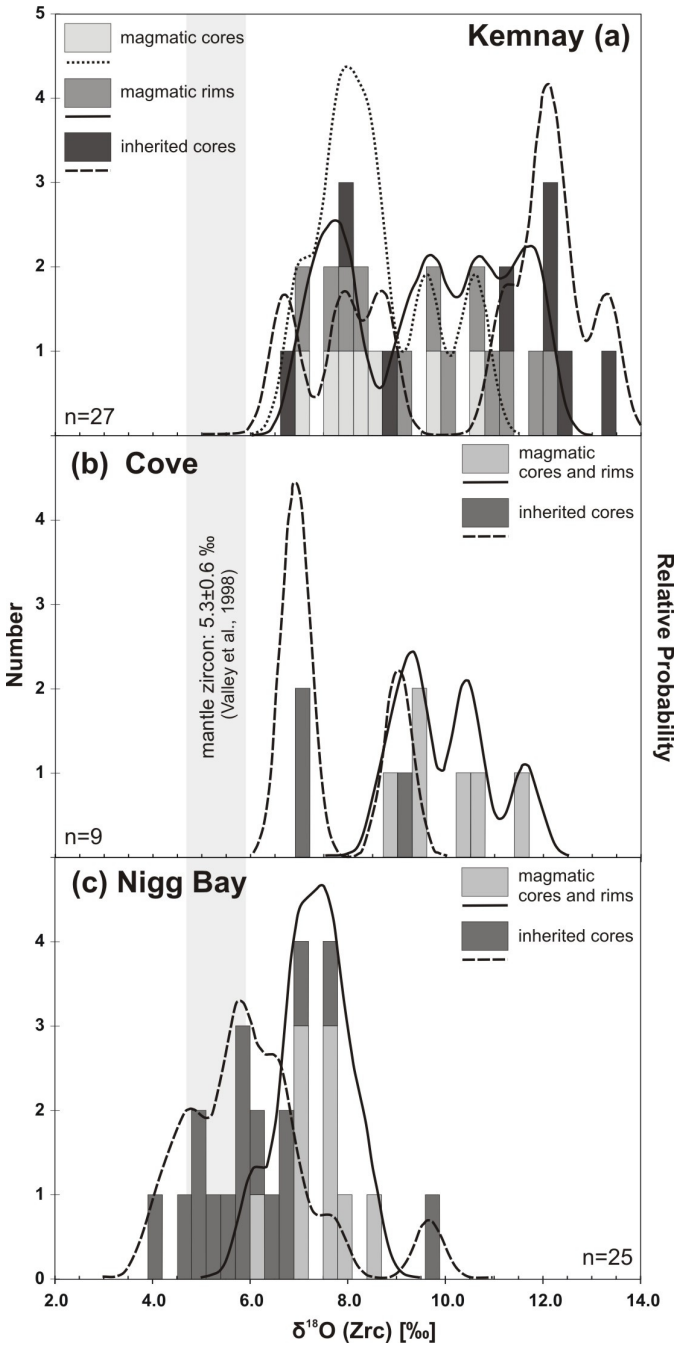

Fig. 4: Cumulative probability plots of zircon oxygen isotope data (probability curves and histograms were calculated at 1σ).

5.2.1. The Kemnay Granite

Magmatic zircons of the Kemnay Granite have a mean oxygen isotope composition of 9.2 ± 3.2 ‰ (2SD; n=19; 7 magmatic cores and 12 rims) and range from 7.0 ‰ to 12 ‰. For comparison, zircon standard 91500 analysed in the same analytical session shows a 2SD uncertainty of ± 0.6 ‰, which approximates the external analytical precision. Some systematic differences exist between magmatic cores and rims (Fig. 4a). Magmatic cores display predominantly low $\delta^{18}O$ values with a mean of 8.6 ± 2.4 ‰, whereas rims cover the entire range and therefore have a mean $\delta^{18}O$ value close to the overall sample mean (9.6 ± 3.4 ‰). Inherited zircons display the highest mean (10.5 ± 4.8 ‰; n=8) and show the largest spread between 6.7 ‰ and 13.3 ‰.

Multiple analyses were made on four magmatic zircon crystals and five crystals comprising an older inherited core. Of these only one magmatic grain (Fig. 2i) and one inherited grain (Fig. 2b) show resolvable intra-grain variations. The magmatic crystal has a core of 7.7 ‰ and a rim of 9.1 ‰; the crystal comprising an inherited core shows a $\delta^{18}O$ value of 13.3 ‰ in the inner part of the core, 12.0 ‰ in the outer part and 11.3 ‰ in the rim.

5.2.2. The Cove Granite

Magmatic zircon cores and rims have a mean $\delta^{18}O$ value of 10.0 ± 2.0 ‰ (2SD, n=6 = 2 cores and 4 rims) (analytical precision = 0.6 ‰ (2σ)). Cores and rims have, within error, the same oxygen isotope composition (cores: 9.8 ± 1.4 ‰; rims: 10.1 ± 2.5 ‰) (Fig. 4b) assuming that this small number of analyses is representative. However, inherited cores are generally less enriched in ^{18}O with a mean $\delta^{18}O$ value of 7.6 ± 2.4 ‰ (n=3). Poor zircon grain quality (cracks, high common Pb, discordance etc.) resulted in many data being rejected, and reliable values for core-rim pairs were obtained from only two crystals. One of these, a wholly magmatic crystal displays no $\delta^{18}O$ variation between core and rim (Fig. 2k), whereas the other displays a large difference (inherited core of 6.9 ‰; magmatic rim of 9.4 ‰) (Fig. 2g; grain 20).

5.2.3. The Nigg Bay Granite

Magmatic zircon rims of the Nigg Bay Granite form a unimodally distributed, relatively tight data cluster (Fig. 4c) with a mean oxygen isotope composition of 7.3 ± 1.4 (2SD, n=9) (analytical precision ± 0.6 ‰ (2σ)). Inherited cores show $\delta^{18}O$ values between 4.1 ‰ and 7.7 ‰ (one outlier at 9.7 ‰) and a mean of 5.8 ± 2.0 (n=15). Resolvable variation between inherited cores and magmatic rims was discovered in one (Fig. 2f) out of four grains where core-rim analyses were carried out. In this crystal (grain 19) the inherited core has a lower $\delta^{18}O$ value (5.9 ‰) than the rim (7.5 ‰).

5.3. Zircon Hf isotope data

5.3.1. The Kemnay Granite

Initial εHf values for magmatic zircons lie between -9.9 ± 1.6 and -17.3 ± 1.9 (quoted errors = 95 % confidence level) (Fig. 5a), with a mean of -13.1 ± 4.4 (2SD, n=11) and a range of 7.4 εHf units. Equivalent two-stage Hf model ages, calculated based on the $^{176}Lu/^{177}Hf$ ratio of the average crust ($^{176}Lu/^{177}Hf$ = 0.015, Griffin et al., 2002), range from 2066 ± 95 to 2531 ± 116 Ma (Fig. 5b). Due to a laser spot size of 50 µm and poor zircon grain quality, it was not possible to carry out multiple analyses on magmatic rims or on magmatic crystals. However, the time-resolved signal revealed a decrease in εHf value from -14.1 ± 0.9 to –11.6 ± 1.8 in one crystal (grain 23, Fig. 2a), which suggests that some intra-grain variation does exist.

Initial εHf values of inherited zircons range from +5.2 ± 1.1 (grain 31, U-Pb age = 1525 ± 11 Ma) to -2.5 ± 1.3 (grain 33, U-Pb age = 1473 ± 16 Ma) (Fig. 5a); Hf model ages vary between 1647 ± 61 Ma (grain 26, U-Pb age = 1047 ± 19 Ma) and 2456 ± 59 Ma (grain 35, U-Pb age = 1793 ± 9 Ma) (Fig. 5c). Re-calculated to 457 Ma, εHf values lie between -9.0 ± 0.8 (grain 26, U-Pb age = 1047 ± 19 Ma) and -29.3 ± 0.8 (grain 35, U-Pb age = 1793 ± 9 Ma).

5.3.2. The Cove Granite

Initial εHf values for magmatic zircon lie between -12.6 ± 0.9 to -20.3 ± 1.1 (Fig. 5a), with a mean of -15.4 ± 5.1 (2SD, n=7) and a range of 7.7 εHf units. Hf model

ages range from 2234 ± 52 Ma to 2718 ± 62 Ma (Fig. 5b). Inherited zircons display initial εHf values of +2.5 ± 1.3 (grain 17, U-Pb age = 1158 ± 32 Ma), +0.7 ± 1.0 (grain 9, U-Pb age: 972 ± 11 Ma) and -21.0 ± 1.2 (grain 20, U-Pb age: 1716 ± 23 Ma) (Fig. 5a). At 458 Ma εHf values are -10.6 ± 0.9, -12.9 ± 0.8 and -49.0 ± 0.8, respectively, and equivalent Hf model ages are 1796 ± 55 Ma, 1825 ± 62 Ma and 3737 ± 59 Ma (Fig. 5c).

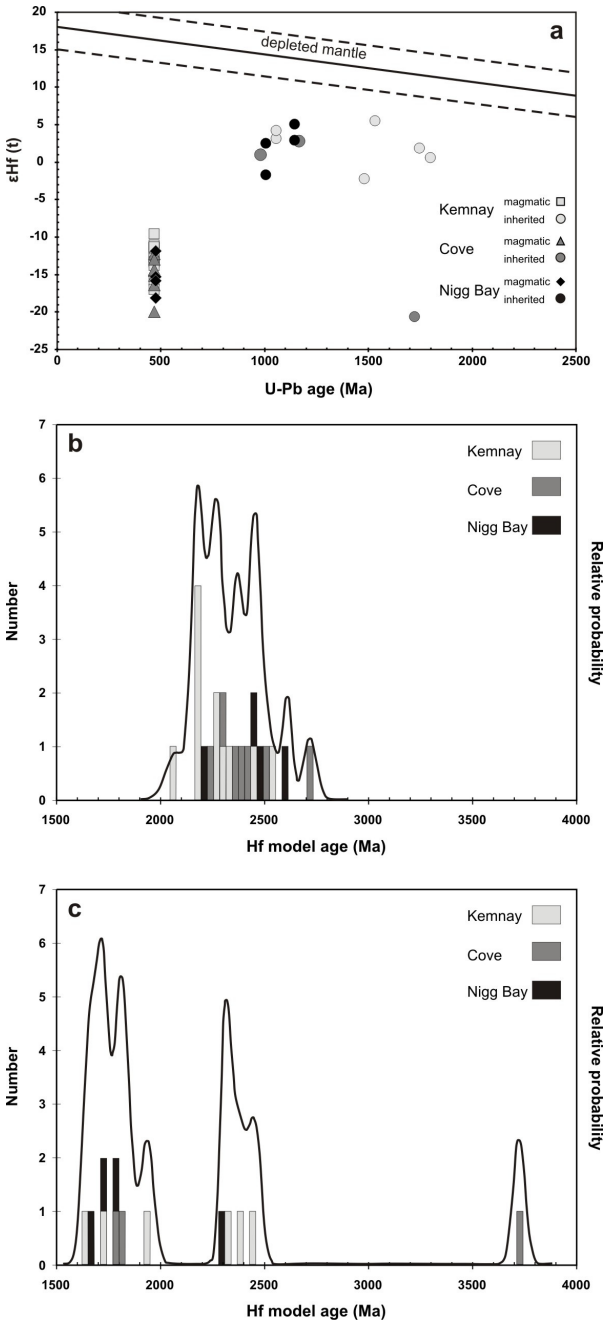

Fig. 5a) U-Pb ages vs. initial εHf values of magmatic and inherited zircons of the Kemnay, Cove and Nigg Bay granites; b) Hf model ages (calculated using average continental crust $^{176}Lu/^{177}Hf$ = 0.015) of magmatic zircons of the Kemnay, Cove and Nigg Bay granites; c) Hf model ages (calculated using average continental crust $^{176}Lu/^{177}Hf$ = 0.015) of inherited zircons of the Kemnay, Cove and Nigg Bay granites.

5.3.3. The Nigg Bay Granite

Magmatic zircons of the Nigg Bay Granite show a spread of 6.3 initial εHf units between -12.2 ± 1.0 and -18.5 ± 0.7 (Fig. 5a), a mean value of -15.6 ± 5.2 (2SD, n=4) and Hf model ages between 2217 ± 58 Ma and 2609 ± 43 Ma (Fig. 5b).

Four inherited cores with U-Pb ages of 997 ± 22 Ma (n=2) and 1136 ± 31 Ma (n=2) show initial εHf values between +4.8 ± 1.4 and -2.0 ± 1.1 (Fig. 5a). At 465 Ma εHf values vary between -9.5 ± 0.8 (grain 25, U-Pb age = 1136 ± 31 Ma) and -13.7 ± 0.8 (grain 31, U-Pb age = 997 ± 22 Ma). Hf model ages range from 1662 ± 67 Ma (grain 25) to 2310 ± 44 Ma (grain 31) (Fig. 5c).

6. Discussion

6.1. Origin and evolution of the Kemnay, Cove and Nigg Bay granites

Zircon crystals in all three granites display a similar range of highly evolved εHf values, typical of ancient continental crust (full range –9.9 to –20.3; Fig. 5a). For comparison, contemporary depleted mantle has an εHf value of approximately +16 ± 3 (Vervoort and Blichert-Toft, 1999). Hf model ages calculated for magmatic and inherited zircon in all three granites are much older than equivalent U-Pb ages, and range from 2.7 to 2.05 Ga in magmatic zircon (Fig. 5b), and from 2.5 Ga and 1.65 Ga (one outlier of 3.75 Ga in the Cove Granite) in inherited zircon (Fig. 5c). Hf model ages are strongly dependent on the $^{176}Lu/^{177}Hf$ ratio used in the calculation, and hence should be considered very rough estimates of the time of separation from the mantle. For example, using the $^{176}Lu/^{177}Hf$ ratio of the granite host ($^{176}Lu/^{177}Hf$ = 0.003-0.004) instead of the average crust ($^{176}Lu/^{177}Hf$ = 0.015; Griffin et al., 2002) results in Hf model ages that are approximately 500 million years younger than those above. The fact that inherited cores have younger model ages than their magmatic rims (with the exception of one inherited core in the Cove Granite, which gave an unrealistic model age of 3.75 Ga) suggests that the $^{176}Lu/^{177}Hf$ ratio of the average crust is not representative here. The actual $^{176}Lu/^{177}Hf$ value(s) of the granite protolith(s) probably lies somewhere between that of the average crust and the host

rock, and may have changed with time as Lu and Hf fractionate during magmatic processes (Nebel et al., 2007). Though the above Hf model ages may not reflect the exact crustal residence ages of protoliths, the data demonstrate that the granite magmas recycled old crust and contain no evidence of a contemporary depleted mantle component.

The absence of published Hf isotope data for Dalradian strata precludes a direct comparison with the granite zircon Hf isotope data. However, several εNd values for the Dalradian have been published from which equivalent εHf values can be calculated using the terrestrial array Hf-Nd correlation (εHf = εNd * 1.36 + 3) of Vervoort et al. (1999). Using the εNd values of Frost et al. (1983) and Frost and O'Nions (1985), calculated at 460 Ma, equivalent εHf values range from -6.1 to -14.0 for the Appin Group (outlier at -27.9; εNd = -6.7 to -12.5), -16.9 to -27.7 for the Argyll Group (εNd = -14.6 to -22.6), and -20.1 to -23.7 for the Southern Highland Group (εNd = -17.0 to -19.6). Thus, magmatic zircons from the Kemnay, Cove and Nigg Bay granites have similar Hf isotope compositions to rocks from the Appin and Argyll groups. In addition, U-Pb age data of inherited zircons found in the granites, which range from c. 1.8 Ga to 1.05 Ga in Kemnay, c. 1.5 Ga to 1.0 in Cove, and 1.6 Ga to c. 0.9 Ga in Nigg Bay, and define dominant peaks at c. 1.05-1.0 Ga and c. 1.45 Ga (discordant age data define an additional small peak at c. 2.7-2.5 Ga) (Fig. 6), are in good agreement with SHRIMP data of detrital zircon from the Grampian, Appin, Argyll and Southern Highland groups of the Dalradian Supergroup (Cawood et al., 2003). The similar Hf isotope compositions between rocks of the Dalradian Supergroup and the granites' magmatic zircons, together with the similar age spectra yielded by inherited and detrital zircon, strongly suggest a Dalradian source and most likely exactly the same source for the magmas, which is consistent with field evidence.

In contrast, large differences exist between the Kemnay, Cove and Nigg Bay granites regarding the oxygen isotope compositions of their magmatic and inherited zircons (Fig. 4). Currently, there are no zircon oxygen isotope data for other Scottish S-type granites, but published whole-rock values (Aberchirder, Aberdeen, Auchedly, Glencroft, Kemnay, Kilmelford, Loch Laggan, Strathspey, Strichen) lie between 9.2 ‰ and 12.1 ‰, with the majority lying above 10 ‰ (Halliday, 1984; Hamilton et al.,

1980; Harmon, 1983; Kay, 1980). Assuming equilibrium between zircons and their host rocks and an oxygen isotope fractionation factor (Δ(WR-Zrc)) of approximately 1.8 at c. 70 wt% SiO_2 (Valley et al., 2005), zircon $\delta^{18}O$ values should range from 7.4-10.3 ‰. Magmatic zircons of the Kemnay and Cove granites show mean values of 9.2 ‰ and 10.0 ‰, typical of S-type granites. However, magmatic zircons of the Nigg Bay Granite have a lower mean $\delta^{18}O$ value (7.3 ‰), similar to those found in I-type granites (e.g. Paper 2). Inherited zircons from the Nigg Bay Granite display even lower $\delta^{18}O$ values (4.1-7.7 ‰, mean = 5.8 ‰) with the majority lying within and even below the field of values for mantle-like zircon (5.3 ± 0.6 ‰, Valley et al., 1998) (Fig. 4c). Thus, even though field, whole-rock geochemical and Hf isotope data for magmatic zircon, and U-Pb isotope data for inherited zircon all provide strong evidence for involvement of a only supracrustal sources in the Kemnay, Cove and Nigg Bay granites, zircon oxygen isotope data show that at least the Nigg Bay Granite contains either additional or entirely different source material.

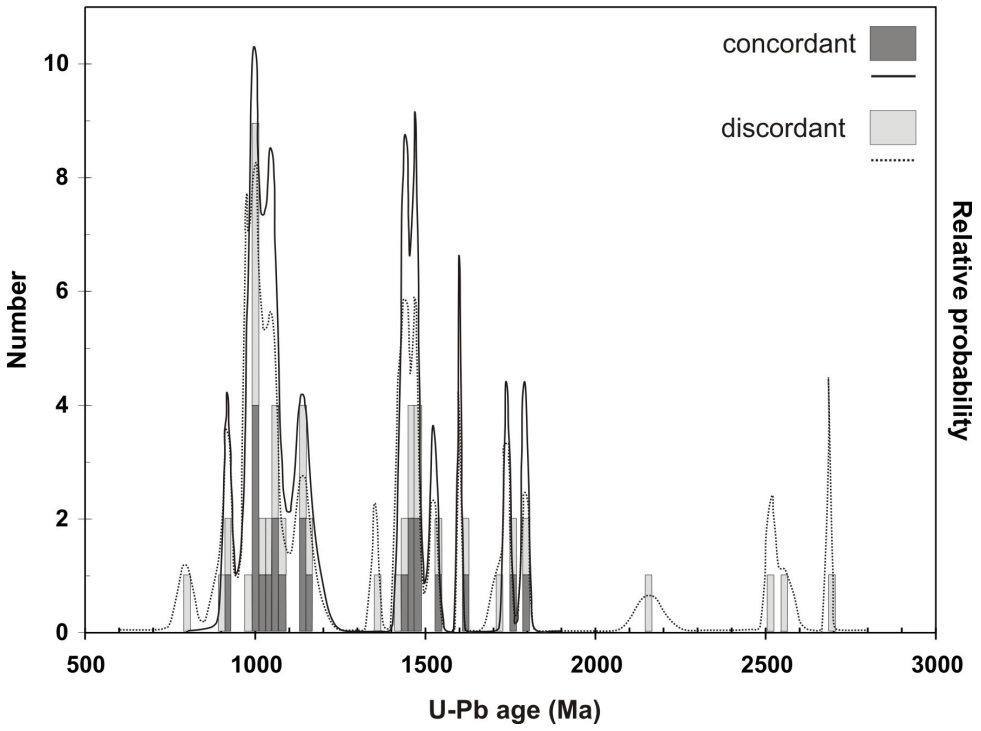

Fig. 6: U-Pb ages of concordant and discordant inherited zircons found in the Kemnay, Cove and Nigg Bay granites.

Combined $\delta^{18}O$ and εHf data for magmatic and inherited zircon in the Kemnay, Cove and Nigg Bay granites define two near-parallel trends; one trend is defined by zircons from the Cove and Kemnay granites, and at lower $\delta^{18}O$ values a second trend is defined by zircons from the Nigg Bay Granite. These trends indicate mixing between at least two components in the granites (Fig. 7). Comparison with published whole-rock oxygen and calculated Hf isotope data for rocks of the Appin, Argyll and Southern Highland groups (Anderson et al., 2004; Frost and O'Nions, 1985; O'Nions et al., 1983) shows good agreement for the Kemnay and Cove granites with those of the Appin Group and to a lesser extent with those of the Argyll Group. Zircons from the Nigg Bay Granite furthermore overlap the field defined by mantle-like zircons.

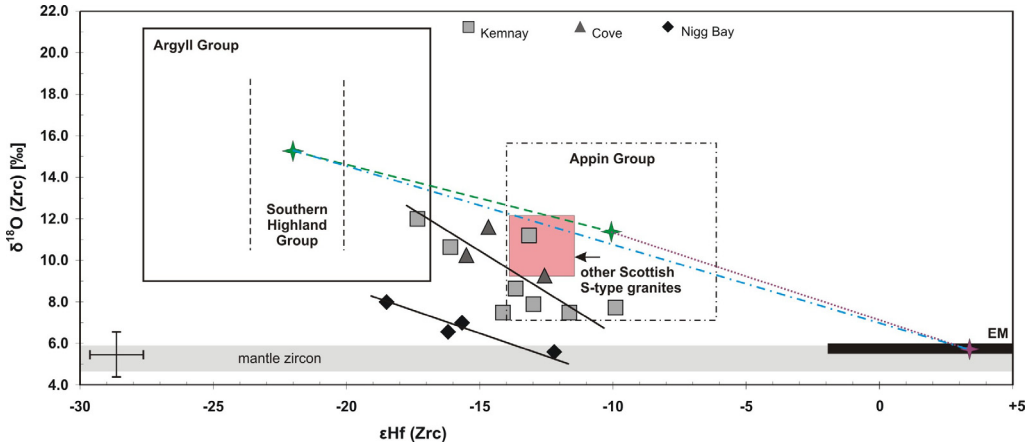

Fig. 7: εHf values (at emplacement age) vs. $\delta^{18}O$ of magmatic zircons of the Kemnay, Cove and Nigg Bay granites (precision on zircon $\delta^{18}O$ and εHf = 0.6 ‰ and 1.0 units (2σ), respectively). Also shown are fields for whole-rock $\delta^{18}O$ and estimated εHf data of the Appin, Argyll and Southern Highland groups, and other Scottish S-type granites (data from Anderson et al., 2004; Frost and O'Nions, 1985; Halliday, 1984; Hamilton et al., 1980; Harmon, 1983; Kay, 1980; O'Nions et al., 1983) and mixing lines (green, purple and blue) between the potential end-members.

Based on these trends three possible petrogenetic models may be proposed for the Kemnay, Cove and Nigg Bay granites: (1) The granites formed by melting of a large proportion of Appin Group and a smaller proportion of Argyll ± Southern Highland Group rocks. Simple two-component magma mixing modelling indicates that zircon $\delta^{18}O$ values of the Kemnay Granite may represent mixing between 35-100 % Appin and 65-0 % Argyll rocks; this ratio changes to 45-100 % Appin and 0-55 % Argyll rocks in the Cove Granite. If field evidence suggesting that the granites were

generated more or less in situ is valid, the low-$\delta^{18}O$ values in magmatic and inherited zircon in the Nigg Bay Granite represent a local low-$\delta^{18}O$, possibly hydrothermally altered, component within the Appin or Argyll groups. (2) Only the Kemnay and Cove granites were generated by melting of Appin Group and Argyll ± Southern Highland Group rocks. The Nigg Bay Granite formed by mixing between Argyll ± Southern Highland Group rocks and an unknown infracrustal source with mantle-like oxygen and crustal Hf isotope characteristics or by mixing with enriched mantle. Based on magma mixing modelling 20-50 % of a mantle-like component may be present in the Nigg Bay Granite. (3) Neither granite involved melting of Appin Group rocks, and all formed by different degrees of mixing between Argyll ± Southern Highland Group rocks and an infracrustal source. In order to produce the observed zircon $\delta^{18}O$ values of the Kemnay and Cove granites 15-65 % of a mantle-like component has to have been incorporated into the supracrustal source rocks.

Several models have been proposed for the nature, age and affinity of the lower crust below the Grampian Highlands, but since appropriate rocks are not exposed in this part of Scotland, these are based on geophysical constraints, geochemical and isotopic data for the late Caledonian granites, U-Pb ages of inherited zircons from the late Caledonian I-type granites and wider geological arguments. Recently, an integrated oxygen, U-Pb and Hf isotope study of zircon in Scottish late Caledonian I-type granites provided evidence that the basement beneath the Grampian Highlands represents a complicated mixture of Archaean- to Neoproterozoic-age material (Paper 3). It may therefore be that the Nigg Bay Granite, and to a lesser extent the Kemnay and Cove granites, comprise mixtures of infracrustal sources rather than one single source.

In addition to varying $\delta^{18}O$ values for magmatic and inherited zircon in the Kemnay, Cove and Nigg Bay granites, the data also differ in the degree of oxygen isotope heterogeneity. An explanation for this may be found in the different body sizes and in the degree of mixing. The Kemnay Granite, by far the largest of the three, shows a 5 ‰ variation in magmatic zircon $\delta^{18}O$ and an even larger spread amongst inherited zircons, whereas the much smaller Cove and Nigg Bay granites display considerably smaller variation (c. 2.5 ‰). The large heterogeneity observed in the Kemnay Granite may result from melting a much larger, and therefore

potentially isotopically more variable, volume of material. Furthermore, inefficient mixing in the Kemnay Granite in contrast to thorough mixing in the isotopically more homogenous Cove and Nigg Bay granites may have also played a role.

6.2. Emplacement of the Kemnay, Cove and Nigg Bay granites

Few reliable ages constrain crystallisation of the Caledonian S-type granites, but published data suggest that those of the northeastern Grampian Highlands crystallised between c. 470 Ma and 465 Ma (Strichen 467 ± 6 Ma (zircon, Oliver, 2001); Aberdeen 470 ± 1 Ma (monazite, Kneller and Aftalion, 1987)). A Rb/Sr mineral age (no isochron) of 411 ± 7 Ma published for the Kemnay Granite (Bell, 1968) is unlikely to be reliable. The new SIMS U-Pb zircon ages for the Kemnay, Cove and Nigg Bay granites (457 ± 3 Ma, 458 ± 5 Ma and 465 ± 5 Ma, respectively) show them to be essentially post-tectonic with respect to the peak Grampian Event deformation (D2) and metamorphism (c. 470 Ma).

6.3. Implications for future studies on I- and S-type granites

The objective of carrying out this study was that S-type granites are believed to be produced by melting of crustal sedimentary rocks, and therefore provide the opportunity to study one of the end-members commonly contributing to I-type granites. Thus, three granites that show typical characteristics of S-type granites (two micas, high proportion of country rock xenoliths and inherited zircon, high SiO_2 contents, peraluminous affinity etc.) were selected. To increase the likelihood of a common source the chosen granites are exposed in the same country rocks, and based on gradational contacts with their current country rocks were thought to have been generated in-situ.

However, based on this integrated oxygen, U-Pb and Hf isotope study of zircons the petrogenetic histories of the granites are not so simple. Rather than forming by melting their current country rocks the granites were probably generated at deeper levels than indicated by field relationships either by: (1) Melting and mixing of at least two supracrustal sources; in the Nigg Bay Granite one supracrustal component

represents local low-$\delta^{18}O$, possibly hydrothermally altered material; Or (2) mixing between one or more supracrustal source(s) and a primitive infracrustal source.

To fully resolve the origin and evolution of the Kemnay, Cove and Nigg Bay granites a more extensive study is required. Nevertheless, this pilot study shows that S-type granites, like I-type granites, may have complex petrogenetic histories and may comprise multiple sources (supracrustal + infracrustal). This raises several important questions: (1) Are the Kemnay, Cove and Nigg Bay S-type granites an exception? Or do the majority of S-type granites in Scotland and worldwide have much more complex petrogenetic histories than recognised by conventional analytical methods? (2) If the low $\delta^{18}O$ (zircon) values observed in Nigg Bay Granite represent a supracrustal rather than an infracrustal source, do I-type granites in reality comprise much larger proportions of supracrustal components, but oxygen isotopes fail to identify them?

6. Conclusions

1) Zircon εHf values of the Kemnay, Cove and Nigg Bay granites suggest an old, probably predominantly Proterozoic-age, supracrustal precursor; no evidence was found of a contemporaneous mantle component. Comparison of zircon εHf values with those calculated for the Dalradian Supergroup show good agreement between the granites and rocks of the Appin Group and to lesser extent with those of the Argyll Group. Furthermore, concordant $^{207}Pb/^{206}Pb$ ages of inherited cores found in the granites match the age spectra determined on detrital zircons of the Appin, Argyll and Southern Highland groups. Based on these data the granites appear to have melted a Dalradian source and most likely exactly the same source, which is consistent with field evidence.
2) The Kemnay and Cove granites show mean zircon oxygen isotope compositions of 9.2 ‰ and 10.0 ‰, hence values typical of S-type granites. However, magmatic zircons of the Nigg Bay Granite have a lower mean $\delta^{18}O$ value (7.3 ‰), similar to those found in I-type granites. Thus, at least the Nigg Bay Granite contains a different source.

3) Combined $\delta^{18}O$ and εHf data for magmatic and inherited zircon in the Kemnay, Cove and Nigg Bay granites define two near-parallel trends, which indicate mixing between at least two components in all three granites, which may be either at least two supracrustal sources, or supracrustal and infracrustal sources. This suggests that the granites did not form in-situ by melting of their current country rocks, but at deeper levels.
4) Large differences can be observed between the granites in the degree of zircon oxygen isotope heterogeneity. An explanation for this may be found in the different body sizes and in the degree of mixing. The Kemnay Granite, by far the largest of the three, shows the most variation, which probably results from melting and inefficient mixing of much larger, and therefore potentially isotopically more variable, volume of material. The much smaller Cove and Nigg Bay granites display considerably less variation (c. 2.5 ‰) suggesting thorough mixing during and after melting.
5) The Kemnay, Cove and Nigg Bay granites were emplaced at 457 ± 3 Ma, 458 ± 5 Ma and 465 ± 5 Ma, respectively; hence they are essentially post-tectonic with respect to the peak Grampian Event deformation (D2) and metamorphism (c. 470 Ma). This observation also supports the formation of the granites at deeper crustal levels.

VI.

CONCLUSIONS

Conclusions

This PhD study aimed to use the isotope and trace element record preserved in zircon crystals from granitic rocks in order to:

- Constrain the contribution made by the voluminous late Caledonian I-type granites to Phanerozoic continental growth.
- Test existing models for, and provide new insights into, granite genesis, ascent and emplacement.
- Evaluate the scales of heterogeneity, and hence the complexity of plutonic systems, by combining information obtained on a range of scales, from whole plutons to intra-crystal.
- Determine the compositions and ages of the sources of Caledonian granite suites in more detail, explaining their observed whole-rock geochemical differences, and test existing models of the nature, ages and origins of the basement underlying the Grampian terrane.
- Assess the applicability - and identify the limitations - of integrated multi-isotope and trace element studies of zircon to answering the above questions.

1. Applicability and limitations of integrated multi-isotope and trace element analyses of zircon

This PhD study shows that the integration of oxygen, U-Pb and Hf isotope data from zircons is a very powerful approach to deciphering the origin and evolution of granites, while trace element/REE data from zircons have been found to be of limited use as petrogenetic indicators. On a regional scale it was possible to resolve questions regarding the sources and emplacement of the Caledonian I- and S-type granites, and the basement beneath the Grampian Highlands. On a wider scale the study makes a significant contribution to our understanding of Phanerozoic crustal growth and the complexity of plutonic systems, and provides strong evidence for recent models of magma generation and pluton assembly.

However, some limitations of this approach have also been recognised:

1. Based on oxygen isotope data alone it was not possible to constrain the proportion of contemporary mantle-derived material. Similarly in order to calculate initial Hf isotope compositions U-Pb isotope data are required. Thus, the origin and evolution of granites can only be resolved by integration of oxygen, U-Pb and Hf isotope data.
2. As analyses by ion microprobe and laser ablation ICPMS are time-consuming as well as very expensive, zircons from only a relatively small number of samples can be analysed, which raises the question whether these samples are representative of an entire pluton.
3. Even though the spatial resolution of modern ion microprobes is already very good it is not possible to analyse every growth zone within a zircon crystal, and thus to investigate its complete growth history. This is further limited by the occurrence of cracks and inclusions within the zircon crystals, which have to be avoided during analysis. Outermost zircon rims are commonly too thin to analyse, which results in an over-representation of data obtained from the zircon's central area.
4. Growth histories of individual crystals or samples may be controlled by local processes, and may not be representative of entire magma bodies.
5. In order to resolve relatively subtle variations in Hf isotope composition a laser beam size of approximately 50 μm is required. Thus, Hf isotope data quite possibly represent a mixture of zones with differing Hf isotope composition. In addition, due to the large beam size it is often impossible to make more than one analysis per zircon crystal.
6. By analysing zircons from mineral separates the relationship to the host rock is lost. However, in thin sections the orientations of zircon crystals are ambiguous, which also makes it difficult to interpret the data in a 3-dimensional context.
7. Studies using zircon are based on the assumption that zircon crystallises early in a magma's history. However, the timing of zircon crystallisation is dependent on

a number of factors, particularly magma composition and to a lesser extent temperature, and not all of these factors are well-constrained.

2. The origin and sources of the Caledonian granites

2.1. Crustal growth vs. crustal differentiation

The majority of the continental crust appears to have formed between late Archaean and late Proterozoic times, perhaps intermittently during several rapid crustal growth events (Hawkesworth and Kemp, 2006a, b). However, it has recently been demonstrated that many Phanerozoic orogenic belts (e.g. Central Asian Orogenic Belt, China; Lachlan Fold Belt, southeastern Australia) also contain significant amounts of juvenile crust (DePaolo et al., 1991; Jahn et al., 2000; Samson et al., 1989; Samson et al., 1995; Wu et al., 2000); an integrated oxygen, U-Pb and Hf isotope study of zircon revealed that between 50 % and 85 % of new crust was added by at least some of the Lachlan Fold Belt 'I-type' granite plutons (Kemp et al., 2007).

Recent thermal models suggest that 'deep crustal hot zones', which develop due to repeated intrusion of mantle-derived hydrous basalt sills into the lower and/or middle crust, may play an important role in the generation of intermediate and silicic igneous rocks (Annen et al., 2006; Annen and Sparks, 2002). In these hot zones melt generation is thought to occur in three different ways: (1) by differentiation of hydrous basaltic magma, (2) by mixing between silicic melts, possibly generated by partial melting of infracrustal and/or supracrustal rocks (e.g. Druitt et al., 1999), and mantle-derived mafic magmas, and (3) by partial melting of pre-existing crustal rocks which may include early basalt sills or older mafic lower crust (Annen et al., 2006). All three models involve crustal growth to some degree. However, in model 3 the basaltic intrusions primarily act as a lower- or mid-crustal heat source and are not necessarily an important component of the resulting intermediate and silicic magmas, which thus largely represent crustal differentiation.

Previous whole-rock studies delivered inconclusive results regarding the origin and sources of the voluminous Scottish late Caledonian I-type granites. Some authors proposed that the granites comprise juvenile (mantle) and infracrustal components (Halliday et al., 1979, 1980; Harmon and Halliday, 1980; Clayburn et al., 1983; Halliday, 1984), and thus possibly played an important role in Phanerozoic crustal growth; others suggested melting of infracrustal and supracrustal sources, and thus recycling of pre-existing material (Frost and O'Nions, 1985). Based on the results of this PhD study a step has been made towards resolving this for two large plutons (the Etive and Lochnagar Plutons) representing the Argyll and Cairngorm suites respectively.

Zircon $\delta^{18}O$ values range from 5.3-8.1 ± 0.6 ‰ (mean=6.6 ‰, 2σ) in the Lochnagar and 4.6-8.2 ± 0.4 ‰ (mean=6.5 ‰, 2σ) in the Etive pluton. Some zircon crystals with mantle-like compositions (5.3 ± 0.6 ‰ (2σ, Valley et al.,1998)) occur within the plutons, but the majority (~80 %) display oxygen isotope compositions that are more ^{18}O-enriched than pristine mantle values. Based on these data a model of magma generation by simple differentiation of basaltic material (model 1) can be ruled out. As the oxygen isotope composition of zircon is insensitive to differentiation (Valley et al., 1994) a much larger proportion of zircons with mantle-like $\delta^{18}O$ values would be expected. Thus, the plutons were either generated by mixing between silicic partial melts and mantle-derived mafic magmas (model 2) or by remelting and recycling of pre-existing crustal rocks (model 3). From oxygen isotope data alone it is impossible to distinguish between contributions made by contemporary mantle-derived material and by old mafic lower crust, thus between models 2 and 3. However, the combination of oxygen and Hf isotope data is a powerful method to resolve this important question. Zircons from the Lochnagar pluton display εHf values of +3.4 to -5.8, and those of the Etive pluton display a less radiogenic range of -3.0 to -10.6, whereas by comparison εHf of depleted mantle at 420 Ma is ~ +16. In addition, Hf model ages calculated for the plutons are considerably older than their zircon U-Pb crystallisation ages as follows: Lochnagar: U-Pb = 424-413 Ma, TDM_C ~ 1.7-1.1 Ga, TDM_W ~ 1.4-1.0 Ga; Etive: U-Pb = 423-407 Ma, TDM_C ~ 2.1-1.3 Ga, TDM_W ~ 1.8-1.2 Ga (where TDM_C is calculated based on the $^{176}Lu/^{177}Hf$ ratio of the average crust and TDM_W on the $^{176}Lu/^{177}Hf$ ratio of

each whole-rock sample). Hence, a significant contribution by melts derived from contemporary depleted mantle can be excluded.

Little is known about the composition of the mantle beneath the Grampian terrane, but it has been suggested that the mantle below Scotland is highly heterogeneous and at least locally enriched (Canning et al., 1998; Thirlwall, 1982). For the Lochnagar pluton involvement of an enriched mantle component cannot be excluded, but the much more negative εHf values of zircons from the Etive pluton make it less likely here. Thus, the integration of zircon oxygen and Hf isotope data provide strong evidence that the Lochnagar and Etive plutons, and possibly the late Caledonian I-type granites as a whole, made some contribution to continental growth, but also comprise a large recycled component (at least the Etive pluton).

2.2. Crustal sources of the Lochnagar and Etive plutons

Based on their differing whole-rock geochemical compositions the Lochnagar and Etive plutons have been interpreted to belong to different granite suites – the Cairngorm and Argyll suites, respectively (Halliday et al., 1984). Using whole-rock analysis alone it was not possible to determine the origin of the differences between the suites, but it was proposed that they either reflect heterogeneities in the composition and age of the underlying lower crust and/or mantle, or differences in the relative contributions made by crust and mantle (Halliday et al., 1984).

Using zircon oxygen and Hf isotope data I have been able to demonstrate (1) that the Lochnagar and Etive plutons comprise similar amounts of mafic material, and (2) that these were predominantly sourced from the lower crust. A supracrustal contribution from Dalradian metasedimentary country rocks cannot be precluded, but given the lack of field evidence (e.g. xenoliths - pristine or partly digested - are very rare) and the plutons' $\delta^{18}O$ (zircon) compositions of 6.6 ± 0.6 ‰ (Lochnagar) and 6.5 ± 0.4 ‰ (Etive), which are much lower than those of typical Dalradian metasediments (e.g. Anderson et al., 2004; Frost and O'Nions, 1985), may not have played an important role. Hence, the whole-rock geochemical differences between the plutons, and on a wider scale between the Cairngorm and Argyll suites, were probably predominantly inherited from their lower crustal and possibly their mantle

sources. Significant differences in the ranges of εHf values and Hf model ages between the plutons indicate that the lower crust beneath the Grampian terrane is a heterogeneous mixture of Archaean- to Neoproterozoic-age material. The contributions from these sources vary between the plutons, with the Lochnagar pluton predominantly representing larger proportions of Mesoproterozoic-age, and the Etive pluton of Palaeo- and Mesoproterozoic-age lower crust. However, as due to lack of outcrop little is known by direct observation about the basement beneath the Grampian Highlands the nature and age of the lower crustal sources currently cannot be constrained in more detail.

2.3. The genesis of the Caledonian Kemnay, Cove and Nigg Bay S-type granites

Based on gradational contacts between the granites and their country rocks it has been suggested that the majority of the Scottish Caledonian S-type granites, including the Kemnay, Cove and Nigg Bay granites, were generated more or less in-situ (Kneller and Aftalion, 1987; Richardson and Powell, 1976), by melting of the host metasedimentary rocks. As the Kemnay, Cove and Nigg Bay granites are currently exposed in the same country rocks, i.e. the Aberdeen Formation of the Dalradian Supergroup, they were thought to have sourced exactly the same supracrustal material. However, as the granites vary greatly in outcrop size (Kemnay: ~36 km^2; Cove: ~1.7 km^2; Nigg Bay: even smaller than the Cove Granite), the possibility that the larger granite bodies contain material of source(s) located at deeper levels in the crust could not be discounted.

Supporting evidence for a dominant Dalradian source was found in the U-Pb ages of inherited zircons from the Kemnay, Cove and Nigg Bay granites, which occur in 60-95 % of all analysed zircon crystals and yield similar ages as those reported for detrital zircons from the Dalradian Supergroup (Cawood et al., 2003), and in the Hf isotope data of magmatic zircons, which match Hf isotope data calculated from published Nd data of the Dalradian Appin and Argyll groups. However, zircon oxygen isotope data provide strong evidence that at least the Nigg Bay Granite sourced different material than the Kemnay and Cove granites. With mean $\delta^{18}O$ (magmatic zircon) values of 9.2 ‰ and 10.0 ‰ the Kemnay and Cove granites most

likely formed by melting of only supracrustal material including their current country rocks. The combination of zircon εHf and $\delta^{18}O$ indicates mixing between at least two components. In contrast, zircons from the Nigg Bay Granite are considerably less enriched in ^{18}O with a mean composition of magmatic zircons of 7.3 ‰, which is similar to the oxygen isotope composition of magmatic zircons found in I-type plutons. Inherited cores display even lower values of 4.1-7.7 ‰ (mean = 5.8 ‰). Based on these data the Nigg Bay Granite formed by mixing between supracrustal, possibly Argyll ± Southern Highland Group rocks and an infracrustal source with mantle-like oxygen and crustal Hf isotope characteristics. Alternatively, the low $\delta^{18}O$ values observed in the Nigg Bay Granite were produced by melting of a local low-$\delta^{18}O$, possibly hydrothermally altered, unit within the Appin or Argyll groups. Differences in the degree of mixing resulted in a large spread in $\delta^{18}O$ in zircons from the Kemnay Granite, and tight data clusters in the Cove and Nigg Bay Granites.

This study shows that all three S-type granites comprise at least two different source components and did not form in-situ by simple melting of their current country rocks, which suggests that S-type granites, like I-type granites, have much more complicated petrogenetic histories than previously recognised. The low $\delta^{18}O$ values found in magmatic and inherited zircons from the Nigg Bay Granite suggest that either (1) the granite is not a true S-type granite, but a mixture of I- and S-type, or (2) Dalradian metasediments comprise at least locally relatively large amounts of low-$\delta^{18}O$ material, which raises the question if the late Caledonian I-type granites perhaps contain a larger proportion of Dalradian supracrustal material than previously recognised.

3. Complexities of plutonic systems

Based on detailed mapping of plutons of the Inyo Batholith, and outlier of the Sierra Nevada batholith in California, Krauskopf (1968) in his paper “A Tale of Ten Plutons” suggested that plutons are extremely complex systems that are generated in the lower crust or the upper mantle from where they ascend, subdivide, differentiate, and mingle in an apparently random manner that fundamentally limits our ability to

rationalise, describe and quantify an unambiguous intrusive history from field and geochemical data. Thus, what may appear to be a single pluton or a phase within a pluton based on criteria such as proximity between outcrops, petrography (mineralogy and texture), abundance of dykes and/or enclaves and contact metamorphic effects, may actually comprise several individual magma batches derived from different sources, with differing petrogenetic histories and even of different ages. This raises the question of the extent to which geological maps really capture the identity and petrogenetic history of plutons, and on a wider scale how meaningful tectonic or crustal evolution models that are based on geological maps or a small number of whole-rock samples are.

Strong evidence for this complexity has been provided by recent studies using information stored in zircon. The most significant contributions to our understanding of the origin and evolution of granites have been made by e.g. Kemp et al. (2007), who integrated zircon oxygen, U-Pb and Hf isotope data of zircons from Lachlan Fold Belt I-type granites to demonstrate that the assumed I-type plutons actually comprise a mixture of mantle-derived juvenile and supracrustal sources, and by Coleman et al. (2004), who used ultra-high precision U-Pb data of granitic rocks of the Tuolomne Intrusive suite (Sierra Nevada) to show that the suite was emplaced over a period of c. 10 m.y., and thus comprises magma batches of differing age that were assembled incrementally.

This PhD study makes a major contribution to our understanding of the scale, nature and complexity of plutons. In the Lochnagar and Etive plutons some of this complexity and also differences in complexity between plutons were recognised at outcrop scale. The Lochnagar pluton has previously been mapped as a simple composite pluton comprising two main granite facies (L1 and L2), a third, locally developed, granite facies (L3), microgranites and several marginal diorites (Oldershaw, 1974; Smith et al., 2001). All phases are at outcrop scale relatively homogeneous and may be distinguished by their mineralogical and textural characteristics. In contrast, the Etive pluton comprises four main intrusive phases (the Meall Odhar, Cruachan, Starav and Quarry intrusions), which range in composition from granite to monzodiorite/diorite (Batchelor, 1987; Clayburn et al., 1983). In particular the Cruachan and Quarry intrusions comprise numerous variants

that differ in grain size, major and accessory phase assemblage (Batchelor, 1987; Stephenson et al., 1999).

Oxygen isotope data of zircons from the Lochnagar and Etive plutons are actually very similar between the plutons. Zircons from the Lochnagar pluton cover a range between 5.3 ‰ and 8.1 ± 0.6 ‰ with a mean of 6.6 ± 0.6 ‰ (2σ, n=230); zircons from the Etive pluton spread between 4.6-8.2 ± 0.4 ‰ with a mean of 6.5 ± 0.4 ‰ (2σ, n=209). Thus, in both plutons the data spread is considerably larger than the analytical uncertainty, which suggests that real variation in oxygen isotope compositions occurs in zircons on a pluton scale. Evidence for this heterogeneity was found when comparing $\delta^{18}O$ values of samples collected within separate mapped units, but also from within a single mapped unit. In the Lochnagar pluton the two samples collected from within the Allt Darrarie diorite differ in their mean oxygen isotope composition and also in their data distribution with zircons from sample AD1 showing a mean $\delta^{18}O$ value of 7.1 ± 0.4 (2σ, n=42) and an apparent bimodal distribution, and those from AD2 having a mean composition of 6.6 ± 0.5 (2σ, n=32) and a unimodal distribution. The same variation can be observed between zircons from three L2 granite samples. In the Etive pluton the most variation occurs between zircons from four different samples collected in the Cruachan Intrusion. Zircons from two of these samples (Cr-11 & Cr-17) are very heterogeneous (range up to 3 ‰) and randomly distributed, whereas those of the other two (Cr-15 & Cr-26) are relatively homogeneous and show a unimodal distribution. Thus, samples from both the Lochnagar and Etive plutons may be homogeneous or heterogeneous in their distribution of zircon $\delta^{18}O$ values. Heterogeneous samples appear to be more abundant in the Etive pluton (6 out of 10 are heterogeneous) in comparison to the Lochnagar pluton (2 out of 10 are heterogeneous). In heterogeneous samples of both plutons, resolvable variations in $\delta^{18}O$ occur between zircon crystals and within zircon crystals of a single sample. Where resolvable intra-grain variations were detected, both decreases and increases of $\delta^{18}O$ with zircon growth were observed, providing evidence for magma mixing.

U-Pb isotope data reveal that the emplacement histories of both plutons are more protracted and complicated than previously recognised with magmatic activity at the Lochnagar pluton lasting for c. 11 m.y. (424 ± 5 Ma to 413± 4 Ma) and at the Etive

pluton for c. 16 m.y. (423 ± 2 Ma and 407 ± 2 Ma). Even individual mapped units like the Allt Darrarie diorite (Lochnagar) or the Cruachan Intrusion (Etive) appear to have been emplaced in multiple magma batches rather than in a single pulse (Allt Darrarie diorite: AD1 = 419 ± 2 Ma, AD2 = 413 ± 4 Ma; Cruachan Intrusion: Cr-11 = 421 ± 5 Ma, Cr-17 = 414 ± 6 Ma, Cr-15 = 413 ± 6 Ma, Cr-26 = 413 ± 4 Ma). This provides strong support for recent models of granite emplacement, which suggest that many (and possibly the majority) of plutons are assembled incrementally as a series of sheet-like intrusions over time spans an order of magnitude longer than the thermal lifetime of large magmatic masses, and never existed as a large molten magma body (Brown and McClelland, 2000; Coleman et al., 1995; Wiebe, 1993; Wiebe and Collins, 1998).

These new data suggest that many plutons may be isotopically heterogeneous at all geological scales, raising important questions about the suitability of traditional sampling strategies, and about where the direction, emphasis and scale(s) of interest of future petrogenetic studies of granitic plutons should lie. On the one hand, the new zircon data of this PhD study and of previous studies support Krauskopf's (1968) view about the complexity of granites and the difficulties of mapping granitoid intrusions. They certainly explain why field and whole-rock studies have often delivered inconclusive results or were not able to resolve the petrogenetic evolution of granites. On the other hand, although Krauskopf (1968) doubted that even high-precision geochemical data would be able to resolve the origin and evolution of granites, by carrying out these detailed micro-analytical studies using zircon it has been possible to set much tighter and more quantitative constraints on granite sources, genesis, evolution and emplacement mechanisms, and therefore on the role granites play in the generation and differentiation of the continental crust.

VII.

FUTURE WORK

Future Work

This PhD project has resolved many regional as well as wider-scale 'granite' questions, and has provided a number of ideas for future studies:

- One of the major outcomes of this project is that the Etive pluton and possibly also the Lochnagar pluton made at most a small contribution to continental growth. Further work, involving similar studies of other plutons, is now required to determine the extent to which these two large plutons are representative of the late Caledonian I-type suites.
- Minor appinitic and lamprophyric intrusions, which are broadly contemporaneous with the I-type plutons, have been reported from numerous locations in the Grampian Highlands (Stephenson et al., 1999 and references therein). In addition, evidence mainly in the form of mafic facies and enclaves for the involvement of contemporaneous (~430-400 Ma) basic mantle-derived magma has been found in some of the Argyll (Strontian, Ratagain, Glen Scaddle, Rogart, Ross of Mull plutons) and South Grampians suite (Glen Tilt, Garabal Hill-Glen Fyne, Glen Doll, Comrie plutons) I-type plutons (Stephenson et al., 1999), which suggests that contemporaneous mantle-derived magmas contributed at least locally to the I-type plutons. In order to place quantitative constraints on the amount of mantle input and to obtain more information on the composition of the mantle beneath the Grampian Highlands it is important to carry out integrated oxygen, U-Pb and Hf isotope studies on zircons from plutons thought to comprise contemporaneous (~430-400 Ma) mafic material, and on selected appinites and lamprophyres. At the same time, a thorough investigation of the age and origin of mafic enclaves in Caledonian granite plutons is required to establish their genetic (cognate) or accidental relationship with the host granites.
- Emplacement ages of juvenile igneous rocks exposed in different parts of the world show peaks at 2.7, 1.9 and 1.2 Ga (Condie, 1998; McCulloch and Bennett, 1994), which has led to the interpretation that much of the continental crust was generated in pulses of relatively rapid growth rather than continuously. This has been confirmed by integrated oxygen, U-Pb and Hf isotope studies of inherited

zircons from Lachlan Fold Belt I- and S-type plutons and detrital zircons of the surrounding Ordovician-age metasedimentary rocks (Hawkesworth and Kemp, 2006a, b; Kemp et al., 2006), which showed that crustal generation in Gondwana probably occurred in two major pulses at 3.3 Ga and 1.9 Ga. A study of major granitic plutonism during these periods of rapid crustal growth using the new methodologies used in this and other very recent studies is now required to characterise the nature, age and processes of periods of rapid crustal growth in more detail and to compare the results for those of this study, where crustal growth as represented by the Caledonian I-type granites appears to have been limited.

- In order to further constrain the complexities of plutonic systems and the scales of heterogeneity of various geochemical signatures, an integrated oxygen, U-Pb and Hf isotope study of zircons on samples from a small area (e.g. 100 x 100 m, or 1 x 1 km) within a single mapped unit of a pluton should be carried out in combination with documentation of field/outcrop scale heterogeneity. On the same samples further independent evidence should be sought for petrological, mineralogical, geochemical and isotopic heterogeneities indicative of multiple magma sources and magma mixing; a detailed CL imaging, and geochemical (e.g. Ginibre et al., 2007 and references therein) and isotopic study of plagioclases (e.g. Davidson et al., 2007 and references therein) in granites and diorites in which isotopic evidence for heterogeneity has been recognised in this study would be an obvious starting point for such studies. For example, the Allt Darrarie diorite of the Lochnagar pluton would be very suitable, as it has already been demonstrated in this PhD study that it comprises at least two magma batches of differing composition and age.
- In order to reach the precision necessary to resolve subtle changes in zircon $\delta^{18}O$ with zircon growth a beam size of ~20 µm is required on the Cameca ims-1270 ion microprobe, which makes it impossible to analyse the complete growth history of a zircon crystal. Recent work by Page et al. (2007) has demonstrated that the Cameca ims-1280 ion microprobe can achieve precisions of 0.3 ‰ (2SD) on 10 µm spots. Even though this spatial resolution still does not permit analysing every growth zone in a zircon crystal it possibly allows making double

the number of analyses. An interesting exercise would be to use the Cameca ims-1280 ion microprobe to analyse some of the zircon crystals from this PhD that show oxygen isotope variation in order to gain further insight into intra-grain scale heterogeneities.

- It has been demonstrated in this project that zircons may contain a cryptic record of magma mixing. No other petrological evidence for magma mixing has been found in either the Lochnagar or Etive plutons. For future work it would be interesting to employ the integrated oxygen, U-Pb and Hf isotope approach on zircons from a pluton known to have experienced extensive magma mixing. A good target would be the Irish late Caledonian Galway Granite, where good evidence for magma mixing has been observed in studies based on field and whole-rock data over several decades.
- To fully resolve the origin and evolution of the Caledonian Kemnay, Cove and Nigg Bay S-type granites, and the extent to which these are representative of the ~475-460 Ma S-type granites of the Scottish Caledonides, a more extensive study is required on a more comprehensive sample suite. Such a study should include detailed mapping of the granites and their country rocks, collection of a much larger number of samples (of the granites, country rock xenoliths and the country rocks), whole-rock oxygen isotope analysis of all samples, and additional oxygen, U-Pb and Hf isotope analysis of zircons.

VIII.

REFERENCES

References

Amelin, Y., Lee, D.-C., Halliday, A.N., Pidgeon, R.T., 1999. Nature of the Earth's earliest crust from hafnium isotopes in single detrital zircons. Nature, 399: 252-255.

Anders, E., Grevesse, N., 1989. Abundances of the elements: Meteoritic and solar Geochimica et Cosmochimica Acta, 53: 197-214.

Andersen, T., Griffin, W.L. 2004. Lu-Hf and U-Pb isotope systematics of zircons from the Storgangen intrusion, Rogaland Intrusive Complex, SW Norway: implications for the composition and evolution of Precambrian lower crust in the Baltic Shield. Lithos, 73: 271-288.

Andersen, T., Griffin, W.L., Pearson, N.J., 2002. Crustal evolution in the SW part of the Baltic Shield: the Hf isotope evidence. Journal of Petrology, 43: 1725-1747.

Anderson, R., Graham, C.M., Boyce, A.J., Fallick, A.E., 2004. Metamorphic and basin fluids in quartz-carbonate-sulphide veins in the SW Scottish Highlands: a stable isotope and fluid inclusion study. Geofluids, 4: 169-185.

Annen, C., Blundy, J.D., Sparks, R.S.J., 2006. The genesis of intermediate and silicic magmas in deep crustal hot zones. Journal of Petrology, 47: 505-539.

Annen, C., Sparks, R.S.J., 2002. Effects of repetitive emplacement of basaltic intrusions on thermal evolution and melt generation in the crust. Earth and Planetary Science Letters, 203: 937-955.

Atherton, M.P., Ghani, A.A., 2002. Slab breakoff: a model for Caledonian, Late Granite syn-collisional magmatism in the orthotectonic (metamorphic) zone of Scotland and Donegal, Ireland. Lithos, 62: 65-85.

Atherton, M.P., Petford, N., 1993. Generation of sodium-rich magmas from newly underplated basaltic crust. Nature, 362: 144-146.

Bailey, E.B., Maufe, A.B., 1960. The Geology of Ben Nevis and Glen Coe. Memoir of the Geological Survey, Sheet 53, 2nd edition.

Baker, D.R., Conte, A.M., Freda, C., Ottolini, L., 2002. The effect of halogens on Zr diffusion and zircon dissolution in hydrous metaluminous granitic melts. Contributions to Mineralogy and Petrology, 142: 666-678.

Barber, A.J., May, F., 1975. The history of the Lewisian in the Glenelg Attadale Inlier, lochalsh, Northern Highlands. Scottish Journal of Geology, 12: 35-50.

Batchelor, R.A., 1987. Geochemical and petrological characteristics of the Etive granitoid complex, Argyll. Scottish Journal of Geology, 23: 227-249.

Bateman, P.C., Chappell, B.W., 1979. Crystallization, fractionation, and solidification of the Tuolomne intrusive series, Yosemite National Park, California. Geological Society of America Bulletin, 90: 465-482.

Bea, F. 1996. Residence of REE, Y, Th and U in granites and crustal protoliths; implications for the chemistry of crustal melts. Journal of Petrology, 37: 521-552.

Bell, K., 1968. Age relations and provenance of the Dalradian series of Scotland. Geological Society of America Bulletin, 79: 1167-1194.

Belousova, E.A., Griffin, W.L., O'Reilly, S.Y., Fisher, N.I., 2002. Igneous zircon: trace element composition as an indicator of source rock type. Chemical Geology, 143: 602-622.

Belousova, E.A., Griffin, W.L., Pearson, N.J., 1998. Trace element composition and cathodoluminescence properties of southern African Kimberlite zircons. Mineralogical Magazine, 62: 355-366.

Benisek, A., Finger, F., 1993. Factors controlling the development of prism faces in granite zircons. Contributions to Mineralogy and Petrology, 114: 441-451.

Bindeman, I.N., Valley, J.W., 2001. Low $\delta^{18}O$ rhyolites from Yellowstone: Magmatic evolution based on analysis of zircons and individual phenocrysts. Journal of Petrology, 42: 1491-1517.

Black, L.P., Williams, I.S., Compston, W., 1986. Four zircon ages from one rock: the history of a 3930 Ma-old granulite from Mount Sones, Enderby Land, Antarctica. Contributions to Mineralogy and Petrology, 94: 427-437.

Blichert-Toft, J., Albarède, F., 1997. The Lu-Hf isotope geochemistry of chondrites and the evolution of the mantle-crust system. Earth and Planetary Science Letters, 148: 243-258.

Bluck, B.J., 1983. Role of the Midland Valley of Scotland in the Caledonian orogeny. Transaction of the Royal Society of Edinburgh, Earth Sciences, 74: 119-136.

Bluck, B.J., 1984. Pre-Carboniferous history of the Midland Valley of Scotland. Transaction of the Royal Society of Edinburgh, Earth Sciences, 75: 279-295.

Bons, P.D., Arnold, J., Elburg, M.A., Kalda, J., Soesoo, A., van Milligen, B.P., 2004. Melt extraction and accumulation from partially molten rocks. Lithos, 78: 25-42.

Booth, A.L., Kolodny, Y., Chamberlain, C.P., McWilliams, M., Schmitt, A.K., Wooden, J., 2005. Oxygen isotopic composition and U-Pb discordance in zircon. Geochimica et Cosmochimica Acta, 69: 4895-4905.

Brewer, T.S., Storey, C.D., Parrish, R.R., Temperley, S., Windley, B.F., 2003. Grenvillian age exhumation of eclogites in the Glenelg-Attadale Inlier, NW Scotland. Journal of the Geological Society, London, 160: 565-574.

Brown, E.H., McClelland, W.C., 2000. Pluton emplacement by sheeting and vertical ballooning in part of the Southeast Coast plutonic complex, British Columbia. Geological Society of America Bulletin, 112: 708-719.

Brown, G.C., Francis, E.H., Kennan, P. Stillman, C.J., 1985. Caledonian igneous rocks of Britain and Ireland. In: A.L. Harris (Editor), The Nature and Timing of Orogenic Activity in the Caledonian Rocks of the British Isles Geological Society, London, pp. 1-15.

Brown, G.C., Locke, C.A., 1979. Space-time variations in British Caledonian granites: some geophysical correlations. Earth and Planetary Science Letters, 45: 69-79.

Brown, J.F., 1975. Rb-Sr studies and related chemistry on the Caledonian calc-alkaline igneous rocks of NW Argyllshire, University of Oxford, Oxford.

Brown, P.E., 1991. Caledonian and earlier magmatism. In: Craig, G.Y. (Editor), Geology of Scotland (3rd edition). Geological Society, London, pp. 229-295.

Brown, P.E., Miller, J.A., Grasty, R.L., 1968. Isotopic ages of late Caledonian granitic intrusions in the British Isles. Proceedings of the Yorkshire geological Society, 36: 251-276.

Buddington, A.F., 1959. Granite emplacement with special reference to North America. Geological Society of America Bulletin, 70: 671-747.

Canning, J.C., Henney, P.J., Morrison, M.A., van Calsteren, P.W.C., Gaskarth, J.W., Swarbrick, A., 1998. The Great Glen Fault: a major vertical lithospheric boundary. Journal of the Geological Society, London, 155: 425-428.

Cavosie, A.J., Valley, J.W., Wilde, S.A., E.I.M.F., 2005. Magmatic $\delta^{18}O$ in 4400-3900 Ma detrital zircons: A record of the alteration and recycling of the crust in the Early Archean. Earth and Planetary Science Letters, 235: 663-681.

Cawood, P.A., Nemchin, A.A., Smith, M., Loewy, S., 2003. Source of the Dalradian Supergroup constrained by U-Pb dating of detrital zircon and implications for the East Laurentian margin. Journal of the Geological Society, London, 160: 231-246.

Chappell, B.W., Stephens, W.E., 1988. Origin of infracrustal (I-type) granite magmas. Transaction of the Royal Society of Edinburgh, Earth Sciences, 79: 71-86.

Chappell, B.W., White, A.J.R., 1974. Two contrasting granite types. Pacific Geology, 8: 173-174.

Chappell, B.W., White, A.J.R., 2001. Two contrasting granite types: 25 years later. Australian Journal of Earth Sciences, 48: 827-831.

Chappell, B.W., White, A.J.R., Williams, I.S., Wyborn, D., Wyborn, L.A.I., 2000. Lachlan Fold Belt granites revisited: high- and low-temperature granites and their implications. Australian Journal of Earth Sciences, 47: 123-138.

Chappell, B.W., White, A.J.R., Wyborn, D., 1987. The importance of residual source material (restite) in granite petrogenesis. Journal of Petrology, 28: 1111-1138.

Chen, Y.D., Williams, I.S., 1990. Zircon inheritance in mafic inclusions from Bega Batholith granites, southeastern Australia: an ion microprobe study. Journal of Geophysical Research, 95: 17787-17796.

Claoué-Long, J.C., Compston, W., Roberts, J., Fanning, C.M., 1995. Two Carboniferous ages: a comparison of SHRIMP zircon dating with conventional zircon ages and 40Ar/39Ar analysis. Geochronology Time Scales and Global Stratigraphic Correlation, SEPM Special Publication, 54: 3-21.

Clayburn, J.A.P., 1981. Age and petrogenetic studies of some magmatic and metamorphic rocks in the Grampian Highlands, University of Oxford, Oxford.

Clayburn, J.A.P., Harmon, R.S., Pankhurst, R.J., Brown, J.F., 1983. Sr, O, and Pb isotope evidence for origin and evolution of Etive Igneous Complex, Scotland. Nature, 303: 492-497.

Clemens, J.D., Mawer, C.K., 1992. Granitic magma transport by fracture propagation. Tectonophysics, 204: 339-360.

Coleman, D.S., Glazner, A.F., Miller, J.S., Bradford, K.J., Frost, T.P., Joye, J.L., Bachl, C.A., 1995. Exposure of a Late Cretaceous layered mafic-felsic magma system in the central Sierra Nevada batholith, California. Contributions to Mineralogy and Petrology, 120: 129-136.

Coleman, D.S., Gray, W., Glazner, A.F., 2004. Rethinking the emplacement and evolution of zoned plutons: Geochronologic evidence for incremental assembly of the Tuolomne Intrusive Suite, California. Geology, 32: 433-436.

Collins, W.J., 1996. Lachlan Fold Belt granitoids: products of three-component mixing. Transactions of the Royal Society of Edinburgh: Earth Sciences, 87: 171-181.

Collins, W.J., 1998. An evaluation of petrogenetic models for Lachlan Fold Belt granitoids: implications for crustal architecture and tectonic models. Australian Journal of Earth Sciences, 45: 483-500.

Collins, W.J., 1999. Evaluation of petrogenetic models for Lachlan Fold Belt granitoids: implications for crustal architecture and tectonic models - Reply. Australian Journal of Earth Sciences, 46: 831-836.

Compston, W., Williams, I.S., 1984. U-Pb Geochronology of Zircons from Lunar Breccia 73217 Using a Sensitive High Mass-Resolution Ion Microprobe. Journal of Geophysical Research, 89: B525-B534.

Condie, K.C., 1998. Episodic continental growth and supercontinents: a mantle avalanche connection? Earth and Planetary Science Letters, 163: 97-108.

Corfu, F., Hanchar, J.M., Hoskin, P.W.O., Kinny, P., 2003. Atlas of zircon textures. In: Hanchar, J.M., Hoskin, P.W.O. (Editors), Zircon. Reviews in Mineralogy & Geochemistry, pp. 468-500.

Coward, M.P., 1990. The Precambrian, Caledonian and Variscan framework to NW Europe. In: Hardman, R.F.P., Brooks, J. (Editors), Tectonic Events Responsible for Britain's Oil and Gas Reserves. Geological Society, London, Special Publications, pp. 1-34.

Criss, R.E., Taylor, H.P.Jr., 1986. Meteoric-hydrothermal systems. In: Valley, J.W., Taylor, H.P.Jr., O'Neil, J.R. (Editors), Stable isotopes in high temperature geological processes. Mineralogical Society of America Reviews in Mineralogy, pp. 373-424.

Dallmeyer, R.D., Strachan, R.A., Rogers, G., Watt, G.R., Friend, C.R.L., 2001. Dating deformation and cooling in the Caledonian thrust nappes of north Sutherland, Scotland: insights from $^{40}Ar/^{39}Ar$ and Rb-Sr chronology. Journal of the Geological Society, London, 158: 501-512.

Davidson, J.P., Morgan, D.J., Charlier, L.A., 2007. Isotopic Microsampling of Magmatic Rocks. Elements, 3: 253-259.

Dempster, T.J., Hudson, N.F.C., Rogers, G., 1995. Metamorphism and cooling of the NE Dalradian. Journal of the Geological Society, London, 152: 383-390.

Dempster, T.J., Rogers, G., Tanner, P.W.G., Bluck, B.J., Muir, R.J., Redwood, S.D., Ireland, T.R., Paterson, B.A., 2002. Timing and deposition, orogenesis and glaciation within the Dalradian rocks of Scotland: constraints from U-Pb ages. Journal of the Geological Society, London, 159: 83-94.

DePaolo, D.J., 1981. Trace-element and isotopic effects of combined wallrock assimilation and fractional crystallisation. Earth and Planetary Science Letters, 53: 189-202.

DePaolo, D.J., Linn, A.M., Schubert, G., 1991. The continental crust age distribution: Methods of determining mantle separation ages from Sm-Nd isotopic data and implication to the southwestern United States. Journal of Geophysical Research, 96.

Detrick, R.S., Mutter, J.C., Buhl, P., Kim, I.I., 1990. No evidence from multichannel reflection data for a crustal magma chamber in the MARK area on the Mid-Atlantic Ridge. Nature, 347: 61-64.

Dewey, J.F., Mange, M., 1999. Petrology of Ordovician and Silurian sediments in the Western Irish Caledonides: tracers of a short-lived Ordovician continent-arc collision orogeny and the evolution of the Laurentian-Appalachian-Caledonian margin. In: MacNiociall, C., Ryan, P.D. (Editors), Continental Tectonics. Geological Society, London, Special Publications, pp. 55-108.

Dewey, J.F., Ryan, P.D., 1990. The Ordovician evolution of the South Mayo Trough, western Ireland. Tectonics, 9: 887-903.

Dewey, J.F., Shackleton, R.J., 1984. A model for the evolution of the Grampian tract in the early Caledonides and Appalachians. Nature, 312: 115-120.

Dickinson, J.E., Jr., Hess, P.C., 1982. Zircon saturation in lunar basalts and granites. Earth and Planetary Science Letters, 57: 336-344.

Dodson, M.H., 1973. Closure temperature in cooling geochronological and petrological systems. Contributions to Mineralogy and Petrology, 40: 259-274.

Dowty, E., 1980. Crystal growth and nucleation theory and the numerical simulation of igneous crystallization In: Hargraves, R.B. (Editor), Physics of Magmatic Processes. Princeton University Press, Princeton, New Jersey, pp. 419-485.

Druitt, T.H., Edwards, L., Mellors, R.M., Pyle, D.M., Sparks, R.S.J., Lanphere, M., Davies, M., Barriero, B., 1999. Santorini Volcano. Geological Society of London, Memoirs, 19.

Eiler, J.M., 2001. Oxygen isotope variations of basaltic lavas and upper mantle rocks. Reviews in Mineralogy and Geochemistry, 43: 319-364.

Farver, J.R., Yund, R.A., 1991. Oxygen diffusion in quartz; dependence on temperature and water fugacity. Chemical Geology, 90: 55-70.

Faure, G., Mensing, T.M., 2004. Isotopes: Principles and Applications. Wiley, 928 pp.

Foden, J.D., Green, D.H., 1992. Possible role of amphibole in the origin of andesite: some experimental and natural evidence. Contributions to Mineralogy and Petrology, 109: 479-493.

Fowler, A., Prokoph, A., Stern, R., Dupuis, C., 2002. Organization of oscillatory zoning in zircon: Analysis, scaling, geochemistry, and model of a zircon from Kipawa, Quebec, Canada. Geochimica et Cosmochimica Acta, 66: 311-328.

Fowler, M.B., Henney, P.J., Darbyshire, D.P.F., Greenwood, P.B., 2001. Petrogenesis of high Ba-Sr granites: the Rogart pluton, Sutherland. Journal of the Geological Society, London, 158: 521-534.

Fraser, G.L., Pattison, D.R.M., Heamann, L.M., 2004. Age of the Ballachulish and Glencoe Igneous Complexes (Scottish Highlands), and paragenesis of zircon, monazite and baddeleyite in the Ballachulish Aureole. Journal of the Geological Society, London, 161: 447-462.

Frondel, C., 1953. Hydroxyl substitution in thorite and zircon. American Mineralogist, 38: 1007-1018.

Frost, C.D., Bel., J.M., Frost, B.R., Chamberlain, K.R., 2001. Crustal growth by magmatic underplating: Isotopic evidence from the northern Sherman batholith. Geology, 29: 515-518.

Frost, C.D., O'Nions, R.K., 1985. Caledonian magma genesis and crustal recycling. Journal of Petrology, 26: 515-544.

Frost, T.P., Mahood, G.A., 1987. Field, chemical, and physical constraints on mafic-felsic magma interaction in the Lamarck Granodiorite, Sierra Nevada, California. Geological Society of America Bulletin, 99: 272-291.

Gill, J., 1981. Orogenic Andesites and Plate Tectonics. Springer, Berlin, 390 pp.

Ginibre, C., Wörner, G., Kronz, A., 2007. Crystal Zoning as an Archive for Magma Evolution. Elements, 3: 261-266.

Glazner, A., Bartley, J.M., Coleman, D.S., Gray, W., Taylor, R.Z., 2004. Are plutons assembled over millions of years by amalgamation from small magma chambers? GSA today, 14: 4-11.

Glazner, A.F., Bartley, J.M., 2006. Is stoping a volumetrically significant pluton emplacement process? GSA Bulletin, 118: 1185-1195.

Gould, D., 1997. Geology of the country around Inverurie and Alford. Memoir of the Geological Survey, Sheets 76E and 76W (Scotland).

Gray, C.M., 1984. An isotopic mixing model for the origin of granitic rocks in southeastern Australia. Earth and Planetary Science Letters, 70: 47-60.

Gray, D.R., Foster, D.A., 1997. Orogenic concepts - application and definition: Lachlan Fold Belt, eastern Australia. American Journal of Science, 297: 859-891.

Griffin, W.L., Belousova, E.A., Shee, S.R., Pearson, N.J., O'Reilly, S.Y., 2004. Archean crustal evolution in the northern Yilgarn Craton: U-Pb and Hf isotope evidence from detrital zircons. Precambrian Research, 131: 231-282.

Griffin, W.L., Pearson, N.J., Belousova, E.A., Jackson, S.E., van Achterbergh, E., O'Reilly, S.Y., Shee, S.R., 2000. The Hf isotope composition of cratonic mantle: LAM-MC-ICPMS analysis of zircon megacrysts in kimberlites. Geochimica et Cosmochimica Acta, 64: 133-147.

Griffin, W.L., Wang, X., Jackson, S.E., Pearson, N.J., O'Reilly, S.Y., Xu, X., Zhou, X., 2002. Zircon chemistry and magma mixing, SE China: In-situ analysis of Hf isotopes, Tonglu and Pingtan igneous complexes. Lithos, 61: 237-269.

Gromet, L.P., Silver, L.T., 1983. Rare earth element distributions among minerals in a granodiorite and their petrogenetic implications. Geochimica and Cosmochimica Acta, 47: 925-939.

Grove, T.L., Donnelly-Nolan, J.M., Housh, T., 1997. Magmatic processes that generated the rhyolite Glass Mountain, Medicine Lake volcano, N California. Contributions to Mineralogy and Petrology, 127: 205-223.

Grove, T.L., Elkins-Tanton, L.T., Parman, S.W., Cjatterjee, N., Müntener, O., Gaetani, G.A., 2003. Fractional crystallisation and mantle-melting controls on calc-alkaline differentiation trends. Contributions to Mineralogy and Petrology, 145: 515-533.

Grove, T.L., Kinzler, R.J., 1986. Petrogenesis of andesites. Annual Review of Earth and Planetary Sciences, 14: 417-454.

Grove, T.L., Parman, S.W., Bowring, S.A., Price, R.C., Baker, M.B., 2002. The role of an H2O-rich fluid component in the generation of primitive basaltic andesites and andesites from Mt. Shasta region, N California. Contributions to Mineralogy and Petrology, 142: 375-396.

Guo, J., O'Reilly, S.Y., Griffin, W.L., 1996. Zircon inclusions in corundum megacrysts: I. Trace element geochemistry and clues to the origin of corundum megacrysts in alkali basalts. Geochimica et Cosmochimica Acta, 60: 2347-2363.

Halliday, A.N., 1984. Coupled Sm-Nd and U-Pb systematics in late Caledonian granites and the basement under northern Britain. Nature, 307: 229-233.

Halliday, A.N., Aftalion, M., van Breemen, O., Jocelyn, J., 1979. Petrogenetic significance of Rb-Sr and U-Pb isotopic systems in the 400 Ma old British Isles granitoids and their hosts. In: Harris, A.L., Holland, C.H., Leake , B.E. (Editors), The Caledonides of the British Isles - Reviewed. Special Publications. Geological Society, London Special Publications, pp. 653-662.

Halliday, A.N., Stephens, W.E., 1984. Crustal controls on the genesis of the 400 Ma old Caledonian granites. Physics of the Earth and Planetary Interiors, 35: 89-104.

Halliday, A.N., Stephens, W.E., Harmon, R.S., 1980. Rb-Sr and O isotopic relationships in 3 zoned Caledonian granitic plutons, Southern Uplands, Scotland: evidence for varied sources and hybridization of magmas. Journal of the Geological Society, London, 137: 329-348.

Halliday, A.N., Stephens, W.E., Hunter, R.H., Menzies, M.A., Dickin, A.P., Hamilton, P.J., 1985. Isotopic and chemical constraints on the building of the deep Scottish lithosphere. Scottish Journal of Geology, 21: 465-491.

Hamilton, P.J., O'Nions, R.K., Pankhurst, R.J., 1980. Isotopic evidence for the provenance of some Caledonian granites. Nature, 287: 279-284.

Hanchar, J.M., Miller, C.F., 1993. Zircon zonation patterns as revealed by cathodoluminescence and backscattered electron images: Implications for interpretation of complex crustal histories. Chemical Geology, 110: 1-13.

Hanchar, J.M., Rudnick, R.L., 1995. Revealing hidden structures: The application of cathodoluminescence and backscattered electron imaging to dating zircons from lower crustal xenoliths. Lithos, 36: 289-303.

Harmon, R.S., 1983. Oxygen and strontium isotope evidence regarding the role of continental crust in the origin and evolution of the British Caledonian granites. In: Atherton, M.P., Gribble, C.D. (Editors), Migmatites, Melting and Metamorphism. Shiva, Orpington, pp. 62-79.

Harmon, R.S., Halliday, A.N., 1980. Oxygen and strontium isotope relationships in the British late Caledonian granites. Nature, 283: 21-25.

Harris, A.L., Baldwin, C.T., Bradbury, H.J., Johnson, H.D., Smith, R.A., 1978. Ensialic basin sedimentation: the Dalradian Supergroup. In: Bowes, D.R., Leake, B.E. (Editors), Crustal Evolution in Northwest Britain and Adjacent Regions. Geological Journal Special Issue, pp. 115-138.

Harris, A.L., Haselock, P.J., Kennedy, M.J., Mendum, J.R., 1994. The Dalradian Supergroup in Scotland, Shetland and Ireland. In: W. Gibbsons, Harris, A.L. (Editor), A Revised Correlation of Precambrian Rocks in the British Isles. Geological Society, London, Special Report, pp. 33-53.

Harrison, T.M., Watson, E.B., Aikman, A.B., 2007. Temperature spectra of zircon crystallisation in plutonic rocks. Geology, 35: 635-638.

Hawkesworth, C.J., Kemp, A.I.S., 2006a. Using hafnium and oxygen isotopes in zircons to unravel the record of crustal evolution. Chemical Geology, 226: 144-162.

Hawkesworth, C.J., Kemp, A.I.S., 2006b. Evolution of the continental crust. Nature, 443: 811-817.

Heaman, L.M., Bowins, R., Crocket, J., 1990. The chemical composition of igneous zircon suites: implications for geochemical tracer studies. Geochimica et Cosmochimica Acta, 54: 1597-1607.

Highton, A.J., Hyslop, E.K., Noble, S.J., 1999. U-Pb geochronology of migmatisation in the Northern Central Highlands: evidence for pre-Caledonian (Neoproterozoic) tectonomorphism in the Grampian block, Scotland. Journal of the Geological Society, London, 156: 1195-1204.

Hinton, R.W., Upton, B.G.J., 1991. The chemistry of zircon: variations within and between large crystals from syenite and alkali basalt xenoliths. Geochimica et Cosmochimica Acta, 55: 3287-3302.

Hoffmann, C., 1981. Chi-square testing of zircon populations from an Archean granite-greenstone terrain, Minas Gerais, Brazil. Neues Jahrbuch Mineralogische Abhandlungen, 140: 202-220.

Hoskin, P.W.O., 1998. Minor and trace element analysis of natural zircon ($ZrSiO_4$) by SIMS and laser ablation ICPMS: a consideration and comparison of two broadly competitive techniques. Journal of Trace and Microprobe Techniques, 16: 301-326.

Hoskin, P.W.O., Ireland, T.R., 2000. Rare earth element chemistry of zircon and its use as a provenance indicator. Geology, 28: 627-630.

Hoskin, P.W.O., Schaltegger, U., 2003. The composition of zircon and igneous and metamorphic petrogenesis. In: Hanchar, J.M., Hoskin, P.W.O. (Editors), Zircon. Reviews in Mineralogy & Geochemistry, pp. 27-62.

Izebekov, P., Gardner, J.E., Eichelberger, J.C., 2004. Comagmatic granophyre and dacite from Karymsky volcanic center, Kamchatka; experimental constraints and magma storage conditions. Journal of Volcanology and Geothermal Research, 131: 1-18.

Iziuka, T., Hirata, T., 2005. Improvements of precision and accuracy in in situ Hf isotope microanalysis of zircon using the laser ablation-MC-ICPMS technique. Chemical Geology, 220: 121-137.

Jackson, M.D., Cheadle, M.J., Atherton, M.P., 2003. Quantative modeling of granitic melt generation and segregation in the continental crust. Journal of Geophysical Research, 108: 2332.

Jacques, J.M., Reavy, R.J., 1994. Caledonian plutonism and major lineaments in the SW Scottish Highlands. Journal of the Geological Society, London, 151: 955-969.

Jahn, B.M., Wu, F.Y., Hong, D.W., 2000. Important crustal growth in the Phanerozoic: Isotopic evidence of granitoids from East-Central Asia. Proceedings of the Indian Academy of Science, 109: 5-20.

John, B.E., Wooden J., 1990. Petrology and geochemistry of the metaluminous to peraluminous Chemehuevi Mountains Plutonic suite, northeastern California. In: Anderson, J.L. (Editor), The Nature and Origin of Cordilleran Magmatism. Geological Society of America, Memoir, pp. 71-98.

John, B.E., Wooden J., 1990. Petrology and geochemistry of the metaluminous to peraluminous Chemehuevi Mountains Plutonic suite, northeastern California. In: J.L. Anderson (Editor), The Nature and Origin of Cordilleran Magmatism. Geological Society of America, Memoir, pp. 71-98.

Kay, L., 1980. Oxygen and hydrogen isotope ratio study of Caledonian rocks from northeast Scotland, PhD thesis, University of Aberdeen.

Kelemen, P.B., 1995. Genesis of high Mg# andesites and the continental crust. Contributions to Mineralogy and Petrology, 120: 1-19.

Kelly N.M., Hinton, R.W., Harley, S.L., Appleby, S.K., (accepted). New SIMS U-Pb zircon ages from the Langavat Belt, South Harris, NW Scotland: implications for the Lewisian Terrane Model. Accepted at Journal of the Geological Society, London.

Kemp, A.I.S., Hawkesworth, C.J., 2003. Granitic perspectives on the generation and secular evolution of the continental crust. In: Holland, H.D., Turekian, K.K. (Editors), Treatise on Geochemistry - The Crust. Elsevier, pp. 349-410.

Kemp, A.I.S., Hawkesworth, C.J., Foster, G.L., Paterson, B.A., Woodhead, J.D., Hergt, J.M., Gray, C.M., Whitehouse, M.J., 2007. Magmatic and crustal differentiation history of granitic rocks from Hf-O isotopes in zircon. Science, 315: 980-983.

Kemp, A.I.S., Hawkesworth, C.J., Paterson, B.A., Kinny, P.D., 2006. Episodic growth of the Gondwana supercontinent from hafnium and oxygen isotopes in zircon. Nature, 439: 580-583.

Kemp, A.I.S., Wormald, R.J., Whitehouse, M.J., Price, R.C., 2005b. Hf isotopes in zircon reveal contrasting sources and crystallization histories for alkaline to peralkaline granites of Temora, southeastern Australia. Geology, 33: 797-800.

Keppler, H., 1993. Influence of fluorine on the enrichment of high field strength trace elements in granitic rocks. Contributions to Mineralogy and Petrology, 114: 479-488.

King, E.M., Barrie, C.T., Valley, J.W., 1997. Hydrothermal alteration of oxygen isotope ratios in quartz phenocrysts, Kidd Creek mine, Ontario: Magmatic values are preserved in zircon. Geology, 25: 1079-1082.

King, E.M., Beard, B.L., Johnson, C.M., Valley, J.W., 2002. Oxygen and strontium isotopic evidence for the abrupt and steeply-dipping suture between lithospheric plates in the Idaho batholith. Geological Society of America, Abstracts with Programs, 34: 180.

King, E.M., Valley, J.W., 2001. The source, magmatic contamination, and alteration of the Idaho batholith. Contributions to Mineralogy and Petrology, 142: 72-88.

King, E.M., Valley, J.W., Davis, D.W., 2000. Oxygen isotope evolution of volcanic rocks at the Sturgeon Lake volcanic complex, Ontario. Canadian Journal of Earth Science, 37: 39-50.

King, E.M., Valley, J.W., Davis, D.W., Edwards, G.R., 1998. Oxygen isotope ratios of Archean plutonic zircons from granite-greenstone belts of the Superior Province: indicator of magmatic source. Precambrian Research, 92: 365-387.

King, E.M., Valley, J.W., Stockli, D.F., Wright, J.E., 2004. Oxygen isotope trends of granitic magmatism in the Great Basin: Location of the Precambrian craton boundary as reflected in zircons. GSA Bulletin, 116: 451-462.

Kinny, P.D., Maas, R., 2003. Lu-Hf and Sm-Nd isotope systems in zircon. In: Hanchar, J.M., Hoskin, P.W.O. (Editors), Zircon. Reviews in Mineralogy & Geochemistry, pp. 327-341.

Kinny, P.D., Strachan, R.A., Rogers, G.R., Friend, C.R.L., Knocks, H., 2003. U-Pb geochronology of deformed meta-granites in central Sutherland, Scotland: evidence for widespread Silurian metamorphism and ductile deformation of the Moine Supergroup during the Caledonian orogeny. Journal of the Geological Society, London, 160: 259-269.

Kistler, R.W., Chappell, B.W., Peck, D.L., Bateman, P.C., 1986. Isotopic variation in the Tuolomne Intrusive Suite, central Sierra Nevada, California. Contributions to Mineralogy and Petrology, 94: 205-220.

Kneller, B.C., Aftalion, M., 1987. The isotopic and structural age of the Aberdeen granite. Journal of the Geological Society, London, 144: 717-722.

Köppel, V., Sommerauer, J., 1974. Trace elements and the behaviour of the U-Pb system in inherited and newly formed zircons. Contributions to Mineralogy and Petrology, 43: 71-82.

Kostov, I., 1973. Zircon morphology as a crystallogenic indicator. Kristall und Technik, 8: 11-19.

Krauskopf, K.B., 1968. A Tale of Ten Plutons. Geological Society of America Bulletin, 79: 1-18.

Lackey, J.S., 2005. The magmatic and alteration history of the Sierra Nevada batholith as recorded by oxygen isotope ratios in zircon, titanite, garnet, and quartz. PhD thesis, University of Wisconsin.

Lackey, J.S., Valley, J.W., Hinke, H.J., 2006. Deciphering the source and contamination history of peraluminous magmas using $\delta^{18}O$ of accessory minerals: examples from garnet-bearing plutons of the Sierra Nevada batholith. Contributions to Mineralogy and Petrology, 151: 20-44.

Lackey, J.S., Valley, J.W., Saleeby, J.B., 2005. Supracrustal input to magmas in the deep crust of Sierra Nevada batholith: Evidence from high $\delta^{18}O$ zircon. Earth and Planetary Science Letters, 235: 315-330.

Larsen, L., 1973. Measurement of solubility of zircon ($ZrSiO_4$) in synthetic granitic melts. EOS, 54: 479.

Larsen, L.H., Poldervaart, A., 1957. Measurement and distribution of zircons in some granitic rocks of magmatic origin. Mineralogical Magazine, 31: 544-564.

Leake, B.E., 1978. Granite emplacement: the granites of Ireland and their origin. In: D.R. Bowes, Leake, B.E. (Editor), Crustal evolution in northwestern Britain and adjacent regions. Journal of the Geological Society, Special Issue, pp. 221-248.

Linnen, R.L., Keppler, H., 2002. Melt composition control of Zr/Hf fractionation in magmatic processes. Geochimica et Cosmochimica Acta, 66: 3293-3301.

Lister, C.R.B., 1983. On the intermittancy and crystallization mechanisms of sub-seafloor magma chambers. Geophysical Journal of the Royal Astronomical Society, 73: 351-365.

Lister, J.R., Kerr, R.C., 1991. Fluid-mechanical models of crack propagation and their application to magma transport in dykes. Journal of Geophysical Research, 96: 10049-10077.

Ludwig, K.R., 2003. Isoplot 3.00. Berkeley Geochronology Center Special Publication No. 4

Macaulay, C.I., Fallick, A. E., Haszeldine, R. S., Graham, C. M, 2000. Methods of laser-based stable isotope measurement applied to diagenetic cements and hydrocarbon reservoir quality. Clay Minerals, 35: 313-322.

Matzel, J.E.P., Bowring, S.A., Miller, R.B., 2006. Time scales of pluton construction at differing crustal levels: Examples from the Mount Stuart and Tenpeak intrusions, North Cascades, Washington. GSA Bulletin, 118: 1412-1430.

Maurice, O.D., 1949. Transport and deposition of the non-sulphide vein minerals. V. Zirconium minerals. Economic Geology, 44: 721-731.

May, F., Peacock, J.D., Smith, D.I., Barber, A.J., 1993. Geology of the Kintail district. Memoir of the Geological Survey, Sheet 72W and Part of 71E.

McCulloch, M.T., Chappell, B.W., 1982. Nd isotopic characteristics of S- and I-type granites. Earth and Planetary Science Letters, 58: 51-64.

McCulloch, M.T., Wasserburg, G.J., 1978. Sm-Nd and Rb-Sr chronology of continental crust formation. Science, 200: 1003-1011.

Miller, C.F., Wooden, J.F., Bennett, V.C., Wright, J.E., Solomon, G.C., Hurst, R.W., 1990. Petrogenesis of the composite peraluminous-metaluminous Old Woman-Piute Range batholith, southeastern California; isotopic constraints. In: J.L. Anderson (Editor), The Nature and Origin of Cordilleran Magmatism. Geological Society of America, Memoir, pp. 99-109.

Monani, S., Valley, J.W., 2001. Oxygen isotope ratios of zircon: magma genesis of low $\delta^{18}O$ granites from the British Tertiary Igneous Province, western Scotland. Earth and Planetary Science Letters, 184: 377-392.

Morris, G.A., Page, L., Martinez, V., 2005. New dates (415 Ma) for the Etive Dyke Swarm and the end of the Caledonian Orogeny in the SW Grampian Highlands of Scotland. Jounal of the Geological Society, London, 162: 741-744.

Mortazavi, M., Sparks, R.S.J., 2004. Origin of rhyolite and rhyodacite lavas and associated mafic inclusions of Cape Akrotiri, Santorini: the role of wet basalt in generating calcalkaline silicic magmas. Contributions to Mineralogy and Petrology, 146: 397-413.

Muir, R.J., 1990. The Precambrian basement and related rocks of the southern Inner Hebrides, Scotland, University of Wales, Aberystwyth.

Muir, R.J., Fitches, W.R., Maltman, A.J., 1994b. The Rhinns Complex: Proterozoic basement on Islay and Colonsay, Inner Hebrides, Scotland, and on Inishtrahull, NW Ireland. Transactions of the Royal Society of Edinburgh: Earth Sciences, 85: 77-90.

Munro, M., 1986. Geology of the country around Aberdeen. Memoir of the British Geological Survey, Sheet 77 (Scotland): 124.

Müntener, O., Kelemen, P.B., Grove, T.L., 2001. The role of H2O during crystallisation of primitive arc magmas under uppermost mantle conditions and genesis of igneous

pyroxenites: an experimental study. Contributions to Mineralogy and Petrology, 141: 643-658.

Murthy, M.V.N., 1958. On the crystallization of accessory zircon in granitic rocks of magmatic origin. Canadian Mineralogist, 6: 260-263.

Musselwhite, D.S., De Paolo, D.J., McCurry, M., 1989. The evolution of a silicic magma system - isotopic and chemical evidence from the Woods Mountain Volcanic Center, Eastern California. Contributions to Mineralogy and Petrology, 101: 19-29.

Nebel, O., Nebel-Jacobsen, Y., Mezger, K., Berndt, J., 2007. Initial Hf isotope compositions in magmatic zircon from early Proterozoic rocks from the Gawler Craton, Australia: A test for zircon model ages. Chemical Geology, 241: 23-37.

Nowell, G.M., Kempton, P.D., Noble, S.R., Fitton, J.G., Saunders, A.D., Mahoney, J.J., Taylor, R.N., 1998. High precision Hf isotope measurements of MORB and OIB by thermal ionization mass spectrometry: insights into the depleted mantle. Chemical Geology, 149: 211-233.

Nowell, G.M., Pearson, D.G., Bell, D.R., Carlson, R.W., Smith, C.B., Kempton, P.D., Noble, S.R., 2004. Hf isotope systematics of kimberlites and their megacrysts: new constraints on their source regions. Journal of Petrology, 45: 1583-1612.

Oldershaw, W., 1974. The Lochnagar granitic ring complex, Aberdeenshire. Scottish Journal of Geology, 10: 297-309.

Oliver, G.J.H., 2001. Reconstruction of the Grampian episode in Scotland: its place in the Caledonian Orogeny. Tectonophysics, 332: 23-49.

Oliver, G.J.H., Chen, F., Buchwald, R., Heger, E., 2000. Fast tectonothermal metamorphism and exhumation in the type area of the Barrovian and Buchan zones. Geology, 28: 459-462.

O'Nions, R.K., Hamilton, P.J., Hooker, P.J., 1983. A Nd isotope investigation of sediments related to crustal development in the British Isles. Earth and Planetary Science Letters, 63: 229-240.

Page, F.Z., Ushikubo, T., Kita, N., Riciputi, L.R., Valley, J.W., 2007. High-precision oxygen isotope analysis of picogram samples reveals 2 μm gradients and slow diffusion in zircon. American Mineralogist, 92: 1772-1775.

Pankhurst, R.J., 1974. Rb-Sr whole-rock chronology of Caledonian events in northeast Scotland. Bulletin of the Geological Society of America, 85: 345-350.

Pankhurst, R.J., 1979. Isotope and trace element evidence for the origin and evolution of Caledonide granites in the Scottish Highlands. In: M.P. Atherton, Tarney, J. (Editor), The Origin of Granite Batholiths: Geochemical Evidence. Shiva Publishing Ltd., Kent, pp. 18-33.

Pankhurst, R.J., Sutherland, D.S., 1982. Caledonian granites and diorites of Scotland and Ireland. In: D.S. Sutherland (Editor), Igneous Rocks of the British Isles Wiley, Chichester, pp. 141-190.

Park, R.G., 1991. The Lewisian Complex. In: G.Y. Craig (Editor), Geology of Scotland. Geological Society of London, London, pp. 25-58.

Park, R.G., Stewart, A.D. Wright, D.T., 2002. The Hebridean terrane. In: N.H. Trewin (Editor), The Geology of Scotland. The Geological Society, London, pp. 45-80.

Patchett, P.J., Kouvo, O., Hedge, C.E., Tatsumo, M., 1981. Evolution of continental crust and mantle heterogeneity: evidence form Hf isotopes. Contributions to Mineralogy and Petrology, 78: 279-297.

Paterson, S.R., Fowler, T.K., Jr., Miller, R.B., 1996. Pluton emplacement in arcs; a crustal-scale exchange process. In: M. Brown, Piccoli, P.M. (Editor), The Third Hutton Symposium on the origin of granites and related rocks: The Geological Society of America Special Paper, pp. 115-123.

Peck, W.H., Valley, J.W., Graham, C.M., 2003. Slow oxygen diffusion rates in igneous zircons from metamorphic rocks. American Mineralogist, 88: 1003-1014.

Peck, W.H., Valley, J.W., Wilde, S.A., Graham, C.M., 2001. Oxygen isotope ratios and rare earth elements in 3.3 to 4.4 Ga zircons: Ion microprobe evidence for high $\delta^{18}O$ continental crust and oceans in the Early Archaean. Geochimica et Cosmochimica Acta, 65: 4215-4229.

Petford, N., Atherton, M., 1996. Na-rich partial melts from newly underplated basaltic crust: the Cordillera Blanca Batholith, Peru. Journal of Petrology, 37: 1491-1521.

Petford, N., Cruden, A.R., McCaffrey, K.J.W., Vigneresse, J.-L., 2000. Granite magma formation, transport and emplacement in the Earth's crust. Nature, 408: 669-673.

Piasecki, M.A.J., 1980. New light on the Moine rocks of the Central Highlands of Scotland. Journal of the Geological Society, London, 137: 47-59.

Pichavant, M., Martel, C., Bourdier, J.L., Scaillet, B., 2002. Physical conditions, structure, and dynamics of a zoned magma chamber: Mount Pelé (Martinique, Lesser Antilees Arc). Journal of Geophysical Research, 107.

Pichavant, M., Montel, J.-M., Richard, L.R., 1992. Apatite solubility in peraluminous liquids: experimental data and an extension of the Harrison-Watson model. Geochimica et Cosmochimica Acta, 56: 3855-3861.

Pickering, K.T., Bassett, M.G., Siveter, D.J., 1988. Late Ordovician-Early Silurian destruction of the Iapetus Ocean: Newfoundland, British Isles and Scandinavia - a discussion. Transactions of the Royal Society of Edinburgh: Earth Sciences, 79: 361-382.

Pidgeon, R.T., Aftalion, M., 1978. Cogenetic and inherited zircon U-Pb systems in granites: Palaeozoic granites of Scotland and England. In: D.R. Bowes, Leake, B.E.

(Editor), Crustal evolution in northwestern Britain and adjacent regions. Geological Journal Special Issues, pp. 183-220.

Pidgeon, R.T., Compston, W., 1992. A SHRIMP ion microprobe study of inherited and magmatic zircons from four Scottish Caledonian granites. Transactions of the Royal Society of Edinburgh: Earth Sciences, 83: 473-483.

Pitcher, W.S., Berger, A.R., 1972. The Geology of Donegal: A Study of Granite Emplacement and Unroofing. Wiley, Interscience, New York.

Poldervaart, A., 1955. Zircons in rocks, 1. Sedimentary rocks. American Journal of Science, 235: 433-461.

Poldervaart, A., 1956. Zircons in rocks, 2. Igneous rocks. American Journal of Science, 254: 521-554.

Prouteau, G., Scaillet, B., 2003. Experimental constraints on the origin of the 1991 Pinatubo dacite. Journal of Petrology, 44: 2203-2241.

Pupin, J.P., 1980. Zircon and granite petrology. Contributions to Mineralogy and Petrology, 73: 207-220.

Pupin, J.P., Turco, G., 1972a. Une typologie originale du zircon accessoire. Bulletin Société Francaise de Minéralogie et de Cristallographie, 95: 348-359.

Pupin, J.P., Turco, G., 1972b. Application des données morphologiques du zircon accessoire en pétrologie endogène. Comptes Rendus de l'Académie des Sciences Paris, 275D: 799-802.

Pupin, J.P., Turco, G., 1972c. Le zircon accessoire en géothermométrie. Comptes Rendus de l'Académie des Sciences Paris, 274D: 2121-2124.

Raia, F., Spera, F.J., 1997. Simulation of the growth and differentiation of continental crust. Journal of Geophysical Research, 102: 22629-22648.

Rapp, R.P., Watson, E.B., 1995. Dehydration melting of metabasalt at 8-32 kbar - implications for continental growth and crust-mantle recycling. Journal of Petrology, 36: 891-931.

Read, H.H., 1961. Aspects of the Caledonian magmatism in Scotland. Proceedings of the Liverpool and Manchester Geological Society, 2: 653-683.

Reid, M.R., Coath, C.D., Harrison, T.M., McKeegan, K.D., 1997. Prolonged residence times for the youngest rhyolites associated with Long Valley Caldera: ^{230}Th-^{238}U ion microprobe dating of young zircons. Earth and Planetary Science Letters, 150: 27-39.

Restrepo-Pace, P.A., Ruiz, J., Gehrels, G., Cosca, M., 1997. Geochronology and Nd isotopic data of Grenville-age rocks in the Colombian Andes: new constraints for Late Proterozoic-Early Paleozoic paleocontinental reconstructions of the Americas. Earth and Planetary Science Letters, 150: 427-441.

Richardson, S.W., Powell, R., 1976. Thermal causes of the Dalradian metamorphism in the Central Highlands of Scotland. Scottish Journal of Geology, 12: 237-268.

Rogers, G., Dunning, G.R., 1991. Geochronology of appinitic and related granitic magmatism in the W. Highlands of Scotland: constraints on the timing of transcurrent fault movement Journal of the Geological Society, London, 148: 17-27.

Rogers, G., Hawkesworth, C.J., 1989. A geochemical traverse across the North Cilean Andes - evidence for crust generation from the mantle wedge. Earth and Planetary Science Letters, 91: 271-285.

Rollin, R.E., 1994. Geophysical correlation of Precambrian rocks in northern Britain. In: W. Gibbons, Harris, A.L. (Editor), A Revised Correlation of Precambrian Rocks in the British Isles. Geological Society, London, Special Report, pp. 65-74.

Rudnick, R.L., Fountain, D.M., 1995. Nature and composition of the continental crust: a lower crustal perspective. Reviews in Geophysics, 33: 267-309.

Samson, S.D., Hibbard, J.P., Wortman, G.L., 1995. Nd isotopic evidence for juvenile crust in the Carolina terrane, southern Appalachians Contributions to Mineralogy and Petrology, 121: 171-184.

Samson, S.D., McClelland, W.C., Patchett, P.J., Gehreless, G.E., Anderson, R.G., 1989. Evidence from neodymium isotopes from mantle contributions to Phanerozoic crustal genesis in the Canadian Cordillera. Nature, 337: 705-709.

Sanders, I.S., van Calsteren, P.W.C., Hawkesworth, C.J., 1984. A Grenville Sm-Nd age for the Glenelg eclogite in northwest Scotland. Nature, 312: 439-440.

Sano, Y., Terado, K., Fukuoka, T., 2002. High mass resolution ion microprobe analysis of rare earth elements in silicate glass, apatite and zircon: lack of matrix dependency. Chemical Geology, 184: 217-230.

Scherer, E., Münker, C., Mezger, K., 2001. Calibration of the Lutetium-Hafnium Clock. Science, 293: 683-687.

Scherer, E., Whitehouse, M.J., Münker, C., 2007. Zircon as a Monitor of Crustal Growth. Elements, 3: 19-24.

Schuhmacher, M., de Chambost, E., McKeegan, K.D., Harrison, T.M. & Migeon, H. 1994. In-situ dating of zircon with the CAMECA ims-1270. In: Secondary Ion Mass Spectrometry, SIMS IX (eds. A. Benninghoven et al.), pp. 919-922. Wiley.

Sharp, Z.D., 1990. A laser-based microanalytical method for the in situ determination of oxygen isotope ratios of silicates and oxides. Geochimica et Cosmochimica Acta, 54: 1353-1357.

Shore, M., Fowler, A.D., 1996. Oscillatory zoning in minerals: a common phenomenon. Canadian Mineralogist, 34: 1111-1126.

Siedner, G., 1965. Geochemical features of a strongly fractionated alkali igneous suite. Geochimica et Cosmochimica Acta, 29: 113-137.

Simpson, P.R., Brown, G.C., Plant, J., Ostle, D., 1979. Uranium mineralization and granite magmatism in the British isles. Philosophical Transactions of the Royal Society of London, A291: 385-412.

Sisson, T.W., Grove, T.L., 1993. Experimental investigations of the role of H_2O in calc-alkaline differentiation and subduction zone magmatism. Contributions to Mineralogy and Petrology, 113: 143-166.

Sisson, T.W., Moore, J.G., 1994. Geologic map of the Giant Forest Quadrangle, Tulare County, California. In: U.S.G. Survey (Editor).

Smith, B.M., 1981. Oxygen and strontium isotopic studies of the Skye intrusive complex, Northwest Scotland, Brown University.

Smith, C.G., Goodman, S., Robertson, S., 2001. Geology of the Ballater district. British Geological Survey - Memoir for 1:50 000 Geological Sheet 65E (Scotland).

Smith, D.R., Leeman, W.P., 1987. Petrogenesis of Mount St. Helens dacitic magmas. Journal of Geophysical Research, 92: 10313-10334.

Soper, N.J., 1986. The Newer Granite problem: a geotectonic view. Geological Magazine, 123: 227-236.

Soper, N.J., Hutton, D.H.W., 1984. Late Caledonian sinistral displacements in Britain: Implications for a three-plate model. Tectonics, 3: 187-190.

Soper, N.J., Ryan, P.D., Dewey, J.F., 1999. Age of the Grampian orogeny in Scotland and Ireland. Journal of the Geological Society of London, 156: 1231-1236.

Soper, N.J., Strachan, R.A., Holdsworth, R.E., Gayer, R.A., Greiling, R.O., 1992. Sinistral transpression and the Silurian closure of Iapetus. Journal of the Geological Society, London, 149: 697-700.

Speer, J.A., 1982. Zircon. Reviews in Mineralogy, pp. 67-112.

Stephens, W.E., 1988. Granitoid plutonism in the Caledonian orogen of Europe. In: A.L. Harris, Fettes, D.J. (Editor), The Caledonian-Appalachian Orogen. Special Publications. Geological Society, London, pp. 389-403.

Stephens, W.E., Halliday, A.N., 1984. Geochemical contrasts between late Caledonian granitoid plutons of northern, central and southern Scotland. Transactions of the Royal Society of Edinburgh: Earth Sciences, 75: 259-273.

Stephenson, D., Gould, D., 1995. The Grampian Highlands. British Regional Geology. HMSO, London.

Stephenson, D.B., R.E., Millward, D., Highton, A.J., Parsons, I., Stone, P., Wadsworth, W.J., 1999. Caledonian igneous rocks of Great Britain. Geological Conservation Review Series, 17. Joint Nature Conservation Committee, 1-648 pp.

Stewart, M., Strachan, R.A., Martin, M.W. Holdsworth, R.E., 2001. Dating early sinistral displacements along the Great Glen Fault Zone, Scotland: structural setting, emplacement and U-Pb geochronology of th syn-tectonic Clunes Tonalite. Journal of the Geological Society, London, 158: 821-830.

Strachan, R.A., Smith, M., Harris, A.L., Fettes, D.J., 2002. The Northern Highland and Grampian terranes. In: N.H. Trewin (Editor), The Geology of Scotland. The Geological Society, London, pp. 81-148.

Sun, S.S., McDonough, W.F., 1989. Chemical and isotopic systematics of oceanic basalts: implications for mantle compositions and processes. Geological Society, London, Special Publications, 42: 313-345.

Tarney, J., Jones, C.E., 1994. Trace element geochemistry of orogenic igneous rocks and crustal growth models. Journal of the Geological Society, London, 151: 855-868.

Taylor, B.E., Huston, D.L., 1998. Hydrothermal alteration of oxygen isotope ratios in quartz phenocrysts, Kidd Creek mine, Ontario: Magmatic values perserved in zircons. Geology: 763-764.

Technology, N.I.o.S., 1992. Reference Materials 8543-8546.

Tepper, J.H., Nelson, B.K., Bergantz, G.W., Irving, A.J., 1993. Petrology of the Chiilwack batholith, North Cascades, Washington. Generation of calc-alkaline granitoids by melting of mafic lower crust with variable water fugacity. Contributions to Mineralogy and Petrology, 113: 333-351.

Thirlwall, M.F., 1981. Implications for Caledonian plate tectonic models of chemical data from volcanic rocks of the British Old Red Sandstone Journal of the Geological Society, London, 138: 123-138.

Thirlwall, M.F., 1982. Systematic variation in chemistry and Nd-Sr isotopes across a Caledonian calc alkaline volcanic arc: implications for source materials. Earth and Planetary Science Letters, 58: 27-50.

Thirlwall, M.F., 1988. Geochronology of Late Caledonian Magmatism in northern Britain. Journal of the Geological Society, London, 145: 951-967.

Thirlwall, M.F., Walder, A.J., 1995. In situ hafnium isotope ratio analysis of zircon by inductively couples plasma mass spectrometry. Chemical Geology, 122: 241-247.

Tindle, A.G., Pearce, A., 1981. Petrogenetic modelling of in situ fractional crystallization in the zoned Loch Doon Pluton, Scotland. Contributions to Mineralogy and Petrology, 78: 196-207.

Valley, J.W., 2003. Oxygen isotopes in zircon. Reviews in Mineralogy & Geochemistry, 53: 343-385.

Valley, J.W., Bindemann, I.N., Peck, W.H., 2003. Empirical calibration of oxygen isotope fractionation in zircon. Geochimica et Cosmochimica Acta, 67: 3257-3266.

Valley, J.W., Chiarenzelli, J.R., McLelland, J.M., 1994. Oxygen isotope geochemistry of zircon. Earth and Planetary Science Letters, 126: 187-206.

Valley, J.W., Graham, C., 1996. Ion microprobe analysis of oxygen isotope ratios in quartz from Skye granite: healed micro-cracks, fluid flow, and hydrothermal exchange. Contributions to Mineralogy and Petrology, 124: 225-234.

Valley, J.W., Kinny, P.D., Schulze, D.J., Spicuzza, M.J., 1998. Zircon megacrysts from kimberlite: oxygen isotope variability among mantle melts. Contributions to Mineralogy and Petrology, 133: 1-11.

Valley, J.W., Kinny, P.D., Schulze, D.J., Spicuzza, M.J., 1998. Zircon megacrysts from kimberlite: oxygen isotope variability among mantle melts. Contributions to Mineralogy and Petrology, 133: 1-11.

Vavra, G., 1990. On the kinematics of zircon growth and its petrogenetic significance: a cathodoluminescence study. Contributions to Mineralogy and Petrology, 106: 90-99.

Vavra, G., 1993. A guide to quantitative morphology of accessory zircon. Chemical Geology, 110: 15-28.

Vavra, G., 1994. Systematics of internal zircon morphology in major Variscan granitoid types. Contributions to Mineralogy and Petrology, 117: 331-344.

Vernon, R.H., 1983. Restite, xenoliths and microgranitoid enclaves in granites. Journal of the Proceedings of the Royal Society of New South Wales, 116: 77-103.

Vervoort, J.D., Blichert-Toft, J., 1999. Evolution of the depleted mantle: Hf isotope evidence from juvenile rocks through time. Geochimica et Cosmochimica Acta, 63: 533-556.

Vervoort, J.D., Patchett, J.P., Albarede, F., Blichert-Toft, J., Rudnick, R., Downes, H., 2000. Hf-Nd isotopic evolution of the lower crust. Earth and Planetary Science Letters, 181: 115-129.

Vervoort, J.D., Patchett, P.J., 1996. Behaviour of hafnium and neodymium idotopes in the crust: Constraints from Precambrian crustally derived granites. Geochimica et Cosmochimica Acta, 60: 3717-3733.

Wall, V.J., Clems, J.D., Clarke, D.B., 1987. Models for granitoid evolution and source compositions. Journal of Geology, 95: 731-749.

Watson, B.E., 1979. Zircon saturation in felsic liquids: Experimental results and applications to trace element geochemistry. Contributions to Mineralogy and Petrology, 70: 407-419.

Watson, B.E., 1996. Dissolution, growth and survival of zircons during crustal fusion: kinetic principles, geological models and implications for isotopic inheritance. Transactions of the Royal Society of Edinburgh: Earth Sciences, 87: 43-56.

Watson, B.E., Harrison, T.M., 1983. Zircon saturation revisited: temperature and composition effects in a variety of crustal magma types. Earth and Planetary Science Letters, 64: 295-304.

Watson, E.B., Cherniak, D.J., 1997. Oxygen diffusion in zircon. Earth and Planetary Science Letters, 148: 527-544.

Watson, E.B., Harrison, T.M., 2005. Zircon Thermometer Reveals Minimum Melting Conditions on Earliest Earth. Science, 308: 841-844.

Watson, E.B., Wark, D.A., Thomas, J.B., 2006. Crystallization thermometers for zircon and rutile. Contributions to Mineralogy and Petrology, 151: 413-433.

Whitehouse, M.J., Claesson, S., Sunde, T. & Vestin, J. 1997. Ion microprobe U-Pb geochronology and correlation of Archaean gneisses from the Lewisian Complex of Gruinard Bay, northwestern Scotland. Geochimica Cosmochimica et Acta, 61, 4429-4438.

Wiebe, R.A., 1993. The Pleasant Bay layered gabbro-diorite, coastal maine; ponding and crystallisation of basaltic injections into a silicic magma chamber. Journal of Petrology, 34: 461-489.

Wiebe, R.A., Collins, W.J., 1998. Depositional features and stratigraphic sections in granitic plutons; implications for the emplacement and crystallization of granitic magma. Journal of Structural Geology, 20: 1273-1289.

Wiedenbeck, M., Alle, P., Corfu, F., Griffin, W.L., Meier, M., Oberli, F., Von Quadt, A., Roddick, J.C. & Spiegel, W. 1995. Three natural zircon standards for U-Th-Pb, Lu-Hf, trace element and REE analyses. Geostandards Newsletter, 19, 1-23.

Wiedenbeck, M., Hanchar, J.M., Peck, W.H., Sylvester, P., Valley, J., Whitehouse, M., Kronz, A., Morishita, Y., Nasdala, L., Fiebig, J., Franchi, I., Girard, J.-P., Greenwood, R.C., Hinton, R., Kita, N., Mason, P.R.D., Norman, M., Ogasawara, M., Piccoli, P.M., Rhede, D., Satoh, H., Schulz-Dobrick, B., Skår, Ø., Spicuzza, M.J., Terada, K., Tindle, A., Togashi, S., Vennemann, T., Xie, Q., Zheng, Y.-F., 2004. Further Characterization of the 91500 Zircon Crystal. Geostandards and Geoanalytical Research, 28: 9-39.

Williams, I.S. 1998. U-Th-Pb geochronology by ion microprobe. In: (Eds. McKibben, M.A., Shanks, W.C., & Ridley, W.I.) Applications of Microanalytical Techniques to Understanding Mineralizing Processes, Socorro, New Mexico, Reviews in Economic Geology, Society of Economic Geologists, 7, 1-35.

Williams, I.S. & Claesson, S. 1987. Isotopic evidence for the Precambrian provenance and Caledonian metamorphism of high-grade paragneisses from the Seve Nappes, Scandinavian Caledonides: 2. Ion microprobe zircon U-Th-Pb. Contributions to Mineralogy and Petrology, 97, 205-217.

Woodhead, J.D., Hergt, J.M., 2005. A preliminary appraisal of seven natural zircon refernce materials for in situ Hf isotope determination. Geostandards and Geoanalytical Research, 29: 183-195.

Wu, F.-Y., Jahn, B.-M., Wilde, S., Sun, D.-Y., 2000. Phanerozoic crustal growth: U-Pb and Sr-Nd isotopic evidence from the granites in northeastern China. Tectonophysics, 328: 89-113.

Zaleski, E., 1983. The geology of Strathspey and Lower Findhorn granitoids - a study involving field relations, petrography, mineralogy, geochemistry and geochronology University of St. Andrews.

IX.

APPENDICES

APPENDIX 1

Supplementary data for Paper 1

Appendix 1a

Zircon oxygen isotope data for CnG (SA04/13) and AD1 (SA04/01) diorites and average values of bracketing zircon standa

analyses no.	grain no.	$^{18}O/^{16}O$ (measured)	2SD	1 s.e.m.	$\delta^{18}O$ [‰] VSMOW	2SD	1 s.e.m.	n	grain area	comment
Session 4 (01.06.2005)										
91500 - 11-20		0.0020157	0.0000010	0.0000002	9.78	0.5	0.075	10		
91500 - 21-30		0.0020159	0.0000008	0.0000001	9.89	0.4	0.067	10		
91500 - 36-45		0.0020160	0.0000007	0.0000001	9.92	0.3	0.051	10		
SA04/01-1	1	0.0020100			6.9				c2a	
SA04/01-2	1	0.0020109			7.4				c2b	rejected, crack
SA04/01-3	2	0.0020085			6.2				rim	rejected, crack
SA04/01-4	2	0.0020089			6.4				c2	rejected, crack
SA04/01-5	3	0.0020103			7.1				c2	
SA04/01-6	3	0.0020094			6.6				c1	
Session 5 (01.06.2005)										
91500 - 46-50		0.0020148	0.0000004	0.0000001	9.92	0.22	0.049	5		
SA04/01-7	4	0.0020095			7.3				?	
SA04/01-8	4	0.0020097			7.4				?	
SA04/01-9	4	0.0020095			7.3				?	
SA04/01-10	4	0.0020103			7.7				?	
SA04/01-11	5	0.0020100			7.5				rim	
SA04/01-12	5	0.0020098			7.4				c1b	
SA04/01-13	5	0.0020092			7.1				c1a	rejected, crack
SA04/01-14	6	0.0020096			7.3				c2a	
SA04/01-15	6	0.0020094			7.3				c2b	
SA04/01-16	7	0.0020092			7.2				c1a	
91500 - 51-55		0.0020145	0.0000010	0.0000002	9.76	0.48	0.107	5		
91500 - 67-70		0.0020148	0.0000012	0.0000003	9.91	0.61	0.152	4		
SA04/01-17	7	0.0020100			7.5				c1b	
SA04/01-18	7	0.0020101			7.6				rim a	
SA04/01-19	7	0.0020099			7.5				rim b	
SA04/01-20	8	0.0020085			6.8				c1	
SA04/01-22	8	0.0020086			6.9				c2a	
SA04/01-23	8	0.0020095			7.3				c2b	
SA04/01-24	8	0.0020092			7.1				c2c	
SA04/01-25	8	0.0020100			7.5				m1	
SA04/01-26	8	0.0020069			6.0				rim	rejected, overlaps epoxy
SA04/01-27	9	0.0020080			6.5				c1	rejected, correction on position of secondary ion beam anomalously large
91500 - 71-75		0.0020147	0.0000008	0.0000002	9.86	0.38	0.084	5		
SA04/01-28	9	0.0020078			6.5				c2a	
SA04/01-29	9	0.0020094			7.3				c2b	
SA04/01-30	10	0.0020095			7.3				rim	rejected, correction on position of secondary ion beam anomalously large
SA04/01-31	10	0.0020081			6.6				c2	
SA04/01-32	10	0.0020106			7.8				c1	
SA04/01-33	11	0.0020112			8.1				rim	
SA04/01-34	11	0.0020094			7.2				c1	
SA04/01-35	12	0.0020098			7.5				c2	
SA04/01-36	12	0.0020096			7.3				c1b	
SA04/01-37	12	0.0020108			8.0				c1c	rejected, convoluted, possibly altered area

Session 6 (01.06.2005)

91500 - 76-80		0.0020156	0.0000006	0.0000001	9.90	0.31	0.070	5		
SA04/01-38	12	0.0020101			7.2				c1d	rejected, crack
SA04/01-39	12	0.0020105			7.4				c1a	
SA04/01-40	12	0.0020110			7.6				c2b	rejected, crack
SA04/01-41	13	0.0020080			6.2				c2a	
SA04/01-42	13	0.0020090			6.6				c2b	
SA04/01-43	14	0.0020094			6.8				c1	
SA04/01-44	14	0.0020090			6.6				c2a	
SA04/01-45	14	0.0020097			7.0				c2b	
SA04/01-46	15	0.0020092			6.7				c1	
SA04/01-47	15	0.0020097			7.0				c3	
91500 - 81-85		0.0020154	0.0000007	0.0000002	9.81	0.32	0.081	4		
SA04/01-48	15	0.0020094			6.8				c2b	
SA04/01-49	15	0.0020090			6.6				c2a	
SA04/01-50	16	0.0020080			6.1				m1	
SA04/01-51	16	0.0020085			6.4				c1	
SA04/01-52	16	0.0020087			6.5				rim	

Session 9 (02.06.2005)

91500 - 140-149		0.0020149	0.0000010	0.0000002	9.96	0.49	0.078	10		
91500 - 150-154		0.0020148	0.0000007	0.0000002	9.88	0.35	0.078	5		
91500 - 155-159		0.0020145	0.0000007	0.0000002	9.77	0.34	0.075	5		
SA04/13-1	1	0.0020093			7.2				c2a	rejected, analytical problem
SA04/13-2	1	0.0020048			4.9				c2b	rejected, analytical problem
SA04/13-3	2	0.0020077			6.4				c2b	
SA04/13-4	2	0.0020067			5.9				c2a	
SA04/13-5	2	0.0020071			6.1				c1	
SA04/13-6	3	0.0020067			5.9				c2	
91500 - 161-164		0.0020148	0.0000013	0.0000003	9.89	0.64	0.16	4		
SA04/13-7	4	0.0020061			5.6				rim	
SA04/13-8	4	0.0020076			6.3				c1a	
SA04/13-9	5	0.0020066			5.9				c2	
SA04/13-10	5	0.0020074			6.2				c1	
SA04/13-11	5	0.0020068			5.9				rim	
SA04/13-12	6	0.0020066			5.8				c1a	
SA04/13-13	6	0.0020051			5.1				c1b	rejected, crack
SA04/13-14	6	0.0020071			6.1				rim	
SA04/13-15	7	0.0020075			6.3				c1a	
SA04/13-16	7	0.0020069			6.0				m1	
SA04/13-17	7	0.0020068			5.9				c1b	
SA04/13-18	8	0.0020068			5.9				rim	
SA04/13-19	8	0.0020067			5.9				m1c	
SA04/13-20	8	0.0020064			5.8				m1b	
SA04/13-21	8	0.0020083			6.7				m1a	rejected, crack
SA04/13-22	8	0.0020065			5.8				c1	
SA04/13-24	9	0.0020066			5.8				c1	
SA04/13-25	9	0.0020071			6.1				rim	
SA04/13-26	10	0.0020059			5.5				c2	rejected, correction on position of secondary ion beam anomalously large
91500 - 170-174		0.0020147	0.0000008	0.0000002	9.87	0.40	0.09	5		
SA04/13-27	10	0.0020072			6.1				c1	rejected, correction on position of secondary ion beam anomalously large
SA04/13-28	11	0.0020073			6.2				c1	
SA04/13-29	12	0.0020066			5.8				rim	
SA04/13-30	12	0.0020059			5.5				c1	
SA04/13-31	13	0.0020064			5.7				c1	
SA04/13-32	13	0.0020063			5.7				c2	
SA04/13-33	13	0.0020064			5.8				rim	
SA04/13-34	14	0.0020060			5.5				c2	
SA04/13-35	15	0.0020061			5.6				c1	
SA04/13-36	15	0.0020073			6.2				rim	
91500 - 175-179		0.0020145	0.0000017	0.0000004	9.74	0.87	0.19	5		

SA04/13-37	16	0.0020066			5.8				c1	
SA04/13-38	17	0.0020077			6.4				c1a	
SA04/13-39	17	0.0020077			6.4				c1b	
SA04/13-40	17	0.0020076			6.3				c2	
SA04/13-41	18	0.0020069			6.0				c2a	rejected, crack
SA04/13-42	18	0.0020063			5.7				c2b	rejected, crack
SA04/13-43	18	0.0020073			6.2				rim	
SA04/13-44	19	0.0020076			6.3				c1	
SA04/13-45	19	0.0020067			5.9				rim	
SA04/13-46	3	0.0020080			6.5				c2c	rejected, crack
91500 - 175-179		0.0020146	0.0000013	0.0000003	9.80	0.66	0.17	4		

c1 = unzoned inner core
c2 = osciallatory zoned outer core
m1-3 = mantle

Appendix 1b
Quartz oxygen isotope data for CnG (SA04/13) and AD1 (SA04/01) diorites and average values of bracketing quartz standard NBS28

	analyses no.	grain no.	$^{18}O/^{16}O$ (measured)	2SD	1 s.e.m.	$^{18}O/^{16}O$ (drift corrected)	$\delta^{18}O$ [‰] VSMOW	2SD	1 s.e.m.	n	grain area	comment
Session 1 (29.05.2007)												
	NBS28 - 20-29		0.0020087	0.0000026	0.0000004	0.0020087	9.87	1.3	0.221	9		
	NBS28 - 30-39		0.0020085	0.0000008	0.0000001	0.0020086	9.76	0.4	0.061	10		
SA04/13	Q13/1-1	1	0.0020110				11.1				centre	
SA04/13	Q13/1-2	1	0.0020113				11.2				rim	
SA04/13	Q13/2-1	2	0.0020108				10.9				centre	
SA04/13	Q13/2-2	2	0.0020128				12.0				rim	rejected, spot in altered area
SA04/13	Q13/2-3	2	0.0020107				10.9				rim	
SA04/13	Q13/3c-1	3	0.0020106				10.9				centre	
SA04/13	Q13/3c-2	3	0.0020106				10.9				rim	
SA04/13	Q13/4-1	4	0.0020103				10.7				centre	
SA04/13	Q13/4-2	4	0.0020104				10.8				centre	
SA04/13	Q13/4-3	4	0.0020106				10.9				rim	
SA04/13	Q13/9-4	9	0.0020097				10.5				towards rim	
SA04/13	Q13/9-5	9	0.0020097				10.4				towards rim	
	NBS28 - 40-49		0.0020080	0.0000024	0.0000004	0.0020085	9.62	1.2	0.189	10		
SA04/13	Q13/9-1	9	0.0020107				11.0				centre	
SA04/13	Q13/9-2	9	0.0020108				11.0				centre	
SA04/13	Q13/7-1	7	0.0020101				10.7				centre	
SA04/13	Q13/7-2	7	0.0020106				11.0				towards rim	
SA04/13	Q13/7-3	7	0.0020116				11.4				rim	
SA04/13	Q13/10-1	10	0.0020098				10.6				centre	
SA04/13	Q13/10-2	10	0.0020105				10.9				towards rim	
SA04/13	Q13/15-1	15	0.0020116				11.4				centre	
SA04/13	Q13/15-2	15	0.0020110				11.2				rim	
SA04/13	Q13/14-1	14	0.0020109				11.1				centre	
SA04/13	Q13/14-3	14	0.0020110				11.2				rim	
							average					
							10.9	0.5	0.057	22		
	NBS28 - 50-59		0.0020093	0.0000022	0.0000003	0.0020083	10.36	1.1	0.172	10		
SA04/01	Q01/1a-1	1	0.0020119				11.7				centre	
SA04/01	Q01/1a-2	1	0.0020127				12.1				towards rim	
SA04/01	Q01/1a-3	1	0.0020127				12.1				rim	
SA04/01	Q01/1c-1	1	0.0020128				12.1				centre	
SA04/01	Q01/1c-3	1	0.0020115				11.5				rim	
SA04/01	Q01/1c-2	1	0.0020124				12.0				rim	
SA04/01	Q01/2-1	2	0.0020116				11.5				centre	
SA04/01	Q01/2-2	2	0.0020119				11.7				centre	
SA04/01	Q01/2-3	2	0.0020110				11.3				rim	
SA04/01	Q01/3-1	3	0.0020111				11.3				centre	
SA04/01	Q01/3-2	3	0.0020117				11.6				rim	
SA04/01	Q01/4-1	4	0.0020126				12.1				centre	
SA04/01	Q01/4-2	4	0.0020129				12.2				towards rim	
SA04/01	Q01/4-3	4	0.0020124				12.0				rim	
SA04/01	Q01/6-1	6	0.0020122				11.9				centre	
SA04/01	Q01/6-2	6	0.0020118				11.7				rim	
	NBS28 - 60-69		0.0020082	0.0000017	0.0000003	0.0020081	9.88	0.8	0.132	10		
SA04/01	Q01/7-1	7	0.0020116				11.6				centre	
SA04/01	Q01/7-2	7	0.0020117				11.7				rim	
SA04/01	Q01/7-3	7	0.0020129				12.3				rim	
SA04/01	Q01/8-1	8	0.0020119				11.8				centre	
SA04/01	Q01/8-2	8	0.0020113				11.5				towards rim	
SA04/01	Q01/8-3	8	0.0020108				11.3				centre	
SA04/01	Q01/10-1	10	0.0020110				11.3				centre	
SA04/01	Q01/10-2	10	0.0020116				11.6				rim	
SA04/01	Q01/13-1	13	0.0020112				11.5				rim	
SA04/01	Q01/13-2	13	0.0020113				11.5				rim	
SA04/01	Q01/16-1	16	0.0020116				11.7				centre	
							average					
							11.7	0.6	0.057	27		
	NBS28 - 70-79		0.0020075	0.0000023	0.0000004	0.0020079	9.66	1.1	0.180	10		

APPENDIX 2

Supplementary data for Paper 2

Appendix 2a
Major, trace and rare earth element whole-rock data of the Lochnagar and Etive plutons

	Lochnagar									Etive									
	AD1	**AD2**	**CnG**	**L1-03**	**L1-06**	**L2-04**	**L2-15**	**L2-12**	**L3**	**MO**	**Cr-11**	**Cr-17**	**Cr-15**	**Cr-26**	**St-05**	**St-06**	**St-01**	**Q-23**	**Q-25**
	SA04/01	SA04/02	SA04/13	SA04/03	SA04/06	SA04/04	SA04/15	SA04/12	SA04/05	SA05/20	SA05/11	SA05/17	SA05/15	SA05/26	SA05/05	SA05/06	SA05/01	SA05/23	SA05/25
SiO_2 [%]	53.0	57.5	54.6	71.8	76.11	71.59	72.9	75.0	68.8	71.8	57.1	68.44	61.53	62.22	71.9		76.1	61.4	57.2
TiO_2	2.06	1.26	1.22	0.35	0.142	0.307	0.29	0.18	0.45	0.35	1.14	0.514	0.882	0.647	0.36		0.14	0.77	1.01
Al_2O_3	17.82	16.51	17.40	14.02	12.24	14.44	13.94	13.40	15.95	14.72	17.59	14.89	18.73	18.48	13.75		12.58	15.73	14.11
Fe_2O_3	9.47	6.65	7.27	1.92	0.92	1.76	1.71	1.06	2.22	1.58	6.06	3.15	4.06	2.98	2.19		0.83	5.17	7.32
MnO	0.12	0.12	0.12	0.04	0.01	0.04	0.03	0.03	0.05	0.04	0.07	0.05	0.06	0.04	0.04		0.03	0.08	0.11
MgO	3.69	4.13	4.90	0.46	0.04	0.5	0.48	0.04	0.48	0.18	2.57	1.69	1.26	0.72	0.73		0.11	3.36	6.15
CaO	6.39	5.80	7.76	1.22	0.35	1.3	1.08	0.34	1.15	0.65	5.46	2.58	3.52	2.46	1.39		0.44	4.60	6.08
Na_2O	3.93	3.41	3.50	3.25	3.19	3.74	3.71	3.64	4.56	4.67	3.90	3.76	5.56	4.94	3.81		3.53	3.94	3.06
K_2O	1.96	2.69	1.65	5.56	5.174	4.457	4.33	5.52	4.73	5.16	2.61	3.886	2.749	4.857	4.13		4.84	3.04	2.12
P_2O_5	0.64	0.22	0.23	0.05	-0.005	0.059	0.06		0.06	0.02	0.32	0.119	0.185	0.112	0.11		0.00	0.24	0.38
LOI	1.11	1.40	0.93	0.52	0.42	0.76	0.77	0.41	0.74	0.49	0.96	0.78	0.79	0.65	0.68		0.39	0.90	1.42
Sum	100.15	99.68	99.56	99.18	98.60	98.95	99.33	99.59	99.20	99.61	97.75	99.86	99.33	98.11	99.12		99.02	99.22	98.97
Sc [ppm]	25		26	4			4	3	4	5	18	8	1	4	4	6	3	13	23
V	176	137	153	16		18	19		7	6	125	46	59	26	24	40	3	92	132
Cr		24	33			1					29	36			8	19		85	191
Ni		6	33								18	9				3		44	82
Ba	870	984	547	864	309	635	523	776	1708	1421	1036	1064	1281	5917	857	1061	192	1104	662
Rb	58	78	43	123	158	165	171	143	141	106	88	101	79	71	125	97	169	69	53
Sr	831	583	775	262	70	268	229	84	325	171	1138	536	911	863	392	625	96	978	981
Y*	27*	21	17*	16*	12	13	11*	12	12*	15*	13*	12	7	9	9	11	7*	11*	16
U*	1*	2	1*	4*	4	6	8*	3	2*	3*	3*	3	2	2	4	3	10*	2*	2
Th*	4*	3	4*	16*	18	17	19*	18	19*	12*	8*	12	8	11	11	12	15*	6*	6
Pb	10	11	8	21	26	28	29	27	25	26	13	18	16	22	22	19	34	14	12
Zr	427	179	230	191	93	144	146	147	339	290	124	144	623	457	140	153	70	121	143
Nb	17	10	13	18	15	16	18	16	18	16	11	11	11	8	13	13	20	10	8
Cu	18	28	31	5	4	10	11	5	5	6	28	8	11	7	7	12	10	17	36
Zn	103	74	79	32	23	39	39	28	50	41	76	46	45	43	42	50	19	65	88
La	39		27	51			30		63	43	31						18	27	
Ce	85		54	90			57		109	77	62						31	53	
Pr	11		6	9			6		10	9	7						3	6	
Nd	44		26	30			21		34	31	30						10	24	
Sm	8		5	5			3		4	5	5						1	4	
Eu	3		2	1			1		2	1	1						0	1	
Tb	1		1	1			0		0	1	1						0	0	
Gd	8		4	4			3		3	4	4						1	3	
Dy	6		4	3			2		2	3	3						1	2	
Ho	1		1	1			0		0	1	1						0	0	
Er	3		2	2			1		1	2	1						1	1	
Tm	0		0	0			0		0	0	0						0	0	
Yb	3		2	2			1		1	1	1						1	1	
Lu	0		0	0			0		0	0	0						0	0	
Hf	7		5	5			4		8	6	3						3	3	
R1	1385	1789	1792	2271	2700	2346	2477	2380	1792	2914	2368	3035	2411	2228	3250		3505	2611	2584
R2	1216	1149	1415	428	280	447	413	301	460	316	924	562	705	577	392		257	833	1047
A/CNK	0.9	0.9	0.8	1.0	1.1	1.1	1.1	1.1	1.1	1.0	0.9	1.0	1.0	1.0	1.0		1.1	0.9	0.8
A/NK	2.1	1.9	2.3	1.2	1.1	1.3	1.3	1.1	1.3	1.1	1.9	1.4	1.5	1.4	1.3		1.1	1.6	1.9
grid	NO 31780	NO 31781	NO 32212	NJ 31780	NO 29893	NO 27717	NO 23830	NO 29053	NO 29660	NN 08328	NN 05740	NN 08407	NN 03710	NN 02225	NN 08559	NN 09480	NN 10307	NN 07761	NN 08172
reference	83993	83993	87858	83994	87174	85606	85133	83656	87121	29977	35478	30073	33167	33768	39219	36685	44834	28095	28066

*** trace elements analysed by ICP-MS**

Appendix 2b

Zircon oxygen isotope data of the Lochnagar pluton and average values of bracketing zircon standard 91500

	analyses no.	grain no.	$^{18}O/^{16}O$ (measured)	1 s.e.m.	$^{18}O/^{16}O$ (drift corrected)	$\delta^{18}O$ [‰] VSMOW	2SD	1 s.e.m.	n	grain area	comment
	Session 2 (31.05.2005)										
	91500 - 1 - 10		0.0020634	0.0000002		9.88	0.5	0.079	10		
AD2	**SA04/02 - 1**	1	0.0020542	0.0000003		5.4		0.078		c2a	rejected, crack
	SA04/02 - 2	2	0.0020577	0.0000004		7.1		0.133		c1a	rejected, crack
	SA04/02 - 3	3	0.0020566	0.0000003		6.6		0.102		c2b	
	SA04/02 - 4	3	0.0020553	0.0000003		5.9		0.080		rim	
	SA04/02 - 5	3	0.0020567	0.0000002		6.6		0.069		c2a	
	SA04/02 - 6	5	0.0020557	0.0000004		6.1		0.106		c2a	rejected, crack
	SA04/02 - 7	5	0.0020569	0.0000003		6.7		0.083		c2b	
	SA04/02 - 8	6	0.0020552	0.0000004		5.9		0.102		c2a	
	SA04/02 - 9	6	0.0020556	0.0000003		6.1		0.086		c2b	
	SA04/02 - 10	7	0.0020559	0.0000004		6.2		0.115		c1	
	91500 - 11 - 14		0.0020634	0.0000005		9.84	0.5	0.128	4		
	SA04/02 - 11	7	0.0020559	0.0000005		6.2				c2b	rejected, partly overlaps
								0.147			epoxy
	SA04/02 - 12	7	0.0020552	0.0000002		5.9		0.065		c2a	rejected, crack
	SA04/02 - 13	8	0.0020552	0.0000004		5.9		0.114		c2c	
	SA04/02 - 14	8	0.0020568	0.0000003		6.7		0.101		c2a	rejected, crack
	SA04/02 - 15	8	0.0020556	0.0000004		6.1		0.106		c2b	rejected, crack
	SA04/02 - 16	9	0.0020559	0.0000004		6.2		0.115		c1b	
	SA04/02 - 17	9	0.0020559	0.0000003		6.2		0.082		c1a	
	SA04/02 - 18	9	0.0020578	0.0000005		7.2		0.157		c2	
	SA04/02 - 19	10	0.0020574	0.0000003		6.9		0.116		c2	
	SA04/02 - 20	10	0.0020565	0.0000002		6.5		0.073		c1	
	91500 - 22 - 25		0.0020634	0.0000004		9.84	0.8	0.207	4		
	SA04/02 - 21	11	0.0020574	0.0000003		8.0		0.133		rim	rejected, crack
	SA04/02 - 22	11	0.0020538	0.0000005		6.3		0.138		c1b	
	SA04/02 - 23	11	0.0020562	0.0000003		7.5		0.121		c1a	
	SA04/02 - 24	11	0.0020557	0.0000003		7.2		0.101		c1c	
	SA04/02 - 25	11	0.0020546	0.0000003		6.7		0.108		c1d	
	SA04/02 - 26	12	0.0020546	0.0000003		6.7		0.108		c1	
	SA04/02 - 27	13	0.0020525	0.0000003		5.7		0.086		rim	rejected, crack
	SA04/02 - 28	13	0.0020542	0.0000003		6.5		0.107		c2b	
	SA04/02 - 29	13	0.0020555	0.0000004		7.1		0.134		c2a	
	SA04/02 - 30	14	0.0020535	0.0000004		6.2		0.113		c1	
	Session 3 (31.05.2005)										
	91500 - 27 - 30		0.0020611	0.0000004		9.87	0.8	0.191	4		
	SA04/02 - 31	15	0.0020546	0.0000003		6.7		0.085		c2a	
	SA04/02 - 32	15	0.0020559	0.0000003		7.3		0.114		c2b	
	SA04/02 - 33	15	0.0020539	0.0000004		6.4		0.121		rim	rejected, crack
	SA04/02 - 34	16	0.0020541	0.0000003		6.4		0.097		c2b	
	SA04/02 - 35	16	0.0020529	0.0000003		5.9		0.084		c2a	
	SA04/02 - 36	16	0.0020552	0.0000004		7.0		0.124		rim	
	SA04/02 - 37	17	0.0020551	0.0000004		6.9		0.120		c1b	
	SA04/02 - 38	17	0.0020544	0.0000004		6.6		0.128		c1a	
	SA04/02 - 39	18	0.0020561	0.0000004		7.4		0.157		rim	
	SA04/02 - 40	18	0.0020533	0.0000002		6.1		0.060		c1	
	91500 - 31 - 35		0.0020611	0.0000001		9.85	0.3	0.069	5		
	Session 4 (01.06.2005)										
	91500/18 - 11 - 20		0.0020157	0.0000002		9.78	0.5	0.079	10		
	91500/18 - 21, 23 - 30		0.0020159	0.0000001		9.89	0.4	0.071	9		
	91500 - 36 - 45		0.0020160	0.0000001		9.92	0.3	0.054	10		
	SA04/02 - 41	19	0.0020087	0.0000002		6.3		0.075		c1	
	SA04/02 - 42	19	0.0020085	0.0000003		6.2		0.093		rim	rejected, crack
	SA04/02 - 43	1	0.0020089	0.0000003		6.4		0.109		c1b	
	SA04/02 - 44	2	0.0020076	0.0000003		5.8		0.087		c2b	rejected, crack
AD1	**SA04/01 - 1**	1	0.0020100	0.0000004		6.9		0.138		c2a	
	SA04/01 - 2	1	0.0020109	0.0000003		7.4		0.126		c2b	rejected, crack
	SA04/01 - 3	2	0.0020085	0.0000002		6.2		0.069		rim	rejected, crack
	SA04/01 - 4	2	0.0020089	0.0000003		6.4		0.092		c2a	rejected, crack
	SA04/01 - 5	3	0.0020103	0.0000003		7.1		0.117		c2	
	SA04/01 - 6	3	0.0020094	0.0000004		6.6		0.126		c1	
	Session 5 (01.06.2005)										
	91500 - 46 - 50		0.0020148	0.0000001		9.92	0.2	0.049	5		
	SA04/01 - 7	4	0.0020095	0.0000002		7.3		0.070		?	
	SA04/01 - 8	4	0.0020097	0.0000002		7.4		0.080		?	
	SA04/01 - 9	4	0.0020095	0.0000004		7.3		0.145		?	
	SA04/01 - 10	4	0.0020103	0.0000003		7.7		0.129		?	
	SA04/01 - 11	5	0.0020100	0.0000003		7.5		0.098		r1	

Appendix 2b

Zircon oxygen isotope data of the Lochnagar pluton and average values of bracketing zircon standard 91500

	analyses no.	grain no.	$^{18}O/^{16}O$ (measured)	1 s.e.m.	$^{18}O/^{16}O$ (drift corrected)	$\delta^{18}O$ [‰] VSMOW	2SD	1 s.e.m.	n	grain area	comment
	SA04/01 - 12	5	0.0020098	0.0000003		7.4		0.124		c1a	
	SA04/01 - 13	5	0.0020092	0.0000002		7.1		0.083		c1b	rejected, crack
	SA04/01 - 14	6	0.0020096	0.0000003		7.3		0.114		c2a	
	SA04/01 - 15	6	0.0020094	0.0000003		7.3		0.126		c2b	
	SA04/01 - 16	7	0.0020092	0.0000003		7.2		0.124		c1a	
	91500 - 51-55		0.0020145	0.0000002		9.76	0.5	0.107	5		
	91500 - 67-70		0.0020148	0.0000003		9.91	0.6	0.152	4		
	SA04/01 - 17	7	0.0020100	0.0000003		7.5		0.106		c1b	
	SA04/01 - 18	7	0.0020101	0.0000002		7.6		0.078		r1a	
	SA04/01 - 19	7	0.0020099	0.0000004		7.5		0.148		r1b	
	SA04/01 - 20	8	0.0020085	0.0000004		6.8		0.130		c1	
	SA04/01 - 22	8	0.0020086	0.0000001		6.9		0.049		c2a	
	SA04/01 - 23	8	0.0020095	0.0000002		7.3		0.084		c2b	
	SA04/01 - 24	8	0.0020092	0.0000003		7.1		0.097		c2c	
	SA04/01 - 25	8	0.0020100	0.0000003		7.5		0.126		r1a	
	SA04/01 - 26	8	0.0020069	0.0000002		6.0		0.048		r1b	rejected, overlaps epoxy
	SA04/01 - 27	9	0.0020080	0.0000002		6.5		0.051		c1	rejected, correction on position of secondary ion beam anomalously large
	91500 - 71-75		0.0020147	0.0000002		9.86	0.4	0.084	5		
	SA04/01 - 28	9	0.0020078	0.0000002		6.5		0.058		c2a	
	SA04/01 - 29	9	0.0020094	0.0000003		7.3		0.116		c2b	
	SA04/01 - 30	10	0.0020095	0.0000003		7.3		0.093		r1	rejected, correction on position of secondary ion beam anomalously large
	SA04/01 - 31	10	0.0020081	0.0000002		6.6		0.059		c2	
	SA04/01 - 32	10	0.0020106	0.0000004		7.8		0.150		c1	
	SA04/01 - 33	11	0.0020112	0.0000002		8.1		0.082		r1	
	SA04/01 - 34	11	0.0020094	0.0000003		7.2		0.118		c1	
	SA04/01 - 35	12	0.0020098	0.0000003		7.5		0.098		c2a	
	SA04/01 - 36	12	0.0020096	0.0000003		7.3		0.092		c1b	
	SA04/01 - 37	12	0.0020108	0.0000003		8.0		0.108		c1c	rejected, convoluted, possibly altered area
	Session 6 (01.06.2005)										
	91500 - 76-80		0.0020156	0.0000001		9.90	0.3	0.070	5		
	SA04/01 - 38	12	0.0020101	0.0000003		7.2		0.104		c1d	rejected, crack
	SA04/01 - 39	12	0.0020105	0.0000003		7.4		0.120		c1a	
	SA04/01 - 40	12	0.0020110	0.0000004		7.6		0.135		c2b	rejected, crack
	SA04/01 - 41	13	0.0020080	0.0000002		6.2		0.060		c2a	
	SA04/01 - 42	13	0.0020090	0.0000003		6.6		0.093		c2b	
	SA04/01 - 43	14	0.0020094	0.0000002		6.8		0.083		c1	
	SA04/01 - 44	14	0.0020090	0.0000003		6.6		0.106		c2a	
	SA04/01 - 45	14	0.0020097	0.0000002		7.0		0.052		c2b	
	SA04/01 - 46	15	0.0020092	0.0000003		6.7		0.102		c1	
	SA04/01 - 47	15	0.0020097	0.0000001		7.0		0.046		c3	
	91500 - 81, 83-85		0.0020154	0.0000002		9.81	0.3	0.081	4		
	SA04/01 - 48	15	0.0020094	0.0000002		6.8		0.064		c2b	
	SA04/01 - 49	15	0.0020090	0.0000002		6.6		0.069		c2a	
	SA04/01 - 50	16	0.0020080	0.0000002		6.1		0.066		r1	
	SA04/01 - 51	16	0.0020085	0.0000003		6.4		0.090		c1	
	SA04/01 - 52	16	0.0020087	0.0000002		6.5		0.074		r3	
L1-03	**S04/03 - 1**	1	0.0020070	0.0000003		5.6		0.094		r2	rejected, analytical problems
	S04/03 - 2	1	0.0020089	0.0000003		6.6		0.111		c2	rejected, analytical problems
	S04/03 - 3	1	0.0020071	0.0000004		5.7		0.124		r1	rejected, analytical problems
	S04/03 - 4	2	0.0020055	0.0000003		4.9		0.083		c2	rejected, analytical problems
	S04/03 - 5	2	0.0020055	0.0000003		4.9		0.066		r2	rejected, analytical problems
	Session 7 (01.06.2005)										
	91500 - 96-100		0.0020147	0.0000002		10.00	0.5	0.105	5		
	S04/03 - 6	3	0.0020090	0.0000003		7.1		0.101		c2	
	S04/03 - 7	4	0.0020085	0.0000004		6.9		0.133		c1	
	S04/03 - 8	4	0.0020085	0.0000002		6.9		0.073		r1	
	S04/03 - 9	6	0.0020077	0.0000002		6.5		0.081		c2a	
	S04/03 - 11	6	0.0020082	0.0000003		6.7		0.092		c2b	
	S04/03 - 12	7	0.0020084	0.0000003		6.8		0.093		c2	
	S04/03 - 13	8	0.0020082	0.0000003		6.8		0.107		c1	
	S04/03 - 14	8	0.0020083	0.0000001		6.8		0.048		r1	
	S04/03 - 15	9	0.0020079	0.0000003		6.6		0.107		c2a	
	S04/03 - 16	9	0.0020083	0.0000003		6.8		0.092		c2b	

Appendix 2b

Zircon oxygen isotope data of the Lochnagar pluton and average values of bracketing zircon standard 91500

	analyses no.	grain no.	$^{18}O/^{16}O$ (measured)	1 s.e.m.	$^{18}O/^{16}O$ (drift corrected)	$\delta^{18}O$ [‰] VSMOW	2SD	1 s.e.m.	n	grain area	comment
	91500 - 101-105		0.0020144	0.0000001		9.81	0.2	0.039	5		
	91500/18 - 31-39		0.0020144	0.0000002		9.82	0.5	0.078	10		
	Session 8 (02.06.2005)										
	91500 - 106-115		0.0020136	0.0000003		9.95	0.8	0.125	10		
	91500 - 120-129		0.0020132	0.0000008		9.77	0.8	0.119	10		
	S04/03 - 17	10	0.0020077	0.0000003		7.0		0.113		c1	
	S04/03 - 18	11	0.0020049	0.0000003		5.6		0.086		c2	
	S04/03 - 19	12	0.0020042	0.0000004		5.3		0.097		rim	
	S04/03 - 20	12	0.0020043	0.0000003		5.3		0.084		c1	rejected, crack
	S04/03 - 21	13	0.0020052	0.0000003		5.8		0.081		c1	rejected, crack
	S04/03 - 22	13	0.0020054	0.0000003		5.9		0.099		rim	
	S04/03 - 23	14	0.0020063	0.0000001		6.3		0.042		c2a	
	S04/03 - 24	14	0.0020051	0.0000003		5.7		0.086		c2b	
	S04/03 - 25	14	0.0020055	0.0000003		5.9		0.086		rim	
	S04/03 - 26	15	0.0020048	0.0000004		5.6		0.110		c1	
	Session 9 (02.06.2005)										
	91500 - 140-149		0.0020149	0.0000002		9.96	0.5	0.082	10		
	S04/03 - 27	15	0.0020073	0.0000002		6.2		0.056		rim	
	S04/03 - 28	16	0.0020078	0.0000003		6.4		0.100		c2	rejected, crack
	S04/03 - 29	16	0.0020087	0.0000002		6.9		0.060		rim	
	S04/03 - 32	18	0.0020093	0.0000002		7.2		0.082		rim	rejected, crack
	S04/03 - 33	18	0.0020120	0.0000003		8.5		0.127		c2	rejected, crack
	S04/03 - 36	20	0.0020063	0.0000003		5.7		0.075		c2a	rejected, correction on position of secondary ion beam anomalously large
	S04/03 - 37	20	0.0020066	0.0000003		5.8		0.086		c2b	
	S04/03 - 38	20	0.0020080	0.0000003		6.5		0.092		r2	
	S04/03 - 39	21	0.0020081	0.0000002		6.6		0.070		r3	
	S04/03 - 40	21	0.0020084	0.0000002		6.7		0.058		r1a	
	91500 - 150-154		0.0020148	0.0000002		9.88	0.4	0.087	5		
	S04/03 - 41	21	0.0020073	0.0000002		6.2		0.053		r1b	
	S04/03 - 42	22	0.0020071	0.0000002		6.1		0.062		c1	
	S04/03 - 43	23	0.0020072	0.0000002		6.1		0.068		c2a	
	S04/03 - 44	23	0.0020082	0.0000002		6.6		0.076		c2b	
	S04/03 - 45	24	0.0020081	0.0000001		6.6		0.044		c2	rejected, crack
	S04/03 - 46	24	0.0020080	0.0000003		6.5		0.103		rim	
	S04/03 - 48	25	0.0020066	0.0000004		5.8		0.112		r2	rejected, crack
	S04/03 - 49	25	0.0020077	0.0000002		6.4		0.072		c2	
	S04/03 - 50	25	0.0020078	0.0000003		6.4		0.094		r3	
	S04/03 - 51	26	0.0020092	0.0000003		7.1		0.094		c1	
	91500 - 155-159		0.0020145	0.0000002		9.77	0.4	0.084	5		
	S04/03 - 52	26	0.0020080	0.0000003		6.5		0.089		c2	
	S04/03 - 53	26	0.0020085	0.0000003		6.8		0.085		rim	
	S04/03 - 54	27	0.0020080	0.0000002		6.6		0.065		c2	
	S04/03 - 55	27	0.0020077	0.0000001		6.4		0.035		c1	
CnG	**SA04/13 - 1**	1	0.0020093	0.0000002		7.2		0.082		c2a	rejected, analytical problem
	SA04/13 - 2	1	0.0020048	0.0000002		4.9		0.058		c2b	rejected, analytical problem
	SA04/13 - 3	2	0.0020077	0.0000002		6.4		0.072		c2b	
	SA04/13 - 4	2	0.0020067	0.0000003		5.9		0.082		c2a	
	SA04/13 - 5	2	0.0020071	0.0000003		6.1		0.085		c1	
	SA04/13 - 6	3	0.0020067	0.0000003		5.9		0.095		c2	
	91500 - 161-164		0.0020148	0.0000003		9.89	0.6	0.161	4		
	SA04/13 - 7	4	0.0020061	0.0000004		5.6		0.099		r1	
	SA04/13 - 8	4	0.0020076	0.0000002		6.3		0.061		c1a	
	SA04/13 - 9	5	0.0020066	0.0000003		5.9		0.077		c2	
	SA04/13 - 10	5	0.0020074	0.0000003		6.2		0.080		c1	
	SA04/13 - 11	5	0.0020068	0.0000003		5.9		0.077		r1	
	SA04/13 - 12	6	0.0020066	0.0000003		5.8		0.076		c1a	
	SA04/13 - 13	6	0.0020051	0.0000005		5.1		0.123		c1b	rejected, crack
	SA04/13 - 14	6	0.0020071	0.0000004		6.1		0.117		r1	
	SA04/13 - 15	7	0.0020075	0.0000001		6.3		0.038		c1a	
	SA04/13 - 16	7	0.0020069	0.0000003		6.0		0.095		r2	
	SA04/13 - 17	7	0.0020068	0.0000001		5.9		0.041		c1b	
	SA04/13 - 18	8	0.0020068	0.0000003		5.9		0.084		r2	
	SA04/13 - 19	8	0.0020067	0.0000003		5.9		0.093		r1c	
	SA04/13 - 20	8	0.0020064	0.0000003		5.8		0.089		r1b	
	SA04/13 - 21	8	0.0020083	0.0000001		6.7		0.048		r1a	rejected, crack
	SA04/13 - 22	8	0.0020065	0.0000001		5.8		0.037		c1	
	SA04/13 - 24	9	0.0020066	0.0000002		5.8		0.049		c1	
	SA04/13 - 25	9	0.0020071	0.0000004		6.1		0.109		r1	

Appendix 2b

Zircon oxygen isotope data of the Lochnagar pluton and average values of bracketing zircon standard 91500

	analyses no.	grain no.	$^{18}O/^{16}O$ (measured)	1 s.e.m.	$^{18}O/^{16}O$ (drift corrected)	$\delta^{18}O$ [‰] VSMOW	2SD	1 s.e.m.	n	grain area	comment
	SA04/13 - 26	10	0.0020059	0.0000001		5.5		0.038		c2	rejected, correction on position of secondary ion beam anomalously large
	91500 - 170-174		0.0020147	0.0000002		9.87	0.4	0.089	5		
	SA04/13 - 27	10	0.0020072	0.0000003		6.1		0.098		c1	rejected, correction on position of secondary ion beam anomalously large
	SA04/13 - 28	11	0.0020073	0.0000003		6.2		0.077		c1	
	SA04/13 - 29	12	0.0020066	0.0000003		5.8		0.077		r1	
	SA04/13 - 30	12	0.0020059	0.0000003		5.5		0.069		c1	
	SA04/13 - 31	13	0.0020064	0.0000002		5.7		0.065		c1	
	SA04/13 - 32	13	0.0020063	0.0000003		5.7		0.090		c2	
	SA04/13 - 33	13	0.0020064	0.0000003		5.8		0.078		r1	
	SA04/13 - 34	14	0.0020060	0.0000002		5.5		0.066		c2	
	SA04/13 - 35	15	0.0020061	0.0000002		5.6		0.061		c1	
	SA04/13 - 36	15	0.0020073	0.0000002		6.2		0.074		r1	
	91500 - 175-179		0.0020145	0.0000004		9.74	0.9	0.193	5		
	SA04/13 - 37	16	0.0020066	0.0000002		5.8		0.057		c1	
	SA04/13 - 38	17	0.0020077	0.0000003		6.4		0.092		c1a	
	SA04/13 - 39	17	0.0020077	0.0000003		6.4		0.107		c1b	
	SA04/13 - 40	17	0.0020076	0.0000002		6.3		0.064		c2	
	SA04/13 - 41	18	0.0020069	0.0000003		6.0		0.080		c2a	rejected, crack
	SA04/13 - 42	18	0.0020063	0.0000003		5.7		0.079		c2b	rejected, crack
	SA04/13 - 43	18	0.0020073	0.0000003		6.2		0.104		r1	
	SA04/13 - 44	19	0.0020076	0.0000003		6.3		0.087		c1	
	SA04/13 - 45	19	0.0020067	0.0000002		5.9		0.051		r1	
	SA04/13 - 46	3	0.0020080	0.0000002		6.5		0.074		c2c	rejected, crack
	91500 - 181-184		0.0020146	0.0000003		9.80	0.7	0.166	4		
	Session 10 (03.06.2005)										
	91500/18 - 42-44, 46-49		0.0020134	0.0000002	0.0020131	10.01	0.4	0.078	7		
	91500 - 11-20		0.0020130	0.0000001	0.0020131	9.79	0.3	0.041	10		
	91500 - 16, 17, 19, 20		0.0020133	0.0000002	0.0020131	9.92	0.4	0.094	4		
L2-04	**SA04/04 - 1**	1	0.0020036	0.0000003		5.1		0.079		c2b	rejected, crack
	SA04/04 - 2	1	0.0020073	0.0000002		7.0		0.063		c2a	
	SA04/04 - 3	2	0.0020091	0.0000006		7.9		0.236		c2a	
	SA04/04 - 4	2	0.0020080	0.0000001		7.3		0.052		c2b	
	SA04/04 - 5	2	0.0020061	0.0000002		6.3		0.060		rim	rejected, crack
	SA04/04 - 6	3	0.0020082	0.0000003		7.4		0.097		c1	rejected, crack
	SA04/04 - 7	3	0.0020090	0.0000005		7.8		0.198		r1	rejected, crack
	91500 - 21-25		0.0020133	0.0000002	0.0020131	9.96	0.6	0.123	5		
	SA04/04 - 10	5	0.0020074	0.0000002		7.0		0.064		c2a	
	SA04/04 - 11	5	0.0020086	0.0000002		7.6		0.080		c2b	
	SA04/04 - 13	7	0.0020077	0.0000003		7.2		0.114		c1	rejected, crack
	SA04/04 - 14	7	0.0020070	0.0000003		6.8		0.103		r1	rejected, crack
	SA04/04 - 15	7	0.0020078	0.0000002		7.2		0.087		r2	rejected, crack
	SA04/04 - 18	9	0.0020077	0.0000004		7.1		0.137		c2	rejected, crack
	SA04/04 - 19	9	0.0020094	0.0000003		8.0		0.112		r1	rejected, crack
	SA04/04 - 20	10	0.0020091	0.0000003		7.9		0.132		c1	
	SA04/04 - 21	10	0.0020122	0.0000003		9.4		0.154		r1	rejected, crack
	SA04/04 - 22	11	0.0020083	0.0000004		7.4		0.141		c1	
	91500 - 31-35		0.0020135	0.0000003	0.0020131	10.03	0.6	0.132	5		
	SA04/04 - 24	13	0.0020081	0.0000003		7.4		0.108		c1	
	SA04/04 - 25	13	0.0020089	0.0000002		7.8		0.091		r1a	
	SA04/04 - 26	13	0.0020087	0.0000002		7.7		0.076		r1b	rejected, crack
	SA04/04 - 28	15	0.0020063	0.0000002		6.5		0.079		c1	inherited
	SA04/04 - 29	15	0.0020054	0.0000002		6.0		0.074		c2a	inherited
	SA04/04 - 30	15	0.0020058	0.0000002		6.2		0.060		c2b	inherited
	SA04/04 - 31	16	0.0020065	0.0000004		6.6		0.116		c1	
	SA04/04 - 32	16	0.0020080	0.0000002		7.3		0.057		rim	
	SA04/04 - 34	18	0.0020075	0.0000003		7.1		0.091		c1	
	SA04/04 - 35	18	0.0020077	0.0000002		7.2		0.077		rim	
	SA04/04 - 21/2	10	0.0020102	0.0000002		8.4		0.072		r1	rejected, crack
	SA04/04 - 37	20	0.0020065	0.0000004		6.6		0.123		c1	rejected, crack
	SA04/04 - 38	20	0.0020079	0.0000002		7.3		0.087		c2	rejected, crack
	SA04/04 - 40	20	0.0020073	0.0000002		7.0		0.063		rim	rejected, crack
	SA04/04 - 43	23	0.0020084	0.0000002		7.5		0.071		c2	
	91500 - 36-40		0.0020133	0.0000003	0.0020131	9.93	0.6	0.124	5		
	SA04/04 - 45	22	0.0020073	0.0000002		6.9		0.062		r1	
L3	**SA04/05 - 1**	1	0.0020065	0.0000004		6.5		0.128		c1	rejected, crack
	SA04/05 - 2	1	0.0020070	0.0000004		6.8		0.136		rim	rejected, crack
	SA04/05 - 9	5	0.0020060	0.0000003		6.3		0.081		c1	

Appendix 2b

Zircon oxygen isotope data of the Lochnagar pluton and average values of bracketing zircon standard 91500

	analyses no.	grain no.	$^{18}O/^{16}O$ (measured)	1 s.e.m.	$^{18}O/^{16}O$ (drift corrected)	$\delta^{18}O$ [‰] VSMOW	2SD	1 s.e.m.	n	grain area	comment
	SA04/05 - 10	5	0.0020064	0.0000004		6.5		0.131		r1+r2	rejected, crack
	SA04/05 - 7	4	0.0020079	0.0000005		7.3		0.165		c1+c2	
	SA04/05 - 8	4	0.0020090	0.0000002		7.8		0.090		c2	
	SA04/05 - 14	8	0.0020077	0.0000002		7.2		0.084		c1	
	SA04/05 - 15	8	0.0020073	0.0000003		6.9		0.108		c2	rejected, crack
	SA04/05 - 16	9	0.0020068	0.0000004		6.7		0.122		c2a	
	91500 - 47, 49-51		0.0020136	0.0000002	0.0020131	10.07	0.5	0.116	4		
	SA04/05 - 17	9	0.0020066	0.0000003		6.6		0.092		c2b	
	SA04/05 - 21	11	0.0020070	0.0000003		6.8		0.103		c2a	
	SA04/05 - 22	11	0.0020055	0.0000002		6.1		0.058		c2b	
	SA04/05 - 26	14	0.0020068	0.0000004		6.7		0.139		c1	
	SA04/05 - 27	14	0.0020066	0.0000002		6.6		0.072		rim	
	SA04/05 - 30	16	0.0020066	0.0000003		6.6		0.100		c1	rejected, crack
	SA04/05 - 31	16	0.0020073	0.0000002		7.0		0.055		rim	
	SA04/05 - 34	18	0.0020046	0.0000003		5.6		0.094		c2a	
	SA04/05 - 35	18	0.0020096	0.0000003		8.1		0.114		c2b	
	SA04/05 - 36	19	0.0020078	0.0000003		7.2		0.106		c2a	
	SA04/05 - 37	19	0.0020074	0.0000002		7.0		0.059		c2b	
	SA04/05 - 40	21	0.0020069	0.0000003		6.7		0.089		c2	
	SA04/05 - 41	21	0.0020058	0.0000002		6.2		0.059		rim	
	SA04/05 - 47	24	0.0020068	0.0000002		6.7		0.064		c2	rejected, crack
	SA04/05 - 48	24	0.0020046	0.0000003		5.6		0.073		rim	
	91500 - 52-56		0.0020132	0.0000002	0.0020131	9.91	0.4	0.098	5		
	SA04/05 - 49	25	0.0020056	0.0000002		6.1		0.065		c2b	
	SA04/05 - 50	25	0.0020079	0.0000002		7.3		0.074		c2a	
	SA04/05 - 51	26	0.0020091	0.0000002		7.9		0.094		c1	rejected, correction on position of secondary ion beam anomalously large
	SA04/05 - 52	26	0.0020062	0.0000003		6.4		0.084		rim	rejected, correction on position of secondary ion beam anomalously large
	SA04/05 - 55	28	0.0020049	0.0000002		5.8		0.068		c2	rejected, crack
	SA04/05 - 56	28	0.0020075	0.0000002		7.1		0.062		rim	rejected, crack
L1-06	**SA04/06 - 1**	1	0.0020063	0.0000004		6.5		0.127		c1	
	SA04/06 - 2	2	0.0020064	0.0000003		6.5		0.099		c1	
	SA04/06 - 3	3	0.0020068	0.0000002		6.7		0.058		c1	
	SA04/06 - 6	5	0.0020070	0.0000002		6.8		0.077		c1	
	SA04/06 - 7	5	0.0020050	0.0000002		5.8		0.064		c2	
	SA04/06 - 10	7	0.0020064	0.0000004		6.5		0.131		c1	
	SA04/06 - 11	7	0.0020064	0.0000002		6.5		0.050		c2	
	SA04/06 - 17	12	0.0020080	0.0000002		7.3		0.079		c1	rejected, crack
	SA04/06 - 18	13	0.0020064	0.0000003		6.5		0.086		c1	
	91500 - 58-61		0.0020133	0.0000004	0.0020131	9.92	0.7	0.175	4		
	SA04/06 - 23	18	0.0020053	0.0000002		5.9		0.050		c2	
	SA04/06 - 44	36	0.0020047	0.0000004		5.7		0.113		c1	
	SA04/06 - 45	36	0.0020063	0.0000001		6.5		0.048		rim	rejected, crack
	SA04/06 - 41	34	0.0020054	0.0000002		6.0		0.052		r2	rejected, crack
	SA04/06 - 42	34	0.0020059	0.0000003		6.3		0.096		r1b	rejected, crack
	SA04/06 - 36	30	0.0020084	0.0000003		7.5		0.118		c1	rejected, crack
	SA04/06 - 37	30	0.0020062	0.0000003		6.4		0.098		c2	
	SA04/06 - 43	35	0.0020030	0.0000004		4.8		0.092		c2	
	SA04/06 - 39	32	0.0020060	0.0000003		6.3		0.082		c1b	
	SA04/06 - 46	32	0.0020068	0.0000003		6.7		0.086		c1a	rejected, crack
	91500 - 62-66		0.0020135	0.0000002	0.0020131	10.03	0.5	0.104	5		
	Session 15 (05.06.2005)										
	91500 - 127-131		0.0020095	0.0000002		9.87	0.5	0.102	5		
L2-12	**SA04/12 - 1**	1	0.0020022			6.2				c1	rejected, correction on position of secondary ion beam anomalously large
				0.0000006				0.179			
	SA04/12 - 2	1	0.0020020	0.0000004		6.1		0.120		c2	
	SA04/12 - 3	2	0.0020020	0.0000005		6.2		0.142		c2	
	SA04/12 - 4	3	0.0020020	0.0000002		6.1		0.075		c2a	
	SA04/12 - 5	3	0.0020017	0.0000002		6.0		0.052		c2b	
	SA04/12 - 6	4	0.0020021	0.0000002		6.2		0.065		c2c	
	SA04/12 - 7	4	0.0020026	0.0000003		6.4		0.112		c2b	rejected, crack
	SA04/12 - 8	4	0.0020033	0.0000004		6.8		0.126		c2a	rejected, crack
	SA04/12 - 9	5	0.0020039	0.0000003		7.1		0.113		c1	
	SA04/12 - 10	5	0.0020031	0.0000004		6.7		0.137		c2	
	SA04/12 - 19	9	0.0020027	0.0000003		6.5		0.104		c2b	
	SA04/12 - 20	9	0.0020039	0.0000003		7.1		0.104		c2a	
	SA04/12 - 24	10	0.0020006	0.0000004		5.5		0.106		c2a	rejected, crack
	91500 - 132-135		0.0020097	0.0000002		9.99	0.3	0.082	4		

Appendix 2b

Zircon oxygen isotope data of the Lochnagar pluton and average values of bracketing zircon standard 91500

	analyses no.	grain no.	$^{18}O/^{16}O$ (measured)	1 s.e.m.	$^{18}O/^{16}O$ (drift corrected)	$\delta^{18}O$ [‰] VSMOW	2SD	1 s.e.m.	n	grain area	comment
	SA04/12 - 22	10	0.0019989	0.0000004		4.6		0.103		c2b	rejected, correction on position of secondary ion beam anomalously large
	SA04/12 - 23	10	0.0020007	0.0000005		5.5		0.142		c1	rejected, crack
	SA04/12 - 25	11	0.0020042	0.0000004		7.3		0.130		c2a	
	SA04/12 - 26	11	0.0020036	0.0000005		6.9		0.166		c2b	
	SA04/12 - 27	11	0.0020031	0.0000003		6.7		0.087		c2c	
	SA04/12 - 32	13	0.0020017	0.0000004		6.0		0.127		c2b	rejected, correction on position of secondary ion beam anomalously large
	SA04/12 - 33	13	0.0020010	0.0000004		5.7		0.120		c2c	rejected, crack
	SA04/12 - 34	14	0.0020002	0.0000004		5.2		0.110		c1b	rejected, crack
	SA04/12 - 35	14	0.0019990	0.0000004		4.6		0.100		c1a	rejected, crack
	SA04/12 - 37	15	0.0020005	0.0000005		5.4		0.141		c1	
	SA04/12 - 38	15	0.0020007	0.0000004		5.5		0.107		c2	
	91500 - 137, 139-141		0.0020092	0.0000001		9.71	0.3	0.064	4		
	Session 2 (24.04.2006)										
	91500/1 - 31-40		0.0020128	0.0000002		9.77	0.7	0.112	10		
	91500/1 - 41-45, 47-50		0.0020121	0.0000003		9.47	0.9	0.142	9		
	91500/2 - 1-10		0.0020133	0.0000002		10.04	0.6	0.094	10		
L2-15	**SA04/15 - 1a**	1	0.0020095			8.2				c1	rejected, correction on position of secondary ion beam anomalously large
				0.0000002				0.089			
	SA04/15 - 2a	2	0.0020047	0.0000002		5.7		0.051		c2b	rejected, crack
	SA04/15 - 3a	3	0.0020054	0.0000003		6.1		0.088		c2a	
	SA04/15 - 4a	4	0.0020033	0.0000003		5.1		0.074		c2a	rejected, possibly altered
	SA04/15 - 5b	5	0.0020062	0.0000004		6.5		0.137		r1b	rejected, crack
	SA04/15 - 5a	5	0.0020067	0.0000003		6.8		0.115		r1a	
	SA04/15 - 6a	6	0.0020051	0.0000003		6.0		0.104		c1	
	SA04/15 - 7a	7	0.0020068	0.0000003		6.8		0.110		c2	rejected, correction on position of secondary ion beam anomalously large
	91500/2 - 11-20		0.0020131	0.0000003		9.93	0.8	0.128	10		
	SA04/15 - 7b	7	0.0020075	0.0000006		7.1		0.221		rim	
	SA04/15 - 8a	8	0.0020049	0.0000002		5.9		0.046		c1	
	SA04/15 - 9a	9	0.0020055	0.0000002		6.2		0.070		c2	
	SA04/15 - 10a	10	0.0020063	0.0000004		6.6		0.131		c2	
	SA04/15 - 12a	12	0.0020073	0.0000003		7.1		0.104		c2	
	SA04/15 - 13a	13	0.0020071	0.0000002		7.0		0.061		c1	
	SA04/15 - 13b	13	0.0020072	0.0000002		7.0		0.067		rim	
	SA04/15 - 14a	14	0.0020072	0.0000003		7.0		0.109		c1	
	SA04/15 - 14b	14	0.0020069	0.0000003		6.9		0.113		rim	rejected, crack
	SA04/15 - 15a	15	0.0020061	0.0000004		6.5		0.114		c1b	rejected, crack
	91500/2 - 21-30		0.0020134	0.0000003		10.11	0.8	0.131	10		
	SA04/15 - 15b	15	0.0020058	0.0000003		6.3		0.109		rim	rejected, correction on position of secondary ion beam anomalously large
	SA04/15 - 16a	16	0.0020014	0.0000003		4.1		0.053		c1a	
	SA04/15 - 17a	17	0.0020072	0.0000003		7.0		0.102		c1	
	SA04/15 - 17b	17	0.0020071	0.0000002		7.0		0.059		c2a	
	SA04/15 - 17c	17	0.0020074	0.0000003		7.1		0.122		c2b	rejected, crack
	SA04/15 - 18a	18	0.0020073	0.0000004		7.1		0.127		c2a	rejected, crack
	SA04/15 - 18b	18	0.0020076	0.0000003		7.2		0.104		r1	rejected, crack
	SA04/15 - 18c	18	0.0020108	0.0000004		8.8		0.156		r2a	rejected, crack
	SA04/15 - 16b	16	0.0020019	0.0000002		4.4		0.037		c1b	
	SA04/15 - 19a	19	0.0020060	0.0000002		6.4		0.059		c1	
	91500/1 - 51-60		0.0020128	0.0000002		9.82	0.5	0.084	10		
	SA04/15 - 20a	20	0.0020064	0.0000003		6.6		0.095		c1	rejected, correction on position of secondary ion beam anomalously large
	SA04/15 - 21a	21	0.0020087	0.0000002		7.8		0.075		c1	
	SA04/15 - 21b	21	0.0020070	0.0000001		6.9		0.040		c2	
	SA04/15 - 22a	22	0.0020046	0.0000003		5.7		0.087		core a	inherited
	SA04/15 - 26a	26	0.0020080	0.0000003		7.4		0.094		c1	rejected, crack
	SA04/15 - 26c	26	0.0020075	0.0000004		7.2		0.128		r2	rejected, correction on position of secondary ion beam anomalously large
	SA04/15 - 27a	27	0.0020033	0.0000004		5.1		0.094		c1a	rejected, possibly altered
	SA04/15 - 27b	27	0.0020037	0.0000005		5.3		0.143		c1b	rejected, possibly altered

Appendix 2b

Zircon oxygen isotope data of the Lochnagar pluton and average values of bracketing zircon standard 91500

analyses no.	grain no.	$^{18}O/^{16}O$ (measured)	1 s.e.m.	$^{18}O/^{16}O$ (drift corrected)	$\delta^{18}O$ [‰] VSMOW	2SD	1 s.e.m.	n	grain area	comment
91500/1 - 61, 63-70		0.0020129	0.0000003		9.85	1.0	0.153	9		
Session 11 (19.06.2006)										
91500/12 - 11-20		0.0020166	0.0000001		9.86	0.4	0.064	10		
91500/12 - 31-40		0.0020166	0.0000001		9.83	0.4	0.071	10		
Mount1/91500 - 1-9		0.0020168	0.0000002		9.93	0.7	0.120	9		
Mount1/91500 - 20-21, 23-25		0.0020166	0.0000001		9.83	0.3	0.064	5		
Mount1/91500 - 26-30		0.0020166	0.0000004		9.83	0.9	0.206	5		
SA04/15 - 3b	3	0.0020092			6.2				c2b	rejected, possibly altered
SA04/15 - 28a	28	0.0020090			6.1				c1	
Session 13 (15.11.2006)										
91500 - 1-10		0.0020195	0.0000001	0.0020197	9.76	0.3	0.052	10		
91500 - 11-20		0.0020195	0.0000001	0.0020195	9.86	0.2	0.035	10		
SA04/15 - 33a	33	0.0020112	0.0000003		5.9		0.095		inh1	inherited
SA04/15 - 29a	29	0.0020106	0.0000005		5.5		0.134		inh1	inherited
SA04/15 - 29b	29	0.0020130	0.0000002		6.8		0.065		rim	rejected, crack
SA04/15 - 2a	2	0.0020131	0.0000003		6.8		0.100		c2b	rejected, crack
SA04/15 - 36a	36	0.0020098	0.0000003		5.2		0.073		c2	inherited
SA04/15 - 3b	3	0.0020129	0.0000003		6.7		0.096		c2b	rejected, crack
SA04/15 - 3a	3	0.0020119	0.0000004		6.2		0.114		c2a	
SA04/15 - 35a	35	0.0020133	0.0000002		6.9		0.074		c2b	rejected, possibly altered
SA04/15 - 35b	35	0.0020119	0.0000003		6.3		0.091		c2a	
SA04/15 - 5c	5	0.0020138	0.0000002		7.2		0.072		r1c	
91500 - 21-25, 27-30		0.0020195	0.0000001	0.0020190	10.11	0.4	0.060	9		
SA04/15 - 4a	4	0.0020113	0.0000002		6.1		0.055		c2a	
SA04/15 - 4b	4	0.0020119	0.0000005		6.4		0.148		c2b	
SA04/15 - 32a	32	0.0020104	0.0000007		5.7		0.208		c2a	inherited
SA04/15 - 32b	32	0.0020122	0.0000004		6.6		0.140		c2b	inherited
SA04/15 - 32c	32	0.0020091	0.0000012		5.0		0.304		c2c	inherited, rejected, crack
SA04/15 - 15c	15	0.0020122	0.0000003		6.6		0.104		c1a	
SA04/15 - 14b	14	0.0020139	0.0000023		7.4		0.832		rim	rejected, crack
SA04/15 - 16a	16	0.0020084	0.0000025		4.8		0.598		c1a	
SA04/15 - 17c	17	0.0020141	0.0000005		7.6		0.201		c2b	rejected, crack
SA04/15 - 18e	18	0.0020134	0.0000002		7.2		0.075		c2b	rejected, crack
SA04/15 - 18d	18	0.0020111	0.0000004		6.1		0.131		r2b	rejected, crack
SA04/15 - 22a	22	0.0020135	0.0000003		7.3		0.127		core a	inherited
SA04/15 - 22b	22	0.0020138	0.0000004		7.5		0.160		core b	inherited
91500 - 31-35		0.0020181	0.0000003	0.0020185	9.64	0.8	0.168	5		
91500 - 36-39		0.0020185	0.0000002	0.0020185	9.88	0.3	0.073	5		
91500 - 42-45		0.0020179	0.0000002	0.0020179	9.80	0.4	0.101	4		

Appendix 2c
Zircon U-Pb data of the Lochnagar pluton

sample	analysis no.	grain no.	U ppm	Th ppm	Pb ppm	Th/U	^{204}Pb ppb	f206 (%)	^{204}Pb/^{206}Pb	corrected ratios									Ages (Ma)								grain area	comment
										^{207}Pb/^{206}Pb	1σ	^{208}Pb/^{206}Pb	1σ	^{207}Pb/^{235}U	1σ	^{206}Pb/^{238}U	1σ	ρ	^{206}Pb/^{238}U	1σ	^{207}Pb/^{235}U	1σ	^{207}Pb/^{206}Pb	1σ	% disc		
AD1	SA04/01 - 3	2	376	126	25	0.34	0.4	0.04	0.0000191	0.0551	0.0004	0.1093	0.0013	0.5084	0.0053	0.0669	0.0005	0.72	417	3	417	4	417	15	0	rim	
	SA04/01 - 4	2	116	46	8	0.41	18.0	4.99	0.0028080	0.0549	0.0035	0.1165	0.0189	0.4879	0.0319	0.0645	0.0010	0.23	403	6	403	22	407	178	1	c2a	rejected, high common Pb
	SA04/01 - 5	3	136	71	10	0.53	0.1	0.01	0.0000064	0.0554	0.0007	0.1683	0.0011	0.5126	0.0079	0.0671	0.0006	0.54	419	3	420	5	427	28	2	c2	
	SA04/01 - 6	3	97	61	7	0.64	1.6	0.53	0.0002868	0.0529	0.0013	0.1942	0.0052	0.4921	0.0126	0.0675	0.0006	0.36	421	4	406	9	322	32	-31	c1	rejected, > 10 % discordant
	SA04/01 - 15	6	141	139	11	1.01	0.3	0.06	0.0000332	0.0546	0.0007	0.3148	0.0023	0.5083	0.0077	0.0676	0.0006	0.57	422	3	417	5	394	25	-7	c1	
	SA04/01 - 14	6	105	75	8	0.73	0.8	0.25	0.0001359	0.0533	0.0008	0.2258	0.0033	0.5004	0.0089	0.0681	0.0006	0.48	424	3	412	6	342	19	-24	c2	rejected, > 10 % discordant
	SA04/01 - 20	8	136	121	10	0.91	0.3	0.06	0.0000335	0.0539	0.0008	0.2814	0.0021	0.4940	0.0084	0.0665	0.0005	0.47	415	3	408	6	365	31	-14	c1	rejected, > 10 % discordant
	SA04/01 - 23	8	79	60	6	0.78	0.0	0.00	0.0000002	0.0551	0.0009	0.2458	0.0022	0.5052	0.0098	0.0665	0.0006	0.47	415	4	415	7	417	38	1	c2	
	SA04/01 - 26	8	173	129	13	0.77	0.2	0.03	0.0000160	0.0548	0.0006	0.2408	0.0013	0.5026	0.0065	0.0666	0.0005	0.57	415	3	413	4	402	23	-3	rim	
	SA04/01 - 27	9	72	60	6	0.85	0.2	0.07	0.0000389	0.0541	0.0011	0.2664	0.0028	0.4992	0.0110	0.0669	0.0007	0.46	417	4	411	7	376	39	-11	c1	rejected, > 10 % discordant
	SA04/01 - 28	9	94	92	7	1.00	0.4	0.14	0.0000726	0.0556	0.0009	0.3129	0.0028	0.5097	0.0094	0.0665	0.0006	0.48	415	4	418	6	436	29	5	c2a	
	SA04/01 - 29	9	101	78	8	0.80	0.3	0.09	0.0000481	0.0546	0.0008	0.2520	0.0022	0.4998	0.0083	0.0664	0.0005	0.48	414	3	412	6	396	27	-5	c2b	
	SA04/01 - 33	11	268	278	22	1.06	0.4	0.05	0.0000247	0.0543	0.0007	0.3308	0.0028	0.5032	0.0073	0.0672	0.0005	0.50	419	3	414	5	383	27	-9	r1	
	SA04/01 - 34	11	157	214	14	1.40	0.6	0.12	0.0000667	0.0561	0.0006	0.4338	0.0046	0.5199	0.0065	0.0673	0.0005	0.61	420	3	425	4	454	15	8	c1	
	SA04/01 - 43	14	89	65	7	0.75	0.0	0.02	0.0000091	0.0560	0.0008	0.2347	0.0022	0.5140	0.0087	0.0666	0.0007	0.58	415	4	421	6	452	29	8	c1	
	SA04/01 - 44	14	76	41	5	0.56	0.2	0.07	0.0000357	0.0547	0.0011	0.1747	0.0022	0.5084	0.0116	0.0675	0.0006	0.40	421	4	417	8	398	43	-6	c2	
	SA04/01 - 46	15	124	226	12	1.87	0.0	0.01	0.0000067	0.0558	0.0006	0.5819	0.0040	0.5157	0.0070	0.0670	0.0006	0.61	418	3	422	5	446	23	6	c1	
	SA04/01 - 48	15	151	130	12	0.88	0.5	0.11	0.0000577	0.0549	0.0010	0.2732	0.0020	0.5059	0.0097	0.0668	0.0005	0.42	417	3	416	7	409	35	-2	c2c	
	SA04/01 - 51	16	446	1050	47	2.41	0.5	0.04	0.0000197	0.0556	0.0005	0.7549	0.0030	0.5176	0.0057	0.0675	0.0005	0.66	421	3	424	4	436	17	3	c1	
	SA04/01 - 52	16	216	448	22	2.12	0.9	0.13	0.0000687	0.0542	0.0005	0.6713	0.0060	0.5094	0.0061	0.0682	0.0005	0.61	425	3	418	4	378	16	-12	rim	rejected, > 10 % discordant
	SA04/01 - 7	4	234	252	19	1.11	0.7	0.10	0.0000540	0.0553	0.0007	0.3467	0.0022	0.5203	0.0081	0.0682	0.0006	0.52	425	3	425	5	425	28	0	?	
	SA04/01 - 9	4	229	280	20	1.25	0.6	0.08	0.0000452	0.0548	0.0005	0.3904	0.0020	0.5278	0.0081	0.0699	0.0009	0.83	435	5	430	5	403	16	-8	?	rejected, crack
	SA04/01 - 10	4	100	87	8	0.89	0.2	0.05	0.0000274	0.0555	0.0010	0.2776	0.0020	0.5223	0.0105	0.0683	0.0006	0.44	426	4	427	7	431	38	1	?	
	SA04/01 - 4.2	2	147	68	10	0.48	0.2	0.04	0.0000203	0.0555	0.0006	0.1504	0.0013	0.5069	0.0077	0.0663	0.0007	0.66	414	4	416	5	431	24	4	c2b	
AD2	SA04/02 - 39	18	1061	994	82	0.96	9.9	0.30	0.0001627	0.0551	0.0004	0.3035	0.0022	0.5033	0.0052	0.0663	0.0005	0.71	414	3	414	3	415	13	0	rim	rejected, > 1000 ppm U
	SA04/02 - 40	18	2590	5221	262	2.07	0.8	0.01	0.0000054	0.0554	0.0001	0.6462	0.0011	0.5264	0.0038	0.0689	0.0005	0.96	429	3	429	3	429	4	0	c1	rejected, > 1000 ppm U
	SA04/02 - 26	12	1960	1839	155	0.96	0.9	0.01	0.0000080	0.0549	0.0002	0.3035	0.0006	0.5123	0.0039	0.0676	0.0005	0.93	422	3	420	3	409	6	-3	c1	rejected, > 1000 ppm U
	SA04/02 - 45	12	617	1760	28	2.93	0.9	0.13	0.0000678	0.0587	0.0002	0.7676	0.0011	0.2120	0.0194	0.0262	0.0024	1.00	167	15	195	16	554	8	70	c1	rejected, crack
	SA04/02 - 45.2	12	3116	7351	327	2.42	71.6	0.71	0.0003839	0.0556	0.0003	0.7732	0.0020	0.5240	0.0062	0.0684	0.0007	0.86	426	4	428	4	435	11	2	c1+rim	rejected, high common Pb
	SA04/02 - 19	10	550	466	42	0.87	1.2	0.07	0.0000367	0.0552	0.0003	0.2762	0.0011	0.5035	0.0058	0.0662	0.0007	0.89	413	4	414	4	418	10	1	c2	
	SA04/02 - 20	10	2000	3675	192	1.89	0.0	0.00	0.0000004	0.0553	0.0002	0.5961	0.0010	0.5197	0.0056	0.0682	0.0007	0.95	425	4	425	4	423	8	-1	c1	rejected, > 1000 ppm U
	SA04/02 - 41	19	962	1273	81	1.36	1.0	0.03	0.0000175	0.0556	0.0003	0.4301	0.0069	0.5089	0.0059	0.0664	0.0007	0.91	414	4	418	4	436	10	5	c1	
	SA04/02 - 42	19	273	67	18	0.25	149.8	15.57	0.0098639	0.0449	0.0037	0.0629	0.0114	0.4030	0.0352	0.0651	0.0017	0.29	407	10	344	25				rim	rejected, high common Pb
	SA04/02 - 30	14	1299	1501	104	1.19	0.9	0.02	0.0000117	0.0556	0.0003	0.3797	0.0029	0.5044	0.0072	0.0657	0.0009	0.93	410	5	415	5	438	11	6	c1	rejected, > 1000 ppm U
	SA04/02 - 10	7	270	212	20	0.81	0.5	0.06	0.0000327	0.0542	0.0006	0.2525	0.0024	0.4835	0.0077	0.0647	0.0008	0.74	404	5	400	5	377	23	-7	c1	rejected, crack
	SA04/02 - 12	7	279	194	20	0.71	0.3	0.03	0.0000172	0.0553	0.0006	0.2260	0.0015	0.5054	0.0074	0.0663	0.0007	0.70	414	4	415	5	423	22	2	c2	
	SA04/02 - 27	13	1891	2685	164	1.46	15.6	0.26	0.0001415	0.0552	0.0002	0.4645	0.0014	0.5110	0.0055	0.0671	0.0007	0.93	419	4	419	4	420	6	0	rim	rejected, > 1000 ppm U
	SA04/02 - 29	13	306	49	20	0.16	0.4	0.05	0.0000250	0.0556	0.0005	0.0509	0.0011	0.5167	0.0074	0.0675	0.0007	0.73	421	4	423	5	434	21	3	c2	
	SA04/02 - 31	15	446	344	34	0.79	0.7	0.05	0.0000273	0.0548	0.0004	0.2494	0.0013	0.5089	0.0068	0.0673	0.0007	0.79	420	4	418	5	404	18	-4	c2a	
	SA04/02 - 32	15	232	153	17	0.68	0.8	0.12	0.0000617	0.0545	0.0008	0.2138	0.0033	0.5014	0.0091	0.0667	0.0008	0.63	417	5	413	6	391	30	-7	c2b	
	SA04/02 - 46	20	1237	1730	111	1.43	0.2	0.01	0.0000028	0.0551	0.0003	0.4517	0.0070	0.5279	0.0060	0.0695	0.0007	0.90	433	4	430	4	414	12	-5	c1	rejected, > 1000 ppm U
	SA04/02 - 22	11	1470	2119	133	1.48	0.5	0.01	0.0000051	0.0553	0.0002	0.4651	0.0009	0.5263	0.0058	0.0690	0.0007	0.92	430	4	429	4	423	10	-2	c1b	rejected, > 1000 ppm U
	SA04/02 - 24	11	354	245	26	0.71	2.1	0.19	0.0001025	0.0542	0.0004	0.2239	0.0016	0.4938	0.0064	0.0661	0.0007	0.80	413	4	408	4	378	15	-9	c1c	
	SA04/02 - 25	11	119	47	8	0.40	0.4	0.12	0.0000649	0.0553	0.0009	0.1273	0.0019	0.4931	0.0097	0.0646	0.0008	0.60	404	5	407	7	426	32	5	c1d	
	SA04/02 - 27.2	13	333	58	21	0.18	0.7	0.07	0.0000362	0.0551	0.0006	0.0556	0.0010	0.4988	0.0074	0.0656	0.0007	0.71	410	4	411	5	418	22	2	c2b	
	SA04/02 - 47	21	305	160	21	0.54	1.5	0.16	0.0000864	0.0554	0.0006	0.1657	0.0040	0.4980	0.0074	0.0652	0.0007	0.73	407	4	410	5	427	21	5	c2a	
	SA04/02 - 48	21	280	208	21	0.76	44.2	4.89	0.0027478	0.0542	0.0012	0.2352	0.0128	0.4971	0.0122	0.0665	0.0007	0.45	415	4	410	8	379	60	-10	c2b	rejected, high common Pb
L1-03	S04/03 - 13	8	934	837	73	0.92	0.9	0.03	0.0000162	0.0554	0.0003	0.2919	0.0023	0.5169	0.0044	0.0677	0.0005	0.82	422	3	423	3	428	10	1	c1+r1	
	S04/03 - 14	8	74	38	5	0.52	0.5	0.23	0.0001230	0.0553	0.0013	0.1592	0.0037	0.4999	0.0123	0.0655	0.0006	0.39	409	4	412	8	424	35	3	r1	rejected, crack
	S04/03 - 23	14	499	557	41	1.15	0.8	0.05	0.0000266	0.0547	0.0004	0.3623	0.0031	0.5049	0.0052	0.0670	0.0005	0.72	418	3	415	3	398	14	-5	c2a	

sample	analysis no.	grain no.	U ppm	Th ppm	Pb ppm	Th/U	^{204}Pb ppb	f206 (%)	^{204}Pb/^{206}Pb	corrected ratios									Ages (Ma)								grain area	comment
										^{207}Pb/^{206}Pb	1σ	^{208}Pb/^{206}Pb	1σ	^{207}Pb/^{235}U	1σ	^{206}Pb/^{238}U	1σ	ρ	^{206}Pb/^{238}U	1σ	^{207}Pb/^{235}U	1σ	^{207}Pb/^{206}Pb	1σ	% disc		
	S04/03 - 24	14	94	53	7	0.58	0.0	0.00	0.0000002	0.0562	0.0007	0.1830	0.0014	0.5175	0.0077	0.0668	0.0006	0.62	417	4	423	5	461	25	10	c2b	
	S04/03 - 28	16	656	262	46	0.41	0.1	0.00	0.0000017	0.0556	0.0003	0.1292	0.0004	0.5232	0.0046	0.0682	0.0005	0.78	425	3	427	3	437	12	3	c1	rejected, crack
	S04/03 - 29	16	57	36	4	0.65	1.1	0.66	0.0003548	0.0518	0.0019	0.1970	0.0076	0.4616	0.0177	0.0647	0.0007	0.28	404	4	385	12	274	39	-47	rim	rejected, > 10 % discordant
	S04/03 - 20	12	2349	1387	135	0.61	465.2	7.44	0.0043001	0.0528	0.0029	0.1860	0.0159	0.3886	0.0223	0.0534	0.0007	0.24	335	5	333	16	321	242	-4	c1	rejected, crack
	S04/03 - 19	12	503	315	37	0.64	0.0	0.00	0.0000000	0.0551	0.0004	0.2025	0.0013	0.5091	0.0054	0.0670	0.0005	0.64	418	3	418	4	417	18	0	rim	
	S04/03 - 56	24	747	481	55	0.66	0.7	0.03	0.0000156	0.0549	0.0004	0.2065	0.0007	0.5100	0.0055	0.0673	0.0005	0.67	420	3	418	4	409	17	-3	c2	
	S04/03 - 46	24	314	199	23	0.65	1.2	0.12	0.0000667	0.0541	0.0005	0.2025	0.0015	0.5058	0.0061	0.0678	0.0005	0.60	423	3	416	4	376	18	-12	r1a	rejected, > 10 % discordant
	S04/03 - 47	24	650	465	42	0.73	22.3	1.20	0.0006519	0.0538	0.0010	0.2627	0.0062	0.4401	0.0086	0.0593	0.0005	0.43	371	3	370	6	363	34	-2	r1b	rejected, crack
	S/04/03 - 6	3	86	48	6	0.57	0.0	0.00	0.0000002	0.0539	0.0010	0.1765	0.0014	0.5118	0.0105	0.0689	0.0006	0.39	429	3	420	7	365	42	-18	c2a	rejected, > 10 % discordant
	S04/03 - 57	3	85	54	6	0.65	0.7	0.26	0.0001389	0.0529	0.0012	0.1971	0.0036	0.4855	0.0119	0.0666	0.0006	0.38	416	4	402	8	322	34	-29	c2b	rejected, > 10 % discordant
	S04/03 - 51	26	284	287	23	1.04	7.0	0.78	0.0004189	0.0547	0.0014	0.3256	0.0067	0.5120	0.0139	0.0679	0.0006	0.32	424	4	420	9	399	49	-6	c1	
	S04/03 - 52	26	207	229	17	1.14	0.5	0.08	0.0000438	0.0548	0.0008	0.3571	0.0025	0.5152	0.0086	0.0682	0.0005	0.48	425	3	422	6	404	30	-5	c2	
	S04/03 - 17	10	80	55	6	0.70	0.0	0.00	0.0000002	0.0568	0.0013	0.2211	0.0039	0.5239	0.0132	0.0669	0.0007	0.39	417	4	428	9	483	50	14	c1	rejected, > 10 % discordant
	S04/03 - 53	26	106	74	8	0.72	0.4	0.12	0.0000621	0.0549	0.0011	0.2274	0.0029	0.5085	0.0108	0.0672	0.0006	0.43	419	4	417	7	408	37	-3	rim	
	S04/03 - 54	27	48	25	3	0.54	0.4	0.27	0.0001424	0.0542	0.0019	0.1633	0.0046	0.5096	0.0191	0.0681	0.0007	0.29	425	4	418	13	380	62	-12	c2	rejected, > 10 % discordant
	S04/03 - 55	27	68	58	5	0.88	0.4	0.19	0.0001004	0.0526	0.0012	0.2708	0.0045	0.4873	0.0113	0.0672	0.0005	0.34	419	3	403	8	311	31	-35	c1	rejected, > 10 % discordant
	S04/03 - 58	28	1930	1125	39	0.60	151.6	6.41	0.0036643	0.0529	0.0016	0.3568	0.0170	0.1591	0.0064	0.0218	0.0006	0.68	139	4	150	6	322	109	57	c2a	rejected, high common Pb
	S04/03 - 59	28	62	36	4	0.60	0.2	0.13	0.0000676	0.0549	0.0017	0.1869	0.0040	0.5071	0.0173	0.0670	0.0009	0.40	418	6	416	12	406	61	-3	c2b	
	S04/03 - 20.2	12	2167	1113	156	0.53	25.6	0.38	0.0002018	0.0555	0.0008	0.1611	0.0028	0.5193	0.0084	0.0678	0.0006	0.53	423	4	425	6	434	30	3	c1	rejected, > 1000 ppm U
	S04/03 - 47.2	24	392	216	28	0.56	0.0	0.00	0.0000001	0.0551	0.0004	0.1750	0.0009	0.5088	0.0056	0.0670	0.0005	0.71	418	3	418	4	414	17	-1	r1c	
	S04/03 - 15	9	83	85	7	1.05	0.6	0.23	0.0001207	0.0537	0.0013	0.3263	0.0038	0.4996	0.0125	0.0674	0.0006	0.37	421	4	411	8	360	36	-17	c2a	rejected, > 10 % discordant
	S04/03 - 16	9	55	32	4	0.59	0.4	0.24	0.0001288	0.0518	0.0018	0.1797	0.0041	0.4819	0.0179	0.0675	0.0008	0.30	421	5	399	12	275	63	-53	c2b	rejected, > 10 % discordant
L2-04	SA04/04 - 31	16	1598	676	114	0.43	0.6	0.01	0.0000058	0.0551	0.0002	0.1358	0.0004	0.5244	0.0058	0.0690	0.0007	0.96	430	4	428	4	417	7	-3	c1	rejected, > 1000 ppm U
	SA04/04 - 32	16	597	242	40	0.42	29.0	1.57	0.0008511	0.0562	0.0009	0.1380	0.0065	0.5066	0.0095	0.0654	0.0007	0.56	408	4	416	6	460	27	11	rim	rejected, high common Pb
	SA04/04 - 34	18	1071	318	74	0.31	2.8	0.08	0.0000441	0.0548	0.0003	0.0940	0.0009	0.5268	0.0064	0.0697	0.0008	0.90	434	5	430	4	405	11	-7	c1	rejected, crack
	SA04/04 - 35	18	758	294	53	0.40	1.4	0.06	0.0000311	0.0551	0.0004	0.1251	0.0012	0.5218	0.0065	0.0686	0.0007	0.85	428	4	426	4	417	14	-3	rim	
	SA04/04 - 21	10	600	94	40	0.16	0.3	0.02	0.0000085	0.0557	0.0003	0.0507	0.0011	0.5361	0.0077	0.0698	0.0009	0.91	435	5	436	5	441	14	1	r1	rejected, crack
	SA04/04 - 20	10	2643	57	169	0.02	0.7	0.01	0.0000045	0.0555	0.0001	0.0069	0.0002	0.5330	0.0055	0.0697	0.0007	0.97	434	4	434	4	431	6	-1	c1	rejected, > 1000 ppm U
	SA04/04 - 22	11	143	65	10	0.46	0.4	0.10	0.0000523	0.0549	0.0006	0.1434	0.0039	0.5010	0.0086	0.0661	0.0008	0.73	413	5	412	6	409	21	-1	c1	
	SA04/04 - 45	11	285	156	20	0.56	0.0	0.00	0.0000001	0.0559	0.0004	0.1744	0.0009	0.5157	0.0066	0.0669	0.0007	0.79	418	4	422	4	447	17	7	r1	
	SA04/04 - 12	6	1470	1042	114	0.73	3.8	0.08	0.0000429	0.0548	0.0002	0.2271	0.0018	0.5267	0.0058	0.0697	0.0007	0.91	434	4	430	4	403	9	-8	c1	
	SA04/04 - 46	6	437	235	32	0.55	0.8	0.06	0.0000306	0.0548	0.0006	0.1722	0.0011	0.5184	0.0081	0.0686	0.0007	0.65	428	4	424	5	402	26	-6	rim	
	SA04/04 - 3	2	92	61	6	0.69	0.3	0.11	0.0000574	0.0549	0.0010	0.2183	0.0033	0.4883	0.0102	0.0645	0.0007	0.53	403	4	404	7	407	34	1	c2a	rejected, crack
	SA04/04 - 4	2	500	266	36	0.55	0.0	0.00	0.0000000	0.0551	0.0002	0.1698	0.0010	0.5227	0.0057	0.0688	0.0007	0.92	429	4	427	4	415	9	-3	c2b	
	SA04/04 - 5	2	10550	1281	788	0.12	2.2	0.01	0.0000030	0.0550	0.0001	0.0385	0.0008	0.5985	0.0060	0.0789	0.0008	0.98	489	5	476	4	413	4	-19	rim	rejected, > 10 % discordant
	SA04/04 - 28	15	70	52	14	0.76	0.0	0.00	0.0000001	0.0750	0.0009	0.2315	0.0017	1.8171	0.0295	0.1758	0.0020	0.70	1044	11	1052	11	1067	23	2	inh1	inherited grain
	SA04/04 - 29	15	174	96	34	0.57	0.4	0.03	0.0000163	0.0747	0.0005	0.1703	0.0010	1.8455	0.0229	0.1793	0.0019	0.84	1063	10	1062	8	1059	13	0	inh2	inherited grain
	SA04/04 - 30	15	272	143	53	0.54	0.1	0.00	0.0000013	0.0739	0.0003	0.1605	0.0006	1.8648	0.0208	0.1831	0.0019	0.93	1084	10	1069	7	1038	8	-4	inh3	inherited grain
	SA04/04 - 24	13	557	295	40	0.54	0.6	0.03	0.0000168	0.0554	0.0003	0.1700	0.0009	0.5233	0.0061	0.0685	0.0007	0.91	427	4	427	4	427	10	0	c1+c2	
	SA04/04 - 25	13	235	116	16	0.51	0.1	0.01	0.0000040	0.0555	0.0006	0.1592	0.0013	0.5108	0.0076	0.0667	0.0007	0.70	416	4	419	5	433	23	4	r1a	
	SA04/04 - 26	13	2687	624	191	0.24	22.6	0.25	0.0001343	0.0552	0.0002	0.0725	0.0015	0.5514	0.0075	0.0724	0.0009	0.95	451	6	446	5	420	9	-7	r1b	rejected, crack
	SA04/04 - 47	25	2869	1128	206	0.40	0.3	0.00	0.0000017	0.0553	0.0002	0.1258	0.0004	0.5349	0.0055	0.0702	0.0007	0.96	437	4	435	4	423	6	-3	c1	rejected, > 1000 ppm U
	SA04/04 - 48	25	1977	732	141	0.38	20.6	0.32	0.0001714	0.0554	0.0003	0.1195	0.0017	0.5362	0.0065	0.0702	0.0007	0.86	437	4	436	4	429	13	-2	rim	rejected, crack
	SA04/04 - 49	26	612	321	44	0.54	17.1	0.91	0.0004897	0.0549	0.0007	0.1431	0.0051	0.5096	0.0081	0.0674	0.0006	0.60	420	4	418	5	406	20	-4	c1	rejected, crack
	SA04/04 - 50	26	1321	502	96	0.39	0.7	0.02	0.0000091	0.0549	0.0002	0.1196	0.0004	0.5386	0.0048	0.0712	0.0006	0.93	443	4	438	3	407	7	-9	c2	rejected, > 1000 ppm U
	SA04/04 - 51	27	499	252	36	0.52	6.4	0.40	0.0002153	0.0549	0.0006	0.1587	0.0031	0.5204	0.0079	0.0688	0.0007	0.66	429	4	425	5	407	20	-5	c1a	
	SA04/04 - 52	27	819	465	63	0.58	8.9	0.33	0.0001773	0.0548	0.0005	0.1791	0.0025	0.5380	0.0090	0.0712	0.0010	0.85	444	6	437	6	402	17	-10	c1b	rejected, > 10 % discordant
	SA04/04 - 5.2	2	840	438	60	0.54	0.4	0.02	0.0000087	0.0546	0.0004	0.1685	0.0010	0.5126	0.0055	0.0681	0.0006	0.77	425	3	420	4	395	15	-8	c2c	
L3	SA04/05 - 1	1	213	212	16	1.02	4.8	0.88	0.0004744	0.0565	0.0013	0.1468	0.0060	0.4889	0.0118	0.0627	0.0006	0.37	392	3	404	8	473	38	17	c1	rejected, crack
	SA04/05 - 2	1	725	531	49	0.75	57.1	2.93	0.0016129	0.0531	0.0008	0.1862	0.0091	0.4289	0.0074	0.0586	0.0005	0.49	367	3	362	5	332	20	-11	rim	rejected, crack
	SA04/05 - 12	7	583	345	42	0.61	1.3	0.07	0.0000401	0.0552	0.0003	0.1890	0.0012	0.5066	0.0058	0.0666	0.0006	0.83	416	4	416	4	419	12	1	c1	
	SA04/05 - 13	7	736	565	55	0.79	0.6	0.02	0.0000133	0.0554	0.0003	0.2456	0.0012	0.5103	0.0052	0.0668	0.0006	0.81	417	3	419	3	426	13	2	c2	
	SA04/05 - 14	8	360	182	26	0.52	0.1	0.00	0.0000026	0.0559	0.0004	0.1630	0.0006	0.5289	0.0062	0.0686	0.0006	0.75	428	4	431	4	448	17	5	c1	

sample	analysis no.	grain no.	U ppm	Th ppm	Pb ppm	Th/U	^{204}Pb ppb	f206 (%)	^{204}Pb/^{206}Pb	corrected ratios									Ages (Ma)								grain area	comment
										^{207}Pb/^{206}Pb	1σ	^{208}Pb/^{206}Pb	1σ	^{207}Pb/^{235}U	1σ	^{206}Pb/^{238}U	1σ	ρ	^{206}Pb/^{238}U	1σ	^{207}Pb/^{235}U	1σ	^{207}Pb/^{206}Pb	1σ	% disc		
	SA04/05 - 15	8	791	454	58	0.59	2.7	0.11	0.0000572	0.0551	0.0004	0.1830	0.0011	0.5209	0.0057	0.0686	0.0006	0.76	428	3	426	4	414	15	-3	c2	
	SA04/05 - 16	9	806	770	66	0.98	0.6	0.02	0.0000119	0.0555	0.0002	0.3051	0.0008	0.5300	0.0050	0.0692	0.0006	0.88	431	3	432	3	433	9	0	c2a	
	SA04/05 - 17	9	567	289	41	0.52	0.1	0.00	0.0000017	0.0552	0.0002	0.1630	0.0005	0.5159	0.0048	0.0678	0.0006	0.89	423	3	422	3	418	9	-1	c2b	
	SA04/05 - 26	14	1829	1044	130	0.59	27.8	0.49	0.0002647	0.0553	0.0003	0.1812	0.0026	0.5069	0.0050	0.0664	0.0006	0.84	415	3	416	3	426	7	3	c1	rejected, crack
	SA04/05 - 27	14	572	307	41	0.55	0.1	0.00	0.0000016	0.0553	0.0004	0.1712	0.0006	0.5186	0.0057	0.0680	0.0006	0.75	424	3	424	4	424	16	0	rim	
	SA04/05 - 34	18	486	385	38	0.81	0.2	0.01	0.0000064	0.0552	0.0003	0.2521	0.0007	0.5195	0.0052	0.0682	0.0006	0.83	425	3	425	3	421	12	-1	c2a	
	SA04/05 - 35	18	613	598	49	1.00	3.2	0.17	0.0000903	0.0556	0.0005	0.3141	0.0015	0.5157	0.0063	0.0673	0.0006	0.67	420	3	422	4	435	18	3	c2b	
	SA04/05 - 38	20	503	358	38	0.73	0.2	0.01	0.0000063	0.0551	0.0004	0.2262	0.0021	0.5108	0.0057	0.0672	0.0006	0.80	419	4	419	4	417	14	-1	c2a	
	SA04/05 - 39	20	712	558	55	0.80	11.1	0.50	0.0002690	0.0553	0.0005	0.2235	0.0034	0.5196	0.0065	0.0682	0.0006	0.66	425	3	425	4	424	15	0	c2b	
	SA04/05 - 41	21	1029	394	67	0.39	47.3	1.53	0.0008334	0.0539	0.0006	0.1219	0.0055	0.4743	0.0067	0.0638	0.0005	0.59	399	3	394	5	366	17	-9	rim	rejected, high common Pb
	SA04/05 - 40	21	1687	1519	135	0.92	0.5	0.01	0.0000044	0.0552	0.0002	0.2947	0.0068	0.5286	0.0047	0.0695	0.0006	0.93	433	3	431	3	419	8	-3	c1	rejected, > 1000 ppm U
	SA04/05 - 49	25	687	562	52	0.84	0.6	0.03	0.0000143	0.0550	0.0003	0.2627	0.0009	0.5065	0.0051	0.0668	0.0006	0.82	417	3	416	3	412	12	-1	c2b	
	SA04/05 - 50	25	647	350	47	0.55	0.7	0.04	0.0000194	0.0546	0.0003	0.1723	0.0009	0.5139	0.0051	0.0682	0.0006	0.84	426	3	421	3	396	11	-7	c2a	
	SA04/05 - 51	26	2210	880	158	0.41	14.1	0.20	0.0001050	0.0554	0.0002	0.1284	0.0012	0.5343	0.0048	0.0699	0.0006	0.89	436	3	435	3	428	7	-2	c1	rejected, > 1000 ppm U
	SA04/05 - 52	26	816	439	59	0.55	1.4	0.05	0.0000293	0.0549	0.0002	0.1701	0.0008	0.5186	0.0048	0.0685	0.0006	0.91	427	3	424	3	407	7	-5	rim	
	SA04/05 - 55	28	66	31	5	0.48	0.0	0.00	0.0000003	0.0558	0.0009	0.1511	0.0022	0.5114	0.0099	0.0665	0.0007	0.55	415	4	419	7	442	36	6	c2a	
	SA04/05 - 56	28	516	507	41	1.01	0.5	0.03	0.0000152	0.0555	0.0003	0.3121	0.0024	0.5123	0.0051	0.0670	0.0006	0.82	418	3	420	3	430	12	3	rim	
	SA04/05 - 64	32	2602	1588	199	0.63	2.3	0.03	0.0000146	0.0549	0.0002	0.1934	0.0006	0.5354	0.0045	0.0708	0.0006	0.94	441	3	435	3	407	6	-8	c1	rejected, > 1000 ppm U
	SA04/05 - 65	32	1101	470	83	0.44	0.0	0.00	0.0000000	0.0556	0.0002	0.1363	0.0004	0.5584	0.0051	0.0728	0.0006	0.91	453	4	450	3	437	9	-4	c1+rim	rejected, > 1000 ppm U
	SA04/05 - 74	36	283	163	21	0.59	0.1	0.01	0.0000037	0.0549	0.0006	0.1834	0.0008	0.5153	0.0069	0.0681	0.0006	0.62	425	3	422	5	407	24	-4	c2a	
	SA04/05 - 75	36	1302	1461	108	1.15	3.1	0.08	0.0000404	0.0553	0.0002	0.3580	0.0011	0.5180	0.0045	0.0679	0.0006	0.93	424	3	424	3	425	5	0	c2b	rejected, crack
	SA04/05 - 76	37	176	102	13	0.60	0.1	0.01	0.0000061	0.0553	0.0008	0.1852	0.0013	0.5151	0.0089	0.0676	0.0006	0.53	421	4	422	6	424	32	1	c1	
	SA04/05 - 77	37	467	320	35	0.70	0.1	0.00	0.0000023	0.0550	0.0004	0.2186	0.0013	0.5114	0.0056	0.0674	0.0006	0.76	421	3	419	4	413	15	-2	c2	rejected, crack
L1-06	SA04/06 - 2.2	2	2279	1197	160	0.54	353.2	4.79	0.0026932	0.0549	0.0007	0.1695	0.0083	0.5027	0.0080	0.0664	0.0007	0.63	414	4	414	5	408	36	-2	c1	rejected, crack
	SA04/06 - 5.6	5	3394	1572	250	0.48	0.9	0.01	0.0000046	0.0551	0.0002	0.1483	0.0005	0.5380	0.0048	0.0708	0.0006	0.93	441	4	437	3	417	7	-6	c1+c2	rejected, > 1000 ppm U
	SA04/06 - 5.7	5	6311	3072	490	0.50	3.6	0.02	0.0000090	0.0550	0.0001	0.1545	0.0003	0.5621	0.0048	0.0741	0.0006	0.99	461	4	453	3	414	3	-11	c2	rejected, > 1000 ppm U
	SA04/06 - 7.10	7	2777	1144	201	0.42	2.1	0.02	0.0000123	0.0551	0.0002	0.1306	0.0005	0.5342	0.0046	0.0704	0.0006	0.94	438	3	435	3	414	6	-6	c1+c2	rejected, > 1000 ppm U
	SA04/06 - 7.11	7	7994	3760	635	0.48	4.1	0.01	0.0000078	0.0552	0.0001	0.1500	0.0002	0.5794	0.0048	0.0762	0.0006	0.98	473	4	464	3	419	4	-13	c1+c2	rejected, > 1000 ppm U
	SA04/06 - 12.17	12	1363	506	93	0.38	9.5	0.22	0.0001191	0.0552	0.0003	0.1187	0.0015	0.5116	0.0051	0.0673	0.0006	0.86	420	3	420	3	418	9	0	c1	rejected, crack
	SA04/06 - 32.46	32	288	73	19	0.26	1.5	0.17	0.0000920	0.0533	0.0005	0.0764	0.0019	0.4842	0.0063	0.0659	0.0006	0.66	412	3	401	4	340	16	-21	c1a	rejected, > 10 % discordant
	SA04/06 - 37.47	37	1486	1083	113	0.75	6.7	0.14	0.0000767	0.0553	0.0003	0.2300	0.0025	0.5177	0.0058	0.0679	0.0007	0.88	423	4	424	4	425	10	0	c1	rejected, crack
	SA04/06 - 37.48	37	2103	1155	155	0.56	0.3	0.00	0.0000025	0.0551	0.0002	0.1744	0.0004	0.5261	0.0048	0.0692	0.0006	0.90	432	3	429	3	416	9	-4	c2	rejected, crack
	SA04/06 - 36.44	36	797	383	56	0.49	13.7	0.55	0.0002973	0.0540	0.0006	0.1488	0.0032	0.4977	0.0067	0.0669	0.0006	0.64	417	3	410	5	370	17	-13	c1	rejected, > 10 % discordant
	SA04/06 - 38.49	38	730	223	49	0.31	6.0	0.26	0.0001414	0.0550	0.0004	0.0957	0.0021	0.5106	0.0055	0.0673	0.0006	0.79	420	3	419	4	412	9	-2	c1a	
	SA04/06 - 38.50	38	2002	1122	143	0.57	526.4	7.88	0.0045766	0.0566	0.0012	0.1747	0.0105	0.5195	0.0122	0.0666	0.0006	0.36	416	3	425	8	474	90	12	c1b	rejected, crack
	SA04/06 - 6.8	6	1331	583	92	0.45	2.0	0.05	0.0000255	0.0550	0.0003	0.1389	0.0010	0.5082	0.0057	0.0671	0.0007	0.91	419	4	417	4	410	9	-2	c1	rejected, > 1000 ppm U
	SA04/06 - 13.18	13	1693	586	113	0.36	10.2	0.20	0.0001057	0.0550	0.0003	0.1083	0.0013	0.5010	0.0058	0.0661	0.0007	0.89	413	4	412	4	411	9	0	c1	rejected, crack
	SA04/06 - 34.41	34	447	110	28	0.25	60.4	4.39	0.0024554	0.0527	0.0012	0.0737	0.0087	0.4650	0.0114	0.0640	0.0007	0.42	400	4	388	8	317	45	-26	r1a	rejected, crack
	SA04/06 - 35.43	35	428	415	34	0.99	1.5	0.11	0.0000606	0.0554	0.0006	0.3094	0.0014	0.5129	0.0074	0.0672	0.0007	0.70	419	4	420	5	428	20	2	c2	rejected, crack
	SA04/06 - 39.51	39	1419	619	98	0.45	0.8	0.02	0.0000098	0.0553	0.0001	0.1386	0.0006	0.5116	0.0053	0.0671	0.0007	0.97	419	4	419	4	423	6	1	c1	rejected, > 1000 ppm U
	SA04/06 - 39.52	39	7481	4283	586	0.59	28.7	0.11	0.0000605	0.0550	0.0001	0.1836	0.0006	0.5550	0.0055	0.0732	0.0007	0.98	455	4	448	4	411	3	-11	c2	rejected, > 10 % discordant
L2-12	SA04/12 - 1.1	1	632	342	45	0.55	1.2	0.06	0.0000332	0.0550	0.0004	0.1751	0.0010	0.5074	0.0055	0.0669	0.0006	0.76	418	3	417	4	411	15	-2	c1	rejected, crack
	SA04/12 - 1.2	1	2664	2304	214	0.89	1.0	0.01	0.0000064	0.0555	0.0002	0.2799	0.0013	0.5348	0.0047	0.0699	0.0006	0.94	435	3	435	3	432	7	-1	c2	rejected, > 1000 ppm U
	SA04/12 - 2.3	2	3124	2745	208	0.90	11.4	0.09	0.0000508	0.0550	0.0001	0.4971	0.0160	0.5391	0.0046	0.0711	0.0006	0.96	443	3	438	3	410	4	-8	c1	rejected, > 1000 ppm U
	SA04/12 - 15.37	15	666	270	46	0.42	1.4	0.07	0.0000358	0.0551	0.0004	0.1311	0.0011	0.5157	0.0068	0.0679	0.0007	0.82	424	4	422	5	415	16	-2	c1	
	SA04/12 - 14.34	14	583	414	45	0.73	12.3	0.67	0.0003624	0.0538	0.0017	0.2117	0.0055	0.5061	0.0166	0.0682	0.0007	0.30	425	4	416	11	362	73	-18	c1b	rejected, > 10 % discordant
	SA04/12 - 14.35	14	687	596	51	0.89	12.4	0.62	0.0003359	0.0551	0.0005	0.2328	0.0035	0.4864	0.0060	0.0640	0.0005	0.68	400	3	402	4	416	10	4	c1a	rejected, crack
	SA04/12 - 3.4	3	958	825	75	0.88	0.7	0.02	0.0000124	0.0552	0.0002	0.2772	0.0009	0.5184	0.0048	0.0681	0.0006	0.88	425	3	424	3	419	10	-1	c2a	
	SA04/12 - 3.5	3	1010	740	77	0.75	0.6	0.02	0.0000095	0.0552	0.0002	0.2349	0.0007	0.5189	0.0048	0.0682	0.0006	0.88	425	3	424	3	419	10	-1	c2b	rejected, > 1000 ppm U
	SA04/12 - 5.10	5	1163	602	82	0.53	5.4	0.15	0.0000801	0.0546	0.0003	0.1641	0.0012	0.5048	0.0047	0.0670	0.0005	0.86	418	3	415	3	396	9	-6	c2	rejected, > 1000 ppm U
	SA04/12 - 4.8	4	1068	871	86	0.84	242.2	6.53	0.0037350	0.0553	0.0007	0.2582	0.0118	0.5355	0.0081	0.0703	0.0006	0.58	438	4	435	5	422	30	-4	c2a	rejected, high common Pb
	SA04/12 - 8.17	8	721	562	55	0.80	0.9	0.04	0.0000203	0.0549	0.0003	0.2514	0.0009	0.5126	0.0053	0.0677	0.0006	0.80	422	3	420	4	407	14	-4	c1	
	SA04/12 - 10.24	10	1206	571	86	0.49	18.9	0.51	0.0002718	0.0552	0.0004	0.1366	0.0025	0.5134	0.0056	0.0675	0.0005	0.75	421	3	421	4	419	12	0	c2a	rejected, crack

sample	analysis no.	grain no.	U ppm	Th ppm	Pb ppm	Th/U	^{204}Pb ppb	f206 (%)	^{204}Pb/^{206}Pb	corrected ratios									Ages (Ma)								grain area	comment
										^{207}Pb/^{206}Pb	1σ	^{208}Pb/^{206}Pb	1σ	^{207}Pb/^{235}U	1σ	^{206}Pb/^{238}U	1σ	ρ	^{206}Pb/^{238}U	1σ	^{207}Pb/^{235}U	1σ	^{207}Pb/^{206}Pb	1σ	% disc		
	SA04/12 - 10.23	10	1083	1142	88	1.08	23.2	0.68	0.0003683	0.0551	0.0006	0.3334	0.0037	0.5115	0.0067	0.0673	0.0006	0.65	420	3	419	5	416	19	-1	c1	rejected, high common Pb
	SA04/12 - 11.25	11	508	351	37	0.71	29.1	1.81	0.0009859	0.0558	0.0009	0.2241	0.0074	0.5142	0.0095	0.0668	0.0006	0.45	417	3	421	6	443	31	6	c2a	rejected, crack
	SA04/12 - 11.26	11	596	438	44	0.75	1.1	0.06	0.0000317	0.0553	0.0003	0.2368	0.0010	0.5081	0.0052	0.0666	0.0006	0.81	416	3	417	4	424	12	2	c2b	
	SA04/12 - 9.20	9	821	733	63	0.92	4.0	0.16	0.0000858	0.0552	0.0002	0.2605	0.0014	0.5033	0.0047	0.0662	0.0005	0.88	413	3	414	3	419	5	1	c2a	
	SA04/12 - 9.21	9	580	330	41	0.58	0.5	0.03	0.0000144	0.0548	0.0004	0.1820	0.0014	0.5048	0.0054	0.0668	0.0005	0.77	417	3	415	4	404	15	-3	c2c	
	SA04/12 - 13.33	13	543	268	38	0.51	5.0	0.30	0.0001591	0.0550	0.0005	0.1563	0.0023	0.5077	0.0062	0.0669	0.0006	0.74	418	4	417	4	413	12	-1	c2a	
	SA04/12 - 7.14	7	337	212	25	0.64	0.7	0.07	0.0000368	0.0549	0.0004	0.2015	0.0018	0.5096	0.0058	0.0673	0.0006	0.74	420	3	418	4	410	14	-2	c1	
	SA04/12 - 6.11	6	2217	1954	176	0.90	2.0	0.03	0.0000155	0.0551	0.0002	0.2828	0.0014	0.5221	0.0045	0.0688	0.0006	0.94	429	3	427	3	414	6	-4	c1	rejected, > 1000 ppm U
	SA04/12 - 6.12	6	2122	1852	167	0.90	0.9	0.01	0.0000068	0.0554	0.0002	0.2772	0.0021	0.5219	0.0045	0.0683	0.0006	0.94	426	3	426	3	429	6	1	c2	rejected, > 1000 ppm U
CnG	SA04/13 - 1	1	239	209	18	0.89	0.3	0.04	0.0000234	0.0545	0.0007	0.2776	0.0021	0.4788	0.0084	0.0637	0.0007	0.66	398	4	397	6	391	28	-2	c2a	rejected, crack
	SA04/13 - 2	1	129	74	9	0.59	0.0	0.00	0.0000001	0.0563	0.0008	0.1823	0.0017	0.4795	0.0085	0.0618	0.0007	0.60	386	4	398	6	463	31	17	c2c	rejected, > 10 % discordant
	SA04/13 - 7	4	316	167	23	0.54	0.3	0.04	0.0000189	0.0546	0.0005	0.1687	0.0006	0.5069	0.0068	0.0674	0.0007	0.78	420	4	416	5	395	18	-6	r1	
	SA04/13 - 8	4	280	214	21	0.78	0.0	0.00	0.0000000	0.0550	0.0004	0.2445	0.0014	0.4996	0.0067	0.0659	0.0007	0.79	412	4	411	5	410	18	0	c1	
	SA04/13 - 9	5	465	286	33	0.63	0.6	0.04	0.0000212	0.0543	0.0003	0.1984	0.0008	0.4969	0.0057	0.0664	0.0007	0.89	414	4	410	4	382	11	-8	c2	
	SA04/13 - 10	5	337	252	26	0.77	0.2	0.02	0.0000088	0.0556	0.0005	0.2439	0.0015	0.5331	0.0077	0.0696	0.0007	0.73	434	4	434	5	434	21	0	c1	rejected, crack
	SA04/13 - 44	19	678	1079	57	1.63	12.3	0.63	0.0003408	0.0501	0.0007	0.4969	0.0037	0.4275	0.0074	0.0619	0.0007	0.64	387	4	361	5	200	26	-93	c1	rejected, high common Pb
	SA04/13 - 45	19	221	107	14	0.50	33.8	5.24	0.0029594	0.0485	0.0016	0.1298	0.0133	0.4081	0.0142	0.0610	0.0007	0.35	382	4	348	10	122	95	-213	r1	rejected, high common Pb
	SA04/13 - 43	18	169	101	11	0.61	0.3	0.07	0.0000354	0.0548	0.0009	0.1853	0.0020	0.4630	0.0106	0.0612	0.0010	0.69	383	6	386	7	405	35	5	r1	rejected, crack
	SA04/13 - 13	6	229	205	18	0.92	0.5	0.07	0.0000360	0.0551	0.0006	0.2735	0.0016	0.5086	0.0097	0.0670	0.0011	0.85	418	7	418	7	414	21	-1	c1	
	SA04/13 - 14	6	533	489	42	0.94	1.3	0.08	0.0000417	0.0550	0.0003	0.2925	0.0013	0.5169	0.0084	0.0682	0.0010	0.94	425	6	423	6	412	11	-3	c2+r1	
	SA04/13 - 35	15	340	258	26	0.78	0.5	0.05	0.0000265	0.0545	0.0004	0.2409	0.0012	0.5109	0.0089	0.0680	0.0011	0.91	424	6	419	6	392	15	-8	c1	
	SA04/13 - 36	15	159	93	11	0.60	0.4	0.09	0.0000475	0.0549	0.0006	0.1890	0.0038	0.4986	0.0101	0.0659	0.0011	0.86	411	7	411	7	408	21	-1	r1	
	SA04/13 - 29	12	174	78	12	0.46	0.5	0.09	0.0000499	0.0555	0.0006	0.1394	0.0015	0.5049	0.0096	0.0660	0.0011	0.84	412	6	415	6	430	21	4	r1	
	SA04/13 - 30	12	344	262	26	0.78	0.9	0.08	0.0000434	0.0549	0.0004	0.2406	0.0021	0.5081	0.0121	0.0671	0.0015	0.94	419	9	417	8	407	17	-3	c1	
	SA04/13 - 46	20	332	354	28	1.09	0.5	0.04	0.0000238	0.0552	0.0006	0.3293	0.0019	0.5240	0.0112	0.0688	0.0013	0.88	429	8	428	7	421	22	-2	c2a	
	SA04/13 - 47	20	362	300	28	0.85	0.4	0.04	0.0000203	0.0546	0.0005	0.2635	0.0011	0.5095	0.0090	0.0677	0.0010	0.88	423	6	418	6	393	19	-8	c2b	
	SA04/13 - 32	13	217	119	16	0.56	0.5	0.08	0.0000423	0.0541	0.0006	0.1715	0.0018	0.5095	0.0097	0.0683	0.0011	0.82	426	6	418	7	375	23	-14	c1	rejected, > 10 % discordant
L2-15	SA04/15 - 29a	29	68	27	14	0.41	0.4	0.06	0.0000310	0.0777	0.0008	0.1265	0.0012	2.0771	0.0284	0.1939	0.0017	0.66	1142	9	1141	9	1139	20	0	inh1	inherited grain
	SA04/15 - 29b	29	394	116	26	0.30	0.2	0.01	0.0000075	0.0558	0.0003	0.0964	0.0008	0.5193	0.0055	0.0675	0.0006	0.82	421	4	425	4	444	13	5	rim	
	SA04/15 - 3a	3	964	542	70	0.58	0.5	0.02	0.0000095	0.0547	0.0003	0.1827	0.0006	0.5127	0.0048	0.0679	0.0005	0.85	424	3	420	3	401	11	-6	c2a	
	SA04/15 - 5a	5	63	40	5	0.64	0.3	0.13	0.0000716	0.0538	0.0010	0.2033	0.0035	0.4971	0.0100	0.0670	0.0006	0.47	418	4	410	7	363	31	-15	r1a	rejected, > 10 % discordant
	SA04/15 - 32a	32	109	64	26	0.60	0.3	0.02	0.0000132	0.0825	0.0006	0.1803	0.0007	2.4930	0.0279	0.2192	0.0018	0.73	1277	9	1270	8	1257	14	-2	inh	inherited grain
	SA04/15 - 31a	31	363	157	25	0.44	18.3	1.61	0.0008737	0.0559	0.0009	0.1435	0.0069	0.5113	0.0093	0.0664	0.0005	0.45	414	3	419	6	447	26	7	c2	rejected, crack
	SA04/15 - 31b	31	4195	1084	301	0.27	31.9	0.22	0.0001202	0.0549	0.0001	0.0837	0.0011	0.5523	0.0046	0.0730	0.0006	0.95	454	3	447	3	407	4	-12	r2	rejected, crack
	SA04/15 - 30a	30	487	221	34	0.47	0.3	0.02	0.0000101	0.0549	0.0004	0.1480	0.0017	0.5144	0.0056	0.0679	0.0006	0.77	424	3	421	4	408	15	-4	c2	
	SA04/15 - 30b	30	139	91	10	0.67	0.5	0.12	0.0000647	0.0544	0.0007	0.2117	0.0018	0.5021	0.0081	0.0670	0.0006	0.53	418	3	413	5	385	26	-9	rim	
	SA04/15 - 6a	6	86	69	6	0.82	0.1	0.05	0.0000269	0.0546	0.0016	0.2624	0.0027	0.4633	0.0577	0.0615	0.0074	0.97	385	45	387	39	397	63	3	c1	rejected, scratch
	SA04/15 - 7a	7	113	84	9	0.76	0.0	0.00	0.0000001	0.0543	0.0006	0.2406	0.0014	0.5123	0.0079	0.0684	0.0007	0.68	427	4	420	5	384	25	-11	c2	rejected, > 10 % discordant
	SA04/15 - 8a	8	5146	2004	382	0.40	0.2	0.00	0.0000006	0.0550	0.0001	0.1250	0.0003	0.5523	0.0045	0.0728	0.0006	0.96	453	3	447	3	412	5	-10	c1	rejected, > 1000 ppm U
	SA04/15 - 22a	22	184	87	46	0.49	0.4	0.02	0.0000112	0.0887	0.0004	0.1455	0.0009	2.8540	0.0312	0.2334	0.0023	0.90	1352	12	1370	8	1397	9	3	inh1	inherited grain
	SA04/15 - 26a	26	193	83	13	0.44	7.9	1.36	0.0007397	0.0547	0.0018	0.1411	0.0083	0.4808	0.0165	0.0638	0.0006	0.27	398	4	399	11	399	69	0	c1	rejected, crack
	SA04/15 - 18a	18	681	255	45	0.38	47.2	2.23	0.0012219	0.0557	0.0007	0.1273	0.0069	0.4995	0.0078	0.0651	0.0005	0.52	406	3	411	5	438	23	7	c2a	rejected, crack
	SA04/15 - 33a	33	117	47	26	0.41	0.3	0.03	0.0000161	0.0813	0.0005	0.1200	0.0022	2.4135	0.0389	0.2154	0.0031	0.91	1258	17	1247	11	1227	13	-3	inh1	inherited grain
	SA04/15 - 34a	34	637	282	41	0.45	27.5	1.46	0.0007946	0.0565	0.0006	0.1550	0.0056	0.4830	0.0064	0.0620	0.0005	0.61	388	3	400	4	470	14	17	r1+r2	rejected, crack
	SA04/15 - 34b	34	352	222	26	0.65	0.1	0.01	0.0000037	0.0557	0.0004	0.2067	0.0023	0.5229	0.0057	0.0681	0.0006	0.76	425	3	427	4	440	16	4	r3	
	SA04/15 - 35a	35	195	79	38	0.41	0.2	0.01	0.0000057	0.0782	0.0004	0.1269	0.0004	2.0504	0.0187	0.1902	0.0014	0.81	1122	8	1132	6	1151	10	2	inh	inherited grain
	SA04/15 - 36a	36	91	75	21	0.85	0.7	0.08	0.0000419	0.0811	0.0006	0.2564	0.0014	2.2620	0.0235	0.2023	0.0016	0.74	1188	8	1201	7	1223	13	3	inh	inherited grain
Session 1 July 2005	91500		83	30	15	0.37	0.5	0.07	0.0000350	0.0734	0.0007	0.1111	0.0010	1.8079	0.0239	0.1788	0.0016	0.66	1060	8	1048	9	1023	19	-4		
	91500		79	28	15	0.37	0.5	0.07	0.0000375	0.0749	0.0006	0.1097	0.0012	1.8552	0.0223	0.1796	0.0016	0.73	1065	9	1065	8	1066	15	0		
	91500		79	27	14	0.36	0.0	0.00	0.0000001	0.0745	0.0008	0.1079	0.0007	1.8176	0.0390	0.1768	0.0032	0.86	1050	18	1052	14	1056	22	1		
	91500		83	29	16	0.36	0.0	0.00	0.0000001	0.0750	0.0004	0.1070	0.0008	1.9212	0.0363	0.1858	0.0033	0.95	1099	18	1088	13	1068	11	-3		
	91500		81	29	15	0.37	0.0	0.00	0.0000001	0.0751	0.0006	0.1107	0.0007	1.8556	0.0350	0.1792	0.0031	0.92	1062	17	1065	12	1071	15	1		

sample	analysis no.	grain no.	U ppm	Th ppm	Pb ppm	Th/U	^{204}Pb ppb	f206 (%)	^{204}Pb/^{206}Pb	corrected ratios									Ages (Ma)							grain area	comment
										^{207}Pb/^{206}Pb	1σ	^{208}Pb/^{206}Pb	1σ	^{207}Pb/^{235}U	1σ	^{206}Pb/^{238}U	1σ	ρ	^{206}Pb/^{238}U	1σ	^{207}Pb/^{235}U	1σ	^{207}Pb/^{206}Pb	1σ	% disc		
	91500		79	28	15	0.36	0.0	0.00	0.0000001	0.0753	0.0006	0.1080	0.0010	1.8541	0.0224	0.1785	0.0016	0.76	1059	9	1065	8	1076	16	2		
	91500		82	29	15	0.36	0.0	0.00	0.0000001	0.0737	0.0006	0.1093	0.0007	1.8057	0.0231	0.1777	0.0018	0.77	1054	10	1048	8	1033	17	-2		
	91500		81	29	15	0.36	0.0	0.01	0.0000035	0.0756	0.0007	0.1078	0.0008	1.8760	0.0246	0.1799	0.0017	0.73	1066	9	1073	9	1085	18	2		
	91500		83	29	15	0.36	0.0	0.00	0.0000001	0.0743	0.0007	0.1083	0.0007	1.8553	0.0266	0.1812	0.0020	0.79	1073	11	1065	9	1049	17	-2		
	91500		82	29	15	0.36	0.0	0.00	0.0000001	0.0757	0.0006	0.1089	0.0009	1.8793	0.0241	0.1800	0.0018	0.77	1067	10	1074	8	1088	16	2		
	91500		80	28	15	0.36	0.0	0.01	0.0000034	0.0750	0.0007	0.1089	0.0008	1.8400	0.0259	0.1778	0.0019	0.76	1055	10	1060	9	1069	18	1		
	91500		83	30	15	0.36	0.3	0.04	0.0000207	0.0753	0.0008	0.1108	0.0009	1.8542	0.0268	0.1785	0.0018	0.72	1059	10	1065	9	1077	19	2		
	91500		83	30	15	0.37	0.0	0.00	0.0000001	0.0753	0.0006	0.1112	0.0005	1.8489	0.0236	0.1780	0.0018	0.81	1056	10	1063	8	1077	15	2		
	91500		79	28	15	0.37	0.0	0.00	0.0000001	0.0746	0.0007	0.1105	0.0010	1.8380	0.0292	0.1788	0.0023	0.80	1060	12	1059	10	1056	19	0		
	91500		79	28	14	0.37	0.3	0.04	0.0000220	0.0752	0.0006	0.1111	0.0010	1.8462	0.0232	0.1780	0.0018	0.81	1056	10	1062	8	1074	13	2		
	91500		82	29	15	0.36	0.0	0.00	0.0000001	0.0748	0.0007	0.1101	0.0007	1.8298	0.0249	0.1774	0.0017	0.72	1053	9	1056	9	1062	19	1		
	91500		83	29	15	0.37	0.0	0.00	0.0000001	0.0750	0.0006	0.1118	0.0005	1.8704	0.0241	0.1810	0.0019	0.80	1072	10	1071	8	1067	15	0		
	91500		80	29	15	0.37	0.5	0.08	0.0000415	0.0742	0.0007	0.1099	0.0013	1.8231	0.0257	0.1783	0.0018	0.71	1057	10	1054	9	1046	18	-1		
	91500		80	29	15	0.37	0.8	0.12	0.0000666	0.0744	0.0007	0.1080	0.0017	1.8815	0.0267	0.1833	0.0020	0.77	1085	11	1075	9	1053	16	-3		
	91500		81	30	15	0.37	0.0	0.00	0.0000001	0.0751	0.0007	0.1125	0.0007	1.8550	0.0336	0.1792	0.0028	0.87	1062	15	1065	12	1070	18	1		
	91500		85	29	16	0.35	0.4	0.06	0.0000311	0.0748	0.0007	0.1059	0.0010	1.9117	0.0331	0.1853	0.0026	0.82	1096	14	1085	11	1063	19	-3		
	91500		80	28	15	0.35	0.0	0.00	0.0000001	0.0749	0.0007	0.1066	0.0008	1.8308	0.0257	0.1772	0.0019	0.75	1052	10	1057	9	1066	19	1		
	91500		79	27	14	0.35	0.0	0.00	0.0000001	0.0741	0.0004	0.1066	0.0010	1.7951	0.0228	0.1757	0.0020	0.88	1043	11	1044	8	1044	12	0		
	91500		82	28	15	0.35	0.2	0.03	0.0000136	0.0743	0.0007	0.1071	0.0007	1.8366	0.0276	0.1793	0.0020	0.75	1063	11	1059	10	1049	20	-1		
	91500		80	28	15	0.36	0.0	0.00	0.0000001	0.0736	0.0007	0.1075	0.0009	1.8308	0.0273	0.1805	0.0020	0.74	1070	11	1057	10	1029	20	-4		
	91500		80	27	14	0.35	0.4	0.06	0.0000343	0.0751	0.0007	0.1045	0.0012	1.8290	0.0253	0.1766	0.0018	0.75	1048	10	1056	9	1071	17	2		
	91500		77	26	14	0.35	0.0	0.00	0.0000001	0.0754	0.0006	0.1074	0.0009	1.8745	0.0257	0.1803	0.0020	0.80	1068	11	1072	9	1079	17	1		
	91500		78	27	14	0.36	0.0	0.00	0.0000001	0.0744	0.0006	0.1073	0.0006	1.8279	0.0257	0.1782	0.0020	0.79	1057	11	1056	9	1052	17	0		
	91500		83	30	15	0.36	0.0	0.00	0.0000001	0.0747	0.0008	0.1095	0.0007	1.8372	0.0269	0.1785	0.0018	0.69	1059	10	1059	10	1059	21	0		
	91500		88	31	16	0.37	0.0	0.00	0.0000001	0.0749	0.0006	0.1117	0.0009	1.8623	0.0259	0.1803	0.0020	0.79	1068	11	1068	9	1066	17	0		
	91500		83	29	15	0.36	0.1	0.01	0.0000042	0.0755	0.0008	0.1086	0.0010	1.8701	0.0269	0.1797	0.0016	0.63	1065	9	1071	9	1081	22	1		
	91500		84	29	15	0.36	0.0	0.00	0.0000001	0.0748	0.0006	0.1091	0.0006	1.8497	0.0231	0.1793	0.0016	0.74	1063	9	1063	8	1063	17	0		
	91500		78	27	14	0.36	0.0	0.00	0.0000001	0.0748	0.0007	0.1057	0.0009	1.8529	0.0244	0.1797	0.0016	0.68	1066	9	1064	9	1062	19	0		
	91500		80	28	15	0.35	0.0	0.00	0.0000001	0.0742	0.0006	0.1056	0.0007	1.8565	0.0232	0.1814	0.0017	0.74	1075	9	1066	8	1047	17	-3		
	91500		79	27	15	0.35	0.0	0.00	0.0000001	0.0756	0.0007	0.1076	0.0008	1.8763	0.0266	0.1800	0.0018	0.72	1067	10	1073	9	1085	19	2		
	91500		84	29	15	0.36	0.0	0.00	0.0000001	0.0736	0.0005	0.1078	0.0009	1.8003	0.0213	0.1775	0.0017	0.83	1053	10	1046	8	1029	14	-2		
	91500		80	27	15	0.35	0.3	0.05	0.0000258	0.0738	0.0006	0.1060	0.0012	1.8156	0.0236	0.1784	0.0017	0.75	1058	10	1051	8	1035	16	-2		
	91500		78	27	14	0.35	0.0	0.00	0.0000001	0.0747	0.0008	0.1052	0.0007	1.8618	0.0281	0.1809	0.0019	0.69	1072	10	1068	10	1059	22	-1		
	91500		80	27	15	0.35	0.0	0.00	0.0000001	0.0741	0.0006	0.1047	0.0010	1.8295	0.0218	0.1791	0.0017	0.78	1062	9	1056	8	1044	15	-2		
	91500		86	30	16	0.35	0.1	0.01	0.0000040	0.0749	0.0005	0.1077	0.0008	1.8145	0.0209	0.1757	0.0017	0.84	1044	9	1051	8	1065	12	2		
	91500		81	28	15	0.35	0.0	0.00	0.0000001	0.0751	0.0006	0.1066	0.0008	1.8461	0.0215	0.1782	0.0014	0.69	1057	8	1062	8	1072	17	1		
	91500		81	28	15	0.35	0.0	0.00	0.0000001	0.0748	0.0008	0.1086	0.0010	1.8431	0.0255	0.1787	0.0016	0.64	1060	9	1061	9	1063	21	0		
	91500		82	28	15	0.36	0.1	0.01	0.0000052	0.0741	0.0009	0.1062	0.0009	1.8357	0.0278	0.1796	0.0015	0.54	1065	8	1058	10	1045	25	-2		
	91500		81	28	15	0.35	0.0	0.00	0.0000001	0.0744	0.0008	0.1058	0.0006	1.8446	0.0236	0.1799	0.0013	0.58	1066	7	1061	8	1051	21	-1		
	91500		80	28	15	0.36	0.0	0.00	0.0000001	0.0763	0.0007	0.1062	0.0007	1.8828	0.0243	0.1791	0.0015	0.67	1062	8	1075	9	1101	19	4		
	91500		81	28	15	0.36	0.0	0.00	0.0000001	0.0736	0.0011	0.1071	0.0009	1.8221	0.0327	0.1796	0.0016	0.51	1065	9	1053	12	1029	31	-3		
	91500		81	28	15	0.35	0.7	0.11	0.0000573	0.0749	0.0008	0.1052	0.0015	1.8543	0.0241	0.1796	0.0015	0.64	1065	8	1065	9	1065	18	0		
	91500		82	28	15	0.35	0.0	0.00	0.0000001	0.0759	0.0006	0.1080	0.0008	1.8746	0.0216	0.1792	0.0015	0.74	1063	8	1072	8	1091	15	3		
	91500		82	28	15	0.35	0.1	0.01	0.0000040	0.0766	0.0006	0.1078	0.0007	1.8937	0.0217	0.1792	0.0015	0.71	1063	8	1079	8	1112	15	4		
	91500		80	28	15	0.35	0.0	0.00	0.0000001	0.0759	0.0005	0.1065	0.0008	1.8583	0.0198	0.1775	0.0014	0.76	1054	8	1066	7	1092	14	4		
	91500		81	28	15	0.36	0.0	0.01	0.0000038	0.0740	0.0007	0.1063	0.0010	1.8327	0.0233	0.1797	0.0015	0.65	1065	8	1057	8	1040	19	-2		
	91500		81	28	15	0.35	0.0	0.01	0.0000039	0.0744	0.0005	0.1055	0.0006	1.8535	0.0195	0.1806	0.0015	0.79	1070	8	1065	7	1053	12	-2		
	91500		81	28	15	0.35	0.3	0.04	0.0000226	0.0735	0.0006	0.1057	0.0011	1.8145	0.0206	0.1790	0.0015	0.72	1061	8	1051	7	1028	15	-3		
	91500		81	28	15	0.35	0.0	0.00	0.0000001	0.0750	0.0004	0.1069	0.0008	1.8469	0.0182	0.1785	0.0014	0.82	1059	8	1062	6	1069	11	1		
	91500		82	28	15	0.35	0.0	0.01	0.0000039	0.0750	0.0006	0.1056	0.0007	1.8385	0.0259	0.1779	0.0020	0.81	1055	11	1059	9	1067	16	1		
	91500		81	28	15	0.35	0.0	0.00	0.0000001	0.0758	0.0008	0.1086	0.0009	1.8327	0.0273	0.1753	0.0019	0.74	1042	11	1057	10	1089	20	4		
	91500		80	27	15	0.35	0.5	0.08	0.0000426	0.0744	0.0009	0.1050	0.0015	1.8644	0.0299	0.1817	0.0019	0.66	1076	11	1069	11	1053	23	-2		
	91500		81	28	15	0.35	0.0	0.00	0.0000000	0.0753	0.0006	0.1067	0.0008	1.8803	0.0270	0.1810	0.0021	0.81	1073	11	1074	9	1077	16	0		
	91500		81	28	15	0.35	0.5	0.07	0.0000373	0.0736	0.0009	0.1068	0.0015	1.7978	0.0307	0.1773	0.0020	0.67	1052	11	1045	11	1029	25	-2		
	91500		82	28	15	0.35	0.3	0.05	0.0000271	0.0738	0.0008	0.1055	0.0011	1.8414	0.0289	0.1809	0.0021	0.74	1072	12	1060	10	1036	20	-3		

sample	analysis no.	grain no.	U ppm	Th ppm	Pb ppm	Th/U	^{204}Pb ppb	f206 (%)	^{204}Pb/^{206}Pb	corrected ratios									Ages (Ma)							grain area	comment
										^{207}Pb/^{206}Pb	1σ	^{208}Pb/^{206}Pb	1σ	^{207}Pb/^{235}U	1σ	^{206}Pb/^{238}U	1σ	ρ	^{206}Pb/^{238}U	1σ	^{207}Pb/^{235}U	1σ	^{207}Pb/^{206}Pb	1σ	% disc		
	91500		81	28	15	0.35	0.8	0.12	0.0000619	0.0739	0.0007	0.1046	0.0014	1.8344	0.0271	0.1800	0.0020	0.76	1067	11	1058	10	1038	19	-3		
	91500		81	28	15	0.36	0.1	0.01	0.0000067	0.0753	0.0006	0.1075	0.0007	1.8605	0.0330	0.1792	0.0028	0.88	1062	15	1067	12	1076	17	1		
Session	91500		79	27	14	0.35	3.0	0.45	0.0002424	0.0735	0.0011	0.1049	0.0038	1.8054	0.0324	0.1781	0.0018	0.55	1057	10	1047	12	1028	24	-3		
3	91500		80	29	14	0.37	0.4	0.06	0.0000331	0.0741	0.0008	0.1098	0.0012	1.7974	0.0252	0.1760	0.0016	0.66	1045	9	1045	9	1043	20	0		
March	91500		84	30	15	0.37	0.0	0.00	0.0000001	0.0756	0.0007	0.1120	0.0008	1.8600	0.0229	0.1784	0.0015	0.70	1058	8	1067	8	1084	18	2		
2006	91500		80	28	15	0.36	0.2	0.02	0.0000129	0.0748	0.0005	0.1080	0.0009	1.8356	0.0208	0.1779	0.0016	0.80	1055	9	1058	7	1064	13	1		
	91500		82	29	15	0.36	0.0	0.00	0.0000001	0.0750	0.0007	0.1099	0.0011	1.8374	0.0250	0.1776	0.0018	0.73	1054	10	1059	9	1069	18	1		
	91500		78	27	14	0.36	0.0	0.00	0.0000001	0.0764	0.0005	0.1084	0.0009	1.8247	0.0215	0.1731	0.0017	0.82	1029	9	1054	8	1106	13	7		
	91500		82	28	15	0.35	0.4	0.05	0.0000277	0.0745	0.0006	0.1071	0.0010	1.8348	0.0228	0.1786	0.0018	0.80	1060	10	1058	8	1054	14	-1		
	91500		81	28	15	0.35	0.3	0.05	0.0000275	0.0733	0.0008	0.1055	0.0009	1.8294	0.0247	0.1809	0.0016	0.65	1072	9	1056	9	1023	20	-5		
	91500		80	28	15	0.35	0.2	0.04	0.0000196	0.0736	0.0004	0.1051	0.0010	1.8523	0.0217	0.1825	0.0019	0.88	1081	10	1064	8	1031	10	-5		
	91500		83	29	15	0.36	0.0	0.00	0.0000001	0.0753	0.0004	0.1065	0.0008	1.8669	0.0190	0.1799	0.0016	0.89	1066	9	1069	7	1075	10	1		
	91500		81	28	15	0.35	0.2	0.04	0.0000199	0.0756	0.0006	0.1080	0.0009	1.8645	0.0241	0.1788	0.0018	0.79	1060	10	1069	8	1085	15	2		
	91500		82	28	15	0.36	0.0	0.00	0.0000001	0.0742	0.0006	0.1083	0.0007	1.8423	0.0236	0.1801	0.0018	0.80	1067	10	1061	8	1046	16	-2		
	91500		82	28	15	0.35	0.4	0.05	0.0000292	0.0748	0.0010	0.1060	0.0012	1.9047	0.0310	0.1847	0.0018	0.61	1092	10	1083	11	1063	25	-3		
	91500		82	28	15	0.35	0.3	0.04	0.0000210	0.0742	0.0005	0.1065	0.0010	1.8494	0.0225	0.1807	0.0018	0.82	1071	10	1063	8	1047	13	-2		
	91500		81	28	15	0.35	0.4	0.06	0.0000308	0.0740	0.0006	0.1068	0.0012	1.8330	0.0228	0.1795	0.0017	0.74	1065	9	1057	8	1042	16	-2		
	91500		81	28	15	0.36	0.0	0.00	0.0000001	0.0755	0.0006	0.1094	0.0007	1.8665	0.0252	0.1793	0.0019	0.77	1063	10	1069	9	1081	17	2		
	91500		81	28	15	0.36	0.0	0.00	0.0000001	0.0746	0.0007	0.1082	0.0010	1.8533	0.0252	0.1802	0.0017	0.71	1068	10	1065	9	1056	20	-1		
	91500		82	29	15	0.36	0.0	0.01	0.0000028	0.0743	0.0007	0.1069	0.0008	1.8233	0.0245	0.1780	0.0016	0.67	1056	9	1054	9	1049	20	-1		
	91500		82	29	15	0.36	0.0	0.00	0.0000001	0.0751	0.0007	0.1072	0.0005	1.8664	0.0249	0.1803	0.0016	0.68	1068	9	1069	9	1070	20	0		
	91500		80	28	15	0.36	0.3	0.04	0.0000234	0.0745	0.0007	0.1066	0.0010	1.8475	0.0235	0.1799	0.0016	0.69	1067	9	1063	8	1054	17	-1		
	91500		81	28	15	0.36	0.0	0.01	0.0000028	0.0742	0.0006	0.1075	0.0007	1.8109	0.0231	0.1769	0.0017	0.73	1050	9	1049	8	1048	17	0		
	91500		82	29	15	0.36	0.0	0.00	0.0000001	0.0751	0.0007	0.1084	0.0008	1.8391	0.0247	0.1776	0.0016	0.69	1054	9	1060	9	1071	19	2		
	91500		83	29	15	0.36	0.0	0.00	0.0000001	0.0748	0.0006	0.1087	0.0009	1.8337	0.0221	0.1779	0.0017	0.77	1055	9	1058	8	1062	15	1		
	91500		83	29	15	0.36	0.0	0.00	0.0000001	0.0758	0.0009	0.1081	0.0012	1.8784	0.0295	0.1798	0.0018	0.62	1066	10	1074	10	1088	24	2		
	91500		82	29	15	0.36	0.5	0.07	0.0000397	0.0738	0.0006	0.1063	0.0014	1.8451	0.0229	0.1814	0.0016	0.71	1075	9	1062	8	1035	16	-4		
	91500		80	28	15	0.35	0.0	0.00	0.0000001	0.0752	0.0007	0.1070	0.0009	1.8848	0.0242	0.1818	0.0017	0.71	1077	9	1076	8	1073	18	0		
	91500		80	28	15	0.36	0.1	0.02	0.0000120	0.0747	0.0007	0.1072	0.0008	1.8564	0.0244	0.1803	0.0018	0.74	1069	10	1066	9	1059	18	-1		
	91500		81	28	15	0.36	0.5	0.08	0.0000412	0.0742	0.0007	0.1061	0.0012	1.8234	0.0240	0.1782	0.0017	0.71	1057	9	1054	9	1046	17	-1		
	91500		82	29	15	0.36	0.0	0.00	0.0000001	0.0742	0.0005	0.1068	0.0008	1.8436	0.0219	0.1801	0.0017	0.80	1068	9	1061	8	1047	14	-2		
	91500		81	28	15	0.36	0.0	0.00	0.0000001	0.0747	0.0008	0.1073	0.0007	1.8485	0.0245	0.1795	0.0015	0.65	1064	8	1063	9	1059	21	-1		
	91500		79	27	14	0.35	0.0	0.00	0.0000001	0.0745	0.0005	0.1073	0.0010	1.8187	0.0201	0.1770	0.0016	0.82	1051	9	1052	7	1055	13	0		
	91500		80	28	15	0.35	0.0	0.01	0.0000027	0.0744	0.0007	0.1075	0.0004	1.8175	0.0232	0.1772	0.0016	0.71	1052	9	1052	8	1052	18	0		
	91500		81	28	15	0.35	0.4	0.06	0.0000326	0.0751	0.0007	0.1065	0.0012	1.8482	0.0242	0.1786	0.0016	0.68	1059	9	1063	9	1070	18	1		
	91500		84	29	15	0.36	0.3	0.04	0.0000224	0.0738	0.0010	0.1078	0.0012	1.8248	0.0287	0.1793	0.0016	0.57	1063	9	1054	10	1036	25	-3		
	91500		80	28	15	0.35	0.0	0.01	0.0000029	0.0751	0.0007	0.1067	0.0008	1.8675	0.0241	0.1804	0.0017	0.73	1069	9	1070	8	1070	17	0		
	91500		80	27	15	0.35	0.6	0.09	0.0000468	0.0746	0.0009	0.1065	0.0015	1.8341	0.0277	0.1783	0.0016	0.60	1058	9	1058	10	1057	23	0		
	91500		81	29	15	0.36	0.0	0.00	0.0000001	0.0756	0.0009	0.1085	0.0011	1.8676	0.0378	0.1792	0.0029	0.79	1062	16	1070	13	1084	25	2		
	91500		83	29	15	0.36	0.5	0.08	0.0000405	0.0747	0.0007	0.1066	0.0014	1.8764	0.0268	0.1821	0.0019	0.72	1078	10	1073	9	1061	18	-2		
	91500		85	29	16	0.36	0.1	0.01	0.0000072	0.0754	0.0008	0.1069	0.0009	1.9060	0.0262	0.1832	0.0017	0.67	1085	9	1083	9	1080	20	0		
	91500		80	28	15	0.35	0.4	0.05	0.0000283	0.0735	0.0007	0.1059	0.0013	1.8569	0.0256	0.1832	0.0018	0.72	1085	10	1066	9	1027	18	-6		
	91500		81	28	15	0.36	0.0	0.00	0.0000001	0.0749	0.0011	0.1053	0.0009	1.8544	0.0338	0.1795	0.0018	0.56	1064	10	1065	12	1066	31	0		
	91500		80	28	15	0.35	0.0	0.00	0.0000001	0.0743	0.0006	0.1081	0.0011	1.8304	0.0261	0.1787	0.0020	0.79	1060	11	1056	9	1048	18	-1		
	91500		83	29	15	0.36	0.5	0.07	0.0000362	0.0758	0.0008	0.1070	0.0016	1.8765	0.0282	0.1795	0.0018	0.67	1064	10	1073	10	1090	21	2		
	91500		83	29	15	0.36	0.6	0.09	0.0000475	0.0733	0.0008	0.1070	0.0015	1.8039	0.0277	0.1786	0.0018	0.67	1059	10	1047	10	1020	21	-4		
	91500		84	29	16	0.36	0.0	0.00	0.0000001	0.0748	0.0006	0.1083	0.0010	1.8725	0.0248	0.1816	0.0019	0.79	1076	10	1071	9	1062	16	-1		
	91500		82	28	15	0.35	0.2	0.03	0.0000168	0.0759	0.0007	0.1070	0.0009	1.8797	0.0244	0.1797	0.0017	0.71	1065	9	1074	9	1091	17	2		
	91500		82	28	15	0.35	0.4	0.05	0.0000283	0.0743	0.0008	0.1068	0.0012	1.8441	0.0260	0.1800	0.0017	0.69	1067	10	1061	9	1050	19	-2		
	91500		80	28	15	0.36	0.4	0.06	0.0000300	0.0750	0.0009	0.1086	0.0013	1.8492	0.0284	0.1789	0.0018	0.64	1061	10	1063	10	1067	22	1		
	91500		80	28	14	0.36	0.0	0.00	0.0000001	0.0747	0.0008	0.1071	0.0010	1.8105	0.0269	0.1759	0.0017	0.65	1045	9	1049	10	1059	22	1		
	91500		76	26	14	0.35	0.4	0.06	0.0000319	0.0754	0.0007	0.1070	0.0012	1.8625	0.0254	0.1793	0.0017	0.69	1063	9	1068	9	1077	19	1		
	91500		80	28	15	0.36	0.6	0.09	0.0000463	0.0736	0.0009	0.1052	0.0015	1.8226	0.0300	0.1795	0.0019	0.64	1065	10	1054	11	1031	23	-3		
	91500		78	27	14	0.35	0.0	0.00	0.0000001	0.0746	0.0010	0.1083	0.0011	1.7915	0.0302	0.1742	0.0019	0.65	1035	10	1042	11	1057	26	2		

sample	analysis no.	grain no.	U ppm	Th ppm	Pb ppm	Th/U	^{204}Pb ppb	f206 (%)	^{204}Pb/^{206}Pb	corrected ratios									Ages (Ma)								grain area	comment
										^{207}Pb/^{206}Pb	1σ	^{208}Pb/^{206}Pb	1σ	^{207}Pb/^{235}U	1σ	^{206}Pb/^{238}U	1σ	ρ	^{206}Pb/^{238}U	1σ	^{207}Pb/^{235}U	1σ	^{207}Pb/^{206}Pb	1σ	% disc		
	91500		81	28	15	0.36	0.0	0.00	0.0000001	0.0741	0.0009	0.1073	0.0010	1.8001	0.0290	0.1763	0.0018	0.62	1047	10	1046	10	1042	26	0		
	91500		82	29	15	0.36	0.0	0.00	0.0000001	0.0740	0.0009	0.1081	0.0009	1.7955	0.0283	0.1759	0.0017	0.62	1044	9	1044	10	1042	25	0		
	91500		82	29	15	0.36	0.3	0.04	0.0000207	0.0747	0.0007	0.1082	0.0012	1.8439	0.0259	0.1789	0.0019	0.74	1061	10	1061	9	1061	18	0		
	91500		79	28	14	0.36	0.2	0.03	0.0000147	0.0749	0.0006	0.1097	0.0009	1.8427	0.0259	0.1783	0.0020	0.80	1058	11	1061	9	1066	16	1		
	91500		81	28	15	0.36	0.7	0.10	0.0000536	0.0766	0.0008	0.1061	0.0016	1.8813	0.0284	0.1782	0.0020	0.73	1057	11	1075	10	1109	19	5		
	91500		81	28	15	0.36	0.0	0.00	0.0000001	0.0741	0.0008	0.1087	0.0010	1.8234	0.0283	0.1784	0.0019	0.70	1058	11	1054	10	1044	22	-1		
	91500		83	29	15	0.36	0.0	0.00	0.0000001	0.0757	0.0007	0.1084	0.0011	1.8966	0.0288	0.1817	0.0021	0.76	1076	11	1080	10	1087	19	1		
Session	temora		155	49	10	0.32	0.4	0.09	0.0000468	0.0559	0.0006	0.1007	0.0015	0.5057	0.0104	0.0656	0.0012	0.86	410	7	416	7	447	19	8		
1	temora		1821	863	131	0.49	0.5	0.01	0.0000050	0.0552	0.0001	0.1529	0.0009	0.5232	0.0093	0.0688	0.0012	0.99	429	7	427	6	419	6	-2		
July	temora		111	57	8	0.53	0.3	0.09	0.0000459	0.0531	0.0006	0.1647	0.0020	0.4936	0.0104	0.0674	0.0012	0.85	420	7	407	7	335	17	-25		
2005	temora		77	22	5	0.30	0.1	0.02	0.0000118	0.0539	0.0010	0.0939	0.0013	0.4942	0.0130	0.0665	0.0012	0.69	415	7	408	9	365	41	-14		
	temora		111	27	7	0.25	0.1	0.02	0.0000084	0.0539	0.0007	0.0794	0.0009	0.5001	0.0110	0.0673	0.0012	0.81	420	7	412	7	366	28	-15		
	temora		104	29	7	0.29	0.0	0.00	0.0000002	0.0549	0.0010	0.0897	0.0014	0.5101	0.0102	0.0674	0.0006	0.45	421	4	419	7	407	39	-3		
	temora		60	19	4	0.32	0.2	0.08	0.0000441	0.0532	0.0010	0.0969	0.0018	0.4980	0.0110	0.0679	0.0007	0.45	424	4	410	7	335	38	-26		
	temora		124	56	9	0.46	0.0	0.00	0.0000001	0.0555	0.0008	0.1427	0.0013	0.5154	0.0090	0.0673	0.0007	0.62	420	4	422	6	432	31	3		
	temora		119	35	8	0.30	0.2	0.07	0.0000352	0.0553	0.0006	0.0912	0.0023	0.5127	0.0080	0.0672	0.0007	0.69	419	4	420	5	425	21	1		
	temora		181	91	13	0.51	0.0	0.01	0.0000041	0.0561	0.0006	0.1581	0.0009	0.5220	0.0075	0.0675	0.0006	0.62	421	4	427	5	456	24	8		
	temora		104	48	7	0.47	0.3	0.11	0.0000563	0.0541	0.0008	0.1460	0.0020	0.4983	0.0087	0.0668	0.0007	0.57	417	4	411	6	374	27	-11		
	temora		117	37	8	0.32	0.1	0.04	0.0000210	0.0562	0.0010	0.1013	0.0015	0.5160	0.0106	0.0666	0.0007	0.51	415	4	422	7	460	38	10		
	temora		102	51	7	0.51	0.3	0.11	0.0000584	0.0551	0.0008	0.1572	0.0020	0.5097	0.0093	0.0671	0.0007	0.55	419	4	418	6	416	29	-1		
	temora		105	33	7	0.32	0.2	0.08	0.0000409	0.0548	0.0007	0.0998	0.0015	0.5064	0.0084	0.0670	0.0007	0.59	418	4	416	6	403	26	-4		
	temora		110	32	7	0.30	0.0	0.01	0.0000073	0.0557	0.0008	0.0923	0.0011	0.5143	0.0096	0.0670	0.0008	0.66	418	5	421	6	440	30	5		
	temora		131	61	9	0.48	0.0	0.00	0.0000001	0.0561	0.0006	0.1475	0.0014	0.5208	0.0077	0.0673	0.0007	0.66	420	4	426	5	457	24	8		
	temora		585	298	41	0.52	0.9	0.05	0.0000270	0.0555	0.0003	0.1631	0.0008	0.5089	0.0057	0.0665	0.0007	0.89	415	4	418	4	432	10	4		
	temora		609	315	43	0.53	0.2	0.01	0.0000050	0.0556	0.0004	0.1662	0.0009	0.5138	0.0064	0.0670	0.0007	0.81	418	4	421	4	437	16	4		
	temora		632	327	45	0.53	0.7	0.03	0.0000183	0.0547	0.0005	0.1646	0.0006	0.5085	0.0068	0.0675	0.0007	0.76	421	4	417	5	398	19	-6		
	temora		672	352	48	0.54	0.2	0.01	0.0000046	0.0550	0.0003	0.1669	0.0007	0.5076	0.0058	0.0670	0.0007	0.88	418	4	417	4	411	12	-2		
	temora		61	28	4	0.47	0.3	0.17	0.0000890	0.0529	0.0014	0.1449	0.0032	0.4741	0.0138	0.0650	0.0008	0.42	406	5	394	9	325	49	-25		
	temora		153	70	11	0.47	0.6	0.12	0.0000641	0.0530	0.0007	0.1443	0.0023	0.4877	0.0083	0.0667	0.0008	0.67	416	5	403	6	329	22	-27		
	temora		100	27	7	0.28	0.7	0.23	0.0001222	0.0537	0.0009	0.0835	0.0030	0.4997	0.0096	0.0675	0.0006	0.50	421	4	411	6	356	22	-18		
	temora		143	66	10	0.47	0.0	0.00	0.0000001	0.0555	0.0008	0.1434	0.0015	0.5188	0.0089	0.0678	0.0006	0.51	423	4	424	6	433	33	2		
	temora		91	28	6	0.32	0.5	0.16	0.0000864	0.0552	0.0011	0.0997	0.0024	0.5152	0.0116	0.0676	0.0007	0.43	422	4	422	8	422	37	0		
	temora		103	33	7	0.32	0.3	0.10	0.0000558	0.0549	0.0010	0.0982	0.0019	0.5133	0.0108	0.0678	0.0007	0.47	423	4	421	7	408	36	-4		
	temora		70	25	5	0.36	0.0	0.00	0.0000002	0.0542	0.0007	0.1023	0.0014	0.4948	0.0088	0.0663	0.0007	0.63	414	5	408	6	377	31	-10		
	temora		63	23	4	0.38	0.6	0.31	0.0001672	0.0535	0.0016	0.1164	0.0042	0.5041	0.0158	0.0683	0.0008	0.36	426	5	415	11	351	48	-21		
	temora		53	17	4	0.34	0.1	0.04	0.0000191	0.0560	0.0009	0.1035	0.0022	0.5157	0.0095	0.0668	0.0006	0.53	417	4	422	6	452	31	8		
	temora		82	39	6	0.49	0.0	0.00	0.0000002	0.0540	0.0008	0.1507	0.0022	0.4983	0.0098	0.0670	0.0008	0.60	418	5	411	7	370	35	-13		
	temora		106	51	7	0.50	0.2	0.06	0.0000299	0.0552	0.0010	0.1578	0.0022	0.4939	0.0102	0.0649	0.0006	0.48	405	4	408	7	419	38	3		
	temora		110	33	7	0.31	0.2	0.06	0.0000337	0.0540	0.0008	0.0964	0.0015	0.4855	0.0086	0.0652	0.0006	0.47	407	3	402	6	371	31	-10		
	temora		136	71	10	0.54	0.1	0.02	0.0000083	0.0559	0.0008	0.1685	0.0018	0.5190	0.0087	0.0673	0.0005	0.43	420	3	424	6	450	32	7		

sample	analysis no.	grain no.	U ppm	Th ppm	Pb ppm	Th/U	^{204}Pb ppb	f206 (%)	^{204}Pb/^{206}Pb	corrected ratios									Ages (Ma)								grain area	comment
										^{207}Pb/^{206}Pb	1σ	^{208}Pb/^{206}Pb	1σ	^{207}Pb/^{235}U	1σ	^{206}Pb/^{238}U	1σ	ρ	^{206}Pb/^{238}U	1σ	^{207}Pb/^{235}U	1σ	^{207}Pb/^{206}Pb	1σ	% disc			
	temora		150	46	10	0.32	0.4	0.08	0.0000452	0.0536	0.0008	0.0993	0.0022	0.5066	0.0087	0.0685	0.0005	0.46	427	3	416	6	354	30	-21			
	temora		72	24	5	0.35	0.2	0.10	0.0000544	0.0538	0.0011	0.1050	0.0023	0.5035	0.0113	0.0678	0.0007	0.43	423	4	414	8	364	37	-16			
	temora		180	89	13	0.51	0.1	0.01	0.0000066	0.0541	0.0007	0.1604	0.0015	0.5080	0.0076	0.0681	0.0005	0.54	425	3	417	5	375	27	-13			
	temora		157	71	11	0.46	0.2	0.05	0.0000264	0.0539	0.0007	0.1416	0.0014	0.5099	0.0080	0.0686	0.0006	0.55	428	4	418	5	367	26	-17			
	temora		174	94	12	0.55	0.0	0.00	0.0000001	0.0544	0.0006	0.1711	0.0016	0.5075	0.0070	0.0676	0.0006	0.59	422	3	417	5	388	24	-9			
	temora		145	39	10	0.28	0.0	0.00	0.0000001	0.0546	0.0006	0.0862	0.0008	0.5018	0.0070	0.0666	0.0005	0.57	416	3	413	5	397	25	-5			
	temora		246	72	16	0.30	0.2	0.02	0.0000114	0.0552	0.0006	0.0945	0.0007	0.5087	0.0064	0.0668	0.0005	0.59	417	3	418	4	420	22	1			
	temora		220	64	14	0.30	0.0	0.01	0.0000039	0.0556	0.0006	0.0936	0.0009	0.5044	0.0069	0.0658	0.0005	0.54	411	3	415	5	434	26	5			
	temora		68	25	5	0.37	0.2	0.08	0.0000406	0.0553	0.0008	0.1150	0.0020	0.5075	0.0088	0.0665	0.0007	0.57	415	4	417	6	425	25	2			
	temora		66	25	4	0.38	0.7	0.35	0.0001900	0.0534	0.0015	0.1138	0.0044	0.4857	0.0144	0.0659	0.0006	0.28	412	3	402	10	347	48	-19			
	temora		76	28	5	0.37	0.3	0.12	0.0000627	0.0553	0.0011	0.1146	0.0024	0.5072	0.0109	0.0666	0.0006	0.40	415	3	417	7	422	37	2			
	temora		61	21	4	0.35	0.4	0.22	0.0001167	0.0525	0.0012	0.1045	0.0032	0.4753	0.0122	0.0656	0.0008	0.47	410	5	395	8	309	35	-33			
	temora		74	26	5	0.36	0.3	0.12	0.0000666	0.0553	0.0012	0.1109	0.0022	0.4940	0.0120	0.0648	0.0007	0.47	404	4	408	8	425	42	5			
	temora		77	30	5	0.40	0.6	0.27	0.0001444	0.0534	0.0012	0.1196	0.0035	0.4851	0.0124	0.0658	0.0007	0.43	411	4	402	8	347	38	-18			
	temora		65	23	4	0.36	0.0	0.00	0.0000001	0.0546	0.0010	0.1139	0.0014	0.4967	0.0113	0.0659	0.0008	0.54	412	5	409	8	397	42	-4			
	temora		89	30	6	0.34	0.6	0.21	0.0001136	0.0533	0.0010	0.1048	0.0045	0.4792	0.0104	0.0652	0.0008	0.54	407	5	397	7	343	35	-19			
	temora		83	22	5	0.27	0.2	0.08	0.0000428	0.0547	0.0007	0.0853	0.0015	0.5047	0.0085	0.0670	0.0008	0.67	418	5	415	6	398	24	-5			
	temora		123	62	9	0.52	0.2	0.06	0.0000310	0.0542	0.0009	0.1586	0.0015	0.5044	0.0117	0.0675	0.0011	0.69	421	7	415	8	379	36	-11			
	temora		146	68	10	0.48	1.0	0.22	0.0001201	0.0550	0.0008	0.1453	0.0027	0.5109	0.0113	0.0674	0.0011	0.76	421	7	419	8	410	28	-3			
Session	temora		624	335	44	0.55	1.9	0.10	0.0000537	0.0548	0.0004	0.1713	0.0011	0.5049	0.0058	0.0669	0.0006	0.73	417	3	415	4	403	15	-4			
3	temora		630	319	44	0.52	0.4	0.02	0.0000119	0.0553	0.0004	0.1607	0.0008	0.5055	0.0053	0.0664	0.0006	0.79	414	3	415	4	422	14	2			
March	temora		164	39	11	0.25	1.0	0.19	0.0001012	0.0540	0.0007	0.0740	0.0021	0.5036	0.0082	0.0676	0.0006	0.55	422	4	414	6	372	24	-13			
2006	temora		150	46	10	0.31	0.1	0.03	0.0000152	0.0553	0.0007	0.0975	0.0008	0.5104	0.0078	0.0669	0.0006	0.61	417	4	419	5	425	26	2			
	temora		199	58	13	0.30	0.8	0.13	0.0000713	0.0555	0.0006	0.0916	0.0017	0.5103	0.0074	0.0667	0.0006	0.59	416	3	419	5	432	22	4			
	temora		162	41	10	0.26	0.6	0.12	0.0000651	0.0550	0.0007	0.0787	0.0017	0.4908	0.0073	0.0648	0.0006	0.59	404	3	405	5	410	22	1			
	temora		224	64	15	0.29	0.0	0.00	0.0000001	0.0555	0.0006	0.0921	0.0007	0.5022	0.0070	0.0656	0.0006	0.65	410	4	413	5	433	24	5			
	temora		176	49	11	0.29	0.2	0.03	0.0000154	0.0554	0.0007	0.0882	0.0010	0.4914	0.0079	0.0644	0.0006	0.55	402	3	406	5	426	29	6			
	temora		178	45	11	0.26	0.0	0.00	0.0000001	0.0548	0.0007	0.0821	0.0007	0.4937	0.0074	0.0653	0.0006	0.60	408	4	407	5	404	27	-1			
	temora		188	66	13	0.36	0.4	0.07	0.0000400	0.0551	0.0005	0.1098	0.0015	0.5019	0.0066	0.0660	0.0006	0.71	412	4	413	4	416	17	1			
	temora		165	65	11	0.40	0.4	0.07	0.0000373	0.0560	0.0006	0.1243	0.0020	0.5094	0.0073	0.0659	0.0006	0.61	412	3	418	5	453	22	9			
	temora		171	85	12	0.51	0.5	0.09	0.0000490	0.0536	0.0006	0.1565	0.0014	0.4796	0.0067	0.0649	0.0005	0.58	405	3	398	5	354	22	-14			
	temora		126	38	8	0.31	0.9	0.25	0.0001341	0.0521	0.0010	0.0907	0.0029	0.4650	0.0098	0.0648	0.0006	0.41	405	3	388	7	287	34	-41			
	temora		132	54	9	0.42	0.7	0.16	0.0000870	0.0536	0.0008	0.1292	0.0026	0.4946	0.0087	0.0669	0.0006	0.50	417	4	408	6	356	26	-17			
	temora		151	72	11	0.49	0.3	0.07	0.0000364	0.0554	0.0013	0.1499	0.0017	0.5106	0.0148	0.0669	0.0011	0.57	417	7	419	10	427	50	2			
	temora		114	34	8	0.31	0.0	0.00	0.0000002	0.0564	0.0009	0.0965	0.0009	0.5164	0.0101	0.0664	0.0007	0.55	414	4	423	7	469	36	12			
	temora		109	29	7	0.27	0.4	0.12	0.0000649	0.0542	0.0012	0.0796	0.0021	0.4971	0.0117	0.0665	0.0007	0.42	415	4	410	8	380	41	-9			
	temora		60	21	4	0.37	0.6	0.34	0.0001832	0.0540	0.0019	0.1110	0.0048	0.4945	0.0192	0.0664	0.0010	0.38	414	6	408	13	372	59	-11			
	temora		80	27	5	0.35	0.7	0.28	0.0001512	0.0544	0.0014	0.1065	0.0039	0.4898	0.0140	0.0653	0.0007	0.37	408	4	405	9	386	45	-6			
	temora		47	16	3	0.36	0.0	0.00	0.0000004	0.0564	0.0009	0.1141	0.0022	0.5085	0.0100	0.0654	0.0007	0.57	409	4	417	7	466	36	12			
	temora		66	23	4	0.36	0.1	0.03	0.0000182	0.0569	0.0011	0.1158	0.0017	0.5191	0.0117	0.0661	0.0008	0.52	413	5	425	8	488	39	15			
	temora		91	50	6	0.56	2.0	0.76	0.0004101	0.0516	0.0017	0.1506	0.0070	0.4555	0.0153	0.0640	0.0007	0.31	400	4	381	11	267	43	-50			
	temora		128	61	9	0.49	0.9	0.23	0.0001259	0.0537	0.0012	0.1446	0.0031	0.4881	0.0117	0.0659	0.0007	0.42	411	4	404	8	359	39	-15			
	temora		94	46	6	0.50	0.8	0.30	0.0001599	0.0534	0.0013	0.1509	0.0037	0.4790	0.0126	0.0650	0.0008	0.45	406	5	397	9	346	39	-17			
	temora		132	54	9	0.42	0.7	0.16	0.0000870	0.0536	0.0008	0.1292	0.0026	0.4946	0.0087	0.0669	0.0006	0.50	417	4	408	6	356	26	-17			
	temora		151	72	11	0.49	0.3	0.07	0.0000364	0.0554	0.0013	0.1499	0.0017	0.5106	0.0148	0.0669	0.0011	0.57	417	7	419	10	427	50	2			
	temora		114	34	8	0.31	0.0	0.00	0.0000002	0.0564	0.0009	0.0965	0.0009	0.5164	0.0101	0.0664	0.0007	0.55	414	4	423	7	469	36	12			
	temora		109	29	7	0.27	0.4	0.12	0.0000649	0.0542	0.0012	0.0796	0.0021	0.4971	0.0117	0.0665	0.0007	0.42	415	4	410	8	380	41	-9			
	temora		60	21	4	0.37	0.6	0.34	0.0001832	0.0540	0.0019	0.1110	0.0048	0.4945	0.0192	0.0664	0.0010	0.38	414	6	408	13	372	59	-11			
	temora		80	27	5	0.35	0.7	0.28	0.0001512	0.0544	0.0014	0.1065	0.0039	0.4898	0.0140	0.0653	0.0007	0.37	408	4	405	9	386	45	-6			
	temora		47	16	3	0.36	0.0	0.00	0.0000004	0.0564	0.0009	0.1141	0.0022	0.5085	0.0100	0.0654	0.0007	0.57	409	4	417	7	466	36	12			
	temora		66	23	4	0.36	0.1	0.03	0.0000182	0.0569	0.0011	0.1158	0.0017	0.5191	0.0117	0.0661	0.0008	0.52	413	5	425	8	488	39	15			
	temora		91	50	6	0.56	2.0	0.76	0.0004101	0.0516	0.0017	0.1506	0.0070	0.4555	0.0153	0.0640	0.0007	0.31	400	4	381	11	267	43	-50			
	temora		128	61	9	0.49	0.9	0.23	0.0001259	0.0537	0.0012	0.1446	0.0031	0.4881	0.0117	0.0659	0.0007	0.42	411	4	404	8	359	39	-15			
	temora		94	46	6	0.50	0.8	0.30	0.0001599	0.0534	0.0013	0.1509	0.0037	0.4790	0.0126	0.0650	0.0008	0.45	406	5	397	9	346	39	-17			

Appendix 2d

Zircon trace element/REE data of the Lochnagar pluton

	AD1																		AD2					
	SA04/01-4.7	SA04/01-4.10	SA04/01-6.14	SA04/01-6.15	SA04/01-11.33	SA04/01-11.34	SA04/01-11.34.2	SA04/01-14.43	SA04/01-14.44	SA04/01-16.51	SA04/01-16.52	SA04/01-8.20	SA04/01-8.25	SA04/01-9.28	SA04/01-9.29	SA04/01-13.41	SA04/01-13.42	SA04/01-10.31	SA04/01-10.32	SA04/02-11.22	SA04/02-11.24	SA04/02-13.27	SA04/02-13.29	SA04/02-18.39	SA04/02-18.40
grain no.	4	4	6	6	11	11	11	14	14	16	16	8	8	9	9	13	13	10	10	11	11	13	13	18	18
Si	140230	140230	140230	140230	140230	140230	140230	140230	140230	140230	140230	140230	140230	140230	140230	140230	140230	140230	140230	140230	140230	140230	140230	140230	140230
P	273	195	172	200	289	225	231	224	206	497	230	376	304	247	372	289	534	377	220	295	234	58	35	207	599
Ca	1	1	1	84	1	17	5	1	1	1	0	3	2	2	1	1	2	2	1	1	5	1	1	21	2
Ti	18	18	9	21	8	10	8	22	17	11	8	26	7	14	11	16	9	18	17	10	4	2	2	12	5
Y	1816	913	487	1260	1875	966	1625	711	601	4174	1316	1069	704	890	775	420	1656	591.60	650	2189	639	197	129	1726	5311
Nb																			2						
Zr	558790	535930	540160	547590	552260	541740	560770	565290	557790	548630	557730	532130	519780	529810	529300	524520	523090	523880	536860	556450	570260	557040	559840	553170	562370
Ba	0.1	0.1	0.0	1.0	0.0	1.3	0.3	0.3	0.2	0.1	0.1	0.1	0.0	0.2	0.2	0.0	0.1	0.1	0.1	0.0	0.7	0.1	0.0	1.5	-0.1
La	0.1	0.1	0.1	0.2	0.1	0.7	0.3	0.1	0.0	0.2	0.1	0.1	0.0	0.1	0.0	0.0	0.0	0.0	0.0	0.1	0.6	0.1	0.0	2.1	0.5
Ce	15.3	9.9	11.9	12.7	38.1	24.9	32.3	7.0	9.7	73.0	29.0	7.9	21.4	11.6	16.9	7.6	52.6	8.6	7.8	73.0	16.4	6.6	3.7	75.1	177.6
Pr	0.6	0.5	0.1	0.5	0.5	0.4	0.5	0.2	0.1	1.1	0.3	0.4	0.1	0.4	0.1	0.1	0.2	0.1	0.2	0.3	0.3	0.0	0.0	2.4	2.9
Nd	7.6	5.9	1.2	6.4	7.5	4.1	6.8	2.9	1.7	15.9	4.0	5.1	1.0	5.7	1.8	1.1	2.7	1.8	3.3	3.5	2.6	0.4	0.2	21.9	40.7
Sm	10.1	6.6	1.8	8.3	9.2	4.8	10.7	3.2	2.6	19.4	6.3	6.2	1.8	6.3	2.5	1.8	4.1	2.3	4.4	7.3	2.7	0.4	0.2	12.8	47.8
Eu	4.8	3.0	0.7	3.5	3.2	1.9	3.6	1.6	1.1	7.4	2.2	3.1	0.8	2.6	1.1	0.7	1.8	1.0	1.9	3.7	1.3	0.2	0.1	5.4	21.2
Gd	56	30	9	40	44	24	42	18	12	110	31	34	12	26	15	9	29	12	21	53	13	2	1	44	194
Tb	19	9	3	12	16	8	14	6	4	37	11	10	5	8	5	3	10	4	6	18	5	1	1	15	59
Dy	209	101	46	144	193	108	183	70	55	460	140	119	63	96	69	39	143	52	75	227	60	16	8	188	662
Ho	73	36	18	50	75	40	66	28	22	169	52	42	26	34	28	15	62	21	27	83	23	7	4	69	218
Er	353	167	98	240	382	206	336	146	122	833	264	195	137	164	157	80	346	113	130	409	125	42	27	348	997
Tm	74	36	24	50	87	48	72	32	28	181	59	42	32	34	39	19	83	26	28	88	30	12	8	77	206
Yb	576	289	193	397	713	384	607	275	246	1465	484	359	288	295	356	165	731	230	236	738	287	114	83	630	1647
Lu	137	65	50	95	175	92	143	70	62	339	119	85	73	69	94	42	181	59	55	173	72	34	27	153	352
Hf	9215	8265	10484	8777	13519	12407	14270	8475	8874	12714	12754	7542	11590	8599	10762	8340	12008	7705	8190	8154	7878	13133	13066	10815	10926
Th	238	78	49	130	301	160	246	56	48	1001	277	96	77	78	76	29	233	39	56	1929	267	66	49	1313	5255
U	249	101	72	153	246	148	175	109	93	461	200	123	121	78	113	45	300	74	75	1517	384	333	297	1344	2935
	Normalised to chondrite (using values from Anders and Grevesse, 1989)																								
La	0.45	0.37	0.23	0.92	0.37	3.04	1.16	0.32	0.13	0.79	0.27	0.49	0.11	0.21	0.11	0.12	0.20	0.11	0.13	0.36	2.45	0.21	0.20	8.90	2.31
Ce	25.38	16.38	19.73	21.11	63.10	41.24	53.62	11.61	16.11	121.07	48.00	13.12	35.53	19.22	28.07	12.64	87.17	14.32	12.92	120.95	27.23	10.91	6.14	124.56	294.50
Pr	6.85	5.17	0.83	5.97	5.75	4.63	5.33	2.25	1.36	11.79	3.21	4.54	0.79	4.04	1.28	0.94	1.84	1.16	2.28	3.45	3.71	0.52	0.48	27.30	32.42
Nd	16.86	13.15	2.71	14.14	16.51	9.08	15.09	6.50	3.79	35.18	8.94	11.18	2.19	12.59	3.93	2.44	6.04	4.04	7.24	7.81	5.64	0.91	0.51	48.33	89.99
Sm	69	45	12	57	63	33	73	22	18	132	43	42	12	43	17	12	28	16	30	50	19	3	1	87	325
Eu	87	54	12	62	57	35	63	28	20	132	39	55	15	46	19	12	32	18	33	67	23	3	2	97	379
Gd	284	155	46	203	224	122	212	92	63	558	158	173	63	134	75	43	149	61	107	270	66	12	6	226	988
Tb	510	246	91	334	439	234	399	160	117	1028	303	284	126	232	145	83	283	115	175	505	126	32	15	415	1620
Dy	860	415	189	592	796	444	754	289	228	1897	578	492	259	395	283	162	588	216	310	934	245	65	34	774	2727
Ho	1318	649	319	893	1341	727	1180	503	400	3045	937	756	466	616	505	274	1115	384	488	1486	408	123	71	1233	3920
Er	2220	1054	617	1509	2407	1295	2115	921	771	5244	1659	1228	864	1031	987	501	2176	710	817	2574	789	264	171	2189	6272
Tm	3045	1504	972	2056	3579	1979	2982	1312	1141	7481	2423	1735	1330	1419	1605	776	3445	1076	1158	3655	1248	481	323	3184	8502
Yb	3546	1780	1189	2441	4390	2363	3734	1693	1516	9018	2978	2211	1772	1818	2190	1018	4501	1415	1454	4542	1764	702	511	3879	10135
Lu	5627	2691	2076	3917	7187	3771	5869	2900	2567	13951	4883	3490	3005	2842	3858	1726	7428	2421	2282	7110	2969	1397	1123	6280	14465
Hf	886077	794712	1008077	843923	1299904	1192981	1372115	814913	853260	1222500	1226346	725212	1114423	826779	1034808	801904	1154615	740827	787490	784048	757452	1262788	1256346	1039904	1050577
Th	96	32	20	53	122	65	99	23	19	405	112	39	31	32	31	12	94	16	23	781	108	27	20	532	2127
U	30747	12527	8867	18873	30354	18214	21584	13409	11433	56922	24710	15228	14894	9635	13949	5589	37026	9166	9273	187222	47404	41117	36631	165877	362370
Th/U	1.0	0.8	0.7	0.9	1.2	1.1	1.4	0.5	0.5	2.2	1.4	0.8	0.6	1.0	0.7	0.6	0.8	0.5	0.7	1.3	0.7	0.2	0.2	1.0	1.8
Yb(n)/La(n)	7931	4807	5240	2648	11790	776	3214	5359	11475	11380	11231	4535	16757	8505	20835	8256	22406	13423	10898	12758	718	3278	2497	436	4389
Yb(n/Gd(n)	12.5	11.5	25.9	12.0	19.6	19.4	17.6	18.5	24.0	16.2	18.9	12.8	28.3	13.6	29.3	23.5	30.1	23.0	13.6	16.8	26.8	60.2	78.6	17.1	10.3
Eu/Eu*	0.6	0.6	0.5	0.6	0.5	0.5	0.5	0.6	0.6	0.5	0.5	0.6	0.5	0.6	0.5	0.5	0.5	0.6	0.6	0.6	0.7	0.6	0.5	0.7	0.7
Ce/Ce*	14.5	11.8	45.3	9.0	43.1	11.0	21.6	13.8	38.0	39.6	52.0	8.8	123.0	20.7	76.6	37.0	143.5	40.9	23.4	109.2	9.0	32.7	19.7	8.0	34.0
HfO_2 [wt%]	1.1	1.0	1.2	1.0	1.6	1.5	1.7	1.0	1.0	1.5	1.5	0.9	1.4	1.0	1.3	1.0	1.4	0.9	1.0	1.0	0.9	1.5	1.5	1.3	1.3
comment							rejected, crack														rejected, crack				
grain area	?	?	c1	c2	r1	c1a	c1b	c1	c2	c1	r3	c1	r1	c2a	c2b	c2a	c2b	c2	c1	c1a	c1b	c2b	c2a	rim	c1

					CnG																	L1-03		
	SA04/02 - 7.12	SA04/02 - 7.10	SA04/02 - 15.32	SA04/02 - 15.31	SA04/13 - 1.1	SA04/13 - 1.2	SA04/13 - 5.9	SA04/13 - 5.10	SA04/13 - 6.13	SA04/13 - 6.14	SA04/13 - 12.29	SA04/13 - 12.30	SA04/13 - 15.35	SA04/13 - 15.36	SA04/13 - 18.42	SA04/13 - 4.7	SA04/13 - 4.8	SA04/13 - 5.11	SA04/13 - 13.31	SA04/13 - 19.44	SA04/13 - 19.44b	SA04/13 - 19.45	S04/03 - 3.6	S04/03 - 3.57	S04/03 - 8.14
grain no.	7	7	15	15	1	1	5	5	6	6	12	12	15	15	18	4	4	5	13	19	19	19	3	3	8
Si	140230	140230	140230	140230	140230	140230	140230	140230	140230	140230	140230	140230	140230	140230	140230	140230	140230	140230	140230	140230	140230	140230	140230	140230	140230
P	176	101	159	125	158	61	206	206	122	230	65	107	120	119	107	115	182	234	103	533	498	104	255	185	189
Ca	149	1	0	3	2	1	0	1	2	1	7	7	1	1	2	2	1	5	2	3	2	19	1	1	6
Ti	56	4	3	3	12	5	8	11	10	11	7	7	7	5	41	4	6	7	5	14	14	8	10	14	10
Y	762	715	696	952	766	196	715	523	586	884	143	644	670	674	390	167	675	450	162	2054	2102	233	537	386	519
Nb																1	2	3	1	4	4	1			
Zr	567990	565750	557200	564630	551440	555060	569270	544810	562230	573120	545100	562530	551470	532660	533430	509380	531930	525950	519520	522280	532620	543600	547000	565860	541200
Ba	10.4	0.0	0.1	0.2	0.3	0.0	0.0	0.0	0.2	0.2	0.1	0.2	0.0	0.1	0.2	0.1	0.1	0.0	0.1	0.1	0.1	1.2	0.0	0.1	0.1
La	0.4	0.1	0.1	0.0	0.2	0.0	0.0	0.0	0.3	0.1	2.1	0.9	0.2	0.1	0.8	0.0	0.1	1.0	0.0	0.2	0.2	3.5	0.0	0.1	0.0
Ce	15.7	15.3	15.2	21.5	12.7	7.2	20.7	11.4	13.7	20.6	15.2	20.3	15.4	16.1	11.8	8.5	15.5	16.3	6.1	18.9	18.1	19.4	14.9	17.0	21.6
Pr	0.5	0.3	0.2	0.2	0.5	0.1	0.1	0.1	0.5	0.2	1.0	0.8	0.4	0.4	0.4	0.0	0.5	0.5	0.1	0.6	0.6	0.5	0.1	0.1	0.1
Nd	5.9	4.3	2.9	3.5	5.0	0.8	1.8	1.1	5.4	2.2	5.2	7.1	5.6	4.9	4.5	0.3	4.6	2.6	0.7	6.7	6.8	2.5	1.6	1.1	1.4
Sm	5.6	4.3	3.4	4.7	4.9	0.6	1.7	1.2	4.9	2.1	0.6	4.7	3.6	3.5	2.9	0.7	4.1	1.7	1.2	12.2	11.6	0.9	2.6	2.0	2.1
Eu	2.0	1.6	1.4	1.7	2.6	0.5	0.7	0.6	2.1	1.2	0.5	1.7	1.8	1.5	1.3	0.2	1.8	0.7	0.4	6.8	7.0	0.3	1.0	0.8	1.0
Gd	22	20	16	24	20	4	8	6	17	12	2	15	14	18	11	3	18	6	3	63	67	3	12	10	13
Tb	7	6	5	8	6	1	4	3	5	5	1	5	5	5	3	1	5	2	1	19	20	1	4	3	5
Dy	81	75	67	94	77	17	57	39	60	74	12	62	63	61	37	13	65	33	13	220	227	17	53	40	55
Ho	28	27	26	36	28	7	25	17	22	30	4	23	23	24	13	5	24	15	6	75	79	7	20	15	20
Er	146	139	136	187	145	37	148	102	114	178	27	125	125	128	69	27	125	86	30	363	385	43	105	76	103
Tm	33	33	34	43	34	10	37	27	28	43	7	29	30	32	17	7	30	22	8	83	86	11	23	16	24
Yb	314	286	300	361	309	89	349	243	243	395	64	256	277	266	159	70	279	212	77	712	762	109	188	143	188
Lu	78	72	75	90	82	23	96	69	68	104	17	68	75	72	40	20	73	58	21	174	177	31	47	34	46
Hf	8828	9696	9440	11540	8115	11173	9648	7824	8590	8757	11053	10095	9073	9370	7743	10535	8791	8913	8834	7238	7601	14119	10319	10964	10359
Th	228	243	235	320	230	51	303	160	197	474	43	245	248	248	93	51	260	146	40	874	928	94	46	55	72
U	316	371	407	477	275	108	543	286	255	583	87	339	340	353	126	120	358	298	80	603	641	234	85	97	118
La	1.74	0.28	0.26	0.18	0.66	0.14	0.12	0.14	1.32	0.30	9.11	3.81	0.91	0.40	3.51	0.06	0.55	4.21	0.10	0.73	0.67	14.74	0.07	0.24	0.20
Ce	26.09	25.40	25.13	35.72	20.98	11.92	34.38	18.89	22.76	34.08	25.22	33.61	25.55	26.76	19.51	14.12	25.73	27.00	10.12	31.26	30.04	32.21	24.65	28.11	35.82
Pr	5.63	3.73	2.76	2.70	5.11	0.73	1.54	1.23	5.42	2.35	10.94	9.09	4.76	4.60	4.45	0.45	5.35	5.67	0.84	6.43	6.51	6.01	0.98	1.08	1.17
Nd	12.98	9.60	6.32	7.76	11.01	1.79	3.88	2.40	11.86	4.77	11.51	15.65	12.43	10.80	9.89	0.67	10.23	5.81	1.64	14.80	15.00	5.56	3.52	2.46	3.02
Sm	38	29	23	32	33	4	12	8	33	14	4	32	25	24	20	5	28	11	8	83	79	6	18	14	14
Eu	36	28	25	30	47	8	13	10	38	22	9	31	31	27	23	3	32	12	8	121	125	6	18	14	19
Gd	111	102	84	124	104	19	38	32	89	63	11	76	73	89	58	13	91	30	17	320	342	17	61	52	65
Tb	194	172	145	212	175	37	100	69	149	133	22	137	142	141	87	26	144	63	29	530	555	33	121	96	126
Dy	334	311	278	389	318	70	237	159	247	306	49	257	259	253	151	53	268	135	55	906	936	71	218	164	225
Ho	510	490	466	646	497	120	447	309	390	542	80	417	418	437	239	90	431	261	104	1345	1417	132	362	273	364
Er	918	872	856	1179	913	233	932	640	718	1121	169	786	787	806	434	172	788	542	192	2287	2425	268	663	479	651
Tm	1369	1372	1386	1784	1418	397	1523	1120	1155	1778	286	1188	1248	1315	697	280	1224	899	344	3414	3547	449	953	663	974
Yb	1930	1761	1847	2223	1904	550	2148	1493	1495	2432	396	1575	1707	1634	980	433	1718	1302	476	4381	4688	669	1155	879	1158
Lu	3195	2962	3066	3687	3375	956	3932	2860	2799	4292	718	2784	3076	2951	1646	819	2994	2389	858	7162	7297	1265	1926	1383	1879
Hf	848856	932346	907644	1109615	780240	1074327	927692	752308	826000	842048	1062788	970673	872433	900942	744529	1012981	845317	857048	849423	696000	730885	1357596	992212	1054231	996058
Th	92	98	95	129	93	21	123	65	80	192	17	99	101	100	38	21	105	59	16	354	376	38	19	22	29
U	39056	45791	50233	58940	33973	13390	66991	35344	31449	72036	10771	41865	41975	43623	15579	14775	44147	36795	9850	74484	79178	28885	10516	12020	14565
Th/U	0.7	0.7	0.6	0.7	0.8	0.5	0.6	0.6	0.8	0.8	0.5	0.7	0.7	0.7	0.7	0.4	0.7	0.5	0.5	1.4	1.4	0.4	0.5	0.6	0.6
Yb(n)/La(n)	1111	6376	7142	12043	2897	3828	18225	10631	1129	8228	44	413	1876	4045	279	6893	3118	310	4817	6012	7023	45	17035	3671	5671
Yb(n/Gd(n)	17.4	17.3	22.1	17.9	18.3	28.8	56.0	46.1	16.8	38.8	35.9	20.7	23.2	18.4	17.0	33.7	19.0	43.2	27.9	13.7	13.7	39.9	18.8	16.9	17.7
Eu/Eu*	0.6	0.5	0.6	0.5	0.8	0.9	0.6	0.6	0.7	0.7	1.3	0.6	0.7	0.6	0.7	0.5	0.6	0.6	0.7	0.7	0.8	0.6	0.5	0.5	0.6
Ce/Ce*	8.3	25.0	29.7	50.6	11.4	36.7	80.8	45.5	8.5	40.9	2.5	5.7	12.3	19.6	4.9	84.3	15.0	5.5	35.1	14.4	14.4	3.4	95.6	55.2	73.2
HfO_2 [wt%]	1.0	1.1	1.1	1.4	1.0	1.3	1.1	0.9	1.0	1.0	1.3	1.2	1.1	1.1	0.9	1.2	1.0	1.1	1.0	0.9	0.9	1.7	1.2	1.3	1.2
comment	rejected, inclusion	rejected, crack							rejected, crack		rejected, crack	rejected, crack			rejected, crack	cycles 1-5		cycles 1-6							
grain area	c2	c1	c2b	c2a	c2a	c2b	c2	c1	c1	r1	r1	c1	c1	r1	c2	r1	c1	r1	c1	c1a	c1b	r1	c2a	c2b	r1

																						L2-04				
	S04/03 - 8.13	S04/03 - 8.14x	S04/03 - 9.15	S04/03 - 9.16	S04/03 - 16.28	S04/03 - 16.29	S04/03 - 27.54	S04/03 - 27.55	SA04/03 - 12.19	SA04/03 - 13.22	SA04/03 - 15.26	SA04/03 - 15.27	SA04/03 - 22.42	SA04/03 - 23.43	SA04/03 - 23.44	SA04/03 - 24.46	SA04/03 - 20.37	SA04/03 - 20.38	SA04/03 - 26.51	SA04/03 - 26.53	SA04/04 - 10.20	SA04/04 - 10.21	SA04/04 - 16.31	SA04/04 - 16.32	SA04/04 - 27.51
grain no.	8	8	9	9	16	16	27	27	12	13	15	15	22	23	23	24	20	20	26	26	10	10	16	16	27
Si	140230	140230	140230	140230	140230	140230	140230	140230	140230	140230	140230	140230	140230	140230	140230	140230	140230	140230	140230	140230	140230	140230	140230	140230	140230
P	558	237	116	85	495	140	136	109	441	3104	225	369	264	808	1016	616	325	209	17024	196	671	281	948	190	238
Ca	7	1513	1	1	8	0	20	1	21	5328	2	8	1	2	1	10	5	13	23900	3	1	9	2	23	22
Ti	7	74	12	9	175	12	15	13	11	6	7	5	8	7	5	16	8	11	15	14	2	10	3	4.05	5.03
Y	2721	497	410	217	1186	361	243	458	1593	1166	1071	1490	541	2192	1318	1527	705	304	1634	273	1822	925	2694	903	1094
Nb									10	10	2	13	3	18	5	11	4	1	2	1					
Zr	547490	589050	553320	547290	560340	549960	561360	568190	546870	522520	530170	540700	534570	528280	526810	531710	525300	526980	507440	536280	552090	556930	541200	549910	538430
Ba	0.9	3.0	0.2	0.1	2.0	0.2	0.3	0.1	12.7	1.1	0.1	0.3	0.1	0.1	0.1	1.9	0.2	0.3	0.8	0.0	0.1	0.4	0.1	2.3	1.6
La	3.0	0.2	0.0	0.0	8.7	0.0	2.0	0.0	12.1	85.2	1.0	0.7	0.0	0.1	0.1	7.7	0.0	0.0	239.6	0.0	0.1	0.5	0.1	4.4	7.1
Ce	120.7	21.9	13.6	10.6	74.9	12.3	14.1	10.0	118.7	269.2	39.1	81.5	23.9	88.4	22.4	88.6	27.4	14.6	611.0	10.3	4.9	17.6	71.7	57.3	41.7
Pr	3.0	0.2	0.2	0.1	6.0	0.1	1.2	0.1	7.0	30.6	1.1	0.6	0.1	0.3	0.1	6.8	0.1	0.1	74.5	0.0	0.1	0.3	0.3	2.8	4.3
Nd	26.3	1.7	2.6	1.1	36.2	1.0	9.0	1.8	36.0	143.9	8.8	5.0	1.5	6.6	2.0	48.4	1.5	0.8	372.9	0.5	0.5	2.6	4.1	19.3	24.0
Sm	22.2	2.7	3.6	1.1	13.3	1.5	3.9	2.7	17.2	31.8	7.4	5.6	2.0	10.7	4.7	22.0	2.1	1.1	76.1	1.0	1.8	6.1	9.2	9.0	15.4
Eu	3.5	1.0	1.2	0.5	2.7	0.7	0.8	1.2	3.8	2.5	2.5	1.3	0.7	2.2	1.2	4.4	0.7	0.4	9.4	0.4	0.4	1.3	1.0	1.4	2.6
Gd	92	14	12	5	30	8	8	13	52	49	35	28	11	62	31	55	12	6	111	6	21	30	61	25	44
Tb	29	5	4	2	9	3	2	4	16	12	10	11	4	21	11	16	5	2	22	2	12	10	23	8	13
Dy	327	55	41	20	117	37	23	51	187	129	119	151	50	257	140	180	60	26	206	25	179	116	294	97	138
Ho	113	20	14	7	43	13	9	18	65	45	43	59	20	90	52	63	24	10	63	10	72	37	108	35	43
Er	527	104	73	37	220	70	46	90	297	217	206	302	105	404	251	290	130	52	269	47	370	158	508	170	192
Tm	107	23	16	10	51	15	11	19	61	46	42	69	25	82	53	58	30	12	53	11	87	30	105	37	40
Yb	828	181	140	93	413	133	95	161	494	373	346	582	225	617	422	451	268	109	402	91	696	220	811	299	307
Lu	190	46	37	24	96	32	24	39	109	84	79	137	56	132	95	100	69	28	88	24	147	46	180	67	67
Hf	11089	11835	10054	10693	12958	10236	10701	10642	12277	12876	10835	13139	10467	11722	11412	12115	9845	10074	8778	9937	29642	13548	12001	13517	13435
Th	774	75	82	36	140	34	36	55	325	250	160	341	86	742	96	251	109	46	164	30	68	126	672	276	172
U	952	131	83	58	468	60	60	76	537	538	224	767	159	997	283	548	190	85	165	57	4419	797	1876	768	465
La	12.99	0.81	0.20	0.10	37.05	0.20	8.43	0.19	51.58	363.02	4.16	2.90	0.13	0.33	0.22	32.93	0.09	0.11	1020.66	0.09	0.44	2.01	0.35	18.90	30.07
Ce	200.17	36.39	22.60	17.60	124.19	20.34	23.32	16.66	196.75	446.34	64.86	135.16	39.64	146.58	37.14	146.82	45.37	24.17	1012.95	17.15	8.05	29.24	118.91	95.01	69.20
Pr	33.78	1.97	1.94	0.82	67.26	0.62	13.71	1.27	78.71	343.91	12.49	6.68	0.94	3.79	1.39	76.13	1.29	0.69	835.72	0.38	0.61	2.95	2.94	31.77	47.76
Nd	58.02	3.76	5.65	2.38	79.97	2.15	19.97	4.07	79.57	317.99	19.49	10.99	3.24	14.61	4.46	107.08	3.34	1.71	824.31	1.10	1.16	5.75	8.95	42.69	53.14
Sm	151	18	24	7	90	10	27	19	117	216	50	38	14	73	32	150	14	8	518	7	12	41	63	61	105
Eu	62	18	22	9	47	12	14	21	68	45	44	23	13	40	21	79	13	6	168	8	7	22	18	25	47
Gd	467	72	60	27	153	38	39	67	265	249	176	141	54	315	155	279	61	30	564	31	104	154	311	125	226
Tb	792	126	98	51	256	77	57	114	449	331	282	295	106	584	305	436	132	58	611	54	328	282	644	220	351
Dy	1346	225	169	84	483	151	97	208	769	531	491	621	205	1057	575	740	245	108	849	104	736	477	1212	400	568
Ho	2028	364	258	134	778	238	159	317	1165	806	770	1062	356	1621	936	1134	430	183	1140	173	1301	657	1944	635	775
Er	3318	652	461	234	1381	438	287	565	1867	1363	1293	1902	660	2545	1580	1825	817	329	1694	297	2330	993	3199	1070	1207
Tm	4441	937	682	405	2100	630	451	794	2502	1894	1754	2841	1036	3370	2202	2388	1239	507	2191	465	3577	1250	4328	1514	1651
Yb	5095	1116	860	570	2544	818	585	988	3039	2297	2132	3580	1383	3799	2599	2776	1647	671	2477	558	4280	1353	4988	1841	1891
Lu	7813	1895	1503	974	3958	1314	1001	1622	4474	3437	3253	5622	2305	5444	3923	4130	2837	1144	3614	981	6065	1907	7398	2778	2773
Hf	1066250	1137981	966731	1028173	1245962	984231	1028942	1023269			1041827	1263365	1006442	1127115	1097308	1164904	946606	968654	844077	955519	2850192	1302692	1153942	1299712	1291827
Th	313	30	33	15	57	14	14	22	1180481	1238077	65	138	35	300	39	102	44	18	66	12	28	51	272	112	70
U	117553	16199	10248	7174	57790	7464	7396	9405	132	101	27654	94706	19690	123063	34905	67685	23454	10497	20379.01	6978	545531	98430	231556	94822	57363
Th/U	0.8	0.6	1.0	0.6	0.3	0.6	0.6	0.7	0.6	0.5	0.7	0.4	0.5	0.7	0.3	0.5	0.6	0.5	1.0	0.5	0.0	0.2	0.4	0.4	0.4
Yb(n)/La(n)	392	1386	4343	5776	69	3998	69	5116	59	6	512	1236	10329	11393	11890	84	18453	5964	2	6059	9623	673	14053	97	63
Yb(n/Gd(n)	10.9	15.4	14.4	21.2	16.7	21.3	14.9	14.8	11.5	9.2	12.1	25.3	25.5	12.1	16.7	10.0	27.2	22.4	4.4	18.1	41.0	8.8	16.1	14.7	8.4
Eu/Eu*	0.2	0.5	0.6	0.7	0.4	0.6	0.4	0.6	0.4	0.2	0.5	0.3	0.5	0.3	0.3	0.4	0.5	0.4	0.3	0.5	0.2	0.3	0.1	0.3	0.3
Ce/Ce*	9.6	28.9	36.5	61.8	2.5	57.3	2.2	33.7	3.1	1.3	9.0	30.7	111.9	130.4	67.4	2.9	133.7	86.9	1.1	91.1	15.5	12.0	116.3	3.9	1.8
HfO_2 [wt%]	1.3	1.4	1.2	1.3	1.5	1.2	1.3	1.3	1.4	1.5	1.3	1.5	1.2	1.4	1.3	1.4	1.2	1.2	1.0	1.2	3.5	1.6	1.4	1.6	1.6
comment	rejected, crack	rejected, apatite inclusion			rejected, crack							cycles 8-10							rejected, apatite inclusion					rejected, crack	rejected, crack
grain area	c1	r1	c2a	c2b	c2	rim	c2	c1	rim	rim	c1	rim	c1	c2a	c2b	rim	c2	rim	c1	rim	c1	r1	c1	rim	c1

	SA04/04 - 15.28 (inh)	SA04/04 - 15.30 (inh)	SA04/04 - 15.29 (inh)	SA04/04 - 18.34	SA04/04 - 18.35	SA04/04 - 11.22	SA04/04 - 11.45	SA04/04 - 1.2
grain no.	15	15	15	18	18	11	11	1
Si	140230	140230	140230	140230	140230	140230	140230	140230
P	360	270	365	730	347	230	9243	659
Ca	1	2	3	16	8	3	8286	3
Ti	25	11	15	7	6	5	28	10
Y	734	862	634	1182	1581	991	947	1891
Nb			5	8	19	2	4	9
Zr	534980	547650	528960	556740	552870	536050	541630	529090
Ba	0.2	0.2	0.1	2.1	0.2	0.1	0.7	-0.1
La	0.1	0.1	0.0	3.9	0.1	0.0	83.1	0.1
Ce	21.5	46.7	32.1	37.4	59.7	30.3	264.4	87.7
Pr	0.1	0.1	0.1	1.7	0.1	0.2	27.8	0.3
Nd	2.5	1.7	1.1	9.3	1.4	3.8	120.5	5.9
Sm	3.9	3.1	2.1	4.9	3.6	6.5	27.6	9.5
Eu	0.6	0.4	0.4	1.1	0.7	1.5	3.4	2.4
Gd	19	18	12	24	28	28	38	49
Tb	6	7	5	9	11	9	10	17
Dy	77	89	59	113	146	107	101	208
Ho	29	34	23	43	60	39	36	77
Er	141	178	117	213	304	178	172	361
Tm	31	39	27	46	69	38	39	76
Yb	243	334	228	389	588	310	330	600
Lu	58	76	55	90	138	73	81	137
Hf	11262	14015	12103	13354	13702	11604	10815	9747
Th	35	173	76	202	359	191	186	711
U	59	398	163	718	1168	299	334	918
La	0.22	0.31	0.05	16.64	0.46	0.10	354.22	0.40
Ce	35.63	77.38	53.18	61.95	98.90	50.24	438.31	145.35
Pr	1.24	1.25	0.81	19.00	1.23	2.31	311.47	3.89
Nd	5.42	3.86	2.50	20.48	3.02	8.38	266.36	12.95
Sm	27	21	14	34	24	44	188	65
Eu	11	7	7	20	13	27	60	43
Gd	99	90	60	123	144	143	193	251
Tb	175	185	125	245	301	254	264	466
Dy	317	365	242	466	603	441	417	858
Ho	524	604	409	779	1079	697	641	1389
Er	888	1120	739	1338	1914	1117	1081	2269
Tm	1268	1629	1118	1915	2837	1582	1595	3133
Yb	1495	2056	1406	2392	3621	1908	2033	3694
Lu	2369	3126	2271	3709	5695	2999	3329	5649
Hf	1082885	1347596	1163750	1284038	1317500	1115769	1039904	937163
Th	14	70	31	82	145	77	75	288
U	7339	49100	20126	88698	144136	36860	41191.36	113322
Th/U	0.6	0.4	0.5	0.3	0.3	0.6	0.6	0.8
Yb(n)/La(n)	6810	6594	29113	144	7904	18351	6	9228
Yb(n/Gd(n)	15.1	22.9	23.3	19.4	25.1	13.4	10.5	14.7
Eu/Eu*	0.2	0.2	0.2	0.3	0.2	0.3	0.3	0.3
Ce/Ce*	68.3	123.8	269.5	3.5	131.8	102.5	1.3	116.5
HfO_2 [wt%]	1.3	1.7	1.4	1.6	1.6	1.4	1.3	1.1
comment	inherited	inherited	inherited				rejected, inclusion	cycles 1-6
grain area	inh1	inh3	inh2	c1	rim	c1	rim	c2

L2-15

	SA04/15 - 4a	SA04/15 - 7b	SA04/15 - 9a	SA04/15 - 13a	SA04/15 - 13b	SA04/15 - 16a	SA04/15 - 16b	SA04/15 - 21a	SA04/15 - 21b	SA04/15 - 28a	SA04/15 - 16c	SA04/15 - 16d	SA04/15 - 29a (inh)	SA04/15 - 35a (inh)	SA04/15 - 32a (inh)	SA04/15 - 36a (inh)	SA04/15 - 33a (inh)
grain no.	4	7	9	13	13	16	16	21	21	28	16	16	29	35	32	36	33
Si	140230	140230	140230	140230	140230	140230	140230	140230	140230	140230	140230	140230	140230	140230	140230	140230	140230
P	651	282	388	1023	354	149	159	849	503	269	144	487	72	332	330	244	279
Ca	6	9	7	13	6	9	9	3	35	17	3	149	41	6	33	33	21
Ti	6	7	3	10	7	3	3	7	8	2	3	464	12	13	15	8	9
Y	1506	526	1040	1748	941	1721	1697	1322	1633	1687	1682	856	1626	767	1075	2260	1229
Nb	9	2	7	7	6	7	8	5	9	12	9	33	10	4	5	8	7
Zr	511380	504900	510500	513340	517670	515170	511110	533470	528290	518800	523730	535040	551590	537410	543130	515510	550860
Ba	0.1	0.1	0.1	0.2	0.1	0.1	0.0	0.1	0.2	0.7	0.1	10.8	0.5	0.1	-0.1	0.3	0.3
La	0.1	0.0	0.0	0.6	0.1	0.3	0.3	0.1	0.4	0.3	0.2	9.6	0.1	0.0	0.0	0.1	0.0
Ce	47.4	22.6	51.0	61.6	37.5	0.1	0.0	36.8	62.4	40.6	0.0	79.6	24.8	12.1	13.8	23.3	15.2
Pr	0.2	0.1	0.1	0.6	0.1	0.0	0.1	0.1	0.4	0.4	0.0	11.7	0.4	0.1	0.2	0.6	0.1
Nd	3.7	1.4	1.9	6.6	1.7	0.0	0.1	3.1	4.0	2.4		71.8	8.3	1.4	1.8	9.4	1.9
Sm	6.9	2.0	3.5	8.3	3.3	0.0		5.9	7.1	3.7	0.0	29.7	12.1	2.7	3.7	14.5	4.4
Eu	1.5	0.6	0.5	2.0	0.9	0.0	0.0	1.7	1.6	0.9	0.0	8.2	2.4	0.2	0.2	0.6	0.2
Gd	39	12	20	43	19	0	0	34	36	27	0	45	54	15	24	64	27
Tb	13	4	7	15	7	1	1	12	13	11	1	11	19	6	10	22	10
Dy	157	47	95	178	86	35	34	138	155	142	34	99	213	77	112	252	131
Ho	58	19	37	65	34	38	38	50	61	57	38	29	71	29	41	89	49
Er	269	89	180	300	167	434	431	242	301	289	428	144	304	139	197	396	236
Tm	54	20	40	64	37	169	168	53	65	68	169	39	57	30	40	75	49
Yb	415	162	321	505	306	2020	2026	416	532	569	2015	429	386	240	315	542	387
Lu	94	40	75	119	72	613	616	103	127	141	616	144	75	56	66	125	87
Hf	10920	9419	11867	9307	10130	17598	17416	9569	10308	14808	18867	17053	8577	12925	12002	9333	12927
Th	216	77	325	357	162	0	0	212	270	512	0	85	37	89	67	83	86
U	422	166	526	670	373	1440	1446	425	570	1561	1465	1179	92	242	124	149	225
La	0.23	0.12	0.11	2.57	0.27	1.13	1.11	0.31	1.86	1.15	1.00	40.88	0.26	0.10	0.21	0.23	0.15
Ce	78.64	37.43	84.60	102.04	62.15	0.15	-0.05	60.96	103.43	67.31	-0.01	131.95	41.18	19.98	22.92	38.67	25.23
Pr	2.11	0.79	1.27	7.23	1.32	0.46	0.59	1.50	3.98	4.00	0.44	131.57	4.44	0.83	1.96	7.18	1.50
Nd	8.28	2.99	4.19	14.69	3.69	0.04	0.18	6.78	8.79	5.28	0.00	158.70	18.24	3.01	3.94	20.87	4.29
Sm	47	14	24	56	22	0	0	40	48	25	0	202	82	19	25	99	30
Eu	26	10	8	35	17	1	0	30	29	16	1	146	43	4	4	10	3
Gd	196	59	102	221	95	2	2	171	181	140	1	227	275	74	122	325	138
Tb	349	108	207	420	187	16	18	325	359	290	18	304	518	156	278	606	288
Dy	648	192	389	735	355	145	139	569	641	583	138	408	878	316	461	1040	541
Ho	1039	334	664	1178	617	689	682	896	1104	1018	675	525	1276	513	743	1594	890
Er	1692	559	1131	1886	1053	2729	2712	1525	1893	1821	2691	905	1912	874	1238	2493	1486
Tm	2218	819	1655	2645	1529	6995	6955	2171	2671	2801	7000	1631	2362	1228	1654	3101	2037
Yb	2553	998	1978	3109	1886	12428	12470	2558	3272	3504	12401	2641	2378	1475	1937	3333	2381
Lu	3856	1637	3090	4893	2973	25223	25355	4248	5222	5820	25354	5912	3082	2313	2733	5150	3573
Hf	1050000	905625	1141058	894885	974038	1692115	1674615	920115	991154	1423846	1814135	1639712	824712	1242788	1154038	897375	1242981
Th	88	31	131	145	65	0	0	86	109	207	0	35	15	36	27	34	35
U	52047	20467	64981	82709	46042	177827	178506	52488	70428	192667	180840	145531	11416	29846	15360	18391	27719
Th/U	0.5	0.5	0.6	0.5	0.4	0.0	0.0	0.5	0.5	0.3	0.0	0.1	0.4	0.4	0.5	0.6	0.4
Yb(n)/La(n)	10942	8097	17351	1208	7088	11018	11249	8205	1757	3052	12362	65	9257	15206	9239	14376	15566
Yb(n/Gd(n)	13.0	16.8	19.4	14.1	19.7	5325.6	7180.5	15.0	18.1	25.1	12899.9	11.7	8.7	19.9	15.8	10.3	17.3
Eu/Eu*	0.3	0.4	0.2	0.3	0.4	1.1	#DIV/0!	0.4	0.3	0.3	1.1	0.7	0.3	0.1	0.1	0.1	0.0
Ce/Ce*	112.2	120.0	222.2	23.6	105.0	0.2	-0.1	89.0	38.0	31.4	0.0	1.8	38.6	70.3	35.8	30.0	52.6
HfO_2 [wt%]	1.3	1.1	1.4	1.1	1.2	2.1	2.1	1.1	1.2	1.7	2.2	2.0	1.0	1.5	1.4	1.1	1.5
comment						rejected, altered	rejected, altered			cycles 1-5	rejected, altered		inherited	inherited	inherited	inherited	inherited
grain area	c2	rim	c2	c1	rim	c1a	c1b	c1	c2	c1	c1c	rim	inh	inh	inh	inh	inh

			L1-06													L2-12								
	SA04/15 - 22a (inh)	SA04/15 - 27b	SA04/06 - 34.41	SA04/06 - 34.42	SA04/06 - 5.6	SA04/06 - 5.7	SA04/06 - 7.10	SA04/06 - 7.11	SA04/06 - 13.18	SA04/06 - 2.2	SA04/06 - 30.36	SA04/06 - 30.37	SA04/06 - 35.43	SA04/06 - 36.44	SA04/06 - 36.45	SA04/06 - 12.17	SA04/12 - 2.3	SA04/12 - 3.4	SA04/12 - 3.5	SA04/12 - 10.22	SA04/12 - 11.25	SA04/12 - 5.10	SA04/12 - 12.30	SA04/12 - 5.9	SA04/12 - 13.33
grain no.	22	27	34	34	5	5	7	7	13	2	30	30	35	36	36	12	2	3	3	10	11	5	12	5	13
Si	140230	140230	140230	140230	140230	140230	140230	140230	140230	140230	140230	140230	140230	140230	140230	140230	140230	140230	140230	140230	140230	140230	140230	140230	140230
P	296	335	145	215	869	573	1200	821	1127	892	1239	579	175	1006	744	1207	734	382	436	579	349	522	550	1286	887
Ca	30	14	30	24	13	44	3	6	18	3	5	15	6	17	164	9	2	2	1	33	1	2	35	12	15
Ti	4	2	6	8	13	5	3	4	14	2	3	4	6	4	8	3	5	5	6	8	8	4	12	5	11
Y	1766	1031	1224	808	5287	5422	3673	6100	5920	2105	2325	2393	676	1614	3154	2565	4248	2881	3392	2741	1261	2360	2612	2098	2657
Nb	3	6									14	31	1	8	50	17								8	18
Zr	580010	510690	551460	535700	522630	529080	543210	530640	532540	539260	530760	514420	522350	528650	535130	540490	536170	540350	540370	543340	544420	537520	539590	524900	506410
Ba	0.8	-0.1	4.0	2.4	3.1	13.6	0.1	0.1	1.1	0.1	0.3	1.3	0.2	1.4	66.8	0.3	0.1	0.1	-0.1	2.5	0.0	0.3	1.0	0.2	0.3
La	0.0	0.0	15.0	11.5	1.5	3.0	0.1	0.4	1.0	0.1	0.2	0.6	0.3	4.3	19.3	0.2	0.1	0.1	0.2	19.0	1.8	0.1	4.9	0.2	1.7
Ce	7.3	23.5	114.2	82.9	141.3	218.6	62.7	162.1	76.3	46.7	46.8	96.8	13.7	710.5	730.1	49.6	184.1	75.2	92.1	215.7	62.1	101.3	176.6	59.6	149.7
Pr	0.2	0.1	12.9	7.8	2.1	4.6	0.1	0.6	1.1	0.1	0.2	0.8	0.5	9.4	23.7	0.2	0.4	1.0	1.2	11.3	0.6	0.3	6.3	0.3	1.2
Nd	3.8	1.2	92.1	52.8	17.2	33.7	2.4	7.8	9.9	2.2	2.4	6.9	5.4	73.5	130.9	2.7	8.1	15.3	19.5	49.8	5.1	4.9	42.4	4.9	12.1
Sm	6.7	2.8	17.3	9.8	26.5	36.3	9.4	20.5	23.2	6.8	6.5	9.3	4.0	35.0	58.3	7.6	18.5	21.4	25.0	19.3	7.0	10.5	25.8	8.8	15.9
Eu	0.8	0.4	13.5	6.9	2.5	2.9	1.1	1.7	1.6	1.0	0.9	1.0	1.9	2.6	4.7	1.1	2.3	4.6	5.2	8.1	1.1	1.6	4.2	1.9	2.6
Gd	44	18	37	18	143	169	72	146	141	42	46	54	17	60	124	51	120	106	118	84	34	63	93	51	83
Tb	16	7	10	5	52	58	29	58	55	17	17	20	5	17	39	21	42	32	37	27	12	23	29	18	27
Dy	189	98	124	71	611	679	393	714	700	222	227	253	60	187	421	270	507	357	421	333	142	273	320	214	289
Ho	71	37	46	29	214	227	145	252	250	82	89	91	23	64	131	103	176	119	139	113	50	96	106	78	100
Er	337	189	239	165	973	1029	718	1178	1171	402	423	425	118	290	585	501	797	531	623	520	236	439	476	374	449
Tm	70	43	54	41	191	202	147	239	237	85	90	87	28	60	120	105	162	104	123	104	49	88	94	81	92
Yb	577	366	472	378	1381	1439	1125	1760	1719	660	701	678	265	472	898	859	1202	780	899	776	368	647	706	627	666
Lu	135	91	116	93	298	303	252	374	375	156	164	153	70	109	199	194	266	170	200	173	84	140	154	151	152
Hf	13635	13337	12988	14686	12764	14214	12963	14016	14010	12542	12771	12987	7383	11104	12736	13446	12090	10774	10637	12228	11253	12098	10954	9604	9800
Th	102	304	504	184	1904	1684	1267	3593	2362	477	550	735	182	317	857	760	1598	613	791	1183	437	1454	1546	478	1574
U	278	1088	645	637	3866	3731	3218	8198	5690	1489	1559	2073	258	755	2086	2259	3801	820	999	2291	753	2336	1846	872	1750
La	0.14	0.20	64.07	48.89	6.44	12.96	0.52	1.84	4.10	0.50	0.78	2.58	1.09	18.27	82.40	0.82	0.53	0.63	0.90	81.05	7.67	0.41	21.01	0.81	7.28
Ce	12.16	38.90	189.26	137.45	234.18	362.45	103.88	268.77	126.57	77.43	77.65	160.48	22.77	1177.90	1210.36	82.23	305.14	124.66	152.75	357.61	103.00	167.87	292.71	98.82	248.23
Pr	2.30	0.75	145.06	87.63	23.33	51.62	1.42	7.13	12.10	1.39	2.43	8.80	5.71	105.49	266.03	2.35	4.82	11.13	13.28	126.88	7.29	3.29	70.88	3.47	13.76
Nd	8.38	2.68	203.51	116.77	38.08	74.43	5.36	17.20	21.85	4.94	5.26	15.25	12.04	162.57	289.41	6.05	17.93	33.86	43.02	110.03	11.36	10.75	93.68	10.84	26.81
Sm	45	19	118	67	180	247	64	140	158	46	44	63	27	238	397	52	126	146	170	131	48	71	176	60	108
Eu	14	8	240	123	44	52	19	30	29	19	17	19	34	46	84	20	41	82	93	144	20	29	75	33	47
Gd	225	90	186	93	728	859	365	745	718	215	235	274	86	305	629	262	611	539	598	426	172	321	474	261	424
Tb	431	204	273	139	1441	1592	802	1589	1506	462	480	559	151	473	1066	574	1164	871	1008	752	331	639	800	483	738
Dy	779	404	512	291	2517	2798	1621	2941	2885	915	936	1044	247	771	1733	1111	2088	1472	1733	1373	585	1124	1319	880	1192
Ho	1278	665	832	527	3849	4086	2604	4524	4495	1476	1593	1635	407	1159	2353	1853	3157	2132	2497	2029	896	1728	1906	1404	1795
Er	2119	1190	1507	1041	6120	6476	4519	7415	7371	2533	2662	2675	744	1826	3679	3155	5016	3341	3922	3276	1487	2760	2993	2356	2823
Tm	2886	1773	2246	1706	7881	8342	6089	9864	9783	3495	3729	3601	1149	2496	4962	4331	6676	4314	5075	4283	2021	3637	3886	3330	3784
Yb	3548	2251	2906	2328	8499	8858	6924	10833	10579	4060	4313	4174	1631	2904	5529	5283	7396	4801	5532	4773	2267	3980	4347	3859	4097
Lu	5572	3761	4782	3840	12249	12466	10357	15392	15447	6413	6729	6282	2868	4501	8179	7979	10959	6980	8224	7127	3441	5772	6355	6228	6252
Hf	1311058	1282404	1248846	1412115	1227308	1366731	1246442	1347692	1347115	1205962	1227981	1248750	709933	1067692	1224615	1292885	1162500	1035962	1022788	1175769	1082019	1163269	1053269	923471	942279
Th	41	123	204	74	771	682	513	1454	956	193	223	298	74	128	347	308	647	248	320	479	177	589	626	194	637
U	34375	134370	79637	78591	477222	460568	397222	1012086	702494	183765	192457	255877	31900	93264	257506	278852	469222	101211	123356	282815	92969	288346	227889	107657	216037
Th/U	0.4	0.3	0.8	0.3	0.5	0.5	0.4	0.4	0.4	0.3	0.4	0.4	0.7	0.4	0.4	0.3	0.4	0.7	0.8	0.5	0.6	0.6	0.8	0.5	0.9
Yb(n)/La(n)	25314	11214	45	48	1320	683	13264	5897	2583	8155	5503	1615	1501	159	67	6460	14050	7635	6146	59	296	9652	207	4789	563
Yb(n/Gd(n)	15.8	25.0	15.6	24.9	11.7	10.3	19.0	14.5	14.7	18.9	18.3	15.2	19.0	9.5	8.8	20.2	12.1	8.9	9.2	11.2	13.2	12.4	9.2	14.8	9.7
Eu/Eu*	0.1	0.2	1.6	1.6	0.1	0.1	0.1	0.1	0.1	0.2	0.2	0.1	0.7	0.2	0.2	0.2	0.1	0.3	0.3	0.6	0.2	0.2	0.3	0.3	0.2
Ce/Ce*	21.4	100.0	2.0	2.1	19.1	14.0	120.5	74.3	18.0	93.0	56.3	33.7	9.1	26.8	8.2	59.4	191.5	47.1	44.2	3.5	13.8	144.2	7.6	59.1	24.8
HfO_2 [wt%]	1.6	1.6	1.5	1.7	1.5	1.7	1.5	1.7	1.7	1.5	1.5	1.5	0.9	1.3	1.5	1.6	1.4	1.3	1.3	1.4	1.3	1.4	1.3	1.1	1.2
comment	inherited, cycles 3-10		rejected, crack	rejected, crack								cycles 1-5		cycles 1-6	cycles 6-10										cycles 1-6
grain area	inh	c1	r2	r1	c1	c2	c1	c2	c1	c1	c1	c2	c2	c1	rim	c1	c2	c2a	c2b	c2	c2	c2	c1	c1	c2

					L3																
	SA04/12 - 14.35	SA04/12 - 15.37	SA04/12 - 15.38	SA04/12 - 11.26	SA04/05 - 21.40	SA04/05 - 21.41	SA04/05 - 14.27	SA04/05 - 9.16	SA04/05 - 9.17	SA04/05 - 25.49	SA04/05 - 25.50	SA04/05 - 18.34	SA04/05 - 18.35	SA04/05 - 28.56	SA04/05 - 10.18	SA04/05 - 4.7	SA04/05 - 5.9	SA04/05 - 11.21	SA04/05 - 11.22	SA04/05 - 24.48
grain no.	14	15	15	11	21	21	14	9	9	25	25	18	18	28	10	4	5	11	11	24
Si	140230	140230	140230	140230	140230	140230	140230	140230	140230	140230	140230	140230	140230	140230	140230	140230	140230	140230	140230	140230
P	446	1142	575	434	914	697	388	429	681	365	370	301	418	419	680	615	1643	659	612	179
Ca	17	8	16	24	9	13	6	4	2	2	1	1	2	1	1	2	12	3	11	4
Ti	20	4	4	7	7	6	11	9	6	8	8	7	11		5	7	3	9	6	14
Y	2704	1866	2030	1278	2457	1425	1824	1555	1421	1197	1795	2371	1482	2091	1433	1937	3185	1795	1896	238
Nb	17	8	17	5												5	18	9	12	0
Zr	545670	510790	517550	544530	551280	530840	550400	549390	557910	547050	555550	551730	550560	559620	562700	544150	528020	531060	536490	536200
Ba	0.3	0.2	0.2	0.1	1.4	1.3	0.5	0.4	0.1	0.2	0.0	0.0	0.2	0.2	0.1	0.0	0.4	0.0	0.8	0.1
La	5.1	0.1	0.8	0.2	3.0	13.5	4.0	0.7	0.1	0.1	0.1	0.1	0.1	0.3	0.1	0.5	1.1	0.4	0.6	0.0
Ce	118.3	47.5	77.4	57.9	98.8	173.5	79.4	82.4	40.5	58.9	73.4	63.0	63.0	83.1	41.2	49.7	64.9	94.9	93.3	8.6
Pr	4.8	0.2	0.3	0.4	1.9	7.3	1.7	0.7	0.2	0.3	0.2	0.9	0.4	0.5	0.2	0.7	0.9	0.4	0.8	0.0
Nd	34.7	3.1	3.7	4.8	14.0	34.6	13.5	7.6	3.5	4.7	4.6	15.1	5.3	5.3	4.0	9.3	6.6	6.3	8.7	0.4
Sm	31.6	6.5	7.3	7.2	14.0	15.7	11.7	9.7	6.3	6.3	8.5	18.3	9.4	9.2	6.5	11.2	9.4	9.9	10.0	0.9
Eu	4.6	1.2	1.1	1.7	3.1	2.5	2.4	2.4	1.8	1.4	1.6	4.5	2.4	2.7	1.8	3.1	1.0	2.4	2.0	0.3
Gd	101	40	51	36	68	40	47	47	36	35	42	88	41	51	37	58	66	51	53	5
Tb	31	15	18	12	23	13	15	16	13	11	14	27	15	19	13	18	25	17	18	2
Dy	337	190	212	142	278	154	187	184	158	137	185	301	176	235	162	211	320	198	210	22
Ho	110	71	78	50	99	56	72	64	58	50	70	100	60	86	60	75	123	71	76	9
Er	473	343	362	227	470	268	368	292	284	230	359	456	293	414	290	333	579	316	344	42
Tm	94	73	75	49	98	57	79	59	61	48	77	89	58	84	62	69	123	65	71	9
Yb	702	573	568	373	791	450	645	451	490	362	624	686	443	651	496	540	955	499	547	76
Lu	153	136	134	88	179	104	151	103	112	82	145	149	95	147	114	123	215	109	124	20
Hf	11348	10217	11494	11241	10972	11034	10647	11177	10930	11123	11131	10982	10683	10516	11110	10356	12209	10299	11407	9514
Th	531	363	484	432	798	275	336	940	275	483	357	477	710	540	281	325	736	1334	718	21
U	725	931	1394	661	1439	778	708	1077	595	699	771	648	778	696	609	509	2295	1308	1195	49
La	21.76	0.52	3.27	0.73	12.79	57.52	16.97	2.96	0.31	0.28	0.28	0.51	0.51	1.46	0.31	2.04	4.90	1.59	2.52	0.10
Ce	196.10	78.79	128.32	95.91	163.78	287.67	131.59	136.62	67.20	97.70	121.61	104.41	104.45	137.69	68.24	82.34	107.66	157.31	154.64	14.31
Pr	54.32	1.88	3.20	4.08	21.75	82.40	19.14	7.77	1.77	2.82	2.62	10.62	4.10	5.13	1.77	8.18	10.40	4.58	9.33	0.34
Nd	76.63	6.96	8.12	10.57	30.93	76.49	29.87	16.73	7.64	10.49	10.10	33.39	11.63	11.67	8.79	20.52	14.62	13.99	19.22	0.90
Sm	215	44	50	49	95	107	80	66	43	43	58	124	64	62	44	76	64	68	68	6
Eu	83	21	19	30	55	44	43	42	32	25	29	80	43	48	33	56	18	43	36	5
Gd	515	204	259	183	344	205	238	238	181	179	214	446	210	261	186	294	336	259	272	27
Tb	841	421	497	336	631	357	421	442	360	310	385	737	418	524	364	509	690	470	496	49
Dy	1388	782	874	585	1146	635	769	758	650	565	763	1240	723	968	667	869	1320	818	866	90
Ho	1978	1276	1401	898	1783	1008	1303	1158	1052	891	1260	1792	1075	1539	1073	1348	2209	1280	1367	159
Er	2974	2158	2276	1426	2958	1686	2317	1839	1787	1445	2261	2867	1844	2606	1826	2099	3645	1986	2164	263
Tm	3890	3007	3099	2014	4066	2351	3276	2448	2520	1980	3173	3689	2399	3455	2572	2861	5067	2685	2949	379
Yb	4320	3527	3493	2297	4866	2772	3968	2774	3014	2230	3837	4219	2724	4006	3055	3321	5879	3071	3368	468
Lu	6307	5603	5498	3640	7349	4279	6221	4244	4609	3388	5982	6127	3928	6060	4682	5056	8841	4503	5085	804
Hf	1091154	982404	1105192	1080865	1055000	1060962	1023750	1074712	1050962	1069519	1070288	1055962	1027212	1011154	1068269	995769	1173942	990288	1096827	914846
Th	215	147	196	175	323	111	136	380	111	195	144	193	288	219	114	132	298	540	291	8
U	89553	114983	172111	81602	177642	96043	87380	132951	73505	86252	95185	79944	96109	85873	75167	62793	283321	161531	147531	6051
Th/U	0.7	0.4	0.3	0.7	0.6	0.4	0.5	0.9	0.5	0.7	0.5	0.7	0.9	0.8	0.5	0.6	0.3	1.0	0.6	0.4
Yb(n)/La(n)	199	6765	1069	3133	380	48	234	937	9668	8058	13487	8258	5316	2747	9851	1626	1201	1926	1339	4776
Yb(n/Gd(n)	8.4	17.3	13.5	12.6	14.2	13.5	16.7	11.7	16.7	12.5	17.9	9.4	13.0	15.3	16.4	11.3	17.5	11.9	12.4	17.5
Eu/Eu*	0.2	0.2	0.2	0.3	0.3	0.3	0.3	0.3	0.4	0.3	0.3	0.3	0.4	0.4	0.4	0.4	0.1	0.3	0.3	0.4
Ce/Ce*	5.7	79.6	39.7	55.5	9.8	4.2	7.3	28.5	90.5	110.6	141.0	44.8	72.1	50.3	92.1	20.1	15.1	58.2	31.9	78.4
HfO_2 [wt%]	1.3	1.2	1.4	1.3	1.3	1.3	1.3	1.3	1.3	1.3	1.3	1.3	1.3	1.2	1.3	1.2	1.4	1.2	1.3	1.1
comment																cycles 5-10				
grain area	c1	c1	c2	c2	c2	rim	rim	c2a	c2b	c2b	c2a	c2a	c2b	rim	c1	c1+c2	c1	c2a	c2b	rim

	Standards								
	Sl1-oct06-2	91500-oct06-2	91500-oct06-3	91500-oct06-4	91500-oct06-5	91500-oct06-6	91500 oct06-7	91500 oct06-8	91500 oct06-9
grain no.									
Si	140230	140230	140230	140230	140230	140230	140230	140230	140230
P	262.16	28.843	25.951	23	21.612	25.393	26.663	24.668	39.04
Ca	3	10	9	5	7	7	8	6	11
Ti	5	5	5	4	4	5	5	4	4
Y	1619	131	140	142	141	143	141	144	137
Nb			1	1	1	1	1	1	2
Zr	515150	520500	528980	536840	545560	547760	536070	538050	522670
Ba	0	0	0	0	0	0	0	0	0
La	0	0	0	0	0	0	0	0	0
Ce	26.6	3	3.1	3.4	3.2	2.9	3.3	3.1	2.9
Pr	0.3	0	0.0	0.0	0.0	0.0	0.0	0.0	0.0
Nd	5.6	0	0.3	0.3	0.2	0.2	0.4	0.3	0.3
Sm	9.4	0	0.4	0.3	0.5	0.4	0.4	0.5	0.5
Eu	0.3	0	0.3	0.2	0.2	0.3	0.2	0.2	0.2
Gd	37.4	2	2.0	2.7	2.4	2.7	2.2	2.4	2.3
Tb	11.7	1	1.0	0.9	0.9	0.9	1.0	1.0	0.9
Dy	136	12	12	12	13	13	12	12	11
Ho	50	5	5	5	5	5	5	5	5
Er	258	27	28	30	29	28	28	28	27
Tm	59	7	7	7	7	7	7	8	7
Yb	514	61	65	68	69	66	65	65	62
Lu	121	15	16	17	16	17	16	17	15
Hf	18270	6273	6473	6812	6944	6962	6659	6869	6302
Th	981	25	28	30	29	29	29	30	26
U	2963	79	85	91	92	93	91	94	79
La	0.12	0.12	0.05	0.05	0.03	0.05	0.06	0.03	12.53
Ce	44.02	5.43	5.16	5.58	5.25	4.87	5.45	5.17	0.02
Pr	3.53	0.20	0.34	0.30	0.15	0.06	0.29	0.23	2.99
Nd	12.45	0.49	0.72	0.71	0.46	0.54	0.81	0.58	1.01
Sm	64	3	2	2	3	3	3	3	1
Eu	6	4	4	3	4	5	4	4	41
Gd	190	11	10	14	12	14	11	12	5
Tb	323	23	27	26	26	25	28	27	307
Dy	559.2089	48.57437	48	50	52	52	49	51	19
Ho	907	86	87	94	92	91	89	95	489
Er	1623	168	179	189	184	178	177	179	43
Tm	2445	284	299	303	287	309	306	315	2555
Yb	3160.185	378.2892	397	419	425	405	402	403	91
Lu	4987.243	615.3498	657	687	674	686	668	709	259325
Hf	1756731	603173	622365	655010	667673	669375	640240	660490	2469
Th	397.3	10.0	11.4	12.2	11.9	11.9	11.9	12.0	32.0
U	365851.85	9740.74	10481.48	11246.91	11417.65	11423.46	11210.49	11665.93	11665.93
Th/U	0.3	0.3	0.3	0.3	0.3	0.3	0.3	0.3	0.3
Yb(n)/La(n)	26852	3208	8504	7664	12240	8188	6541	14697	7
Yb(n/Gd(n)	16.6	35.1	39.2	30.5	34.7	30.0	36.1	33.4	20.0
Eu/Eu*	0.1	0.7	0.9	0.6	0.7	0.8	0.7	0.6	15.9
Ce/Ce*	68.3	35.8	41.1	43.5	72.3	87.2	41.0	65.5	0.0
HfO_2 [wt%]	2.2	0.7	0.8	0.8	0.8	0.8	0.8	0.8	0.7
comment									
grain area									

Appendix 2e
Zircon oxygen isotope data of the Etive pluton and average values of bracketing zircon standard 91500

	analyses no.	grain no.	$^{18}O/^{16}O$ (measured)	2SD	1 s.e.m.	$^{18}O/^{16}O$ (drift corrected)	$\delta^{18}O$ [‰] VSMOW	2SD	1 s.e.m.	n	grain area	comment
	Session 2 (24.04.2006)											
	91500/1 - 31-40		0.0020128	0.0000015	0.0000002		9.77	0.7	0.112	10		
	91500/1 - 41-45, 47-50		0.0020121	0.0000018	0.0000003		9.47	0.9	0.142	9		
	91500/2 - 1-10		0.0020133	0.0000012	0.0000002		10.04	0.6	0.094	10		
	91500/2 - 11-20		0.0020131	0.0000017	0.0000003		9.93	0.8	0.128	10		
	91500/2 - 21-30		0.0020134	0.0000018	0.0000003		10.11	0.8	0.131	10		
	91500/1 - 51-60		0.0020128	0.0000011	0.0000002		9.82	0.5	0.084	10		
MO	**SA05-20_1a**	1	0.0020019		0.0000004		4.4		0.080		c2a	rejected, scratch
	SA05-20_2a	2	0.0020022		0.0000002		4.5		0.044		c1	rejected, crack
	91500/1 - 61, 63-70		0.0020129	0.0000021	0.0000003		9.85	1.0	0.153	9		
	Session 3 (25.04.2006)											
	91500/14 - 52-61		0.0020157	0.0000007	0.0000001		9.74	0.4	0.055	10		
	91500/1 - 1-10		0.0020162	0.0000014	0.0000002		9.98	0.7	0.109	10		
St-01	**SA05/01 - 1a**	1	0.0020087		0.0000002		6.3		0.051		c1	rejected, crack
	SA05/01 - 2a	2	0.0020108		0.0000001		7.3		0.042		c2	rejected, grain altered
	SA05/01 - 2b	2	0.0020129		0.0000002		8.3		0.078		c2+rim	rejected, crack
	SA05/01 - 3a	3	0.0020100		0.0000002		6.9		0.085		c2	rejected, crack
	SA05/01 - 4a	4	0.0020111		0.0000003		7.4		0.112		c1	
	SA05/01 - 6a	6	0.0020102		0.0000002		7.0		0.060		c2a	
	SA05/01 - 5b	5	0.0020110		0.0000001		7.4		0.054		c1	
	SA05/01 - 5c	5	0.0020108		0.0000003		7.3		0.110		rim	
	SA05/01 - 7a	7	0.0020106		0.0000003		7.2		0.091		c2	
	SA05/01 - 8a	8	0.0020104		0.0000002		7.1		0.078		c1	
	Session 4 (25.04.2006)											
	91500/1 - 11-15, 17-20		0.0020170	0.0000007	0.0000001		9.91	0.4	0.061	9		
	SA05/01 - 8b	8	0.0020094		0.0000002		6.1		0.072		c2	rejected, crack
	SA05/01 - 9a	9	0.0020111		0.0000003		7.0		0.106		c1	
	SA05/01 - 11a	11	0.0020102		0.0000002		6.6		0.058		c2	rejected, crack
	SA05/01 - 11c	11	0.0020101		0.0000002		6.5		0.052		rim	
	SA05/01 - 12a	12	0.0020113		0.0000003		7.1		0.100		c2	
	SA05/01 - 13a	13	0.0020110		0.0000002		6.9		0.072		c2	
	SA05/01 - 13b	13	0.0020098		0.0000002		6.3		0.071		rim	
	SA05/01 - 14a	14	0.0020111		0.0000003		7.0		0.101		rim	
	SA05/01 - 15a	15	0.0020104		0.0000001		6.6		0.040		r1	
	SA05/01 - 15b	15	0.0020119		0.0000003		7.4		0.113		r2	rejected, crack
	91500/1 - 21b, 22, 24-30		0.0020169	0.0000007	0.0000001		9.88	0.4	0.060	9		
	SA05/01 - 16a	16	0.0020104		0.0000002		6.63		0.068		c2	rejected, correction on position of secondary ion beam anomalously large
	SA05/01 - 17a	17	0.0020102		0.0000002		6.5		0.054		c2	rejected, crack
	SA05/01 - 18a	18	0.0020104		0.0000002		6.7		0.071		c2a	
	SA05/01 - 18b	18	0.0020103		0.0000003		6.6		0.086		c2b	
	SA05/01 - 19c	19	0.0020102		0.0000002		6.6		0.081		c1	rejected, crack
	SA05/01 - 19b	19	0.0020101		0.0000001		6.5		0.040		rim	
	SA05/01 - 20a	20	0.0020113		0.0000002		7.1		0.060		c2	
St-05	**SA05/05 - 1a**	1	0.0020100		0.0000002		6.4		0.053		c1	
	SA05/05 - 2a	2	0.0020112		0.0000002		7.1		0.081		rim	
	SA05/05 - 3b	3	0.0020104		0.0000003		6.6		0.095		rim	
	SA05/05 - 4a	4	0.0020116		0.0000002		7.2		0.072		c2	
	SA05/05 - 4b	4	0.0020072		0.0000004		5.0		0.089		rim	rejected, grain altered
	SA05/05 - 5a	5	0.0020111		0.0000003		7.0		0.121		rim	rejected, crack
	SA05/05 - 6a	6	0.0020102		0.0000003		6.5		0.099		rim	
	SA05/05 - 7a	7	0.0020107		0.0000002		6.8		0.056		rim	
	SA05/05 - 8a	8	0.0020101		0.0000002		6.5		0.070		c1	rejected, crack
	SA05/05 - 9a	9	0.0020109		0.0000003		6.9		0.112		c2	
	SA05/05 - 10a	10	0.0020113		0.0000001		7.1		0.043		c2	
	SA05/05 - 10b	10	0.0020112		0.0000002		7.0		0.080		rim	
	SA05/05 - 11a	11	0.0020192		0.0000003		11.0		0.144		c2a	analytical problem
	91500/1 - 36-40		0.0020165	0.0000005	0.0000001		9.67	0.3	0.059	5		
	91500/1 - 41-45		0.0020170	0.0000008	0.0000002		9.92	0.4	0.089	5		
	SA05/05 - 11b	11	0.0020113		0.0000003		7.1		0.107		rim	
	SA05/05 - 11c	11	0.0020126		0.0000002		7.7		0.090		c2b	
	SA05/05 - 12a	12	0.0020101		0.0000003		6.5		0.088		c2	rejected, crack
	SA05/05 - 13a	13	0.0020107		0.0000002		6.8		0.071		c2a	
	SA05/05 - 13b	13	0.0020112		0.0000001		7.1		0.040		c2b	rejected, crack
	SA05/05 - 14c	14	0.0020114		0.0000003		7.1		0.104		r1a	
	SA05/05 - 14b	14	0.0020104		0.0000002		6.7		0.074		r1b	
	SA05/05 - 15a	15	0.0020110		0.0000002		6.9		0.081		c1	rejected, crack
	SA05/05 - 15b	15	0.0020114		0.0000002		7.2		0.071		rim	
	SA05/05 - 16a	16	0.0020099		0.0000003		6.4		0.090		c2	
	SA05/05 - 23a	23	0.0020106		0.0000002		6.8		0.067		c2	
	SA05/05 - 17a	17	0.0020106		0.0000001		6.7		0.030		rim	
	SA05/05 - 18a	18	0.0020105		0.0000003		6.7		0.104		c1	
	SA05/05 - 18b	18	0.0020103		0.0000003		6.6		0.094		c2	
	SA05/05 - 19a	19	0.0020106		0.0000003		6.8		0.094		c1	
	SA05/05 - 19b	19	0.0020104		0.0000002		6.7		0.053		c2	
	SA05/05 - 20a	20	0.0020112		0.0000003		7.1		0.091		rim	

Appendix 2e
Zircon oxygen isotope data of the Etive pluton and average values of bracketing zircon standard 91500

	analyses no.	grain no.	$^{18}O/^{16}O$ (measured)	2SD	1 s.e.m.	$^{18}O/^{16}O$ (drift corrected)	$\delta^{18}O$ [‰] VSMOW	2SD	1 s.e.m.	n	grain area	comment
	Session 5 (25.04.2006)											
	91500/1 - 46-50		0.0020157	0.0000009	0.0000002		9.86	0.4	0.100	5		
	SA05/05 - 21a	21	0.0019430		0.0000012		-26.3		-1.643		c2a	instrument failure
	SA05/05 - 21b	21	0.0019749		0.0000007		-10.5		-0.382		c2b	instrument failure
	SA05/05 - 22a	22	0.0019254		0.0000007		-35.1		-1.188		rim	instrument failure
	Session 6 (12.06.2006)											
	Mount4/91500 - 1-3, 5-10		0.0020222	0.0000008	0.0000001	0.0020222	9.85	0.395	0.066	9		
Cr-15	**SA05/15 - 2a**	2	0.0020148		0.0000003		6.2		0.098		c1	
	SA05/15 - 3a	3	0.0020153		0.0000003		6.4		0.101		c2	
	SA05/15 - 3b	3	0.0020152		0.0000002		6.3		0.065		c1	
	SA05/15 - 4a	4	0.0020164		0.0000002		7.0		0.061		inh1	inherited
	SA05/15 - 4b	4	0.0020140		0.0000002		5.8		0.046		rim	
	SA05/15 - 4c	4	0.0020165		0.0000005		7.0		0.159		inh2	inherited
	SA05/15 - 8a	8	0.0020143		0.0000004		5.9		0.107		inh1	inherited
	SA05/15 - 8b	8	0.0020153		0.0000003		6.4		0.080		rim	rejected, crack
	SA05/15 - 9a	9	0.0020131				5.3				c2	rejected, > 20 %
					0.0000002				0.051			discordant
	SA05/15 - 11a	11	0.0020151		0.0000005		6.3		0.166		c2a	
	Mount4/91500 - 12-15		0.0020225	0.0000006	0.0000001	0.0020223	9.93	0.3	0.069	4		
	SA05/15 - 11b	11	0.0020156		0.0000003		6.5		0.113		c2b	
	SA05/15 - 15a	15	0.0020149		0.0000004		6.2		0.130		c2a	
	SA05/15 - 15b	15	0.0020133		0.0000002		5.4		0.041		c2b	rejected, crack
	SA05/15 - 19a	19	0.0020163		0.0000005		6.9		0.157		c1	
	SA05/15 - 19b	19	0.0020153		0.0000003		6.4		0.095		c2	
	SA05/15 - 22a	22	0.0020161		0.0000006		6.8		0.201		c1	
	SA05/15 - 22b	22	0.0020148		0.0000003		6.1		0.099		c2	
	SA05/15 - 25a	25	0.0020152		0.0000003		6.3		0.099		c1	rejected, crack
	SA05/15 - 25b	25	0.0020140		0.0000003		5.7		0.088		c2	
	SA05/15 - 26a	26	0.0020144		0.0000004		5.9		0.127		c1	
	Mount4/91500 - 16-20		0.0020223	0.0000007	0.0000002	0.0020224	9.79	0.4	0.079	5		
	SA05/15 - 26b	26	0.0020141		0.0000005		5.7		0.129		c2	rejected, correction on position of secondary ion beam anomalously large
	SA05/15 - 29a	29	0.0020133		0.0000004		5.3		0.096		c2	
	SA05/15 - 29b	29	0.0020142		0.0000004		5.8		0.108		rim	
	SA05/15 - 1a	1	0.0020149		0.0000004		6.1		0.127		c1	rejected, correction on position of secondary ion beam anomalously large
	SA05/15 - 5a	5	0.0020151		0.0000003		6.2		0.108		c1	rejected, crack
	SA05/15 - 5b	5	0.0020149		0.0000005		6.1		0.144		rim	
Cr-26	**SA05/26 - 1b**	1	0.0020145		0.0000002		5.9		0.064		rim	rejected, > 20 % discordant
	SA05/26 - 1a	1	0.0020152		0.0000003		6.3		0.078		c1+rim	
	SA05/26 - 2a	2	0.0020151		0.0000002		6.2		0.056		c1	
	SA05/26 - 2b	2	0.0020147		0.0000002		6.0		0.067		rim	
	Mount4/91500 - 21-25		0.0020227	0.0000009	0.0000002	0.0020225	9.94	0.5	0.103	5		
	SA05/26 - 3a	3	0.0020146		0.0000005		5.9		0.135		c2a	rejected, > 20 % discordant
	SA05/26 - 3b	3	0.0020145		0.0000003		5.9		0.089		c2b	
	SA05/26 - 5a	5	0.0020139		0.0000005		5.6		0.138		c1	
	SA05/26 - 6a	6	0.0020149		0.0000004		6.1		0.127		c1	
	SA05/26 - 6b	6	0.0020157		0.0000004		6.5		0.117		c2	
	SA05/26 - 7a	7	0.0020164		0.0000006		6.8		0.200		c2a	
	SA05/26 - 7b	7	0.0020162		0.0000002		6.7		0.071		c2b	
	SA05/26 - 8a	8	0.0020150		0.0000004		6.1		0.134		c2	
	SA05/26 - 8b	8	0.0020135		0.0000005		5.4		0.141		rim	rejected, correction on position of secondary ion beam anomalously large
	SA05/26 - 10a	10	0.0020147		0.0000003		6.0		0.101		c2	rejected, crack
	Mount4/91500 - 27, 28, 30		0.0020224	0.0000001	0.0000000	0.0020226	9.79	0.1	0.017	3		
	Session 7 (12.06.2006)											
	Mount4/91500 - 31-35		0.0020231	0.0000008	0.0000002		9.89	0.4	0.089	5		
	SA05/26 - 11b.2	11	0.0020168		0.0000002		6.8		0.063		c2b	
	SA05/26 - 11b	11	NaN									analytical problem
	SA05/26 - 11a	11	0.0020163		0.0000003		6.5		0.110		c2a	
	SA05/26 - 12a	12	0.0020185		0.0000003		7.6		0.108		c2b	
	SA05/26 - 12b	12	0.0020156		0.0000003		6.2		0.097		c2c	rejected, correction on position of secondary ion beam anomalously large
	SA05/26 - 12c	12	0.0020181		0.0000002		7.4		0.090		c2a	rejected, correction on position of secondary ion beam anomalously large
	SA05/26 - 13a	13	0.0020174		0.0000004		7.1		0.132		c1	rejected, crack
	SA05/26 - 13b	13	0.0020153		0.0000002		6.0		0.054		c2	
	SA05/26 - 14a	14	0.0020161		0.0000003		6.4		0.104		c1	
	SA05/26 - 14b	14	0.0020158		0.0000004		6.3		0.115		c2	
	Mount4/91500 - 36-40		0.0020231	0.0000007	0.0000002		9.90	0.3	0.075	5		
	SA05/26 - 15b	15	0.0020171		0.0000004		6.9		0.151		r1a	rejected, correction on position of secondary ion beam anomalously large
	SA05/26 - 15c	15	0.0020161		0.0000002		6.4		0.056		r1b	rejected, correction on position of secondary ion beam anomalously large
	SA05/26 - 15a	15	0.0020149		0.0000002		5.8		0.054		c1	rejected, crack

Appendix 2e

Zircon oxygen isotope data of the Etive pluton and average values of bracketing zircon standard 91500

	analyses no.	grain no.	$^{18}O/^{16}O$ (measured)	2SD	1 s.e.m.	$^{18}O/^{16}O$ (drift corrected)	$\delta^{18}O$ [‰] VSMOW	2SD	1 s.e.m.	n	grain area	comment
	SA05/26 - 16a	16	0.0020176		0.0000003		7.2		0.102		c2	
	SA05/26 - 16b	16	0.0020164		0.0000003		6.6		0.113		rim	
	SA05/26 - 17a	17	0.0020156		0.0000003		6.2		0.079		rim	
	SA05/26 - 17b	17	0.0020154		0.0000004		6.1		0.131		c2	rejected, crack
	SA05/26 - 19a	19	0.0020166		0.0000002		6.7		0.067		c1	rejected, crack
	SA05/26 - 19b	19	0.0020145		0.0000003		5.7		0.087		c2	rejected, crack
	SA05/26 - 20a	20	0.0020114		0.0000002		4.1		0.046		c1b	rejected, correction on position of secondary ion beam anomalously large
	Mount4/91500 - 46-47, 49-50		0.0020230	0.0000006	0.0000002		9.70	0.6	0.157	4		
	SA05/26 - 20c	20	0.0020153		0.0000002		6.0		0.065		c1a	
	SA05/26 - 20b	20	0.0020163		0.0000003		6.5		0.091		rim	
	SA05/26 - 21a	21	0.0020157		0.0000002		6.2		0.074		c2a	
	SA05/26 - 21b	21	0.0020162		0.0000003		6.5		0.104		c2b	
	SA05/26 - 23a	23	0.0020155		0.0000003		6.1		0.102		c1	rejected, crack
	SA05/26 - 25a	25	0.0020160		0.0000004		6.4		0.130		rim	
	SA05/26 - 27a	27	0.0020163		0.0000002		6.5		0.069		c2	
	SA05/26 - 27b	27	0.0020138		0.0000003		5.3		0.091		r1a	
	SA05/26 - 27c	27	0.0020144		0.0000004		5.6		0.110		r1b	rejected, crack
Q-23	**SA05/23 - 22a**	22	0.0020166		0.0000004		6.7		0.139		c1	
	SA05/23 - 22b	22	0.0020144		0.0000003		5.6		0.082		c2b	rejected, crack
	SA05/23 - 21a	21	0.0020157		0.0000004		6.2		0.115		c2	
	SA05/23 - 20a	20	0.0020164		0.0000002		6.6		0.057		c2a	rejected, crack
	SA05/23 - 20b	20	0.0020139		0.0000002		5.4		0.058		c2b	rejected, correction on position of secondary ion beam anomalously large
	SA05/23 - 19a	19	0.0020160		0.0000004		6.4		0.119		c1	rejected, crack
	Mount4/91500 - 56-60		0.0020231	0.0000005	0.0000001		9.88	0.2	0.051	5		
	SA05/23 - 19b	19	0.0020110		0.0000003		3.9		0.060		c2	rejected, correction on position of secondary ion beam anomalously large
	SA05/23 - 18a	18	0.0020157		0.0000003		6.2		0.105		c2	
	SA05/23 - 17a	17	0.0020166		0.0000002		6.7		0.076		c1a	rejected, correction on position of secondary ion beam anomalously large
	SA05/23 - 17b	17	0.0020149		0.0000004		5.8		0.107		c1b	rejected, grain altered
	SA05/23 - 16a	16	0.0020177		0.0000002		7.2		0.074		c2a	
	SA05/23 - 16b	16	0.0020166		0.0000005		6.7		0.167		c2b	
	SA05/23 - 15a	15	0.0020150		0.0000003		5.9		0.078		c1	
	SA05/23 - 14a	14	0.0020132		0.0000004		5.0		0.089		c1b	rejected, crack
	SA05/23 - 13a	13	0.0020170		0.0000002		6.9		0.082		c1	rejected, inclusion
	SA05/23 - 14c	14	0.0020144		0.0000003		5.6		0.091		c1a	rejected, crack
	Mount4/91500 - 61-65		0.0020231	0.0000010	0.0000002		9.87	0.5	0.106	5		
	SA05/23 - 12a	12	0.0020137		0.0000004		5.3		0.096		c1b	rejected, correction on position of secondary ion beam anomalously large
	SA05/23 - 12b	12	0.0020169		0.0000002		6.8		0.083		c1a	
	SA05/23 - 11a	11	0.0020155		0.0000005		6.1		0.161		c2	
	SA05/23 - 10a	10	0.0020149		0.0000003		5.8		0.088		c2b	
	SA05/23 - 10b	10	0.0020162		0.0000004		6.5		0.126		c2a	
	SA05/23 - 9a	9	0.0020152		0.0000002		6.0		0.059		c2	
	SA05/23 - 8a	8	0.0020154		0.0000004		6.1		0.134		c2	
	SA05/23 - 7a	7	0.0020166		0.0000001		6.7		0.048		c1	
	SA05/23 - 6a	6	0.0020143		0.0000002		5.5		0.054		c2a	
	SA05/23 - 5a	5	0.0020156		0.0000004		6.2		0.123		c2	
	Mount4/91500 - 66-67, 69-70		0.0020228	0.0000003	0.0000001		9.55	0.7	0.170	4		
	Session 8 (13.06.2006)											
	Mount4/91500 - 81-84, 86-90		0.0020207	0.0000006	0.0000001		9.76	0.3	0.046	9		
	SA05/23 - 6b	6	0.0020127		0.0000003		5.8		0.053		c2b	rejected, correction on position of secondary ion beam anomalously large
	SA05/23 - 2a	2	0.0020134		0.0000003		6.2		0.090		c2	rejected, crack
	SA05/23 - 1a	1	0.0020129		0.0000003		5.9		0.093		c1	
	SA05/23 - 23a	23	0.0020138		0.0000003		6.4		0.070		c1	rejected, correction on position of secondary ion beam anomalously large
									0.083			
	Mount4/91500 - 91-95		0.0020211	0.0000006	0.0000001		9.98	0.3	0.115	5		
Q-25	**SA05/25 - 1a**	1	0.0020133		0.0000004		6.1		0.114		c2a	rejected, crack
	SA05/25 - 1b	1	0.0020098		0.0000003		4.4		0.059		c2b	rejected, crack
	SA05/25 - 2a	2	0.0020108		0.0000004		4.9		0.090		c2	rejected, crack
	SA05/25 - 3a	3	0.0020103		0.0000002		4.6		0.056		c2	rejected, correction on position of secondary ion beam anomalously large
	SA05/25 - 4a	4	0.0020129		0.0000005		5.9		0.150		c2	
	SA05/25 - 6a	6	0.0020142		0.0000003		6.5		0.093		c2	
	SA05/25 - 7a	7	0.0020111		0.0000002		5.0		0.052		c2	rejected, crack
	SA05/25 - 8a	8	0.0020117		0.0000003		5.3		0.071		c2	rejected, crack
	SA05/25 - 9a	9	0.0020123		0.0000002		5.6		0.044		c1	
	SA05/25 - 10a	10	0.0020109		0.0000005		4.9		0.134		c2b	
	Mount4/91500 - 96-100		0.0020209	0.0000010	0.0000002		9.90	0.5	0.107	5		
	SA05/25 - 11a	11	0.0020147		0.0000004		6.8		0.125		c2	
	SA05/25 - 12a	12	0.0020121		0.0000005		5.5		0.131		c2	rejected, crack
	SA05/25 - 14a	14	0.0020134		0.0000003		6.2		0.084		c2	rejected, crack
	SA05/25 - 15a	15	0.0020110		0.0000004		5.0		0.106			
	SA05/25 - 16a	16	0.0020133		0.0000004		6.1		0.116		c2	

Appendix 2e
Zircon oxygen isotope data of the Etive pluton and average values of bracketing zircon standard 91500

	analyses no.	grain no.	$^{18}O/^{16}O$ (measured)	2SD	1 s.e.m.	$^{18}O/^{16}O$ (drift corrected)	$\delta^{18}O$ [‰] VSMOW	2SD	1 s.e.m.	n	grain area	comment
	SA05/25 - 17a	17	0.0020110		0.0000005		5.0		0.135		c2	rejected, correction on position of secondary ion beam anomalously large
	SA05/25 - 18b	18	0.0020129		0.0000003		5.9		0.097		c2	rejected, crack
	SA05/25 - 19b	19	0.0020126		0.0000005		5.8		0.151		c2	rejected, crack
	SA05/25 - 20c	20	0.0020130		0.0000004		5.9		0.116		c2	rejected, correction on position of secondary ion beam anomalously large
	SA05/25 - 21a	21	0.0020113		0.0000003		5.1		0.086		c2a	rejected, crack
	Mount4/91500 - 106-110		0.0020209	0.0000004	0.0000001		9.87	0.2	0.039	5		
	SA05/25 - 21b	21	0.0020136		0.0000004		6.3		0.120		c2b	rejected, correction on position of secondary ion beam anomalously large
	SA05/25 - 22a	22	0.0020138		0.0000004		6.4		0.122		c2	rejected, correction on position of secondary ion beam anomalously large
	SA05/25 - 23a	23	0.0020120		0.0000004		5.5		0.096		c2	rejected, crack
	SA05/25 - 24a	24	0.0020159		0.0000002		7.4		0.063		c2a	rejected, crack
	SA05/25 - 24b	24	0.0020149		0.0000004		6.9		0.138		c2b	
	SA05/25 - 25a	25	0.0020136		0.0000004		6.3		0.112		c2	
	Session 9 (13.06.2006)											
	Mount4/91500 - 111-115		0.0020203	0.0000008	0.0000002		9.82	0.4	0.088	5		
	Mount3/91500 - 1-5, 7-9		0.0020204	0.0000013	0.0000002		9.84	0.7	0.117	8		
Cr-11	**SA05/11 - 1a**	1	0.0020136		0.0000002		6.5		0.060		c1	
	SA05/11 - 1b	1	0.0020120		0.0000004		5.7		0.113		rim	
	SA05/11 - 3a	3	0.0020136		0.0000003		6.5		0.092		c1	
	SA05/11 - 3b	3	0.0020123		0.0000002		5.8		0.059		rim	
	SA05/11 - 2a	2	0.0020134		0.0000004		6.4		0.117		c1	
	SA05/11 - 2b	2	0.0020106		0.0000004		5.0		0.109		c2	rejected, correction on position of secondary ion beam anomalously large
	SA05/11 - 6a	6	0.0020140		0.0000004		6.7		0.128		c2	rejected, correction on position of secondary ion beam anomalously large
	SA05/11 - 8a	8	0.0020161		0.0000003		7.7		0.133		c2a	
	SA05/11 - 8b	8	0.0020126		0.0000003		6.0		0.102		c2b	
	SA05/11 - 9b	9	0.0020147		0.0000003		7.0		0.093		rim	
	Mount3/91500 - 16-20		0.0020206	0.0000009	0.0000002		9.93	0.4	0.098	5		
	SA05/11 - 5a	5	0.0020143		0.0000003		6.8		0.100		c2	
	SA05/11 - 5b	5	0.0020146		0.0000006		7.0		0.202		rim	
	SA05/11 - 7a	7	0.0020148		0.0000004		7.1		0.137		c1	
	SA05/11 - 7b	7	0.0020136		0.0000003		6.5		0.102		c2	
	SA05/11 - 9a	9	0.0020157		0.0000003		7.5		0.121		c1	
	SA05/11 - 10a	10	0.0020155		0.0000002		7.4		0.066		c2a	rejected, scratch
	SA05/11 - 10b	10	0.0020139		0.0000005		6.6		0.165		c2b	
	SA05/11 - 11a	11	0.0020087		0.0000003		4.1		0.069		c1b	rejected, correction on position of secondary ion beam anomalously large
	SA05/11 - 11b	11	0.0020933		0.0000323		45.9		70.902		r1a	rejected, crack
	SA05/11 - 14a	14	0.0020155		0.0000003		7.4		0.107		c2a	rejected, correction on position of secondary ion beam anomalously large
	Mount3/91500 - 23-25		0.0020205	0.0000003	0.0000001		9.89	0.1	0.033	3		
	SA05/11 - 14c	14	0.0020105		0.0000002		4.9		0.044		c2b	rejected, correction on position of secondary ion beam anomalously large
	SA05/11 - 11c	11	0.0020097		0.0000003		4.6		0.067		c1a	rejected, crack
	SA05/11 - 11d	11	0.0020360		0.0000009		17.6		0.761		r1b	rejected, crack
	SA05/11 - 17a	17	0.0020142		0.0000003		6.8		0.096		c2a	rejected, crack
	SA05/11 - 17b	17	0.0020153		0.0000004		7.3		0.136		c2b	
	SA05/11 - 20a	20	0.0020164		0.0000004		7.9		0.173		c2a	
	SA05/11 - 20b	20	0.0020161		0.0000002		7.7		0.079		c2b	
	SA05/11 - 20c	20	0.0020158		0.0000003		7.6		0.113		c2c	
	SA05/11 - 20d	20	0.0020163		0.0000004		7.8		0.142		c2d	
	SA05/11 - 23a	23	0.0020147		0.0000002		7.0		0.054		c2	
	Mount3/91500 - 26-30		0.0020205	0.0000008	0.0000002		9.89	0.4	0.093	5		
	SA05/11 - 21a	21	0.0020095		0.0000005		4.5		0.100		c2a	rejected, correction on position of secondary ion beam anomalously large
	SA05/11 - 21c	21	0.0020141		0.0000004		6.8		0.144		c2c	rejected, correction on position of secondary ion beam anomalously large
	SA05/11 - 21b	21	0.0020080		0.0000003		3.7		0.050		c2d	rejected, correction on position of secondary ion beam anomalously large
	SA05/11 - 21d	21	0.0020074		0.0000003		3.4		0.051		c2b	rejected, crack
	SA05/11 - 24a	24	0.0020050		0.0000003		2.2		0.036		c2a	rejected, crack
	SA05/11 - 17c	17	0.0020160		0.0000003		7.7		0.108		c2c	rejected, correction on position of secondary ion beam anomalously large
					0.0000006				0.131			rejected, correction on position of
Cr-17	**SA05/17 - 3a**	3	0.0020100				4.7				c2c	secondary ion beam anomalously large

Appendix 2e

Zircon oxygen isotope data of the Etive pluton and average values of bracketing zircon standard 91500

	analyses no.	grain no.	$^{18}O/^{16}O$ (measured)	2SD	1 s.e.m.	$^{18}O/^{16}O$ (drift corrected)	$\delta^{18}O$ [‰] VSMOW	2SD	1 s.e.m.	n	grain area	comment
	SA05/17 - 3b	3	0.0020104		0.0000004		4.9		0.100		c2a	
	SA05/17 - 4a	4	0.0020106		0.0000005		5.0		0.129		c1a	
	SA05/17 - 4b	4	0.0020122		0.0000004		5.8		0.109		c1b	
	Mount3/91500 - 31-33, 35		0.0020203	0.0000002	0.0000001		9.81	0.1	0.031	4		
	SA05/17 - 5a	5	0.0020113		0.0000002		5.4		0.062		c2a	rejected, crack
	SA05/17 - 5b	5	0.0020123		0.0000005		5.8		0.151		c2b	
	SA05/17 - 6a	6	0.0020129		0.0000004		6.2		0.120		inh	inherited
	SA05/17 - 6b	6	0.0020100		0.0000004		4.7		0.085		r1a	
	SA05/17 - 7a	7	0.0020118		0.0000004		5.6		0.110		c2a	rejected, > 20 % discordant
	SA05/17 - 7b	7	0.0020144		0.0000006		6.9		0.217		c2b	
	SA05/17 - 7c	7	0.0020121		0.0000006		5.8		0.159		rim	
	SA05/17 - 8a	8	0.0020097		0.0000005		4.6		0.103		c2a	
	SA05/17 - 8c	8	0.0020097		0.0000005		4.6		0.111		c2c	
	SA05/17 - 10a	10	0.0020120		0.0000004		5.7		0.114		c1b	
	Session 10 (14.06.2006)											
	Mount2/91500 - 1-4, 6-9		0.0020210	0.0000010	0.0000002	0.0020214	9.64	0.4	0.075	9		
	Mount2/91500 - 11-20		0.0020221	0.0000011	0.0000002	0.0020216	10.12	0.5	0.084	10		
St-06	**SA05/06 - 1a**	1	0.0020146		0.0000002		6.4		0.065		c1	
	SA05/06 - 1b	1	0.0020150		0.0000002		6.6		0.077		rim	
	SA05/06 - 2a	2	0.0020132		0.0000003		5.6		0.073		c1	rejected, crack
	SA05/06 - 3a	3	0.0020156		0.0000002		6.8		0.076		c1	rejected, correction on position of secondary ion beam anomalously large
	SA05/06 - 4a	4	0.0020153		0.0000003		6.7		0.094		c1	rejected, crack
	SA05/06 - 5a	5	0.0020149		0.0000003		6.5		0.082		c1	rejected, crack
	SA05/06 - 5b	5	0.0020158		0.0000002		6.9		0.079		c2	
	SA05/06 - 6a	6	0.0020161		0.0000002		7.0		0.068		c2	
	SA05/06 - 7a	7	0.0020158		0.0000003		6.9		0.108		rim	
	SA05/06 - 8a	8	0.0020145		0.0000003		6.2		0.088		c2a	rejected, crack
	Mount2/91500 - 21-25		0.0020218	0.0000010	0.0000002	0.0020219	9.82	0.5	0.108	5		
	SA05/06 - 8b	8	0.0020138		0.0000003		5.8		0.073		c2b	rejected, correction on position of secondary ion beam anomalously large
	SA05/06 - 9a	9	0.0020158		0.0000001		6.8		0.048		c1	
	SA05/06 - 10a	10	0.0020146		0.0000003		6.2		0.080		c2	rejected, crack
	SA05/06 - 11a	11	0.0020151		0.0000003		6.5		0.082		c1	
	SA05/06 - 11c	11	0.0020131		0.0000003		5.4		0.086		c2	rejected, crack
	SA05/06 - 12a	12	0.0020136		0.0000003		5.7		0.075		c2	rejected, crack
	SA05/06 - 13b	13	0.0020101		0.0000003		3.9		0.063		c2	rejected, correction on position of secondary ion beam anomalously large
	SA05/06 - 14a	14	0.0020158		0.0000003		6.8		0.112		c2a	rejected, correction on position of secondary ion beam anomalously large
	SA05/06 - 14b	14	0.0020143		0.0000003		6.0		0.081		c2b	
	SA05/06 - 15a	15	0.0020146		0.0000003		6.1		0.099		c2a	
	Mount2/91500 - 26-30		0.0020224	0.0000008	0.0000002	0.0020222	9.96	0.4	0.089	5		
	SA05/06 - 15b	15	0.0020147		0.0000003		6.1		0.103		c2b	
	SA05/06 - 16a	16	0.0020151		0.0000002		6.3		0.071		r1a	
	SA05/06 - 16b	16	0.0020152		0.0000003		6.3		0.106		r1b	rejected, crack
	SA05/06 - 17a	17	0.0020144		0.0000003		5.9		0.078		c1	
	SA05/06 - 18a	18	0.0020139		0.0000003		5.7		0.082		r1a	rejected, correction on position of secondary ion beam anomalously large
	SA05/06 - 18b	18	0.0020138		0.0000002		5.6		0.056		r1b	
	SA05/06 - 18c	18	0.0020156		0.0000002		6.5		0.080		r2	
	SA05/06 - 19a	19	0.0020130		0.0000002		5.2		0.049		c2	rejected, correction on position of secondary ion beam anomalously large
	SA05/06 - 19b	19	0.0020155		0.0000002		6.5		0.060		rim	rejected, correction on position of secondary ion beam anomalously large
	SA05/06 - 20a	20	0.0020116		0.0000003		4.5		0.060		c1	rejected, crack
	Mount2/91500 - 31-34		0.0020223	0.0000011	0.0000003	0.0020225	9.78	0.5	0.137	4		
	SA05/06 - 20b	20	0.0020110		0.0000001		4.1		0.026		rim	rejected, crack
	SA05/06 - 21a	21	0.0020131		0.0000001		5.2		0.036		c1	rejected, crack
	SA05/06 - 21b	21	0.0020132		0.0000001		5.2		0.033		rim	rejected, crack
	Mount2/91500 - 36-40		0.0020227	0.0000008	0.0000002	0.0020226	9.89	0.4	0.085	5		
	Mount3/91500 - 41-50		0.0020227	0.0000009	0.0000001	0.0020228	9.78	0.5	0.074	10		
Cr-17	**SA05/17 - 10b**	10	0.0020165		0.0000002		6.7		0.062		c1c	
	SA05/17 - 12a	12	0.0020170		0.0000001		6.9		0.033		r1a	
	SA05/17 - 12b	12	0.0020173		0.0000003		7.0		0.094		r1b	rejected, crack
	SA05/17 - 10c	10	0.0020153		0.0000002		6.1		0.063		c1a	
	SA05/17 - 13a	13	0.0020165		0.0000002		6.6		0.061		c2	
	SA05/17 - 14a	14	0.0020162		0.0000002		6.5		0.069		c1a	
	SA05/17 - 14b	14	0.0020185		0.0000002		7.6		0.070		c2a	
	SA05/17 - 17a	17	0.0020169		0.0000002		6.8		0.057		c1	
	SA05/17 - 17b	17	0.0020178		0.0000002		7.2		0.055		c2	
	SA05/17 - 19a	19	0.0020151		0.0000002		5.9		0.064		r1a	
	Mount3/91500 - 51-55		0.0020235	0.0000008	0.0000002	0.0020232	10.02	0.4	0.086	5		
	SA05/17 - 19c	19	0.0020151		0.0000003		5.9		0.075		r1b	rejected, correction on position of secondary ion beam anomalously large
	SA05/17 - 20a	20	0.0020185		0.0000003		7.5		0.107		c1	
	SA05/17 - 24a	24	0.0020160		0.0000003		6.2		0.096		c2	

Appendix 2e
Zircon oxygen isotope data of the Etive pluton and average values of bracketing zircon standard 91500

	analyses no.	grain no.	$^{18}O/^{16}O$ (measured)	2SD	1 s.e.m.	$^{18}O/^{16}O$ (drift corrected)	$\delta^{18}O$ [‰] VSMOW	2SD	1 s.e.m.	n	grain area	comment
	SA05/17 - 24b	24	0.0020156		0.0000001		6.1		0.030		rim	
	SA05/17 - 3c	3	0.0020157		0.0000004		6.1		0.107		c2b	rejected, crack
	SA05/17 - 4c	4	0.0020154		0.0000002		5.9		0.069		c1c	
	SA05/17 - 6c	6	0.0020186		0.0000002		7.5		0.073		r1a	
	Session 11 (19.06.2006)											
	91500/12 - 11-20		0.0020166	0.0000008	0.0000001		9.86	0.4	0.064	10		
	91500/12 - 31-40		0.0020166	0.0000009	0.0000001		9.83	0.4	0.071	10		
	Mount1/91500 - 1-9		0.0020168	0.0000015	0.0000002		9.93	0.7	0.120	9		
MO	**SA05/20 - 2b**	2	0.0020083		0.0000003		5.7		0.077		c2	
	SA05/20 - 3a	3	0.0020107		0.0000003		6.9		0.100		c2	
	SA05/20 - 3b	3	-0.0012666		0.0000152		-1618.2				rim	analytical problem
	SA05/20 - 4a	4	-0.0010095		0.0000129		-1490.7				c2a	analytical problem
	SA05/20 - 4c	4	0.0020123		0.0000005		7.1		0.174		c2b	rejected, correction on position of secondary ion beam anomalously large
	SA05/20 - 5a	5	0.0020141		0.0000004		8.0		0.148		c2a	rejected, correction on position of secondary ion beam anomalously large
	SA05/20 - 6a	6	0.0020115		0.0000004		6.6		0.141		c2	
	SA05/20 - 6b	6	0.0020104		0.0000003		6.1		0.093		rim	
	SA05/20 - 7a	7	0.0020137		0.0000003		7.7		0.117		c2	
	SA05/20 - 8a	8	0.0020106		0.0000004		6.2		0.133		c2a	
	SA05/20 - 8b	8	0.0020103		0.0000003		6.1		0.101		c2b	
	SA05/20 - 9a	9	0.0020099		0.0000006		5.8		0.169		c1	
	SA05/20 - 9b	9	0.0020091		0.0000004		5.5		0.110		c2	
	SA05/20 - 10a	10	0.0020098		0.0000004		5.8		0.120		c1	rejected, crack
	Mount1/91500 - 20-21, 23-25		0.0020166	0.0000006	0.0000001		9.83	0.3	0.064	5		
	SA05/20 - 10b	10	0.0020093		0.0000003		6.2		0.103		c2b	
	SA05/20 - 11a	11	0.0020093		0.0000005		6.2		0.165		c1	
	SA05/20 - 11b	11	0.0020128		0.0000005		7.9		0.196		c2	rejected, crack
	SA05/20 - 12a	12	0.0020096		0.0000004		6.3		0.140		r1a	rejected, correction on position of secondary ion beam anomalously large
	SA05/20 - 12b	12	0.0020090		0.0000005		6.1		0.155		r1b	
	SA05/20 - 13a	13	0.0020107		0.0000003		6.9		0.092		rim	
	SA05/20 - 14a	14	0.0020133		0.0000003		8.2		0.107		c2b	
	SA05/20 - 15a	15	0.0020106		0.0000005		6.9		0.171		c2a	

Appendix 2e
Zircon oxygen isotope data of the Etive pluton and average values of bracketing zircon standard 91500

	analyses no.	grain no.	$^{18}O/^{16}O$ (measured)	2SD	1 s.e.m.	$^{18}O/^{16}O$ (drift corrected)	$\delta^{18}O$ [‰] VSMOW	2SD	1 s.e.m.	n	grain area	comment
	SA05/20 - 14b	14	0.0020089		0.0000003		6.0		0.092		c2a	rejected, correction on position of secondary ion beam anomalously large
	SA05/20 - 15b	15	0.0020102		0.0000004		6.6		0.128		c2b	
	Mount1/91500 - 26-30		0.0020166	0.0000019	0.0000004		9.83	0.9	0.206	5		
	SA05/20 - 16a	16	0.0020100		0.0000005		6.6		0.159		r1a	rejected, correction on position of secondary ion beam anomalously large
	SA05/20 - 16b	16	0.0020100		0.0000004		6.6		0.126		r1b	rejected, correction on position of secondary ion beam anomalously large
	SA05/20 - 17a	17	0.0020090		0.0000006		6.1		0.189		c1	rejected, correction on position of secondary ion beam anomalously large
	SA05/20 - 17b	17	0.0020084		0.0000004		5.8		0.106		c2	rejected, correction on position of secondary ion beam anomalously large
	SA05/20 - 18a	18	0.0020069		0.0000004		5.0		0.092		c1	rejected, crack
	SA05/20 - 18b	18	0.0020081		0.0000005		5.6		0.135		c2	
	SA05/20 - 19a	19	0.0020099		0.0000004		6.5		0.143		c2a	
	SA05/20 - 19b	19	0.0020085		0.0000004		5.8		0.112		rim	
	Session 12 (19.06.2006)											
	Mount1/91500 - 26-30		0.0020155	0.0000013	0.0000003		9.86	0.6	0.145	5		
	Session 13 (15.11.2006)											
	Mount1/91500 - 1-10		0.0020195	0.0000006	0.0000001	0.0020197	9.76	0.3	0.052	10		
	Mount1/91500 - 11-20		0.0020195	0.0000004	0.0000001	0.0020195	9.86	0.2	0.035	10		
	Mount1/91500 - 21-25, 27-30		0.0020195	0.0000007	0.0000001	0.0020190	10.11	0.4	0.060	9		
	SA05/20 - 17a.2	17	0.0020124		0.0000013		6.8		0.451		c1	
	SA05/20 - 17b.2	17	0.0020119		0.0000004		6.6		0.132		c2	
	Mount1/91500 - 31-35		0.0020181	0.0000015	0.0000003	0.0020185	9.64	0.8	0.168	5		
	Mount1/91500 - 36-39		0.0020185	0.0000006	0.0000002	0.0020184	9.88	0.3	0.073	4		
	SA05/20 - 14b.2	14	0.0020128		0.0000002		7.1		0.078		c2a	
	SA05/20 - 14a.2	14	0.0020122		0.0000002		6.8		0.068		c2b	
	SA05/20 - 12a.2	12	0.0020138		0.0000007		7.6		0.267		r1a	rejected, crack
	SA05/20 - 12b.2	12	0.0020122		0.0000011		6.9		0.367		r1b	
	SA05/20 - 10c	10	0.0020116		0.0000005		6.6		0.166		c2a	
	SA05/20 - 5a.2	5	0.0020114		0.0000012		6.5		0.386		c2a	
	SA05/20 - 5c	5	0.0020122		0.0000009		6.9		0.293		c2b	
	SA05/20 - 4c.2	4	0.0020130		0.0000011		7.3		0.403		c2b	
	SA05/20 - 4a.2	4	0.0020113		0.0000006		6.5		0.208		c2a	
	SA05/20 - 1c	1	0.0020107		0.0000006		6.2		0.170			
	Mount1/91500 - 42-45		0.0020179	0.0000008	0.0000002	0.0020181	9.80	0.4	0.101	4		
	Session 14 (15.11.2006)											
	Mount3/91500 - 46-49		0.0020176	0.0000005	0.0000001		9.78	0.3	0.065	4		
	91500 - 0-4		0.0020177	0.0000002	0.0000001		9.85	0.1	0.028	4		
Cr-17	**SA05/17 - 3d**	3	0.0020077		0.0000014		4.9		0.352		c2d	rejected, crack
	SA05/17 - 3b	3	0.0020110		0.0000004		6.5		0.114		c2a	
	SA05/17 - 4d	4	0.0020117		0.0000003		6.9		0.089		c1b	
	SA05/17 - 4e	4	0.0020096		0.0000003		5.8		0.095		c2b	rejected, crack
	SA05/17 - 6c	6	0.0020115		0.0000003		6.8		0.115		r1a	
	SA05/17 - 6d	6	0.0020109		0.0000002		6.5		0.057		r1c	
	SA05/17 - 10a	10	0.0020114		0.0000007		6.7		0.242		c1b	
	SA05/17 - 10c	10	0.0020123		0.0000029		7.2		1.026		c1a	
	SA05/17 - 10b	10	0.0020105		0.0000032		6.3		0.997		c1c	
	SA05/17 - 14d	14	0.0020116		0.0000003		6.8		0.087		c1b	rejected, crack
	Mount3/91500 - 51-55		0.0020178	0.0000006	0.0000001		9.91	0.3	0.062	5		
	SA05/17 - 14e	14	0.0020114		0.0000002		6.7		0.051		c2b	
	SA05/17 - 14f	14	0.0020118		0.0000002		6.9		0.080		c2c	
Cr-11	**SA05/11 - 10a**	10	0.0020120		0.0000004		7.0		0.145		c2a	
	SA05/11 - 10b	10	0.0020108		0.0000003		6.4		0.108		c2b	
	SA05/11 - 11a	11	0.0020122		0.0000002		7.1		0.088		c1b	
	SA05/11 - 11b	11	0.0020110		0.0000006		6.5		0.205		r1a	
	SA05/11 - 11e	11	0.0020120		0.0000004		7.0		0.151		c1c	
	SA05/11 - 11d	11	0.0020128		0.0000013		7.4		0.483		r1b	
	SA05/11 - 17a	17	0.0020123		0.0000016		7.2		0.587		c2a	rejected, crack
	SA05/11 - 17b	17	0.0020135		0.0000002		7.7		0.095		c2b	rejected, crack
	SA05/11 - 21a	21	0.0020102		0.0000003		6.2		0.089		c2a	rejected, correction on position of secondary ion beam anomalously large
	SA05/11 - 21c	21	0.0020097		0.0000003		5.9		0.083		c2c	rejected, correction on position of secondary ion beam anomalously large
	SA05/11 - 21d	21	0.0020104		0.0000005		6.2		0.141		c2b	rejected, correction on position of secondary ion beam anomalously large
	SA05/11 - 24a	24	0.0020127		0.0000003		7.4		0.102		c2a	rejected, crack
	SA05/11 - 24b	24	0.0020112		0.0000003		6.6		0.089		c2b	rejected, grain altered
	Mount3/91500 - 56-60		0.0020178	0.0000005	0.0000001		9.88	0.2	0.051	5		

Appendix 2f

Zircon U-Pb data of the Etive pluton

sample	analysis no.	grain no.	U ppm	Th ppm	Pb ppm	Th/U	^{204}Pb ppb	f206 (%)	^{204}Pb/^{206}Pb	corrected ratios									Ages (Ma)								grain area	comment
										^{207}Pb/^{206}Pb	1σ	^{208}Pb/^{206}Pb	1σ	^{207}Pb/^{235}U	1σ	^{206}Pb/^{238}U	1σ	ρ	^{206}Pb/^{238}U	1σ	^{207}Pb/^{235}U	1σ	^{207}Pb/^{206}Pb	1σ	% disc		
St-01	SA05/01 - 1a	1	232	225	18	0.99	0.4	0.06	0.0000322	0.0551	0.0008	0.2995	0.0056	0.4906	0.0083	0.0646	0.0006	0.55	404	4	405	6	414	30	2	c1	
	SA05/01 - 3a	3	257	134	18	0.54	0.2	0.03	0.0000171	0.0563	0.0007	0.1668	0.0050	0.5035	0.0078	0.0649	0.0006	0.55	405	3	414	5	463	28	12	c2	rejected, crack
	SA05/01 - 2a	2	214	93	21	0.45	0.4	0.04	0.0000214	0.0584	0.0004	0.1384	0.0010	0.7572	0.0081	0.0940	0.0008	0.80	579	5	572	5	544	12	-6	c2	rejected, crack
	SA05/01 - 6a	6	350	449	30	1.32	0.9	0.08	0.0000447	0.0535	0.0005	0.4070	0.0032	0.4917	0.0122	0.0666	0.0015	0.91	416	9	406	8	351	21	-18	c2a	rejected, > 10 % discordant
	SA05/01 - 5b	5	250	111	17	0.46	1.2	0.16	0.0000834	0.0540	0.0008	0.1393	0.0022	0.4900	0.0134	0.0658	0.0015	0.84	411	9	405	9	369	29	-11	c1	rejected, > 10 % discordant
	SA05/01 - 5c	5	1193	499	79	0.43	0.5	0.01	0.0000074	0.0551	0.0003	0.1362	0.0006	0.4869	0.0108	0.0641	0.0014	0.97	400	8	403	7	416	12	4	rim	rejected, > 1000 ppm U
	SA05/01 - 21a	21	301	132	19	0.45	0.1	0.01	0.0000076	0.0552	0.0006	0.1398	0.0012	0.4689	0.0111	0.0616	0.0013	0.91	385	8	390	8	420	22	8	c1	rejected, crack
	SA05/01 - 19c	19	4711	5870	426	1.28	1.6	0.01	0.0000055	0.0548	0.0001	0.4024	0.0028	0.5465	0.0117	0.0723	0.0015	1.00	450	9	443	8	406	4	-11	c1	rejected, > 1000 ppm U
	SA05/01 - 19b	19	221	91	15	0.43	0.2	0.02	0.0000131	0.0543	0.0006	0.1333	0.0009	0.4969	0.0121	0.0663	0.0015	0.90	414	9	410	8	384	23	-8	rim	
	SA05/01 - 18a	18	284	124	20	0.45	0.0	0.00	0.0000000	0.0545	0.0004	0.1409	0.0007	0.5029	0.0118	0.0669	0.0015	0.94	418	9	414	8	391	18	-7	c2a	
	SA05/01 - 18b	18	175	76	12	0.44	0.4	0.08	0.0000414	0.0558	0.0007	0.1400	0.0016	0.4986	0.0124	0.0648	0.0014	0.88	405	9	411	8	444	24	9	c2b	
	SA05/01 - 11a	11	266	212	20	0.82	0.4	0.05	0.0000272	0.0538	0.0005	0.2539	0.0015	0.4850	0.0064	0.0654	0.0006	0.65	409	3	402	4	360	21	-14	c2	rejected, > 10 % discordant
	SA05/01 - 9a	9	307	113	20	0.38	0.6	0.06	0.0000341	0.0551	0.0005	0.1160	0.0012	0.4981	0.0059	0.0656	0.0005	0.69	410	3	410	4	415	17	1	c1	
St-05	SA05/05 - 1a	1	107	61	8	0.59	0.0	0.00	0.0000002	0.0551	0.0007	0.1874	0.0030	0.5144	0.0084	0.0677	0.0007	0.66	422	4	421	6	416	27	-2	c1	rejected, crack
	SA05/05 - 4a	4	181	102	13	0.58	0.0	0.00	0.0000001	0.0545	0.0005	0.1842	0.0012	0.4913	0.0057	0.0654	0.0005	0.68	408	3	406	4	391	19	-4	c2	
	SA05/05 - 4b	4	3855	1518	279	0.40	132.5	1.04	0.0005630	0.0544	0.0002	0.1228	0.0029	0.5304	0.0048	0.0707	0.0006	0.87	440	3	432	3	387	7	-14	rim	rejected, > 10 % discordant
	SA05/05 - 6a	6	207	102	15	0.51	0.1	0.02	0.0000081	0.0549	0.0005	0.1575	0.0010	0.5097	0.0064	0.0674	0.0005	0.64	420	3	418	4	407	21	-3	rim	rejected, crack
	SA05/05 - 6b	6	314	200	23	0.65	0.7	0.07	0.0000381	0.0545	0.0005	0.2012	0.0012	0.5026	0.0063	0.0670	0.0006	0.69	418	3	413	4	389	19	-7	c1	
	SA05/05 - 8a	8	215	123	15	0.59	0.3	0.05	0.0000246	0.0546	0.0006	0.1837	0.0059	0.5002	0.0071	0.0664	0.0006	0.65	414	4	412	5	396	23	-5	c1	
	SA05/05 - 24a	24	291	156	20	0.55	0.1	0.01	0.0000059	0.0545	0.0004	0.1724	0.0031	0.4948	0.0057	0.0659	0.0006	0.79	411	4	408	4	391	15	-5	c1	
	SA05/05 - 14c	14	134	47	9	0.36	0.1	0.03	0.0000136	0.0555	0.0005	0.1150	0.0014	0.5203	0.0067	0.0680	0.0006	0.66	424	3	425	4	431	20	2	r1a	rejected, crack
	SA05/05 - 18b	18	250	132	17	0.54	0.0	0.00	0.0000001	0.0551	0.0007	0.1731	0.0012	0.4886	0.0073	0.0644	0.0005	0.57	402	3	404	5	414	27	3	c2a	
	SA05/05 - 18c	18	170	69	11	0.41	0.1	0.02	0.0000107	0.0542	0.0006	0.1285	0.0012	0.4910	0.0076	0.0657	0.0007	0.64	410	4	406	5	379	26	-8	c2a	
	SA05/05 - 22c	22	1627	2745	153	1.73	26.1	0.50	0.0002702	0.0549	0.0003	0.5437	0.0023	0.5180	0.0051	0.0684	0.0006	0.83	427	3	424	3	407	9	-5	c2b	rejected, high common Pb
	SA05/05 - 22a	22	121	66	8	0.56	0.0	0.00	0.0000001	0.0547	0.0006	0.1810	0.0015	0.4833	0.0069	0.0641	0.0005	0.58	400	3	400	5	399	26	0	rim	
	SA05/05 - 19a	19	95	56	7	0.61	0.2	0.06	0.0000312	0.0543	0.0007	0.1916	0.0019	0.4828	0.0078	0.0645	0.0006	0.56	403	3	400	5	383	27	-5	c1	
St-06	SA05/06 - 20a	20	91	76	7	0.85	0.7	0.25	0.0001319	0.0527	0.0010	0.2615	0.0032	0.4649	0.0096	0.0640	0.0006	0.44	400	4	388	7	316	30	-27	c1	rejected, > 10 % discordant
	SA05/06 - 19a	19	183	91	12	0.51	0.0	0.00	0.0000001	0.0550	0.0003	0.1617	0.0008	0.4930	0.0049	0.0650	0.0005	0.82	406	3	407	3	411	13	1	c2	
	SA05/06 - 18c	18	150	148	12	1.01	0.4	0.09	0.0000507	0.0551	0.0007	0.3209	0.0021	0.4935	0.0075	0.0649	0.0006	0.62	405	4	407	5	417	24	3	r2	
	SA05/06 - 17a	17	203	108	14	0.55	0.5	0.08	0.0000434	0.0541	0.0007	0.1741	0.0015	0.4813	0.0074	0.0646	0.0005	0.52	403	3	399	5	373	27	-8	c1	
	SA05/06 - 16a	16	201	150	15	0.76	0.2	0.03	0.0000147	0.0543	0.0005	0.2408	0.0012	0.4881	0.0061	0.0652	0.0005	0.64	407	3	404	4	383	21	-6	r1a	
	SA05/06 - 21a	21	1955	2964	174	1.56	131.9	2.12	0.0011590	0.0532	0.0012	0.4893	0.0058	0.4915	0.0124	0.0670	0.0006	0.37	418	4	406	8	335	66	-25	c1	rejected, high common Pb
	SA05/06 - 9a	9	160	75	11	0.48	0.1	0.02	0.0000086	0.0541	0.0007	0.1502	0.0013	0.4933	0.0087	0.0661	0.0008	0.69	413	5	407	6	375	28	-10	c1	rejected, > 10 % discordant
	SA05/06 - 5a	5	184	87	13	0.48	0.6	0.11	0.0000596	0.0542	0.0006	0.1516	0.0046	0.4886	0.0076	0.0654	0.0007	0.68	408	4	404	5	378	22	-8	c1	
	SA05/06 - 3a	3	242	116	17	0.49	0.4	0.06	0.0000322	0.0541	0.0005	0.1563	0.0015	0.4900	0.0061	0.0657	0.0006	0.67	410	3	405	4	373	19	-10	c1	
	SA05/06 - 1a	1	182	146	13	0.82	0.5	0.10	0.0000517	0.0542	0.0006	0.2574	0.0022	0.4858	0.0074	0.0650	0.0007	0.67	406	4	402	5	380	22	-7	c1	
Cr-11	SA05/11 - 1b	1	149	158	12	1.09	0.5	0.12	0.0000622	0.0545	0.0009	0.3369	0.0020	0.5017	0.0100	0.0668	0.0008	0.61	417	5	413	7	390	31	-7	rim	
	SA05/11 - 2b	2	117	130	10	1.14	0.7	0.19	0.0001039	0.0557	0.0009	0.3522	0.0031	0.5104	0.0097	0.0664	0.0006	0.44	415	3	419	6	441	30	6	c2	
	SA05/11 - 4a	4	106	118	9	1.14	1.4	0.42	0.0002267	0.0528	0.0012	0.3484	0.0046	0.4904	0.0117	0.0673	0.0006	0.36	420	4	405	8	321	34	-31	c2	rejected, > 10 % discordant
	SA05/11 - 5a	5	211	200	17	0.97	0.0	0.00	0.0000001	0.0561	0.0007	0.3041	0.0027	0.5450	0.0262	0.0704	0.0033	0.97	439	20	442	17	457	28	4	c2	
	SA05/11 - 7a	7	94	68	7	0.74	0.9	0.30	0.0001631	0.0559	0.0016	0.2208	0.0046	0.5122	0.0161	0.0664	0.0009	0.42	415	5	420	11	449	45	8	c1	
	SA05/11 - 8a	8	137	164	12	1.23	0.2	0.05	0.0000253	0.0558	0.0010	0.3772	0.0034	0.5192	0.0104	0.0675	0.0007	0.49	421	4	425	7	444	35	5	c2a	
	SA05/11 - 25a	25	113	134	10	1.22	0.7	0.19	0.0001009	0.0546	0.0012	0.3714	0.0039	0.5177	0.0124	0.0688	0.0006	0.37	429	4	424	8	394	37	-9	c1	
	SA05/11 - 10a	10	128	156	11	1.25	0.6	0.16	0.0000876	0.0565	0.0011	0.3908	0.0035	0.5152	0.0116	0.0662	0.0007	0.50	413	4	422	8	471	33	12	c2a	rejected, > 10 % discordant
	SA05/11 - 11a	11	228	315	20	1.42	0.2	0.03	0.0000168	0.0573	0.0005	0.4320	0.0046	0.5372	0.0079	0.0680	0.0008	0.77	424	5	437	5	504	18	16	c1b	rejected, > 10 % discordant
	SA05/11 - 14a	14	116	139	10	1.23	1.3	0.34	0.0001830	0.0561	0.0016	0.3740	0.0053	0.5331	0.0167	0.0689	0.0008	0.36	430	5	434	11	456	48	6	c2a	
	SA05/11 - 26a	26	287	467	26	1.67	0.5	0.05	0.0000278	0.0563	0.0009	0.5110	0.0042	0.5216	0.0099	0.0671	0.0007	0.52	419	4	426	7	466	34	10	c1	rejected, > 10 % discordant
	SA05/11 - 17a	17	65	44	5	0.70	0.2	0.10	0.0000557	0.0599	0.0017	0.2211	0.0031	0.5602	0.0169	0.0679	0.0007	0.33	423	4	452	11	599	53	29	c2a	rejected, > 10 % discordant
	SA05/11 - 21a	21	274	407	25	1.53	1.5	0.18	0.0000948	0.0549	0.0009	0.4659	0.0037	0.5126	0.0094	0.0677	0.0006	0.48	422	4	420	6	408	28	-4	c2a	
Cr-15	SA05/15 - 1a	1	270	273	21	1.04	0.1	0.01	0.0000051	0.0553	0.0006	0.3251	0.0024	0.5088	0.0068	0.0667	0.0006	0.62	416	3	418	5	425	23	2	c1	
	SA05/15 - 2a	2	26	24	2	0.96	12.0	0.73	Th Corrd	0.0506	0.0061	Th Corrc	Th Corr	0.4486	0.0133	0.0644	0.0008	0.40	402	5	376	9	220	266	-83	c1	rejected, > 10 % discordant
	SA05/15 - 4a	4	25	13	5	0.54	0.2	0.12	0.0000621	0.0728	0.0009	0.1606	0.0021	1.7756	0.0286	0.1768	0.0017	0.61	1050	9	1037	10	1008	22	-4	inh1	inherited grain
	SA05/15 - 4b	4	52	42	4	0.83	0.2	0.15	0.0000806	0.0549	0.0010	0.2603	0.0032	0.4890	0.0102	0.0646	0.0007	0.50	403	4	404	7	409	29	1	rim	
	SA05/15 - 5a	5	218	154	16	0.72	0.5	0.07	0.0000370	0.0542	0.0006	0.2290	0.0011	0.4912	0.0065	0.0657	0.0005	0.62	410	3	406	4	379	21	-8	c1	rejected, crack
	SA05/15 - 8a	8	62	57	21	0.94	0.7	0.08	0.0000453	0.1010	0.0006	0.2772	0.0015	3.9680	0.0402	0.2849	0.0024	0.83	1616	12	1628	8	1642	10	2	inh1	inherited grain
	SA05/15 - 8b	8	406	234	27	0.59	3.7	0.31	0.0001685	0.0551	0.0007	0.1858	0.0201	0.4749	0.0081	0.0625	0.0007	0.69	391	5	395	6	417	24	6	rim	rejected, crack

sample	analysis no.	grain no.	U ppm	Th ppm	Pb ppm	Th/U	^{204}Pb ppb	f206 (%)	^{204}Pb/^{206}Pb	corrected ratios									Ages (Ma)								grain area	comment
										^{207}Pb/^{206}Pb	1σ	^{208}Pb/^{206}Pb	1σ	^{207}Pb/^{235}U	1σ	^{206}Pb/^{238}U	1σ	ρ	^{206}Pb/^{238}U	1σ	^{207}Pb/^{235}U	1σ	^{207}Pb/^{206}Pb	1σ	% disc		
	SA05/15 - 9a	9	113	141	10	1.28	0.4	0.10	0.0000554	0.0533	0.0008	0.3861	0.0035	0.4937	0.0098	0.0671	0.0008	0.62	419	5	407	7	343	31	-22	c2	rejected, > 10 % discordant
	SA05/15 - 15a	15	400	578	35	1.48	1.1	0.09	0.0000494	0.0536	0.0005	0.4602	0.0050	0.4944	0.0063	0.0669	0.0005	0.63	418	3	408	4	353	21	-18	c2a	rejected, > 10 % discordant
	SA05/15 - 15b	15	163	185	11	1.17	23.7	6.24	0.0035568	0.0524	0.0018	0.2780	0.0203	0.3650	0.0132	0.0505	0.0005	0.26	318	3	316	10	304	67	-4	c2b	rejected, high common Pb
	SA05/15 - 22a	22	94	121	8	1.33	1.7	0.59	0.0003163	0.0549	0.0014	0.4076	0.0061	0.5060	0.0134	0.0669	0.0006	0.36	417	4	416	9	407	32	-3	c1	
	SA05/15 - 25a	25	135	179	11	1.36	0.6	0.14	0.0000739	0.0549	0.0009	0.4180	0.0045	0.4958	0.0097	0.0655	0.0007	0.58	409	5	409	7	409	30	0	c1	rejected, crack
	SA05/15 - 25b	25	94	90	7	0.98	0.5	0.16	0.0000875	0.0533	0.0009	0.2990	0.0030	0.4897	0.0107	0.0666	0.0009	0.59	416	5	405	7	342	33	-22	c2	rejected, > 10 % discordant
	SA05/15 - 26a	26	328	229	24	0.72	0.4	0.04	0.0000235	0.0555	0.0004	0.2240	0.0011	0.5078	0.0069	0.0664	0.0007	0.81	414	4	417	5	431	17	4	c1	
	SA05/15 - 11a	11	94	73	7	0.79	0.4	0.13	0.0000710	0.0553	0.0010	0.2472	0.0027	0.5017	0.0105	0.0658	0.0008	0.57	411	5	413	7	424	33	3	c2a	
	SA05/15 - 29a	29	81	63	6	0.79	0.4	0.15	0.0000829	0.0530	0.0011	0.2427	0.0028	0.4723	0.0118	0.0646	0.0008	0.50	404	5	393	8	329	42	-23	c2	rejected, > 10 % discordant
	SA05/15 - 15b.2	15	174	168	13	0.99	0.2	0.04	0.0000196	0.0550	0.0006	0.3146	0.0020	0.5013	0.0084	0.0661	0.0008	0.72	412	5	413	6	413	25	0	c2b	
	SA05/15 - 27a	27	87	83	7	0.98	0.4	0.14	0.0000733	0.0531	0.0011	0.3044	0.0037	0.4782	0.0112	0.0654	0.0008	0.52	408	5	397	8	331	40	-23	c2	rejected, > 10 % discordant
	SA05/15 - 8c	8	68	74	24	1.13	0.0	0.00	0.0000001	0.1015	0.0007	0.3321	0.0016	4.0026	0.0481	0.2861	0.0028	0.80	1622	14	1635	10	1651	13	2	c2b	inherited grain
	SA05/15 - 4c	4	304	71	52	0.24	0.8	0.04	0.0000188	0.0739	0.0003	0.0733	0.0005	1.7424	0.0169	0.1709	0.0015	0.92	1017	8	1024	6	1039	7	2	inh2	inherited grain
	SA05/15 - 19a	19	86	116	7	1.38	0.2	0.08	0.0000413	0.0561	0.0008	0.4345	0.0034	0.4998	0.0083	0.0647	0.0006	0.58	404	4	412	6	455	24	11	c1	rejected, > 10 % discordant
Cr-17	SA05/17 - 3a	3	114	69	8	0.62	0.2	0.07	0.0000349	0.0545	0.0009	0.1925	0.0016	0.4926	0.0093	0.0655	0.0006	0.47	409	4	407	6	393	34	-4	c2c	
	SA05/17 - 4a	4	115	107	9	0.96	0.5	0.13	0.0000718	0.0553	0.0010	0.2983	0.0041	0.5156	0.0103	0.0677	0.0007	0.49	422	4	422	7	422	33	0	c1a	
	SA05/17 - 5a	5	146	194	12	1.37	0.4	0.11	0.0000563	0.0543	0.0008	0.4326	0.0099	0.4724	0.0079	0.0631	0.0006	0.54	394	3	393	5	383	27	-3	c2a	rejected, crack
	SA05/17 - 5b	5	93	88	7	0.97	0.8	0.28	0.0001503	0.0532	0.0012	0.2925	0.0040	0.4974	0.0119	0.0678	0.0006	0.40	423	4	410	8	337	34	-26	c2b	rejected, > 10 % discordant
	SA05/17 - 6a	6	86	37	15	0.44	0.9	0.13	0.0000695	0.0739	0.0010	0.1335	0.0019	1.7631	0.0288	0.1729	0.0016	0.56	1028	9	1032	11	1040	25	1	inh	inherited grain
	SA05/17 - 6b	6	90	55	6	0.63	0.4	0.14	0.0000745	0.0544	0.0009	0.1982	0.0027	0.4946	0.0096	0.0659	0.0006	0.49	412	4	408	6	388	27	-6	r1a	
	SA05/17 - 7a	7	60	34	4	0.57	0.5	0.26	0.0001409	0.0527	0.0014	0.1762	0.0040	0.4862	0.0138	0.0669	0.0007	0.37	417	4	402	9	317	43	-32	c2a	rejected, > 10 % discordant
	SA05/17 - 7c	7	162	164	13	1.04	0.4	0.07	0.0000375	0.0542	0.0007	0.3199	0.0017	0.5119	0.0078	0.0685	0.0006	0.56	427	4	420	5	380	25	-12	rim	rejected, > 10 % discordant
	SA05/17 - 8a	8	74	49	5	0.68	0.5	0.22	0.0001172	0.0545	0.0013	0.2125	0.0044	0.4891	0.0128	0.0651	0.0007	0.40	407	4	404	9	389	43	-5	c2a	
	SA05/17 - 12c	12	205	163	16	0.82	24.0	3.55	0.0019697	0.0562	0.0016	0.2579	0.0143	0.5317	0.0162	0.0686	0.0006	0.29	428	4	433	11	461	48	7	c2	rejected, high common Pb
	SA05/17 - 26a	26	206	125	14	0.62	4.0	0.63	0.0003415	0.0534	0.0009	0.1940	0.0052	0.4793	0.0092	0.0651	0.0005	0.41	406	3	398	6	346	24	-17	c2	rejected, > 10 % discordant
	SA05/17 - 25a	25	179	145	14	0.83	0.7	0.12	0.0000657	0.0539	0.0010	0.2557	0.0019	0.4933	0.0098	0.0663	0.0006	0.44	414	4	407	7	368	37	-13	c2	rejected, > 10 % discordant
	SA05/17 - 23a	23	88	68	7	0.80	0.2	0.08	0.0000453	0.0555	0.0010	0.2518	0.0028	0.5082	0.0105	0.0665	0.0006	0.42	415	3	417	7	431	37	4	c1	
	SA05/17 - 14a	14	206	219	17	1.09	0.8	0.12	0.0000666	0.0549	0.0007	0.3363	0.0033	0.5135	0.0084	0.0678	0.0006	0.55	423	4	421	6	407	27	-4	rim	
	SA05/17 - 13a	13	83	56	6	0.69	0.2	0.09	0.0000472	0.0546	0.0012	0.2168	0.0021	0.4960	0.0114	0.0659	0.0006	0.38	411	3	409	8	396	43	-4	c2	
MO	SA05/20 - 2a	2	149	149	12	1.03	0.8	0.18	0.0000973	0.0534	0.0007	0.3171	0.0043	0.4995	0.0079	0.0678	0.0006	0.53	423	3	411	5	346	23	-22	c1	rejected, > 10 % discordant
	SA05/20 - 3a	3	92	66	7	0.73	0.2	0.07	0.0000395	0.0549	0.0009	0.2292	0.0024	0.5060	0.0096	0.0668	0.0006	0.48	417	4	416	6	409	34	-2	c2	
	SA05/20 - 5a	5	154	88	11	0.59	0.0	0.00	0.0000001	0.0566	0.0005	0.1856	0.0012	0.5232	0.0090	0.0671	0.0010	0.87	419	6	427	6	474	18	12	c2a	rejected, > 10 % discordant
	SA05/20 - 6a	6	256	333	22	1.34	0.0	0.00	0.0000001	0.0561	0.0007	0.4189	0.0024	0.5188	0.0136	0.0671	0.0015	0.86	419	9	424	9	455	29	8	c2	
	SA05/20 - 9a	9	153	156	12	1.04	0.0	0.00	0.0000001	0.0552	0.0008	0.3255	0.0021	0.5161	0.0083	0.0678	0.0005	0.49	423	3	423	6	419	31	-1	c1	
	SA05/20 - 11b	11	77	57	6	0.76	2.9	1.17	0.0006304	0.0517	0.0026	0.2308	0.0126	0.4901	0.0254	0.0688	0.0007	0.19	429	4	405	17	271	99	-58	c2	rejected, high common Pb
	SA05/20 - 12a	12	103	63	8	0.62	0.1	0.03	0.0000173	0.0556	0.0008	0.1975	0.0012	0.5199	0.0087	0.0678	0.0006	0.52	423	4	425	6	435	30	3	rim	
	SA05/20 - 14b	14	236	182	18	0.79	0.2	0.03	0.0000157	0.0544	0.0008	0.2476	0.0015	0.5110	0.0083	0.0681	0.0005	0.43	425	3	419	6	389	32	-9	c2a	
	SA05/20 - 15a	15	140	143	12	1.05	0.0	0.00	0.0000001	0.0544	0.0005	0.3238	0.0023	0.5204	0.0066	0.0694	0.0005	0.62	433	3	425	4	385	23	-12	c2a	rejected, > 10 % discordant
	SA05/20 - 15b	15	165	182	14	1.13	0.0	0.00	0.0000001	0.0559	0.0004	0.3505	0.0022	0.5269	0.0054	0.0684	0.0005	0.77	427	3	430	4	446	15	4	c2b	
	SA05/20 - 17a	17	154	158	13	1.06	0.2	0.05	0.0000253	0.0544	0.0007	0.3277	0.0015	0.5106	0.0077	0.0680	0.0005	0.52	424	3	419	5	388	27	-9	c1	
	SA05/20 - 17b	17	53	32	4	0.61	0.0	0.00	0.0000003	0.0554	0.0012	0.1941	0.0025	0.5151	0.0124	0.0674	0.0007	0.41	420	4	422	8	430	48	2	c2	
	SA05/20 - 1a	1	135	149	11	1.14	0.5	0.13	0.0000701	0.0553	0.0009	0.3556	0.0021	0.5119	0.0093	0.0671	0.0005	0.44	419	3	420	6	424	31	1	c2a	
	SA05/20 - 7a	7	212	220	17	1.06	0.0	0.00	0.0000001	0.0548	0.0005	0.3318	0.0016	0.5149	0.0061	0.0681	0.0005	0.63	425	3	422	4	404	20	-5	c2	
	SA05/20 - 10a	10	233	245	19	1.08	0.6	0.08	0.0000421	0.0544	0.0005	0.3345	0.0032	0.5166	0.0064	0.0688	0.0005	0.62	429	3	423	4	389	18	-10	c1	rejected, > 10 % discordant
Q-23	SA05/23 - 1a	1	177	143	13	0.83	0.4	0.07	0.0000369	0.0554	0.0006	0.2647	0.0024	0.4896	0.0081	0.0642	0.0008	0.75	401	5	405	6	426	22	6	c1	
	SA05/23 - 2a	2	794	1049	69	1.35	7.8	0.31	0.0001672	0.0532	0.0003	0.4193	0.0019	0.4962	0.0063	0.0677	0.0008	0.87	422	5	409	4	336	10	-26	c2	rejected, crack
	SA05/23 - 6a	6	368	433	30	1.21	0.7	0.06	0.0000330	0.0545	0.0003	0.3786	0.0019	0.4957	0.0062	0.0660	0.0007	0.88	412	4	409	4	390	11	-6	c2a	
	SA05/23 - 12a	12	808	1066	68	1.35	0.7	0.03	0.0000161	0.0551	0.0003	0.4242	0.0038	0.4984	0.0102	0.0656	0.0013	0.97	409	8	411	7	417	11	2	c1b	
	SA05/23 - 13a	13	255	264	20	1.06	1.0	0.13	0.0000694	0.0555	0.0006	0.3313	0.0018	0.4997	0.0077	0.0653	0.0007	0.74	408	5	412	5	433	19	6	c1	rejected, hit inclusion
	SA05/23 - 14a	14	105	85	8	0.84	1.2	0.38	0.0002033	0.0555	0.0010	0.2611	0.0041	0.5003	0.0110	0.0654	0.0007	0.52	408	5	412	7	431	28	5	c1b	
	SA05/23 - 15a	15	97	96	8	1.01	0.2	0.06	0.0000337	0.0544	0.0009	0.3146	0.0021	0.4942	0.0105	0.0659	0.0009	0.62	411	5	408	7	388	34	-6	c1	
	SA05/23 - 16a	16	199	194	15	1.00	0.4	0.07	0.0000350	0.0546	0.0009	0.3089	0.0064	0.4830	0.0160	0.0642	0.0019	0.88	401	11	400	11	395	34	-2	c2a	
	SA05/23 - 16b	16	286	346	23	1.24	0.5	0.06	0.0000299	0.0543	0.0005	0.3868	0.0014	0.4857	0.0072	0.0648	0.0007	0.76	405	4	402	5	385	20	-5	c2b	
	SA05/23 - 19a	19	105	103	8	1.01	7.4	2.34	0.0012831	0.0565	0.0016	0.3143	0.0119	0.4930	0.0151	0.0633	0.0007	0.37	396	4	407	10	470	38	16	c1	rejected, high common Pb
	SA05/23 - 22a	22	72	59	5	0.84	0.3	0.12	0.0000625	0.0549	0.0010	0.2571	0.0023	0.4973	0.0106	0.0657	0.0008	0.56	410	5	410	7	408	33	-1	c1	
	SA05/23 - 21a	21	851	1209	72	1.46	0.7	0.03	0.0000147	0.0552	0.0003	0.4590	0.0011	0.4955	0.0061	0.0651	0.0007	0.89	407	4	409	4	420	13	3	c2	
	SA05/23 - 23a	23	102	94	7	0.94	0.2	0.05	0.0000289	0.0558	0.0004	0.2978	0.0014	0.4840	0.0068	0.0629	0.0007	0.82	393	4	401	5	445	13	12	c1	rejected, > 10 % discordant
	SA05/23 - 20a	20	438	536	36	1.26	1.1	0.08	0.0000447	0.0547	0.0004	0.3967	0.0015	0.4943	0.0057	0.0655	0.0006	0.77	409	4	408	4	400	15	-2	c2a	
	SA05/23 - 17a	17	1761	2080	150	1.21	0.6	0.01	0.0000061	0.0546	0.0002	0.3812	0.0012	0.5186	0.0048	0.0688	0.0006	0.95	429	4	424	3	397	7	-8	c1a	rejected, > 1000 ppm U

sample	analysis no.	grain no.	U ppm	Th ppm	Pb ppm	Th/U	^{204}Pb ppb	f206 (%)	^{204}Pb/^{206}Pb	corrected ratios									Ages (Ma)								grain area	comment
										^{207}Pb/^{206}Pb	1σ	^{208}Pb/^{206}Pb	1σ	^{207}Pb/^{235}U	1σ	^{206}Pb/^{238}U	1σ	ρ	^{206}Pb/^{238}U	1σ	^{207}Pb/^{235}U	1σ	^{207}Pb/^{206}Pb	1σ	% disc		
Q-25	SA05/25 - 2a	2	320	315	24	1.01	0.6	0.07	0.0000364	0.0546	0.0004	0.3208	0.0020	0.4816	0.0057	0.0640	0.0006	0.76	400	3	399	4	395	15	-1	c2	rejected, crack
	SA05/25 - 3a	3	1134	1830	103	1.66	0.6	0.02	0.0000089	0.0548	0.0002	0.5270	0.0016	0.5085	0.0050	0.0673	0.0006	0.89	420	4	417	3	405	10	-4	c2	
	SA05/25 - 4a	4	1631	2223	140	1.40	16.3	0.32	0.0001734	0.0549	0.0006	0.4374	0.0067	0.5038	0.0088	0.0666	0.0009	0.81	416	6	414	6	406	22	-2	c2	
	SA05/25 - 7a	7	3699	7064	358	1.96	7.1	0.06	0.0000325	0.0553	0.0003	0.6245	0.0051	0.5193	0.0062	0.0681	0.0007	0.87	425	4	425	4	424	13	0	c2	rejected, crack
	SA05/25 - 8a	8	2512	2386	176	0.97	31.9	0.39	0.0002119	0.0553	0.0004	0.3969	0.0025	0.4945	0.0055	0.0649	0.0006	0.81	405	4	408	4	424	13	4	c2	rejected, crack
	SA05/25 - 11a	11	216	221	16	1.05	0.1	0.02	0.0000086	0.0551	0.0006	0.3363	0.0019	0.4857	0.0067	0.0640	0.0006	0.67	400	4	402	5	415	22	4	c2	
	SA05/25 - 12a	12	2432	3362	196	1.42	434.0	5.88	0.0033406	0.0390	0.0018	0.4332	0.0110	0.3341	0.0162	0.0621	0.0007	0.24	389	4	293	12				c2	rejected, crack
	SA05/25 - 14a	14	483	605	39	1.28	5.8	0.40	0.0002128	0.0551	0.0006	0.4067	0.0046	0.4912	0.0078	0.0647	0.0007	0.68	404	4	406	5	415	20	3	c2	rejected, crack
	SA05/25 - 15a	15	1617	2392	139	1.52	1.2	0.02	0.0000129	0.0547	0.0002	0.4872	0.0026	0.4968	0.0047	0.0658	0.0006	0.91	411	3	410	3	400	9	-3	c2	
	SA05/25 - 17a	17	1757	1836	140	1.07	1.0	0.02	0.0000095	0.0549	0.0002	0.3428	0.0012	0.5039	0.0048	0.0666	0.0006	0.92	416	4	414	3	407	8	-2	c2	
	SA05/25 - 21a	21	5974	####	410	1.92	39.9	0.29	0.0001553	0.0281	0.0579	0.6155	0.3873	0.1907	0.3953	0.0493	0.0104	0.10	310	64	177	291				c2a	rejected, high common Pb
	SA05/25 - 20c	20	332	379	26	1.17	0.0	0.00	0.0000001	0.0556	0.0004	0.3715	0.0056	0.4867	0.0065	0.0635	0.0007	0.83	397	4	403	4	434	17	9	c2	
	SA05/25 - 23a	23	2112	2920	180	1.42	13.7	0.21	0.0001128	0.0545	0.0002	0.4479	0.0012	0.4959	0.0047	0.0660	0.0006	0.92	412	3	409	3	392	6	-5	c2	rejected, crack
	SA05/25 - 24b	24	639	1103	60	1.77	4.2	0.21	0.0001137	0.0551	0.0004	0.5537	0.0020	0.5098	0.0060	0.0671	0.0006	0.82	419	4	418	4	415	11	-1	c2b	
Cr-26	SA05/26 - 1a	1	221	286	19	1.33	0.0	0.00	0.0000001	0.0555	0.0006	0.4183	0.0027	0.5267	0.0072	0.0689	0.0006	0.65	429	4	430	5	430	24	0	c1+rim	rejected, crack
	SA05/26 - 1b	1	53	49	4	0.94	0.5	0.28	0.0001513	0.0527	0.0013	0.2928	0.0042	0.4825	0.0133	0.0665	0.0007	0.38	415	4	400	9	313	37	-33	rim	rejected, > 10 % discordant
	SA05/26 - 3a	3	70	78	6	1.14	0.4	0.19	0.0001042	0.0528	0.0011	0.3534	0.0033	0.4908	0.0113	0.0674	0.0007	0.44	421	4	405	8	319	35	-32	c2a	rejected, > 10 % discordant
	SA05/26 - 5a	5	1835	1675	147	0.94	0.3	0.01	0.0000028	0.0552	0.0002	0.2977	0.0022	0.5254	0.0048	0.0691	0.0006	0.94	430	4	429	3	419	7	-3	c1	rejected, > 1000 ppm U
	SA05/26 - 6a	6	246	400	23	1.66	0.0	0.00	0.0000001	0.0553	0.0003	0.5304	0.0026	0.5172	0.0058	0.0679	0.0007	0.87	423	4	423	4	422	13	0	c1	
	SA05/26 - 7a	7	166	238	14	1.47	0.2	0.04	0.0000220	0.0553	0.0006	0.4654	0.0045	0.5091	0.0072	0.0668	0.0006	0.68	417	4	418	5	424	22	2	c2a	
	SA05/26 - 10a	10	86	64	4	0.76	15.4	7.96	Th Corrd	0.0466	-0.0192	Th Corrc	Th Corr	0.4054	0.2449	0.0631	0.0026	0.07	394	16	346	163				c2	rejected, high common Pb
	SA05/26 - 12a	12	73	68	6	0.95	0.0	0.00	0.0000002	0.0550	0.0008	0.3046	0.0025	0.4989	0.0084	0.0658	0.0006	0.57	411	4	411	6	411	31	0	c2b	
	SA05/26 - 12b	12	58	52	4	0.92	0.1	0.05	0.0000278	0.0565	0.0013	0.2914	0.0029	0.5078	0.0131	0.0652	0.0007	0.41	407	4	417	9	471	49	14	c2c	rejected, > 10 % discordant
	SA05/26 - 11a	11	187	122	14	0.67	0.3	0.05	0.0000277	0.0544	0.0005	0.2110	0.0015	0.5003	0.0070	0.0667	0.0007	0.72	416	4	412	5	388	19	-7	c2a	
	SA05/26 - 16a	16	119	114	9	0.98	0.0	0.00	0.0000001	0.0550	0.0004	0.3050	0.0034	0.5028	0.0059	0.0663	0.0006	0.80	414	4	414	4	413	15	0	c2	
	SA05/26 - 17b	17	169	135	13	0.82	0.2	0.04	0.0000201	0.0545	0.0008	0.2547	0.0014	0.4961	0.0083	0.0660	0.0006	0.57	412	4	409	6	393	29	-5	c2	
	SA05/26 - 21a	21	327	300	25	0.94	0.6	0.06	0.0000304	0.0550	0.0004	0.2994	0.0014	0.5003	0.0060	0.0660	0.0006	0.75	412	4	412	4	412	16	0	c2a	
	SA05/26 - 27a	27	130	82	9	0.65	0.0	0.00	0.0000001	0.0556	0.0006	0.2074	0.0018	0.4942	0.0076	0.0644	0.0007	0.71	402	4	408	5	437	24	8	c2	
	SA05/26 - 28a	28	225	266	18	1.21	0.0	0.00	0.0000001	0.0552	0.0005	0.3850	0.0027	0.5048	0.0064	0.0664	0.0006	0.74	414	4	415	4	418	19	1	c1	
	SA05/26 - 13a	13	156	250	14	1.65	0.0	0.00	0.0000001	0.0558	0.0005	0.5183	0.0067	0.5083	0.0066	0.0660	0.0006	0.71	412	4	417	4	446	20	8	c1	
Standards																												
Session	91500		81	27	15	0.34	0.2	0.04	0.0000190	0.0747	0.0005	0.1017	0.0009	1.8442	0.0313	0.1792	0.0028	0.91	1062	15	1061	11	1059	13	0		
2	91500		81	28	15	0.36	0.2	0.04	0.0000195	0.0736	0.0007	0.1083	0.0010	1.8184	0.0343	0.1792	0.0029	0.86	1062	16	1052	12	1030	19	-3		
July	91500		75	26	14	0.36	0.0	0.00	0.0000001	0.0747	0.0007	0.1089	0.0006	1.8293	0.0230	0.1777	0.0015	0.69	1054	8	1056	8	1059	19	0		
2005	91500		81	28	15	0.35	0.3	0.05	0.0000273	0.0742	0.0005	0.1048	0.0009	1.8355	0.0195	0.1794	0.0015	0.80	1064	8	1058	7	1046	12	-2		
	91500		82	28	15	0.35	0.1	0.01	0.0000060	0.0745	0.0005	0.1066	0.0005	1.8364	0.0205	0.1788	0.0015	0.77	1060	8	1059	7	1054	14	-1		
	91500		82	28	15	0.35	0.3	0.04	0.0000198	0.0747	0.0005	0.1052	0.0010	1.8641	0.0198	0.1810	0.0015	0.80	1072	8	1068	7	1060	12	-1		
	91500		81	27	15	0.35	0.6	0.09	0.0000471	0.0734	0.0005	0.1038	0.0013	1.7961	0.0213	0.1776	0.0017	0.80	1054	9	1044	8	1023	13	-3		
	91500		83	28	15	0.35	0.2	0.03	0.0000137	0.0744	0.0007	0.1056	0.0008	1.8406	0.0225	0.1794	0.0015	0.70	1064	8	1060	8	1052	17	-1		
	91500		85	29	16	0.35	0.2	0.03	0.0000176	0.0747	0.0006	0.1061	0.0014	1.8579	0.0341	0.1803	0.0030	0.90	1069	16	1066	12	1061	15	-1		
	91500		77	27	14	0.36	0.0	0.00	0.0000001	0.0757	0.0004	0.1098	0.0010	1.8801	0.0259	0.1801	0.0023	0.91	1067	12	1074	9	1087	12	2		
	91500		82	28	15	0.35	0.0	0.00	0.0000001	0.0752	0.0005	0.1070	0.0008	1.8964	0.0255	0.1828	0.0021	0.86	1082	12	1080	9	1075	13	-1		
	91500		82	28	15	0.35	0.3	0.04	0.0000229	0.0744	0.0008	0.1065	0.0011	1.8159	0.0292	0.1770	0.0021	0.72	1051	11	1051	10	1052	22	0		
	91500		81	28	15	0.35	0.2	0.03	0.0000149	0.0748	0.0007	0.1054	0.0009	1.8310	0.0278	0.1774	0.0021	0.77	1053	11	1057	10	1064	19	1		
	91500		83	29	15	0.36	0.0	0.00	0.0000001	0.0746	0.0006	0.1075	0.0009	1.8523	0.0260	0.1800	0.0021	0.82	1067	11	1064	9	1058	16	-1		
	91500		81	28	15	0.35	0.0	0.00	0.0000001	0.0745	0.0006	0.1076	0.0006	1.7992	0.0253	0.1751	0.0021	0.84	1040	11	1045	9	1055	16	1		
	91500		82	28	15	0.35	0.0	0.00	0.0000001	0.0752	0.0005	0.1060	0.0009	1.8840	0.0254	0.1818	0.0022	0.89	1077	12	1075	9	1073	12	0		
	91500		85	29	16	0.35	0.0	0.00	0.0000001	0.0737	0.0005	0.1074	0.0008	1.8378	0.0206	0.1809	0.0017	0.84	1072	9	1059	7	1033	12	-4		
	91500		82	28	15	0.35	0.0	0.00	0.0000001	0.0747	0.0006	0.1065	0.0009	1.8551	0.0235	0.1801	0.0017	0.75	1068	9	1065	8	1060	16	-1		
	91500		83	28	15	0.35	0.1	0.01	0.0000073	0.0748	0.0006	0.1058	0.0009	1.8409	0.0224	0.1785	0.0017	0.77	1059	9	1060	8	1063	15	0		
	91500		83	29	16	0.35	0.0	0.00	0.0000001	0.0747	0.0006	0.1066	0.0008	1.8815	0.0234	0.1827	0.0017	0.76	1082	9	1075	8	1060	16	-2		
	91500		79	27	14	0.35	0.0	0.00	0.0000001	0.0742	0.0007	0.1064	0.0007	1.8270	0.0238	0.1786	0.0017	0.73	1059	9	1055	9	1046	18	-1		
	91500		83	28	15	0.35	0.0	0.00	0.0000001	0.0738	0.0006	0.1055	0.0006	1.8354	0.0221	0.1803	0.0016	0.76	1069	9	1058	8	1036	16	-3		
	91500		80	27	15	0.35	0.0	0.00	0.0000001	0.0749	0.0006	0.1045	0.0008	1.8595	0.0240	0.1800	0.0018	0.78	1067	10	1067	9	1066	16	0		
	91500		80	27	15	0.35	0.2	0.03	0.0000184	0.0753	0.0006	0.1051	0.0011	1.8682	0.0228	0.1801	0.0017	0.79	1067	10	1070	8	1075	14	1		
	91500		80	27	15	0.35	0.0	0.00	0.0000001	0.0756	0.0006	0.1049	0.0010	1.9006	0.0231	0.1824	0.0017	0.78	1080	9	1081	8	1084	15	0		
	91500		80	27	15	0.35	0.0	0.00	0.0000001	0.0748	0.0007	0.1049	0.0005	1.8424	0.0270	0.1786	0.0019	0.74	1060	11	1061	10	1063	19	0		
	91500		83	28	15	0.35	0.0	0.00	0.0000001	0.0744	0.0005	0.1067	0.0009	1.8362	0.0222	0.1790	0.0018	0.83	1062	10	1058	8	1052	13	-1		
	91500		82	28	15	0.35	0.1	0.02	0.0000093	0.0748	0.0008	0.1052	0.0009	1.7961	0.0260	0.1740	0.0018	0.71	1034	10	1044	9	1064	20	3		

sample	analysis no.	grain no.	U ppm	Th ppm	Pb ppm	Th/U	^{204}Pb ppb	f206 (%)	^{204}Pb/^{206}Pb	corrected ratios									Ages (Ma)								grain area	comment
										^{207}Pb/^{206}Pb	1σ	^{208}Pb/^{206}Pb	1σ	^{207}Pb/^{235}U	1σ	^{206}Pb/^{238}U	1σ	ρ	^{206}Pb/^{238}U	1σ	^{207}Pb/^{235}U	1σ	^{207}Pb/^{206}Pb	1σ	% disc			
	91500		79	27	14	0.35	0.0	0.00	0.0000001	0.0753	0.0008	0.1051	0.0008	1.8416	0.0276	0.1775	0.0017	0.66	1053	10	1060	10	1075	22	2		
	91500		78	26	14	0.35	0.0	0.00	0.0000001	0.0747	0.0008	0.1051	0.0009	1.8089	0.0268	0.1757	0.0017	0.67	1044	10	1049	10	1059	22	1		
	91500		85	30	16	0.36	0.0	0.00	0.0000001	0.0753	0.0007	0.1101	0.0006	1.8682	0.0253	0.1799	0.0018	0.74	1067	10	1070	9	1076	18	1		
	91500		84	30	15	0.37	0.0	0.00	0.0000001	0.0750	0.0006	0.1100	0.0005	1.8553	0.0208	0.1794	0.0015	0.75	1064	8	1065	7	1068	14	0		
	91500		82	29	15	0.36	0.0	0.00	0.0000001	0.0747	0.0006	0.1088	0.0008	1.8474	0.0206	0.1794	0.0014	0.72	1064	8	1062	7	1059	16	0		
	91500		84	29	15	0.36	0.0	0.00	0.0000001	0.0759	0.0007	0.1113	0.0009	1.8838	0.0235	0.1800	0.0014	0.64	1067	8	1075	8	1091	20	2		
	91500		81	28	15	0.36	0.1	0.01	0.0000079	0.0745	0.0005	0.1089	0.0008	1.8519	0.0196	0.1802	0.0015	0.78	1068	8	1064	7	1056	13	-1		
	91500		81	29	15	0.36	0.0	0.00	0.0000001	0.0755	0.0006	0.1107	0.0010	1.8539	0.0204	0.1781	0.0015	0.75	1056	8	1065	7	1082	14	2		
	91500		81	29	15	0.36	0.4	0.06	0.0000335	0.0740	0.0005	0.1078	0.0011	1.8196	0.0190	0.1783	0.0014	0.73	1057	7	1053	7	1042	13	-1		
	91500		80	28	15	0.36	0.0	0.00	0.0000001	0.0748	0.0006	0.1082	0.0006	1.8447	0.0208	0.1789	0.0014	0.70	1061	8	1062	7	1063	16	0		
	91500		81	29	15	0.36	0.0	0.00	0.0000001	0.0744	0.0007	0.1084	0.0007	1.8257	0.0224	0.1780	0.0015	0.67	1056	8	1055	8	1052	18	0		
	91500		76	27	14	0.36	0.0	0.00	0.0000001	0.0749	0.0007	0.1089	0.0010	1.8417	0.0217	0.1784	0.0014	0.65	1058	8	1060	8	1065	18	1		
	91500		78	27	14	0.36	0.0	0.00	0.0000001	0.0760	0.0006	0.1074	0.0008	1.8895	0.0291	0.1803	0.0023	0.85	1069	13	1077	10	1095	16	2		
	91500		77	27	14	0.36	0.3	0.04	0.0000212	0.0740	0.0004	0.1073	0.0009	1.8229	0.0205	0.1787	0.0017	0.85	1060	9	1054	7	1041	11	-2		
	91500		80	28	15	0.36	0.2	0.03	0.0000143	0.0749	0.0006	0.1082	0.0007	1.8423	0.0222	0.1783	0.0016	0.74	1058	9	1061	8	1066	16	1		
	91500		80	28	15	0.36	0.4	0.07	0.0000356	0.0747	0.0007	0.1069	0.0011	1.8374	0.0234	0.1783	0.0016	0.71	1058	9	1059	8	1061	17	0		
	91500		77	27	14	0.36	0.0	0.00	0.0000001	0.0741	0.0004	0.1087	0.0006	1.8314	0.0188	0.1793	0.0016	0.88	1063	9	1057	7	1043	10	-2		
	91500		79	28	14	0.36	0.0	0.00	0.0000001	0.0738	0.0005	0.1091	0.0009	1.7933	0.0197	0.1762	0.0016	0.82	1046	9	1043	7	1036	13	-1		
	91500		80	29	15	0.37	0.3	0.05	0.0000283	0.0736	0.0008	0.1095	0.0012	1.8044	0.0259	0.1778	0.0017	0.66	1055	9	1047	9	1030	21	-2		
	91500		82	30	15	0.37	0.0	0.00	0.0000001	0.0754	0.0007	0.1115	0.0006	1.8699	0.0255	0.1798	0.0017	0.69	1066	9	1071	9	1079	20	1		
	91500		81	29	15	0.37	0.0	0.00	0.0000001	0.0752	0.0006	0.1110	0.0012	1.8839	0.0226	0.1817	0.0017	0.77	1076	9	1075	8	1073	16	0		
	91500		81	29	15	0.37	0.8	0.12	0.0000630	0.0736	0.0009	0.1098	0.0017	1.8221	0.0308	0.1795	0.0022	0.71	1064	12	1053	11	1030	22	-3		
	91500		79	29	15	0.37	0.0	0.00	0.0000001	0.0746	0.0005	0.1111	0.0008	1.8650	0.0204	0.1814	0.0016	0.81	1075	9	1069	7	1056	13	-2		
	91500		97	35	18	0.37	0.0	0.00	0.0000001	0.0751	0.0006	0.1114	0.0008	1.8611	0.0222	0.1797	0.0016	0.76	1065	9	1067	8	1071	15	1		
	91500		80	29	15	0.37	0.0	0.00	0.0000001	0.0762	0.0008	0.1099	0.0008	1.9141	0.0459	0.1821	0.0040	0.91	1078	22	1086	16	1101	19	2		
	91500		82	30	15	0.37	0.0	0.00	0.0000001	0.0748	0.0006	0.1116	0.0007	1.8185	0.0425	0.1762	0.0039	0.95	1046	21	1052	15	1064	15	2		
	91500		89	32	16	0.37	0.0	0.00	0.0000001	0.0758	0.0006	0.1112	0.0006	1.8654	0.0220	0.1785	0.0016	0.74	1059	9	1069	8	1089	16	3		
	91500		90	32	17	0.37	0.0	0.00	0.0000001	0.0755	0.0005	0.1118	0.0006	1.8992	0.0215	0.1824	0.0016	0.80	1080	9	1081	7	1082	14	0		
	91500		86	30	16	0.36	0.0	0.00	0.0000001	0.0739	0.0007	0.1096	0.0008	1.8343	0.0217	0.1800	0.0014	0.66	1067	8	1058	8	1039	18	-3		
	91500		86	31	16	0.37	0.0	0.00	0.0000001	0.0754	0.0008	0.1097	0.0008	1.8475	0.0240	0.1777	0.0014	0.62	1054	8	1063	9	1079	20	2		
	91500		90	32	17	0.37	0.3	0.05	0.0000251	0.0744	0.0005	0.1103	0.0011	1.8312	0.0211	0.1785	0.0016	0.77	1059	9	1057	8	1052	13	-1		
	91500		88	32	16	0.37	0.3	0.04	0.0000208	0.0749	0.0006	0.1110	0.0008	1.8396	0.0212	0.1780	0.0014	0.68	1056	8	1060	8	1066	17	1		
	91500		85	30	16	0.37	0.0	0.00	0.0000001	0.0750	0.0005	0.1108	0.0007	1.8423	0.0194	0.1782	0.0015	0.78	1057	8	1061	7	1067	14	1		
	91500		92	33	17	0.37	0.1	0.01	0.0000062	0.0743	0.0005	0.1116	0.0011	1.8400	0.0194	0.1795	0.0014	0.75	1064	8	1060	7	1050	14	-1		
	91500		92	33	17	0.37	0.1	0.01	0.0000064	0.0744	0.0006	0.1114	0.0008	1.8687	0.0206	0.1822	0.0014	0.71	1079	8	1070	7	1052	15	-3		
	91500		88	31	16	0.37	0.0	0.00	0.0000001	0.0741	0.0005	0.1121	0.0009	1.8517	0.0197	0.1813	0.0015	0.78	1074	8	1064	7	1043	14	-3		
	91500		57	19	11	0.35	0.0	0.00	0.0000001	0.0752	0.0008	0.1058	0.0009	1.8702	0.0268	0.1803	0.0017	0.64	1068	9	1071	9	1075	22	1		
	91500		69	24	13	0.36	0.2	0.04	0.0000207	0.0745	0.0009	0.1099	0.0012	1.8253	0.0281	0.1776	0.0017	0.60	1054	9	1055	10	1055	24	0		
	91500		71	25	13	0.37	0.3	0.06	0.0000307	0.0730	0.0006	0.1094	0.0013	1.7819	0.0234	0.1769	0.0018	0.78	1050	10	1039	8	1015	15	-3		
	91500		72	26	13	0.37	0.0	0.00	0.0000001	0.0746	0.0006	0.1123	0.0007	1.8264	0.0214	0.1775	0.0014	0.68	1053	8	1055	8	1058	17	0		
	91500		75	27	14	0.38	1.1	0.17	0.0000930	0.0745	0.0011	0.1097	0.0026	1.8554	0.0345	0.1807	0.0022	0.64	1071	12	1065	12	1054	24	-2		
	91500		75	28	14	0.38	0.4	0.07	0.0000349	0.0763	0.0011	0.1127	0.0014	1.8717	0.0326	0.1779	0.0016	0.53	1055	9	1071	11	1103	28	4		
	91500		78	29	14	0.38	0.0	0.00	0.0000001	0.0744	0.0008	0.1147	0.0015	1.8307	0.0291	0.1786	0.0021	0.76	1059	12	1057	10	1051	20	-1		
Session 3 March 2006	91500		79	27	14	0.35	3.0	0.45	0.0002424	0.0735	0.0011	0.1049	0.0038	1.8054	0.0324	0.1781	0.0018	0.55	1057	10	1047	12	1028	24	-2.8		
	91500		80	29	14	0.37	0.4	0.06	0.0000331	0.0741	0.0008	0.1098	0.0012	1.7974	0.0252	0.1760	0.0016	0.66	1045	9	1045	9	1043	20	-0.2		
	91500		84	30	15	0.37	0.0	0.00	0.0000001	0.0756	0.0007	0.1120	0.0008	1.8600	0.0229	0.1784	0.0015	0.70	1058	8	1067	8	1084	18	2.4		
	91500		80	28	15	0.36	0.2	0.02	0.0000129	0.0748	0.0005	0.1080	0.0009	1.8356	0.0208	0.1779	0.0016	0.80	1055	9	1058	7	1064	13	0.8		
	91500		82	29	15	0.36	0.0	0.00	0.0000001	0.0750	0.0007	0.1099	0.0011	1.8374	0.0250	0.1776	0.0018	0.73	1054	10	1059	9	1069	18	1.4		
	91500		78	27	14	0.36	0.0	0.00	0.0000001	0.0764	0.0005	0.1084	0.0009	1.8247	0.0215	0.1731	0.0017	0.82	1029	9	1054	8	1106	13	6.9		
	91500		82	28	15	0.35	0.4	0.05	0.0000277	0.0745	0.0006	0.1071	0.0010	1.8348	0.0228	0.1786	0.0018	0.80	1060	10	1058	8	1054	14	-0.5		
	91500		81	28	15	0.35	0.3	0.05	0.0000275	0.0733	0.0008	0.1055	0.0009	1.8294	0.0247	0.1809	0.0016	0.65	1072	9	1056	9	1023	20	-4.8		
	91500		80	28	15	0.35	0.2	0.04	0.0000196	0.0736	0.0004	0.1051	0.0010	1.8523	0.0217	0.1825	0.0019	0.88	1081	10	1064	8	1031	10	-4.8		
	91500		83	29	15	0.36	0.0	0.00	0.0000001	0.0753	0.0004	0.1065	0.0008	1.8669	0.0190	0.1799	0.0016	0.89	1066	9	1069	7	1075	10	0.8		
	91500		81	28	15	0.35	0.2	0.04	0.0000199	0.0756	0.0006	0.1080	0.0009	1.8645	0.0241	0.1788	0.0018	0.79	1060	10	1069	8	1085	15	2.3		
	91500		82	28	15	0.36	0.0	0.00	0.0000001	0.0742	0.0006	0.1083	0.0007	1.8423	0.0236	0.1801	0.0018	0.80	1067	10	1061	8	1046	16	-2.0		
	91500		82	28	15	0.35	0.4	0.05	0.0000292	0.0748	0.0010	0.1060	0.0012	1.9047	0.0310	0.1847	0.0018	0.61	1092	10	1083	11	1063	25	-2.8		
	91500		82	28	15	0.35	0.3	0.04	0.0000210	0.0742	0.0005	0.1065	0.0010	1.8494	0.0225	0.1807	0.0018	0.82	1071	10	1063	8	1047	13	-2.3		
	91500		81	28	15	0.35	0.4	0.06	0.0000308	0.0740	0.0006	0.1068	0.0012	1.8330	0.0228	0.1795	0.0017	0.74	1065	9	1057	8	1042	16	-2.2		
	91500		81	28	15	0.36	0.0	0.00	0.0000001	0.0755	0.0006	0.1094	0.0007	1.8665	0.0252	0.1793	0.0019	0.77	1063	10	1069	9	1081	17	1.6		
	91500		81	28	15	0.36	0.0	0.00	0.0000001	0.0746	0.0007	0.1082	0.0010	1.8533	0.0252	0.1802	0.0017	0.71	1068	10	1065	9	1056	20	-1.2		
	91500		82	29	15	0.36	0.0	0.01	0.0000028	0.0743	0.0007	0.1069	0.0008	1.8233	0.0245	0.1780	0.0016	0.67	1056	9	1054	9	1049	20	-0.7		
	91500		82	29	15	0.36	0.0	0.00	0.0000001	0.0751	0.0007	0.1072	0.0005	1.8664	0.0249	0.1803	0.0016	0.68	1068	9	1069	9	1070	20	0.1		

sample	analysis no.	grain no.	U ppm	Th ppm	Pb ppm	Th/U	^{204}Pb ppb	f206 (%)	^{204}Pb/^{206}Pb	corrected ratios									Ages (Ma)								grain area	comment
										^{207}Pb/^{206}Pb	1σ	^{208}Pb/^{206}Pb	1σ	^{207}Pb/^{235}U	1σ	^{206}Pb/^{238}U	1σ	ρ	^{206}Pb/^{238}U	1σ	^{207}Pb/^{235}U	1σ	^{207}Pb/^{206}Pb	1σ	% disc			
	91500		80	28	15	0.36	0.3	0.04	0.0000234	0.0745	0.0007	0.1066	0.0010	1.8475	0.0235	0.1799	0.0016	0.69	1067	9	1063	8	1054	17	-1.2		
	91500		81	28	15	0.36	0.0	0.01	0.0000028	0.0742	0.0006	0.1075	0.0007	1.8109	0.0231	0.1769	0.0017	0.73	1050	9	1049	8	1048	17	-0.2		
	91500		82	29	15	0.36	0.0	0.00	0.0000001	0.0751	0.0007	0.1084	0.0008	1.8391	0.0247	0.1776	0.0016	0.69	1054	9	1060	9	1071	19	1.6		
	91500		83	29	15	0.36	0.0	0.00	0.0000001	0.0748	0.0006	0.1087	0.0009	1.8337	0.0221	0.1779	0.0017	0.77	1055	9	1058	8	1062	15	0.6		
	91500		83	29	15	0.36	0.0	0.00	0.0000001	0.0758	0.0009	0.1081	0.0012	1.8784	0.0295	0.1798	0.0018	0.62	1066	10	1074	10	1088	24	2.0		
	91500		82	29	15	0.36	0.5	0.07	0.0000397	0.0738	0.0006	0.1063	0.0014	1.8451	0.0229	0.1814	0.0016	0.71	1075	9	1062	8	1035	16	-3.8		
	91500		80	28	15	0.35	0.0	0.00	0.0000001	0.0752	0.0007	0.1070	0.0009	1.8848	0.0242	0.1818	0.0017	0.71	1077	9	1076	8	1073	18	-0.3		
	91500		80	28	15	0.36	0.1	0.02	0.0000120	0.0747	0.0007	0.1072	0.0008	1.8564	0.0244	0.1803	0.0018	0.74	1069	10	1066	9	1059	18	-0.9		
	91500		81	28	15	0.36	0.5	0.08	0.0000412	0.0742	0.0007	0.1061	0.0012	1.8234	0.0240	0.1782	0.0017	0.71	1057	9	1054	9	1046	17	-1.1		
	91500		82	29	15	0.36	0.0	0.00	0.0000001	0.0742	0.0005	0.1068	0.0008	1.8436	0.0219	0.1801	0.0017	0.80	1068	9	1061	8	1047	14	-2.0		
	91500		81	28	15	0.36	0.0	0.00	0.0000001	0.0747	0.0008	0.1073	0.0007	1.8485	0.0245	0.1795	0.0015	0.65	1064	8	1063	9	1059	21	-0.5		
	91500		79	27	14	0.35	0.0	0.00	0.0000001	0.0745	0.0005	0.1073	0.0010	1.8187	0.0201	0.1770	0.0016	0.82	1051	9	1052	7	1055	13	0.4		
	91500		80	28	15	0.35	0.0	0.01	0.0000027	0.0744	0.0007	0.1075	0.0004	1.8175	0.0232	0.1772	0.0016	0.71	1052	9	1052	8	1052	18	0.0		
	91500		81	28	15	0.35	0.4	0.06	0.0000326	0.0751	0.0007	0.1065	0.0012	1.8482	0.0242	0.1786	0.0016	0.68	1059	9	1063	9	1070	18	1.0		
	91500		84	29	15	0.36	0.3	0.04	0.0000224	0.0738	0.0010	0.1078	0.0012	1.8248	0.0287	0.1793	0.0016	0.57	1063	9	1054	10	1036	25	-2.6		
	91500		80	28	15	0.35	0.0	0.01	0.0000029	0.0751	0.0007	0.1067	0.0008	1.8675	0.0241	0.1804	0.0017	0.73	1069	9	1070	8	1070	17	0.1		
	91500		80	27	15	0.35	0.6	0.09	0.0000468	0.0746	0.0009	0.1065	0.0015	1.8341	0.0277	0.1783	0.0016	0.60	1058	9	1058	10	1057	23	-0.1		
	91500		81	29	15	0.36	0.0	0.00	0.0000001	0.0756	0.0009	0.1085	0.0011	1.8676	0.0378	0.1792	0.0029	0.79	1062	16	1070	13	1084	25	2.0		
	91500		83	29	15	0.36	0.5	0.08	0.0000405	0.0747	0.0007	0.1066	0.0014	1.8764	0.0268	0.1821	0.0019	0.72	1078	10	1073	9	1061	18	-1.6		
	91500		85	29	16	0.36	0.1	0.01	0.0000072	0.0754	0.0008	0.1069	0.0009	1.9060	0.0262	0.1832	0.0017	0.67	1085	9	1083	9	1080	20	-0.4		
	91500		80	28	15	0.35	0.4	0.05	0.0000283	0.0735	0.0007	0.1059	0.0013	1.8569	0.0256	0.1832	0.0018	0.72	1085	10	1066	9	1027	18	-5.6		
	91500		81	28	15	0.36	0.0	0.00	0.0000001	0.0749	0.0011	0.1053	0.0009	1.8544	0.0338	0.1795	0.0018	0.56	1064	10	1065	12	1066	31	0.2		
	91500		80	28	15	0.35	0.0	0.00	0.0000001	0.0743	0.0006	0.1081	0.0011	1.8304	0.0261	0.1787	0.0020	0.79	1060	11	1056	9	1048	18	-1.1		
	91500		83	29	15	0.36	0.5	0.07	0.0000362	0.0758	0.0008	0.1070	0.0016	1.8765	0.0282	0.1795	0.0018	0.67	1064	10	1073	10	1090	21	2.4		
	91500		83	29	15	0.36	0.6	0.09	0.0000475	0.0733	0.0008	0.1070	0.0015	1.8039	0.0277	0.1786	0.0018	0.67	1059	10	1047	10	1020	21	-3.9		
	91500		84	29	16	0.36	0.0	0.00	0.0000001	0.0748	0.0006	0.1083	0.0010	1.8725	0.0248	0.1816	0.0019	0.79	1076	10	1071	9	1062	16	-1.3		
	91500		82	28	15	0.35	0.2	0.03	0.0000168	0.0759	0.0007	0.1070	0.0009	1.8797	0.0244	0.1797	0.0017	0.71	1065	9	1074	9	1091	17	2.3		
	91500		82	28	15	0.35	0.4	0.05	0.0000283	0.0743	0.0008	0.1068	0.0012	1.8441	0.0260	0.1800	0.0017	0.69	1067	10	1061	9	1050	19	-1.6		
	91500		80	28	15	0.36	0.4	0.06	0.0000300	0.0750	0.0009	0.1086	0.0013	1.8492	0.0284	0.1789	0.0018	0.64	1061	10	1063	10	1067	22	0.6		
	91500		80	28	14	0.36	0.0	0.00	0.0000001	0.0747	0.0008	0.1071	0.0010	1.8105	0.0269	0.1759	0.0017	0.65	1045	9	1049	10	1059	22	1.4		
	91500		76	26	14	0.35	0.4	0.06	0.0000319	0.0754	0.0007	0.1070	0.0012	1.8625	0.0254	0.1793	0.0017	0.69	1063	9	1068	9	1077	19	1.3		
	91500		80	28	15	0.36	0.6	0.09	0.0000463	0.0736	0.0009	0.1052	0.0015	1.8226	0.0300	0.1795	0.0019	0.64	1065	10	1054	11	1031	23	-3.3		
	91500		78	27	14	0.35	0.0	0.00	0.0000001	0.0746	0.0010	0.1083	0.0011	1.7915	0.0302	0.1742	0.0019	0.65	1035	10	1042	11	1057	26	2.1		
	91500		81	28	15	0.36	0.0	0.00	0.0000001	0.0741	0.0009	0.1073	0.0010	1.8001	0.0290	0.1763	0.0018	0.62	1047	10	1046	10	1042	26	-0.5		
	91500		82	29	15	0.36	0.0	0.00	0.0000001	0.0740	0.0009	0.1081	0.0009	1.7955	0.0283	0.1759	0.0017	0.62	1044	9	1044	10	1042	25	-0.2		
	91500		82	29	15	0.36	0.3	0.04	0.0000207	0.0747	0.0007	0.1082	0.0012	1.8439	0.0259	0.1789	0.0019	0.74	1061	10	1061	9	1061	18	0.0		
	91500		79	28	14	0.36	0.2	0.03	0.0000147	0.0749	0.0006	0.1097	0.0009	1.8427	0.0259	0.1783	0.0020	0.80	1058	11	1061	9	1066	16	0.8		
	91500		81	28	15	0.36	0.7	0.10	0.0000536	0.0766	0.0008	0.1061	0.0016	1.8813	0.0284	0.1782	0.0020	0.73	1057	11	1075	10	1109	19	4.7		
	91500		81	28	15	0.36	0.0	0.00	0.0000001	0.0741	0.0008	0.1087	0.0010	1.8234	0.0283	0.1784	0.0019	0.70	1058	11	1054	10	1044	22	-1.4		
	91500		83	29	15	0.36	0.0	0.00	0.0000001	0.0757	0.0007	0.1084	0.0011	1.8966	0.0288	0.1817	0.0021	0.76	1076	11	1080	10	1087	19	1.0		
Session 1	temora		106	53	7	0.51	0.3	0.11	0.0000573	0.0542	0.0007	0.1625	0.0019	0.4785	0.0076	0.0640	0.0006	0.57	400	4	397	5	378	24	-5.9		
	temora		114	57	8	0.51	0.1	0.02	0.0000132	0.0554	0.0007	0.1593	0.0012	0.5185	0.0089	0.0678	0.0008	0.67	423	5	424	6	430	27	1.6		

sample	analysis no.	grain no.	U ppm	Th ppm	Pb ppm	Th/U	^{204}Pb ppb	f206 (%)	^{204}Pb/^{206}Pb	corrected ratios									Ages (Ma)								grain area	comment
										^{207}Pb/^{206}Pb	1σ	^{208}Pb/^{206}Pb	1σ	^{207}Pb/^{235}U	1σ	^{206}Pb/^{238}U	1σ	ρ	^{206}Pb/^{238}U	1σ	^{207}Pb/^{235}U	1σ	^{207}Pb/^{206}Pb	1σ	% disc		
July 2005	temora		118	59	8	0.51	0.1	0.02	0.0000126	0.0566	0.0008	0.1588	0.0011	0.5125	0.0093	0.0657	0.0008	0.66	410	5	420	6	476	29	13.9		
	temora		105	55	7	0.54	0.0	0.00	0.0000001	0.0540	0.0007	0.1671	0.0011	0.4950	0.0089	0.0665	0.0008	0.64	415	5	408	6	370	31	-12.2		
	temora		117	58	8	0.51	0.0	0.00	0.0000001	0.0552	0.0009	0.1578	0.0011	0.5131	0.0096	0.0674	0.0006	0.50	421	4	421	6	420	36	-0.1		
	temora		102	51	7	0.51	0.2	0.06	0.0000335	0.0543	0.0008	0.1604	0.0019	0.5100	0.0088	0.0682	0.0007	0.58	425	4	418	6	382	28	-11.3		
	temora		104	52	7	0.51	0.0	0.00	0.0000001	0.0564	0.0005	0.1612	0.0012	0.5200	0.0071	0.0669	0.0006	0.70	417	4	425	5	468	21	10.9		
	temora		110	58	8	0.55	0.0	0.00	0.0000001	0.0540	0.0005	0.1708	0.0012	0.4993	0.0063	0.0670	0.0006	0.72	418	4	411	4	371	20	-12.7		
	temora		109	54	7	0.51	0.2	0.07	0.0000378	0.0555	0.0011	0.1579	0.0022	0.4998	0.0116	0.0653	0.0007	0.46	408	4	412	8	434	43	6.1		
	temora		290	89	19	0.31	0.2	0.02	0.0000122	0.0544	0.0005	0.0987	0.0009	0.5009	0.0066	0.0668	0.0006	0.70	417	4	412	4	386	21	-8.0		
	temora		111	50	8	0.46	0.0	0.00	0.0000002	0.0548	0.0012	0.1428	0.0013	0.5097	0.0115	0.0674	0.0006	0.36	421	3	418	8	405	46	-3.9		
	temora		152	67	11	0.45	0.0	0.00	0.0000001	0.0555	0.0007	0.1414	0.0008	0.5120	0.0079	0.0669	0.0006	0.56	418	3	420	5	432	28	3.3		
	temora		81	39	6	0.49	0.0	0.00	0.0000002	0.0555	0.0007	0.1525	0.0012	0.5188	0.0088	0.0678	0.0007	0.61	423	4	424	6	432	29	2.1		
	temora		164	72	11	0.45	0.0	0.00	0.0000001	0.0562	0.0006	0.1412	0.0009	0.5212	0.0066	0.0672	0.0005	0.63	420	3	426	4	460	22	8.8		
	temora		86	27	6	0.32	0.0	0.00	0.0000001	0.0565	0.0009	0.1021	0.0011	0.5190	0.0101	0.0666	0.0007	0.52	416	4	425	7	473	36	12.1		
	temora		81	25	6	0.32	0.2	0.07	0.0000373	0.0540	0.0010	0.0981	0.0014	0.5073	0.0106	0.0682	0.0006	0.42	425	4	417	7	369	39	-15.2		
	temora		92	28	6	0.31	0.0	0.00	0.0000001	0.0553	0.0008	0.0981	0.0010	0.5047	0.0090	0.0661	0.0006	0.52	413	4	415	6	426	33	3.1		
	temora		283	88	19	0.32	0.4	0.05	0.0000251	0.0554	0.0005	0.0995	0.0010	0.5248	0.0067	0.0687	0.0006	0.63	428	3	428	4	428	21	-0.1		
	temora		406	131	28	0.33	0.0	0.00	0.0000000	0.0560	0.0003	0.1031	0.0006	0.5320	0.0054	0.0689	0.0006	0.83	430	4	433	4	451	13	4.7		
	temora		283	93	20	0.34	0.0	0.00	0.0000001	0.0560	0.0004	0.1055	0.0008	0.5317	0.0057	0.0689	0.0006	0.76	430	3	433	4	450	16	4.5		
	temora		172	42	12	0.25	0.0	0.00	0.0000001	0.0553	0.0006	0.0786	0.0006	0.5222	0.0128	0.0685	0.0015	0.89	427	9	427	8	422	25	-1.3		
	temora		203	105	14	0.53	0.3	0.05	0.0000245	0.0547	0.0009	0.1630	0.0015	0.5073	0.0099	0.0673	0.0008	0.58	420	5	417	7	398	34	-5.5		
	temora		190	98	14	0.53	0.4	0.07	0.0000382	0.0543	0.0006	0.1661	0.0014	0.5051	0.0077	0.0675	0.0007	0.64	421	4	415	5	383	23	-9.9		
	temora		192	82	13	0.44	0.2	0.03	0.0000174	0.0549	0.0004	0.1360	0.0011	0.5062	0.0057	0.0669	0.0005	0.72	418	3	416	4	406	16	-2.8		
	temora		354	130	24	0.38	0.9	0.08	0.0000416	0.0547	0.0005	0.1164	0.0011	0.5080	0.0058	0.0674	0.0005	0.69	420	3	417	4	398	16	-5.6		
	temora		272	105	19	0.40	2.3	0.26	0.0001412	0.0551	0.0011	0.1186	0.0030	0.5298	0.0115	0.0698	0.0007	0.47	435	4	432	8	414	34	-5.0		
Session 3 March 2006	temora		624	335	44	0.55	1.9	0.10	0.0000537	0.0548	0.0004	0.1713	0.0011	0.5049	0.0058	0.0669	0.0006	0.73	417	3	415	4	403	15	-3.5		
	temora		630	319	44	0.52	0.4	0.02	0.0000119	0.0553	0.0004	0.1607	0.0008	0.5055	0.0053	0.0664	0.0006	0.79	414	3	415	4	422	14	1.9		
	temora		164	39	11	0.25	1.0	0.19	0.0001012	0.0540	0.0007	0.0740	0.0021	0.5036	0.0082	0.0676	0.0006	0.55	422	4	414	6	372	24	-13.3		
	temora		150	46	10	0.31	0.1	0.03	0.0000152	0.0553	0.0007	0.0975	0.0008	0.5104	0.0078	0.0669	0.0006	0.61	417	4	419	5	425	26	1.8		
	temora		199	58	13	0.30	0.8	0.13	0.0000713	0.0555	0.0006	0.0916	0.0017	0.5103	0.0074	0.0667	0.0006	0.59	416	3	419	5	432	22	3.7		
	temora		162	41	10	0.26	0.6	0.12	0.0000651	0.0550	0.0007	0.0787	0.0017	0.4908	0.0073	0.0648	0.0006	0.59	404	3	405	5	410	22	1.3		
	temora		224	64	15	0.29	0.0	0.00	0.0000001	0.0555	0.0006	0.0921	0.0007	0.5022	0.0070	0.0656	0.0006	0.65	410	4	413	5	433	24	5.4		
	temora		176	49	11	0.29	0.2	0.03	0.0000154	0.0554	0.0007	0.0882	0.0010	0.4914	0.0079	0.0644	0.0006	0.55	402	3	406	5	426	29	5.6		
	temora		178	45	11	0.26	0.0	0.00	0.0000001	0.0548	0.0007	0.0821	0.0007	0.4937	0.0074	0.0653	0.0006	0.60	408	4	407	5	404	27	-1.0		
	temora		188	66	13	0.36	0.4	0.07	0.0000400	0.0551	0.0005	0.1098	0.0015	0.5019	0.0066	0.0660	0.0006	0.71	412	4	413	4	416	17	0.9		
	temora		165	65	11	0.40	0.4	0.07	0.0000373	0.0560	0.0006	0.1243	0.0020	0.5094	0.0073	0.0659	0.0006	0.61	412	3	418	5	453	22	9.1		
	temora		171	85	12	0.51	0.5	0.09	0.0000490	0.0536	0.0006	0.1565	0.0014	0.4796	0.0067	0.0649	0.0005	0.58	405	3	398	5	354	22	-14.5		
	temora		126	38	8	0.31	0.9	0.25	0.0001341	0.0521	0.0010	0.0907	0.0029	0.4650	0.0098	0.0648	0.0006	0.41	405	3	388	7	287	34	-41.0		
	temora		132	54	9	0.42	0.7	0.16	0.0000870	0.0536	0.0008	0.1292	0.0026	0.4946	0.0087	0.0669	0.0006	0.50	417	4	408	6	356	26	-17.2		
	temora		151	72	11	0.49	0.3	0.07	0.0000364	0.0554	0.0013	0.1499	0.0017	0.5106	0.0148	0.0669	0.0011	0.57	417	7	419	10	427	50	2.3		
	temora		114	34	8	0.31	0.0	0.00	0.0000002	0.0564	0.0009	0.0965	0.0009	0.5164	0.0101	0.0664	0.0007	0.55	414	4	423	7	469	36	11.7		
	temora		109	29	7	0.27	0.4	0.12	0.0000649	0.0542	0.0012	0.0796	0.0021	0.4971	0.0117	0.0665	0.0007	0.42	415	4	410	8	380	41	-9.2		
	temora		60	21	4	0.37	0.6	0.34	0.0001832	0.0540	0.0019	0.1110	0.0048	0.4945	0.0192	0.0664	0.0010	0.38	414	6	408	13	372	59	-11.4		
	temora		80	27	5	0.35	0.7	0.28	0.0001512	0.0544	0.0014	0.1065	0.0039	0.4898	0.0140	0.0653	0.0007	0.37	408	4	405	9	386	45	-5.7		
	temora		47	16	3	0.36	0.0	0.00	0.0000004	0.0564	0.0009	0.1141	0.0022	0.5085	0.0100	0.0654	0.0007	0.57	409	4	417	7	466	36	12.3		
	temora		66	23	4	0.36	0.1	0.03	0.0000182	0.0569	0.0011	0.1158	0.0017	0.5191	0.0117	0.0661	0.0008	0.52	413	5	425	8	488	39	15.4		
	temora		91	50	6	0.56	2.0	0.76	0.0004101	0.0516	0.0017	0.1506	0.0070	0.4555	0.0153	0.0640	0.0007	0.31	400	4	381	11	267	43	-49.8		
	temora		128	61	9	0.49	0.9	0.23	0.0001259	0.0537	0.0012	0.1446	0.0031	0.4881	0.0117	0.0659	0.0007	0.42	411	4	404	8	359	39	-14.6		
	temora		94	46	6	0.50	0.8	0.30	0.0001599	0.0534	0.0013	0.1509	0.0037	0.4790	0.0126	0.0650	0.0008	0.45	406	5	397	9	346	39	-17.4		
	temora		132	54	9	0.42	0.7	0.16	0.0000870	0.0536	0.0008	0.1292	0.0026	0.4946	0.0087	0.0669	0.0006	0.50	417	4	408	6	356	26	-17.2		
	temora		151	72	11	0.49	0.3	0.07	0.0000364	0.0554	0.0013	0.1499	0.0017	0.5106	0.0148	0.0669	0.0011	0.57	417	7	419	10	427	50	2.3		
	temora		114	34	8	0.31	0.0	0.00	0.0000002	0.0564	0.0009	0.0965	0.0009	0.5164	0.0101	0.0664	0.0007	0.55	414	4	423	7	469	36	11.7		
	temora		109	29	7	0.27	0.4	0.12	0.0000649	0.0542	0.0012	0.0796	0.0021	0.4971	0.0117	0.0665	0.0007	0.42	415	4	410	8	380	41	-9.2		
	temora		60	21	4	0.37	0.6	0.34	0.0001832	0.0540	0.0019	0.1110	0.0048	0.4945	0.0192	0.0664	0.0010	0.38	414	6	408	13	372	59	-11.4		
	temora		80	27	5	0.35	0.7	0.28	0.0001512	0.0544	0.0014	0.1065	0.0039	0.4898	0.0140	0.0653	0.0007	0.37	408	4	405	9	386	45	-5.7		
	temora		47	16	3	0.36	0.0	0.00	0.0000004	0.0564	0.0009	0.1141	0.0022	0.5085	0.0100	0.0654	0.0007	0.57	409	4	417	7	466	36	12.3		
	temora		66	23	4	0.36	0.1	0.03	0.0000182	0.0569	0.0011	0.1158	0.0017	0.5191	0.0117	0.0661	0.0008	0.52	413	5	425	8	488	39	15.4		
	temora		91	50	6	0.56	2.0	0.76	0.0004101	0.0516	0.0017	0.1506	0.0070	0.4555	0.0153	0.0640	0.0007	0.31	400	4	381	11	267	43	-49.8		
	temora		128	61	9	0.49	0.9	0.23	0.0001259	0.0537	0.0012	0.1446	0.0031	0.4881	0.0117	0.0659	0.0007	0.42	411	4	404	8	359	39	-14.6		
	temora		94	46	6	0.50	0.8	0.30	0.0001599	0.0534	0.0013	0.1509	0.0037	0.4790	0.0126	0.0650	0.0008	0.45	406	5	397	9	346	39	-17.4		

Appendix 2g
Zircon trace element/REE data of the Etive pluton

	St-01											St-05											Cr-15	
	SA05/01 4a	SA05/01 5b	SA05/01 5c	SA05/01 11c	SA05/01 13a	SA05/01 13b	SA05/01 18a	SA05/01 18b	SA05/01 19b	SA05/01 20a	SA05/01 14a	SA05/05 9a	SA05/05 10a	SA05/05 10b	SA05/05 11b	SA05/05 11c	SA05/05 14c	SA05/05 14b	SA05/05 23a	SA05/05 18a	SA05/05 18b	SA05/05 7a	SA05/15 2a	SA05/15 4b
grain no.	4	5	5	11	13	13	18	18	19	20	14	9	10	10	11	11	14	14	23	18	18	7	2	4
Si	140230	140230	140230	140230	140230	140230	140230	140230	140230	140230	140230	140230	140230	140230	140230	140230	140230	140230	140230	140230	140230	140230	140230	140230
P	507	291	315	304	204	90	292	144	207	197	313	207	142	338	3014	272	41	138	111	234	85	335	241	169
Ca	5	10	686	21	4	12	5	6	5	6	5	13	8	8	5104	18	4	10	4	6	8	252	11	13
Ti	2.10	3.10	9.58	9.74	2.97	3.88	2.96	3.81	2.84	3.63	6	3.59	3.79	5.08	2.76	5.32	1.49	3.05	2.20	2.09	2.35	3	26.52	9.56
Y	1199	669	2363	1418	981	637	764	602	401	664	980	990	599	654	640	1283	208	571	477	462	336	483	857	400
Nb	10	3	30	14	2	4	5	5	3	4	4	8	4	2	1	8	1	4	4	3	2	2	0	0
Zr	521700	548100	528880	513150	530840	526990	538900	542070	531220	537430	524950	530690	518950	528790	525550	538180	553490	540890	535530	530850	560550	517320	558360	567400
Ba	0.0	0.1	12.6	0.3	0.0	0.1	0.2	0.1	0.1	0.1	0	0.2	0.1	0.1	0.7	0.1	0.0	0.0	0.1	0.2	0.1	0	2.4	0.2
La	0.1	0.0	5.6	2.4	0.0	0.7	0.1	0.1	0.0	0.0	0	0.1	1.0	0.3	24.7	0.2	0.0	0.0	0.1	0.0	0.0	1	0.1	0.0
Ce	45.0	34.9	139.8	108.7	43.2	29.5	47.5	38.2	24.1	39.9	55	73.7	55.3	31.0	85.4	85.9	14.9	37.0	46.4	26.4	31.6	34	19.2	30.2
Pr	0.1	0.1	3.3	2.4	0.2	0.3	0.1	0.1	0.0	0.0	0	0.1	0.3	0.1	6.0	0.2	0.0	0.1	0.1	0.0	0.0	0	0.5	0.1
Nd	0.9	1.5	18.1	16.3	2.5	2.0	0.9	1.2	0.6	1.0	2	1.1	2.0	1.3	27.1	2.5	0.1	0.8	0.8	0.6	0.4	3	7.0	1.2
Sm	1.7	2.6	6.8	6.8	4.7	2.0	2.4	2.2	1.6	2.2	4	2.4	2.0	2.4	6.5	4.3	0.4	1.5	1.0	1.2	1.1	1	8.2	2.1
Eu	0.4	0.8	1.2	0.9	1.3	0.6	0.8	0.6	0.3	0.6	1	0.7	0.5	0.7	1.4	1.5	0.2	0.6	0.4	0.4	0.3	0	3.3	0.8
Gd	13	16	29	24	24	10	13	11	7	13	22	14	9	12	16	24	2	9	7	7	5	7	29	10
Tb	5	5	11	8	7	4	5	4	3	5	8	5	3	4	5	9	1	4	2	3	2	3	10	3
Dy	74	63	149	111	91	48	63	49	32	59	94	73	44	56	61	117	12	44	33	35	27	38	105	42
Ho	35	25	70	46	33	19	25	21	13	24	36	32	19	22	23	47	6	19	15	15	11	16	36	16
Er	212	128	425	246	163	109	141	113	73	126	178	182	107	114	114	235	37	105	84	88	61	87	157	76
Tm	56	29	111	60	38	29	35	28	18	29	40	45	27	27	27	53	10	26	22	22	15	21	32	16
Yb	548	274	1120	513	323	290	322	272	171	268	324	428	255	237	221	449	114	258	222	212	152	200	255	141
Lu	156	70	307	137	85	87	90	76	47	69	82	119	73	62	57	110	36	71	64	59	44	52	58	35
Hf	13522	12831	15599	12286	12010	13889	12173	11838	11708	11857	9635	11990	12037	10244	12106	10965	15431	12350	13426	11939	14392	11337	9026	11029
Th	528	118	1307	1078	179	203	186	99	69	91	103	293	220	108	112	205	59	106	369	80	188	75	67	51
U	1372	275	3059	1643	302	411	446	253	178	220	165	585	420	216	207	362	192	269	587	200	381	184	60	71
	Normalised to chondrite (using values from Anders and Grevesse, 1989)																							
La	0.43	0.15	23.91	10.14	0.20	3.14	0.21	0.28	0.08	0.13	0.22	0.23	4.41	1.29	105.28	0.82	0.05	0.17	0.43	0.21	0.11	6.36	0.42	0.21
Ce	74.6	57.9	231.7	180.3	71.6	48.9	78.7	63.4	39.9	66.1	91.9	122.2	91.6	51.4	141.5	142.5	24.7	61.4	76.9	43.8	52.4	55.8	31.8	50.1
Pr	0.94	0.98	37.01	26.59	1.80	3.45	0.80	0.82	0.39	0.51	1.13	1.03	3.76	1.17	67.70	2.18	0.22	0.69	0.86	0.48	0.46	4.45	5.50	0.96
Nd	2.02	3.35	40.06	35.97	5.62	4.52	1.93	2.60	1.34	2.13	4.47	2.39	4.53	2.94	59.92	5.42	0.31	1.86	1.82	1.36	0.98	5.80	15.48	2.55
Sm	12	18	46	46	32	14	16	15	11	15	27	16	14	16	44	30	2	10	7	8	7	10	56	14
Eu	6	15	21	16	23	11	14	11	6	11	22	13	10	13	25	26	3	10	8	8	6	7	60	14
Gd	67	80	149	122	123	52	67	55	35	65	113	70	44	63	79	121	11	47	35	33	28	38	149	50
Tb	146	139	290	233	206	101	130	103	69	125	215	145	89	123	140	246	24	99	67	71	55	76	271	96
Dy	305	262	613	458	375	196	259	201	132	244	386	302	182	232	252	484	51	183	135	144	112	156	431	172
Ho	635	441	1265	828	601	347	457	379	239	426	649	580	348	402	411	840	104	344	263	271	198	282	643	281
Er	1334	804	2675	1547	1024	689	890	710	458	790	1120	1143	671	717	721	1481	231	659	529	551	382	546	986	478
Tm	2326	1210	4591	2468	1558	1181	1446	1158	730	1196	1638	1854	1121	1114	1101	2197	431	1074	901	910	636	878	1329	659
Yb	3371	1687	6894	3156	1985	1786	1984	1671	1050	1648	1992	2633	1569	1461	1359	2764	703	1588	1364	1306	938	1229	1572	867
Lu	6428	2868	12626	5643	3482	3598	3699	3145	1933	2831	3359	4886	2994	2567	2348	4516	1479	2902	2620	2427	1821	2150	2383	1424
Hf	1300192	1233750	1499904	1181346	1154808	1335481	1170481	1138269	1125769	1140096	926481	1152885	1157404	985000	1164038	1054327	1483750	1187500	1290962	1147981	1383846	1090096	867885	1060481
Th	214	48	529	437	72	82	75	40	28	37	42	119	89	44	46	83	24	43	150	32	76	30	27	21
U	169420	34000	377667	202889	37335	50696	55121	31231	21996	27167	20330	72240	51846	26700	25578	44635	23691	33210	72472	24740	46991	22733	7432	8752
Th/U	0.39	0.43	0.43	0.66	0.59	0.49	0.42	0.39	0.38	0.41	0.63	0.50	0.52	0.50	0.54	0.57	0.31	0.39	0.63	0.40	0.49	0.41	1.11	0.72
Yb(n)/La(n)	7846	11024	288	311	9921	568	9291	6005	13800	12796	8949	11231	355	1133	13	3352	15320	9565	3180	6200	8225	193	3737	4112
Yb(n/Gd(n)	50.5	21.1	46.2	25.9	16.2	34.3	29.5	30.7	30.2	25.5	17.6	37.5	35.4	23.3	17.2	22.9	62.7	34.1	39.5	39.5	34.1	32.5	10.5	17.2
Eu/Eu*	0.2	0.4	0.3	0.2	0.4	0.4	0.4	0.4	0.3	0.4	0.4	0.4	0.4	0.4	0.4	0.4	0.6	0.5	0.5	0.5	0.4	0.4	0.7	0.5
Ce/Ce*	117.3	149.8	7.8	11.0	119.3	14.8	190.2	132.7	231.0	257.8	183.3	248.4	22.5	41.9	1.7	106.2	243.5	180.9	126.5	137.6	229.6	10.5	20.9	111.2
HfO_2 [wt%]	1.6	1.5	1.8	1.4	1.4	1.6	1.4	1.4	1.4	1.4	1.1	1.4	1.4	1.2	1.4	1.3	1.8	1.5	1.6	1.4	1.7	1.3	1.1	1.3
comment			rejected, inclusion	rejected, inclusion											rejected, inclusion							rejected, inclusion		
grain area	c1	c1	rim	rim	c2	rim	c2a	c2b	rim	c2	rim	c2	c2	rim	rim	c2b	r1a	r1b	c2	c1	c2	rim	c1	inh1

											Cr-26											**Q-23**			
	SA05/15 4a	SA05/15 8a	SA05/15 9a	SA05/15 11a	SA05/15 11b	SA05/15 19a	SA05/15 19b	SA05/15 22a	SA05/15 22b	SA05/15 26a	SA05/26 5a	SA05/26 6a	SA05/26 6b	SA05/26 12a	SA05/26 16a	SA05/26 16b	SA05/26 20c	SA05/26 20b	SA05/26 27a	SA05/26 27b	SA05/23 5a	SA05/23 8a	SA05/23 9a	SA05/23 10a
grain no.	4	8	9	11	11	19	19	22	22	26	5	6	6	12	16	16	20	20	27	27	5	8	9	10
Si	140230	140230	140230	140230	140230	140230	140230	140230	140230	140230	140230	140230	140230	140230	140230	140230	140230	140230	140230	140230	140230	140230	140230	140230	140230	140230
P	470	307	161	298	349	205	252	246	331	392	812	406	284	285	281	262	273	131	162	473	538	769	439	337
Ca	21	20	9	16	5	87	5	6	7	2	17	13	6	14	13	3	5	5	5	28	5	6	5	12
Ti	35.29	21.89	6.28	16.54	8.64	36.90	9.60	10.44	11.99	4.76	12	11.14	8.74	15.68	12.00	7.42	10.95	7.73	7.42	7.85	11	17.69	22.03	13.43
Y	827	658	657	911	519	1090	723	1234	886	1195	3909	1184	651	566	819	843	1147	266	394	2190	2948	4027	1933	744
Nb	2	3	2	2	1	1	1	2	2	6	42	3	2	2	2	3	1	1	1	21	5	6	2	1
Zr	569060	570070	565580	567410	543560	535940	533740	526830	528090	596670	556790	549980	531160	544370	576150	558510	558140	556240	570300	532030	542230	533380	536270	549350
Ba	0.1	0.2	0.1	0.0	0.1	6.3	0.0	0.0	0.0	0.0	0	0.2	0.1	0.1	0.1	0.1	0.1	0.0	-0.1	0.7	0	0.0	0.1	0.2
La	0.0	0.0	0.0	0.0	0.0	0.1	0.0	0.1	0.1	0.1	0	0.1	0.0	0.0	0.0	0.0	0.2	0.0	0.0	8.5	0	0.5	0.2	0.0
Ce	21.6	35.7	42.0	39.1	25.1	41.2	31.7	36.7	37.2	80.2	282	89.6	52.0	30.7	52.9	56.8	39.3	25.2	25.6	182.5	90	91.0	39.3	44.7
Pr	0.2	0.1	0.1	0.2	0.1	0.5	0.2	0.5	0.2	0.1	0	0.3	0.1	0.2	0.2	0.1	0.5	0.0	0.1	1.6	1	1.5	1.3	0.1
Nd	2.9	1.7	1.9	3.2	1.3	8.5	3.0	8.2	2.6	2.2	5	4.9	2.6	2.9	3.1	1.8	8.1	0.5	1.0	11.1	13	18.3	11.8	2.7
Sm	5.3	3.0	3.6	4.8	1.8	9.2	4.2	8.5	4.4	4.0	13	6.6	3.7	3.0	4.4	3.0	9.4	1.1	2.0	8.7	16	23.7	13.5	4.0
Eu	1.3	0.6	1.1	1.6	0.9	3.3	1.5	3.0	1.3	1.3	2	2.2	1.3	1.1	1.7	1.1	3.2	0.4	0.7	1.2	2	3.3	2.1	0.6
Gd	24	15	17	20	11	38	18	38	18	14	79	29	16	15	22	17	39	6	9	49	84	134	65	20
Tb	8	6	6	7	4	12	6	12	7	9	32	10	6	5	7	6	12	2	3	18	27	42	19	7
Dy	94	67	69	89	52	132	76	140	82	117	412	126	65	57	84	72	129	25	36	220	309	466	214	78
Ho	33	25	25	36	19	44	28	48	33	46	155	47	24	21	32	27	45	11	14	83	112	160	76	29
Er	145	123	125	183	95	197	132	218	165	237	740	222	116	101	156	129	200	50	73	398	508	692	331	135
Tm	30	28	26	41	21	40	29	45	37	55	156	48	25	23	34	28	41	12	17	85	100	136	65	29
Yb	238	238	219	352	175	312	234	344	308	495	1262	395	195	194	295	243	317	100	161	698	773	1012	501	240
Lu	53	57	52	87	45	74	59	84	78	121	277	92	49	48	72	55	74	25	39	155	168	217	111	56
Hf	12318	12413	12606	9711	10225	9685	9505	9005	8989	14103	14324	10134	10140	9045	10606	11856	10168	11270	11825	13568	12929	10685	10105	11977
Th	14	71	81	92	44	128	66	130	82	286	2680	386	123	69	129	136	122	30	88	1550	922	1261	355	198
U	30	86	110	126	63	105	78	114	110	473	2933	300	131	82	157	178	116	48	155	1718	786	889	319	269
La	0.17	0.18	0.15	0.20	0.10	0.48	0.20	0.26	0.26	0.22	0.60	0.33	0.20	0.13	0.17	0.20	0.81	0.10	0.06	36.19	0.49	2.22	0.68	0.10
Ce	35.8	59.2	69.6	64.8	41.6	68.3	52.5	60.9	61.6	132.9	466.8	148.6	86.2	50.9	87.7	94.2	65.1	41.8	42.4	302.6	149.3	150.9	65.1	74.2
Pr	1.81	1.04	1.37	2.19	0.95	6.00	2.14	5.80	1.78	1.29	3.06	3.00	1.60	1.92	2.17	1.15	5.44	0.38	0.80	17.76	9.44	16.52	14.38	1.51
Nd	6.40	3.83	4.28	7.05	2.84	18.69	6.65	18.20	5.84	4.89	11.90	10.81	5.66	6.33	6.82	3.96	17.99	1.14	2.27	24.46	29.02	40.49	26.01	5.98
Sm	36	20	24	33	12	62	29	58	30	27	90	45	25	20	30	21	64	8	14	59	112	162	92	28
Eu	23	10	19	29	16	59	26	54	24	23	29	39	22	20	31	19	57	6	13	21	32	58	37	11
Gd	124	76	84	103	55	192	93	191	92	71	404	147	82	75	110	88	199	28	45	249	426	681	333	99
Tb	220	152	154	190	114	317	175	321	182	237	893	283	154	125	196	168	326	62	82	490	740	1149	533	180
Dy	388	276	285	368	215	543	312	576	339	480	1696	519	268	235	347	297	532	105	150	906	1274	1921	883	321
Ho	585	457	456	641	347	797	503	861	593	833	2791	844	434	372	571	487	812	190	259	1489	2012	2882	1359	524
Er	914	777	785	1154	600	1243	832	1372	1040	1491	4659	1399	730	637	979	812	1261	317	459	2502	3200	4356	2083	850
Tm	1240	1162	1072	1692	868	1662	1187	1856	1540	2272	6461	1967	1018	944	1400	1149	1690	479	684	3529	4143	5630	2672	1195
Yb	1465	1465	1347	2163	1075	1922	1439	2118	1897	3045	7763	2428	1201	1194	1818	1495	1950	614	991	4296	4758	6230	3086	1475
Lu	2197	2358	2156	3592	1842	3066	2443	3447	3220	4993	11400	3801	2026	1988	2977	2284	3059	1017	1620	6366	6929	8940	4574	2300
Hf	1184423	1193558	1212115	933731	983173	931221	913904	865827	864327	1356058	1377308	974423	975000	869692	1019808	1140000	977692	1083654	1137019	1304615	1243173	1027404	971635	1151635
Th	6	29	33	37	18	52	27	53	33	116	1085	156	50	28	52	55	49	12	35	628	373	511	144	80
U	3683	10558	13610	15543	7720	12981	9594	14049	13522	58373	362136	36977	16125	10130	19362	21958	14269	5892	19179	212049	97007	109743	39328	33160
Th/U	0.47	0.83	0.73	0.73	0.70	1.22	0.85	1.15	0.74	0.61	0.91	1.29	0.94	0.84	0.83	0.76	1.05	0.64	0.56	0.90	1.17	1.42	1.11	0.74
Yb(n)/La(n)	8713	7937	9116	11080	11203	4031	7089	8232	7209	13806	13033	7464	6025	9183	10592	7458	2403	6314	16849	119	9730	2809	4532	14721
Yb(n/Gd(n)	11.8	19.4	16.0	20.9	19.5	10.0	15.5	11.1	20.6	42.7	19.2	16.5	14.6	16.0	16.5	17.0	9.8	21.8	22.0	17.2	11.2	9.1	9.3	14.9
Eu/Eu*	0.3	0.3	0.4	0.5	0.6	0.5	0.5	0.5	0.4	0.5	0.2	0.5	0.5	0.5	0.5	0.5	0.5	0.4	0.5	0.2	0.1	0.2	0.2	0.2
Ce/Ce*	64.9	135.0	154.5	99.0	138.3	40.4	79.7	49.8	89.9	249.3	345.6	150.4	152.7	102.0	143.8	196.0	31.0	218.7	195.1	11.9	69.5	24.9	20.8	190.5
HfO_2 [wt%]	1.5	1.5	1.5	1.1	1.2	1.1	1.1	1.1	1.1	1.7	1.7	1.2	1.2	1.1	1.3	1.4	1.2	1.3	1.4	1.6	1.5	1.3	1.2	1.4
comment	inherited	inherited				rejected, inclusion										rejected, Hf2+ wrong mass				rejected, inclusion				
grain area	rim	inh1	c2	c2a	c2b	c1	c2	c1	c2	c1	c1	c1	c2	c2b	c2	rim	c1a	rim	c2	r1a	c2	c2	c2	c2b

	SA05/23 10b	SA05/23 7a	SA05/23 12b	SA05/23 14a	SA05/23 14c	SA05/23 16a	SA05/23 16b	SA05/23 22a	SA05/23 22b	Cr-11 SA05/11 1a	SA05/11 1b	SA05/11 5a	SA05/11 5b	SA05/11 8a	SA05/11 8b	SA05/11 9a	SA05/11 9b	SA05/11 11c	SA05/11 20a	SA05/11 20d
grain no.	10	7	12	14	14	16	16	22	22	1	1	5	5	8	8	9	9	11	20	20
Si	140230	140230	140230	140230	140230	140230	140230	140230	140230	140230	140230	140230	140230	140230	140230	140230	140230	140230	140230	140230
P	617	312	920	332	346	391	345	268	145	208	203	311	253	213	252	345	170	362	480	282
Ca	7	8	178	19	5	21	24	18	14	12	3	4	3	3	3	3	3	3	4	9
Ti	19.17	21.73	11.34	20.58	20.32	16	14.21	27.96	4.33	6	8	11	7.91	9.11	9.63	11.62	5.16	11.20	12.20	8.99
Y	2203	515	5009	615	535	1637	1849	514	364	1097	1243	1467	783	1324	1393	1146	1050	2173	2839	931
Nb	3	2	9	1	1	2	3	2	1	4	1	4	2	2	2	3	1	2	4	3
Zr	540770	547180	536030	558630	540360	549310	549660	566080	543710	550700	535900	554830	546300	552380	539850	541380	546260	544060	549680	542900
Ba	0.2	0.1	0.3	0.2	0.2	0	0.1	0.1	0.3	0	0	0	0.0	0.1	0.1	0.3	0.0	0.1	0.2	0.1
La	0.1	0.2	3.0	0.0	0.0	2	0.1	0	1	0	0	0	0.0	0.1	0.1	0.1	0.0	0.1	0.2	0.0
Ce	67.1	18.7	193.8	26.6	22.5	63	59.3	22	23	37	38	61	35.2	40.3	39.4	48.6	40.4	59.2	85.0	41.7
Pr	0.9	0.2	2.9	0.1	0.1	2	0.8	0	1	0	1	0	0.1	0.6	0.7	0.2	0.3	1.0	1.2	0.1
Nd	12.6	2.8	30.5	2.5	2.5	20	11.5	2	4	6	8	5	2.2	9.4	10.5	3.5	5.7	13.8	17.1	2.5
Sm	15.6	3.2	31.8	4.3	3.5	15	14.7	3	2	8	9	7	3.4	11.5	12.4	5.0	7.6	17.0	23.7	3.8
Eu	2.4	0.6	4.1	0.7	0.6	2	1.7	1	0	3	3	3	1.0	3.8	4.1	1.6	2.4	6.1	8.1	1.1
Gd	80	15	161	19	16	59	66	15	8	33	39	34	17	48	52	26	35	84	110	19
Tb	23	5	51	6	5	18	20	5	3	10	11	12	6	14	15	10	10	24	32	6
Dy	255	53	566	69	54	200	223	55	33	117	133	142	71	152	165	112	113	256	337	82
Ho	88	19	196	24	20	70	76	19	13	43	48	55	29	53	56	44	41	88	115	34
Er	388	86	877	114	93	311	342	90	66	197	223	273	150	236	248	215	194	395	504	176
Tm	78	19	177	24	19	61	67	19	16	42	46	60	34	49	52	47	41	79	103	40
Yb	588	152	1334	200	159	492	522	157	147	343	378	497	297	397	411	398	338	629	812	345
Lu	133	35	282	46	37	108	114	36	38	81	92	121	77	92	97	100	80	146	186	90
Hf	10732	11523	12693	11151	10543	11619	11895	11510	13425	11744	10723	10393	10489	10588	9531	9360	12094	9385	9546	10027
Th	581	54	2130	82	65	475	430	46	67	180	211	243	120	199	199	178	185	382	564	122
U	506	91	1598	131	92	429	423	79	819	187	210	291	188	192	184	215	188	307	412	204
La	0.63	0.67	12.81	0.12	0.17	6.57	0.36	0.11	6.27	0.19	0.37	0.36	0.18	0.28	0.48	0.22	0.20	0.56	0.79	0.19
Ce	111.3	31.0	321.3	44.0	37.3	103.9	98.4	35.9	38.4	61.8	62.7	100.3	58.3	66.8	65.2	80.6	67.0	98.1	140.9	69.1
Pr	9.67	2.49	32.51	1.35	1.61	25.88	8.93	1.08	8.35	4.60	6.66	3.83	1.29	7.04	7.41	2.11	3.25	11.09	13.05	1.35
Nd	27.79	6.19	67.39	5.47	5.45	44.94	25.52	4.24	8.85	14.15	18.54	11.92	4.76	20.83	23.21	7.82	12.54	30.43	37.80	5.49
Sm	106	22	216	29	24	100	100	18	15	55	63	48	23	78	85	34	51	116	161	26
Eu	43	10	72	12	10	41	31	9	7	49	54	45	19	68	73	29	43	109	144	20
Gd	406	76	818	97	80	302	335	74	41	170	197	174	85	247	265	134	177	426	559	95
Tb	646	126	1395	162	138	490	545	133	72	280	316	321	155	393	416	271	276	650	868	176
Dy	1053	220	2332	283	224	823	919	227	134	481	547	587	292	628	679	460	466	1056	1387	338
Ho	1588	337	3518	437	367	1257	1369	350	232	770	857	998	513	953	1014	790	730	1585	2076	604
Er	2445	542	5520	718	587	1956	2151	567	414	1241	1405	1717	945	1483	1562	1353	1223	2483	3173	1105
Tm	3235	775	7305	982	790	2527	2776	785	647	1728	1920	2484	1404	2005	2133	1958	1701	3273	4244	1671
Yb	3620	933	8209	1228	980	3029	3211	968	904	2111	2324	3060	1827	2440	2531	2450	2081	3868	4997	2126
Lu	5483	1449	11587	1913	1527	4425	4699	1469	1581	3336	3772	4970	3156	3805	3975	4105	3297	6023	7648	3688
Hf	1031923	1107981	1220481	1072212	1013750	1117212	1143750	1106731	1290865	1129231	1031058	999327	1008558	1018077	916442	900038	1162885	902413	917856	964135
Th	235	22	862	33	26	192	174	19	27	73	86	98	49	80	81	72	75	155	228	49
U	62522	11220	197333	16226	11301	52995	52236	9731	101120	23069	25967	35930	23235	23678	22667	26600	23152	37912	50874	25142
Th/U	1.15	0.60	1.33	0.63	0.71	1.11	1.02	0.58	0.08	0.96	1.00	0.84	0.64	1.04	1.09	0.83	0.99	1.25	1.37	0.60
Yb(n)/La(n)	5725	1396	641	10202	5692	461	8895	8825	144	11210	6287	8586	10297	8699	5289	11188	10450	6939	6358	11012
Yb(n/Gd(n)	8.9	12.2	10.0	12.7	12.3	10.0	9.6	13.1	21.9	12.4	11.8	17.6	21.6	9.9	9.5	18.3	11.8	9.1	8.9	22.4
Eu/Eu*	0.2	0.2	0.2	0.2	0.2	0.2	0.2	0.2	0.3	0.5	0.5	0.5	0.4	0.5	0.5	0.4	0.5	0.5	0.5	0.4
Ce/Ce*	45.0	24.0	15.7	109.2	70.9	8.0	54.8	104.2	5.3	66.3	39.9	85.9	121.7	47.5	34.7	118.4	83.3	39.5	44.0	135.6
HfO_2 [wt%]	1.3	1.4	1.5	1.3	1.2	1.4	1.4	1.4	1.6	1.4	1.3	1.2	1.2	1.2	1.1	1.1	1.4	1.1	1.1	1.2
comment			rejected, inclusion																	
grain area	c2a	c1	c1a	c1b	c1a	c2a	c2b	c1	c2b	c1	rim	c2	rim	c2a	c2b	c1	rim	c1a	c2a	c2d

	MO										
	SA05/20 2a	SA05/20 2b	SA05/20 6a	SA05/20 7a	SA05/20 9a	SA05/20 9b	SA05/20 14a	SA05/20 18a	SA05/20 18b	SA05/20 19a	SA05/20 19b
grain no.	2	2	6	7	9	9	14	18	18	19	19
Si	140230	140230	140230	140230	140230	140230	140230	140230	140230	140230	140230
P	285	304	435	394	306	291	505	333	324	534	297
Ca	44	5	16	23	17	7	4	5	4	4	5
Ti	11.28	9.80	17.11	106.94	12.89	10.91	13.02	10.93	10.51	11.59	11.12
Y	1196	851	1505	1365	1333	760	1871	1096	811	742	1143
Nb	3	3	4	4	3	2	7	2	2	1	3
Zr	552690	542600	575770	578690	565440	537440	546260	542540	549220	548450	539730
Ba	0.2	0.1	0.1	17.6	0.1	0.2	0.0	0.0	0.2	0.2	0.2
La	0.1	0.0	0.1	0.1	0.1	0.1	0.1	0.1	0.0	0.0	0.1
Ce	43.1	44.5	76.9	66.3	49.8	38.0	101.1	41.5	54.3	23.5	48.3
Pr	0.3	0.1	0.3	0.2	0.3	0.1	0.2	0.3	0.1	0.1	0.2
Nd	5.7	2.1	4.9	4.2	6.4	2.1	4.1	5.4	2.6	1.7	4.6
Sm	8.0	3.7	7.5	5.9	9.2	3.8	7.3	7.1	4.4	3.7	6.8
Eu	2.2	1.1	2.2	1.9	2.5	1.1	1.9	1.8	1.1	1.2	1.7
Gd	37	22	40	32	41	21	43	32	23	19	34
Tb	11	7	13	11	13	6	15	10	7	6	11
Dy	127	88	165	134	146	78	186	118	87	78	124
Ho	46	34	61	53	53	29	73	43	31	28	44
Er	209	164	281	263	249	140	351	195	144	134	203
Tm	43	36	59	56	51	29	74	41	31	29	43
Yb	337	291	469	463	413	243	594	320	236	226	326
Lu	79	69	107	110	94	58	138	74	56	54	76
Hf	9774	9876	10235	10319	10409	9780	9726	10387	10526	9725	9981
Th	97	79	325	156	121	64	225	122	148	53	109
U	127	132	315	228	161	103	293	159	176	82	137
La	0.51	0.17	0.29	0.26	0.22	0.26	0.31	0.22	0.20	0.14	0.31
Ce	71.4	73.7	127.4	110.0	82.6	63.0	167.6	68.8	89.9	39.0	80.1
Pr	3.73	1.32	3.02	2.30	3.87	1.39	2.64	3.25	1.51	1.18	2.63
Nd	12.69	4.74	10.74	9.31	14.09	4.74	9.10	11.90	5.81	3.66	10.15
Sm	54	25	51	40	63	26	50	48	30	25	46
Eu	40	19	39	34	44	19	34	32	19	21	30
Gd	186	113	202	165	207	105	216	164	115	98	171
Tb	309	204	368	299	356	179	402	285	206	178	293
Dy	522	363	680	550	603	323	765	485	359	323	512
Ho	820	610	1095	957	955	519	1311	765	565	508	790
Er	1315	1035	1771	1655	1565	879	2210	1226	904	843	1275
Tm	1769	1481	2438	2307	2108	1193	3078	1693	1280	1195	1763
Yb	2073	1791	2885	2848	2542	1496	3654	1969	1450	1393	2006
Lu	3256	2858	4422	4545	3887	2368	5680	3042	2318	2234	3146
Hf	939846	949596	984135	992212	1000865	940375	935202	998750	1012115	935087	959721
Th	39	32	132	63	49	26	91	50	60	21	44
U	15683	16299	38946	28115	19878	12737	36178	19642	21763	10143	16877
Th/U	0.77	0.60	1.03	0.69	0.75	0.63	0.77	0.77	0.84	0.64	0.80
Yb(n)/La(n)	4025	10815	9953	11095	11414	5651	11637	8947	7269	9935	6478
Yb(n/Gd(n)	11.2	15.8	14.3	17.3	12.3	14.3	16.9	12.0	12.6	14.1	11.8
Eu/Eu*	0.4	0.4	0.4	0.4	0.4	0.4	0.3	0.4	0.3	0.4	0.3
Ce/Ce*	51.6	157.7	136.3	143.3	89.0	103.8	184.2	81.4	163.9	95.9	88.7
HfO_2 [wt%]	1.2	1.2	1.2	1.2	1.2	1.2	1.1	1.2	1.2	1.1	1.2
comment	cycles 1-7										
grain area	c1	c2	c2	c2	c1	c2	c2b	c1	c2	c2a	rim

Appendix 2h: Zircon saturation and 'Ti-in-zircon' thermometry

1. Zircon saturation thermometry

In the past 30 years numerous studies have discussed the occurrence, stability and chemistry of zircon in crustal rocks (e.g. Baker et al., 2002; Keppler, 1993; Larsen, 1973; Maurice, 1949; Murthy, 1958; Poldervaart, 1955, 1956; Siedner, 1965; Speer, 1982; Watson, 1979). A major contribution was made by Watson (1979), who based on an experimental study concluded that in the system SiO_2-Al_2O_3-Na_2O-K_2O the Zr saturation level strongly depends on the molar proportions of $(Na_2O+K_2O)/Al_2O_3$ of the melt, and only little on temperature, SiO_2 content or on the ratio Na_2O/K_2O. He further determined that for peraluminous melts less than 100 ppm Zr are required to saturate the melt and crystallise zircon. In a subsequent experimental study Watson and Harrison (1983) re-investigated the relationship between zircon crystallisation, melt composition and temperature and proposed the following solubility model:

$$\ln D_{Zr}^{zircon/melt} = (-3.80 - [0.85(M-1)\}) + 12900/T$$

where $D_{Zr}^{zircon/melt}$ describes the concentration of Zr in zircon to Zr in the melt, M the cation ratio (Na+K+2 Ca)/(Al*Si), and T the temperature (in Kelvin). Based on this solubility model Watson and Harrison (1983) showed that zircon solubility is largely insensitive to pressure, deviates from the above equation only for dry (< ~1.5 wt% H_2O) or peralkaline melts, and hence should apply to most intermediate to felsic crustal magmas. However, they also proposed that zircon solubilities vary in natural granitic systems due to the wide range of whole-rock geochemical compositions (M values), Zr concentrations and crystallisation temperatures.

Rearranging the above equation to *T* yields a geothermometer:

$$T_{Zr} = 12900 / [2.95+0.85*M + \ln (496000/Zr_{melt})]$$

However, calculated zircon saturation temperatures only give meaningful estimates, if (1) the unknown samples have M values equivalent to those used in the Watson and Harrison (1983) experiments (i.e. M=0.9-2.1), (2) the melt was saturated in Zr,

(3) textural evidence suggests early saturation (i.e. zircons are interstitial and not predominantly located within other minerals such as micas), and (4) presence of inherited zircons suggests saturation throughout the magma's evolution.

Table 1
Zircon saturation temperatures for the Lochnagar and Etive plutons

		Zr [ppm]	M	T [°C]			Zr [ppm]	M	T [°C]
Lochnagar					**Etive**				
SA04/01	**AD1**	427	2.3	808	SA05/20	**MO**	290	1.0	870
SA04/02	**AD2**	179	2.1	744	SA05/11	**Cr-11**	124	1.7	745
SA04/13	**CnG**	230	2.4	744	SA05/17	**Cr-17**	144	1.2	788
SA04/03	**L1-03**	191	1.4	800	SA05/15	**Cr-15**	623	1.3	928
SA04/06	**L1-06**	93	1.3	748	SA05/26	**Cr-26**	457	1.2	900
SA04/04	**L2-04**	144	1.4	780	SA05/05	**St-05**	140	1.1	799
SA04/15	**L2-15**	146	1.3	784	SA05/01	**St-01**	70	1.0	749
SA04/12	**L2-12**	147	1.3	784	SA05/23	**Q-23**	121	1.6	745
SA04/05	**L3**	339	1.4	853	SA05/25	**Q-25**	143	2.1	728

For the Lochnagar pluton the calculated zircon saturation temperatures range from 744°C to 808°C (Table 1, error on the calculation = ~50°C) with a mean temperature of 783±71°C (2SD, n=9). Samples of the Etive pluton yield a similar mean temperature of 806±150°C (2SD, n=9), but cover a larger temperature range between 728°C and 928°C. Both plutons show temperatures similar to those observed in other plutonic systems (e.g. Miller, 2003). In both plutons the majority of samples have M values within the calibrated range. However, in the Lochnagar pluton the Allt Darrarie (AD1 and AD2) and Cul nan Gad (CnG) diorites have higher M values suggesting their temperatures may not be reliable. An ambiguity affecting all the Lochnagar and Etive samples is that at present the zircons' textural relationships within the samples have not been investigated in great detail making it impossible to assess the degree of interaction between zircon and melt. In addition, only two samples in each pluton (Lochnagar: L2-04 and L2-15; Etive: Cr-15 and Cr-17) contain pre-magmatic inherited zircons, hence Zr saturation cannot be guaranteed throughout magma evolution. As further and much more detailed information is

required to eliminate these ambiguities and to calculate reliable saturation temperatures the above temperatures were not included into the main body of the text or integrated with the zircon oxygen, Hf isotope and/or REE/trace element data.

2. 'Ti-in-zircon' thermometry

Recently Watson and Harrison (2005) established that in rutile-bearing rocks the Ti content in zircon is highly dependent on temperature making it suitable as a geothermometer:

$$T(°C)_{zircon} = (5080\pm30 / (6.01\pm0.03) - \log (Ti)) - 273$$

The tetravalent nature of Ti allows it to substitute into the zircon crystal lattice for Zr^{4+} or Si^{4+}. In TiO_2-saturated samples (i.e. rutile is present), the thermodynamic basis of the thermometer is the reaction TiO_2 (rutile) = TiO_2 (zircon). As rutile represents nearly pure TiO_2 rutile-bearing rocks show a TiO_2 activity that equals unity; this value decreases in rocks lacking or containing other TiO_2 phases. In general, rutile predominantly occurs in metamorphic rocks, but is not common in igneous rocks. In the latter other TiO_2-bearing phases (e.g. ilmenite, titanite) constrain the TiO_2 activity, which will be smaller than unity. Hence, 'Ti-in-zircon' temperatures calculated for igneous rocks will most likely represent minimum temperatures.

In the Lochnagar pluton the mean 'Ti-in-zircon' temperatures range from 669±119°C (2SD, n=7, error on calculation ~ 10°C) in the AD2 diorite to 769±74°C (2SD, n=18) in the AD1 diorite (Table 2). The Etive plutons shows similar mean temperatures between 645±62°C (St-05, n=9) and 786±87°C (Q-23, n=12) (Table 2). Some variation occurs between each unit within the plutons. However, at least in the Lochnagar plutons this variation does not appear to be systematic. In the Etive pluton samples of the Starav Intrusion have lower 'Ti-in-zircon' temperatures than the Meall Odhar, Cruachan and Quarry intrusion samples. Variation also occurs between zircon crystals of a single sample as well as within individual crystals. Most commonly temperature decreases with zircon growth. However, the opposite trend can also be observed (e.g. AD1 grain 6). This may be further evidence for the

complexity of the Lochnagar and Etive plutonic systems as indicated by zircon oxygen and U-Pb isotope data. However, as the TiO_2 activity has not been constrained in the Lochnagar and Etive samples temperatures are most likely underestimated and can therefore only be seen as preliminary results. In order to obtain reliable temperatures the nature and abundance of all TiO_2-bearing phases has to be constrained in great detail. As this has not been carried out at this point the temperatures were not incorporated into the main body of the thesis.

Table 2
'Ti-in-zircon' temperatures for the Lochnagar and Etive plutons

Lochnagar

	grain no.	analysis no.	Ti [ppm]	T [ºC]	grain area
AD1	4	4.7	18	793	?
	4	4.10	18	795	?
	6	6.14	9	734	c1
	6	6.15	21	808	c2
	11	11.33	8	727	r1
	11	11.34	10	738	c1a
	14	14.43	22	815	c1
	14	14.44	17	792	c2
	16	16.51	11	748	c1
	16	16.52	8	721	r3
	8	8.20	26	832	c1
	8	8.25	7	707	r1
	9	9.28	14	771	c2a
	9	9.29	11	746	c2b
	13	13.41	16	787	c2a
	13	13.42	9	731	c2b
	10	10.31	18	798	c2
	10	10.32	17	790	c1
mean				**769**	
2SD				**74**	

AD2	11	11.22	10	741	c1a
	13	13.27	2	612	c2b
	13	13.29	2	606	c2a
	18	18.39	12	756	rim
	18	18.40	5	682	c1
	15	15.32	3	643	c2b
	15	15.31	3	644	c2a
mean				**669**	
2SD				**119**	

CnG	1	1.1	12	756	c2a
	1	1.2	5	678	c2b
	5	5.9	8	724	c2
	5	5.10	11	747	c1
	6	6.14	11	750	r1
	15	15.35	7	709	c1
	15	15.36	5	684	r1
	4	4.7	4	657	r1
	4	4.8	6	699	c1
	5	5.11	7	706	r1
	13	13.31	5	690	c1
	19	19.44	14	772	c1a
	19	19.44b	14	771	c1b
	19	19.45	8	720	r1
mean				**719**	
2SD				**72**	

L1-03	3	3.6	10	744	c2a
	3	3.57	14	770	c2b
	8	8.14	10	745	r1
	9	9.15	12	759	c2a
	9	9.16	9	732	c2b
	16	16.29	12	755	rim
	27	27.54	15	777	c2
	27	27.55	13	765	c1
	12	12.19	11	746	rim
	13	13.22	6	691	rim
	15	15.26	7	710	c1
	15	15.27	5	683	rim
	22	22.42	8	724	c1
	23	23.43	7	705	c2a
	23	23.44	5	683	c2b
	20	20.37	8	726	rim
	20	20.38	11	747	c2
	26	26.53	14	774	rim
	24	24.46	16	786	rim
mean				**738**	
2SD				**64**	

L1-06	5	5.6	13	763	c1
	5	5.7	5	688	c2
	7	7.10	3	642	c1
	7	7.11	4	666	c2
	13	13.18	14	769	c1
	2	2.2	2	630	c1
	30	30.36	3	645	c1
	30	30.37	4	674	c2
	25	35.43	6	700	c2
	36	36.44	4	659	c1
	36	36.45	8	719	rim
	12	12.17	3	637	c1
mean				**683**	
2SD				**94**	

L2-04	10	10.20	2	617	c1
	10	10.21	10	738	r1
	16	16.31	3	650	c1
	18	18.34	7	706	c1
	18	18.35	6	693	rim
	11	11.22	5	688	c1
	1	1.2	10	739	c2
mean				**690**	
2SD				**89**	

	grain no.	analysis no.	Ti [ppm]	T [ºC]	grain area
L2-12	2	2.3	5	682	c2
	3	3.4	5	687	c2a
	3	3.5	6	703	c2b
	10	10.22	8	719	c2
	11	11.25	8	723	c2
	5	5.10	4	674	c2
	12	12.30	12	756	c1
	5	5.9	5	686	c1
	13	13.33	11	746	c2
	14	14.35	20	805	c1
	15	15.37	4	662	c1
	15	15.38	4	662	c2
	11	11.26	7	705	c2
mean				**709**	
2SD				**83**	
L2-15	4	4a	6	696	c2
	7	7b	7	715	rim
	9	9a	3	655	c2
	13	13a	10	743	c1
	13	13b	7	709	rim
	21	21a	7	708	c1
	21	21b	8	722	c2
	28	28a	2	625	c1
	16	16d	464	**1246**	rim
	27	27b	2	629	c1
mean				**689**	
2SD				**84**	

	grain no.	analysis no.	Ti [ppm]	T [ºC]	grain area
L3	21	21.40	7	708	c2
	21	21.41	6	701	rim
	14	14.27	11	746	rim
	9	9.16	9	729	c2a
	9	9.17	6	691	c2b
	25	25.49	8	719	c2b
	25	25.50	8	717	c2a
	18	18.34	7	710	c2a
	18	18.35	11	748	c2b
	28	28.56	15	777	rim
	10	10.18	5	691	c1
	4	4.7	7	709	c1+c2
	5	5.9	3	651	c1
	11	11.21	9	731	c2a
	11	11.22	6	700	c2b
	24	24.48	14	769	rim
mean				**719**	
2SD				**63**	

Etive

	grain no.	analysis no.	Ti [ppm]	T [ºC]	grain area
St-01	4	4a	2	620	c1
	5	5b	3	648	c1
	13	13a	3	645	c2
	13	13b	4	664	rim
	18	18a	3	644	c2a
	18	18b	4	663	c2b
	19	19b	3	641	rim
	20	20a	4	659	c2
	14	14a	6	699	rim
mean				**654**	
2SD				**43**	

	grain no.	analysis no.	Ti [ppm]	T [ºC]	grain area
St-05	9	9a	4	658	c2
	10	10a	4	662	c2
	10	10b	5	685	rim
	11	11c	5	688	c2b
	14	14c	1	597	r1a
	14	14b	3	646	r1b
	23	23a	2	623	c2
	18	18a	2	620	c1
	18	18b	2	628	c2
mean				**645**	
2SD				**62**	

	grain no.	analysis no.	Ti [ppm]	T [ºC]	grain area
Cr-11	1	1a	6	703	c1
	1	1b	8	723	rim
	5	5a	11	748	c2
	5	5b	8	721	rim
	8	8a	9	733	c2a
	8	8b	10	738	c2b
	9	9a	12	754	c1
	9	9b	5	686	rim
	11	11c	11	751	c1a
	20	20a	12	759	c2a
	20	20d	9	732	c2d
mean				**731**	
2SD				**45**	
Cr-15	2	2a	27	835	c1
	4	4b	10	737	inh1
	9	9a	6	702	c2
	11	11a	17	787	c2a
	11	11b	9	728	c2b
	19	19b	10	737	c2
	22	22a	10	745	c1
	22	22b	12	757	c2
	26	26a	5	680	c1
mean				**745**	
2SD				**91**	
Cr-26	5	5a	12	755	c1
	6	6a	11	751	c1
	6	6b	9	729	c2
	12	12a	16	782	c2b
	16	16a	12	757	c2
	20	20c	11	749	c1a
	20	20b	8	719	rim
	27	27a	7	715	c2
mean				**745**	
2SD				**45**	

	grain no.	analysis no.	Ti [ppm]	T [ºC]	grain area
Q-23	5	5a	11	749	c2
	8	8a	18	794	c2
	9	9a	22	816	c2
	10	10a	13	768	c2b
	10	10b	19	802	c2a
	7	7a	22	814	c1
	14	14a	21	809	c1b
	14	14c	20	807	c1a
	16	16a	16	785	c2a
	16	16b	14	773	c2b
	22	22a	28	840	c1
	22	22b	4	672	c2b
mean				**786**	
2SD				**87**	
MO	2	2a	11	752	c1
	2	2b	10	739	c2
	6	6a	17	790	c2
	7	7a	107	1003	c2
	9	9a	13	764	c1
	9	9b	11	749	c2
	14	14a	13	765	c2b
	18	18a	11	749	c1
	18	18b	11	745	c2
	19	19a	12	754	c2a
	19	19b	11	750	rim
mean				**778**	
2SD				**152**	

Appendix 2i: A comparison of measured whole-rock REE data and melt compositions calculated from zircon REE data

Accessory minerals (e.g. zircon, apatite) typically make up less than one modal percent in a whole-rock sample. Nevertheless, they host the majority of trace elements and REEs useful as petrogenetic indicators (e.g. Bea, 1996; Gromet and Silver, 1983). In order to assess the controls accessory minerals have on the whole-rock REE budget back-calculations may be made from accessory mineral REE data.

For the Lochnagar and Etive plutons these calculations were made for zircon and whole-rock using the partition coefficients by Sano et al. (2002) (Table 1). The measured whole-rock and average back-calculated REE data of each sample (Tables 2 & 3) are plotted normalised to chondrite using normalising values by Sun and McDonough (1989).

In both plutons good agreement was found for the MREEs and HREEs (Fig. 1). Larger discrepancies were observed in the LREE. This may be the result of (1) the overall low LREE abundances in zircon leading to lower accuracy and reproducibility, (2) may have been caused by accidental analysis of small inclusions enriched in LREE (e.g. apatite) in zircon, (3) is evidence that other accessory minerals (e.g. apatite) provide the majority of the whole-rock's LREEs and MREEs. This comparison of measured whole-rock REE data and melt compositions calculated from zircon REE data supports the conclusion by Sano et al. (2002) that, as long as the correct zircon/melt partition coefficients are used, melt compositions may be successfully back-calculated from zircon REE data.

Table 1
Partition coefficients of REEs in zircon/melt

Element	La	Ce	Pr	Nd	Sm	Eu	Gd	Tb	Dy	Ho	Er	Tm	Yb	Lu
zircon/melt	0.0005	0.4	0.0172	0.1	0.8	1.2	8	21	46	80	136	2	277	325
±	0.0003	0.1	0.0088	0	0.2	0.3	1.7	4.8	9.5	19	27	40	55	62

*data from Sano et al. (2002)

Table 2

Measured and calculated REE data for the Lochnagar pluton

	AD1	AD1 calc	CnG	CnG calc	L1-03	L1-03 calc	L2-15	L2-15 calc	L3	L3 calc
La	39	237	27	865	51	12492	30	2434	63	3350
Ce	85	56	54	41	90	131	57	129	109	203
Pr	11	19	6	19	9	149	6	80	10	62
Nd	44	58	26	42	30	188	21	127	34	116
Sm	8	7	5	4	5	8	3	9	4	12
Eu	2.6	1.9	1.6	1.5	1.0	1.2	0.6	1.5	1.6	1.8
Tb	1.1	0.5	0.7	0.3	0.5	0.3	0.4	0.5	0.4	0.8
Gd	7.7	3.7	4.2	2.2	3.6	2.8	2.6	3.6	3.0	6.0
Dy	6.3	2.6	3.7	1.5	3.0	1.9	2.0	2.6	2.2	4.2
Ho	1.1	0.6	0.7	0.3	0.6	0.4	0.4	0.6	0.5	0.9
Er	2.9	1.7	2.0	1.0	1.8	1.1	1.1	1.6	1.2	2.5
Tm	0.5	0.3	0.3	0.2	0.3	0.2	0.2	0.2	0.2	0.4
Yb	2.7	1.5	1.7	1.1	1.8	1.0	1.2	1.5	1.3	2.0
Lu	0.4	0.3	0.2	0.2	0.3	0.2	0.2	0.3	0.2	0.4

Table 3

Measured and calculated REE data for the Etive pluton

	MO	MO calc	Cr-11	Cr-11 calc	St-01	St-01 calc	Q-23	Q-23 calc
La	43	134	31	177	18	275	27	782
Ce	77	148	62	133	31	110	53	131
Pr	9	13	7	29	3	6	6	44
Nd	31	52	30	100	10	18	24	113
Sm	5	8	5	12	1	3	4	12
Eu	1.1	1.4	1.4	2.7	0.3	0.6	1.1	1.2
Tb	0.6	0.5	0.5	0.7	0.2	0.2	0.4	0.7
Gd	3.6	3.9	4.2	5.6	1.2	1.8	3.2	6.0
Dy	3.3	2.6	3.0	3.3	1.2	1.4	2.4	3.6
Ho	0.6	0.6	0.5	0.7	0.2	0.3	0.4	0.7
Er	1.7	1.6	1.3	1.9	0.7	1.0	1.2	1.9
Tm	0.2	0.2	0.2	0.3	0.1	0.2	0.2	0.3
Yb	1.5	1.3	1.2	1.6	1.0	1.1	1.2	1.5
Lu	0.2	0.3	0.2	0.3	0.2	0.3	0.2	0.3

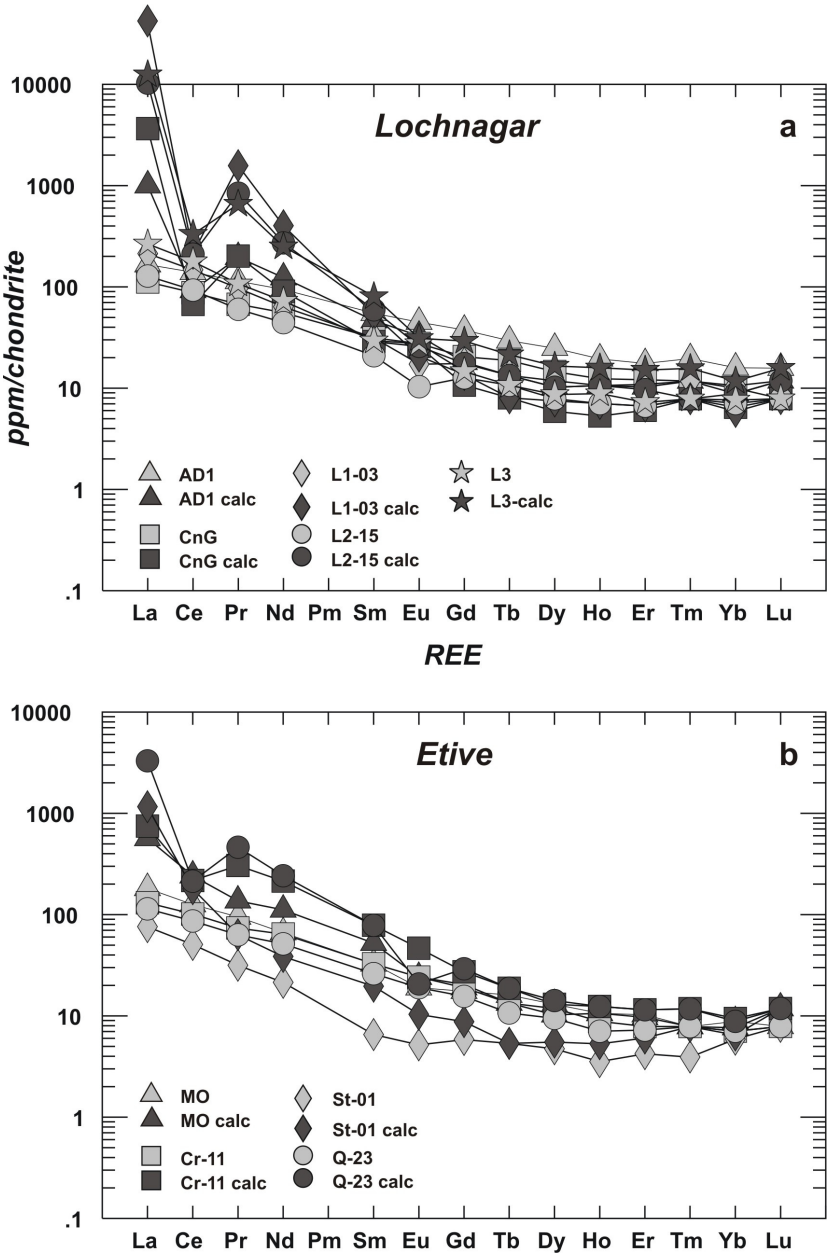

Fig. 1: Chondrite-normalised REE patterns (values from Sun and McDonough, 1989) of measured and back-calculated zircon REE data for the (a) the Lochnagar and (b) the Etive plutons.

Appendix 2j
Two-component magma mixing modelling

% Dalradian	$\delta^{18}O$ [‰]	% enriched mantle
0	5.5*	1
0.1	6.4	0.9
0.2	7.2	0.8
0.3	8.1	0.7
0.4	9.0	0.6
0.5	9.9	0.5
0.6	10.7	0.4
0.7	11.6	0.3
0.8	12.5	0.2
0.9	13.3	0.1
1	14.2*	0

*Average enriched mantle and average Dalradian (data from Anderson et al., 2004; Eiler , 2001; Frost and O'Nions, 1985; O'Nions et al., 1983)

APPENDIX 3

Supplementary data for Paper 3

Appendix 3a
Hf isotope data of zircons from the Lochnagar and Etive plutons

Analysis no.	grain no.	grain area	age	1 SD	$\delta^{18}O$ [‰]	2σ	$^{176}Lu/^{177}Hf$ (WR)	total Hf	Yb/Hf	$^{178}Hf/^{177}Hf$	1s%	$^{176}Hf/^{177}Hf$	1s%	$^{176}Yb/^{177}Hf$	1s%	$^{176}Lu/^{177}Hf$	1s%	$^{176}Hf/^{177}Hf$ (initial)	εHf	95% conf.	TDM_C	95% conf.	TDM_W	95% conf.
Lochnagar																								
AD1																								
SA04/01 - 1.1b	1	c2	419	4	6.9	0.6	0.008	3.93	0.15	1.467270	0.0038	0.282516	0.0078	0.37217	7.5	0.00147	5.3	0.282504	-0.3	0.9	1428	53	1197	40
SA04/01 - 3.6b	3	c1	419	4	6.6	0.6	0.008	3.66	0.13	1.467130	0.0045	0.282489	0.0073	0.32758	7.6	0.00133	5.0	0.282478	-1.2	0.8	1486	50	1242	38
SA04/01 - 4.10b	4	?	419	4	7.7	0.6	0.008	3.40	0.05	1.467320	0.0047	0.282501	0.0083	0.13111	9.1	0.00055	7.0	0.282497	-0.5	0.9	1445	56	1211	42
SA04/01 - 7.17b	7	c1	419	4	7.5	0.6	0.008	4.10	0.14	1.467240	0.0048	0.282391	0.0083	0.35798	7.8	0.00132	5.0	0.282381	-4.6	0.9	1705	56	1412	42
SA04/01 - 8.20b	8	c1	419	4	6.8	0.6	0.008	2.94	0.08	1.467290	0.0060	0.282599	0.0103	0.19478	7.5	0.00084	5.4	0.282592	2.9	1.1	1230	69	1044	52
SA04/01 - 9.27b	9	c1	419	4	6.5	0.6	0.008	2.63	0.09	1.467250	0.0040	0.282614	0.0097	0.23707	7.6	0.00096	5.1	0.282606	3.4	1.1	1198	65	1020	50
SA04/01 - 9.29b	9	c2	419	4	7.3	0.6	0.008	3.24	0.06	1.467290	0.0037	0.282473	0.0078	0.15657	7.4	0.00067	4.9	0.282468	-1.6	0.9	1510	52	1261	40
SA04/01 - 10.32b	10	c1	419	4	7.8	0.6	0.008	2.98	0.08	1.467290	0.0048	0.282525	0.0113	0.20886	8.4	0.00090	6.3	0.282518	0.2	1.2	1398	75	1174	57
SA04/01 - 10.31b	10	c2	419	4	6.6	0.6	0.008	3.09	0.10	1.467230	0.0053	0.282544	0.0086	0.26180	7.4	0.00112	4.9	0.282535	0.8	1.0	1359	58	1144	44
SA04/01 - 11.34b	11	c1	419	4	7.2	0.6	0.008	4.44	0.11	1.467150	0.0064	0.282449	0.0113	0.28000	7.9	0.00114	6.2	0.282440	-2.5	1.2	1573	75	1309	57
SA04/01 - 15.49	15	c2	419	4	6.6	0.6	0.008	4.15	0.09	1.467250	0.0042	0.282384	0.0081	0.23131	7.5	0.00096	5.0	0.282376	-4.8	0.9	1715	54	1419	41
SA04/01 - 16.51b	16	c1	419	4	6.4	0.6	0.008	4.39	0.26	1.467220	0.0043	0.282511	0.0075	0.65764	7.4	0.00248	4.9	0.282491	-0.7	0.9	1457	52	1220	39
CnG																								
SA04/13 - 13.32	13	c2	418	6	5.7	0.4	0.007	2.82	0.03	1.467180	0.0051	0.282495	0.0092	0.06450	7.6	0.00031	5.3	0.282492	-0.7	1.1	1455	62	1193	45
SA04/13 - 14.34	14	c2	418	6	5.5	0.4	0.007	3.24	0.04	1.467310	0.0048	0.282560	0.0078	0.10874	7.5	0.00051	5.0	0.282556	1.5	0.9	1312	54	1086	39
SA04/13 - 15.35	15	c1	418	6	5.6	0.4	0.007	3.18	0.10	1.467190	0.0043	0.282545	0.0100	0.25757	7.8	0.00110	6.1	0.282536	0.9	1.2	1357	68	1119	50
SA04/13 - 16.37	16	c1	418	6	5.8	0.4	0.007	3.00	0.08	1.467190	0.0046	0.282545	0.0089	0.20330	7.6	0.00086	4.9	0.282538	0.9	1.0	1352	61	1116	44
SA04/13 - 17.39	17	c1	418	6	6.4	0.4	0.007	2.90	0.04	1.467230	0.0056	0.282575	0.0106	0.10524	9.9	0.00044	6.7	0.282571	2.1	1.2	1277	72	1060	52
SA04/13 - 19.44	19	c1	418	6	6.3	0.4	0.007	2.19	0.21	1.467190	0.0048	0.282572	0.0095	0.53290	7.4	0.00205	4.9	0.282556	1.5	1.1	1312	65	1086	47
SA04/13 - 11.28	11	c1	418	6	6.2	0.4	0.007	2.83	0.07	1.467350	0.0044	0.282584	0.0086	0.18442	7.4	0.00082	5.0	0.282577	2.3	1.0	1264	59	1050	43
SA04/13 - 9.24	9	c1	418	6	5.8	0.4	0.007	2.05	0.04	1.467310	0.0054	0.282563	0.0089	0.09790	7.6	0.00040	5.1	0.282560	1.7	1.0	1304	61	1079	44
SA04/13 - 2.4	2	c2	418	6	5.9	0.4	0.007	2.72	0.10	1.467170	0.0046	0.282581	0.0083	0.24187	7.5	0.00110	5.1	0.282572	2.1	1.0	1276	57	1058	42
SA04/13 - 4.8	4	c1	418	6	6.3	0.4	0.007	3.13	0.08	1.467300	0.0047	0.282515	0.0095	0.18998	7.9	0.00087	5.7	0.282508	-0.1	1.1	1420	64	1167	47
SA04/13 - 6.12	6	c2	418	6	5.8	0.4	0.007	3.37	0.04	1.467180	0.0049	0.282542	0.0089	0.10449	7.7	0.00051	5.3	0.282538	0.9	1.0	1353	61	1116	44
SA04/13 - 8.20	8	r1	418	6	5.8	0.4	0.007	3.15	0.05	1.467200	0.0044	0.282556	0.0078	0.12494	7.8	0.00065	5.9	0.282551	1.4	0.9	1324	54	1095	39
L1-03																								
SA04/03 - 3.6	3	c2	420	3	7.1	0.4	0.007	2.95	0.04	1.467190	0.0042	0.282464	0.0073	0.10446	7.4	0.00042	5.1	0.282461	-1.8	0.8	1525	48	1246	36
SA04/03 - 7.12	7	c2	420	3	6.8	0.4	0.007	3.78	0.09	1.467250	0.0052	0.282393	0.0081	0.23719	7.4	0.00088	5.3	0.282386	-4.4	0.9	1693	53	1371	39
SA04/03 - 8.14	8	r1	420	3	6.8	0.4	0.007	2.90	0.04	1.467180	0.0052	0.282450	0.0083	0.10402	8.0	0.00054	8.6	0.282446	-2.3	0.9	1559	55	1271	41
SA04/03 - 8.13	8	c1	420	3	6.8	0.4	0.007	3.24	0.10	1.467160	0.0046	0.282427	0.0081	0.25437	11.1	0.00092	8.3	0.282420	-3.2	0.9	1617	54	1315	40
SA04/03 - 9.15	9	c2	420	3	6.6	0.4	0.007	2.83	0.07	1.467320	0.0046	0.282423	0.0103	0.18585	8.0	0.00076	6.2	0.282417	-3.3	1.1	1624	68	1319	50
SA04/03 - 16.29	16	rim	420	3	6.9	0.6	0.007	3.40	0.03	1.467210	0.0046	0.282419	0.0075	0.07894	7.6	0.00031	5.3	0.282416	-3.3	0.8	1625	50	1320	37
SA04/03 - 16.28	16	c1+c2	420	3	6.9	0.6	0.007	3.86	0.13	1.467190	0.0039	0.282466	0.0078	0.31852	7.6	0.00118	5.0	0.282457	-1.9	0.9	1534	52	1253	38
SA04/03 - 20.37	20	c2	420	3	5.8	0.6	0.007	3.14	0.05	1.467270	0.0048	0.282473	0.0075	0.13395	7.7	0.00052	5.2	0.282469	-1.5	0.8	1507	50	1232	37
SA04/03 - 20.38	20	r2	420	3	6.5	0.6	0.007	2.95	0.03	1.467130	0.0042	0.282457	0.0092	0.07626	7.4	0.00031	5.2	0.282454	-2.0	1.0	1539	60	1256	44
SA04/03 - 21.41	21	r1	420	3	6.2	0.6	0.007	2.95	0.04	1.467260	0.0046	0.282464	0.0075	0.09044	7.5	0.00038	5.0	0.282461	-1.8	0.8	1525	50	1245	37
SA04/03 - 22.42	22	?	420	3	6.1	0.6	0.007	2.98	0.04	1.467260	0.0042	0.282463	0.0075	0.10724	7.4	0.00044	5.1	0.282459	-1.8	0.8	1528	50	1248	37
SA04/03 - 23.43	23	c2a	420	3	6.1	0.6	0.007	3.50	0.11	1.467190	0.0056	0.282355	0.0092	0.26479	7.5	0.00094	5.0	0.282347	-5.8	1.0	1779	60	1436	45
SA04/03 - 23.44	23	c2b	420	3	6.6	0.6	0.007	3.35	0.09	1.467240	0.0041	0.282390	0.0089	0.22958	7.5	0.00086	5.1	0.282383	-4.5	1.0	1699	59	1376	43
SA04/03 - 26.51	26	c1	420	3	7.1	0.6	0.007	2.76	0.06	1.467110	0.0062	0.282459	0.0110	0.16216	8.1	0.00061	6.1	0.282454	-2.0	1.2	1540	72	1257	53

Analysis no.	grain no.	grain area	age	1 SD	$\delta^{18}O$ [‰]	2σ	$^{176}Lu/^{177}Hf$ (WR)	total Hf	Yb/Hf	$^{178}Hf/^{177}Hf$	1s%	$^{176}Hf/^{177}Hf$	1s%	$^{176}Yb/^{177}Hf$	1s%	$^{176}Lu/^{177}Hf$	1s%	$^{176}Hf/^{177}Hf$ (initial)	εHf	95% conf.	TDM_C	95% conf.	TDM_W	95% conf.
L2-04																								
SA04/04 - 15.28	15	c1	1046	15	6.5	0.4	0.006*	4.52	0.05	1.467190	0.0037	0.282147	0.0059	0.12311	10.6	0.00049	11.2	0.282138	0.7	0.96	1855	50	1632	32
SA04/04 - 15.29	15	c2	1046	15	6.0	0.4	0.006*	4.92	0.04	1.467270	0.0033	0.282157	0.0074	0.10438	10.7	0.00042	11.2	0.282149	1.1	1.10	1829	59	1613	38
SA04/04 - 16.31	16	c1	424	6	6.6	0.4	0.006*	5.14	0.16	1.467260	0.0051	0.282494	0.0140	0.39673	10.7	0.00147	11.4	0.282483	-0.9	1.6	1473	95	1184	67
L2-15																								
SA04/15 - 3a	3	c2	422	3	6.1	0.9	0.006	2.74	0.17	1.467170	0.0044	0.282587	0.0105	0.40847	12.6	0.00120	10.6	0.282578	2.4	1.2	1260	71	1029	51
SA04/15 - 4b	4	c2	422	3	6.4	0.5	0.006	3.83	0.09	1.467290	0.0046	0.282435	0.0100	0.23524	12.6	0.00070	10.6	0.282430	-2.8	1.1	1593	66	1270	47
SA04/15 - 6a	6	c1	422	3	6.0	0.9	0.006	3.12	0.03	1.467140	0.0051	0.282499	0.0098	0.07446	12.5	0.00025	10.6	0.282497	-0.4	1.1	1442	64	1160	46
SA04/15 - 12a	12	c2	422	3	7.1	0.9	0.006	3.04	0.11	1.467270	0.0050	0.282591	0.0113	0.26839	12.5	0.00086	10.6	0.282585	2.7	1.2	1245	76	1018	54
SA04/15 - 22a	22	core a	422	3	7.3	0.5	0.006	4.77	0.04	1.467030	0.0061	0.282513	0.0137	0.11013	14.1	0.00036	13.7	0.282511	0.0	1.4	1412	89	1139	64
SA04/15 - 22b	22	core b	422	3	7.5	0.5	0.006	5.19	0.23	1.467230	0.0139	0.282551	0.0271	0.58234	14.5	0.00187	11.3	0.282537	1.0	2.8	1353	178	1096	128
SA04/15 - 29a	29	inh core	1149	8	5.5	0.5	0.006	2.54	0.14	1.467040	0.0045	0.282355	0.0122	0.35307	13.9	0.00097	11.7	0.282334	10.0	1.5	1341	89	1288	62
SA04/15 - 29b	29	rim	422	3			0.006	3.35	0.13	1.467230	0.0049	0.282492	0.0103	0.33927	17.9	0.00086	14.9	0.282486	-0.9	1.1	1468	69	1180	49
SA04/15 - 36a	36	inh core	1235	19	5.2	0.5	0.006	3.27	0.11	1.467300	0.0055	0.281760	0.0105	0.27049	12.4	0.00078	10.6	0.281742	-9.1	1.5	2622	82	2240	54
SA04/15 - 32a	32	inh core	1235	19	5.7	0.5	0.006	3.54	0.07	1.467160	0.0039	0.282173	0.0125	0.18227	14.0	0.00048	12.1	0.282162	5.8	1.7	1676	95	1554	64
SA04/15 - 35b	35	inh core	1149	8	6.3	0.5	0.006	3.17	0.04	1.467240	0.0047	0.282198	0.0105	0.08883	12.6	0.00027	10.6	0.282192	4.9	1.3	1664	74	1521	51
SA04/15 - 10a	10	c2	422	3	6.6	0.9	0.006	3.67	0.07	1.467210	0.0045	0.282499	0.0113	0.18292	13.4	0.00057	11.1	0.282495	-0.5	1.2	1447	75	1164	54
																					1403	86		62
L3																								
SA04/05 - 8.14	8	c1+c2	423	5	7.2	0.5	0.004	5.13	0.08	1.467210	0.0061	0.282549	0.0086	0.21303	11.5	0.00081	12.0	0.282543	1.2	1.0	1339	60	1047	39
SA04/05 - 5.9	5	c1	423	5	6.3	0.5	0.004	5.77	0.11	1.467290	0.0065	0.282546	0.0119	0.27705	12.0	0.00099	13.2	0.282539	1.0	1.3	1348	81	1054	54
SA04/05 - 9.17	9	c2	423	5	6.6	0.5	0.004	4.14	0.11	1.467210	0.0038	0.282583	0.0071	0.27596	10.6	0.00112	11.2	0.282574	2.3	0.8	1267	50	999	33
SA04/05 - 11.21	11	c2	423	5	6.8	0.5	0.004	4.75	0.10	1.467200	0.0038	0.282512	0.0065	0.24876	10.6	0.00097	11.2	0.282505	-0.2	0.8	1425	46	1106	30
SA04/05 - 18.34	18	c2a	423	5	5.6	0.5	0.004	4.17	0.14	1.467240	0.0040	0.282517	0.0059	0.35386	11.4	0.00136	11.6	0.282507	-0.1	0.7	1420	43	1103	28
SA04/05 - 18.35	18	c2b	423	5	8.1	0.5	0.004	4.08	0.12	1.467220	0.0042	0.282508	0.0074	0.29035	11.1	0.00113	11.6	0.282499	-0.3	0.9	1436	52	1114	34
SA04/05 - 21.40	21	c1	423	5	6.7	0.5	0.004	5.06	0.14	1.467260	0.0042	0.282503	0.0077	0.35546	10.7	0.00141	11.2	0.282492	-0.6	0.9	1453	54	1126	36
SA04/05 - 24.48	24	c2+rim	423	5	5.6	0.5	0.004	4.03	0.06	1.467300	0.0036	0.282512	0.0083	0.13929	10.6	0.00055	11.2	0.282508	0.0	1.0	1417	57	1101	37
SA04/05 - 25.49	25	c2	423	5	6.1	0.5	0.004	3.90	0.10	1.467340	0.0041	0.282545	0.0083	0.26160	11.1	0.00110	12.0	0.282537	1.0	1.0	1353	58	1057	38
SA04/05 - 32.64	32	c1	423	5			0.004	5.50	0.13	1.467250	0.0037	0.282488	0.0065	0.32727	10.6	0.00129	11.2	0.282478	-1.1	0.8	1484	47	1147	30
L1-06																								
SA04/06 - 5.6	5	c1	420	4	6.8	0.5	0.004*	6.55	0.20	1.467130	0.0093	0.282509	0.0126	0.51407	11.5	0.00199	12.4	0.282494	-0.6	1.4	1451	86	1123	58
SA04/06 - 7.10	7	c1	420	4	6.5	0.5	0.004*	6.32	0.23	1.467350	0.0071	0.282562	0.0113	0.56821	11.2	0.00219	11.7	0.282545	1.2	1.3	1335	78	1044	52
SA04/06 - 18.23	18	c1+c2	420	4	5.9	0.5	0.004*	6.34	0.27	1.467370	0.0073	0.282561	0.0160	0.68749	10.7	0.00247	11.3	0.282542	1.1	1.8	1343	109	1049	73
SA04/06 - 32.46	32	c1	420	4	6.3	0.5	0.004*	3.96	0.19	1.467270	0.0042	0.282515	0.0071	0.47830	12.4	0.00169	13.0	0.282502	-0.3	0.9	1432	51	1111	34
SA04/06 - 38.49	38	c1	420	4			0.004*	5.83	0.09	1.467090	0.0055	0.282452	0.0096	0.23289	11.7	0.00092	11.7	0.282445	-2.3	1.1	1560	65	1198	43
L2-12																								
SA04/12 - 2.3	2	c2	419	4	6.2	0.5	0.004*	6.89	0.17	1.467220	0.0057	0.282527	0.0106	0.43366	10.6	0.00168	11.2	0.282514	0.1	1.2	1406	73	1092	49
SA04/12 - 3.4	3	c2	419	4	6.1	0.5	0.004*	5.28	0.18	1.467190	0.0051	0.282530	0.0093	0.44886	10.8	0.00180	11.3	0.282516	0.2	1.1	1401	65	1089	43
SA04/12 - 4.7	4	c2	419	4	6.2	0.5	0.004*	5.86	0.13	1.467250	0.0045	0.282531	0.0083	0.32600	11.1	0.00132	11.9	0.282521	0.3	1.0	1390	58	1082	38
SA04/12 - 5.9	5	c2	419	4	7.1	0.5	0.004*	4.76	0.19	1.467190	0.0044	0.282548	0.0059	0.47319	10.6	0.00185	11.2	0.282534	0.8	0.7	1362	44	1062	29
SA04/12 - 11.26	11	c2	419	4	6.9	0.5	0.004*	5.24	0.13	1.467250	0.0038	0.282531	0.0062	0.31881	10.7	0.00127	11.4	0.282521	0.3	0.7	1390	44	1081	29
SA04/12 - 15.38	15	c2	419	4	5.5	0.5	0.004*	6.56	0.13	1.467180	0.0056	0.282520	0.0086	0.32383	10.8	0.00132	11.3	0.282510	-0.1	1.0	1415	60	1099	40

Analysis no.	grain no.	grain area	age	1 SD	$\delta^{18}O$ [‰]	2σ	$^{176}Lu/^{177}Hf$ (WR)	total Hf	Yb/Hf	$^{178}Hf/^{177}Hf$	1s%	$^{176}Hf/^{177}Hf$	1s%	$^{176}Yb/^{177}Hf$	1s%	$^{176}Lu/^{177}Hf$	1s%	$^{176}Hf/^{177}Hf$ (initial)	εHf	95% conf.	TDM_C	95% conf.	TDM_W	95% conf.
Etive																								
SA05/20 - 1c	1	c2	423	3	6.2	0.5	0.005	2.75	0.08	1.467220	0.0041	0.282374	0.0103	0.21191	12.5	0.00066	10.6	0.282369	-5.0	1.11	1729	68	1341	47
SA05/20 - 5a	5	c2	423	3	6.5	0.5	0.005	3.05	0.07	1.467180	0.0049	0.282416	0.0087	0.17122	12.4	0.00055	10.6	0.282412	-3.4	0.95	1633	58	1273	40
SA05/20 - 10c	10	c2	423	3	6.6	0.5	0.005	3.95	0.08	1.467200	0.0037	0.282354	0.0089	0.21310	12.4	0.00065	10.6	0.282349	-5.7	0.97	1773	59	1372	41
SA05/20 - 14a	14	c2	423	3	6.8	0.5	0.005	3.89	0.12	1.467210	0.0047	0.282432	0.0103	0.31326	12.7	0.00099	10.8	0.282425	-3.0	1.12	1605	69	1253	48
SA05/20 - 17a	17	c1	423	3	6.8	0.5	0.005	3.88	0.08	1.467260	0.0033	0.282425	0.0103	0.20267	13.5	0.00063	11.9	0.282420	-3.1	1.11	1614	68	1260	47
SA05/20 - 18a	17	c2	423	3	5.6	0.5	0.005	3.63	0.06	1.467260	0.0037	0.282382	0.0087	0.16231	12.4	0.00055	10.8	0.282378	-4.6	0.95	1709	57	1327	40
SA05/20 - 15a	15	c2	423	3	6.9	0.5	0.005	3.79	0.06	1.467230	0.0041	0.282418	0.0089	0.15410	13.5	0.00050	11.4	0.282414	-3.4	0.97	1627	59	1270	41
SA05/20 - 13a	13	rim	423	3	6.9	0.5	0.005	4.87	0.08	1.467270	0.0051	0.282368	0.0100	0.20715	12.4	0.00064	10.6	0.282363	-5.2	1.09	1742	66	1350	46
SA05/20 - 11a	11	c1	423	3	6.2	0.5	0.005	3.99	0.08	1.467280	0.0042	0.282383	0.0089	0.20096	12.6	0.00064	10.7	0.282378	-4.6	0.97	1708	59	1326	41
SA05/20 - 9a	9	c2	423	3	5.8	0.5	0.005	4.11	0.06	1.467190	0.0040	0.282359	0.0098	0.15910	12.6	0.00049	10.8	0.282355	-5.4	1.06	1759	64	1363	45
SA05/20 - 8a	8	c2	423	3	6.2	0.5	0.005	4.15	0.04	1.467080	0.0037	0.282366	0.0091	0.10838	12.4	0.00034	10.6	0.282364	-5.1	0.98	1741	60	1350	41
SA05/20 - 6a	6	c2	423	3	6.6	0.5	0.005	4.07	0.09	1.467160	0.0044	0.282404	0.0085	0.22009	13.0	0.00068	11.1	0.282399	-3.9	0.93	1662	57	1294	39
SA05/11 - 2a	2	c1+c2	421	9	6.4	0.4	0.009	5.35	0.05	1.467180	0.0037	0.282319	0.0057	0.11391	11.5	0.00057	11.6	0.282315	-6.9	0.78	1851	41	1562	32
SA05/11 - 3a	3	c1	421	9	6.5	0.4	0.009	5.46	0.04	1.467170	0.0038	0.282336	0.0065	0.11356	11.1	0.00052	11.5	0.282332	-6.3	0.86	1812	47	1531	36
SA05/11 - 7b	7	c1+c2	421	9	6.5	0.4	0.009	6.29	0.03	1.467230	0.0054	0.282315	0.0071	0.07857	10.6	0.00039	11.2	0.282312	-7.0	0.92	1857	50	1567	39
SA05/11 - 8a	8	c2	421	9	7.7	0.4	0.009	5.02	0.12	1.467270	0.0037	0.282349	0.0059	0.29645	10.6	0.00137	11.2	0.282339	-6.1	0.83	1798	44	1520	34
SA05/11 - 9a	9	c1	421	9	7.5	0.4	0.009	4.93	0.11	1.467290	0.0037	0.282370	0.0065	0.27239	10.7	0.00124	11.2	0.282361	-5.3	0.88	1749	48	1481	37
SA05/11 - 9b	9	c2	421	9	7.0	0.4	0.009	5.84	0.05	1.467240	0.0036	0.282334	0.0050	0.12449	10.6	0.00058	11.2	0.282330	-6.4	0.72	1818	38	1536	28
SA05/11 - 10a	10	c2a	421	9	7.0	0.2	0.009	4.69	0.07	1.467230	0.0036	0.282354	0.0054	0.17041	11.1	0.00082	11.8	0.282348	-5.8	0.76	1777	40	1503	31
SA05/11 - 10b	10	c2b	421	9	6.4	0.2	0.009	5.20	0.04	1.467250	0.0036	0.282340	0.0052	0.10649	11.2	0.00054	11.5	0.282336	-6.2	0.73	1804	38	1524	29
SA05/11 - 11a	11	c1	421	9	7.1	0.2	0.009	4.73	0.13	1.467220	0.0047	0.282352	0.0065	0.33270	11.4	0.00146	11.8	0.282341	-6.0	0.89	1793	48	1516	37
SA05/11 - 11d	11	rim	421	9	7.4	0.2	0.009	5.55	0.04	1.467220	0.0036	0.282331	0.0057	0.10151	10.7	0.00050	11.2	0.282327	-6.5	0.78	1823	41	1540	31
SA05/11 - 17b	17	c2	421	9	7.3	0.4	0.009	5.40	0.08	1.467210	0.0045	0.282341	0.0059	0.19750	10.6	0.00093	11.2	0.282334	-6.2	0.81	1808	44	1528	33
SA05/11 - 20a	20	c2	421	9	7.9	0.4	0.009	5.41	0.12	1.467210	0.0036	0.282316	0.0057	0.29653	10.7	0.00139	11.2	0.282305	-7.3	0.80	1872	43	1579	33
SA05/11 - 23a	23	c2	421	9	7.0	0.4	0.009	5.63	0.10	1.467210	0.0034	0.282340	0.0071	0.25352	10.6	0.00122	11.3	0.282331	-6.4	0.94	1815	51	1534	40
SA05/17 - 7b	7	rim	414	6	6.9	0.4	0.009*	5.01	0.04	1.467200	0.0046	0.282363	0.0068	0.10710	10.6	0.00051	11.4	0.282359	-5.5	0.82	1756	47	1485	37
SA05/17 - 8a	8	c2	414	6	4.6	0.4	0.009*	5.89	0.05	1.467240	0.0042	0.282390	0.0083	0.12478	10.9	0.00058	11.6	0.282386	-4.6	0.98	1697	57	1437	45
SA05/17 - 10a	10	c1+rim	414	6	6.7	0.4	0.009*	4.90	0.05	1.467270	0.0038	0.282357	0.0080	0.13396	10.7	0.00062	11.3	0.282353	-5.7	0.95	1771	55	1497	43
SA05/17 - 10c	10	c1+rim	414	6	7.2	0.5	0.009*	4.97	0.05	1.467230	0.0051	0.282349	0.0077	0.13658	10.7	0.00060	11.2	0.282345	-6.0	0.92	1789	53	1511	41
SA05/17 - 13a	13	c2	414	6	6.6	0.5	0.009*	4.64	0.04	1.467200	0.0047	0.282332	0.0057	0.10205	10.6	0.00046	11.2	0.282329	-6.6	0.71	1824	40	1539	31
SA05/17 - 14e	14	c2	414	6	6.7	0.2	0.009*	4.54	0.03	1.467230	0.0040	0.282335	0.0068	0.07012	11.5	0.00034	11.8	0.282333	-6.4	0.82	1815	47	1532	36
SA05/17 - 17b	17	c2	414	6	7.2	0.5	0.009*	4.18	0.05	1.467210	0.0047	0.282371	0.0071	0.12011	11.3	0.00052	11.7	0.282367	-5.2	0.86	1738	49	1471	38
SA05/17 - 19a	19	rim	414	6	5.9	0.5	0.009*	4.70	0.05	1.467170	0.0042	0.282349	0.0065	0.11520	11.0	0.00049	11.3	0.282346	-6.0	0.79	1787	45	1509	35
SA05/17 - 20a	20	c1+c2	414	6	7.5	0.5	0.009*	4.49	0.04	1.467210	0.0038	0.282331	0.0065	0.09837	10.7	0.00046	11.4	0.282328	-6.6	0.79	1827	45	1541	35
SA05/17 - 24a	24	c2	414	6	6.2	0.5	0.009*	4.78	0.05	1.467230	0.0035	0.282345	0.0057	0.12867	10.6	0.00058	11.2	0.282341	-6.2	0.71	1797	40	1518	31
SA05/17 - 3d	3	c2	414	6	6.5	0.2	0.009*	5.81	0.04	1.467170	0.0063	0.282361	0.0099	0.10660	10.9	0.00049	11.7	0.282358	-5.6	1.14	1760	67	1488	53
SA05/26 - 2c	2	c2	413	5	6.2	0.3	0.009*	3.21	0.05	1.46723	0.0036	0.282333	0.0095	0.13760	21.6	0.00055	20.4	0.282329	-6.6	1.1	1824	66	1539	51
SA05/26 - 1b	1	rim	413	5			0.009*	2.80	0.04	1.46728	0.0039	0.282352	0.0082	0.11285	21.2	0.00046	19.8	0.282349	-5.9	1.0	1780	57	1504	44
SA05/26 - 6a	6	c1	413	5	6.1	0.3	0.009*	3.00	0.10	1.4672	0.0040	0.282324	0.0087	0.25106	21.1	0.00105	19.8	0.282316	-7.1	1.0	1853	62	1562	48
SA05/26 - 7a	7	c2	413	5	6.8	0.3	0.009*	2.80	0.12	1.46736	0.0038	0.282367	0.0075	0.29222	21.2	0.00118	19.9	0.282358	-5.6	0.9	1759	55	1487	43
SA05/26 - 8a	8	c2	413	5	6.1	0.3	0.009*	3.07	0.07	1.46732	0.0035	0.282373	0.0079	0.16583	21.1	0.00068	19.8	0.282368	-5.2	0.9	1737	56	1470	44
SA05/26 - 11b	11	c2	413	5	6.8	0.3	0.009*	2.92	0.07	1.46727	0.0033	0.282362	0.0098	0.16639	21.1	0.00071	19.8	0.282357	-5.6	1.1	1762	68	1490	53
SA05/26 - 12a	12	c2	413	5	7.6	0.3	0.009*	2.45	0.06	1.46721	0.0037	0.282351	0.0095	0.15146	21.1	0.00067	19.9	0.282346	-6.0	1.1	1786	66	1509	52
SA05/26 - 16a	16	c2	413	5	7.2	0.3	0.009*	2.93	0.06	1.46727	0.0039	0.282367	0.0084	0.14670	21.2	0.00062	19.9	0.282362	-5.4	1.0	1750	59	1480	46
SA05/26 - 20c	20	c1	413	5	6.0	0.3	0.009*	3.99	0.06	1.46733	0.0031	0.282379	0.0082	0.15531	21.3	0.00071	20.0	0.282374	-5.0	1.0	1724	58	1459	45
SA05/26 - 27a	27	c2	413	5	6.5	0.3	0.009*	3.58	0.04	1.46731	0.0038	0.282351	0.0077	0.09035	21.4	0.00036	20.0	0.282348	-5.9	0.9	1781	54	1505	42
SA05/26 - 27d	27	rim	413	5	5.3	0.3	0.009*	4.36	0.10	1.46728	0.0035	0.282353	0.0084	0.26296	21.5	0.00097	20.1	0.282346	-6.0	1.0	1787	60	1509	47

Analysis no.	grain no.	grain area	age	1 SD	$\delta^{18}O$ [‰]	2σ	$^{176}Lu/^{177}Hf$ (WR)	total Hf	Yb/Hf	$^{178}Hf/^{177}Hf$	1s%	$^{176}Hf/^{177}Hf$	1s%	$^{176}Yb/^{177}Hf$	1s%	$^{176}Lu/^{177}Hf$	1s%	$^{176}Hf/^{177}Hf$ (initial)	εHf	95% conf.	TDM_C	95% conf.	TDM_W	95% conf.
SA05/15 - 4a (inh)	4	inh	1036	22	7.0	0.4	0.009*	4.47	0.04	1.467260	0.0042	0.282256	0.0079	0.09480	21.2	0.00039	19.8	0.282249	4.4	1.33	1611	73	1494	52
SA05/15 - 8a (inh)	8	inh	1646	6	5.9	0.4	0.009*	4.10	0.05	1.467260	0.0033	0.281749	0.0080	0.12292	21.2	0.00053	19.8	0.281733	-0.1	1.04	2374	75	2227	55
SA05/15 - 11a	11	c2	413	5	6.3	0.4	0.009*	3.44	0.08	1.467320	0.0043	0.282407	0.0090	0.19225	21.2	0.00085	19.8	0.282401	-4.1	1.05	1664	62	1411	49
SA05/15 - 19a	19	c1	413	5	6.9	0.4	0.009*	2.49	0.05	1.467260	0.0045	0.282383	0.0101	0.13428	21.5	0.00059	19.9	0.282379	-4.8	1.15	1713	68	1450	54
SA05/15 - 22a	22	c1+c2	413	5	6.8	0.4	0.009*	2.94	0.06	1.467250	0.0043	0.282413	0.0082	0.14185	21.2	0.00064	19.8	0.282408	-3.8	0.96	1647	57	1397	44
SA05/15 - 25b	25	c2+rim	413	5	5.7	0.4	0.009*	3.67	0.05	1.467310	0.0036	0.282350	0.0087	0.13485	21.2	0.00064	19.9	0.282345	-6.0	1.01	1788	60	1510	47
SA05/15 - 29a	29	c2	413	5	5.3	0.4	0.009*	3.21	0.05	1.467280	0.0038	0.282333	0.0079	0.11945	21.2	0.00049	19.8	0.282329	-6.6	0.93	1823	55	1539	43
SA05/15 - 26a	26	c1+c2	413	5	5.9	0.4	0.009*	5.13	0.07	1.467260	0.0032	0.282366	0.0073	0.17216	21.1	0.00083	19.8	0.282360	-5.5	0.88	1755	52	1484	40
SA05/15 - 15a	15	c2	413	5	6.2	0.4	0.009*	2.98	0.09	1.467240	0.0032	0.282381	0.0084	0.21755	21.2	0.00096	19.9	0.282374	-5.0	1.00	1724	59	1459	46
SA05/15 - 3b	3	c1	413	5	6.3	0.4	0.009*	3.22	0.12	1.467110	0.0048	0.282391	0.0118	0.30769	21.1	0.00115	19.8	0.282382	-4.7	1.35	1705	81	1444	64
SA05/05 - 4a	4	c2	412	6	7.2	0.4	0.008*	6.15	0.07	1.467250	0.0036	0.282290	0.0074	0.18907	10.6	0.00099	11.2	0.282283	-8.3	0.90	1928	52	1583	39
SA05/05 - 9a	9	c2+rim	412	6	6.9	0.4	0.008*	6.74	0.11	1.467200	0.0041	0.282275	0.0062	0.27014	11.3	0.00138	12.0	0.282265	-8.9	0.79	1968	45	1614	34
SA05/05 - 11d	11	rim	412	6	7.1	0.4	0.008*	7.45	0.03	1.467230	0.0046	0.282278	0.0057	0.06728	10.8	0.00039	11.2	0.282275	-8.5	0.71	1945	40	1596	30
SA05/01 - 6a	6	c2	408	6	7.0	0.6	0.008	6.47	0.10	1.467220	0.0044	0.282293	0.0059	0.25028	10.7	0.00123	11.3	0.282284	-8.3	0.76	1928	43	1582	32
SA05/01 - 5b	5	c1+c2	408	6	7.4	0.6	0.008	7.11	0.06	1.467170	0.0039	0.282266	0.0059	0.15473	10.8	0.00077	11.6	0.282260	-9.1	0.75	1980	42	1622	31
SA05/01 - 7a	7	c2	408	6	7.2	0.6	0.008	6.98	0.04	1.467220	0.0045	0.282255	0.0057	0.11092	10.7	0.00056	11.2	0.282251	-9.5	0.71	2001	40	1638	30
SA05/01 - 8a	8	c1	408	6	7.1	0.6	0.008	6.49	0.04	1.467220	0.0042	0.282284	0.0065	0.10581	10.7	0.00055	11.3	0.282280	-8.4	0.80	1936	45	1588	34
SA05/01 - 9a	9	c1	408	6	7.0	0.4	0.008	4.96	0.11	1.467210	0.0037	0.282229	0.0062	0.28582	11.4	0.00129	12.3	0.282219	###	0.79	2071	45	1693	33
SA05/01 - 14a	14	rim	408	6	7.0	0.4	0.008	5.91	0.08	1.467270	0.0043	0.282273	0.0057	0.19611	10.6	0.00097	11.3	0.282266	-8.9	0.72	1968	41	1613	30
SA05/01 - 18a	18	c2+rim	408	6	6.7	0.4	0.008	5.59	0.05	1.467250	0.0049	0.282250	0.0074	0.13544	10.9	0.00065	11.7	0.282245	-9.7	0.89	2014	51	1648	38
SA05/01 - 18b	18	rim+c2	408	6	6.6	0.4	0.008	6.07	0.04	1.467170	0.0042	0.282259	0.0059	0.10556	10.6	0.00058	11.2	0.282255	-9.3	0.74	1992	42	1632	31
SA05/01 - 19b	19	rim	408	6	6.5	0.4	0.008	6.11	0.04	1.467210	0.0057	0.282278	0.0065	0.09172	10.7	0.00051	11.2	0.282274	-8.6	0.79	1949	45	1598	34
SA05/01 - 20a	20	c2	408	6	7.1	0.4	0.008	5.85	0.05	1.467180	0.0051	0.282267	0.0062	0.12736	11.2	0.00062	11.4	0.282263	-9.1	0.77	1975	44	1619	32
SA05/23 - 1a	1	c1	408	4	5.9	0.3	0.007	3.34	0.12	1.467080	0.0045	0.282344	0.0104	0.29991	21.1	0.00108	19.8	0.282336	-6.5	1.18	1812	71	1458	52
SA05/23 - 5a	5	c2	408	4	6.2	0.3	0.007	4.00	0.15	1.467410	0.0079	0.282385	0.0134	0.36980	21.2	0.00134	19.8	0.282375	-5.1	1.50	1725	91	1392	67
SA05/23 - 6a	6	c2	408	4	5.5	0.3	0.007	3.83	0.10	1.467500	0.0054	0.282330	0.0118	0.24101	21.3	0.00085	20.0	0.282324	-6.9	1.32	1839	80	1478	59
SA05/23 - 10b	10	c2	408	4	6.5	0.3	0.007	4.34	0.08	1.467320	0.0048	0.282377	0.0098	0.21192	21.2	0.00085	19.9	0.282371	-5.2	1.11	1734	67	1399	49
SA05/23 - 11a	11	c2	408	4	6.1	0.3	0.007	3.80	0.08	1.467280	0.0040	0.282364	0.0087	0.19851	21.6	0.00090	20.1	0.282357	-5.7	1.00	1764	60	1422	44
SA05/23 - 15a	15	c1	408	4	5.9	0.3	0.007	3.55	0.03	1.467240	0.0039	0.282351	0.0092	0.08658	21.1	0.00039	19.8	0.282348	-6.0	1.03	1784	62	1437	45
SA05/23 - 16b	16	c2	408	4	6.7	0.3	0.007	3.92	0.08	1.467240	0.0040	0.282350	0.0077	0.20446	21.5	0.00098	19.9	0.282343	-6.2	0.91	1797	54	1446	40
SA05/23 - 22a	22	c1	408	4	6.7	0.3	0.007	2.85	0.03	1.467300	0.0037	0.282384	0.0084	0.07854	21.1	0.00033	19.8	0.282382	-4.8	0.95	1710	57	1381	42
SA05/25 - 4a	4	c2	405	12	5.9	0.3	0.007*	3.84	0.14	1.467090	0.0055	0.282331	0.0131	0.34746	21.5	0.00142	19.8	0.282320	-7.1	1.64	1848	94	1484	67
SA05/25 - 6a	6	c2	405	12	6.5	0.3	0.007*	2.78	0.11	1.467230	0.0047	0.282403	0.0125	0.28364	21.7	0.00108	19.9	0.282395	-4.4	1.56	1682	89	1359	64
SA05/25 - 9a	9	c1	405	12	5.6	0.3	0.007*	1.94	0.08	1.467350	0.0050	0.282401	0.0128	0.21122	22.7	0.00088	21.4	0.282395	-4.4	1.58	1683	91	1360	65
SA05/25 - 10b	10	c2	405	12	4.9	0.3	0.007*	2.53	0.19	1.467290	0.0112	0.282565	0.0134	0.47931	21.7	0.00167	19.9	0.282553	1.1	1.68	1328	97	1094	70
SA05/25 - 16a	16	c2	405	12	6.1	0.3	0.007*	3.94	0.07	1.467260	0.0049	0.282415	0.0101	0.18452	21.9	0.00076	20.5	0.282410	-3.9	1.31	1649	73	1335	52
SA05/25 - 24b	24	c2	405	12	6.9	0.3	0.007*	3.11	0.14	1.467270	0.0048	0.282384	0.0092	0.35801	21.2	0.00154	19.9	0.282373	-5.2	1.25	1732	70	1397	49
SA05/25 - 25b	25	c2	405	12	6.3	0.3	0.007*	3.18	0.16	1.467200	0.0035	0.282415	0.0087	0.40569	21.1	0.00162	19.8	0.282403	-4.2	1.20	1664	67	1346	47

c1 = unzoned inner core
c2 = osciallatory zoned outer core
r1-2 = rim

*$^{176}Lu/^{177}Hf$ (WR) ratio not calculated based on the Lu/Hf ratio of the whole-rock; assumed to be similar to other samples of same mapped unit showing the same εHf value

Appendix 3b
Hf isotope data of Mud Tank zircon standard

	total Hf	1σ	Yb/Hf	1σ	$^{176}Yb/^{177}Hf$	1σ	$^{176}Lu/^{177}Hf$	1σ	$^{176}Hf/^{177}Hf$	1σ
13/12/06										
mud tank 1	5.1	0.10	0.004	0.000021	0.011160	0.000053	0.0002361	0.0000006	0.282506	0.000010
mud tank 2	5.1	0.11	0.004	0.000017	0.011142	0.000042	0.0002357	0.0000006	0.282491	0.000020
mud tank 3	5.0	0.12	0.004	0.000014	0.011173	0.000036	0.0002362	0.0000006	0.282500	0.000011
mud tank 4	4.8	0.12	0.004	0.000013	0.011376	0.000034	0.0002417	0.0000007	0.282496	0.000015
mud tank 5	4.6	0.11	0.005	0.000013	0.012351	0.000032	0.0002621	0.0000006	0.282507	0.000013
mud tank 6	4.8	0.11	0.005	0.000012	0.012265	0.000032	0.0002617	0.0000006	0.282468	0.000016
mud tank 7	4.8	0.11	0.004	0.000014	0.010731	0.000035	0.0002302	0.0000009	0.282471	0.000015
mud tank 8	5.0	0.11	0.005	0.000015	0.011413	0.000039	0.0002419	0.0000007	0.282500	0.000016
Mud tank 9	4.6	0.08	0.004	0.000014	0.010985	0.000036	0.0002305	0.0000008	0.282468	0.000011
Mud tank 10	4.6	0.08	0.004	0.000018	0.010848	0.000045	0.0002237	0.0000007	0.282489	0.000014
Mud tank 11	4.9	0.08	0.004	0.000021	0.010938	0.000053	0.0002355	0.0000006	0.282480	0.000015
Mud tank 12	4.7	0.07	0.004	0.000022	0.010834	0.000055	0.0002290	0.0000007	0.282484	0.000011
Mud tank 13	4.5	0.07	0.004	0.000018	0.010878	0.000045	0.0002259	0.0000007	0.282489	0.000011
Mud tank 14	4.4	0.06	0.004	0.000020	0.010882	0.000050	0.0002262	0.0000005	0.282479	0.000016
Mud Tank 15	4.3	0.06	0.004	0.000014	0.011049	0.000035	0.0002249	0.0000005	0.282476	0.000012
Mud Tank 16	4.7	0.06	0.004	0.000017	0.011119	0.000043	0.0002244	0.0000004	0.282473	0.000010
Mud Tank 17	4.2	0.05	0.004	0.000022	0.009601	0.000054	0.0002182	0.0000006	0.282465	0.000017
Mud Tank 18	4.3	0.07	0.004	0.000019	0.009433	0.000047	0.0002171	0.0000006	0.282470	0.000013
Mud Tank 19	4.3	0.07	0.004	0.000021	0.009833	0.000052	0.0002323	0.0000007	0.282491	0.000017
Mud Tank 20	4.3	0.07	0.004	0.000022	0.009699	0.000055	0.0002258	0.0000005	0.282477	0.000012
Mud Tank 21	4.1	0.06	0.004	0.000019	0.009767	0.000049	0.0002307	0.0000008	0.282492	0.000012
Mud Tank 22	3.9	0.05	0.004	0.000023	0.009857	0.000057	0.0002310	0.0000006	0.282523	0.000018
14/12/06										
Mud tank 1	4.5	0.07	0.004	0.000024	0.010034	0.000061	0.0002261	0.0000006	0.282521	0.000018
Mud tank 2	4.2	0.09	0.005	0.000031	0.011716	0.000077	0.0002588	0.0000007	0.282512	0.000012
Mud tank 3	4.2	0.10	0.004	0.000025	0.010480	0.000064	0.0002376	0.0000007	0.282526	0.000012
Mud tank 4	3.9	0.10	0.005	0.000026	0.011611	0.000065	0.0002580	0.0000007	0.282530	0.000015
Mud tank 5	4.3	0.11	0.004	0.000028	0.009822	0.000070	0.0002259	0.0000009	0.282483	0.000014
Mud tank 6	4.3	0.11	0.004	0.000020	0.010564	0.000051	0.0002402	0.0000007	0.282505	0.000016
Mud Tank 7	4.2	0.10	0.005	0.000024	0.012785	0.000061	0.0002913	0.0000006	0.282496	0.000019
Mu Tank 8	4.1	0.09	0.005	0.000033	0.012129	0.000084	0.0002767	0.0000008	0.282473	0.000015
Mud Tank 9	3.9	0.08	0.004	0.000020	0.009684	0.000051	0.0002143	0.0000006	0.282499	0.000010
Mud tank 10	4.0	0.08	0.005	0.000025	0.011990	0.000063	0.0002432	0.0000007	0.282475	0.000009
Mud tank 11	4.2	0.09	0.004	0.000021	0.011072	0.000053	0.0002289	0.0000008	0.282511	0.000011
Mud Tank 12	4.5	0.09	0.006	0.000017	0.014095	0.000044	0.0002946	0.0000008	0.282510	0.000012
Mud Tank 13	4.5	0.10	0.006	0.000018	0.014799	0.000046	0.0003048	0.0000006	0.282518	0.000011
Mud Tank 14	4.4	0.10	0.006	0.000023	0.014029	0.000058	0.0002912	0.0000008	0.282509	0.000015
Mud Tank 15	3.9	0.08	0.005	0.000027	0.013356	0.000069	0.0002685	0.0000006	0.282470	0.000019
Mud Tank 16	3.7	0.06	0.004	0.000022	0.011311	0.000056	0.0002248	0.0000008	0.282544	0.000021
Mud Tank 17	4.5	0.10	0.005	0.000021	0.013512	0.000053	0.0002609	0.0000006	0.282486	0.000014
Mud Tank 18	4.6	0.09	0.005	0.000023	0.011856	0.000059	0.0002322	0.0000005	0.282498	0.000013
Mud Tank 19	4.7	0.10	0.005	0.000028	0.012116	0.000072	0.0002408	0.0000007	0.282517	0.000012
Mud Tank 20	4.6	0.11	0.005	0.000021	0.012959	0.000051	0.0002510	0.0000005	0.282490	0.000015
15/12/06										
Mud Tank 1	4.2	0.11	0.005	0.000023	0.011431	0.000059	0.0002110	0.0000006	0.282525	0.000012
Mud Tank 2	4.2	0.11	0.005	0.000016	0.011759	0.000040	0.0002154	0.0000006	0.282512	0.000016
Mud Tank 3	4.2	0.10	0.004	0.000024	0.011171	0.000061	0.0002062	0.0000006	0.282506	0.000016
Mud Tank 4	4.3	0.11	0.005	0.000023	0.011675	0.000058	0.0002131	0.0000006	0.282521	0.000016
Mud Tank 5	4.6	0.08	0.004	0.000035	0.010439	0.000087	0.0001952	0.0000006	0.282502	0.000016
Mud Tank 6	4.6	0.10	0.004	0.000029	0.010255	0.000073	0.0001896	0.0000004	0.282496	0.000015
Mud Tank 7	4.2	0.10	0.004	0.000021	0.010795	0.000053	0.0001937	0.0000006	0.282518	0.000010
Mud Tank 8	4.1	0.10	0.005	0.000025	0.011456	0.000062	0.0002132	0.0000007	0.282512	0.000018
Mud Tank 9	4.6	0.09	0.004	0.000034	0.010616	0.000086	0.0002143	0.0000005	0.282514	0.000015
Mud Tank 10	4.4	0.08	0.004	0.000031	0.010665	0.000077	0.0002070	0.0000005	0.282495	0.000016
Mud Tank 11	4.0	0.09	0.004	0.000028	0.011202	0.000070	0.0002035	0.0000006	0.282499	0.000013
Mud Tank 12	4.0	0.10	0.004	0.000037	0.011085	0.000093	0.0002024	0.0000005	0.282517	0.000018
Mud Tank 13	3.8	0.08	0.004	0.000028	0.010938	0.000070	0.0002069	0.0000008	0.282505	0.000016
Mud Tank 14	3.8	0.06	0.004	0.000035	0.010800	0.000089	0.0002007	0.0000006	0.282510	0.000015
Mud Tank 15	5.4	0.11	0.004	0.000017	0.009333	0.000044	0.0001994	0.0000005	0.282524	0.000015
Mud Tank 16	5.3	0.11	0.005	0.000022	0.013619	0.000056	0.0002869	0.0000007	0.282493	0.000013
Mud Tank 17	5.0	0.10	0.005	0.000041	0.013523	0.000100	0.0002764	0.0000005	0.282510	0.000012
Mud Tank 18	5.6	0.10	0.004	0.000026	0.009330	0.000066	0.0001970	0.0000004	0.282516	0.000014
Mud Tank 19	5.6	0.11	0.004	0.000023	0.009149	0.000058	0.0001957	0.0000004	0.282497	0.000010
Mud Tank 20	5.4	0.11	0.004	0.000027	0.010034	0.000068	0.0002185	0.0000006	0.282501	0.000014
Mud Tank 21	5.1	0.11	0.004	0.000028	0.009546	0.000071	0.0002083	0.0000006	0.282496	0.000012
Mud Tank 22	5.1	0.10	0.004	0.000025	0.010261	0.000063	0.0002171	0.0000006	0.282517	0.000013
Mud Tank 23	5.0	0.12	0.004	0.000029	0.010007	0.000072	0.0002113	0.0000006	0.282497	0.000012
Mud Tank 24	6.3	0.12	0.004	0.000019	0.010792	0.000048	0.0002332	0.0000004	0.282526	0.000012
Mud Tank 25	5.1	0.11	0.005	0.000030	0.011935	0.000076	0.0002383	0.0000006	0.282520	0.000011
Mud Tank 26	4.9	0.11	0.005	0.000033	0.011741	0.000083	0.0002323	0.0000006	0.282525	0.000013
Mud Tank 27	5.0	0.11	0.004	0.000022	0.009070	0.000054	0.0001769	0.0000004	0.282507	0.000013
average (n=69)	**4.6**		**0.004417**		**0.011158**		**0.000231**		**0.282500**	
2SD	**1.0**		**0.000986**		**0.002515**		**0.000054**		**0.000036**	

	total Hf	1σ	Yb/Hf	1σ	$^{176}Yb/^{177}Hf$	1σ	$^{176}Lu/^{177}Hf$	1σ	$^{176}Hf/^{177}Hf$	1σ
07/02/07										
Mud Tank 1	4.6	0.10	0.005	0.000019	0.012201	0.000047	0.0002353	0.0000009	0.282540	0.000014
Mud Tank 2	5.3	0.09	0.005	0.000028	0.012417	0.000071	0.0002389	0.0000006	0.282519	0.000013
Mud Tank 3	4.9	0.12	0.005	0.000018	0.011950	0.000044	0.0002322	0.0000005	0.282509	0.000012
Mud Tank 4	4.9	0.11	0.005	0.000018	0.011886	0.000045	0.0002251	0.0000007	0.282484	0.000010
Mud Tank 5	5.1	0.11	0.005	0.000022	0.013796	0.000056	0.0002575	0.0000006	0.282515	0.000012
Mud Tank 6	5.0	0.09	0.006	0.000029	0.014386	0.000074	0.0002678	0.0000008	0.282537	0.000009
Mud Tank 7	4.7	0.05	0.002	0.000015	0.005273	0.000038	0.0001138	0.0000007	0.282519	0.000014
Mud Tank 8	4.5	0.05	0.003	0.000020	0.006572	0.000049	0.0001482	0.0000006	0.282499	0.000012
Mud Tank 9	4.1	0.05	0.003	0.000017	0.006295	0.000044	0.0001374	0.0000006	0.282489	0.000012
Mud Tank 10	3.6	0.04	0.004	0.000018	0.008921	0.000044	0.0001936	0.0000009	0.282525	0.000019
Mud Tank 11	5.2	0.06	0.004	0.000030	0.011259	0.000076	0.0002182	0.0000009	0.282504	0.000016
Mud Tank 12	5.0	0.04	0.005	0.000040	0.011808	0.000100	0.0002242	0.0000005	0.282477	0.000008
Mud Tank 13	5.2	0.09	0.005	0.000022	0.011457	0.000055	0.0002248	0.0000005	0.282537	0.000012
Mud Tank 14	4.5	0.08	0.005	0.000019	0.012323	0.000047	0.0002356	0.0000006	0.282515	0.000014
Mud Tank 15	4.7	0.09	0.005	0.000028	0.011898	0.000070	0.0002270	0.0000006	0.282517	0.000010
Mud Tank 16	4.7	0.08	0.005	0.000026	0.013125	0.000066	0.0002512	0.0000006	0.282484	0.000009
Mud Tank 17	4.6	0.08	0.005	0.000025	0.012249	0.000064	0.0002357	0.0000006	0.282515	0.000013
Mud Tank 18	4.8	0.08	0.005	0.000034	0.011919	0.000084	0.0002247	0.0000006	0.282496	0.000011
Mud Tank 19	4.7	0.10	0.005	0.000029	0.011839	0.000072	0.0002294	0.0000007	0.282511	0.000011
Mud Tank 20	4.3	0.09	0.004	0.000020	0.010578	0.000049	0.0002246	0.0000006	0.282500	0.000014
Mud Tank 21	4.4	0.09	0.004	0.000022	0.010775	0.000055	0.0002321	0.0000006	0.282531	0.000015
Mud Tank 22	4.1	0.10	0.004	0.000018	0.011108	0.000046	0.0002271	0.0000007	0.282505	0.000013
08/02/07										
Mud Tank 1	5.9	0.06	0.007	0.000052	0.017588	0.000130	0.0002956	0.0000006	0.282508	0.000012
Mud Tank 2	6.0	0.07	0.007	0.000043	0.017752	0.000110	0.0003006	0.0000003	0.282486	0.000010
Mud Tank 3	6.2	0.11	0.007	0.000035	0.017047	0.000088	0.0002987	0.0000006	0.282514	0.000012
Mud Tank 4	6.2	0.10	0.007	0.000030	0.016695	0.000075	0.0002905	0.0000005	0.282513	0.000012
Mud Tank 5	6.2	0.11	0.007	0.000038	0.017507	0.000095	0.0003028	0.0000006	0.282498	0.000010
Mud Tank 6	4.9	0.10	0.007	0.000034	0.018183	0.000085	0.0003054	0.0000005	0.282515	0.000010
Mud Tank 7	5.3	0.10	0.007	0.000034	0.017745	0.000086	0.0003025	0.0000005	0.282499	0.000012
Mud Tank 8	4.5	0.07	0.007	0.000041	0.018170	0.000100	0.0003037	0.0000006	0.282492	0.000012
Mud Tank 9	4.9	0.09	0.007	0.000044	0.018256	0.000110	0.0003046	0.0000005	0.282486	0.000010
Mud Tank 10	4.7	0.09	0.007	0.000032	0.017485	0.000081	0.0002925	0.0000007	0.282537	0.000013
Mud Tank 11	5.2	0.09	0.007	0.000036	0.016926	0.000091	0.0002910	0.0000005	0.282518	0.000012
Mud Tank 12	5.1	0.06	0.008	0.000060	0.019555	0.000150	0.0003241	0.0000008	0.282527	0.000013
Mud Tank 13	5.5	0.06	0.008	0.000040	0.019314	0.000099	0.0003218	0.0000006	0.282506	0.000013
Mud Tank 14	4.7	0.08	0.008	0.000079	0.019078	0.000200	0.0003131	0.0000007	0.282513	0.000013
Mud Tank 15	5.4	0.06	0.007	0.000051	0.018439	0.000130	0.0003052	0.0000007	0.282512	0.000010
Mud Tank 16	5.7	0.05	0.007	0.000053	0.017897	0.000130	0.0002976	0.0000005	0.282510	0.000011
Mud Tank 17	5.8	0.06	0.005	0.000040	0.013722	0.000100	0.0002295	0.0000006	0.282505	0.000009
Mud Tank 18	6.1	0.13	0.006	0.000042	0.015670	0.000110	0.0002612	0.0000007	0.282535	0.000011
Mud Tank 19	6.1	0.13	0.007	0.000051	0.017408	0.000130	0.0002881	0.0000005	0.282509	0.000012
Mud Tank 20	6.1	0.10	0.006	0.000047	0.016142	0.000120	0.0002672	0.0000005	0.282521	0.000009
Mud Tank 21	5.9	0.05	0.007	0.000052	0.016741	0.000130	0.0002779	0.0000005	0.282530	0.000013
Mud Tank 22	5.5	0.06	0.007	0.000052	0.016853	0.000130	0.0002804	0.0000008	0.282513	0.000011
Mud Tank 23	5.2	0.08	0.007	0.000058	0.017852	0.000150	0.0002953	0.0000006	0.282511	0.000016
Mud Tank 24	4.6	0.08	0.007	0.000062	0.017262	0.000160	0.0002815	0.0000008	0.282540	0.000014
Mud Tank 25	5.3	0.09	0.006	0.000030	0.015944	0.000076	0.0002574	0.0000005	0.282508	0.000010
Mud Tank 26	5.7	0.10	0.007	0.000033	0.017936	0.000082	0.0002951	0.0000004	0.282525	0.000012
average (n=48)	**5.1**		**0.005761**		**0.014525**		**0.000258**		**0.282512**	
2SD	**1.3**		**0.002869**		**0.007246**		**0.000093**		**0.000031**	

Appendix 3c: Hf isotope methodology – Correction for isobaric Yb interference

In order to obtain accurate $^{176}Hf/^{177}Hf$ ratios for zircons corrections for the interference of ^{176}Lu and ^{176}Yb on ^{176}Hf have to be carried out. These may be made by monitoring the signal intensities of the interference-free isotopes ^{175}Lu and ^{173}Yb, ^{172}Yb or ^{171}Yb, which are used to calculate the intensities for ^{176}Lu and ^{176}Yb. At the NERC Isotope Geosciences Laboratory (NIGL) in Nottingham corrections were applied based on the signal intensities of ^{175}Lu using the $^{176}Lu/^{175}Lu$ ratio of 0.02653 and ^{173}Yb. The appropriate value of $^{176}Yb/^{173}Yb$ (0.79488) was determined by successively spiking the JMC475 Hf standard with Yb. This method of Yb correction has been shown to provide accurate Hf isotope data, if the difference between the Yb mass bias factor (β(Yb)) and Hf mass bias factor (β(Hf)) is constant between different samples (solution standard and zircon) (Thirlwall and Walder, 1995; Griffin et al., 2000, 2002, 2004; Andersen et al., 2002; Andersen and Griffin, 2004). However, Iziuka and Hirata (2005) demonstrated by analysing a mixed solution of Hf standard JMC475 and Yb standard Cica-Merck, and solid samples of NIST SRM 610 glass and zircon standard 91500 that data from all samples deviate from the line β(Yb) = β(Hf) indicating that β(Yb) must be determined separately from β(Hf). In addition, they found that both β(Yb) and β(Hf) changed with analysis time, and that all samples formed different regression lines with differing slopes. Based on these results they suggested that β(Yb) based on solution data cannot be applied to in-situ Hf isotope analysis of zircons.

At NIGL a peak jumping routine including ^{172}Yb to allow assessment of the effect of using a Yb mass bias correction for the Yb interference correction in addition to a Hf mass bias correction, has been investigated but was nevertheless found unnecessary with the data for both being equivalent within the increased uncertainty reflected by the low Yb concentrations. Therefore, the Yb interference correction was solely based on solution data. To illustrate the appropriateness of this correction method the measured $^{176}Hf/^{177}Hf$ and $^{176}Yb/^{177}Hf$ ratios determined on all unknown zircons are plotted (Fig. 1). This shows that as no positively sloping trend can be observed, correctness of the method may be assumed. Supporting evidence is

that Yb-doped JMC475 solutions gave $^{176}Hf/^{177}Hf$ ratios indistinguishable of undoped solutions (Table 1) and within analytical uncertainty (2SD) of the accepted value of JMC475 ($^{176}Hf/^{177}Hf = 0.28216$ (Nowell et al., 1998)).

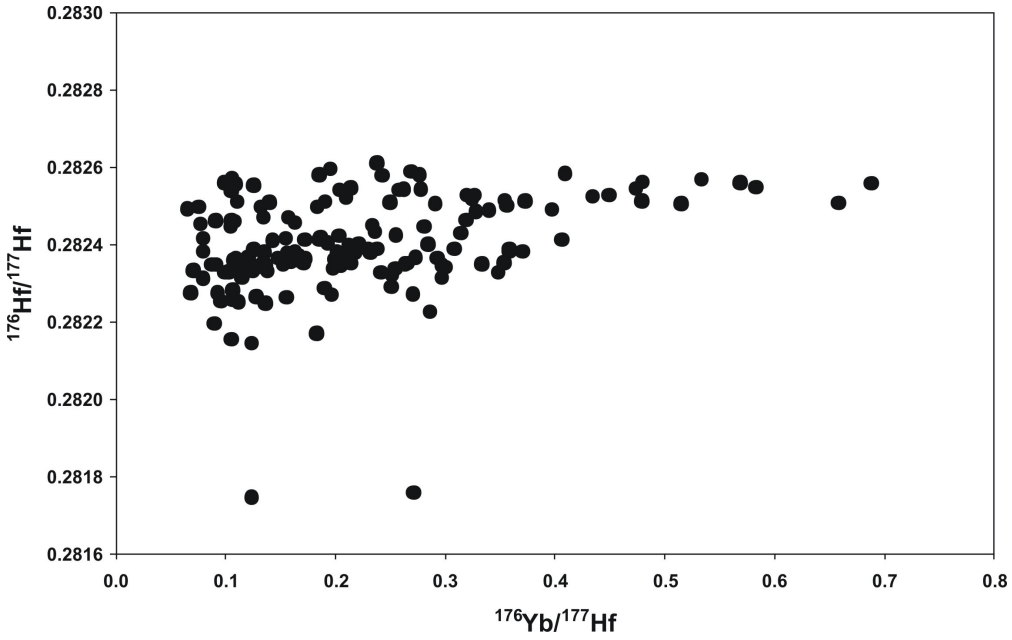

Fig. 1: $^{176}Yb/^{177}Hf$ vs. $^{176}Hf/^{177}Hf$ plot demonstrating the correctness of the Yb interference method.

Table 1
Hf isotope data of undoped and doped JMC475 solution standard

	total Hf	1σ	Yb/Hf	1σ	$^{176}Yb/^{177}Hf$	1σ	$^{176}Lu/^{177}Hf$	1σ	$^{176}Hf/^{177}Hf$	1σ
13/12/06										
JMC475 - undoped	11.9	0.02	0.000	0.000001	-0.000023	0.000003	-0.0000001	0.0000001	0.282143	0.000004
JMC475 - undoped	12.0	0.02	0.000	0.000001	-0.000021	0.000003	-0.0000009	0.0000001	0.282147	0.000004
JMC475 - undoped	11.9	0.02	0.000	0.000001	-0.000016	0.000003	0.0000000	0.0000001	0.282137	0.000004
JMC475 - undoped	11.8	0.02	0.000	0.000001	0.000003	0.000003	0.0000001	0.0000001	0.282138	0.000003
JMC475 - undoped	11.8	0.02	0.000	0.000001	-0.000008	0.000003	-0.0000002	0.0000001	0.282140	0.000004
JMC475 - undoped	12.0	0.02	0.000	0.000001	0.000005	0.000003	0.0000002	0.0000001	0.282134	0.000003
JMC475 - undoped	12.1	0.02	0.000	0.000001	0.000009	0.000003	-0.0000003	0.0000001	0.282128	0.000004
JMC475 - undoped	11.9	0.02	0.000	0.000001	0.000013	0.000003	0.0000006	0.0000001	0.282123	0.000004
JMC475 - undoped	12.1	0.02	0.000	0.000001	0.000031	0.000003	0.0000005	0.0000001	0.282129	0.000004
JMC475 - undoped	12.0	0.02	0.000	0.000001	0.000018	0.000003	0.0000003	0.0000001	0.282128	0.000003
JMC475 - undoped	9.9	0.02	0.000	0.000001	0.000015	0.000004	0.0000002	0.0000001	0.282128	0.000004
JMC475 - undoped	9.8	0.01	0.000	0.000001	0.000002	0.000003	-0.0000001	0.0000001	0.282133	0.000003
JMC475 - undoped	9.7	0.02	0.000	0.000002	0.000013	0.000005	-0.0000003	0.0000001	0.282129	0.000003
average (n=13)	**11.5**		**0.000**		**0.000003**		**0.0000000**		**0.282134**	
2SD	**1.9**		**0.000**		**0.000032**		**0.0000007**		**0.000014**	
JMC475 - doped	11.9	0.02	0.271	0.000108	0.683869	0.000287	0.0055566	0.0000008	0.282149	0.000005
JMC475 - doped	11.7	0.02	0.270	0.000135	0.681534	0.000354	0.0055502	0.0000007	0.282151	0.000005
JMC475 - doped	9.9	0.01	0.251	0.000062	0.633844	0.000184	0.0053795	0.0000005	0.282143	0.000006
JMC475 - doped	9.8	0.01	0.251	0.000071	0.633122	0.000191	0.0053777	0.0000004	0.282131	0.000004
average (n=4)	**10.8**		**0.260**		**0.658093**		**0.0054660**		**0.282143**	
2SD	**2.2**		**0.022**		**0.056868**		**0.0002019**		**0.000018**	
14/12/06										
JMC475 - undoped	9.4	0.02	0.000	0.000001	0.000009	0.000004	0.0000000	0.0000001	0.282156	0.000004
JMC475 - undoped	9.3	0.02	0.000	0.000001	0.000008	0.000004	-0.0000005	0.0000002	0.282158	0.000005
JMC475 - undoped	9.2	0.02	0.000	0.000002	0.000002	0.000004	-0.0000002	0.0000001	0.282148	0.000005
JMC475 - undoped	9.3	0.01	0.000	0.000002	0.000008	0.000004	-0.0000005	0.0000001	0.282148	0.000006
JMC475 - undoped	9.3	0.01	0.000	0.000001	0.000016	0.000003	-0.0000002	0.0000001	0.282141	0.000004
JMC475 - undoped	9.2	0.02	0.000	0.000002	0.000006	0.000004	-0.0000001	0.0000001	0.282158	0.000004
JMC475 - undoped	9.2	0.02	0.000	0.000002	-0.000003	0.000005	0.0000002	0.0000002	0.282151	0.000005
JMC475 - undoped	9.2	0.01	0.000	0.000002	0.000007	0.000004	-0.0000005	0.0000001	0.282140	0.000004
JMC475 - undoped	9.2	0.01	0.000	0.000001	0.000004	0.000003	0.0000007	0.0000001	0.282153	0.000004
JMC475 - undoped	9.1	0.01	0.000	0.000001	0.000008	0.000003	-0.0000001	0.0000001	0.282151	0.000005
JMC475 - undoped	8.5	0.01	0.000	0.000002	0.000011	0.000004	0.0000001	0.0000002	0.282148	0.000005
JMC475 - undoped	8.4	0.01	0.000	0.000002	-0.000003	0.000004	0.0000002	0.0000002	0.282141	0.000005
JMC475 - undoped	8.4	0.02	0.000	0.000001	0.000012	0.000004	-0.0000001	0.0000002	0.282150	0.000005
JMC475 - undoped	8.5	0.01	0.000	0.000002	0.000025	0.000004	0.0000009	0.0000002	0.282132	0.000004
JMC475 - undoped	8.9	0.01	0.000	0.000002	0.000005	0.000004	-0.0000001	0.0000001	0.282148	0.000004
JMC475 - undoped	9.1	0.02	0.000	0.000001	-0.000005	0.000003	0.0000009	0.0000001	0.282164	0.000005
average (n=16)	**9.0**		**0.000**		**0.000007**		**0.0000000**		**0.282149**	
2SD	**0.7**		**0.000**		**0.000015**		**0.0000009**		**0.000016**	
JMC475 - doped	9.2	0.01	0.237	0.000051	0.599317	0.000140	0.0053919	0.0000004	0.282135	0.000005
JMC475 - doped	9.2	0.01	0.238	0.000043	0.600950	0.000119	0.0053919	0.0000004	0.282150	0.000005
JMC475 - doped	9.2	0.01	0.237	0.000041	0.599273	0.000121	0.0053861	0.0000004	0.282143	0.000005
JMC475 - doped	9.2	0.01	0.237	0.000058	0.598782	0.000155	0.0053840	0.0000004	0.282167	0.000005
JMC475 - doped	9.1	0.01	0.237	0.000049	0.598935	0.000142	0.0053858	0.0000004	0.282162	0.000004
JMC475 - doped	9.2	0.01	0.236	0.000047	0.597413	0.000123	0.0053779	0.0000004	0.282149	0.000006
JMC475 - doped	8.7	0.01	0.232	0.000038	0.587203	0.000106	0.0053348	0.0000003	0.282156	0.000006
JMC475 - doped	8.6	0.01	0.233	0.000034	0.587649	0.000100	0.0053372	0.0000003	0.282154	0.000005
average (n=8)	**9.1**		**0.236**		**0.596190**		**0.0053737**		**0.282152**	
2SD	**0.5**		**0.004**		**0.010991**		**0.0000474**		**0.000021**	
15/12/06										
JMC475 - undoped	8.9	0.02	0.000	0.000001	0.000006	0.000004	0.0000000	0.0000001	0.282148	0.000004
JMC475 - undoped	8.9	0.02	0.000	0.000002	0.000007	0.000004	-0.0000004	0.0000002	0.282148	0.000004
JMC475 - undoped	8.9	0.02	0.000	0.000001	-0.000009	0.000003	0.0000001	0.0000001	0.282154	0.000004
average (n=3)	**8.9**		**0.000**		**0.000002**		**-0.0000001**		**0.282150**	
2SD	**0.0**		**0.000**		**0.000018**		**0.0000004**		**0.000007**	
JMC475 - doped	9.2	0.03	0.241	0.000099	0.610867	0.000264	0.0054659	0.0000007	0.282148	0.000005
JMC475 - doped	9.3	0.02	0.241	0.000069	0.610453	0.000190	0.0054602	0.0000007	0.282146	0.000004
average (n=2)	**9.2**		**0.241**		**0.610660**		**0.0054631**		**0.282147**	
2SD	**0.1**		**0.000**		**0.000585**		**0.0000081**		**0.000003**	
07/02/07										
JMC475 - undoped	8.1	0.01	0.000	0.000001	-0.000006	0.000004	0.0000003	0.0000002	0.282163	0.000006
JMC475 - undoped	8.0	0.01	0.000	0.000002	0.000013	0.000005	0.0000004	0.0000001	0.282165	0.000004
JMC475 - undoped	8.2	0.01	0.000	0.000001	-0.000006	0.000004	-0.0000002	0.0000002	0.282170	0.000004
JMC475 - undoped	8.1	0.03	0.000	0.000002	0.000006	0.000004	0.0000002	0.0000001	0.282152	0.000004

	total Hf	1σ	Yb/Hf	1σ	$^{176}Yb/^{177}Hf$	1σ	$^{176}Lu/^{177}Hf$	1σ	$^{176}Hf/^{177}Hf$	1σ
JMC475 - undoped	7.8	0.01	0.000	0.000002	-0.000002	0.000005	0.0000008	0.0000002	0.282160	0.000005
JMC475 - undoped	7.7	0.01	0.000	0.000002	0.000002	0.000004	0.0000006	0.0000002	0.282166	0.000004
JMC475 - undoped	8.0	0.02	0.000	0.000002	0.000024	0.000005	0.0000000	0.0000002	0.282160	0.000005
average (n=7)	**8.0**		**0.000**		**0.000004**		**0.0000003**		**0.282162**	
2SD	**0.4**		**0.000**		**0.000021**		**0.0000007**		**0.000012**	
JMC475 - doped	9.5	0.02	0.262	0.000162	0.664747	0.000430	0.0050835	0.0000016	0.282152	0.000004
JMC475 - doped	9.7	0.02	0.262	0.000115	0.662352	0.000289	0.0050752	0.0000007	0.282177	0.000005
JMC475 - doped	9.1	0.01	0.259	0.000089	0.655427	0.000236	0.0050364	0.0000005	0.282190	0.000004
JMC475 - doped	9.3	0.02	0.258	0.000087	0.653079	0.000247	0.0050311	0.0000006	0.282168	0.000006
average (n=4)	**9.4**		**0.260**		**0.658901**		**0.0050565**		**0.282172**	
2SD	**0.5**		**0.004**		**0.011079**		**0.0000532**		**0.000031**	
08/02/07										
JMC475 - undoped	9.4	0.02	0.000	0.000002	-0.000003	0.000004	-0.0000010	0.0000001	0.282148	0.000004
JMC475 - undoped	9.3	0.02	0.000	0.000002	0.000000	0.000004	-0.0000004	0.0000001	0.282157	0.000004
JMC475 - undoped	8.9	0.02	0.000	0.000001	0.000013	0.000004	0.0000013	0.0000001	0.282156	0.000004
JMC475 - undoped	9.2	0.02	0.000	0.000002	-0.000010	0.000004	-0.0000001	0.0000001	0.282161	0.000004
average (n=4)	**9.2**		**0.000**		**0.000000**		**-0.0000001**		**0.282155**	
2SD	**0.4**		**0.000**		**0.000020**		**0.0000019**		**0.000011**	
JMC475 - doped	11.0	0.02	0.289	0.000176	0.729128	0.000451	0.0051518	0.0000009	0.282160	0.000005
JMC475 - doped	10.4	0.02	0.286	0.000129	0.720559	0.000332	0.0051092	0.0000010	0.282168	0.000005
JMC475 - doped	10.9	0.02	0.288	0.000218	0.725945	0.000567	0.0051252	0.0000009	0.282157	0.000005
JMC475 - doped	10.9	0.02	0.287	0.000173	0.722760	0.000423	0.0051206	0.0000007	0.282169	0.000005
average (n=4)	**10.8**		**0.287**		**0.724598**		**0.0051267**		**0.282163**	
2SD	**0.6**		**0.003**		**0.007486**		**0.0000360**		**0.000012**	

Appendix 3d
Two-component magma mixing modelling

% Dalradian	$\delta^{18}O$ [‰]	εHf_T	εHf_C	% enriched mantle
0	5.5*	1.3*	3.4*	1
0.1	6.4	-0.5	1.4	0.9
0.2	7.2	-2.3	-0.7	0.8
0.3	8.1	-4.2	-2.7	0.7
0.4	9.0	-6.0	-4.7	0.6
0.5	9.9	-7.8	-6.8	0.5
0.6	10.7	-9.6	-8.8	0.4
0.7	11.6	-11.4	-10.8	0.3
0.8	12.5	-13.3	-12.8	0.2
0.9	13.3	-15.1	-14.9	0.1
1	14.2*	-16.9*	-16.9*	0

*Average enriched mantle and average Dalradian

(data from Anderson et al., 2004; Canning et al., 1998; Eiler , 2001; Frost and O'Nions, 1985; O'Nions et al., 1983; Thirlwall, 1982)

εHf_T = data from Thirlwall (1982)

εHf_C = data from Canning et al. (1998)

APPENDIX 4

Supplementary data for Paper 4

Appendix 4a
Major, trace and rare earth element whole-rock data

	Kemnay SA04/07	**Cove** SA04/10	**Nigg Bay** SA04/11
SiO_2 [%]	73.4	70.2	71.2
TiO_2	0.2	0.4	0.3
Al_2O_3	14.0	14.8	14.7
Fe_2O_3	1.4	2.5	2.6
MnO	0.0	0.0	0.0
MgO	0.1	0.6	0.6
CaO	1.2	1.3	1.6
Na_2O	3.3	3.0	3.4
K_2O	4.6	4.3	3.9
P_2O_5	0.0	0.1	0.1
LOI	0.7	1.2	1.0
Sum	99.0	98.4	99.3
Sc [ppm]	3	3	5
V		10	20
Cr			9
Ni			
Ba	1126	989	774
Rb	111	117	107
Sr	344	297	219
Y*	6	12	13
U*	3	2	3
Th*	12	14	14
Pb	36	17	25
Zr	108	203	194
Nb	9	16	17
Cu	5	5	10
Zn	40	41	37
La	35.08	56.71	48.77
Ce	67.0	108.2	96.9
Pr	7.17	12.41	10.93
Nd	25.7	45.7	40.0
Sm	4.07	7.63	7.04
Eu	0.95	1.37	1.19
Tb	0.34	0.64	0.65
Gd	2.55	5.37	4.96
Dy	1.46	3.02	3.30
Ho	0.25	0.46	0.49
Er	0.70	1.08	1.22
Tm	0.09	0.14	0.15
Yb	0.58	0.84	0.82
Lu	0.09	0.11	0.11
Hf	3.1	5.2	5.3
R1	3389	3239	3308
R2	357	396	418
A/CNK	1.12	1.23	1.16
A/NK	1.35	1.54	1.50
grid reference	NJ 73788 16821	NJ 95259 00268	NJ 96940 05083

* trace elements analysed by ICP-MS

Appendix 4b: Analytical protocols

1. Whole-rock analyses

REEs and some trace elements were analysed at the British Geological Survey (BGS) in Nottingham. The samples were fused with Na_2O_2 and then leached with deionised water and HCl before analysis using a ThermoElemental PQ Excel quadrupole ICP-MS. Matrix-matched calibration standards were used throughout.

2. Zircon sample preparation

Zircon separation was carried out in the University of St. Andrews Mineral Separation Facility. Rock samples of approximately 5 kg were crushed and sieved to obtain the < 500 µm fraction from which zircon crystals were separated using a Wilfley Table, heavy liquids and a Frantz magnetic separator. Approximately 100 zircon crystals were hand-picked from the remaining heavy, non-magnetic fraction, providing a range of grain size, morphology, transparency, alteration and occurrence of inclusions or cracks. The crystals were mounted into epoxy (Araldite) and the zircon mounts polished to about half thickness to expose the crystal interiors. The polished surfaces were imaged in back-scattered electron (BSE) and cathodoluminescence (CL) mode using a Philips XL30CP Scanning Electron Microscope (SEM) at the University of Edinburgh to identify internal zoning features, inherited material, inclusions and cracks. Suitable crystals for in-situ oxygen isotope analysis were selected using this information.

3. Zircon oxygen isotope analysis

Zircon oxygen isotope data were obtained using a Cameca ims-1270 ion microprobe at the University of Edinburgh following the methods of Cavosie et al. (2005) and Kemp et al. (2006). A 6nA primary $^{133}Cs^+$ ion beam with a diameter of c. 20 µm was used, charge was neutralised using a normal-incidence electron flood gun, secondary ions were extracted at 10 kV, and $^{18}O^-$ and $^{16}O^-$ ions were monitored simultaneously on dual Faraday cups. Secondary ion beam centring, pre-sputtering for 50 seconds and subsequent data collection over 10 cycles (total counting time: 40 seconds = 4 seconds per cycle) resulted in a total acquisition time of c. 200 seconds.

The secondary yield of ^{18}O under these conditions was typically between 4.5 x 10^6 and 5.5 x 10^6 counts per second. To correct for instrumental mass fractionation (IMF) and instrumental drift, all data were normalised to zircon standard 91500 ($\delta^{18}O$ = 9.86 ‰) (Wiedenbeck et al., 2004), which was analysed in blocks of 5 to 10 after every 10 to 15 unknown zircon analyses. During stable instrument conditions the unknown zircon analyses were normalised to the daily average $^{18}O/^{16}O$ value obtained for 91500. In cases where instrumental drift was recognised, the analytical conditions changed or sample exchange was carried out, the data were divided into sessions in which unknowns were normalised to the linearly interpolated $^{18}O/^{16}O$ value derived from analyses of the bracketing 91500 standard.

Prior to oxygen isotope analysis, HfO_2 concentrations in the zircons were measured by electron microprobe as variations in HfO_2 have been shown to cause variations in IMF (Peck et al., 2001). This has been shown to be particularly important when conducting analysis using e.g. a Cameca ims-4f at high-energy offset. However, in this study oxygen isotope analysis were carried out using a Cameca ims-1270 ion microprobe, and in both diorite samples HfO_2 variations in zircons were $\leq$ 0.5 wt %; therefore corrections for IMF were unnecessary. The internal precision of the analyses based on counting statistics varied between 0.1-0.4 ‰ (1SD). External precision based on the reproducibility of standard 91500 ranged from 0.2-0.7 ‰ (2SD) and 0.031-0.145 (1 s.e.m.).

Analyses were conducted in clear, crack- and inclusion-free areas of representative zircon crystals. Where possible, multiple analyses (core to rim) were carried out on single zircon crystals to document zircon growth histories, and occasionally also in adjacent spots within crystals to assess reproducibility. The ion probe pits were subsequently imaged in BSE and SE mode using an SEM to determine the exact position of the analyses and to ensure that no cracks in the bottom of the pit might have influenced the results. Data obtained from suspect locations were rejected. In addition, data were excluded when the correction on the position of the secondary ion beam was anomalously large.

4. U-Th-Pb analysis

Subsequent to oxygen isotope analysis, U-Th-Pb analyses were carried out also using the Cameca ims-1270 at the EIMF. Analytical procedures are similar to those described by Schuhmacher et al. (1994) and Whitehouse et al. (1997), and are described in detail in Kelly et al. (accepted). Zircons were analysed using a ~4nA O_2^- primary ion source with 22.5 keV net impact energy. The beam was focused using Köhler illumination, with primary beam alignment giving ellipsoidal analysis pits (~25 µm max. dimension). Spatial resolution of the analysed area was further limited by the use of the field aperture. U, Th and Pb were analysed at a mass resolution (M/ΔM) of ~4000R using a peak switching routine. An energy window of 60 eV was used throughout, with energy centring on each analysis using the HfO peak. Oxygen flooding on the surface of the sample was employed to enhance Pb ion yields. Prior to analysis the sample surface was pre-rastered over an area of ~40 µm for 120 seconds to remove any surface contamination.

Calibration of Pb/U ratios followed procedures employed by other SHRIMP and/or Cameca ims-1270 laboratories and were based on the observed relationship between Pb/U and ratios of UO/U (e.g. Claoué-Long et al., 1995; Compston et al., 1984; Schuhmacher et al., 1994; Williams, 1998; Williams and Claesson, 1987; Whitehouse et al., 1997). However, the relationship ln(Pb/U) vs. ln(UO_2/UO) was found to give a better within-session reproducibility than the conventional ln(Pb/U) vs. ln(UO/U) or ln(Pb/U) vs. ln(UO_2/U) methods.

U/Pb ratios were calibrated against measurements on standard 91500 (Wiedenbeck et al., 1995: ~1062.5 Ma; assumed $^{206}Pb/^{238}U$ ratio = 0.17917), which is measured after 3-4 unknowns. Temora 2 was analysed as a secondary standard after every 10-15 analyses. Th/U ratios in unknowns were calculated by reference to measurements of Th/U and $^{208}Pb/^{206}Pb$ on the 91500 standard (Th/U = 0.362), assuming closed system behaviour. Elemental concentrations were determined based on the observed oxide ratios of the standard (UO_2/Zr_2O_2 and HfO/Zr_2O_2; assuming U = 81.2 ppm, Hf = 5880 ppm).

Corrections were carried out for dead time, detector background (~0.025 counts/second) and common Pb. Common Pb corrections were made using the measured ^{204}Pb counts above detector background and the modern day composition

of common Pb. Typically ^{204}Pb count rates approached the background, which led to corrections of < 15 ppb on ^{206}Pb.

Uncertainties on the Pb/U ratios include an error based on observed uncertainty from each measured ratio, which is generally close to that expected from counting statistics. Observed uncertainties on the U/Pb ratio of 91500 are generally an additional 0.3% in excess of that expected from counting statistics alone. This is assumed to be a random error (see also Ireland and Williams, 2003) and has been propagated (in both standards and unknowns) together with the observed variation in Pb/U ratios measured for each analysis (typically close to the counting errors). For measurement of the 91500 standard, uncertainties are typically between 0.7-1.0 % per analysis. Uncertainties on ^{207}Pb/^{206}Pb ratios are based on observed variations from cycle to cycle during each analysis and commonly approach those expected from counting statistics. Uncertainties on ages quoted in the text and in tables for *individual analyses* (ratios and ages) are at the 1σ level. All uncertainties in calculated *group* ages are reported at 2σ level or 95 % confidence.

Plots and age calculations have been made using the computer program ISOPLOT/EX v3 (Ludwig, 2003). Ages of magmatic grains are presented as weighted mean ^{206}Pb/^{238}U average ages and include only concordant data points; ages of inherited grains (> 1000 Ma) are ^{207}Pb/^{206}Pb ages. Following analysis, the ion probe pits were imaged in BSE and SE mode to check for inclusions and cracks in the bottom of the pit. Data obtained from dubious locations were rejected. During data processing we noticed that zircons with high U concentrations (>1000 ppm) commonly give older ages or lie off Concordia. Electron back-scatter diffractometry (EBSD) of these zircons showed disturbance and even complete destruction of their crystal structure. To provide a robust data set we excluded all data obtained from zircons showing above 1000 ppm U. In addition, zircons displaying high common Pb concentrations and/or > 10 % discordance were also rejected (summarised data are presented in Table 1; full data sets in Appendix 3).

5. Hf isotope analysis

Hafnium isotope analysis was carried out at the NERC Isotope Geosciences Laboratory (NIGL) in Nottingham, using a Nu Instruments Nu-Plasma HR multi-

collector ICP-MS coupled to a New Wave Research UP193SS 193nm solid state laser ablation system. For an improved wash-out a low volume ablation cell (NIGL zircon cell) was employed. Ablation was conducted in a He atmosphere (0.8-1.0 l/min). Ar make-up gas was sourced from a Nu Instruments DSN-100 desolvating nebuliser whilst aspirating 2 % HNO_3 and 0.1 molar HF to maintain constant plasma conditions.

At the time of analysis the mass spectrometer was fitted with a specially designed U-Pb collector block, which limits the number of Faraday cups available for Hf isotope analysis to seven. The instrument is therefore restricted to measuring ^{173}Yb, ^{174}Lu, ^{175}Lu, ^{176}(Yb, Lu, Hf), ^{177}Hf, ^{178}Hf and ^{179}Hf. The stable isotopes ^{180}Hf and ^{181}Hf are not analysed and emphasis is placed on the ^{178}Hf/^{177}Hf stable isotope ratio for monitoring of data quality. A peak jumping routine including ^{172}Yb, to allow assessment of the effect of using a Yb mass bias correction for the Yb interference correction rather than the Hf mass bias correction, has been investigated but was found unnecessary with the data for both being equivalent within the increased uncertainty reflected by the low Yb concentrations.

The isobaric interference correction for ^{176}Yb was determined prior to each analytical session using Yb doped JMC475 Hf standards. This correction was determined for total Yb/Hf ratios of up to 0.3. These data were used to calculate a true ratio for the ^{176}Yb/^{173}Yb of 0.79488. The Lu interference correction used the accepted ratio of ^{176}Lu/^{175}Lu = 0.02653. During measurement the ^{173}Yb and ^{175}Lu peaks were monitored and corrections applied according to these ratios. Each day spiked and unspiked solution standards were analysed to monitor instrument performance and effectiveness of the corrections.

Ablation data were acquired using a static spot ablation protocol, a 50 µm beam and a 5-10 Hz laser pulse repetition rate. A fluence of 4-6 J/cm^2 and ablation time of 70 seconds resulted in an ablation rate of 0.05-0.09 µm/pulse (0.5-0.9 µm/sec). Total Hf signals varied between 4.5-6.5 V resulting in reproducibilities of the Mud Tank reference material between 0.7 and 1.0 εHf units (2σ). The Mud Tank zircon reference material was used to normalise the sample zircons and assess the reproducibility of all ratios. This included normalisation of the Lu-Hf ratio required for age correction. All values for Mud Tank were taken from Woodhead and Hergt

(2005). All uncertainty components, including those for age and normalisation, were factored into the expanded uncertainty quoted.

For Hf isotope analysis zircons were selected for which U-Pb and (in most cases) oxygen isotope data already existed in order to enable correlation of the different data sets. Where possible multiple analyses were made on a single crystal. However, due to the much larger spot size of the laser in comparison to the ion probe this was seldom possible. Most data were obtained from crystal cores, which were easier to analyse as they often define the largest part of the crystal, and only rarely of the rim. Cracks and inclusions were always avoided and all analyses were carried out on the already existing SIMS spots or at least within the same CL growth zone. The ablation data were normalised to Mud Tank ($^{176}Hf/^{177}Hf_{solution}$= 0.282507 ± 6 and $^{176}Lu/^{177}Hf_{solution}$ = 0.000042 (Woodhead and Hergt, 2005)). Reproducibility of the Mud Tank standard was propagated into the uncertainty of the sample analysis.

In the rare cases where the laser drilled through the zircon grains or from an older inherited core into the surrounding magmatic rim, the analyses were examined using NIGL's time-resolved software, which allowed identification of the most stable parts of the profile and of distinguishable Hf isotope zones.

εHf values were calculated using a ^{176}Lu decay constant of 1.865 x $10^{-11}y^{-1}$ (Scherer et al., 2001), the present-day chondritic $^{176}Lu/^{177}Hf$ value of 0.0332 and $^{176}Hf/^{177}Hf$ ratio of 0.282772 (Blichert-Toft and Albarède, 1997). To calculate two-stage Hf model ages the $^{176}Lu/^{177}Hf$ ratios of the average crust (TDM_C) ($^{176}Lu/^{177}Hf$ = 0.015 (Griffin et al., 2002)) and of the depleted mantle ($^{176}Lu/^{177}Hf$ = 0.0384 (Griffin et al., 2000)), the initial $^{176}Hf/^{177}Hf$ ratios of the zircon and the depleted mantle (present-day $^{176}Hf/^{177}Hf$ ratio of the depleted mantle = 0.28325 (Nowell et al., 1998)), and the U-Pb SIMS age were used. For comparison, two-stage Hf model ages were also calculated based on the whole-rock $^{176}Lu/^{177}Hf$ ratio of each sample (TDM_W) (summarised data in Table 1; full data set in Appendix 5).

Appendix 4c

Zircon U-Pb data of the Kemnay, Cove and Nigg Bay granites

sample	analysis no.	grain no.	U ppm	Th ppm	Pb ppm	Th/U	^{204}Pb ppb	f206 (%)	^{204}Pb/^{206}Pb	corrected ratios									Ages (Ma)								grain area	comment
										^{207}Pb/^{206}Pb	1σ	^{208}Pb/^{206}Pb	1σ	^{207}Pb/^{235}U	1σ	^{206}Pb/^{238}U	1σ	ρ	^{206}Pb/^{238}U	1σ	^{207}Pb/^{235}U	1σ	^{207}Pb/^{206}Pb	1σ	% disc		
Kemnay Granite	SA04/07 - 23.48	23	140	59	26	0.44	0.6	0.06	0.0000298	0.0744	0.0005	0.1313	0.0010	1.8020	0.0199	0.1758	0.0015	0.79	1044	8	1046	7	1051	13	1	inh	
	SA04/07 - 23.49	23	1769	171	122	0.10	6.9	0.11	0.0000609	0.0564	0.0002	0.0323	0.0010	0.5709	0.0050	0.0734	0.0006	0.93	456	4	459	3	469	6	3	rim1	rejected, U > 1000 ppm
	SA04/07 - 26.55	26	98	31	17	0.32	1.2	0.15	0.0000814	0.0741	0.0006	0.0940	0.0017	1.7819	0.0223	0.1745	0.0016	0.74	1037	9	1039	8	1043	15	1	inh	
	SA04/07 - 26.56	26	1695	98	118	0.06	210	3.44	0.0019069	0.0554	0.0009	0.0205	0.0025	0.5718	0.0100	0.0749	0.0006	0.46	466	4	459	6	426	45	-9	rim	rejected, high common Pb
	SA04/07 - 27.58	27	93	38	17	0.42	0.5	0.07	0.0000382	0.0736	0.0016	0.1257	0.0035	1.7761	0.0581	0.1750	0.0042	0.74	1040	23	1037	21	1030	44	-1	inh	
	SA04/07 - 27.57	27	793	48	59	0.06	0.8	0.03	0.0000152	0.0577	0.0003	0.0234	0.0004	0.6357	0.0072	0.0799	0.0008	0.88	496	5	500	4	517	11	4	inh+rim	rejected, crack
	SA04/07 - 31.66	31	144	37	38	0.26	0.7	0.04	0.0000214	0.0949	0.0006	0.0778	0.0008	3.3903	0.0394	0.2592	0.0026	0.85	1486	13	1502	9	1525	11	3	inh1	
	SA04/07 - 31.68	31	614	111	99	0.18	0.9	0.02	0.0000106	0.0896	0.0004	0.0637	0.0004	2.0142	0.0213	0.1630	0.0016	0.90	973	9	1120	7	1417	9	31	inh2	inherited core, > 10 % discordant
	SA04/07 - 33.71	33	52	58	15	1.14	0.2	0.03	0.0000139	0.0923	0.0008	0.3427	0.0031	3.0512	0.0418	0.2398	0.0025	0.77	1386	13	1421	10	1473	16	6	inh	
	SA04/07 - 33.73	33	1845	135	129	0.07	2.1	0.03	0.0000174	0.0567	0.0002	0.0238	0.0010	0.5843	0.0070	0.0748	0.0008	0.94	465	5	467	4	477	9	3	rim	rejected, U > 1000 ppm
	SA04/07 - 34.76	34	206	46	15	0.23	0.5	0.07	0.0000358	0.0561	0.0006	0.0717	0.0011	0.5650	0.0076	0.0730	0.0006	0.63	454	4	455	5	456	21	0	c2b	
	SA04/07 - 34.77	34	991	459	70	0.48	6.8	0.22	0.0001155	0.0559	0.0003	0.1546	0.0019	0.5234	0.0051	0.0678	0.0006	0.84	423	3	427	3	450	8	6	c2a	rejected, crack
	SA04/07 - 35.78	35	105	35	33	0.35	1.1	0.07	0.0000392	0.1097	0.0005	0.0991	0.0011	4.4935	0.0539	0.2972	0.0032	0.91	1677	16	1730	10	1793	9	6	inh	
	SA04/07 - 35.81	35	2124	152	151	0.07	3.5	0.05	0.0000253	0.0563	0.0002	0.0168	0.0004	0.5913	0.0055	0.0761	0.0006	0.90	473	4	472	3	464	9	-2	rim	rejected, crack
	SA04/07 - 18.37	18	120	42	8	0.36	1.8	0.54	0.0002886	0.0568	0.0013	0.0704	0.0047	0.4830	0.0122	0.0617	0.0006	0.42	386	4	400	8	484	36	20	c1a	rejected, > 10 % discordant
	SA04/07 - 18.38	18	539	138	37	0.26	2.1	0.12	0.0000656	0.0562	0.0005	0.0476	0.0013	0.5386	0.0069	0.0695	0.0006	0.70	433	4	438	5	461	19	6	rim	rejected, crack
	SA04/07 - 19.39	19	233	54	16	0.24	9.6	1.26	0.0006830	0.0469	0.0010	0.0501	0.0056	0.4607	0.0112	0.0713	0.0007	0.40	444	4	385	8	41	33	-983	c1	rejected, > 10 % discordant
	SA04/07 - 19.40	19	1855	409	133	0.23	0.5	0.01	0.0000045	0.0562	0.0002	0.0690	0.0017	0.5691	0.0050	0.0734	0.0006	0.93	457	4	457	3	461	7	1	c2	rejected, crack
	SA04/07 - 13.26	13	266	80	51	0.31	0.8	0.03	0.0000176	0.0866	0.0005	0.1153	0.0015	2.2793	0.0296	0.1908	0.0022	0.89	1126	12	1206	9	1352	11	17	inh	inherited core, > 10 % discordant
	SA04/07 - 13.27	13	2014	85	143	0.04	0.9	0.01	0.0000069	0.0559	0.0002	0.0134	0.0002	0.5900	0.0053	0.0766	0.0006	0.92	476	4	471	3	448	7	-6	rim	rejected, U > 1000 ppm
	SA04/07 - 11.22	11	173	44	23	0.26	2.5	0.23	0.0001244	0.0690	0.0008	0.0838	0.0023	1.2720	0.0201	0.1336	0.0014	0.64	809	8	833	9	899	23	10	inh	inherited core, > 10 % discordant
	SA04/07 - 11.23	11	2767	116	199	0.04	1.6	0.02	0.0000086	0.0565	0.0002	0.0133	0.0003	0.6062	0.0054	0.0778	0.0006	0.92	483	4	481	3	471	8	-3	rim	rejected, U > 1000 ppm
	SA04/07 - 9.18	9	213	46	15	0.22	0.7	0.09	0.0000495	0.0554	0.0005	0.0676	0.0014	0.5683	0.0081	0.0744	0.0008	0.73	462	5	457	5	429	18	-8	c1	
	SA04/07 - 9.19	9	138	40	10	0.30	0.0	0.00	0.0000001	0.0569	0.0004	0.0927	0.0008	0.5785	0.0068	0.0737	0.0007	0.82	458	4	463	4	488	15	6	rim	
	SA04/07 - 8.15	8	361	607	31	1.73	83.5	11.2	0.0067677	0.0527	0.0016	0.1575	0.0168	0.3779	0.0123	0.0520	0.0005	0.32	327	3	326	9	316	135	-3	c1	rejected, high common Pb
	SA04/07 - 8.16	8	175	38	11	0.22	0.3	0.05	0.0000275	0.0583	0.0006	0.1090	0.0015	0.5287	0.0072	0.0658	0.0006	0.65	411	4	431	5	540	20	24	c2	rejected, > 10 % discordant
	SA04/07 - 6.11	6	274	74	15	0.28	67.8	8.21	0.0047826	0.0585	0.0020	0.1515	0.0172	0.4575	0.0163	0.0567	0.0005	0.26	355	3	383	11	549	114	35	c1	rejected, > 10 % discordant
	SA04/07 - 6.12	6	558	209	25	0.39	694	28.4	0.0211902	0.0541	0.0019	0.3719	0.0303	0.4173	0.0187	0.0559	0.0015	0.61	351	9	354	13	375	344	6	c2	rejected, high common Pb
	SA04/07 - 36.82	36	314	179	25	0.58	0.4	0.04	0.0000203	0.0567	0.0004	0.1801	0.0011	0.5736	0.0060	0.0734	0.0006	0.80	456	4	460	4	480	12	5	c2	
	SA04/07 - 36.83	36	153	89	12	0.60	1.1	0.22	0.0001190	0.0560	0.0008	0.1824	0.0028	0.5636	0.0096	0.0730	0.0007	0.54	454	4	454	6	451	24	-1	rim	
	SA04/07 - 32.69	32	87	77	25	0.91	1.0	0.11	0.0000564	0.0904	0.0006	0.2645	0.0026	3.0555	0.0415	0.2453	0.0029	0.86	1414	15	1422	10	1433	12	1	inh	inherited core
	SA04/07 - 32.70	32	427	12	29	0.03	1.6	0.11	0.0000586	0.0554	0.0004	0.0070	0.0009	0.5681	0.0065	0.0743	0.0006	0.76	462	4	457	4	429	13	-8	rim1	
	SA04/07 - 29.61	29	95	50	31	0.54	2.9	0.22	0.0001202	0.1699	0.0024	0.1651	0.0043	6.7605	0.1337	0.2886	0.0040	0.69	1634	20	2081	17	2556	24	36	inh	inherited core, > 10 % discordant
	SA04/07 - 28.59	28	101	27	11	0.27	1.0	0.18	0.0000962	0.0656	0.0009	0.1223	0.0025	1.0190	0.0165	0.1126	0.0011	0.58	688	6	713	8	794	22	13	inh	inherited core, > 10 % discordant
	SA04/07 - 28.60	28	1519	60	110	0.04	0.7	0.01	0.0000063	0.0572	0.0002	0.0143	0.0002	0.6206	0.0058	0.0787	0.0007	0.92	488	4	490	4	499	8	2	rim	rejected, U > 1000 ppm
	SA04/07 - 37.84	37	393	234	32	0.61	0.7	0.05	0.0000259	0.0562	0.0004	0.1888	0.0011	0.5759	0.0065	0.0743	0.0007	0.78	462	4	462	4	461	13	0	c1	
	SA04/07 - 37.85	37	524	165	38	0.32	1.4	0.08	0.0000423	0.0558	0.0004	0.0999	0.0011	0.5630	0.0064	0.0732	0.0007	0.82	455	4	453	4	444	12	-3	c2	
	SA04/07 - 38.86	38	190	128	53	0.69	1.4	0.06	0.0000335	0.0907	0.0005	0.2011	0.0009	3.0859	0.0338	0.2467	0.0023	0.85	1422	12	1429	8	1440	11	1	inh1	inherited core
	SA04/07 - 38.87	38	250	126	67	0.52	0.4	0.01	0.0000067	0.0913	0.0005	0.1534	0.0008	3.1279	0.0347	0.2485	0.0023	0.85	1431	12	1440	9	1452	12	1	inh2	inherited core
	SA04/07 - 39.88	39	156	40	21	0.26	0.4	0.04	0.0000212	0.0724	0.0007	0.0912	0.0012	1.3679	0.0190	0.1370	0.0014	0.73	828	8	875	8	997	19	17	inh	inherited core, > 10 % discordant
	SA04/07 - 39.89	39	2547	175	171	0.07	344	3.87	0.0021556	0.0550	0.0008	0.0238	0.0028	0.5477	0.0100	0.0722	0.0007	0.55	450	4	443	7	411	45	-9	rim	rejected, high common Pb
	SA04/07 - 29.62	29	1816	45	126	0.03	28.4	0.45	0.0002396	0.0556	0.0004	0.0066	0.0011	0.5783	0.0063	0.0754	0.0006	0.79	469	4	463	4	437	12	-7	rim	rejected, high common Pb
	SA04/07 - 24.50	24	521	158	38	0.31	8.7	0.49	0.0002657	0.0548	0.0006	0.0944	0.0034	0.5517	0.0080	0.0730	0.0007	0.64	454	4	446	5	404	15	-12	c2 a	rejected, crack
	SA04/07 - 24.51	24	267	94	18	0.36	6.3	0.75	0.0004030	0.0551	0.0011	0.1176	0.0055	0.5094	0.0111	0.0670	0.0007	0.48	418	4	418	7	417	25	0	c2 b	rejected, crack
	SA04/07 - 25.52	25	185	96	56	0.53	0.8	0.04	0.0000189	0.1065	0.0005	0.1558	0.0008	4.0887	0.0444	0.2784	0.0027	0.89	1583	14	1652	9	1740	9	9	inh	inherited core
	SA04/07 - 25.54	25	2119	407	155	0.20	6.7	0.09	0.0000486	0.0558	0.0003	0.0551	0.0008	0.5796	0.0060	0.0754	0.0007	0.86	468	4	464	4	443	11	-6	rim	rejected, crack
	SA04/07 - 40.90	40	428	123	31	0.30	0.8	0.05	0.0000282	0.0564	0.0004	0.0892	0.0010	0.5671	0.0070	0.0730	0.0007	0.76	454	4	456	5	466	16	3	c2	
	SA04/07 - 40.91	40	533	175	39	0.34	0.6	0.03	0.0000174	0.0568	0.0004	0.1053	0.0008	0.5730	0.0067	0.0732	0.0007	0.77	455	4	460	4	483	16	6	rim	
Cove Granite	SA04/10 - 3.3	3	820	868	47	1.09	569	35.53	0.0294778	0.0201	0.0017	-0.0082	-0.0013	0.1014	0.0118	0.0366	0.0028	0.66	232	18	98	11	#N/A	#N/A	#N/A	c1	rejected, > 10 % discordant
	SA04/10 - 4.5	4	630	68	40	0.11	69.1	3.55	0.0019660	0.0437	0.0021	-0.0006	-0.0001	0.4012	0.0207	0.0666	0.0013	0.37	416	8	343	15	#N/A	#N/A	#N/A	c1	rejected, > 10 % discordant
	SA04/10 - 5.7	5	1118	196	70	0.18	380	10.62	0.0063519	0.0549	0.0019	0.0298	0.0037	0.4794	0.0171	0.0633	0.0006	0.27	396	4	398	12	408	175	3	rim	rejected, high common Pb
	SA04/10 - 5.8	5	85	71	7	0.85	0.2	0.08	0.0000449	0.0555	0.0008	0.2648	0.0026	0.5706	0.0097	0.0746	0.0007	0.55	464	4	458	6	431	26	-8	c2c	

sample	analysis no.	grain no.	U ppm	Th ppm	Pb ppm	Th/U	^{204}Pb ppb	f206 (%)	^{204}Pb/^{206}Pb	corrected ratios									Ages (Ma)								grain area	comment
										^{207}Pb/^{206}Pb	1σ	^{208}Pb/^{206}Pb	1σ	^{207}Pb/^{235}U	1σ	^{206}Pb/^{238}U	1σ	ρ	^{206}Pb/^{238}U	1σ	^{207}Pb/^{235}U	1σ	^{207}Pb/^{206}Pb	1σ	% disc		
	SA04/10 - 9.17	9	50	31	9	0.63	1.5	0.38	0.0002019	0.0722	0.0011	0.1854	0.0037	1.6786	0.0301	0.1686	0.0016	0.52	1004	9	1000	11	992	24	-1	inh	inherited core
	SA04/10 - 9.18	9	1430	52	95	0.04	18.4	0.39	0.0002068	0.0556	0.0003	0.0108	0.0013	0.5508	0.0052	0.0719	0.0006	0.85	447	3	445	3	435	8	-3	rim	rejected, high common Pb
	SA04/10 - 7.13	7	1908	74	136	0.04	33.3	0.49	0.0002620	0.0556	0.0007	0.0095	0.0014	0.5905	0.0089	0.0771	0.0006	0.53	479	4	471	6	434	29	-10	c1	rejected, high common Pb
	SA04/10 - 7.14	7	146	9	10	0.06	1.1	0.22	0.0001168	0.0551	0.0008	0.0163	0.0020	0.5500	0.0095	0.0724	0.0006	0.49	450	4	445	6	416	27	-8	rim	
	SA04/10 - 12.22	12	44	21	5	0.50	146.7	38.34	0.0332459	0.0536	0.0014	0.1518	0.0201	0.8597	0.0283	0.1164	0.0025	0.64	710	14	630	15	353	191	-101	inh	rejected, high common Pb
	SA04/10 - 12.24	12	235	68	17	0.29	1.2	0.16	0.0000831	0.0558	0.0006	0.0901	0.0017	0.5621	0.0078	0.0731	0.0006	0.59	455	4	453	5	444	20	-2	rim	
	SA04/10 - 20.46	20	25	14	8	0.56	0.4	0.10	0.0000540	0.1346	0.0031	0.2215	0.0110	5.5165	0.1623	0.2972	0.0053	0.61	1677	26	1903	25	2159	40	22	inh	inherited core, > 10 % discordant
	SA04/10 - 20.47	20	317	70	69	0.23	0.6	0.02	0.0000096	0.1051	0.0013	0.0628	0.0008	3.1271	0.0571	0.2157	0.0029	0.74	1259	15	1439	14	1716	23	27	inh	inherited core, > 10 % discordant
	SA04/10 - 19.43	19	139	62	10	0.46	532.8	60.31	0.0812751	0.0264	0.0004	0.0203	0.0023	0.2217	0.0043	0.0609	0.0008	0.70	381	5	203	4	#N/A	#N/A	#N/A	c2b	rejected, > 10 % discordant
	SA04/10 - 19.45	19	45	29	4	0.66	1.3	0.85	0.0004598	0.0518	0.0020	0.1901	0.0082	0.5094	0.0203	0.0714	0.0008	0.27	444	5	418	14	275	52	-62	c2a	rejected, > 10 % discordant
	SA04/10 - 16.33	16	299	179	81	0.61	13.8	0.40	0.0002138	0.1093	0.0005	0.1959	0.0023	3.7212	0.0358	0.2468	0.0021	0.88	1422	11	1576	8	1788	7	20	inh	rejected, crack
	SA04/10 - 16.34	16	815	30	56	0.04	18.1	0.65	0.0003481	0.0570	0.0004	0.0117	0.0017	0.5788	0.0064	0.0736	0.0006	0.73	458	4	464	4	492	10	7	rim	rejected, crack
	SA04/10 - 14.28	14	74	50	6	0.69	1.9	0.79	0.0004275	0.0517	0.0015	0.2065	0.0072	0.5096	0.0155	0.0715	0.0008	0.36	445	5	418	10	270	33	-65	c1	rejected, > 10 % discordant
	SA04/10 - 14.28B	14	105	59	8	0.58	0.6	0.16	0.0000863	0.0571	0.0008	0.1800	0.0025	0.5697	0.0097	0.0724	0.0007	0.57	451	4	458	6	494	23	9	c2	
	SA04/10 - 14.30	14	220	54	16	0.25	14.1	1.92	0.0010443	0.0533	0.0012	0.0684	0.0072	0.5265	0.0125	0.0717	0.0006	0.36	446	4	429	8	339	34	-32	rim	rejected, > 10 % discordant
	SA04/10 - 15.31	15	224	84	16	0.38	1.8	0.24	0.0001273	0.0561	0.0006	0.1199	0.0023	0.5594	0.0077	0.0723	0.0007	0.65	450	4	451	5	456	16	1	c2	
	SA04/10 - 15.32	15	75	41	6	0.56	0.9	0.37	0.0001963	0.0545	0.0015	0.1724	0.0042	0.5324	0.0153	0.0709	0.0008	0.38	441	5	433	10	391	47	-13	c1	rejected, crack
	SA04/10 - 13.25	13	56	20	8	0.37	121.7	26.29	0.0190742	0.0628	0.0015	0.0857	0.0127	1.1725	0.0325	0.1353	0.0018	0.49	818	10	788	15	702	79	-17	inh	inherited core, > 10 % discordant
	SA04/10 - 17.36	17	661	220	120	0.34	1.7	0.03	0.0000170	0.0766	0.0002	0.1024	0.0004	1.8700	0.0159	0.1770	0.0014	0.95	1051	8	1071	6	1111	5	5	inh	rejected, crack
	SA04/10 - 17.35	17	526	9	36	0.02	2.2	0.12	0.0000654	0.0553	0.0003	0.0035	0.0007	0.5676	0.0058	0.0745	0.0006	0.80	463	4	456	4	422	11	-10	rim	
	SA04/10 - 7.14B	7	124	9	8	0.08	4.7	1.12	0.0006045	0.0591	0.0016	0.0283	0.0051	0.5933	0.0169	0.0728	0.0007	0.32	453	4	473	11	570	43	21	rim	rejected, high common Pb
	SA04/10 - 20.46B	20	120	42	53	0.36	0.3	0.01	0.0000067	0.1658	0.0012	0.1015	0.0008	9.1538	0.1140	0.4005	0.0040	0.81	2171	19	2354	11	2515	12	14	inh	inherited core, > 10 % discordant
	SA04/10 - 20.47B	20	294	76	51	0.26	13.8	0.59	0.0003176	0.0995	0.0009	0.0756	0.0041	2.3442	0.0539	0.1708	0.0036	0.92	1017	20	1226	16	1615	15	37	inh	rejected, high common Pb
	SA04/10 - 15.32B	15	133	108	11	0.84	1.0	0.22	0.0001156	0.0557	0.0008	0.2592	0.0027	0.5761	0.0103	0.0751	0.0007	0.52	467	4	462	7	439	26	-6	c1	
	SA04/10 - 17.36B	17	296	70	54	0.24	0.8	0.03	0.0000164	0.0785	0.0013	0.0744	0.0012	1.9763	0.0373	0.1827	0.0017	0.51	1082	10	1107	13	1158	32	7	inh	
	SA04/10 - 17.35B	17	896	10	63	0.01	129.7	3.93	0.0021888	0.0531	0.0011	0.0000	0.0000	0.5614	0.0125	0.0767	0.0007	0.41	476	4	452	8	332	58	-44	rim	rejected, > 10 % discordant
	SA04/10 - 5.8B	5	99	72	8	0.75	0.6	0.18	0.0000964	0.0566	0.0011	0.2310	0.0032	0.5720	0.0124	0.0733	0.0008	0.47	456	5	459	8	475	34	4	c2a	
	SA05/10 - 5.8C	5	65	52	6	0.82	0.3	0.15	0.0000798	0.0567	0.0011	0.2554	0.0032	0.5857	0.0129	0.0749	0.0008	0.48	466	5	468	8	480	33	3	c2b	
	SA04/10 - 9.17B	9	42	23	8	0.55	0.6	0.18	0.0000946	0.0747	0.0012	0.1698	0.0027	1.7825	0.0365	0.1731	0.0021	0.58	1029	11	1039	13	1060	29	3	inh	
	SA04/10 - 13.25B	13	39	18	6	0.48	137.8	35.15	0.0289898	0.0694	0.0018	0.1208	0.0179	1.3667	0.0411	0.1428	0.0022	0.51	860	12	875	17	911	92	6	inh	rejected, crack
	SA04/10 - 21.49	21	370	178	100	0.49	2.6	0.06	0.0000322	0.0922	0.0004	0.1457	0.0007	3.2080	0.0302	0.2522	0.0022	0.91	1450	11	1459	7	1472	7	2	inh	
	SA04/10 - 21.50	21	1419	93	78	0.07	212.8	5.23	0.0029506	0.0616	0.0033	0.0218	0.0038	0.4987	0.0278	0.0587	0.0008	0.25	368	5	411	19	661	178	44	rim	rejected, > 10 % discordant
	SA05/10 - 22.51	22	190	74	90	0.40	0.9	0.02	0.0000131	0.1836	0.0007	0.1098	0.0005	10.6569	0.1304	0.4211	0.0049	0.94	2265	22	2494	11	2685	6	16	inh	inherited core, > 10 % discordant
	SA05/10 - 8.15	8	344	143	98	0.43	6.6	0.16	0.0000835	0.1081	0.0005	0.1276	0.0014	3.9733	0.0382	0.2666	0.0023	0.90	1524	12	1629	8	1767	7	14	inh	rejected, crack
	SA05/10 - 8.16	8	1185	28	81	0.02	146.8	3.48	0.0019275	0.0549	0.0008	0.0063	0.0010	0.5626	0.0091	0.0743	0.0006	0.52	462	4	453	6	408	31	-13	rim	rejected, high common Pb
	SA05/10 - 10.19	10	1154	136	170	0.12	1.6	0.02	0.0000105	0.0715	0.0002	0.0364	0.0003	1.5169	0.0135	0.1539	0.0013	0.94	923	7	937	5	971	6	5	inh	rejected, U > 1000 ppm
	SA05/10 - 10.20	10	1423	17	98	0.01	17.6	0.35	0.0001896	0.0564	0.0004	0.0028	0.0006	0.5857	0.0065	0.0753	0.0006	0.78	468	4	468	4	469	12	0	rim	rejected, crack
	SA05/10 - 11.21	11	1005	43	69	0.04	62.5	1.76	0.0009588	0.0567	0.0007	0.0161	0.0025	0.5840	0.0085	0.0747	0.0006	0.60	465	4	467	5	478	19	3	rim	
Nigg Bay Granite	SA04/11 - 3.5	3	112	29	20	0.26	1.9	0.21	0.0001111	0.0777	0.0008	0.0922	0.0030	1.9097	0.0314	0.1784	0.0023	0.78	1058	13	1084	11	1138	17	7	inh	
	SA04/11 - 3.6	3	505	30	77	0.06	7.9	0.21	0.0001138	0.0725	0.0004	0.0120	0.0013	1.6053	0.0227	0.1607	0.0021	0.94	960	12	972	9	999	8	4	inh	
	SA04/11 - 10.22	10	76	34	44	0.46	1.2	0.07	0.0000350	0.1986	0.0018	0.1288	0.0014	13.6990	0.2087	0.5003	0.0062	0.81	2615	27	2729	14	2814	14	7	inh	rejected, crack
	SA04/11 - 10.21	10	660	64	121	0.10	29.7	0.52	0.0002789	0.0992	0.0004	0.0254	0.0019	2.5612	0.0248	0.1873	0.0017	0.92	1107	9	1290	7	1608	6	31	inh	rejected, high common Pb
	SA04/11 - 14.32	14	1048	61	78	0.06	6.6	0.17	0.0000919	0.0562	0.0003	0.0179	0.0011	0.6172	0.0060	0.0796	0.0006	0.82	494	4	488	4	462	10	-7	rim	rejected, crack
	SA04/11 - 14.34	14	111	22	18	0.20	1.3	0.15	0.0000800	0.0844	0.0011	0.0819	0.0022	1.8825	0.0601	0.1617	0.0047	0.92	966	26	1075	21	1302	23	26	inh	rejected, crack
	SA04/11 - 26.69a	26	81	99	18	1.27	0.5	0.08	0.0000405	0.0758	0.0009	0.3786	0.0035	1.8367	0.0375	0.1757	0.0029	0.80	1043	16	1059	13	1090	22	4	inh	rejected, crack
	SA04/11 - 26.69b	26	95	77	19	0.82	8.2	1.06	0.0005732	0.0772	0.0016	0.2403	0.0074	1.8664	0.0487	0.1753	0.0029	0.63	1041	16	1069	17	1126	29	8	inh	rejected, crack
	SA04/11 - 26.67	26	497	22	34	0.04	25.2	1.47	0.0008003	0.0577	0.0010	0.0106	0.0024	0.5853	0.0136	0.0735	0.0012	0.67	457	7	468	9	519	21	12	rim	rejected, high common Pb
	SA04/11 - 28.73	28	568	4	39	0.01	1.9	0.10	0.0000515	0.0555	0.0004	0.0009	0.0003	0.5662	0.0065	0.0740	0.0007	0.78	460	4	456	4	432	14	-6	rim	
	SA04/11 - 28.74	28	17	9	3	0.56	0.9	0.66	0.0003558	0.0723	0.0028	0.1597	0.0081	1.7222	0.0732	0.1729	0.0028	0.38	1028	15	1017	27	993	59	-4	inh	
	SA04/11 - 38.97	38	11	32	3	2.99	1.3	1.55	0.0008413	0.0806	0.0043	0.9151	0.0125	1.8313	0.1009	0.1649	0.0026	0.29	984	14	1057	36	1210	57	19	inh	rejected, high common Pb
	SA04/11 - 38.98	38	404	5	28	0.01	3.7	0.26	0.0001419	0.0565	0.0005	0.0038	0.0010	0.5813	0.0073	0.0746	0.0006	0.70	464	4	465	5	473	15	2	rim	
	SA04/11 - 33.86	33	798	128	139	0.16	7.2	0.11	0.0000582	0.0772	0.0004	0.0487	0.0011	1.9036	0.0275	0.1789	0.0024	0.95	1061	13	1082	10	1125	9	6	inh	rejected, crack
	SA04/11 - 33.87	33	655	73	90	0.12	36.2	0.81	0.0004386	0.0731	0.0006	0.0417	0.0031	1.4577	0.0186	0.1446	0.0015	0.79	871	8	913	8	1016	14	14	inh	rejected, crack
	SA04/11 - 35.90	35	236	102	46	0.44	0.7	0.03	0.0000179	0.0761	0.0006	0.1348	0.0006	1.9595	0.0232	0.1867	0.0017	0.78	1103	9	1102	8	1098	14	0	inh	rejected, crack
	SA04/11 - 35.92	35	311	11	22	0.04	6.4	0.59	0.0003175	0.0557	0.0008	0.0093	0.0021	0.5773	0.0096	0.0751	0.0007	0.52	467	4	463	6	441	20	-6	rim	

sample	analysis no.	grain no.	U ppm	Th ppm	Pb ppm	Th/U	^{204}Pb ppb	f206 (%)	^{204}Pb/^{206}Pb	corrected ratios									Ages (Ma)								grain area	comment
										^{207}Pb/^{206}Pb	1σ	^{208}Pb/^{206}Pb	1σ	^{207}Pb/^{235}U	1σ	^{206}Pb/^{238}U	1σ	ρ	^{206}Pb/^{238}U	1σ	^{207}Pb/^{235}U	1σ	^{207}Pb/^{206}Pb	1σ	% disc		
	SA04/11 - 31.81	31	231	146	43	0.65	1.1	0.06	0.0000336	0.0731	0.0005	0.1960	0.0012	1.6985	0.0202	0.1685	0.0017	0.84	1004	9	1008	8	1017	12	1	inh	
	SA04/11 - 31.82	31	424	4	30	0.01	1.5	0.10	0.0000540	0.0560	0.0006	0.0019	0.0006	0.5863	0.0078	0.0760	0.0007	0.67	472	4	469	5	451	19	-5	rim	
	SA04/11 - 2.4	2	387	3	27	0.01	0.5	0.04	0.0000195	0.0572	0.0007	0.0029	0.0005	0.5982	0.0091	0.0758	0.0007	0.58	471	4	476	6	499	26	6	c1	rejected, crack
	SA04/11 - 2.3	2	580	9	41	0.02	3.4	0.16	0.0000873	0.0552	0.0006	0.0029	0.0008	0.5881	0.0082	0.0772	0.0007	0.65	479	4	470	5	422	20	-14	rim	rejected, crack
	SA04/11 - 39.99	39	171	87	28	0.52	4.8	0.40	0.0002138	0.0688	0.0008	0.1551	0.0033	1.4456	0.0210	0.1523	0.0014	0.63	914	8	908	9	893	16	-2	inh	rejected, crack
	SA04/11 - 39.100	39	501	175	78	0.36	0.6	0.02	0.0000098	0.0697	0.0003	0.1080	0.0005	1.4685	0.0149	0.1528	0.0014	0.87	917	8	918	6	919	10	0	inh	
	SA04/11 - 25.99	25	588	5	40	0.01	3.1	0.15	0.0000807	0.0565	0.0005	0.0014	0.0005	0.5813	0.0073	0.0747	0.0006	0.69	464	4	465	5	470	17	1	rim	
	SA04/11 - 25.66	25	17	7	3	0.41	0.3	0.17	0.0000906	0.0771	0.0022	0.1236	0.0034	2.1417	0.0675	0.2014	0.0029	0.45	1183	15	1162	22	1124	49	-5	inh	
	SA04/11 - 24.60	24	635	6	44	0.01	4.7	0.21	0.0001138	0.0555	0.0004	0.0005	0.0002	0.5779	0.0070	0.0755	0.0007	0.74	469	4	463	4	432	13	-9	rim	
	SA04/11 - 24.63	24	439	424	137	0.99	3.2	0.06	0.0000322	0.0987	0.0003	0.3041	0.0013	3.5584	0.0404	0.2614	0.0028	0.95	1497	14	1540	9	1600	6	6	c2	
	SA04/11 - 27.70	27	498	8	34	0.02	1.1	0.06	0.0000337	0.0566	0.0004	0.0035	0.0006	0.5741	0.0067	0.0735	0.0006	0.74	457	4	461	4	476	16	4	rim	
	SA04/11 - 5.11	5	272	114	47	0.43	16.9	0.81	0.0004344	0.0713	0.0008	0.1266	0.0045	1.6281	0.0226	0.1656	0.0015	0.65	988	8	981	9	966	15	-2	inh	rejected, high common Pb
	SA04/11 - 5.10	5	597	142	101	0.24	0.6	0.01	0.0000069	0.0719	0.0003	0.0731	0.0005	1.6921	0.0171	0.1706	0.0015	0.90	1015	9	1006	6	984	9	-3	inh	
Standards																												
91500	91500	91500	79.4	27.2	14.5	0.35	3.0	0.45	0.0002424	0.0735	0.0011	0.1049	0.0038	1.8054	0.0324	0.1781	0.0018	0.55	1057	10	1047	12	1028	24	-2.8		
	91500	1	80.0	28.6	14.5	0.37	0.4	0.06	0.0000331	0.0741	0.0008	0.1098	0.0012	1.7974	0.0252	0.1760	0.0016	0.66	1045	9	1045	9	1043	20	-0.2		
	91500	6	84.1	30.2	15.4	0.37	0.0	0.00	0.0000001	0.0756	0.0007	0.1120	0.0008	1.8600	0.0229	0.1784	0.0015	0.70	1058	8	1067	8	1084	18	2.4		
	91500	11	80.1	28.3	14.6	0.36	0.2	0.02	0.0000129	0.0748	0.0005	0.1080	0.0009	1.8356	0.0208	0.1779	0.0016	0.80	1055	9	1058	7	1064	13	0.8		
	91500	15	81.6	28.8	14.8	0.36	0.0	0.00	0.0000001	0.0750	0.0007	0.1099	0.0011	1.8374	0.0250	0.1776	0.0018	0.73	1054	10	1059	9	1069	18	1.4		
	91500	20	78.2	27.4	13.9	0.36	0.0	0.00	0.0000001	0.0764	0.0005	0.1084	0.0009	1.8247	0.0215	0.1731	0.0017	0.82	1029	9	1054	8	1106	13	6.9		
	91500	21	82.1	28.2	15.0	0.35	0.4	0.05	0.0000277	0.0745	0.0006	0.1071	0.0010	1.8348	0.0228	0.1786	0.0018	0.80	1060	10	1058	8	1054	14	-0.5		
	91500	25	80.9	27.9	15.0	0.35	0.3	0.05	0.0000275	0.0733	0.0008	0.1055	0.0009	1.8294	0.0247	0.1809	0.0016	0.65	1072	9	1056	9	1023	20	-4.8		
	91500	30	80.0	27.6	14.9	0.35	0.2	0.04	0.0000196	0.0736	0.0004	0.1051	0.0010	1.8523	0.0217	0.1825	0.0019	0.88	1081	10	1064	8	1031	10	-4.8		
	91500	34	82.8	28.7	15.2	0.36	0.0	0.00	0.0000001	0.0753	0.0004	0.1065	0.0008	1.8669	0.0190	0.1799	0.0016	0.89	1066	9	1069	7	1075	10	0.8		
	91500	39	80.8	27.9	14.8	0.35	0.2	0.04	0.0000199	0.0756	0.0006	0.1080	0.0009	1.8645	0.0241	0.1788	0.0018	0.79	1060	10	1069	8	1085	15	2.3		
	91500	43	81.7	28.3	15.0	0.36	0.0	0.00	0.0000001	0.0742	0.0006	0.1083	0.0007	1.8423	0.0236	0.1801	0.0018	0.80	1067	10	1061	8	1046	16	-2.0		
	91500	48	81.6	28.2	15.4	0.35	0.4	0.05	0.0000292	0.0748	0.0010	0.1060	0.0012	1.9047	0.0310	0.1847	0.0018	0.61	1092	10	1083	11	1063	25	-2.8		
	91500	52	81.6	28.2	15.1	0.35	0.3	0.04	0.0000210	0.0742	0.0005	0.1065	0.0010	1.8494	0.0225	0.1807	0.0018	0.82	1071	10	1063	8	1047	13	-2.3		
	91500	56	81.0	28.0	14.9	0.35	0.4	0.06	0.0000308	0.0740	0.0006	0.1068	0.0012	1.8330	0.0228	0.1795	0.0017	0.74	1065	9	1057	8	1042	16	-2.2		
	91500	61	81.2	28.2	14.9	0.36	0.0	0.00	0.0000001	0.0755	0.0006	0.1094	0.0007	1.8665	0.0252	0.1793	0.0019	0.77	1063	10	1069	9	1081	17	1.6		
	91500	65	81.2	28.2	15.0	0.36	0.0	0.00	0.0000001	0.0746	0.0007	0.1082	0.0010	1.8533	0.0252	0.1802	0.0017	0.71	1068	10	1065	9	1056	20	-1.2		
	91500	70	82.1	28.6	14.9	0.36	0.0	0.01	0.0000028	0.0743	0.0007	0.1069	0.0008	1.8233	0.0245	0.1780	0.0016	0.67	1056	9	1054	9	1049	20	-0.7		
	91500	74	82.2	28.7	15.2	0.36	0.0	0.00	0.0000001	0.0751	0.0007	0.1072	0.0005	1.8664	0.0249	0.1803	0.0016	0.68	1068	9	1069	9	1070	20	0.1		
	91500	79	79.8	27.7	14.7	0.36	0.3	0.04	0.0000234	0.0745	0.0007	0.1066	0.0010	1.8475	0.0235	0.1799	0.0016	0.69	1067	9	1063	8	1054	17	-1.2		
	91500	83	81.0	28.2	14.7	0.36	0.0	0.01	0.0000028	0.0742	0.0006	0.1075	0.0007	1.8109	0.0231	0.1769	0.0017	0.73	1050	9	1049	8	1048	17	-0.2		
	91500	91500	82.3	28.8	15.0	0.36	0.0	0.00	0.0000001	0.0751	0.0007	0.1084	0.0008	1.8391	0.0247	0.1776	0.0016	0.69	1054	9	1060	9	1071	19	1.6		
	91500	91500	83.1	29.0	15.1	0.36	0.0	0.00	0.0000001	0.0748	0.0006	0.1087	0.0009	1.8337	0.0221	0.1779	0.0017	0.77	1055	9	1058	8	1062	15	0.6		
	91500	91500	82.8	29.1	15.3	0.36	0.0	0.00	0.0000001	0.0758	0.0009	0.1081	0.0012	1.8784	0.0295	0.1798	0.0018	0.62	1066	10	1074	10	1088	24	2.0		
	91500	91500	82.5	28.7	15.3	0.36	0.5	0.07	0.0000397	0.0738	0.0006	0.1063	0.0014	1.8451	0.0229	0.1814	0.0016	0.71	1075	9	1062	8	1035	16	-3.8		
	91500	91500	80.2	27.6	14.9	0.35	0.0	0.00	0.0000001	0.0752	0.0007	0.1070	0.0009	1.8848	0.0242	0.1818	0.0017	0.71	1077	9	1076	8	1073	18	-0.3		
	91500	91500	79.7	27.6	14.7	0.36	0.1	0.02	0.0000120	0.0747	0.0007	0.1072	0.0008	1.8564	0.0244	0.1803	0.0018	0.74	1069	10	1066	9	1059	18	-0.9		
	91500	91500	80.5	27.9	14.7	0.36	0.5	0.08	0.0000412	0.0742	0.0007	0.1061	0.0012	1.8234	0.0240	0.1782	0.0017	0.71	1057	9	1054	9	1046	17	-1.1		
	91500	91500	82.1	28.5	15.1	0.36	0.0	0.00	0.0000001	0.0742	0.0005	0.1068	0.0008	1.8436	0.0219	0.1801	0.0017	0.80	1068	9	1061	8	1047	14	-2.0		
	91500	91500	80.6	27.9	14.8	0.36	0.0	0.00	0.0000001	0.0747	0.0008	0.1073	0.0007	1.8485	0.0245	0.1795	0.0015	0.65	1064	8	1063	9	1059	21	-0.5		
	91500	91500	79.0	27.2	14.3	0.35	0.0	0.00	0.0000001	0.0745	0.0005	0.1073	0.0010	1.8187	0.0201	0.1770	0.0016	0.82	1051	9	1052	7	1055	13	0.4		
	91500	91500	80.4	27.8	14.6	0.35	0.0	0.01	0.0000027	0.0744	0.0007	0.1075	0.0004	1.8175	0.0232	0.1772	0.0016	0.71	1052	9	1052	8	1052	18	0.0		
	91500	91500	80.7	27.9	14.7	0.35	0.4	0.06	0.0000326	0.0751	0.0007	0.1065	0.0012	1.8482	0.0242	0.1786	0.0016	0.68	1059	9	1063	9	1070	18	1.0		
	91500	91500	83.8	29.1	15.4	0.36	0.3	0.04	0.0000224	0.0738	0.0010	0.1078	0.0012	1.8248	0.0287	0.1793	0.0016	0.57	1063	9	1054	10	1036	25	-2.6		
	91500	91500	80.5	27.8	14.9	0.35	0.0	0.01	0.0000029	0.0751	0.0007	0.1067	0.0008	1.8675	0.0241	0.1804	0.0017	0.73	1069	9	1070	8	1070	17	0.1		
	91500	91500	79.8	27.5	14.5	0.35	0.6	0.09	0.0000468	0.0746	0.0009	0.1065	0.0015	1.8341	0.0277	0.1783	0.0016	0.60	1058	9	1058	10	1057	23	-0.1		
	91500	91500	81.2	28.5	14.9	0.36	0.0	0.00	0.0000001	0.0756	0.0009	0.1085	0.0011	1.8676	0.0378	0.1792	0.0029	0.79	1062	16	1070	13	1084	25	2.0		
	91500	158	82.9	28.9	15.5	0.36	0.5	0.08	0.0000405	0.0747	0.0007	0.1066	0.0014	1.8764	0.0268	0.1821	0.0019	0.72	1078	10	1073	9	1061	18	-1.6		
	91500	163	84.9	29.5	15.9	0.36	0.1	0.01	0.0000072	0.0754	0.0008	0.1069	0.0009	1.9060	0.0262	0.1832	0.0017	0.67	1085	9	1083	9	1080	20	-0.4		

sample	analysis no.	grain no.	U ppm	Th ppm	Pb ppm	Th/U	^{204}Pb ppb	f206 (%)	^{204}Pb/^{206}Pb	corrected ratios									Ages (Ma)								grain area	comment
										^{207}Pb/^{206}Pb	1σ	^{208}Pb/^{206}Pb	1σ	^{207}Pb/^{235}U	1σ	^{206}Pb/^{238}U	1σ	ρ	^{206}Pb/^{238}U	1σ	^{207}Pb/^{235}U	1σ	^{207}Pb/^{206}Pb	1σ	% disc			
	91500	167	80.1	27.5	15.0	0.35	0.4	0.05	0.0000283	0.0735	0.0007	0.1059	0.0013	1.8569	0.0256	0.1832	0.0018	0.72	1085	10	1066	9	1027	18	-5.6			
	91500	172	80.9	28.0	14.9	0.36	0.0	0.00	0.0000001	0.0749	0.0011	0.1053	0.0009	1.8544	0.0338	0.1795	0.0018	0.56	1064	10	1065	12	1066	31	0.2			
	91500	176	80.0	27.6	14.6	0.35	0.0	0.00	0.0000001	0.0743	0.0006	0.1081	0.0011	1.8304	0.0261	0.1787	0.0020	0.79	1060	11	1056	9	1048	18	-1.1			
	91500	181	83.1	29.1	15.3	0.36	0.5	0.07	0.0000362	0.0758	0.0008	0.1070	0.0016	1.8765	0.0282	0.1795	0.0018	0.67	1064	10	1073	10	1090	21	2.4			
	91500	185	83.3	29.0	15.2	0.36	0.6	0.09	0.0000475	0.0733	0.0008	0.1070	0.0015	1.8039	0.0277	0.1786	0.0018	0.67	1059	10	1047	10	1020	21	-3.9			
	91500	190	83.8	29.2	15.6	0.36	0.0	0.00	0.0000001	0.0748	0.0006	0.1083	0.0010	1.8725	0.0248	0.1816	0.0019	0.79	1076	10	1071	9	1062	16	-1.3			
	91500	194	81.6	28.2	15.0	0.35	0.2	0.03	0.0000168	0.0759	0.0007	0.1070	0.0009	1.8797	0.0244	0.1797	0.0017	0.71	1065	9	1074	9	1091	17	2.3			
	91500	199	82.4	28.4	15.2	0.35	0.4	0.05	0.0000283	0.0743	0.0008	0.1068	0.0012	1.8441	0.0260	0.1800	0.0017	0.69	1067	10	1061	9	1050	19	-1.6			
	91500	203	80.0	27.7	14.6	0.36	0.4	0.06	0.0000300	0.0750	0.0009	0.1086	0.0013	1.8492	0.0284	0.1789	0.0018	0.64	1061	10	1063	10	1067	22	0.6			
	91500	208	79.6	27.5	14.3	0.36	0.0	0.00	0.0000001	0.0747	0.0008	0.1071	0.0010	1.8105	0.0269	0.1759	0.0017	0.65	1045	9	1049	10	1059	22	1.4			
	91500	212	76.3	26.2	14.0	0.35	0.4	0.06	0.0000319	0.0754	0.0007	0.1070	0.0012	1.8625	0.0254	0.1793	0.0017	0.69	1063	9	1068	9	1077	19	1.3			
	91500	217	80.3	27.8	14.8	0.36	0.6	0.09	0.0000463	0.0736	0.0009	0.1052	0.0015	1.8226	0.0300	0.1795	0.0019	0.64	1065	10	1054	11	1031	23	-3.3			
	91500	221	77.6	26.7	13.8	0.35	0.0	0.00	0.0000001	0.0746	0.0010	0.1083	0.0011	1.7915	0.0302	0.1742	0.0019	0.65	1035	10	1042	11	1057	26	2.1			
	91500	226	80.6	28.1	14.5	0.36	0.0	0.00	0.0000001	0.0741	0.0009	0.1073	0.0010	1.8001	0.0290	0.1763	0.0018	0.62	1047	10	1046	10	1042	26	-0.5			
	91500	230	82.2	28.6	14.8	0.36	0.0	0.00	0.0000001	0.0740	0.0009	0.1081	0.0009	1.7955	0.0283	0.1759	0.0017	0.62	1044	9	1044	10	1042	25	-0.2			
	91500	234	82.0	28.6	15.0	0.36	0.3	0.04	0.0000207	0.0747	0.0007	0.1082	0.0012	1.8439	0.0259	0.1789	0.0019	0.74	1061	10	1061	9	1061	18	0.0			
	91500	0	79.0	27.7	14.4	0.36	0.2	0.03	0.0000147	0.0749	0.0006	0.1097	0.0009	1.8427	0.0259	0.1783	0.0020	0.80	1058	11	1061	9	1066	16	0.8			
	91500	239	81.3	28.5	14.9	0.36	0.7	0.10	0.0000536	0.0766	0.0008	0.1061	0.0016	1.8813	0.0284	0.1782	0.0020	0.73	1057	11	1075	10	1109	19	4.7			
	91500	240	81.5	28.5	14.9	0.36	0.0	0.00	0.0000001	0.0741	0.0008	0.1087	0.0010	1.8234	0.0283	0.1784	0.0019	0.70	1058	11	1054	10	1044	22	-1.4			
	91500	243	83.0	29.1	15.5	0.36	0.0	0.00	0.0000001	0.0757	0.0007	0.1084	0.0011	1.8966	0.0288	0.1817	0.0021	0.76	1076	11	1080	10	1087	19	1.0			
temora	temora	10	624.0	334.6	44.3	0.55	1.9	0.10	0.0000537	0.0548	0.0004	0.1713	0.0011	0.5049	0.0058	0.0669	0.0006	0.73	417	3	415	4	403	15	-3.5			
	temora	19	630.4	319.0	44.1	0.52	0.4	0.02	0.0000119	0.0553	0.0004	0.1607	0.0008	0.5055	0.0053	0.0664	0.0006	0.79	414	3	415	4	422	14	1.9			
	temora	29	163.6	39.2	10.8	0.25	1.0	0.19	0.0001012	0.0540	0.0007	0.0740	0.0021	0.5036	0.0082	0.0676	0.0006	0.55	422	4	414	6	372	24	-13.3			
	temora	38	149.6	45.7	10.0	0.31	0.1	0.03	0.0000152	0.0553	0.0007	0.0975	0.0008	0.5104	0.0078	0.0669	0.0006	0.61	417	4	419	5	425	26	1.8			
	temora	47	198.8	57.9	13.2	0.30	0.8	0.13	0.0000713	0.0555	0.0006	0.0916	0.0017	0.5103	0.0074	0.0667	0.0006	0.59	416	3	419	5	432	22	3.7			
	temora	60	161.6	41.2	10.3	0.26	0.6	0.12	0.0000651	0.0550	0.0007	0.0787	0.0017	0.4908	0.0073	0.0648	0.0006	0.59	404	3	405	5	410	22	1.3			
	temora	69	223.9	64.2	14.6	0.29	0.0	0.00	0.0000001	0.0555	0.0006	0.0921	0.0007	0.5022	0.0070	0.0656	0.0006	0.65	410	4	413	5	433	24	5.4			
	temora	78	176.2	49.1	11.2	0.29	0.2	0.03	0.0000154	0.0554	0.0007	0.0882	0.0010	0.4914	0.0079	0.0644	0.0006	0.55	402	3	406	5	426	29	5.6			
	temora	87	178.4	45.4	11.5	0.26	0.0	0.00	0.0000001	0.0548	0.0007	0.0821	0.0007	0.4937	0.0074	0.0653	0.0006	0.60	408	4	407	5	404	27	-1.0			
	temora	TEM	187.8	65.8	12.5	0.36	0.4	0.07	0.0000400	0.0551	0.0005	0.1098	0.0015	0.5019	0.0066	0.0660	0.0006	0.71	412	4	413	4	416	17	0.9			
	temora	TEM	165.4	64.6	11.2	0.40	0.4	0.07	0.0000373	0.0560	0.0006	0.1243	0.0020	0.5094	0.0073	0.0659	0.0006	0.61	412	3	418	5	453	22	9.1			
	temora	TEM	170.9	84.7	11.7	0.51	0.5	0.09	0.0000490	0.0536	0.0006	0.1565	0.0014	0.4796	0.0067	0.0649	0.0005	0.58	405	3	398	5	354	22	-14.5			
	temora	TEM	126.4	37.6	8.2	0.31	0.9	0.25	0.0001341	0.0521	0.0010	0.0907	0.0029	0.4650	0.0098	0.0648	0.0006	0.41	405	3	388	7	287	34	-41.0			
	temora	TEM	131.5	53.8	9.0	0.42	0.7	0.16	0.0000870	0.0536	0.0008	0.1292	0.0026	0.4946	0.0087	0.0669	0.0006	0.50	417	4	408	6	356	26	-17.2			
	temora	TEM	150.5	72.4	10.5	0.49	0.3	0.07	0.0000364	0.0554	0.0013	0.1499	0.0017	0.5106	0.0148	0.0669	0.0011	0.57	417	7	419	10	427	50	2.3			
	temora	162	113.7	34.1	7.5	0.31	0.0	0.00	0.0000002	0.0564	0.0009	0.0965	0.0009	0.5164	0.0101	0.0664	0.0007	0.55	414	4	423	7	469	36	11.7			
	temora	171	108.6	28.6	7.1	0.27	0.4	0.12	0.0000649	0.0542	0.0012	0.0796	0.0021	0.4971	0.0117	0.0665	0.0007	0.42	415	4	410	8	380	41	-9.2			
	temora	180	59.7	21.5	4.0	0.37	0.6	0.34	0.0001832	0.0540	0.0019	0.1110	0.0048	0.4945	0.0192	0.0664	0.0010	0.38	414	6	408	13	372	59	-11.4			
	temora	189	80.0	27.5	5.3	0.35	0.7	0.28	0.0001512	0.0544	0.0014	0.1065	0.0039	0.4898	0.0140	0.0653	0.0007	0.37	408	4	405	9	386	45	-5.7			
	temora	198	46.6	16.4	3.1	0.36	0.0	0.00	0.0000004	0.0564	0.0009	0.1141	0.0022	0.5085	0.0100	0.0654	0.0007	0.57	409	4	417	7	466	36	12.3			
	temora	207	65.9	22.9	4.4	0.36	0.1	0.03	0.0000182	0.0569	0.0011	0.1158	0.0017	0.5191	0.0117	0.0661	0.0008	0.52	413	5	425	8	488	39	15.4			
	temora	216	90.8	49.5	6.3	0.56	2.0	0.76	0.0004101	0.0516	0.0017	0.1506	0.0070	0.4555	0.0153	0.0640	0.0007	0.31	400	4	381	11	267	43	-49.8			
	temora	225	128.1	60.7	8.8	0.49	0.9	0.23	0.0001259	0.0537	0.0012	0.1446	0.0031	0.4881	0.0117	0.0659	0.0007	0.42	411	4	404	8	359	39	-14.6			
	temora	238	93.9	46.1	6.4	0.50	0.8	0.30	0.0001599	0.0534	0.0013	0.1509	0.0037	0.4790	0.0126	0.0650	0.0008	0.45	406	5	397	9	346	39	-17.4			
	temora	TEM	131.5	53.8	9.0	0.42	0.7	0.16	0.0000870	0.0536	0.0008	0.1292	0.0026	0.4946	0.0087	0.0669	0.0006	0.50	417	4	408	6	356	26	-17			
	temora	TEM	150.5	72.4	10.5	0.49	0.3	0.07	0.0000364	0.0554	0.0013	0.1499	0.0017	0.5106	0.0148	0.0669	0.0011	0.57	417	7	419	10	427	50	2			
	temora	162	113.7	34.1	7.5	0.31	0.0	0.00	0.0000002	0.0564	0.0009	0.0965	0.0009	0.5164	0.0101	0.0664	0.0007	0.55	414	4	423	7	469	36	12			
	temora	171	108.6	28.6	7.1	0.27	0.4	0.12	0.0000649	0.0542	0.0012	0.0796	0.0021	0.4971	0.0117	0.0665	0.0007	0.42	415	4	410	8	380	41	-9			
	temora	180	59.7	21.5	4.0	0.37	0.6	0.34	0.0001832	0.0540	0.0019	0.1110	0.0048	0.4945	0.0192	0.0664	0.0010	0.38	414	6	408	13	372	59	-11			
	temora	189	80.0	27.5	5.3	0.35	0.7	0.28	0.0001512	0.0544	0.0014	0.1065	0.0039	0.4898	0.0140	0.0653	0.0007	0.37	408	4	405	9	386	45	-6			
	temora	198	46.6	16.4	3.1	0.36	0.0	0.00	0.0000004	0.0564	0.0009	0.1141	0.0022	0.5085	0.0100	0.0654	0.0007	0.57	409	4	417	7	466	36	12			
	temora	207	65.9	22.9	4.4	0.36	0.1	0.03	0.0000182	0.0569	0.0011	0.1158	0.0017	0.5191	0.0117	0.0661	0.0008	0.52	413	5	425	8	488	39	15			
	temora	216	90.8	49.5	6.3	0.56	2.0	0.76	0.0004101	0.0516	0.0017	0.1506	0.0070	0.4555	0.0153	0.0640	0.0007	0.31	400	4	381	11	267	43	-50			
	temora	225	128.1	60.7	8.8	0.49	0.9	0.23	0.0001259	0.0537	0.0012	0.1446	0.0031	0.4881	0.0117	0.0659	0.0007	0.42	411	4	404	8	359	39	-15			
	temora	238	93.9	46.1	6.4	0.50	0.8	0.30	0.0001599	0.0534	0.0013	0.1509	0.0037	0.4790	0.0126	0.0650	0.0008	0.45	406	5	397	9	346	39	-17			

Appendix 4d
Zircon oxygen isotope data and average values of bracketing zircon standard 91500

	analyses no.	grain no.	$^{18}O/^{16}O$ (measured)	2SD	1 s.e.m.	$\delta^{18}O$ [‰] VSMOW	2SD	1 s.e.m.	n	grain area	comment
	Session 11 (04.06.2005)										
	91500-3 - 1-9		0.0020133	0.0000011	0.0000002	10.02	0.54	0.090	9		
	91500-3 - 11-15, 17-18, 20		0.0020127	0.0000006	0.0000001	9.68	0.28	0.049	8		
Kemnay	**SA04/07 - 1**	1	0.0020091		0.0000003	7.9		0.101		c1	
	SA04/07 - 2	2	0.0020099		0.0000003	8.3		0.124		c1	
	SA04/07 - 4	2	0.0020094		0.0000004	8.1		0.147		rim	
	SA04/07 - 6	4	0.0020036		0.0000002	5.2		0.049		c1	rejected, grain plucked
	SA04/07 - 7	4	0.0020054		0.0000002	6.1		0.065		rim	rejected, grain plucked
	SA04/07 - 9	5	0.0020075		0.0000002	7.1		0.060		c2	
	SA04/07 - 10	5	0.0020049		0.0000002	5.8		0.065		c1	rejected, crack
	SA04/07 - 11	6	0.0020091		0.0000002	7.9		0.071		c1	rejected, crack
	SA04/07 - 12	6	0.0020089		0.0000003	7.8		0.121		c2	rejected, crack
	SA04/07 - 15	8	0.0020089		0.0000004	7.8		0.139		c1	rejected, crack
	91500-3 - 21-25		0.0020127	0.0000008	0.0000002	9.69	0.37	0.084	5		
	SA04/07 - 16	8	0.0020093		0.0000003	8.0		0.100		c2	rejected, crack
	SA04/07 - 18	9	0.0020087		0.0000004	7.7		0.147		c1	
	SA04/07 - 19	9	0.0020115		0.0000002	9.1		0.090		c2	
	SA04/07 - 22	11	0.0020022		0.0000002	4.5		0.053		c1	rejected, grain plucked
	SA04/07 - 23	11	0.0020069		0.0000003	6.8		0.099		rim	rejected, grain plucked
	SA04/07 - 24	12	0.0020073		0.0000003	7.0		0.091		c1	
	SA04/07 - 26	13	0.0020067		0.0000003	6.7		0.092		inh	
	SA04/07 - 27	13	0.0020088		0.0000002	7.8		0.079		rim	
	SA04/07 - 33	16	0.0020066		0.0000003	6.7		0.093		c1	
	SA04/07 - 34	16	0.0020074		0.0000003	7.1		0.113		rim	rejected, grain plucked
	91500-3 - 26-30		0.0020133	0.0000006	0.0000001	10.01	0.28	0.062	5		
	SA04/07 - 37	18	0.0020106		0.0000003	8.6		0.110		c1	
	SA04/07 - 38	18	0.0020125		0.0000003	9.6		0.128		c1+rim	
	SA04/07 - 39	19	0.0020109		0.0000002	8.8		0.089		c1	rejected, crack
	SA04/07 - 40	19	0.0020107		0.0000003	8.7		0.131		c2	rejected, crack
	SA04/07 - 46	22	0.0020125		0.0000003	9.6		0.143		c1	
	SA04/07 - 47	22	0.0020106		0.0000003	8.7		0.146		rim	rejected, crack
	SA04/07 - 48	23	0.0020092		0.0000004	7.9		0.176		inh	
	SA04/07 - 49	23	0.0020082		0.0000004	7.5		0.140		rim	
	SA04/07 - 50	24	0.0020146		0.0000004	10.6		0.188		c2a	
	SA04/07 - 51	24	0.0020130		0.0000003	9.9		0.151		c2b	
	91500-3 - 31-32, 35		0.0020131	0.0000011	0.0000003	9.90	0.57	0.164	3		
	Session 12 (05.06.2005)										
	91500-18 - 60-69		0.0020107	0.0000018	0.0000003	9.85	0.91	0.151	10		
	91500-3 - 82-91		0.0020104	0.0000010	0.0000002	9.68	0.48	0.076	10		
	SA04/07 - 55	26	0.0020084		0.0000004	8.7		0.160		inh	rejected, correction on position of secondary ion beam anomalously large
	SA04/07 - 56	26	0.0020152		0.0000004	12.1		0.211		rim	rejected, crack
	SA04/07 - 59	28	0.0020134		0.0000005	11.2		0.250		inh	
	SA04/07 - 60	28	0.0020121		0.0000007	10.5		0.358		rim	
	SA04/07 - 61	29	0.0020110		0.0000004	10.0		0.176		c1	rejected, crack
	SA04/07 - 62	29	0.0020126		0.0000003	10.8		0.141		rim	
	SA04/07 - 63	30	0.0020159		0.0000004	12.4		0.219		c2	
	SA04/07 - 72	33	0.0020151		0.0000006	12.0		0.337		c2	
	SA04/07 - 73	33	0.0020150		0.0000004	12.0		0.224		rim	
	SA04/07 - 74	34	0.0020166		0.0000002	12.8		0.152		c2c	rejected, crack
	SA04/07 - 75	34	0.0020144		0.0000003	11.7		0.195		rim	
	91500-3 - 93-96		0.0020111	0.0000006	0.0000002	10.05	0.30	0.076	4		
	SA04/07 - 76	34	0.0020117		0.0000003	10.3		0.170		c2b	rejected, correction on position of secondary ion beam anomalously large
	SA04/07 - 77	34	0.0020143		0.0000003	11.6		0.200		c2a	rejected, crack
	SA04/07 - 78	35	0.0020176		0.0000005	13.3		0.331		inh1	
	SA04/07 - 79	35	0.0020150		0.0000003	12.0		0.154		inh2	
	SA04/07 - 80	35	0.0020137		0.0000002	11.3		0.137		r1	
	SA04/07 - 81	35	0.0020131		0.0000004	11.0		0.192		r2	rejected, crack
Cove	**SA04/10 - 2**	2	0.0020104		0.0000005	9.7		0.225		c1	rejected, correction on position of secondary ion beam anomalously large
	SA04/10 - 3	3	0.0020094		0.0000003	9.2		0.119		c1	rejected, crack
	SA04/10 - 7	5	0.0020091		0.0000002	9.0		0.111		rim	rejected, crack
	SA04/10 - 8	5	0.0020095		0.0000003	9.3		0.155		c2c	
	91500-3 - 97-101		0.0020110	0.0000011	0.0000002	9.98	0.43	0.097	5		
	SA04/10 - 13	7	0.0020115		0.0000002	10.3		0.095		c1	
	SA04/10 - 14	7	0.0020120		0.0000003	10.5		0.153		rim	
	SA04/10 - 15	8	0.0020094		0.0000002	9.2		0.103		inh	rejected, crack
	SA04/10 - 16	8	0.0020086		0.0000003	8.8		0.137		inh	rejected, crack
	SA04/10 - 17	9	0.0020090		0.0000002	9.0		0.111		inh	
	SA04/10 - 18	9	0.0020114		0.0000002	10.2		0.117		rim	rejected, crack
	SA04/10 - 23	12	0.0020054		0.0000004	7.2		0.152		inh	rejected, crack
	SA04/10 - 22	12	0.0020068		0.0000002	7.9		0.082		inh	
	SA04/10 - 24	12	0.0020142		0.0000002	11.6		0.110		rim	
	SA04/10 - 39	18	0.0020103		0.0000003	9.6		0.123		rim	rejected, crack
	91500-3 - 102-106		0.0020112	0.0000007	0.0000002	10.09	0.34	0.085	5		

	analyses no.	grain no.	$^{18}O/^{16}O$ (measured)	2SD	1 s.e.m.	$\delta^{18}O$ [‰] VSMOW	2SD	1 s.e.m.	n	grain area	comment
	SA04/10 - 41	18	0.0020060		0.0000003	6.9		0.116		inh1	rejected, crack
	SA04/10 - 42	18	0.0020060		0.0000003	6.9		0.090		inh2	
	SA04/10 - 43	19	0.0020091		0.0000003	8.4		0.139		c2b	rejected, crack
	SA04/10 - 44	19	0.0020086		0.0000003	8.2		0.107		c2c	rejected, crack
	SA04/10 - 45	19	0.0020104		0.0000002	9.1		0.090		c2a	
	SA04/10 - 46	20	0.0020061		0.0000004	6.9		0.155		inh	
	SA04/10 - 47	20	0.0020051		0.0000002	6.5		0.058		inh	rejected, > 20 % discordant
	SA04/10 - 48	20	0.0020111		0.0000003	9.4		0.139		rim	
Nigg Bay	SA04/11 - 3	2	0.0020053		0.0000002	6.5		0.068		c1	rejected, correction on position of secondary ion beam anomalously large
	SA04/11 - 4	2	0.0020045		0.0000005	6.2		0.148		rim	rejected, crack
	Session 13 (05.06.2005)										
	91500-3 - 107-111		0.0020117	0.0000005	0.0000001	9.75	0.26	0.057	5		
	SA04/11 - 5	3	0.0020011		0.0000003	4.5		0.067		inh	rejected, correction on position of secondary ion beam anomalously large
	SA04/11 - 6	3	0.0020003		0.0000002	4.1		0.050		inh	
	SA04/11 - 10	5	0.0020033		0.0000002	5.6		0.052		inh	
	SA04/11 - 11	5	0.0020029		0.0000003	5.4		0.091		inh	rejected, crack
	SA04/11 - 15	7	0.0020008		0.0000002	4.3		0.048		?	rejected, crack
	SA04/11 - 21	10	0.0020025		0.0000004	5.2		0.114		inh	rejected, crack
	SA04/11 - 22	10	0.0020011		0.0000003	4.5		0.062		inh	rejected, crack
	SA04/11 - 32	14	0.0020075		0.0000004	7.7		0.153		rim	rejected, crack
	SA04/11 - 33	14	0.0020028		0.0000003	5.3		0.074		inh	
	SA04/11 - 34	14	0.0020034		0.0000002	5.6		0.067		inh	rejected, crack
	91500-3 - 112-116		0.0020122	0.0000001	0.0000000	10.00	0.07	0.016	5		
	SA04/11 - 35	15	0.0020017		0.0000004	4.8		0.085		c2a	
	SA04/11 - 36	15	0.0020020		0.0000004	4.9		0.100		c2b	
	SA04/11 - 37	16	0.0020085		0.0000003	8.1		0.135		c2	rejected, crack
	SA04/11 - 38	16	0.0020035		0.0000004	5.7		0.117		rim	rejected, > 20 % discordant
	SA04/11 - 40	17	0.0020075		0.0000003	7.6		0.111		c2a	
	SA04/11 - 41	17	0.0020061		0.0000002	7.0		0.073		c2b	
	SA04/11 - 42	17	0.0020071		0.0000003	7.5		0.113		rim	rejected, crack
	SA04/11 - 47	19	0.0020071		0.0000003	7.5		0.105		rim	
	SA04/11 - 48	19	0.0020034		0.0000005	5.6		0.142		inh	rejected, crack
	SA04/11 - 49	19	0.0020039		0.0000002	5.9		0.067		inh	
	Session 14 (05.06.2005)										
	91500-3 - 117-121		0.0020106	0.0000016	0.0000003	9.84	0.67	0.151	5		
	SA04/11 - 52	21	0.0020023		0.0000002	5.7		0.064		inh	rejected, correction on position of secondary ion beam anomalously large
	SA04/11 - 53	21	0.0020061		0.0000003	7.6		0.100		rim	
	SA04/11 - 66	25	0.0020038		0.0000002	6.5		0.076		inh	
	SA04/11 - 99	25	0.0020048		0.0000003	7.0		0.110		rim	
	SA04/11 - 67	26	0.0020073		0.0000003	8.2		0.128		rim	rejected, crack
	SA04/11 - 68	26	0.0020062		0.0000003	7.7		0.123		inh	
	SA04/11 - 69	26	0.0020081		0.0000003	8.6		0.121		inh	rejected, crack
	SA04/11 - 73	28	0.0020068		0.0000005	8.0		0.180		rim	
	SA04/11 - 74	28	0.0020049		0.0000003	7.0		0.122		rim	
	SA04/11 - 75	29	0.0020047		0.0000002	6.9		0.069		c1	
	91500-3 - 122-126		0.0020107	0.0000016	0.0000003	9.88	0.56	0.126	5		
	SA04/11 - 76	29	0.0020049		0.0000004	7.0		0.125		rim	rejected, correction on position of secondary ion beam anomalously large
	SA04/11 - 81	31	0.0020040		0.0000003	6.6		0.114		inh	
	SA04/11 - 82	31	0.0020040		0.0000003	6.6		0.082		rim	
	SA04/11 - 86	33	0.0020103		0.0000002	9.7		0.083		inh	
	SA04/11 - 87	33	0.0020047		0.0000004	6.9		0.138		inh	rejected, crack
	SA04/11 - 88	34	0.0020025		0.0000003	5.8		0.075		inh	
	SA04/11 - 89	34	0.0020063		0.0000004	7.7		0.156		rim	rejected, crack
	SA04/11 - 90	35	0.0020025		0.0000002	5.8		0.055		inh	
	SA04/11 - 91	35	0.0020031		0.0000004	6.1		0.109		inh	
	SA04/11 - 92	35	0.0020031		0.0000005	6.1		0.164		rim	
	Session 15 (05.06.2005)										
	91500 - 127-131		0.0020095	0.0000009	0.0000002	9.87	0.5	0.102	5		
	SA04/11 - 97	38		0.0020016	0.0000004	5.9		0.129		inh	rejected, correction on position of secondary ion beam anomalously large
	SA04/11 - 98	38		0.0020066	0.0000003	8.4		0.121		rim	
	91500 - 132-135		0.0020097	0.0000007	0.0000002	9.99	0.3	0.082	4		
	91500 - 137, 139-141		0.0020092	0.0000005	0.0000001	9.71	0.3	0.064	4		

c1 = unzoned inner core
c2 = osciallatory zoned outer core
r1-2 = rim

Appendix 4e
Hf isotope data of zircons from the Kemnay, Cove and Nigg Bay granites

Analysis no.	grain no.	grain area	age	1 SD	$\delta^{18}O$ [‰]	2σ	$^{176}Lu/^{177}Hf$ (WR)	total Hf	Yb/Hf	$^{178}Hf/^{177}Hf$	1s%	$^{176}Hf/^{177}Hf$	1s%	$^{176}Yb/^{177}Hf$	1s%	$^{176}Lu/^{177}Hf$	1s%	$^{176}Hf/^{177}Hf$ (initial)	εHf	95% conf.	TDM_C	95% conf.	TDM_W	95% conf.
Kemnay																								
SA04-07_1.1	1	c1	457	4	7.9	0.6	0.004	7.40	0.06	1.467180	0.0074	0.282124	0.0110	0.14833	8.2	0.00037	8.2	0.282121	-13.0	1.2	2259	73	1690	49
SA04-07_9.18	9	c1	457	4	7.7	0.6	0.004	5.18	0.05	1.467270	0.0080	0.282211	0.0146	0.13516	7.8	0.00037	7.9	0.282208	-9.9	1.6	2066	95	1557	64
SA04-07_24.50	24	c2	457	4	10.6	0.6	0.004	6.05	0.05	1.467330	0.0032	0.282036	0.0059	0.13219	7.8	0.00039	7.6	0.282033	-16.1	0.7	2454	40	1824	26
SA04-07_23.48	23	inh	457	4	7.9	0.6	0.004	6.00	0.05	1.467240	0.0035	0.282206	0.0067	0.13606	7.0	0.00040	7.1	0.282203	-10.1	0.8	1716	58	1496	40
SA04-07_25.52	25	inh	457	4			0.004	7.50	0.07	1.467230	0.0036	0.281737	0.0092	0.17200	7.1	0.00047	7.2	0.281733	-26.7	1.0	2333	70	2127	63
SA04-07_26.55	26	inh	457	4	8.7	0.6	0.004	6.17	0.05	1.467260	0.0038	0.282235	0.0072	0.13099	7.3	0.00033	7.4	0.282232	-9.0	0.8	1647	61	1450	41
SA04-07_28.59	28	rim	457	4	11.2	0.6	0.004	6.84	0.08	1.467200	0.0036	0.282121	0.0062	0.21221	12.9	0.00057	13.3	0.282116	-13.2	0.7	2270	43	1697	28
SA04-07_31.66	31	inh	457	4			0.004	8.46	0.13	1.467260	0.0041	0.281988	0.0077	0.33110	7.2	0.00092	7.3	0.281980	-18.0	0.9	1934	63	1775	69
SA04-07_36.82	36	c2	457	4			0.004	5.94	0.07	1.467260	0.0038	0.282159	0.0058	0.19016	7.8	0.00053	7.8	0.282155	-11.8	0.7	2185	40	1638	27
SA04-07_35.78	35	inh	457	4	13.3	0.6	0.004	6.50	0.05	1.467280	0.0034	0.281662	0.0074	0.13339	11.4	0.00031	11.2	0.281660	-29.3	0.8	2456	59	2233	50
SA04-07_40.90	40	c2	457	4			0.004	6.41	0.05	1.467270	0.0035	0.282161	0.0069	0.12671	8.1	0.00033	8.8	0.282158	-11.7	0.8	2176	47	1633	31
SA04-07_37.84	37	c2	457	4			0.004	5.98	0.08	1.467240	0.0035	0.282170	0.0060	0.20786	7.5	0.00054	7.6	0.282166	-11.4	0.7	2160	41	1622	27
SA04-07_18.37	18	c1	457	4	8.6	0.6	0.004	5.29	0.06	1.467090	0.0093	0.282105	0.0120	0.14372	9.5	0.00035	8.6	0.282102	-13.6	1.3	2301	79	1718	53
SA04-07_23.49 (1)	23	rim	457	4	7.5	0.6	0.004	9.91	0.19	1.467280	0.0044	0.282099	0.0077	0.47027	7.0	0.00122	7.0	0.282089	-14.1	0.9	2331	53	1739	35
SA04-07_23.49 (2)	23	rim	457	4	7.5	0.6	0.004	2.67		1.467570	0.0074	0.282178	0.0167	0.59385	7.1	0.00223	7.1	0.282159	-11.6	1.8	2175	110	1632	74
SA04-07_33.72 (1)	33	inh	457	4	12.4	0.6	0.004	6.40	0.09	1.467240	0.0043	0.281790	0.0089	0.20370	7.0	0.00050	7.1	0.281786	-24.8	1.0	2389	71	2083	58
SA04-07_33.73	33	rim	457	4	12.0	0.6	0.004	3.71	0.31	1.467460	0.0064	0.282024	0.0177	0.97430	7.1	0.00306	7.1	0.281998	-17.3	1.9	2531	116	1877	79
Cove																								
SA04-10_5.8	5	c2	458	7	9.3	0.6	0.004	4.41	0.03	1.467260	0.0038	0.282134	0.0074	0.08757	9.1	0.00023	9.0	0.282132	-12.6	0.9	2234	52	1672	33
SA04-10_9.17	9	inh	458	7	9.0	0.6	0.004	5.32	0.05	1.467280	0.0032	0.282190	0.0072	0.11826	7.1	0.00032	7.3	0.282188	-10.6	0.9	1796	55	1529	39
SA04-10_17.36	17	inh	458	7			0.004	6.83	0.04	1.467220	0.0034	0.282124	0.0060	0.11231	7.4	0.00028	7.3	0.282122	-12.9	0.8	1825	62	1606	38
SA04-10_17.35	17	rim	458	7			0.004	10.45	0.07	1.467240	0.0038	0.282072	0.0058	0.18960	7.6	0.00050	7.9	0.282068	-14.8	0.7	2376	42	1770	27
SA04-10_19.45	19	c2	458	7			0.004	4.52	0.06	1.467230	0.0036	0.282052	0.0072	0.14044	7.1	0.00033	7.2	0.282049	-15.5	0.9	2417	50	1799	32
SA04-10_21.49	21	rim	458	7			0.004	6.97	0.11	1.467240	0.0035	0.282079	0.0064	0.27602	7.1	0.00076	7.1	0.282073	-14.7	0.8	2366	46	1763	29
SA04-10_7.13	7	c1	458	7	10.3	0.6	0.004	5.96	0.36	1.467260	0.0040	0.282037	0.0107	1.14409	7.9	0.00265	7.8	0.282015	-16.7	1.3	2494	75	1851	49
SA04-10_12.24	12	rim	458	7	11.6	0.6	0.004	7.72	0.10	1.467110	0.0051	0.281915	0.0092	0.10142	9.3	0.00025	8.4	0.281913	-20.3	1.1	2718	62	2005	41
SA04-10_14.28	14	c1	458	7			0.004	7.04	0.07	1.467240	0.0038	0.282115	0.0072	0.16782	9.2	0.00047	9.5	0.282111	-13.3	0.9	2281	50	1704	32
SA04-10_20.47	20	inh	458	7			0.004	6.38	0.03	1.467250	0.0063	0.281105	0.0067	0.04461	7.2	0.00013	7.1	0.281104	-49.0	0.8	3737	59	3094	38
Nigg Bay																								
SA04-11_3.5	3	inh	465	5	4.5	0.6	0.003	6.59	0.11	1.467060	0.0062	0.282149	0.0163	0.26913	7.1	0.00064	7.1	0.282144	-12.0	1.8	1799	128	1576	90
SA04-11_25.66	25	inh	465	5	6.5	0.6	0.003	5.42	0.04	1.467290	0.0042	0.282201	0.0069	0.09024	7.0	0.00024	7.0	0.282199	-10.0	0.8	1662	67	1490	41
SA04-11_25.99	25	rim	465	5	7.0	0.6	0.003	5.02	0.11	1.467390	0.0046	0.282049	0.0086	0.28335	8.2	0.00101	9.3	0.282040	-15.7	1.0	2433	59	1774	38
SA04-11_28.74	28	inh	465	5	7.0	0.6	0.003	4.86	0.04	1.467250	0.0035	0.282216	0.0067	0.09736	8.1	0.00025	8.0	0.282214	-9.5	0.8	1718	59	1485	37
SA04-11_28.73	28	rim	465	5	8.0	0.6	0.003	8.80	0.10	1.467240	0.0034	0.281966	0.0062	0.26380	7.0	0.00067	7.0	0.281960	-18.5	0.7	2609	43	1892	27
SA04-11_31.82	31	rim	465	5	6.6	0.6	0.003	7.42	0.10	1.467290	0.0035	0.282031	0.0069	0.24363	7.2	0.00065	8.4	0.282026	-16.2	0.8	2466	48	1796	30
SA04-11_31.81	31	inh	465	5	6.6	0.6	0.003	4.83	0.06	1.467290	0.0036	0.282099	0.0064	0.14142	7.4	0.00036	7.3	0.282096	-13.7	0.8	2850	-806	2259	-554
SA04-11_5.10	5	rim	465	5	5.6	0.6	0.003	6.01	0.09	1.467160	0.0061	0.282142	0.0086	0.19840	8.6	0.00047	8.7	0.282138	-12.2	1.0	2217	58	1629	37

Appendix 4f
Hf isotope data of Mud Tank zircon standard

	total Hf	1σ	Yb/Hf	1σ	$^{176}Yb/^{176}Hf$	1σ	$^{176}Lu/^{176}Hf$	1σ	$^{176}Hf/^{177}Hf$	1σ
08/02/07										
Mud Tank 1	5.9	0.06	0.007	0.000052	0.017588	0.000130	0.0002956	0.0000006	0.282508	0.000012
Mud Tank 2	6.0	0.07	0.007	0.000043	0.017752	0.000110	0.0003006	0.0000003	0.282486	0.000010
Mud Tank 3	6.2	0.11	0.007	0.000035	0.017047	0.000088	0.0002987	0.0000006	0.282514	0.000012
Mud Tank 4	6.2	0.10	0.007	0.000030	0.016695	0.000075	0.0002905	0.0000005	0.282513	0.000012
Mud Tank 5	6.2	0.11	0.007	0.000038	0.017507	0.000095	0.0003028	0.0000006	0.282498	0.000010
Mud Tank 6	4.9	0.10	0.007	0.000034	0.018183	0.000085	0.0003054	0.0000005	0.282515	0.000010
Mud Tank 7	5.3	0.10	0.007	0.000034	0.017745	0.000086	0.0003025	0.0000005	0.282499	0.000012
Mud Tank 8	4.5	0.07	0.007	0.000041	0.018170	0.000100	0.0003037	0.0000006	0.282492	0.000012
Mud Tank 9	4.9	0.09	0.007	0.000044	0.018256	0.000110	0.0003046	0.0000005	0.282486	0.000010
Mud Tank 10	4.7	0.09	0.007	0.000032	0.017485	0.000081	0.0002925	0.0000007	0.282537	0.000013
Mud Tank 11	5.2	0.09	0.007	0.000036	0.016926	0.000091	0.0002910	0.0000005	0.282518	0.000012
Mud Tank 12	5.1	0.06	0.008	0.000060	0.019555	0.000150	0.0003241	0.0000008	0.282527	0.000013
Mud Tank 13	5.5	0.06	0.008	0.000040	0.019314	0.000099	0.0003218	0.0000006	0.282506	0.000013
Mud Tank 14	4.7	0.08	0.008	0.000079	0.019078	0.000200	0.0003131	0.0000007	0.282513	0.000013
Mud Tank 15	5.4	0.06	0.007	0.000051	0.018439	0.000130	0.0003052	0.0000007	0.282512	0.000010
Mud Tank 16	5.7	0.05	0.007	0.000053	0.017897	0.000130	0.0002976	0.0000005	0.282510	0.000011
Mud Tank 17	5.8	0.06	0.005	0.000040	0.013722	0.000100	0.0002295	0.0000006	0.282505	0.000009
Mud Tank 18	6.1	0.13	0.006	0.000042	0.015670	0.000110	0.0002612	0.0000007	0.282535	0.000011
Mud Tank 19	6.1	0.13	0.007	0.000051	0.017408	0.000130	0.0002881	0.0000005	0.282509	0.000012
Mud Tank 20	6.1	0.10	0.006	0.000047	0.016142	0.000120	0.0002672	0.0000005	0.282521	0.000009
Mud Tank 21	5.9	0.05	0.007	0.000052	0.016741	0.000130	0.0002779	0.0000005	0.282530	0.000013
Mud Tank 22	5.5	0.06	0.007	0.000052	0.016853	0.000130	0.0002804	0.0000008	0.282513	0.000011
Mud Tank 23	5.2	0.08	0.007	0.000058	0.017852	0.000150	0.0002953	0.0000006	0.282511	0.000016
Mud Tank 24	4.6	0.08	0.007	0.000062	0.017262	0.000160	0.0002815	0.0000008	0.282540	0.000014
Mud Tank 25	5.3	0.09	0.006	0.000030	0.015944	0.000076	0.0002574	0.0000005	0.282508	0.000010
Mud Tank 26	5.7	0.10	0.007	0.000033	0.017936	0.000082	0.0002951	0.0000004	0.282525	0.000012
average (n=48)	**5.5**		**0.007**		**0.017430**		**0.000292**		**0.282513**	
2SD	**1.1**		**0.001**		**0.002432**		**0.000041**		**0.000028**	

Appendix 4g
Two-component magma mixing modelling

% Dalradian	$\delta^{18}O$ [‰]	εHf_T	εHf_C	% enriched mantle
0	5.5*	1.3*	3.4*	1
0.1	6.4	-0.5	1.4	0.9
0.2	7.2	-2.3	-0.7	0.8
0.3	8.1	-4.2	-2.7	0.7
0.4	9.0	-6.0	-4.7	0.6
0.5	9.9	-7.8	-6.8	0.5
0.6	10.7	-9.6	-8.8	0.4
0.7	11.6	-11.4	-10.8	0.3
0.8	12.5	-13.3	-12.8	0.2
0.9	13.3	-15.1	-14.9	0.1
1	14.2*	-16.9*	-16.9*	0

% Appin Group	$\delta^{18}O$ [‰]	εHf_T	εHf_C	% enriched mantle
0	5.5	1.3	3.4	1
0.1	6.1	0.2	2.1	0.9
0.2	6.7	-1.0	0.7	0.8
0.3	7.3	-2.1	-0.7	0.7
0.4	7.9	-3.3	-2.0	0.6
0.5	8.5	-4.4	-3.4	0.5
0.6	9.0	-5.5	-4.7	0.4
0.7	9.6	-6.7	-6.1	0.3
0.8	10.2	-7.8	-7.4	0.2
0.9	10.8	-9.0	-8.8	0.1
1	11.4	-10.1	-10.1	0

% Argyll Group	$\delta^{18}O$ [‰]	εHf_T	εHf_C	% enriched mantle
0	5.5	1.3	3.4	1
0.1	6.5	-1.1	0.8	0.9
0.2	7.4	-3.4	-1.7	0.8
0.3	8.4	-5.8	-4.3	0.7
0.4	9.3	-8.1	-6.9	0.6
0.5	10.3	-10.5	-9.5	0.5
0.6	11.3	-12.9	-12.0	0.4
0.7	12.2	-15.2	-14.6	0.3
0.8	13.2	-17.6	-17.2	0.2
0.9	14.1	-19.9	-19.7	0.1
1	15.1	-22.3	-22.3	0

% Appin Group	$\delta^{18}O$ [‰]	εHf_T	% Argyll
0	15.1	-22.3	1
0.1	14.7	-21.1	0.9
0.2	14.4	-19.9	0.8
0.3	14.0	-18.6	0.7
0.4	13.6	-17.4	0.6
0.5	13.3	-16.2	0.5
0.6	12.9	-15.0	0.4
0.7	12.5	-13.8	0.3
0.8	12.1	-12.5	0.2
0.9	11.8	-11.3	0.1
1	11.4	-10.1	0

*Average enriched mantle and average Dalradian

(data from Anderson et al., 2004; Canning et al., 1998; Eiler , 2001; Frost and O'Nions, 1985; O'Nions et al., 1983; Thirlwall, 1982)

εHf_T = data from Thirlwall (1982)

εHf_C = data from Canning et al. (1998)